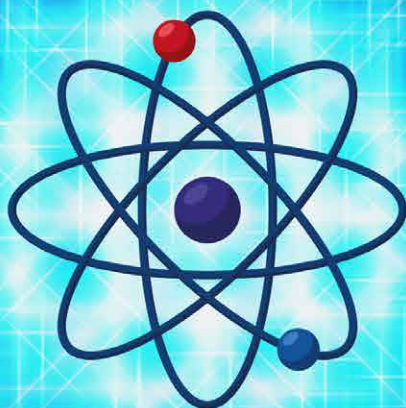


17th Biennial DAE-BRNS Symposium on NUCLEAR AND RADIOCHEMISTRY

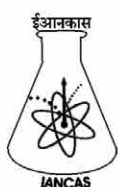
NUCAR - 2025

April 23 - 26, 2025

DAE Convention Centre, Anushaktinagar, Mumbai, India



BOOK OF ABSTRACTS



Editors

Aishwarya S. Kar
S. B. Deb
Seraj Ansari
S. K. Rakshit

S. Jeyakumar
M. K. Saxena
Y. K. Bhardwaj

न्यूकार- २०२५

१७वीं द्विवार्षिक डीएई-बीआरएनएस
नाभिकीय एवं रेडियोरसायनिकी संगोष्ठी

प ऊ वि सम्मेलन केन्द्र, अणुशक्तिनगर, मुंबई
अप्रैल २३ – २६, २०२५

आयोजक

भाभा परमाणु अनुसंधान केन्द्र
एवं
इंडियन असोसियन ऑफ न्युकिलियर केमिस्ट्स एंड
अलाईड साइंटिस्ट्स (ईआनकास)

संपादक मंडल

ऐश्वर्या एस. कर, एस. बी. देव, सेराज ए. अंसारी, एस. के. रक्षित,
एस. जयकुमार, एम. के. सक्सेना, वाई. के. भारद्वाज

प्रायोजक

नाभिकीय विज्ञान अनुसंधान बोर्ड (बीआरएनएस)
परमाणु ऊर्जा विभाग

Title:

17th Biennial DAE-BRNS Symposium
on Nuclear and Radiochemistry (NUCAR – 2025)

Editors:

Aishwarya S. Kar, S. B. Deb., Seraj Ansari, S. K. Rakshit,
S. Jeyakumar, M. K. Saxena, Y. K. Bhardwaj

Disclaimer

The abstracts included in this book have been provided by the individual authors and are published as submitted. The editors are not responsible for the accuracy, content, or views expressed in the abstracts. Inclusion in this abstracts book does not imply endorsement of the methods, results, or conclusions by the editors.

Printed by:

Prudent Art & Fab Pvt Ltd
A-221, TTC Industrial Area,
MIDC., Mahape, Navi Mumbai - 400701

डॉ. अजित कुमार मोहान्ती
Dr. Ajit Kumar Mohanty



अध्यक्ष, परमाणु ऊर्जा आयोग
व
सचिव, परमाणु ऊर्जा विभाग
Chairman, Atomic Energy Commission
&
Secretary, Department of Atomic Energy

MESSAGE

I am pleased to learn that the 17th Biennial DAE-BRNS Symposium on “Nuclear and Radiochemistry” (NUCAR-2025) is being organised at DAE Convention Centre, Anushakti Nagar, during 23rd-26th April, 2025. This symposium remains a prominent platform for sharing knowledge and working together in the domain of nuclear and radiochemistry, uniting professionals, researchers and academics from around the nation as well as globally.

NUCAR-2025 provides an important platform for the DAE scientific community and academics to engage in substantive discussions and collaborations, thereby enhancing India's nuclear science and technology framework and inspiring young scientists and researchers to take up the associated challenges as their research endeavours.

The participation of nearly 300 researchers is commendable, as their contributions are vital in shaping the future of nuclear and radiochemistry and the applications of radiation and radioisotopes. The invited talks and the contributory abstracts on both fundamental and applied research will be significant in establishing India's leadership in peaceful nuclear advancements.

I extend my best wishes for the success of NUCAR-2025 and look forward to the contributions that will emerge from this symposium, furthering our collective pursuit of excellence in nuclear science and technology.

Ajit Kumar Mohanty
(Ajit Kumar Mohanty)

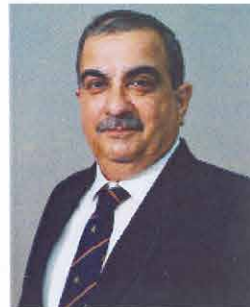


विवेक भसीन
Vivek Bhasin



भारत सरकार
Government of India

निदेशक, भाभा परमाणु अनुसंधान केंद्र
Director, Bhabha Atomic Research Centre
सदस्य, परमाणु ऊर्जा आयोग
Member, Atomic Energy Commission



MESSAGE

I am delighted to know that the 17th Biennial DAE-BRNS Symposium on Nuclear and Radiochemistry (NUCAR-2025) is being held at DAE Convention Centre, Anushakti Nagar, during 23rd-26th April, 2025.

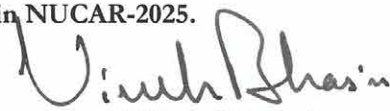
It is gratifying to witness the continued progress of the NUCAR series of symposia as a premier gathering for researchers and professionals in the field of nuclear & radiochemistry and allied sciences. Over the years, this symposium has played an important role in fostering the exchange of scientific ideas and advancements in nuclear and radiochemistry. The symposium has consistently garnered wide participation from researchers across India, with over 250 contributory papers, reflecting the growing interest and engagement in nuclear sciences.

NUCAR-2025 covers topics, such as nuclear reactions, actinide chemistry, materials for reactors, Radioanalytical techniques, the chemistry of nuclear fuel cycle, uses of radiation technology, environmental radioactivity, nuclear safety measures, and forensic science. It also intends to address challenges in nuclear waste management, artificial intelligence in nuclear applications, and radiation-based technologies. The, symposium serves as an avenue to acknowledge the multidisciplinary nature of nuclear research to drive progress in atomic energy applications. NUCAR facilitates insightful discussions through invited talks by eminent scientists, oral and poster presentations and panel discussions on emerging challenges and future directions. I am sure that these deliberations align with India's long-term vision of leveraging nuclear science for sustainable development and technological self-reliance

It is remarkable that a commemorative special session in memory of Dr. M. V. Ramaniah has been scheduled in NUCAR. It will further enrich the scientific discourse to remember his landmark achievements in formulating the radiochemistry programme at BARC.

The exchange of knowledge at NUCAR-2025 will contribute significantly to scientific progress and further strengthen India's capabilities in nuclear science and technology. The research insights and discussions during this event will help drive forward innovations that are crucial to the progress of nuclear and radiochemistry.

I extend my best wishes for fruitful and scientifically enriching sessions in NUCAR-2025.


(Vivek Bhasin)

08.04.2025



भाभा परमाणु अनुसंधान केंद्र, ट्रॉम्बे, मुंबई- 400 085, भारत • Bhabha Atomic Research Centre, Trombay, Mumbai 400 085, India
दूरभाष/Phone: +(91) (22) 2550 5300, 2551 1910 • फैक्स/Fax: +(91) (22) 2559 2107, 2550 5151
ई-मेल/E-mail: director@barc.gov.in



Dr. R. B. Grover
Chairman

Government of India
Department of Atomic Energy (DAE)
Board of Research in Nuclear Sciences (BRNS)

16 April 2025

MESSAGE

I am pleased to know that the 17th Biennial DAE-BRNS Symposium on Nuclear and Radiochemistry (NUCAR-2025), a prestigious symposium of DAE, is being organised at the DAE Convention Centre, Anushakti Nagar, during 23rd-26th April, 2025. The NUCAR series of symposium covers a wide range of topics related to nuclear and radiochemistry, including the nuclear fuel cycle, nuclear reactions, the chemistry of materials used in reactors their by-products, actinide chemistry and spectroscopy, nuclear and radioanalytical techniques, and applications of radiation technology and radioisotopes for non-power applications in industry, food, agriculture and healthcare.

I am delighted to note that the symposium has received an overwhelming participation, which includes more than 250 contributory papers and around 26 invited talks by experts. It is heartwarming to know that a special session is dedicated to Dr. M. V. Ramaniah, the architect of the radiochemistry program at BARC. Dr. Ramaniah's foresight and vision paved the way for nuclear and radiochemistry research, and his immense contributions and able guidance nurtured many stalwarts in this field of research.

The Board of Research in Nuclear Sciences (BRNS) plays a crucial role in providing financial support for research initiatives within universities and institutions. Participation in the symposium will offer university researchers an opportunity to collaborate with their DAE counterparts and gain insights into the research needs of the DAE's mission.

I compliment the organisers, and I must say that this symposium will benefit scientists, researchers, and students through deliberations and possible collaborations.

I extend my best wishes for the grand success of NUCAR 2025.

(R B Grover)

PREFACE

It is our pleasure to bring to you all the technical proceedings of the 17th biennial DAE-BRNS Symposium on Nuclear and Radiochemistry (NUCAR-2025) being held during 23rd – 26th April 2025 at the DAE Convention Centre, Anushaktinagar, Mumbai. The venue is in a well-planned self-contained community situated near hills, lakes, and abundant green natural environment.

NUCAR 2025 is organized by the Board of Research in Nuclear Sciences (BRNS) under the aegis of Bhabha Atomic Research Centre (BARC) in association with the Indian Association of Nuclear Chemists and Allied Scientists (IANCAS), which aims to promote high-quality research, facilitate professional interactions among academia, researchers, scientists & industry and discuss new advancements across nine key fields of nuclear and radiochemistry.

IANCAS plays a key role in shaping the scope and quality of NUCAR series of symposium, ensuring a technical program that encompasses recent developments and challenges in the subject domain. The financial support of BRNS, Department of Atomic Energy, India, is integral and backbone to the success of this event.

A total of more than 325 abstracts received underwent a thorough single-blind critical review by esteemed reviewers. Post review 265 abstracts have been accepted for presentation. The program spans diverse topics, including Nuclear & Radiochemistry, Nuclear Probes, Chemistry & Spectroscopy of Actinides, Nuclear & Radioanalytical Techniques, Chemistry of Reactor Materials and applications of Artificial Intelligence in Nuclear Instrumentation, among others.

Since its inception in 1993, NUCAR has been held biennially at various premier institutions across India. Details of the present symposia, including its proceedings, can be found in the NUCAR website at <https://www.iancas.org.in/nucar2025/>

It is anticipated that this symposium will bring together leading experts, researchers, and students, providing a relaxed yet focused setting for the exchange of new ideas and the discussions on emerging technologies and solutions in nuclear and radiochemistry.

It is an honour to host distinguished scientists from India and around the world for delivering their invited talks through which they will present their innovative research and ideas, sparking insightful discussions and kindling multidisciplinary collaborations. In addition, theme based Invited Short Presentations (ISP) by emerging specialists have been arranged in the symposium.

Mumbai, India's financial capital is a city where tradition meets modernity. It offers visitors a unique cultural experience, boasts a rich history, vibrant performing arts, and a rich and eclectic cuisine. During your stay, we hope you also take time to explore the natural beauty of Mumbai.

We record our sincere gratitude to Dr. A. K. Mohanty, Chairman, AEC & Secretary, DAE and Dr. R. B. Grover, Chairman, BRNS, DAE for being our patrons of NUCAR – 2025 and also for their kind support. We are highly indebted to Shri Vivek Bhasin, Director, BARC for his whole hearted support and guidance as the Chairman of the National Advisory Committee of NUCAR -2025. Our sincere thanks are due to BRNS for providing the financial support. We record our heartfelt thanks to all the members of National Advisory Committee and Symposium Organizing Committee for their constant support and guidance. We are grateful to Indian Association of Nuclear Chemists and Allied Scientists (IANCAS) for shouldering the responsibilities and encouraging the young scientists by best paper presentation awards.

Our heartfelt gratitude to all participants of NUCAR 2025 and invited speakers, contributed abstract authors, technical committee members, the symposium organizing team and of course, the local organising committee members, who are meticulously taking care of every aspect of the symposium. Special thanks go to the NUCAR 2025 secretariat members for their diligent efforts behind the scenes to ensure smooth execution of this technical event.

We put on record our sincere thanks to Shri Manish Singh (FCD), Ms. Swarnima Rawat (RTDD), Ms. Debarati Das (RCD), Shri Sunil Kumar (RACD), Shri Shishu Kant Suman (RPhD) and Shri Abhishek Sharma (PDD) for their untiring efforts towards preparation of the "*Book of Abstracts*".

We are excited to welcome you to Mumbai and look forward to the impactful exchanges that will shape the future research and possible collaborations.

Have a wonderful stay and scientifically stimulating interactions!

With best wishes.

Editors

प्रस्तावना

“सत्रहवीं द्विवार्षिक डीई-बीआरएनएस नाभिकीय और रेडियोरसायनिकी संगोष्ठी, न्यूकार – २०२५” भाभा परमाणु अनुसंधान केंद्र एवं भारतीय परमाणु रसायनज्ञ और संबद्ध वैज्ञानिकों के संघ(ईआनकास) द्वारा आयोजित हो रही है जो आमंत्रित शोधकर्ताओं और विभिन्न वैज्ञानिकों के “नाभिकीय और रेडियोरसायनिकी” पर आधारित नए निष्कर्षों / खोजों से संबंधित है। संगोष्ठी के कार्यकलाप नाभिकीय विज्ञान अनुसंधान मंडल (बीआरएनएस), परमाणु ऊर्जा विभाग की ओर से प्रायोजित है और इसमें ईआनकास भी एक अग्रणी भूमिका निभा रही है। संगोष्ठी आयोजन स्थल “प ऊ वि सम्मेलन केन्द्र, अणुशक्तिनगर, मुंबई” जोपहाड़ियों, झीलों और प्रचुर हरे प्राकृतिक वातावरण के पास स्थित एक सुनियोजित आत्मनिर्भर समुदाय में है। यह संगोष्ठी “नाभिकीय और रेडियोरसायनिकी” के क्षेत्र में काम करने वाले शोधकर्ताओं के अपने नए निष्कर्षों / खोजों पर चर्चा और नवीनतम जानकारी के साथ अपने ज्ञान को अद्यतन करने के लिए एक साझा मंच प्रदान करती है। “नाभिकीय और रेडियोरसायनिकी” विभिन्न विषयों जैसे चिकित्सा, इंजीनियरिंग, कृषि, उद्योगों और जल विज्ञान में रेडियोसमस्थानिकों की बढ़ती मांग एवं विकिरण प्रौद्योगिकी की वजह से आधुनिक विज्ञान के क्षेत्र में बुनियादी और अनुप्रयुक्त अनुसंधान के एक महत्वपूर्ण क्षेत्र का प्रतिनिधित्व करता है।

आईएनसीएस के सहयोग से परमाणु विज्ञान अनुसंधान मंडल (बीआरएनएस) और भाभा परमाणु अनुसंधान केंद्र (बीएआरसी) द्वारा संयुक्त रूप से आयोजित न्यूकार-२०२५ का उद्देश्य उच्च गुणवत्ता वाले अनुसंधान को बढ़ावा देना, शिक्षाविदों, शोधकर्ताओं, वैज्ञानिकों और उद्योग के बीच पेशेवर बातचीत को सुविधाजनक बनाना और परमाणु और रेडियोरसायनिकी के नौ प्रमुख क्षेत्रों में नई प्रगति पर चर्चा करना है। इस संगोष्ठी में कुल 325 से अधिक सोध पत्र के सार प्राप्त हुए, जिन्हें सम्मानित समीक्षकों द्वारा गहन आलोचनात्मक समीक्षा से गुज़ारा गया। समीक्षा के बाद 265 सोध पत्र के सार प्रस्तुतीकरण के लिए स्वीकार किए गए हैं। इस संगोष्ठी के तकनीकी कार्यक्रम में चर्चा के लिए परमाणु और रेडियोरसायन विज्ञान, परमाणु प्रोब्स, एक्टिनाइड्स की रसायन विज्ञान और स्पेक्ट्रोस्कोपी, परमाणु और रेडियोविश्लेषण तकनीक, रिएक्टर सामग्री की रसायन विज्ञान और परमाणु इंस्ट्रूमेंटेशन में कृत्रिम बुद्धिमत्ता के अनुप्रयोग इत्यादिजैसे विभिन्न विषयों को शामिल किया गया है।

१९९३ में अपनी स्थापना के बाद से, न्यूकार संगोष्ठी को भारत भर के विभिन्न प्रमुख संस्थानों में द्विवार्षिक रूप से आयोजित किया जाता रहा है। वर्तमान संगोष्ठी का विवरण और कार्यवाही, न्यूकार – २०२५ की वेबसाइट <https://www.iancas.org.in/nucar2025/> पर पाया जा सकता है। यह संगोष्ठी अग्रणी विशेषज्ञों, शोधकर्ताओं और छात्रों को परमाणु और रेडियोरसायनिकी विषय में उभरती प्रौद्योगिकियों और समाधानों पर नए विचारों के आदान-प्रदान और चर्चा के लिए एक सुनहरा अवसर एवं मंच प्रदान करेगी। भारत और दुनिया भर के प्रतिष्ठित वैज्ञानिकों को वार्ता देने के लिए आमंत्रित करना एक सम्मान की बात है, जिसके माध्यम से वे अपने अभिनव शोध और विचारों को प्रस्तुत करेंगे, व्यावहारिक चर्चाओं को बढ़ावा देंगे और बहु-विषयक सहयोग को

बढ़ावा देंगे। इसके अलावा, संगोष्ठी में उभरते विशेषज्ञों द्वारा विषय पर आधारित आमंत्रित लघु व्याख्यान की भी व्यवस्था की गई है।

भारत की वित्तीय राजधानी “मुंबई” एक ऐसा शहर है जहाँ परंपरा आधुनिकता से मिलती है। यह आगंतुकों को एक समृद्ध इतिहास, जीवंत प्रदर्शन कलाएँ, विविध व्यंजन एवं एक अनूठा सांस्कृतिक अनुभव प्रदान करता है। अपने प्रवास के दौरान, हम आशा करते हैं कि आप मुंबई की प्राकृतिक सुंदरता को देखने के लिए भी समय निकालेंगे।

सम्पादक मंडली न्यूकार – २०२५ के सभी प्रतिभागियों और आमंत्रित वक्ताओं, योगदान देने वाले सार लेखकों एवं तकनीकी समिति के सदस्यों के प्रति हार्दिक आभार अभिव्यक्त करते हैं। इस तकनीकी कार्यक्रम के सुचारुरूप से निष्पादन को सुनिश्चित करने के लिए पर्दे के पीछे काम करने वाले संगोष्ठी आयोजन समिति और स्थानीय आयोजन समिति के सदस्यों के प्रति हम हार्दिक आभार अभिव्यक्त करते हैं, जो संगोष्ठी के सफल परिचालन के लिए हर पहलू का सावधानी पूर्वक ध्यान रख रहे हैं।

हम आईसी के अध्यक्ष और डीईई के सचिव डॉ ए के मोहंती और बीआरएनएस, डीईई के अध्यक्ष डॉ आर बी ग्रोवर जी के न्यूकार - २०२५ में संरक्षक बनने और उनके सहयोग के लिए अपनी हार्दिक कृतज्ञता व्यक्त करते हैं। हम बीएआरसी के निदेशक श्री विवेक भसीन के न्यूकार - २०२५ की राष्ट्रीय सलाहकार समिति के अध्यक्ष के रूप में उनके पूरे दिल से समर्थन और मार्गदर्शन के लिए बहुत आभारी हैं। वित्तीय सहायता प्रदान करने के लिए हम बीआरएनएस के प्रति अपना हार्दिक आभार व्यक्त करते हैं। हम राष्ट्रीय सलाहकार समिति और संगोष्ठी आयोजन समिति के सभी सदस्यों को उनके निरंतर समर्थन और मार्गदर्शन के लिए हार्दिक धन्यवाद देते हैं। सम्पादक मंडली इंडियन एसोसिएशन ऑफ न्यूक्लियर केमिस्ट्स एंड अलाइड साइंटिस्ट्स (आईएनसीएस) को हमारी जिम्मेदारियों को साझा करने के लिए और युवा वैज्ञानिकों को सर्वश्रेष्ठ शोधपत्र प्रस्तुतिकारकों के पुरस्कारों द्वारा सम्मानित कर उन्हें प्रोत्साहित करने के लिए के लिए बहुत आभारी हैं।

सम्पादक मंडली सार पुस्तिका तैयार करने के लिए न्यूकार – २०२५ सचिवालय के सदस्य, श्री मनीष सिंह (एफसीडी), सुश्री स्वर्णिमा रावत (आरटीडीडी), सुश्री देबारती दास (आरसीडी), श्री सुनील कुमार (आरएसीडी), श्री शिशुकांत सुमन (आरपीएचडी) और श्री अभिषेक शर्मा (पीडीडी) को उनके अथक प्रयासों के लिए हार्दिक धन्यवाद देते हैं।

हम मुंबई की इस संगोष्ठी में आपका स्वागत करने के लिए उत्साहित हैं और भविष्य के शोध और संभावित सहयोग को आकार देने वाले प्रभावशाली आदान-प्रदान की प्रतीक्षा कर रहे हैं।

आपके शानदार प्रवास और वैज्ञानिक रूप से उत्साहवर्धक बातचीत की कामना करते हुए!

शुभकामनाओं के साथ
सम्पादक मंडली

NUCAR – 2025 Organizers

PATRONS

Mohanty A.K., Chairman, AEC

Grover, R.B. Chairman, BRNS, DAE

NATIONAL ADVISORY COMMITTEE

Bhasin V., Director, BARC, Mumbai

Bhardwaj Y. K., Associate Director, RC & IG, BARC, Mumbai

Aswal D. K., Director, HS&EG, BARC, Mumbai

Bhasikuttan A.C., Associate Director, CG, BARC, Mumbai

Bagla H. K., Vice Chancellor, HSNC University, Mumbai

Dani U., CE, NRB, BARC, Mumbai

Ghosh H.N., NISER, Bhubaneswar

Hassan P.A., Associate Director, BSG, BARC, Mumbai

Kapoor K, CE, NFC, Hyderabad

Karhadkar C.G., Director, IGCAR, Kalpakkam

Manohar S., Director, NRG, BARC

Malshe U.D., Director, RRCAT, Indore

Mohan J., Associate Director, RPG, BARC, Mumbai

Mudali U. K., Vice Chancellor, HBNI, Mumbai

Mukherjee P., CE, BRIT, Mumbai

Nayak A.K., Head NCPW, DAE Mumbai

Pathak B.C., CMD, NPCIL, Mumbai

Rajan K., Director, RPG, IGCAR, Kalpakkam

Saravanan B., Director, AMDER, Hyderabad

Satpati S.K., C&MD, UCIL, Jaduguda, Jharkhand

Satyakumar S., Chairman and CE, HWB, Mumbai

Shenoy K. T., Director, ChEG, BARC, Mumbai

Shukla D. K., Chairman, AERB, Mumbai

Singh D., CMD, IREL, Mumbai

Jayaraman V., Associate Director, MC&MFCG, IGCAR, Kalpakkam

Som Sumit, Director, VECC, Kolkata

Tewari R., Director, MG, BARC, Mumbai

Tilara M., Assoc. Director, RG, BARC, Mumbai

Tyagi A. K., Dean, HBNI, Mumbai

Yusuf S. M., Director, PG, BARC, Mumbai

Chairman

Convener

NUCAR – 2025 Organizers

SYMPOSIUM ORGANISING COMMITTEE

Bhardwaj Y.K., RC & IG, BARC, Mumbai
Rakshit S.K., PDD, BARC, Mumbai
Amrit Prakash, RMD, BARC, Mumbai
Acharya R., IRAD, BARC, Mumbai
Balaji Rao, Y, NFC Hyderabad
Basu, S., RMC, Mumbai
Baghel N. S. RMC, Mumbai
Bhanja, K., HWD, BARC, Mumbai
Chaudhury P., RSSD, BARC, Mumbai
Choudhury N., ChD, BARC, Mumbai
Das Tapas, RPhD, BARC, Mumbai
Dash K, NCCCM, Hyderabad
Gangadharan A., WMD, BARC, Mumbai
Ganesan R., MCD, IGCAR, Kalpakkam
Gautam S., FTD, BARC, Mumbai
Ghosh S., MF&PPD, IGCAR, Kalpakkam
Jeyakumar S., RCD, BARC, Mumbai
Joshi G.C., G. B. Pant University, Uttarakhand
Mukherjee J., BRNS, Mumbai
Mukhopadhyay S., ChED, BARC, Mumbai
Pai R.V., FCD, BARC, Mumbai
Parida S. C., PDD, BARC, Mumbai
Pandey Usha, BRIT, Mumbai
Patra C. N., ACD, BARC, Mumbai
Rao C. V. S. B., FCD, IGCAR, Kalpakkam
Sapra B. K., RP&AD, BARC, Mumbai
Saxena M. K., RACD, BARC, Mumbai
Shivakumar Y. C., TDD, BARC, Mumbai
Singh M, SIRD, BARC, Mumbai
Sugilal G., FRD, BARC, Mumbai
Suresh A., FCD, IGCAR, Kalpakkam
Umesh Kumar, ITIS, BARC, Mumbai
Virendra Kumar, RTDD, BARC, Mumbai
Venkatesan K.A., PRRR&DD, IGCAR, Kalpakkam
Vincent T., PSDD, BARC, Mumbai
Kar Aishwarya S., RACD, BARC, Mumbai
Ansari S.A., RCD BARC, Mumbai

**Chairman
Convener**

**Secretary
Joint Secretary**

NUCAR – 2025 Organizers

TECHNICAL COMMITTEE

Saxena M. K., Head, RACD, BARC, Mumbai

Jeyakumar, S., Head, RCD, BARC, Mumbai

Acharya R. V., ITIS, BARC

Agarwal Chhavi, RCD, BARC

Ashok Kumar G. V. S., ACSD, IGCAR

Ashokkumar P., HPD, BARC

Biswal Jayashree, IRAD, BARC

Chattaraj D., PDD, BARC

Deb S. B., RACD, BARC

Goel N.K., RTDD

Gupta Ruma, FCD, BARC

Gupta S. K., RCD, BARC

Kelkar Anoop, FF, BARC

Kumar Sumit, RACD, BARC

Mathur Anupam, BRIT

Meena G., RCD, BARC

Mishra S., EMAD, BARC

Mishra V.G., RACD, BARC

Mohanty Bholanath, RCD, BARC

Panja Surajit, FRD, BARC

Patra S., RCD, BARC

Paul Sumana, FCD, BARC

Pranaw Kumar, FCD, BARC

Ramanathan N., FChD, IGCAR

Rao Ankita, RCD, BARC

Remya P. S., ACD, BARC

Rout S., EMAD, BARC

Sahoo, S. K., HPD, BARC

Samui Pradeep, PDD, BARC

Satendra Kumar, ACSD, IGCAR

Sengupta Arijit, RCD, BARC

Sharma S. K., RCD, BARC

Sreenivasulu Balija, FChD, IGCAR

Vats Kusum, RPhD, BARC

Chairman

Co-Chairman

NUCAR – 2025 Organizers

Local Organizing Committee

Dr. Arnab Sarkar, FCD, BARC, Chairman

<u>Accommodation Committee</u>
Dr. Pranaw Kumar, FCD, Coordinator
Shri Dharmendra B Sharma, RCD
Shri Nitin Gumber, FCD
Shri Sunil Kumar, RACD
Shri Ginish Kumar P, PDD

<u>Hall Management Committee</u>
Dr. Sumana Paul, FCD, Coordinator
Kum. Anannya Banerjee, FCD
Kum. Debarati DAS, RCD
Dr. Ruma S. Gupta, FCD
Smt. Swarnima Rawat, RTDD
Kum. Khushboo Kumari, RACD
Kum P. S. Shetty, RPhD

<u>Hall Communication Committee</u>
Shri Manish Singh, FCD, Coordinator
Shri Sanjay Y. Salunkhe, PDD
Shri Anand R. Devlekar, RCD
Shri Vishal S. Choughule, RCD
Shri Sibu Soren, RCD

<u>Catering Committee</u>
Dr. Arvind S Ambolkar, FCD, Coordinator
Shri Lukman Ahamad, FCD
Shri Amit S. Kulkarni, RACD

<u>NUCAR - 2025 Secretariat</u>
Shri Manish Singh, FCD, Coordinator
Ms. Swarnima Rawat, RTDD
Ms. Debarati Das, RCD
Shri Sunil Kumar, RACD
Shri Shishu Kant Suman, RPhD
Shri Abhishek Sharma, PDD
Dr. Vijay Telmore, FCD
Ms. Khushboo Kumari, RACD
Dr. Seraj Ansari, RCD, Joint Secretary
Dr. Aishwarya S Kar, RACD, Secretary

<u>Poster Management Committee</u>
Dr. Sabyasachi Patra, RCD, Coordinator
Dr. Ashutosh Srivastava, RCD
Shri U. K. Thakur, RACD
Shri Sharath Babu M, PDD

<u>Registration Committee</u>
Dr. Ankita Rao, RCD, Coordinator
Smt. Soumi Kolay, RPhD
Kum. Rohini Agarwal, RTDD
Kum Annapurna R Chandane, RTDD
Dr. Kavitha Jayachandran, FCD
Dr. Shiny Suresh Kumar, RCD
Kum. Priya Goyal, RCD
Smt. Vishakha S. Uchale, FCD

<u>Transport Committee</u>
Shri Viju Chirayil, RPhD, Coordinator
Shri Sahiralam Khan Md., RPhD
Shri Umesh Kumar, RPhD
Shri Arijit Ghoshal, RTDD
Shri Arkaprava Layek, FCD

<u>Exhibition Committee</u>
Dr. P. S. Ramanjaneyulu, RACD, Coordinator
Dr. S. B. Deb, RACD,
Dr. Manoj Mohapatra, RCD
Dr. Narendra Goel, RTDD
Dr. Rajesh Acharya, ITIS
Dr. Suresh Subramaniam, RPhD
Dr. Ram Avatar Jat, PDD
Dr. Sunil Goswami, IRAD
Dr. Vijay Karki, FCD

Table of Contents

Invited Talks (IT) and Invited Short Presentations (ISP)

IT-1	Fabrication of Fast Reactor Fuels and their Characterization <i>Amrit Prakash</i>	1
IT-2	Research and Development of Microsphere based Fuels for Advanced Reactor Concept <i>Rajesh V. Pai</i>	3
IT-3	Development of Solvents for Nuclear Fuel Cycle <i>C.V.S. Brahmananda Rao</i>	5
IT-4	New Methodologies and Substrates for the Assay of Actinides using Nuclear Radiations <i>Rahul Tripathi</i>	6
IT-5	High-precision Mass Spectrometry Methods for Environmental Radionuclide Analysis <i>Norbert Kavasi, Tatsuo Aono</i>	8
IT-6	Isotopic Separations at Heavy Water Board <i>S. Satyakumar, V.V.S.A. Prasad, K.V. Tale, S.R. Gaidhani, Ajit R. Dusane</i>	10
IT-7	The Approaches to Design the Ligands for Separation of f-elements <i>V. G. Petrov</i>	12
IT-8	Production and Applications of Radioisotopes at RIKEN RI Beam Factory - Search for New Elements through Therapy of Cancer <i>H. Haba</i>	13
IT-9	Physics Safety and Utilization Aspects of Research Reactors <i>Tej Singh</i>	15
IT-10	Climate Change Impacts on Global Water Resources – Role of Nuclear Techniques <i>Chidambaram Sabarathinam, Khaled Hadi, Adnan Akber, S.V.V. Dhanuradha, Amjad Al Rashidi</i>	17
IT-11	Delayed Molecular Hydrogen Production in Portlandite Under Irradiation: Reaction Mechanisms and Consequences for the Storage of Radioactive Waste <i>Thibaut Herin, Stéphane Poyet, Pascal Bouniol, Sophie Le Caër</i>	19
IT-12	Back End Fuel Cycle- Status and Current Trends <i>Madhuri Shetty</i>	21
IT-13	Recent Advances in Nuclear Waste Management Practices in India <i>D. Banerjee</i>	22

IT-14	Advanced Materials for Selective Capture and Removal of Radionuclides in Nuclear Waste Management <i>Debajit Sarma</i>	23
IT-15	Research and Development of Molten Salt Fuels <i>S.C. Parida</i>	25
IT-16	Regulatory Clearance and Hot Commissioning Experience of DFRP <i>K. Rajan</i>	26
ISP-1	Direct Solid Sampling of Nuclear Materials for Chemical Quality Assurance – An Advanced ETV-ICP-OES Application <i>S.B. Deb, Abhijit Saha</i>	27
ISP-2	Development of Ion Chromatography as an Analytical Tool in the Nuclear Material Fabrication Process at Nuclear Fuel Complex <i>Shehanaz Bano, A.K. Nayak, Y. Balaji Rao</i>	29
ISP-3	Radiation Detection using Scintillators for Multiple Applications <i>Liviu Matei, Arnold Burger</i>	31
ISP-4	Calibration free Laser ablation Molecular Isotopic Spectrometry – A New Outlook to the Isotopic Composition Determination of Boron <i>Arnab Sarkar, Anandhu Mohan, Anannya Banerjee</i>	32
ISP-5	Dynamics of Neck-rupture in Nuclear Fission using Particle Emission as a Probe <i>Y.K. Gupta</i>	34
ISP-6	Nuclear Instrumentation and Application of AI <i>P.P. Shete</i>	35
ISP-7	Molten Salt-based Electrochemical De-oxidation of Uranium and Thorium Oxides <i>R. Kumaresan</i>	36
ISP-8	Fissile Zone Identification System (FIZIDS) <i>K. Sundararajan</i>	37
ISP-9	Development of Potentiometric Sensors for Lanthanides and Actinides <i>Bholanath Mahanty</i>	38
ISP-10	Recent Advances in Industrial Applications of Radiotracers for Process Optimization in Glass Production and Waste Water Treatment <i>Jayashree Biswal</i>	39
ISP-11	Medical Cyclotrons: An Essential Need for Cancer Management <i>M.R.A. Pillai</i>	41
ISP-12	Radiolabeled Somatostatin Analogs for Diagnosis and Therapy of Neuroendocrine Cancers: In-house Synthesis, Quality Control and Preliminary Clinical Investigation <i>V. Kusum Vats</i>	42

Contributory Papers

A: Nuclear Chemistry and Nuclear Probes

- | | | |
|-------------|--|----|
| A-1 | To Investigate the Fission Timescale of $^{206}\text{Rn}^*$ Utilizing Neutron Multiplicity as a Probe
<i>Punit Dubey, Mahima Upadhyay, Mahesh Choudhary, Namrata Singh, Shweta Singh, Sriya Paul, Utkarsha Mishra, N. Saneesh, Mohit Kumar, Rishabh Prajapati, K. S. Golda, Akhil Jhingan, P. Sugathan, Jhilam Sadhukhan, Raghav Agarwal, Kiran, Ajay Kumar</i> | 43 |
| A-2 | Positron Annihilation Lifetime Spectroscopic (PALS) Study on SBA-15 Nano-pores Under High CO_2 Gas Pressure in Presence of [BmIm][NTf2] Ionic Liquid
<i>Shapath Bhandari, Dhanadeep Dutta</i> | 44 |
| A-3 | Compression Induced Crystalline to Porous Glass Transformation of Zeolitic Imidazolate Framework-62: A Positron Annihilation Spectroscopy Study
<i>J. Mor, Renjith B. Nelliyil, S. K. Sharma</i> | 45 |
| A-4 | CO_2 Pressure Induced Flexibility of Pure and Hybrid ZIF-7: An in-situ PALS Study
<i>R. B. Nelliyil, J. Mor, S. K. Sharma</i> | 46 |
| A-5 | Role of Defects in Light Emission of $\text{Zn}_2\text{Ge}_{1-x}\text{Sn}_x\text{O}_4$: A Combined Positron Annihilation Lifetime and Photoluminescence Spectroscopic Study
<i>Bhavana Bharti, Annu Balhara, Santosh K. Gupta, K. Sudarshan</i> | 47 |
| A-6 | Study of fission product mass distribution in $^{11}\text{B} + ^{237}\text{Np}$ reaction to investigate the role of shell closure
<i>S. Kumar, S. Patra, A. Mhatre, A. Kumar, K. Ramachandran, R. Tripathi</i> | 48 |
| A-7 | Neutron Capture Cross Section of ^{68}Zn: Uncertainty Analysis and Comparison with γ-Ray Strength Functions
<i>Monika, Sumit Bamal, A. Gandhi, S. Lawitlang, B. Lalremruata, A. Kumar, Rajeev Kumar, K. Umasankari, L.S. Danu, S. Santra, B.K. Nayak, Rebecca Lalnuntluangi</i> | 49 |
| A-8 | Neutron Yield from Stable Heavy Ion on high Z Beam Dump
<i>Vitisha Suman, Biju K.</i> | 50 |
| A-9 | Investigation of Site-selective Doping Induced Defects in CaSnO_3 Perovskite: A Positron Annihilation Spectroscopic Study
<i>D. Das, S.K. Gupta, K. Sudarshan</i> | 51 |
| A-10 | Simulations for Proton Induced Positron Annihilation Facility
<i>K. Dhankar, S. Kulkarni, K. Shastry, S. Mukherjee</i> | 52 |
| A-11 | Influence of Electron Beam Irradiation on Free Volume of LLDPE/POE Blends: A Positron Annihilation Lifetime Spectroscopic Study
<i>M. Singh, R. Agarwal, D. Dutta, S. Ray Chowdhury</i> | 53 |

A-12	Measurement of Activation Cross Sections of Alpha Induced Reactions on ^{nat}Ta up to 40 MeV <i>Sk Wasim Raja</i>	54
A-13	Quark-Gluon Interactions and Color Confinement: An Algebraic Approach to Theoretical Modeling <i>B.C. Chanyal, V.K. Sharma, Neeraj Bisht</i>	55
A-14	Measurement of Production Cross Sections of ¹⁹⁶Au Produced From ¹⁹⁷Au + ²⁰Ne Reactions from 108 To 171 MeV Projectile Energy <i>S. Mukherjee, S. Lahiri, C. Barman, S. Bhattacharyya, S. Chatterjee, S. Dasgupta, J. Datta, G. Mukherjee</i>	56
A-15	Spectroscopic Investigation of Defects in Natural Zircon Irradiated with 10 MeV Electron Beam <i>Rumu H. Banerjee, Nishant Chaudhary, Rajath Alexander, Kulwant Singh, Pranesh Sengupta</i>	57
A-16	Study of Uncertainty Propagation of ⁵⁸Ni(N, P)⁵⁸Co Reaction <i>Namrata Singh, Mahesh Choudhary, Mahima Upadhyay, Punit Dubey, Shweta Singh, Sriya Paul, G. Mishra, Sukanya De, L. S. Danu, Ajay Kumar, R. G. Thomas, A. Kumar</i>	58
A-17	Induced Air Activity Studies in a Photo-Fission Experimental Vault <i>K. Biju, V.S. Dagle, P. Srinivasan</i>	59

B: Chemistry of Reactor Materials

B-1	Effect of Ions and Oxides on Hydrogen Peroxide Yield <i>Muniasamy. L, Puspallata Rajesh, R. Ramakrishnan, S. Bera, I.V.N.S. Kamaraju, T.V. Krishna Mohan</i>	60
B-2	Electrochemical Conversion of UO₂-ZrO₂ Mixture to U and Zr by Direct Oxide Electrochemical Reduction (DOER) <i>N. Sanil, L. Shakila, V. Arunkumar, R. Kumaresan</i>	61
B-3	Electrochemical Behavior of Gd⁺³ in LiCl-KCl at W and Fe Electrodes <i>Suvra Sil, S. Nedumaran, Patoju Sai Dilip, Anwesha Mukherjee, Gurudas Pakhui, R. Kumaresan</i>	62
B-4	Ion Chromatographic Determination of Phosphorous in Stainless steel <i>U.K. Thakur, Poonam Verma, S. Jeyakumar</i>	63
B-5	Analysis of Gases in Sodium-Limestone Concrete Interactions by Gas Chromatography <i>Venkat Reddy G, Arjun Pradeep, Malarvizhi B., Sanjay Kumar Das, Sreedhar B.K.</i>	64
B-6	Electrical Conductivity Measurement of LiCl-Li₂O Molten Salts <i>N. Sanil, V. Arunkumar, R. Kumaresan</i>	65
B-7	Measurement of Dielectric Constant and Loss Tangent of Uranium Compounds at 2.45 GHz by Rectangular Waveguide Cavity Resonator <i>Pasupuleti Kalpana, Jayanta Mondal, A.N. Patil, S.K. Satpati, Rishi Verma</i>	66
B-8	Determination of Trace Thorium in Uranium Oxide via Direct Solid Sampling in Electrothermal Vaporization Coupled ICP-OES <i>Abhijit Saha, S.B. Deb, Khushboo Kumari</i>	67

B-9	Addictive White Gaussian Noise (AWGN) Incorporated Calibration-Free LAMIS for Improved Direct Boron Isotopic Analysis <i>Anandhu Mohan, Anannya Banerjee, Arnab Sarkar</i>	68
B-10	Application of Electrothermal Vapourization Coupled ICP-OES for Preparing In-House Reference Materials of Gd₂Zr₂O₇ <i>S.B. Deb, Khushboo Kumari, Abhijit Saha</i>	69
B-11	Characterizing Isotopic Fractionation in Boron Plasma Plume Produced by Laser Ablation <i>Anandhu Mohan, Anannya Banerjee, Arnab Sarkar</i>	70
B-12	High-Precision Measurement of ⁶Li / ⁷Li Isotopic Abundance in Highly Depleted ⁶LiF for Molten Salt Reactor <i>Preeti Goswami, K. Sasi Bhushan, P.G. Jaison</i>	71
B-13	Trace Boron Determination in Graphite by Isotope Dilution-Thermal Ionization Mass Spectrometry <i>K. Sasi Bhushan, Preeti Goswami, P.G. Jaison</i>	72
B-14	Determination of Impurities in Helium Bond Gas of FBTR Fuel Pins <i>M. Phanindra Kumar, P.S. Ramanjaneyulu, Sunil Kumar, A.S. Kulkarni, B.K. Nagar, M.K. Saxena</i>	73
B-15	Studies on the Kinetic Effect of Hydrogen Isotope Oxidation using Copper Oxide Beads <i>Jitendra Singh, Sandeep K.C., Kalyan Bhanja</i>	74
B-16	Application of Fluoro-Phosphate Salts for Uranium Determination in Tin Slag, Zircon and Sillimanite Minerals via LED Fluorimetry <i>C. Santosh Reddy and V.V. Hanuman</i>	75
B-17	Effect of Annealing Conditions on Diffusion of Deuterium in Zircaloy-4 Clad Material <i>Sunil Kumar, P.S. Ramanjaneyulu, M. Phanindra Kumar, A.S. Kulkarni, B.K. Nagar, M.K. Saxena</i>	76
B-18	Thermophysical Properties of Intermediate Ternary Compounds relevant to LiF-ThF₄-UF₄ System <i>Abhishek Kumar Rai, M.K. Sharma, S.K. Rakshit</i>	77
B-19	Liquid Chromatography Separation of Rare Earths Impurities in Gadolinium Zirconate, A Burnable Poison Material <i>Vaibhavi V. Raut, S. Jeyakumar, M.K. Saxena</i>	78
B-20	Solubility of Nickel in Molten Sodium Hydroxide <i>S.M. Bhojane, V. Chandanshive, E.D. Shiny Sam, H.V. Khadilkar, P. Ginish Kumar, B.D. Thakur, P. Samui, A. Saha, S.K. Rakshit, S.C. Parida</i>	79
B-21	Quality Control of Materials for Reactor Applications <i>S. Sriram, Manisankar Palai, V. Hemalatha, S Maji, K. Sundararajan</i>	80
B-22	A Single Method Approach for Chemical Characterization of PHWR Steam Generator Tube Material using RF GDOES <i>Y. Balaji Rao, S.N.V.M.S. Gupta, P.V. Nagendra Kumar, Dinesh Srivastava</i>	81

C: Chemistry & Spectroscopy of Actinides

C-1	Evaluation of Hydrodynamic Properties of Phosphate and Phosphonate Ligands	82
	<i>K.N. Bikash, S. Rajeswari, B. Sreenivasulu, C.V.S. Brahmananda Rao</i>	
C-2	Acid Free, Ligand Free, Selective, Room Temperature Dissolution of UO₃ into Ionic Liquid with Subsequent Electro-Deposition	83
	<i>D. Karmakar, A. Nagar, A. Srivastava, R.M.R Dumpala, A. Sengupta</i>	
C-3	Evaluation of Electrocatalytic Performance of RGO-Pt Catalyst for U(IV) Generation	84
	<i>Kuntal Kumar Pal, Chanchal Ghosh, Sandip Kumar Dhara</i>	
C-4	Green Route for Uranium Recovery from Solid Analytical Waste using Supercritical Carbon Dioxide Extraction	85
	<i>A.S. Kanekar, A. Rao, S.S. Kumar, S. Dhara</i>	
C-5	Electrodeposition Study of Uranium from Non-aqueous Methane Sulphonic Acid Medium	86
	<i>A. Srivastav, A. Rao, S.S. Kumar, P. Agarkar</i>	
C-6	Complexation of UO₂²⁺ ion with DGA & CMPO Functionalized Ionic Liquids	87
	<i>Priya Goyal, A. Sengupta, P. K. Mohapatra</i>	
C-7	Speciation of Uranium in K₂MgGeO₄ and its Implication on Photochemistry	88
	<i>Annu Balhara, J. Balasurendran, B. Modak, A.K. Yadav, Santosh K. Gupta</i>	
C-8	Demonstration of Mixer-Settler Runs for the Processing of U-Pu-Zr Feed Solutions using Tri-iso-Amyl Phosphate	89
	<i>B. Sreenivasulu, P. Amarendiran, A. Suresh, C.V.S. Brahmananda Rao</i>	
C-9	Nitridation and Dissolution Behavior of U-Zr Alloy with Different wt% of Zirconium	90
	<i>M. Bootharajan, Suranjan Bera, B. Sreenivasulu, K. Sundararajan, C.V.S. Brahmananda Rao</i>	
C-10	Separation of Uranium, Thorium and Lanthanides for the Processing of Monazite feed Solutions using Tri-iso-amyl Phosphate	91
	<i>B. Sreenivasulu, N. Navamani, A. Suresh, C.V.S. Brahmananda Rao</i>	
C-11	Trap Level Spectroscopic Properties of Uranium Incorporated Li₂B₄O₇	92
	<i>Hemachandar V., Saparya Chattaraj, D.K. Patre, D.P. Rath, Ashokkumar P., M. Mohapatra</i>	
C-12	Direct Uranium Extraction from Solid Oxides Employing Novel Supercritical CO₂-Phylic Extractants	93
	<i>N. Nayak, A.S. Kanekar, Shiny S., P. Agarkar, A. Rao, S. Jeyakumar</i>	
C-13	Understanding the Plutonium Transient Profiles in the Stripping Bank for Minimizing the Retention of Plutonium in Lean Organic Phase	94
	<i>S. Balasubramonian, N. Desigan, K.A. Venkatesan</i>	
C-14	Application of Tetra Alkyl Ammonium Hydrogen Phthalate Ionic Liquid for the Extraction of Pu⁴⁺ And UO₂²⁺ from Aqueous Hydrochloric Acid	95
	<i>S.D. Chowta, A. Sengupta, S. Biswas, K.K. Gupta, G. Sugilal, P.K. Mohapatra</i>	

C-15	Feasibility Study on Simultaneous Acid Killing cum Catalytic Oxalate Destruction cum Volume Reduction in the RA Cycle Evaporator <i>Arvind Prasad, Satyabrata Mishra, N. Desigan, P. Sivakumar, K.A. Venkatesan</i>	96
C-16	Conditions Prior to Acidification of Carbonate Waste Generated during Clean-Up of Degraded PUREX Solvent for Metal Recovery <i>Satyabrata Mishra, Rudrashis Bhattacharja, N. Desigan, J. Kodandaraman, K.A. Venkatesan</i>	97
C-17	Plutonium Estimation by Spectrophotometry Using 2-(5-Bromo-2-pyridylazo)-5-(diethylamino) phenol <i>P. Chakraborty, V.K.M. Kutty, G. Srinivasa Rao, J. Mohandas, D. Gogoi, A. Das</i>	98
C-18	Spectrophotometric Determination of Plutonium using $KMnO_4$ <i>Parichay Chakraborty, V.K.M. Kutty, Jaya Mohandas, C. Krishna Kumar, G. Srinivasa Rao, Arindam Das</i>	99
C-19	Estimation of Plutonium (IV) by Spectrophotometric Methods to Explore An Alternative Method for Online Determination of Plutonium in Oxalate Supernatant <i>Suman Panja, S.K. Gupta, N.S. Rathore, A. Kelkar, D.B. Sathe, R B Bhatt</i>	100
C-20	Computational Studies of U(VI) and Th (IV) Metal Complexes with TAP and DAAP Ligands <i>Vemuri Lakshmi Ganesh, T. Revathy, B. Sreenivasulu, C.V.S. Brahmananda Rao, Gopinadhanpillai Gopakumar</i>	101
C-21	Solvent Extraction Study of Irradiated U-Zr Feed Solution using Phosphate and Phosphonate Based Solvents <i>K.N. Bikash, B. Sreenivasulu, C.V.S. Brahmananda Rao</i>	102
C-22	Aggregate Size based Evaluation of Nature of Gel Formed during the Reaction between Citric Acid and Uranyl Nitrate <i>G. Jogeswara Rao, A.S. Suneesh, S. Balakrishnan, Rajesh Ganesan</i>	103
C-23	Effect of Aqueous Phase Acidity on Gamma Radiolysis of TBP/N-DD System <i>Chandan Mukhopadhyay, Satyabrata Mishra, R. Karthick, Debasish Saha, Pabitra Ghosh, Pushpalata Rajesh, K. Dhamodharan, K.A. Venkatesan</i>	104
C-24	Speciation of Uranium in Barium Molybdate Host through Time Resolved Photoluminescence Spectroscopy <i>Ritu Singh, T.P. Reshmi, M. Mohapatra</i>	105
C-25	Highly Efficient Pertraction of Np(IV) and Pu(IV) using Two Alkyl Substituted Diglycolamides in Octanol Medium <i>R.B. Gujar, B. Mahanty, P.K. Mohapatra, W. Verboom</i>	106
C-26	Routing Behaviour of Neptunium in PUREX Process Streams during Reprocessing of Fast Reactor Spent Nuclear Fuel at DFRP <i>K. Dhamodharan, T. Aneesh, K.A. Venkatesan, K. Rajan</i>	107
C-27	Tailored Polyethersulfone Beads with TiAP/DEHPA for Enhanced Plutonium (IV) Separation from Aqueous Acidic Feed <i>S.R. Guchhait, P.J. Wagh, Partha Sarathi, A. Kelkar, D.B. Sathe, R.B. Bhatt, Kartikey K. Yadav, D.K. Singh</i>	108

C-28	An Offline Conjugation of Cloud Point Extraction with Inductively Coupled Plasma Optical Emission Spectrometry for Determination of Trace Lanthanides in Uranium Matrix <i>Khushboo Kumari, Abhijit Saha, S.B. Deb</i>	109
C-29	An Accurate and Precise Isotope Dilution Mass Spectrometry Method for the Determination of U in High Active Liquid Sample <i>Ananda Karak, A.K. Tiwari, M.A. Kesarkar, P. Banerjee, P.S. Mukherjee, A. Kelkar, D.B. Sathe, R.B. Bhatt</i>	110
C-30	Electrochemical Study of Uranium at Bimetallic Ni Zn based MOFs Modified Electrode <i>Nitin Gumber, Apeksha Kadam, Ashutosh Srivastava, Rajesh V. Pai</i>	111
C-31	Speciation and Decorporation of Uranium with Pyrazine-2-Amidoxime Chelate <i>Ashutosh Srivastava, Manjoor Ali, Shikha Sharma, Pranaw Kumar, Rama Mohan Rao Dumpala, Amit Kumar</i>	112
C-32	A Sensitive Differential Pulse Voltammetry Method for Dissolution and Destructive Assay of Uranium Oxide in Acidic Media <i>Shiny S. Kumar, Pooja Agarkar, Ashutosh Srivastava, S. Jeyakumar</i>	113
C-33	Development of Amide-Based Resin for Rapid Uranium Sorption <i>Vinita Kumari, Ritesh Ruhela, Mahesh Tiwari, S.K. Sahu</i>	114
C-34	Separation of Plutonium, Thorium and Uranium in MSBR Fuel using HPLC <i>Vijay M. Telmore, Raju V. Shah, Pranaw Kumar, P.G. Jaison</i>	115
C-35	Development of Functionalized Aluminosilicate Composites from Fly Ash for Efficient Sorption of Am(III) <i>Atanu Das, Ranjeet Saket, Aishwarya S. Kar</i>	116
C-36	Sorption Properties of Eco-friendly Fly Ash-based Geopolymer for Am(III) Ion Removal in Nuclear Waste Management <i>Atanu Das, Aishwarya S. Kar, M.K. Saxena</i>	117
C-37	Complexation Thermodynamics Studies of UO₂²⁺/DGA Complexes Optical Spectroscopy and Microcalorimetry: Effect of Alkyl Chain Branching <i>D.B. Sharma, A.P. Wadawale, S.A. Ansari, A. Bhattacharyya</i>	118
C-38	Diluent Free Solvent Extraction of Uranium with Higher Analogue of TOPO-DEHPA Eutectic <i>M. Sharathbabu, Prashant Patil, Sachin Pathak, Ashutosh Srivastava, S.K. Rakshit</i>	119
C-39	Extraction Behaviour of Pu(IV) into Hydrophobic DES of TBACl:DA <i>Prashant Patil, Sachin Pathak, M. Sharathbabu, Ashutosh Srivastava, S.K. Rakshit</i>	120
C-40	XAFS Study of Isostructural Sulphate Salts of Tetravalent Actinides and Lanthanides <i>Sumit Kumar, Meera Keskar</i>	121
C-41	Uranyl Complexation by Hydroxy-pyridine Dicarboxylic Acid: Thermodynamic and Theoretical Studies <i>Diksha P. Dalvi, Shiny S. Kumar, Rama Mohana Rao Dumpala, S. Jeyakumar</i>	122

C-42	Novel Tri-copolymerized Pyridinium Functionalized Polymeric Resins for Removal of Pb From Lanthanum Chloride Solution <i>Nikhilesh Nav Vigyan, Ritesh Ruhela</i>	123
C-43	Reverse Phase Liquid Chromatographic Method with online Pre-Concentrator for Trace Level Uranium Determination in Active Liquid Waste Generated from Uranium Production Facility <i>Y. Balaji Rao, Shehanaz Bano, P.V. Nagendra Kumar, Dinesh Srivastava</i>	124
D: Chemistry of Fission and Activation Products		
D-1	Complexation Behavior of Terpyridine Ligands with Am(III) and Eu(III) <i>Femina F.N., Vemuri Lakshmi Ganesh, C.V.S. Brahmananda Rao, Gopinadhanpillai Gopakumar</i>	125
D-2	Computational Prediction of Enthalpy of Extraction for Zr Complexes with Tri-Amyl Phosphate and Diamyl Amyl Phosphonate <i>Gopinadhanpillai Gopakumar, T. Revathy, B. Sreenivasulu, Vemuri Lakshmi Ganesh, C.V.S. Brahmananda Rao</i>	126
D-3	Spectroscopic Studies on Irradiated La₂O₃ and BaO-Doped Sodium Borosilicate (NBS) Glass for Application in Radioactive Waste Immobilization <i>Nimai Pathak, Prithwish Sinharoy, Dayamoy Banerjee, Manoj Mohapatra</i>	127
D-4	Synthesis, Characterization and Phase Transitions in Ca_xTh_xCe_{1-2x}PO₄ <i>Bal Govind Vats, Geeta R. Patkare, Muhammed Shafeeq</i>	128
D-5	Synergism in extraction of ²⁴¹Am from acidic feed using Combined Ligand Polymer Inclusion Membrane <i>Soumitra Panda, Bholanath Mahanty, Smita Thakur, Pramilla D. Sawant, A. Bhattacharyya</i>	129
D-6	Understanding the Complexation of CMPO and DGA functionalized Task Specific Ionic Liquids (TSILs) with Trivalent f-cations <i>Adityamani Nagar, A. Sengupta, P.K. Mohapatra</i>	130
D-7	Selective Separation of Cesium from a Mixture of Alpha and Beta-Gamma Activities using Ammonium Phosphomolybdate Modified Nafion Membrane <i>Amol Mhatre, Chhavi Agarwal</i>	131
D-8	Effect of γ - Radiation on Structural and Dissolution Behaviour of Fission Product Doped Chromium Ferrites <i>B. Padma Shruti, V. Balaji, P Chandramohan, R. Puspallata, T.V. Krishna Mohan</i>	132
D-9	Studies on Selective Separation of Palladium (Pd) from High Level Radioactive Liquid Waste (HLW) using Bis-Triazinyl-Pyridine <i>Kumari Anshul, Pawan Kumar Cheeta, J. Selvakumar, S. Srinivasan, G. Srinivasa Rao, J.K. Gayen</i>	133
D-10	Comparative Adsorption Behavior of Sr²⁺ Ions on Kaolinite and Lizardite Clay Minerals in the Presence of Sulphate Ions using Molecular Dynamics <i>Shelly Goel, Manish Chopra, Niharendu Choudhury</i>	134

D-11	Extraordinarily High Mutual Separation of Nd-Pr by Selective Dissolution of Nd into Ionic Liquid Containing Furyl Trifluoroacetone (FTA)	135
	<i>Dipita Karmakar, Adityamani Nagar, Priya Goyal, A. Sengupta, P.K. Mohapatra</i>	
D-12	DFT Approach to Elucidate Eu³⁺ Complexation with TOPO-Decanoic Acid Deep Eutectic Solvent	136
	<i>Pratyasha Panda, Bibek Dash, Pratyusha Parida, Sujata Mishra</i>	
D-13	Extraction of Platinum Group Metals with Dialkyl H-Phosphonates	137
	<i>Somnath Sengupta, B. Sreenivasulu, C.V.S. Brahmananda Rao</i>	
D-14	Comparing the Extraction Behavior of Actinides and Fission Products with Phosphates and Phosphonates	138
	<i>T. Revathy, B. Sreenivasulu, C.V.S. Brahmananda Rao</i>	
D-15	Advanced Separation of Radioactive Pertechnetate (TcO₄⁻) from Low Level Waste using MOF-808(Zr): A Cutting-Edge Approach	139
	<i>Kankan Patra, V.K. Mittal, Arijit Sengupta, A.K. Sahu, Anoop Kelkar, D.B. Sathe, R. B. Bhatt</i>	
D-16	Ion Exchange Behavior of Sodium Titanium Phosphate towards Exchanging Cesium	140
	<i>B. Robert Selvan, A. S. Suneesh, M. Amutha Suba, N. Ramanathan</i>	
D-17	Extraction and Stripping Behavior of Nd(III) in TODGA+TBP/N-Dodecane Phase in using Six Stage Annular Centrifugal Extractor	141
	<i>Jammu Ravi, M. Balamurugan, N. Desigan, R. Rajeev</i>	
D-18	Assay of Leached Hulls of FBTR Irradiated fuel for Plutonium at DFRP	142
	<i>J.S. Brahmaji Rao, G.V.S. Ashok Kumar, Debasish Saha, K. Sundararajan, V. Jayaraman, V. Anandhanarayanan, S. Sudhagar, P. Sivakumar, N. Desigan, K. Rajan</i>	
D-19	Conformational Studies of Tri-Amyl Phosphate (TAP) and its Branched Derivatives	143
	<i>Vemuri Lakshmi Ganesh, C.V.S. Brahmananda Rao, Gopinadhanpillai Gopakumar</i>	
D-20	Synthesis of Ion-Imprinted Polymer Gels for Selective Separation of Strontium Ions	144
	<i>Aditi Chourasia, Amol Mhatre, Chhavi Agarwal, R. Tripathi</i>	
D-21	Tailoring the Electrochemical Behavior and Speciation of Eu(III) in Choline Chloride-Based Deep Eutectic Solvents	145
	<i>Arkaprava Layek, Kavitha Jayachandran, Annu Balhara, Ruma Gupta</i>	
D-22	Separation of Lanthanides using a Mixed Ion Exchange Column with α-HIBA as Eluent	146
	<i>M.K. Das, V.G. Mishra</i>	
D-23	Study of Effect of Linker Behavior on the Iodine Adsorption Capacity of Thorium based UiO-66/67 MOFs	147
	<i>Abhishek Sharma, Bal Govind Vats, S.C. Parida</i>	
D-24	Fe (II)-Induced Immobilization of Selenium(VI) Oxyanion in Presence of Uranyl Ions	148
	<i>Snigdha Srabanee, Sumit Kumar</i>	

D-25	Neodymium Complexation by Tridentate Chelators: Speciation Studies by Absorbance and Calorimetry <i>Rama Mohana Rao Dumpala, Diksha P. Dalvi, Shiny S. Kumar, S. Jeyakumar</i>	149
D-26	Studies on Simultaneous Removal of Tc⁹⁹ & Ru¹⁰⁶ from Radioactive Low-Level Waste using Mild Steel Wool in Acidic Conditions <i>Adwitiya Kar, Anupkumar Bhaskarapillai, A.G. Shanmugamani, S. Srinivasan, G. Srinivasa Rao, J.K. Gayen</i>	150
E: Nuclear & Radioanalytical Techniques		
E-1	Measurement of Nuclear Reaction Rates for Neutron Spectrum Characterization at the Maximum Flux Location in the Dry Tube of the KAMINI Reactor <i>Alakananda S.G, Manish Chand, G.V.S. Ashok Kumar, K. Sundararajan</i>	151
E-2	Quantification of Minor and Trace Elements in Antidiabetic Herbal Formulations by Instrumental Neutron Activation Analysis Utilizing Self-Serve Facility of Dhruva Reactor <i>Arpita Datta, Reetta Sara George, S.K. Samanta, R. Acharya</i>	152
E-3	Influence of Organic and Inorganic Nutrients on Soil Physio-Chemical Parameters and Maize Yield Utilizing Instrumental Neutron Activation Analysis <i>Vaishali Dadwal, Deep Shikha, Sonika Gupta, Aditi Dalvi, Vimal Mehta, R. Acharya</i>	153
E-4	Neutron Attenuation Measurements in Borated Concrete and Comparison with Normal Concrete <i>D.V. Subramanian, Adish Haridas, D. Sunil Kumar, J. Ashok Kumar, M. Elumalai, Himanshu Gupta, R. Preetha</i>	154
E-5	Semi-Quantitative Direct Non-Destructive Determination of Fe, Sn and Ni in Zirconium Alloy Samples using Wavelength Dispersive X-ray Fluorescence Spectrometer <i>M. Singh, L. Pradhan, A. D. Jadhav, A. Pandey, V.R. Sonar, A. Kelkar, D. B. Sathe, Aniruddha Kumar, R. B. Bhatt</i>	155
E-6	Assessment of Photo Peak Efficiency of BEGe Detector in Comparison with p-Type Co-axial HPGe Detector <i>S.J. Sartandel, V.A. Pulhani</i>	156
E-7	Investigating the Concentrations and Spatial Variability of Key Elements in Soil from Haryana India <i>R.C. Bhargare, M. Tiwari, P.Y. Ajmal, T.D. Rathod, S.K. Sahu, V.A. Pulhani</i>	157
E-8	Evaluation of Experimental Detection Limit of B in Varying Matrices in External (in air) PIGE Using 3.5 MeV Proton Beam from FOTIA <i>Sonika Gupta, Priya Girikar, Suparna Sodaye, R. Acharya</i>	158
E-9	EDXRF-Based Green Methodology for Direct Compositional Characterization of Actinides in UF₄-ThF₄-LiF <i>Kaushik Sanyal, Sangita Dhara, Pratik Das, R.V. Pai</i>	159
E-10	Assessment of Heavy Metals in Roadside Agricultural Field Soil around Trombay <i>Rupali C., K. Kamat, Sujata Gothankar, Sunita Singh, Vandana A. Pulhani</i>	160

E-11	SRXRF Analysis of Serum Trace Elements in Breast Cancer Subtypes <i>B. Gowrinaidu, P. Sarita, G.J. Naga Raju, S. Srikanth, N. Srinivasa Rao, M.K. Tiwari</i>	161
E-12	Estimation of KAMINI PFTS Neutron flux Uncertainty by Foil Activation Method <i>G. Pandikumar, D.V. Subramanian, Adish Haridas</i>	162
E-13	Development of Direct X-Ray Fluorescence based Methodology for the Determination of Fissile Atom Content in Fluoride Salt for Molten Salt Fuel Applications <i>K. Sanyal, B. Kanrar, R.V. Pai</i>	163
E-14	Discoloration of Acidic Solution of Yellow 6 Lake Dye With 8 MeV ¹H Beam <i>A.A. Shanbhag, Sabyasachi Paul, S.C. Sharma, P. Srinivasan</i>	164
E-15	Hydrogen Estimation for Post LOCA Tested Fuel Clads using Neutron Imaging <i>Shefali Shukla, T. Roy, Y.S. Kashyap, T. Sawarn, M. Shukla, P. Singh</i>	165
E-16	Determination of Am-243 in the Fast Reactor Fuel Reprocessing Stream <i>T. Aneesh, Suraj Mondal, Sagunthala Devi, Bhavya S. Nair, K. Dhamodharan, K.A. Venkatesan, K. Rajan</i>	166
E-17	Determination of Neptunium-237 Concentration of by Extractive Alpha Spectrometry Method <i>T. Aneesh, S. Usha, Neeraja Chandran, K. Dhamodharan, K.A. Venkatesan, K. Rajan</i>	167
E-18	Introduction of Oxygen Non-stoichiometry in Oxides and its Determination by Particle Induced Gamma-Ray Emission: A Feasibility Study <i>Y. Sunitha, D.V. Lakshmiopathy, A.A. Sukumar, Sk. Jayabun, G.L.N. Reddy</i>	168
E-19	Non-destructive Evaluation of Accelerator Cathode Assembly <i>Anant Mitra, Dhruva Bhattacharjee, Lakshminarayana Y., Rajesh Acharya, S. Khader, Amitava Roy, Virendra Kumar, Umesh Kumar</i>	169
E-20	Comparative Study of Air Borne Uranium Estimation using Radioanalytical and Chemical Methods <i>Nitin Kumari, Swaroopa Lakshmi, Amrit Pal Singh, K. Vishwa Prasad, Aditi C. Patra, Probal Chaudhury, V.V. Mahesh Kumar, Komal Kapoor</i>	170
E-21	Simultaneous Determination of Uranium, Thorium and Plutonium in Nitric Acid Solution by K-edge Densitometry <i>M. Bootharajan, R. Gangadevi, B. Sreenivasulu, K. Sundararajan, C.V.S. Brahmananda Rao</i>	171
E-22	Non-destructive EDXRF Analysis of LaMnO₃-BaTiO₃ Multi-functional Oxide Powders: Addressing the spectral overlaps <i>T.A. Chavan, P.S. Remya Devi, K.K. Swain</i>	172
E-23	Estimation of ²²⁷Ac Activity in Lanthanum Samples using Gamma Spectrometry <i>Amar D. Pant, Ritesh Ruhela, Anilkumar S. Pillai</i>	173

E-24	Occurrence of Trace Metals in Popularly Consuming Fruits and their Health Risk Assessment	174
	<i>Sugandhi Suresh, Harshali S. Suryavanshi, Mahesh Tiwari, Vandana A. Pulhani</i>	
E-25	Plutonium Estimation using Functionalized Nuclear Track Detector	175
	<i>Amol Mhatre, Chhavi Agarwal, R. Tripathi</i>	
E-26	Development of Scintillating Phosphate based Polystyrene Polymer Inclusion Films (PIFs) for Ultra-Trace Detection of Pu	176
	<i>Amol Mhatre, Chhavi Agarwal, R. Tripathi</i>	
E-27	Exploring Gamma Peak Identification for Sb, Eu, Co, and Zr in Cs Rich Condition: Challenges and Breakthroughs	177
	<i>Gopal Sharma, Chanchal Solanki, Kankan Patra, V.K. Mittal, Anoop Kelkar, D.B. Sathe, R.B. Bhatt</i>	
E-28	Determination of Boron concentration and its Isotopic composition (IC) in BORAL by PIGE	178
	<i>Purbali Das, Sudeep Kumar Samanta, Suparna Sodaye</i>	
E-29	Polyoxometalate (POM) based Composite Material for the Determination of Americium in Synthetic Urine Samples	179
	<i>Suja A. Kumar, B. Mahanty, A. Bhattacharyya, P.D. Sawant</i>	
E-30	Determination of U²³⁵ Content in UO₂ Pellet by Gamma Ray Spectrometer with HPGe Detector using Enrichment Meter Principle	180
	<i>Vinod. K. Ray, U.B. Misra, Y. Balaji Rao</i>	

F: Radioisotopes & Radiation Technology

F-1	N-13 Ammonia Production in Standard Niobium Target used for F-18 Production: Radiosynthesis and Quality Control	181
	<i>S.K. Nandy, A. Gopalkrishna, S. Chinnaessaki, S.P. Kulkarni, N.S. Baghel</i>	
F-2	Pre-clinical Studies for Clinical Translation of 16-α-¹⁸F – Fluoroestradiol	182
	<i>S.K. Nandy, Y. Shete, S. Rakshit, Y. Dhekale, S.P. Kulkarni, N.S. Baghel</i>	
F-3	¹⁸F-Flutamide & Nilutamide: PET Diagnostic Tool for Benign Prostate Disorders and Prostate Cancer: Development, Radiosynthesis & PET/CT Evaluation in Rabbit	183
	<i>S.K. Nandy, S. Rakshit, Y. Shete, S.P. Kulkarni, N.S. Baghel</i>	
F-4	¹⁸F-Sodium Tetra Fluoro Borate for Thyroid disorder and Thyroid Cancer: Radiosynthesis, Bio-evaluation & Histopathological Correlation	184
	<i>S.K. Nandy, Y. Shete, S. Rakshit, S.P. Kulkarni, N.S. Baghel</i>	
F-5	¹⁸F-Labelled Phytochemicals for Breast Cancer Diagnosis	185
	<i>S.K. Nandy, S. Rakshit, Y. Shete, S.P. Kulkarni, N.S. Baghel</i>	
F-6	Development of Radiation Grafted Bio-degradable Adsorbent for Ammonia Remediation in Water	186
	<i>N. Misra, M.G. Patil, S. Rawat, S.A. Shelkar, V. Kumar</i>	

F-7	Ensuring Consistency in Fluorine-18 Radiopharmaceuticals Production under GMP for Cancer Diagnosis: Lessons from Retrospective Analysis <i>R. Nanabala, A.K. Puthiyottumkara, T. George, A.K. Muhammed, D. Kottuparamban, J. Pokkat, S.K. Maniyoth, V. Pazhakkal, A.K. Joy, M.R.A. Pillai</i>	187
F-8	Extended Surface Modification of Silicone-Based Materials for Biomedical Application <i>R. Agarwal, S. Ray Chowdhury, Y. K. Bhardwaj</i>	188
F-9	Intercomparison of Reference Standard Ionization Chamber of BARC for Dosimetry of Ir-192 Brachytherapy Source with IAEA <i>Greeshma K.A., Sougata Rakshit, Sneha Chandrasekhar</i>	189
F-10	Preparation of Ethylene Vinyl Acetate/Jute Fabric Bio-Composites with Improved Properties <i>A. Jha, S. A. Khader, S. Ray Chowdhury</i>	190
F-11	Formulation, Quality Control and Pre-Clinical Evaluation of [¹⁷⁷Lu] Lu- Labeled Glucuronic Acid Functionalized Hydroxyapatite Nanoparticles using Cold Kit for Potent Application of Nanoscale Brachytherapy <i>Sourav Patra, K.V. Vimalnath, Khajan Singh, Shishukant Suman, Rubel Chakravarty, Sudipta Chakraborty</i>	191
F-12	Studies on the Complexation Kinetics and Mechanism of Bone Uptake of ¹⁷⁷Lu-Complex of Bisphosphonate Amide of DOTA <i>Priyalata S.S. Shetty, K.V. Vimalnath, Sharad P. Lohar, Sudipta Chakraborty</i>	192
F-13	Indigenous Synthesis of Fibroblast Activation Protein Targeted [⁶⁸Ga/¹⁷⁷Lu]-FAPI-2286 Peptide <i>Akanksha Jain, Manoj Kumar, Drishty Satpati</i>	193
F-14	Effect of Vegetation on Hydraulic Performance of A Horizontal Flow Constructed Wetland using Radiotracer <i>Sunil Goswami, J.S. Samantray, V.K. Sharma, R. Acharya</i>	194
F-15	Radiochemical Separation of Multi-Curie Quantity of ¹³¹I for Human Clinical Use in A Newly Installed Facility: Methodologies and Operational Insights <i>Rajwardhan N. Ambade, Bharat R. Ganjave, Sachin B. Jadhav, Sahiralam Khan, Ramu Ram, Rubel Chakravarty, Sudipta Chakraborty, Tapas Das</i>	195
F-16	Post-Harvest Quality Assessment of Litchi Fruits (Litchi Chinensis Sonn.) through Edible Coatings and Gamma Irradiation <i>Mani Gopal, Singh Omveer, Rai Ratna, Lal Surendra, G.C. Joshi</i>	196
F-17	Gamma Rays Induced Morphological and Biochemical Mutants in Bael (Aegle Marmelos) <i>M. Rawat, V.P. Singh, S. Aswal, G.C. Joshi and J. Das</i>	197
F-18	Corrosion Monitoring of Borosilicate Glass by Thin Layer Activation Method Utilizing Proton Beam from Pelletron <i>Jayashree Biswal, S.C. Sharma, A.K. Gupta, V.K. Sharma, R. Acharya</i>	198

F-19	In-Situ Monitoring of Natural Radioactivity Present in Sediments of Jampore Beach, Daman, India <i>Jayashree Biswal, Sunil Goswami, V.B. Yadav, S.J. Sartandel, J.S. Samantray, V. Pulhani, V.K. Sharma, R. Acharya</i>	199
F-20	Pr³⁺-Activated Phosphor for X-ray Imaging <i>Annu Balhara, Priyansu Mishra, Mohit Tyagi, Santosh K. Gupta</i>	200
F-21	Radioluminescent and Persistent Phosphor for Potential X-ray Scintillator <i>Reshmi T. Parayil, Nitesh Kanojia, Mohit Tyagi, M. Mohapatra, Santosh K. Gupta</i>	201
F-22	Optimization of Peptide-based Chelators for ^{99m}Tc-labeling <i>Sonal Gupta, Manoj Kumar, Ajit A. Kengar, Drishty Satpati</i>	202
F-23	Synthesis of [¹⁷⁷Lu]Lu-labeled-PCNA-Directed Dual Modal Conjugate for Treatment of Triple Negative Breast Cancer (TNBC) <i>Soumi Kolay, V. Kusum Vats, Sandeep B. Shelar, Mohini Guleria, Tapas Das</i>	203
F-24	Studying the Effect of Administration of Cold Antibody on Bio-Distribution of [¹⁷⁷Lu]Lu-Labeled-Antibody in Small Animal Model <i>Jeyachitra Amirdhanayagam, Soumi Kolay, Samrudhi Kar, Rohini P. E., Mohini Guleria, Tapas Das</i>	204
F-25	Expression of Sodium-Iodide Symporter in Patients with Thyroglobulin Elevated and Negative ¹³¹Iodine Scan in Various Thyroid Cancer Types <i>Chandrakala Gholve, Vividh Raje, Yogita Shete, Swapnil Rane, Asawari Patil, Smita Gawandi, Roopal Agrawal, Sandip Basu, Nawab Singh Baghel</i>	205
F-26	Radiation and Plasma Fabricated Reusable Catalytic System for Catalytic Reduction of Cr(VI) to Cr(III) <i>S. Rawat, N. Misra, S.A. Shelkar, V. Kumar</i>	206
F-27	Sorption of Actinide by Phosphate Functionalized Teflon Scrap <i>R.B. Gujar, S.A. Ansari, A. Bhattacharyya, C.V. Chaudhari, K.A. Dubey and Y.K. Bhardwaj</i>	207
F-28	Indigenous Development of ¹⁴¹Ce-Point Source for Radiometry Assay of Nuclear Fuels <i>Manoj Kumar, Drishty Satpati, Tapas Das</i>	208
F-29	[¹⁷⁷Lu]Lu-Doxorubicin Loaded DHF-I Cross-linked Radiopaque Microspheres towards Radio-Chemoembolization of Hepatocellular Carcinoma <i>Sayan Das, Mohini Guleria, Saikat Biswas, Santanu Dhara, Tapas Das</i>	209
F-30	Comparative Analysis of Serum Thyroglobulin Quantification Using Indigenous Developed Immunoradiometric Assay Kit with Electrochemiluminescence Immunoassay in Thyroid Cancer Patients <i>C.S. Gholve, S.N. Gawandi, S. Raut, K. Ghosh, N.S. Baghel</i>	210
F-31	Boron-Doped Bismuth Zinc Erbium Tellurite (TBBZE) Glass Matrix for Radiation Shielding Applications <i>Mo. Anas Ahmad, Virendra Singha, Neeraj Singh, Neeraj Bisht, Yogendra Kumar Singh</i>	211

Index

F-32	Studies on Gamma Radiation Stability of Curcumin <i>S. Show, S. Mitra, S. Lahiri, R.K. Nandi, P. Banerjee</i>	212
F-33	A Large-Scale Radiotracer Investigation in Heat Exchanger System of Refinery <i>Sunil Goswami, J. Biswal, J.S. Samantray, V.K. Sharma, R. Acharya</i>	213
F-34	Production of ⁸⁹Zr via Indigenously Developed Solid Target: Evaluation of Radiation Safety Parameters using the FLUKA Code <i>K. Kushwaha, B. Keshavkumar, N. S. Baghel, S. Banerjee</i>	214
F-35	Effects of Gamma Radiation on Corrosion Behaviour and Hardness Properties of AA6061-T6 <i>Deepa Singh, Neeraj Bisht, Virendra Singh, B.C. Chanyal</i>	215
F-36	Increased Efficacy of ¹⁷⁷Lu-DOTA-BASS Antagonist Peptide over ¹⁷⁷Lu- DOTA-TATE Agonist Peptide Using ¹⁷⁷Lu of Low to Medium Specific Activity in AR42J Cells <i>Rani G., Shalaka Paradkar, Sheela M., Navin Sakhare, Laxman Ram, Sanjeev Kumar</i>	216
F-37	Role of PET-CT Imaging in Neurobehavioral Studies Influenced by Pheromones in C57BL/6 Mice <i>Yogita Shete, Anushka Patil, Swati Baghul, Avik Chakraborty, Sandip Basu</i>	217
F-38	Radiation Grafting: An Innovative Strategy for Designing Tailored Surfaces <i>N.K. Goel, S.A. Shelkar, Sanju Francis, Virendra Kumar, Y.K. Bhardwaj</i>	218
F-39	Performance Assessment of X-ray DRCT Image Display and Interpretation System for NDT Analysis of Concrete Specimens <i>Janaki S. Nair, Lakshminarayana Y., Anant Mitra, Rajesh Acharya, Umesh Kumar</i>	219
F-40	Influence of Gamma Irradiation on Physico-Chemical, Thermodynamic, Electro-Chemical and Surface Properties of Superhydrophobic Coatings <i>Sonali B. Jadhavar, Prashant P. Chikode, Satish A. Mahadik, Rajiv S. Vhatkar</i>	220
F-41	Investigating the Correlation between Mechanical Properties and Water Absorption in Gamma-Irradiated Jute/SiC Composites for Enhanced Durability in Moisture-Sensitive Applications <i>Deepa Singh, Neeraj Bisht, Deepak Yadav, Sonika Chauhan</i>	221
F-42	Ultraviolet and Visible-Emitting Bi³⁺-Activated Phosphor with Efficient Radioluminescence under X-ray Excitation <i>Annu Balhara, Priyansu Mishra, Mohit Tyagi, Santosh K. Gupta, K. Sudarshan, S. Jeyakumar</i>	222
F-43	Design and Fabrication of an Automated Module for Formulating Clinical Doses [¹⁷⁷Lu]Lu-DOTA-Trastuzumab using Medium Specific Activity, Carrier Added [¹⁷⁷Lu]LuCl₃ <i>Aaditya Shah, Arpit Mitra, Varun Nair, Mohini Guleria, Jeyachitra Amirdhanayagam, Anupam Mathur, Usha Pandey, Tapas Das</i>	223

- F-44** **Single Optimized Protocol for Formulation of Multiple Patient Doses of Different [177Lu]Lu- based Radiopharmaceuticals using Low Specific Activity, Carrier Added [177Lu]LuCl₃** 224
Sudeep Kumar Sahu, Sangita Lad, Avik Chakraborty, Arpit Mitra, Megha Tawate, Mukti Kanta Ray, Sandip Basu
- F-45** **Energy-Dependent Attenuation Properties of Water-Soluble Inorganic Compounds in the 10 keV–1333 keV Gamma-Ray Regime: A Shielding-Oriented Study** 225
Sneha Dinkar Sanap, S.R. Mitkari, Anil V. Raut, Pravina P. Pawar
- F-46** **Gamma Radiolytic Synthesis of Polybis[2-(Methacryloyloxy)Ethyl] Phosphate Stabilized Gold Nanoparticles: An Efficient Sensor for LSPR Shift Based Detection of U(VI)** 226
S.A. Shelkar, N. Misra, S. Rawat, V. Kumar

G: Environmental Radioactivity

- G-1** **Analysis of Sedimentary Organic Carbon Sources in Mumbai Harbour Bay** 227
V.B. Yadav, Vandana A. Pulhani, A. Vinod Kumar
- G-2** **Trend Analysis of Gross Alpha and Gross Beta Activities in the Environment of Rawatbhata Rajasthan** 228
S.N. Tiwari, A.K. Jain, M. Sisodia, Tejpal Menaria, M.C. Meena, I.V. Saradhi
- G-3** **Assessment of Radiation Hazard Indices in Soil Samples and ²²²Rn in Drinking Water of Southern Gulbarga District** 229
S. Rajesh, R. Archanadevi, B.R. Kerur
- G-4** **Optimization of Parameters for the Determination of ²²⁶Ra in Water Via Cherenkov Radiation** 230
Sudeshna Goswami, N. Chitra, Kothai Parthasarathy
- G-5** **Radionuclide Transfer in Rice: Assessing Uptake in the Uranium-Mineralized Singhbhum Region, Jharkhand, India** 231
Samim Molla, Ranjit Kumar, V.S. Srivastava, Aditi C. Patra, P. Chaudhury
- G-6** **Short Term Prediction of Radon in a dwelling using an ARIMA Model** 232
C.G. Sumesh, R. Shrivastava, P. Singhal, A.C. Patra, P. Chaudhury
- G-7** **Radiological Assessment of Building Materials around the Tummalapalle uranium Mining Site** 233
M.R. Dhumale, B.K. Rana, S.V. Bara, S. Chinnaesakki, A.C. Patra, P. Chaudhury
- G-8** **Long-Term Monitoring of ²²⁶Ra Activity in Groundwater around the Uranium Mill Tailings Pond, Turamdih, Jharkhand** 234
Ranjit Kumar, Samim Molla, V.S. Srivastava, A.C. Patra, P. Chaudhury
- G-9** **Bio Accumulation of ⁴⁰K in Seaweed Samples** 235
B. S. Selvi, Thomas George, B. Vijayakumar, I.V. Saradhi

G-10	Assessment of Radiological Impact for Utilization of Uranium Mining Waste Rock in Paver Block Construction	236
	<i>Raghvendra Rathore, Pallavi Singhal, Aditi C. Patra, Pradeep Bhargava</i>	
G-11	Cs Sorption Study on Different Organic Phases in Organic Rich Soil	237
	<i>Sukanta Maity, P. Sandeep, Suchismita Mishra, C.B. Dusane, Anilkumar S. Pillai</i>	
G-12	Long-Term Trends in Environmental Gamma Radiation Monitoring using Thermoluminescent Dosimeters (TLDs) around Variable Energy Cyclotron Centre, Kolkata	238
	<i>R.A. Takale, P.G. Shetty, M. Swarnakar, S.K. Sahu, V. Pulhani</i>	
G-13	Distribution of Primordial Radionuclides in Soil Samples from Haryana, India and their Radiological Significance	239
	<i>M. Tiwari, S.K. Sahu, S.J. Sartandel, T.D. Rathod, M. Swarnakar, R.C. Bhangare, P.Y. Ajmal, M.K. Mishra, V. Pulhani</i>	
G-14	Environmental Gamma Radiation Monitoring Around Upcoming NFC-Kota	240
	<i>P.G. Shetty, R.A. Takale, M. Swarnakar, S.K. Sahu, V. Pulhani</i>	
G-15	Radiological Assessment of U-Mill Tailings and Mine Waste Rock-Based Construction Materials for Societal Applications	241
	<i>B.K. Rana, Samim Molla, B.K. Sahoo, Arshad Khan, B.K. Sapra</i>	
G-16	Measurement of Radon Concentration in Air over the Eastern Coast of India: Implications of Heavy Mineral Deposits on Natural Background Radiation	242
	<i>Abinash Sahu, P. Prusty, A. Rout, P. Sahu, R.P. Patra, A.C. Patra, P. Choudhury</i>	
G-17	Comparative Assessment of Uranium in Groundwater around Operating Uranium Mining Facilities in Singhbhum Region, Jharkhand	243
	<i>S.K. Sahoo, V.N. Jha, Rajesh Kumar, A.M. Gupta, A.C. Patra, P. Chaudhury</i>	
G-18	Natural Radio Nuclides in Fish Consumed at Visakhapatnam	244
	<i>P. Padma Savitri, B. Ramesh, J. Sudhakar, R. Balaram, Manoj Warriar, A.D.P. Rao</i>	
G-19	Weathered Microplastics as Uranium Carriers: Sorption Behavior in Simulated Marine Conditions	245
	<i>Sonali Yadav, Sabyasachi Rout, Vandana Pulhani</i>	
G-20	Indigenously Developed Sampling System for Radiocarbon Species in Air	246
	<i>Sabyasachi Rout, Sonali Yadav, Vandana Pulhani</i>	
G-21	Modifying the UiO-66 (Ce) Functionality to Boost Uranium Sorption from Real Water Samples	247
	<i>Jay Singh Dubey, Adish Tyagi, Pallavi Singhal, Gourab Karmakar, Aditi C. Patra</i>	
G-22	Modifying the ZIF-8 Functionality to Boost Uranium Sorption from Real Water Samples	248
	<i>Pallavi Singhal, Jay Singh Dubey, Adish Tyagi, Gourab Karmakar, Aditi C. Patra</i>	

- G-23 Measurement of Naturally Occurring Radioactive Materials (NORM) in Kutni Village near South Purulia Shear Zone** 249
Sayantan Mitra, Sumana Mukherjee, Anil Sharma, Soumalya Kundu, Aditi Das, Pankaj K. Giri, Rajarshi Raut, Sandeep S. Ghugre, Chiranjib Barman
- G-24 Evaluation of Step-wise Decontamination of Actinide Spiked Soil Sample** 250
Saparya Chattaraj, Hemachandar V., Dinesh K. Patre, D.P. Rath, Ashokkumar P.
- G-25 Radiological Mapping of Environment around the Upcoming Fuel Fabrication Facility at Kota** 251
Anil Goyal, Daksha, Anshi, Richa Sharma, S.K. Srivastava, C.G. Sumesh, Aditi C. Patra, Probal Chaudhury
- G-26 Assessment of Radon, Thoron Concentration and Inhalation Dose in Rural and Urban Dwellings of Aligarh District** 252
R.L. Sharma, A.K. Mahur, S. Sharma, S.A. Ali
- G-27 Influence of Soil Organic Matter on the Distribution of Radionuclides in Soil Systems around Kaiga: A Correlation Study** 253
Sanyam Jain, S. Rout, V. Pulhani, M.S. Vishnu, I.V. Saradhi
- G-28 Assessment of Groundwater Recharge through Defunct Dug Wells using Environmental Stable and Radioisotopes** 254
Anushree Ghosh, Tirumalesh Keesari, A. Jaryal, A. Roy, D. Pant, H.V. Mohokar, S.N. Kamble, R Acharya
- G-29 A Study on the Groundwater Dynamics in Coastal Aquifers of Eastern India using Environmental Tritium and Radiocarbon Dating Techniques** 255
Annadasankar Roy, Diksha Pant, H.V. Mohokar, Ajay Jaryal, Sanjit Kumar Sahu, Anushree Ghosh, Prakash Chandra Mishra, Raghunath Acharya, Tirumalesh Keesari
- G-30 Measurement of Activity Size Distribution of Radon Progeny using SSNTD- Based Cascade Impactor** 256
R.P. Rout, R. Mishra, R. Prajith, S. Jalaluddin, Arshad Khan, B.K. Sapra
- G-31 Measurement of Radon Mitigation Factor of Synthetic and Natural Fibers** 257
R. Prajith, R.P. Roul, R. Mishra, Arshad Khan, B.K. Sapra
- G-32 Distribution of ^{210}Po and ^{210}Pb Activity in Soil of Chittorgarh, Rajasthan** 258
Tejpal Menaria, D.S. Rathore, S.N. Tiwari, I.V. Saradhi
- G-33 Radiocarbon Dating of Tree Rings using Accelerator Mass Spectrometry** 259
Anushree Ghosh, Tirumalesh Keesari, Pankaj Kumar, Leema Saikia, Shreyas Managave, Chandra Kant Salunke, Himanshu Mishra
- G-34 Measurement of $^{232+228}\text{Th}$ in Fine and Coarse Fractions of Airborne Aerosols in Monazite Mining and Processing Facilities** 260
P. Prusty, A. Sahu, A. Chakrabarty, A. Rout, R.P. Patra, P. Chaudhury

G-35	Assessment of ²¹⁰Po Activity in Stream Sediments Around a Uranium Ore Processing Facility, India <i>Sarjan Singh, N.K. Sethy, N.M. Soren, A.C. Patra, P. Chaudhury</i>	261
G-36	Radiological Parameters of Environmental Water Samples: Radiological Safety at OSCOM, Chhatarpur, Odisha <i>Annapurna Rout, A. Sahu, P. Prusty, R. Patra, Aditi C. Patra, P. Chaudhury</i>	262
G-37	Study of Elemental Profile of Soil and Plant Samples using EDXRF Technique near National Highway Pantnagar, Uttarakhand <i>Smriti Kandpal, G.C. Joshi, Mahesh Tiwari, R.S. Srivastava, Anil Kumar</i>	263
G-38	Baseline Radiological Assessment in Soil Samples from Uranium Mining Site at Rohil <i>S.V. Bara, M.R. Dhumale, S. Chinnaesakki, P. Lenka, A.C. Patra and Probal Chaudhury</i>	264
G-39	Particle Size Distribution and Dose Estimation in Uranium and Rare Earth Chloride Processing Plants <i>Ajesh Kumar, S.M. Harikumar, Aditi C. Patra, Probal Chaudhury</i>	265
G-40	Fly Ash to Pollucite: A Long-Term Storage Option for Cesium of Low-Level Radioactive Waste <i>Y. Raghavendra, Jayaprakasam Selvakumar, Anupkumar Bhaskarapillai, A.L. Rufus, T.V. Krishna Mohan, S.N. Achary</i>	266
G-41	Estimation of Effective Radiation Dose Due to ²²²Rn in Groundwater of Gogi Region, Yadgir District <i>R. Archanadevi, B.R. Kerur</i>	267
G-42	Environmental Aspects of Release of Iodine-129, Performance of Mitigation Processes and Management of Secondary Waste <i>Umadevi K., Prasad Dabhade, Pradeep Kumar Sharma, Santhosh Kumar Satpati</i>	268
G-43	Assessment of the Activity Concentrations of ²³⁸U, ²³²Th, and ⁴⁰K in Stone Samples from the Koppal Districts of Karnataka, India <i>Nagraj Channappa, Jayashri B. Mutugar, Basavaraj Rachappa Kerur</i>	269
G-44	Assessment of Radioactivity in Solid Waste Generated Due to Operation of Rare Earth Extraction Plant in Odisha <i>Rajendra P. Patra, A. Sahu, A. Rout, P. Prusty, A.C. Patra, P. Choudhury</i>	270
G-45	Variation of Outdoor Natural Gamma Absorbed Dose Rate in Air Across the Indian Himalayan Region <i>Hasem Ali, Pratip Mitra, Saurabh Srivastava, G. Priyanka Reddy, Saurabh Garg</i>	271
G-46	Understanding the Groundwater-Surface Water Interactions in Yamuna Plains of Noida Region using Environmental Tritium <i>Diksha Pant, H.V. Mohokar, A. Roy, Tirumalesh Keesari, Dipankar Saha</i>	272
G-47	Natural Radioactivity Levels in Some Environmental Soil Samples of the Belagavi Region, North West Karnataka, India <i>Jayashri B. Mutugar, Nagraj Channappa, Basavaraj Rachappa Kerur</i>	273

G-48	Studying Back Diffusion in Accumulators for Radon Flux Measurements Using OpenFOAM	274
	<i>D. Rana, N.K. Sethy, R.L. Patnaik, M.K. Singh, A.C. Patra, P. Choudhuri</i>	
G-49	Study of Seasonal Variation of Outdoor ²²²Rn Concentration at a Location nearby Uranium Mining and Milling Facility	275
	<i>R.L. Patnaik, M.K. Singh, Dibyendu Rana, N.K. Sethy, V.N. Jha, A.C. Patra</i>	
G-50	⁷Be in Fresh Water Sediment in Kadra Reservoir at Kaiga Region	276
	<i>R.M. Joshi, M.S. Vishnu, I.V. Saradhi</i>	
G-51	Assessment of Radon Levels and their Correlation with Physiochemical Parameters in Water Sources of Dakshina Kannada District	277
	<i>Neha S, Latha T., Rishika, Greeshma K V., Rita Crasta, Suresh S.</i>	
G-52	Pre operational Environmental Radiation Mapping around Gorakhpur Haryana Anu Vidyut Pariyojana (GHAVP)	278
	<i>Vaibhav Bhujbal, M.V.R. Narsaiah, Jaivendra Kumar, Anil Kumar, Deepak Kumar, Shashank S. Saindane</i>	
G-53	Uranium Partitioning in Soils from NFC Kota Campus	279
	<i>V.K. Thakur, P. Lenka, Gopal P. Verma, S.K. Srivastava, A.C. Patra, P. Chaudhury</i>	
G-54	Phosphonate Modified MOF-808 (Ce) for the Remediation of Uranium from Aqueous Solution	280
	<i>Nitin Gumber, Rajesh V. Pai</i>	
G-55	Characterization of Contaminated Water using Stable and Radioisotope Signatures	281
	<i>Bhumika Kumari, Hemant Mohokar, Diksha Pant, Tirumalesh Keesari</i>	
G-56	Estimation of ⁴⁰K in the Human Body using Shadow Shield Whole Body Counter	282
	<i>Jayan M.P., Krishnakumar P., Amit Bhatnagar, Sureshkumar M.K.</i>	
G-57	Electrochemical Decontamination of Radioactive Metallic Surfaces with Fixed Contamination	283
	<i>Arkaprava Layek, Ruma Gupta</i>	
H: Nuclear Safeguards & Nuclear Forensics		
H-1	Advanced Statistical Approach for Tracing Uranium Yellow Cake Origins via Coupled LIBS-Chemometrics Analysis	284
	<i>Anannya Banerjee, Subhankar Manna, Anandhu Mohan, Santosh K. Satpati, Rajesh V. Pai, Arnab Sarkar</i>	
H-2	Development of A Supervised Machine Learning Algorithm for Non-Destructive Burn-Up Verification of Simulated PHWR Spent Fuel Pin	285
	<i>Sabyasachi Patra, Satyam Kumar, Y.S. Rana, Rahul Tripathi</i>	

H-3	Development of a Monte Carlo Methodology for Response Function Analysis of Plutonium Alpha Spectra	286
	<i>Sabyasachi Patra, R. Suvethaa, Satyam Kumar, Rahul Tripathi</i>	
H-4	Radiochemical Separation of Protactinium using Anion Exchange Method in Uranium Rich Matrices for Application in Chronometry	287
	<i>Prabhath Ravi K., Suchismita Mishra, Sathyapriya R Sreejith</i>	
I: Nuclear Instrumentation & Application of AI		
I-1	Implementing Artificial Neural Network Base Modelling for Estimating Elemental Concentration from Overlapping Line of Rb/U	288
	<i>B. Kanrar, K. Sanyal, R.V. Pai</i>	
I-2	Development of Instrumentation for On-Line Measurement of DC Current using Non-Contact Method for the Electrolytic Conversion of Metal Oxide into Metal	289
	<i>Ajay Kumar Keshari, J. Prabhakar Rao, N. Sanil, V. Arunkumar, L. Shakilaand R. Kumaresan</i>	
I-3	Coincidence Ion Beam Analysis (CIBA) Facility	290
	<i>A. A Sukumar, D.V. Lakshmipathy, Y. Sunitha, Sk. Jayabun, G.L.N. Reddy</i>	
I-4	Characterization of ASIC based Indigenous Neutron Area Flux Monitor with BARC-Make BF₃ filled Neutron Detector	291
	<i>P. Bahre, M.K. Jha, T. Bhattacharjee, P. Maity, S. Ghosh, A. Banerjee, S. Mazumder, T. Samanta, S.S. Desai</i>	
I-5	Automation of Indigenous Integrated Segmented & Tomography Gamma Ray Scanning System	292
	<i>Rajesh T. Jadhav, Chhavi Agarwal, Rahul Tripathi, Suparna Sodaye</i>	
I-6	Measurement of Radiation and Transmutation in H₂O & D₂O Electrolysis	293
	<i>Ankit Kumar, K.P. Rajeev, Pankaj Jain, R.G.S. Pala</i>	
I-7	Glove Box Adaptation, Performance Evaluation of O-N, O-H Twin Determinator System and Related Studies at FRFCF	294
	<i>S. Sasmal, B. Sivakumar, P. Kumarsekaran, P.K. Singh, G. Sivasankaran, R.B. Bhatt</i>	
I-8	Integrator Circuit to Measure Giga-ohm Resistor of Charge Sensitive Loop of HPGe Detector	295
	<i>N. Tawade, S. Vishwasrao, C. Datrik, S. Sodaye</i>	
I-9	Performance Study of Indigenous Readout Electronics for Hpge Detectors in Low Level Gamma Spectroscopy and Counting Applications	296
	<i>Tushar A. Kesarkar, Saikat Das, Sudheer K.M., Sourav Mukhopadhyay, V.B. Chandratre, R.S. Shastrakar, Vaishali Shedam, Sandeep Kumar, K. Hari Prasad, Menka Sukhwani, P.V. Bhatnagar, S. Chinnaesakki</i>	
I-10	Neutron Measurement in 10 MeV Electron Accelerator Environment using CR-39 Track Detector	297
	<i>G.S. Sahoo, Sabyasachi Paul, S.P. Tripathy, N. Chaudhary, P. Srinivasan</i>	

I-11	Development of Instrumentation for the Fabrication of Fuel Microspheres using the Sol-Gel Method	298
	<i>Ajay Kumar Keshari, S. Balakrishnan, J. Prabhakar Rao, Dasarath Maji, Abhiram Senapati, V. Suresh Kumar, T.V. Prabhu, V. Jayaraman</i>	
I-12	Validation of an Automated FBTR End Plug Metrology System	299
	<i>Rajashree Dixit, Gagan Deep Kaur, Amrit Prakash</i>	
I-13	Removal and Scraping of Two Nos. of 110 kW Furnace No. 1 & 2, at ADU Facility by using ALARA Principle	300
	<i>Akhilesh Panigrahi, Kumar Awinash, Rajkumar, Rohit Ameta, K.S. Vasudevan</i>	
I-14	Comprehensive Quality Assurance Tests for Large Area Dual Phosphor Contamination Monitors as per Standards	301
	<i>I. Vijayalakshmi, A. Dhanasekaran, Kothai Parthasarathy</i>	
I-15	Control Instrumentation for Fuel Cell Based Hydrogen Mitigation System for Secondary Cold Trap Regeneration	302
	<i>R. Karunakaran, M. Lavanya, V.A Faizal, N. Murugesan, P. Manikandan, Hrudananda Jena, Rajesh Ganesan, V. Jayaraman</i>	
I-16	Design and Fabrication of Segmented Temperature Controller with a Furnace to Study Positron Annihilation Lifetime Spectroscopy at High Temperatures	303
	<i>Ghanshyam Meena, Sandeep Vishwasrao, Chhaya P. Koli, Siby Soren, Vishal Chougule, Suparna Sodaye</i>	
I-17	Comparative Analysis on Efficiency Variation for Alpha Spectrometry System	304
	<i>Riya Gupta, Anish A. Ansari, D. K. Pandey, U.V. Deokar, J.P.N. Pandey</i>	
I-18	Low Resolution Gamma Spectroscopy (LRGS) for Waste Drum Assay	305
	<i>J. A. Mason, S. Ramesh, A.C.N. Towner, N.A. Troughton, H.R. Turner</i>	
I-19	In-house Design and Development of a Bi-amperometer to Analyse Uranium and Plutonium using Redox Titrimetric Method	306
	<i>Ghanshyam Meena, Sandeep Vishwasrao, Chhaya P. Koli, Siby Soren, Vishal Chougule, Suparna Sodaye, Jayashree S. Gamare, Kavita Jayachandran</i>	
I-20	Refurbishment of Preamplifier in HPGe Detectors	307
	<i>C. Datrik, S.Vishwasrao, N. Tawade, Suparna Sodaye</i>	
	Author Index	309

Fabrication of Fast Reactor Fuels and their Characterisation

Amrit Prakash

Radiometallurgy Division, Bhabha Atomic Research Centre, Mumbai, India

Email: amritp@barc.gov.in, mrt_prakash@yahoo.co.in

Fast Reactor Fuel Program in India can be traced back to 1985 when the Fast Breeder Test Reactor (FBTR) was commissioned at Kalpakkam. The first choice of fuel for FBTR was 70% UO_2 (85% enriched U)-20% PuO_2 . However, the unavailability of enriched uranium led to the consideration of plutonium-enriched mixed oxide fuel as a second choice, i.e., 76% PuO_2 -24% UO_2 (natural U). Since chemical compatibility with sodium coolant was an issue, this fuel was also not pursued further. The third choice was development of plutonium enriched mixed carbide fuel, e.g., 70% PuC -30% UC (natural U). This fuel was found to be compatible with both sodium coolant and SS316 cladding material. Subsequently FBTR was fuelled with the Mark I fuel of composition $(\text{U}_{0.3}\text{Pu}_{0.7})\text{C}$ for the initial core, which was followed by Mark II fuel of composition $(\text{U}_{0.45}\text{Pu}_{0.55})\text{C}$ for the extended core. For the first time in the world, plutonium rich mixed carbide fuel was fabricated and used in a reactor as driver fuel. The mixed carbide fuel has performed exceedingly well and its burn-up has exceeded 1.65 GWd/Te without any fuel failure, thereby achieving a new milestone. The reactor has recently achieved its target power of 40 Mwd (Th.).

Oxide fuels, however, are already well established as safe for fast reactors, rendering a large scale irradiation experience worldwide. The fabrication flow sheet is easier as compared to carbide fuel, and the reprocessing technology is well established. Keeping this in mind, uranium-plutonium mixed oxide fuel has been chosen as the driver fuel for the forthcoming Prototype Fast Breeder Reactor (PFBR) at Kalpakkam. The 500 MWe PFBR is almost ready to become operational soon. The MOX fuel pins for PFBR have been manufactured at Advanced Fuel Fabrication Facility (AFFF), Tarapur (now known as FF, NRB, BARC, Tarapur).

Metallic fuels are planned to be deployed in large scale in future Indian FBRs. Metallic fuels have high fissile atom density and higher thermal conductivity as compared to MOX fuel and carbide fuel. Hence these fuels have higher breeding ratio and are also inherently safe. Studies related to development of fast reactor fuels based on metallic fuels have been initiated. This consists of development of technology for metallic fuel fabrication, building a data base on thermophysical properties of various fuel alloys, studies on thermodynamics and fuel-cladding compatibility, etc. Both U-Pu binary fuels and U-Pu-Zr ternary fuels are the candidate fuels for future Indian fast reactors. In this respect, both mechanically bonded binary fuel and sodium-bonded ternary fuel designs are under consideration.

The characterization of nuclear fuel loaded in the reactors is an important factor, which ensures safe and economic operation of nuclear reactors and the useful life of the fuel elements/assemblies. Various techniques/methodologies are being used for assuring the quality of the fuel elements fabricated in a fabrication facility. The physical quality control involves the inspection of fuel pellets, which means the inspection of pellets to evaluate physical characteristics, such as density, linear mass, dimensions, and surface defects. Several equipment have been developed and deployed for these analyses inside Glove box. The pellets of accepted dimensions are subjected to visual inspection under illumination for detecting the presence of any surface defects, such as chips, pits, metallic or non-metallic inclusions, cracks. Metallography is a destructive test used for checking the quality of the end plug welds on a statistical basis during qualification and production of end plug welding. The

test gives an idea about the depth of penetration, cracks, porosities and other defects in the welds. The top and bottom end plug welds are checked by X-Ray radiographic technique to assess the integrity of welds. Digital radiography, which is faster and more sensitive than film-based radiography, is being widely utilized in fabrication facilities.

The fast reactor fuel has to conform to stringent chemical specifications like boron, cadmium, rare earths, hydrogen, oxygen to metal ratio, total gas, heavy metal content, chlorine and fluorine, etc. Selection of technique is very important to evaluate the true specification. This is important particularly when the analyses have to be performed inside leak tight enclosure. However, analysis of nuclear materials poses challenges due to the complexity of the materials and the absence of relevant standards or reference materials. Advanced analytical techniques based on titrimetry, spectroscopy, thermogravimetry, XRF, and XRD have largely been used for this purpose. Since they have to be handled inside special enclosures, extreme care is being taken during handling. Instruments are being developed/modified for ease of handling and maintenance. The method should be fast to reduce the total analytical time. The instruments are chosen in such a way that a single instrument could do as many elements as possible. Inter laboratory comparison experiments are carried out to validate the method as well as to prepare certified reference materials. Regular analyses are carried out only after a satisfactory performance evaluation of the instruments.



Dr. Amrit Prakash is an Outstanding Scientist and Head of the Radiometallurgy Division at the Bhabha Atomic Research Centre (BARC), Mumbai. His expertise lies in the fabrication and process control of mixed carbide fuels for the Fast Breeder Test Reactor (FBTR) and in the quality control of various types of nuclear fuels, including mixed oxide fuels for PHWRs, BWRs, and PFBRs, using a range of analytical methods. Dr. Prakash has also been instrumental in the design and development of systems and components for glove box adaptation,

and in setting up a microfocus digital radiography system for accurate and rapid evaluation of end plug welds in fuel assemblies. He is a recipient of the DAE Scientific and Technical Excellence Award (2012) and has received multiple group achievement awards. With more than 150 publications in national and international journals and conferences, he has made significant scholarly contributions, including authoring a chapter in the book Nuclear Fuel Cycle, published by Springer.

Research and Development of Microsphere based Fuels for Advanced Reactor Concept

Rajesh V. Pai^{1,2}

¹Fuel Chemistry Division, Bhabha Atomic Research Centre, Mumbai, India

²Homi Bhabha National Institute, Mumbai, India

Email: rajeshvp@barc.gov.in

Most of the present nuclear reactors use ceramic pellet fuel formulations, which are conventionally derived by the powder metallurgical route [1–2]. But these conventional fuel fabrication routes pose many disadvantages and challenges [3], while processing many of the advanced fuel concepts, such as kernel fuel for high-temperature reactors, sphere-pac fuel for fast reactors, etc. [4]. Because of this, the fabrication of advanced fuel concepts has attracted attention toward special techniques, such as the sol–gel process. The sol–gel process is a dust-free method that uses liquids or free-flowing solids, devoid of radiotoxic dust hazards. Also, this technique is highly amenable to remotization and automation. It is particularly advantageous in the fabrication of mixed oxide/nitride/carbide kernel-type fuels with high homogeneity and excellent aspect ratio. The sol–gel process has been developed for particulate fuels, such as (Th,U)O₂ and (Th,Pu)O₂ (Th,U,Gd)O₂ solid solutions.

Microsphere-based fuels for TRISO (tri-structural isotropic) fuel particles are a promising fuel concept for advanced nuclear reactors, designed to withstand high temperatures of ~1500–1600°C without any disintegration of the fuel particles and coatings, which enhances safety and reliability, particularly in high-temperature gas-cooled reactors (HTGRs) and other advanced reactor types. This type of fuel, with its robust ceramic coatings, is also being explored as Accident-Tolerant Fuel (ATF) for advanced nuclear reactors, offering improved safety and performance under extreme conditions [5]. There is a need for optimizing TRISO fuel particle design, manufacturing processes, and understanding the performance of SiC layers under oxidizing and extreme conditions for their utmost in-pile performance. Thermal stability and oxidation resistance are also important to evaluate the integrity of the coating layers for successful performance [6].

Sphere-pac fuel is an attractive alternative fuel concept in place of pellet fuel due to its improved fuel utilization and irradiation performance. Development of high-plutonium-containing, phase-pure sphere-pac fuel with an optimum O/M ratio requires many heat treatment schemes and sintering conditions [7]. Inert matrix fuels (IMFs) [8], which are composite fuels with high thermal conductivity and the potential for high burnup, are being investigated for use in advanced nuclear reactors, including for plutonium and minor actinide incineration and waste disposal. Recent studies carried out on microsphere-based inert matrix fuels will also be discussed.

References:

- [1] O. Gotzmann and H. Kleykamp, *J. Nucl. Mater.*, **89** (1980) 79.
- [2] T.R.G. Kutty et al., *J. Nucl. Mater.*, **282** (2000) 54.
- [3] X. Zhao et al., *Trans. Am. Nucl. Soc.*, **80** (1999) 43.
- [4] D.D. Sood, *J. Sol-Gel Sci. Technol.*, **59** (2011) 404.
- [5] Z. Shao et al., *J. Phys.: Conf. Ser.*, **2749** (2024) 012012.
- [6] R.V. Pai et al., *J. Nucl. Mater.*, **473** (2016) 229.
- [7] A. Kumaret al., *J. Nucl. Mater.*, **434** (2013) 162.
- [8] N. Gumber et al., *J. Alloys Compd.*, **1002** (2024) 175146.



Dr. Rajesh V. Pai, joined Fuel Chemistry Division in 1997 through 40th batch of Training School after completion of his M.Sc. from Cochin University of Science and Technology. Since then he has been working on development of nuclear fuel materials by sol gel process. He obtained his PhD from Mumbai University. He has developed many flow sheets suitable for fabrication of advanced nuclear fuel materials and special fuels by sol-gel process. He is an expert in synthesizing many technologically important materials such as perovskites, pyrochlores, layered perovskites etc. which are used as peizo electric, catalytic, chemical sensors in different applications. He has published about 45 papers in international journals, 3 book chapters and one monograph. His current interest includes the development and functional studies of various advanced porous materials like Metal-organic Frameworks (MOFs) and composite materials. Currently, he is a Professor at HBNI, DAE and Head, Fuel Chemistry Division, BARC.

Development of Solvents for Nuclear Fuel Cycle

C.V.S. Brahmananda Rao

FChD, Indira Gandhi Centre for Atomic Research, Kalpakkam, India

Email: brahma@igcar.gov.in

Solvent extraction, as a separation method, has played a pivotal role in the development of nuclear technology and it is employed in various stages of nuclear fuel cycle. This presentation will dwell on the historical perspective of separation techniques in nuclear industry for various applications. The importance of Tri-n-butyl phosphate (TBP) in the fuel cycle and the possibilities of the alternate extractants in the front and the back end will be presented. It is reported in literature that phosphonates are superior to phosphates, and can be employed as ligands for actinide extraction. In this category, two ligands such as dialkylalkyl and dialkyl hydrogen phosphonates are studied for actinide separations. Among these, dialkyl hydrogen phosphonates show dual performance upon variation of acid concentration. These phosphonates have been less explored for the actinide separation, but show promise in the extraction of PGMs from high level liquid waste in the back end of the fuel cycle. It is important to understand the extraction and complexation behaviour of these classes of compounds for potential applications in metal extraction. Most of the experimental studies were dedicated to synthesizing and studying numerous molecules for various applications. Understanding actinide extraction from a theoretical point of view provides insights crucial for tailoring extractants for specific applications. Solvent extraction being a complex process is influenced by various factors and presents challenges for theoretical studies. Nonetheless, the formation of complexes between ligands and metal nitrates at the aqueous-organic interface constitutes a molecular process amenable to modelling through quantum computational chemistry tools.



Dr. C.V.S. Brahmanand Rao completed his B.Sc. (Hons.) in Chemistry from Delhi University and M.Sc. in Chemistry from the University of Hyderabad. He joined the 38th batch of the BARC Training School in 1994. After completing his training, he joined the Radiochemistry Laboratory at IGCAR in 1995. He earned his Ph.D. from the University of Madras in the field of organic ligand synthesis and its application in actinide recovery. He is currently the Head of the Solution Chemistry and Mass Spectrometric Studies Section in the Fuel Chemistry Division at IGCAR.

He has authored over 120 publications in journals, seminars, and symposia. He also serves as the Dean of Chemical Sciences at IGCAR under the Homi Bhabha National Institute, Mumbai. His research interests include synthetic organic chemistry, the development of alternative extractants for actinide recovery, computational chemistry, and high-temperature mass spectrometry.

New Methodologies and Substrates for the Assay of Actinides using Nuclear Radiations

Rahul Tripathi

Radiochemistry Division, Bhabha Atomic Research Centre, Mumbai, India-400085

Email: rahult@barc.gov.in

Use of nuclear radiations for detection and quantification of radionuclides is the most common and oldest approach. Techniques such as gamma-ray spectrometry, alpha spectrometry, neutron counting and calorimetry are widely employed for the quantification of actinides over the past several decades and are now well established [1]. However, due to the complexity of samples in terms of size, shape, matrix, containment and signal interferences, continuous efforts are being made to develop new need-based methodologies by addressing these challenges to meet the requirements of nuclear security and safeguards.

High resolution gamma-ray spectrometry is most commonly employed for the determination of the relative isotopic amounts and can also be used for absolute quantification if absolute efficiency and attenuation of the gamma rays from the sample can be determined with reasonable accuracy. Significant efforts have been made in the recent past to address these challenges, thereby developing high resolution gamma ray spectrometry as a technique for absolute quantification of actinides in complex samples by taking care of non-standard geometry, sample attenuation and heterogeneous matrix [2-4].

For detection and quantification of actinides at extremely low level, among different radiations, alpha particle detection is usually employed. Recently, extractive scintillating substrates based on polyethersulphone were developed to pre-concentrate and quantify plutonium activity as low as ~100 mBq [5]. A dedicated low background PMT based scintillation counting system was setup in house for this purpose. Subsequently, polystyrene based extractive scintillation film was developed for selective uptake and quantification of plutonium activity as low as ~1.3 mBq [6]. In another study, an actinide-hydrolysis based sequestration approach has been developed for actinide pre-concentration without selectivity followed by subsequent quantification of gross alpha activity using scintillation counting [7]. It should be mentioned here that all the pre-concentrated samples made using these novel platforms can be used for alpha spectrometry thereby showing a potential for elemental/isotopic quantification.

Acknowledgements: I would like to thank all my co-workers especially Dr. Chhavi Agarwal, Dr. Sabyasachi Patra, Dr. Amol Mhatre and Shri Satyam Kumar, on whose behalf I am making this presentation.

References:

- [1] D Reilly, N Ensslin, H Smith Jr, S Kreiner Eds, Passive nondestructive assay of nuclear materials 1991; <https://doi.org/10.2172/5428834>
- [2] Satyam Kumar et.al., *Analytical Chemistry*, **95** (2023) 3247
- [3] S. Patra et. al., *Analytical Chemistry*, **96** (2024) 2857
- [4] S. Patra et. al., *ACS Omega*, **9** (2024) 44658
- A. Mhatre et. al., *Sensors and Actuators B*, **390** (2023) 134021
- [5] Mhatre et. al., *Analytical Chemistry* (2025) (In press)
- [6] S. Patra et. al., *Environ. Sci.: Nano* (2025) DOI: 10.1039/D4EN01159G



Dr. Rahul Tripathi joined Radiochemistry Division, BARC in the year 2000 after completing one year orientation course from BARC training school. His area of research mainly includes nuclear fission and assay of nuclear materials using nuclear radiations. He has about 100 publications in the peer reviewed journals.

High-precision Mass Spectrometry Methods for Environmental Radionuclide Analysis

Norbert Kavasi[§], Tatsuo Aono

Regional Environmental Co-Creation Unit, Fukushima Institute for Research, Education and Innovation (F-REI), Fukushima, Japan

[§]Email: kavasinorbert@resfrei.onmicrosoft.com

The Fukushima Institute for Research, Education and Innovation (F-REI) is a special corporation established on April 1, 2023, under the Act on Special Measures for the Reconstruction and Revitalization of Fukushima. In addition to providing dreams and hopes for realizing the reconstruction of Fukushima and other prefectures in the Tohoku region, F-REI aims to become a world-renowned “central institute for creative reconstruction” which drives forward with enhancing the scientific capabilities, technological capabilities and industrial competitiveness of Japan, and contributes to economic growth and improvement of the daily lives of people living in Japan. Regional Environmental Co-Creation Unit is one of the research units of F-REI and its aim is to conduct research and analysis on the natural environment and local communities in the areas affected by the nuclear disaster, and also, to accumulate and disseminate scientific knowledge for enhancing local safety.

In recent years, inductively coupled plasma mass spectrometry (ICP-MS), including triple quadrupole, tandem, and high-resolution techniques, as well as thermal ionization mass spectrometry (TIMS) and multi-collector inductively coupled plasma mass spectrometry (MC-ICP MS) with various ion counters capable of detecting low ion currents below 10-13 A, have been employed to analyse different radionuclides (such as Sr-90, Cs-137, Ra-226, Am-241, U and Pu isotopes, etc.)

Mass spectrometry provides several significant advantages over radiometric methods, such as shortens analysis time, enhanced sample throughput, and lowered sample input necessities. Nevertheless, utilising mass spectrometry instruments to analyse low-level radioactive concentrations in environmental materials may present challenges.

The primary issue is the isobaric interference, which refers to the existence of isotopes from various elements that possess identical atomic mass. Examples include Zr-90 being interfere for Sr-90, U-238 for Pu-238, Am-241 for Pu-241, Ba-137 for Cs-137, and so on.

The second issue pertains to peak tailing and fronting, resulting from ion beam scattering, which manifests as asymmetrical peak shapes in the mass spectra. This distortion appears on either the upper or lower mass side of an abundant isotope, such as Sr-88 for Sr-90, U-238 for U-235, Cs-133 for Cs-135, and so on.

The third issue is that certified standards of radionuclide standards are specifically designed for radiometric measurement, not for mass spectrometry. Nonetheless, all standards contain a mixture of different isotopes, and the ratios of these isotopes are not validated. For instance, Sr-90 standards contain Sr-88, Am-241 standards contain Am-243, Ra-228 standards contain Ra-226, and so on.



Norbert Kavasi is an accomplished researcher from Hungary at Regional Environmental Co-Creation Unit, Fukushima Institute for Research, Fukushima, Japan. He has over 15 years of experience collaborating with prestigious research institutes across Japan and Europe. He has served as a postdoctoral fellow under both the Japan Society for the Promotion of Science (JSPS) and the Marie Skłodowska-Curie Actions (MSCA). His core expertise lies in the field of radioecology and the analysis of radionuclides using advanced radiometric and mass spectrometric techniques. Norbert is known for his positive outlook and tireless energy, which he brings to his professional environment, motivating colleagues and inspiring high performance. He is actively engaged in the testing and analysis of various samples, where radioactive contamination is suspected.

Isotopic Separations at Heavy Water Board

S. Satyakumar, V.V.S.A. Prasad, K.V. Tale, S.R. Gaidhani, Ajit R. Dusane[§]

Heavy Water Board, Mumbai, India

[§]Email: arduane@hwb.gov.in

Heavy Water Board(HWB) is primarily mandated with production of deuterium oxide, commonly known as heavy water, through the separation of deuterium from hydrogen and its enrichment to nuclear-grade purity. This heavy water is suitable for use as coolant and moderator in Pressurised Heavy Water Reactors (PHWR). Isotope separation methods such as diffusion, distillation, centrifugation, thermal diffusion, exchange reactions, and electrolysis are employed on case-to-case basis, to achieve effective separation and enrichment. HWB is engaged in industrial-scale separation of isotopes of hydrogen, boron, and oxygen, using chemical exchange, distillation, and electrolysis processes, as the other viable processes were not found economical on larger scale industrial facilities. HWB also employs multiple isotopic separation techniques to achieve extraction and enrichment of given isotope based on optimized separation duty. Accordingly, cascade theory is adopted for designing and operation of isotopic separation facilities. HWB has successfully implemented H₂S-H₂O and NH₃-H₂ based chemical exchange process facilities for production of Heavy Water on industrial scale.

Hydrogen has three isotopes, i.e., hydrogen, deuterium, and tritium, where hydrogen and deuterium are stable isotopes while tritium is radioactive. Natural abundance of deuterium is around 150 ppm D/(D+H) a/a Isotopic Purity (IP), in hydrogen and its naturally occurring compounds. Deuterium is enriched through a chemical exchange process up to a sizable IP and then exposed to vacuum distillation for final enrichment up to nuclear grade HW.

Boron has two stable isotopes, i.e., B-10 and B-11, where B-10 is ~20 % (a/a IP) naturally abundant. Since many of the boron compounds are in solid form in ambient conditions, it is necessary to select certain specialty compound for achieving isotopic separation of B-10 and B-11 through conventionally available isotope separation methods. Accordingly, boron trifluoride-diethyl ether complex, commonly known as BF₃-complex is employed for isotopic separation and further enrichment. HWB is equipped with facilities for converting the BF₃ complex into useful B-10 enriched compounds required for Fast Breeder Reactor program. While, B-10 enriched compounds finds application in Nuclear field, B-11 which, is getting simultaneously enriched during B-10 enrichment, finds applications in the field of semiconductor industry. HWB is exploring potential to support Indian semiconductor industry by sourcing the B-11 compounds for production of B-11 enriched BF₃ gas used in doping of semiconductor chips and other applications. Isotopic separation technique used is exchange distillation of BF₃ complex. HWB is equipped with facilities for converting the BF₃ complex into useful B-11 enriched compounds required for semiconductor industries.

Oxygen has three stable isotopes, i.e., O-16, O-17 and O-18 with their natural abundance being 99.763%, 0.037%, and 0.200%, respectively. O-17 has application in biomedical research, where determination of cerebral metabolic rate of oxygen utilization is monitored by assessing the changes of metabolically generated H₂¹⁷O in brain tissue from inhaled ¹⁷O-labeled oxygen gas. O-18 enriched water also finds application in the field of nuclear medicine and biomedical research. 10% O-18 enriched water has applications in human metabolism studies and >97 % O-18 enriched water is used as precursor of F-18, a Positron Emission Tomography (PET) imaging isotope, used in detection and staging of cancer. The product O-18 water at end of distillation cascade usually gets simultaneously enriched with

deuterium, in the form of $D_2^{18}O$. Deuterium is replaced with hydrogen using combination of electrolytic splitting and catalytic re-combination.

Isotope separation technologies require specially designed contacting devices due to the limited thermodynamic driving forces and minimal differences in chemical and physical properties between isotopes. These processes are often energy-intensive, and to achieve high separation factors, a combination of multiple separation techniques and novel contacting devices is employed to meet industrial-scale demands efficiently.



Shri Ajit Ramesh Dusane joined the Heavy Water Board (HWB) in 1998 after completing his B.Tech in Chemical Engineering. He has served at HWP-Manuguru and HWP-Tuticorin and is presently working in the Operation Group at HWB (Central Office). He has extensive experience in both H_2S-H_2O and NH_3-H_2 chemical exchange processes, as well as in the vacuum distillation of off-grade water for the production of heavy water. He has been instrumental in process development for Oxygen-18 enriched water and was actively involved in the design and development of India's first H_2O^{18} plant at HWP-Manuguru. Currently, he is engaged in various ongoing projects of HWB and serves as the Unit Project Coordinator for Capital Scheme Projects. He is also actively involved in the restart-up activities at HWP-Tuticorin, the production of deuterium-labelled compounds at HWBF-Vadodara, the establishment of a hydrogen production facility at HWBF-Mumbai, and the augmentation of Heavy Water Plants in line with the Amritkal Vision – 2047.

The Approaches to Design the Ligands for Separation of F-Elements

V.G. Petrov

Department of Chemistry, Lomonosov Moscow State University, Moscow, Russia

Email: vladimir.g.petrov@gmail.com

To meet the requirements of sustainable development, humanity has no other choice but to utilize and advance nuclear energy. After 70 years of development, it is time to transition not just to Generation IV reactors, but also to establish the Generation IV nuclear systems. A key element of such systems is the closure of the nuclear fuel cycle, which involves the extraction and reuse of valuable components from spent nuclear fuel. This will significantly improve the efficiency of natural uranium and thorium utilization, while also reducing the volume of radioactive waste.

However, to establish sustainable nuclear energy, it is necessary to address not only the issue of fissile materials, but also other long-lived elements, such as technetium and iodine, which pose significant environmental risks due to their long half-lives and high mobility in the environment. Spent nuclear fuel contains more than 50 chemical elements, and their extraction and separation require the development of highly efficient and selective industrial chemical processes. One of the most challenging tasks in this field is the separation of trivalent f-elements, particularly americium and curium, due to their extremely similar chemical properties, electronic structures, and ionic radii. One of the most promising methods for separating such elements is liquid-liquid extraction. Extraction systems (extractant + diluent) must meet stringent requirements: high selectivity, radiation and thermal stability, as well as chemical durability. Therefore, the search for extractants that combine high efficiency, selectivity, solubility, and stability remains critically important.

During the talk, an overview of recent advancements in the development of extraction systems for the separation of Am/Ln/Cm pairs as well as other actinides will be provided. The development of such technologies is a crucial step toward the creation of the Gen-IV nuclear systems, which will ensure a sustainable and safe future for nuclear energy. Addressing the challenges associated with long-lived elements, such as technetium and iodine, will also make a significant contribution in minimizing the environmental impact of nuclear energy and establishing a closed fuel cycle. The ongoing research and development in this field are essential to overcome the technical and environmental challenges associated with nuclear energy, thereby ensuring its role in the global transition to a low-carbon economy.



Dr. Vladimir Petrov is currently serving as an Associate Professor at Lomonosov Moscow State University. His research focuses on radiochemistry, separation of f-elements, radioactive waste management, spent fuel processing, and environmental radioactivity. Over the course of his academic career, Dr. Petrov has been recognized with several prestigious honors, including the Acad. I.P. Alimarin Award for successful scientific work (2009), a DAAD scholarship (August 2009 – July 2010), the

President's Stipendium for Young Scientists (2015–2017), the MSU Stipendium for Young Scientists (2015), and the MSU Award for Young Professors and Scientists (2018). Dr. Petrov has an extensive publication record, with 74 documents indexed in Web of Science (848 citations, H-index 15) and 102 documents indexed in Scopus (983 citations, H-index 18), reflecting his significant contributions to the field of nuclear and radiochemical science.

Production and Applications of Radioisotopes at RIKEN RI Beam Factory – Search for New Elements through Therapy of Cancer –

H. Haba

Nishina Center for Accelerator-Based Science, RIKEN, Wako, Saitama 351-0198, Japan
Email: haba@riken.jp

At RIKEN RI Beam Factory, Wako, Japan, we have been developing production technologies of radioisotopes (RIs) and conducting RI application studies in the fields of physics, chemistry, biology, engineering, medicine, pharmaceutical and environmental sciences [1]. Utilizing light- to heavy-ion beams from the RIKEN AVF cyclotron, we produce more than 100 RIs, ranging from ^7Be (atomic number $Z = 4$) to ^{262}Db ($Z = 105$).

In chemistry of super heavy elements (SHEs), chemical properties of Rf ($Z = 104$) and Db in aqueous solutions were investigated in collaboration with Osaka University, Kanazawa University, Niigata University, and Japan Atomic Energy Agency. In nuclear medicine, we have been developing a production technology for ^{211}At via $^{209}\text{Bi}(\alpha, 2n)^{211}\text{At}$ reaction for targeted α -particle therapy (TAT) and supplying ^{211}At to 20 research groups in Japan for the development of new nuclear medicines.

RIs of a large number of elements (multitracer) are simultaneously produced from metallic targets such as ^{nat}Ti , ^{nat}Ag , ^{nat}Hf , and ^{197}Au irradiated with a 135-MeV/nucleon ^{14}N beam from RIKEN Ring Cyclotron (RRC). The multitracer is useful to trace the behavior of many elements simultaneously under identical experimental conditions. Recently, we have devised a large-scale ^{211}At production system using a rotating ^{209}Bi target and a dry distiller for chemical separation of ^{211}At on the beamline of RRC. ^{225}Ac has also been produced via the $^{232}\text{Th}(^{14}\text{N}, xny)^{225}\text{Ac}$ reaction for TAT applications.

An isotope of element 113 was synthesized via the cold fusion reaction of $^{209}\text{Bi}(^{70}\text{Zn}, n)^{278}113$ using the RIKEN gas-filled recoil ion separator (GARIS) at the RIKEN linear accelerator (RILAC) facility. The name nihonium and symbol Nh were approved for the new element, completing the 7th period of the periodic table. A synthesis experiment for new element 119 is ongoing using the $^{248}\text{Cm}(^{51}\text{V}, xn)^{299-x}119$ reaction at GARIS-III, located at the upgraded superconducting RILAC facility (SRILAC). A gas-jet transport system has been installed at GARIS as a novel technique for SHE chemistry. Long-lived SHE RIs, such as ^{261}Rf , ^{262}Db , ^{265}Sg ($Z = 106$), and ^{266}Bh ($Z = 107$), which are useful for chemistry experiments, were produced via the heavy-ion induced reactions on a ^{248}Cm target. Their decay properties were investigated in detail using a rotating wheel apparatus for α and spontaneous fission spectrometry. Following the successful chemical synthesis of $\text{Sg}(\text{CO})_6$ led by the Univ. Mainz and GSI Helmholtzzentrum für Schwerionenforschung groups, a detailed experiment is underway to investigate the stability of the metal carbon bond in $\text{Sg}(\text{CO})_6$, using a thermal decomposition setup led by the Paul Scherrer Institute group. Additionally, the syntheses and properties of Tc, Ru, Rh, and Re carbonyls were studied using a ^{252}Cf fission source at Institute of Modern Physics and GARIS, laying the groundwork for future investigations on Bh, Hs ($Z = 108$), and Mt ($Z = 109$) carbonyls.

Reference:

[1] RIKEN Accelerator Progress Report, Sect. Radiochemistry and Nuclear Chemistry in each volume (https://www.nishina.riken.jp/researcher/APR/index_e.html).



Dr. Hiromitsu Haba earned his Ph.D. from Kanazawa University, Kanazawa, Japan, in 1999. He worked at the Japan Atomic Energy Research Institute (1999–2001) as a postdoctoral researcher and at RIKEN as a Special Postdoctoral Researcher (2002–2004), Research Scientist (2004–2006), and Senior Research Scientist (2007–2010). He was appointed Team Leader of the RI Applications Team, Nishina Center for Accelerator-Based Science, RIKEN (2011–2017), and served as Director of the RI Application Research Group (2018–2023), Super heavy Element Research Group (2022–present), and Nuclear Chemistry Group (2023–present). His research focuses on the nuclear chemistry of super-heavy elements and the production and application of radioisotopes using heavy-ion accelerators at the RIKEN RI Beam Factory. He has authored about 300 publications in reputed international journals and books. He received the Young Scientist Award from the Japan Society of Nuclear and Radiochemical Sciences in 2001, the Science Council of Japan President's Award, the 2nd Japan Open Innovation Prize from the Cabinet Office in 2020, and the Science and Technology Award (Commendation for Science and Technology by the Minister of Education, Culture, Sports, Science and Technology) in 2023. He has also served as Visiting Associate Professor (2013–2022) and Visiting Professor (2023–present) at the Graduate School of Science and Technology, Niigata University, Japan; Visiting Professor (2017–2019) at the Faculty of Science, Graduate School of Science, Kyushu University, Japan; Professor (2015–2016) at the Graduate School of Science and Engineering, Tokyo Institute of Technology, Japan; and Visiting Professor (2019–2022) at the Institute of Modern Physics, Chinese Academy of Sciences, China.

Physics Safety and Utilization Aspects of Research Reactors

Tej Singh^{1,2, §}

¹*Reactor Physics and Nuclear Engineering Section, BARC, Mumbai, India*

²*Homi Bhabha National Institute, Mumbai India*

[§]Email: t_singh@barc.gov.in

Research reactors are mainly utilized for radioisotope production, fundamental research, testing various nuclear and structural materials, etc. Radioisotopes are important in various fields, such as nuclear medicine, industries, agriculture and other R&D activities. Beam-tubes are another type of specialised positions providing neutron source, which are utilized for research work in the area of condensed matter physics, neutron radiography, fission fragment studies, neutron scattering studies, etc. Utilization of research reactors in a safe and efficient manner requires continuous technical support from operational reactor physicists. At BARC, Trombay, three research reactors are currently operational: 100 MW_{th} Dhruva, 100 W_{th} Critical Facility (CF) for Advanced Heavy Water Reactor (AHWR) and 2 MW_{th} upgraded Apsara, i.e., Apsara-U. Dhruva contains two on-power rods and one off-power tray rod, pneumatic carrier facility (PCF), self-serve facility for radioisotope production, and experimental beam holes (including two through tubes) for neutron beam research. The maximum thermal neutron flux available in Dhruva tray rod position is about 2.0×10^{14} n/cm²/s. Apsara-U has 1 in-core and 7 out-of-core irradiation positions (situated in the BeO reflector region), wherein tray rods can be loaded for radioisotope production. The maximum thermal and fast neutron flux available at in-core irradiation position is 6.2×10^{13} and 1.5×10^{13} n/cm²/s, respectively. Apsara-U also contains eight beam tubes. CF has an average thermal neutron flux of 10^8 n/cm²/sec. Graphite reflector position of this reactor has facilities for testing neutron detectors and also, to irradiate samples for neutron activation analysis (NAA). Other than these, research reactors in Trombay are also used for novel activities, such as generation of Neutron Transmutation Doping of Silicon (NTD-Si), irradiation of antimony to be used as Sb-Be startup neutron source, production of fission moly of high specific activity in specially designed fission moly tray rod, irradiation of special fuel assemblies to test fuel and clad material at high burnup level, etc.

Reactor physics analysis has to be performed before the target sample is cleared for irradiation for radioisotope production. Any sample loaded in the core perturbs the reactor due to absorption of neutrons, it is very important to evaluate the reactivity effects due to loading of the target sample. Neutron diffusion equation is solved for a given sample geometry with appropriate boundary conditions to estimate neutron flux depression and associated reactivity changes via perturbation theory. The rate of heat generation is determined to ensure it stays within the safety limit of the reactor. In reactor, target nuclide inside the reactor transmutes due to a series of neutron induced nuclear reactions, generating new radioisotopes in the process. Resulting induced radioactivity is estimated by solving a large set of coupled differential equations, governing temporal rate of change in the number of each nuclei, using a semi-analytic model by discretization of total time duration into fine time steps. Optimization of the irradiation position and duration is important to maximize the specific activity of the target isotope. Estimation of sufficient cooling period, as well as necessary shielding needed during post-irradiation transportation for reducing the dose to below acceptable limit is very important. In this regard, an interactive code system: Operational Reactor Physics Analysis Code, or ORPAC-2 had been developed. It consists of different sets of one-group spectrum-averaged cross-sections for various type of neutronic reactions

corresponding to spectrum at the irradiation positions of Dhruva and Apsara-U. It also incorporates photon data library, as used in ORIGEN-2 code, for estimating dose rate.

Furthermore, any core loading changes involves estimation of changes in power distribution in core and necessary optimization must be carried out to avoid power peaking in fuel. Such core changes may also involve change in detector response, requiring recalibration and may alter the worth of shutoff rods. Therefore, reactor physics analysis is necessary to ensure compliance with technical specifications. Various reactor physics codes, many of which are developed in-house, are regularly used for such safety analyses.



Dr. Tej Singh is an Outstanding Scientist and Head of the Reactor Physics and Nuclear Engineering Services (RPNES) section at the Bhabha Atomic Research Centre (BARC), Mumbai. His core expertise lies in reactor physics, safety analysis, and shielding. He has played a pivotal role in providing reactor physics support for the safe and efficient operation of research reactors at Trombay. Dr. Singh has developed several advanced computational tools for core design, safety, and shielding analyses. Notable among these are NEMSQR and HEXNEM, nodal expansion method-based codes for reactor core design and management; IQSHEX and DINHEX, space-time kinetics codes based on nodal expansion methods; and RITAC and SACRIT, point kinetics codes coupled with thermal hydraulics for analyzing reactivity-initiated accidents in research and power reactors. He also developed MANTRA, a 2D Method of Characteristics (MOC)-based neutron transport code for lattice cell calculations, and MCBLD, a Monte Carlo-based shielding code.

Climate Change Impacts on Global Water Resources – Role of Nuclear Techniques

Chidambaram Sabarathinam[§], Khaled Hadi, Adnan Akber, S.V.V. Dhanuradha,
Amjad Al Rashidi

*Hydrology and water resources management, Water Research Center, Kuwait Institute for
Scientific Research, Kuwait*

[§]Email: sabarathinam@kisir.edu.kw

Climate change is one of our most significant environmental challenges, affecting water resources globally. Water isotopes are components of the water molecule and travel through the hydrological cycle. The origin, mobility, and history of water are ascertained by analysing stable isotopes in water samples. The radioactive isotopes provide insight into the ages of reservoir water, aiding in assessment of replenishment rates and water sustainability. The isotopic composition of water reflects climate change-induced variations in temperature, precipitation, and extreme weather events. These isotopic markers can demonstrate the impact of climate change on water availability and distribution by addressing the water source and tracking the hydrological cycle, using predictive climate models, identifying regional and local effects, and assisting in paleoclimate reconstruction. Analysis of precipitation, river water, groundwater, and other water bodies' isotopic compositions can reveal water origins and pathways, particularly in areas affected by climate change with altered precipitation, providing information on moisture sources and runoff patterns. Isotope-based climate change models elucidate the climate phenomena, such as the Pacific Walker Circulation (PWC) and El Niño–Southern Oscillation (ENSO) and their influence the global water cycle. Consequently, the isotopic signatures unveil groundwater recharge patterns, sources, climate conditions, and timelines. Temperature-based estimates in groundwater help in assessing recharge temperatures, and noble gas isotopes also play a crucial role in dating recent groundwater. Furthermore, isotopic studies quantify the contributions of glacial and snowmelts to river flow and monitor their evolution. Advances in isotope-enabled climate models have improved the precision of hydrological and climate projections. Models that simulate the distribution of water isotopes in vapour and precipitation reduce forecast uncertainty and enhance simulations. Additionally, incorporating isotope signatures into general circulation models increases the accuracy of predictions. Hence, monitoring the isotope signatures will assist in managing and sustaining the global water resources under the climate change scenario.



Dr. Chidambaram Sabarathinam is currently serving as a Research Scientist at the Water Research Center, Kuwait Institute for Scientific Research (KISR), Kuwait. With specialized expertise in hydro-geochemistry and geochemical modelling, he has contributed extensively to the understanding of groundwater systems and environmental geochemistry. His notable achievements include receiving the Best Research Article of the Year 2013 award from Applied Water Science (Springer) for his publication titled "A study on the defluoridation in water by using natural soil." He was also honored with the Dr. Sudarshan

Pani – Dr. (Smt) Rama Dwivedy Medal in 2016 by the Indian Society of Applied Geochemists, Hyderabad, for his significant contributions to hydrogeology and environmental

geochemistry. In recognition of his academic excellence, he was awarded the Dr. Héctor Mayagoitia Domínguez Lecture Series Award for the academic year 2018–2019 by IPN, Mexico, for his work on climate change perspectives and the environment. Mr. Sabarathinam was also listed among the top 2% of scientists worldwide for the years 2023 and 2024, according to Stanford University's global research rankings.

Delayed Molecular Hydrogen Production in Portlandite under Irradiation: Reaction Mechanisms and Consequences for the Storage of Radioactive Waste

Thibaut Herin^{1,2}, Stéphane Poyet², Pascal Bouniol², Sophie Le Caër^{1,§}

¹Université Paris-Saclay, CEA, Service de recherche en Corrosion et Comportement des Matériaux, 91191 Gif-sur-Yvette, France

²Université Paris-Saclay, CEA, CNRS, NIMBE UMR 3685, 91191 Gif-sur-Yvette, France

§Email: sophie.le-caer@cea.fr

Calcium hydroxide, or portlandite ($\text{Ca}(\text{OH})_2$) is the second most abundant hydrate in cementitious materials. The latter form the basis of coating matrices for certain radioactive wastes. Under ionizing radiation, this results in the production of radiolytic molecular hydrogen, which, when it accumulates in the environment, may raise safety concerns. Therefore, it is important, to understand how radiation interacts with these materials, and particularly with portlandite. This hydroxide displays a unique behaviour: upon irradiation, it not only leads to the immediate production of molecular hydrogen but also to a delayed production over long periods of time (days or even weeks) after the irradiation has stopped [1]. In fact, the di-hydrogen formed within the material moves by sub-diffusion (a non-Fickéan diffusion) to the surface, which then leads to its release into the atmosphere, although this process is very slow [1, 2].

We have also determined the reaction mechanisms operating in this system by means of electron paramagnetic resonance (EPR) spectroscopy experiments, in order to identify the different radicals generated under radiation. Thus, we have shown that the immediate production of H_2 is due to the stabilization of electrons on the surface of the portlandite, followed by surface reactions that promote the immediate release of H_2 into the gaseous atmosphere. As the radiation dose increases, the number of these sites decreases, leading to a reduction in the immediate production of the molecular hydrogen. The delayed production of H_2 is due to the formation of hydrogen atoms, followed by their dimerization within the portlandite crystal lattice, resulting in the trapping of molecular hydrogen molecules. In this case, the movement of the hydrogen atoms in the crystal lattice also mobilizes the CaO^\bullet radicals. At low doses, these radicals dimerize to form CaO-OCa peroxides. At high doses, the CaO^\bullet radicals can react with hydrogen atoms, thereby limiting the formation of the trapped H_2 [3]. The range of the different reaction intermediates identified reflects the richness of the chemical processes involved in the mechanisms, which accounts for the behaviour of portlandite on exposure to irradiation.

References:

- [1] T. Herin et al., *J. Phys. Chem. C*, **127** (2023) 20245.
- [2] T. Honorio et al., *J. Phys. Chem. C*, **128** (2024) 19085.
- [3] T. Herinet al., *J. Phys. Chem. C*, **128** (2024) 19529.



Dr. Sophie Le Caer is a researcher at NIMBE UMR 3685, CEA, CNRS, Université Paris-Saclay, France. Her expertise lies in radiation chemistry, particularly in materials characterization, confinement effects, radiation chemistry in heterogeneous media, and processes relevant to the storage of nuclear waste. Her research also explores energy transfer phenomena in nanostructures and the use of radiolysis to study ageing mechanisms in batteries. Dr. Le Caer was awarded the Young Researcher Prize by the Physical Chemistry Division of the French Chemical Society. Her recent work includes investigations into reaction mechanisms triggered by irradiation in model nuclear waste storage materials, studies on energy transfer in one-dimensional nanostructures, and the application of radiation chemistry to simulate and understand battery ageing processes in a highly accelerated manner.

Back End Fuel Cycle- Status and Current Trends

Madhuri Shetty

Fuel Reprocessing Division, Bhabha Atomic Research Centre, Mumbai, India

Email: mskittad@barc.gov.in

India has opted for an ambitious three-stage nuclear power program aimed at the optimal utilization of its available uranium resources and transition to thorium-based nuclear technology. The recovery and recycling of fissile materials generated during nuclear fuel irradiation (Pu^{239} and U^{233}) will aid self-sustaining energy program. In this context, the closed fuel cycle approach is particularly well-suited for our country, towards realization of goal of three stage nuclear power program.

India has demonstrated its Indigenous capability in the field of PHWR spent fuel management by designing, constructing and operating PUREX based reprocessing plants as well as associated radioactive waste management facilities at Tarapur and Kalpakkam. Over the years, significant advancements in reprocessing flow sheets have been achieved, leading to standardized and enhanced operating capacities, improved product recoveries and purity, as well as reductions in waste volumes and personnel exposure. Recent developments in radioactive waste management have enabled the recovery of valuable radionuclides, substantial minimization of waste volumes, and effective reduction in radioactive discharges.



Smt. Madhuri Shetty is currently working at Bhabha Atomic Research Centre (BARC), Mumbai as Scientific Officer–H and specializing in the back-end fuel cycle. With significant expertise in this critical area of the nuclear fuel cycle, she has made impactful contributions to the field. In recognition of her work, she has been honoured with the prestigious Scientific & Technical Excellence Award.

Recent Advances in Nuclear Waste Management Practices in India

D. Banerjee

Process Development Division, Nuclear Recycle Group, BARC, Mumbai, India

Email: daya@barc.gov.in

Efficient nuclear waste management is critical for the sustainable growth of atomic energy programs. From the outset, India has established a robust R&D framework to implement best-in-class waste management strategies aligned with global standards. High-level liquid waste (HLLW), which contains nearly 99% of total radioactivity, has conventionally been managed through vitrification using sodium borosilicate-based matrices. This immobilization process has been instrumental in ensuring safe disposal. However, recent advancements in partitioning technology have revolutionized nuclear waste management by significantly reducing waste volumes, while enabling the recovery of valuable radioisotopes. Some of these extracted isotopes have found extensive applications in cancer treatment and industrial radiation technologies. Furthermore, India has pioneered the development of innovative melter technologies for vitrification, which are essential for the long-term stabilization of HLLW. These advancements have enhanced vitrification efficiency and ensured greater operational reliability.

Significant progress has also been made in the management of low and intermediate-level radioactive waste. The development of innovative ion exchange, sequestration and membrane-based processes has effectively minimized radioactive discharges, ensuring adherence to the strictest environmental safety norms. India's nuclear waste management practices are now well-poised to address future challenges, including those arising from next-generation nuclear reactors. With a strong infrastructure, indigenous technological innovations, and an unwavering commitment to sustainability, India has established itself as a global leader in nuclear waste management, setting benchmarks for safe and efficient waste disposal. This talk reviews India's latest scientific and technological progress in the field, highlighting innovations that ensure secure and sustainable management of nuclear waste.



Dr. D. Banerjee is the Head of the Process and Matrix Development Section at the Process Development Division, Nuclear Recycle Group, BARC. He joined BARC in 1999 after completing the 42nd batch of the BARC Training School. He obtained his PhD in Chemistry from Homi Bhabha National Institute (HBNI), Mumbai, in 2012. With over 25 years of research experience, Dr. Banerjee has made significant contributions to the development of processes and matrices for the treatment of radioactive liquid waste. His research interests also extend to the development of radiation sources for technological applications. Dr. Banerjee's contributions to nuclear science have been recognized with several prestigious awards, including the Scientific and Technical Excellence Award (2008) and the Prof. H.J. Arnikar Best Thesis Award (2012). He has authored over 100 publications in leading international journals and conference proceedings.

Advanced Materials for Selective Capture and Removal of Radionuclides in Nuclear Waste Management

Debajit Sarma

Department of Chemistry, IIT Patna, Bihta, India

Email: debajit@iitp.ac.in

In this talk, recent developments in the design of advanced materials for the selective capture, removal, and recovery of radionuclides from nuclear waste will be described [1-8]. Emphasis will be placed on the use of functional frameworks such as open-framework oxysulfides, layered metal sulfides, and organic-inorganic hybrid thioantimonates to address the challenges associated with radioactive contamination. Key topics will include the highly selective capture of cesium-137 using super-tetrahedral cluster-based materials, along with efficient removal strategies for radionuclides such as uranium, strontium, technetium, and iodine. The role of radiation-resistant materials like gallium thioantimonates and ion-exchangeable molybdenum sulphide chalcogels in the development of next-generation separation technologies will also be highlighted. The talk will underscore how these materials, capable of operating under extreme conditions, offer significant promise for environmental remediation and the long-term management of nuclear waste.

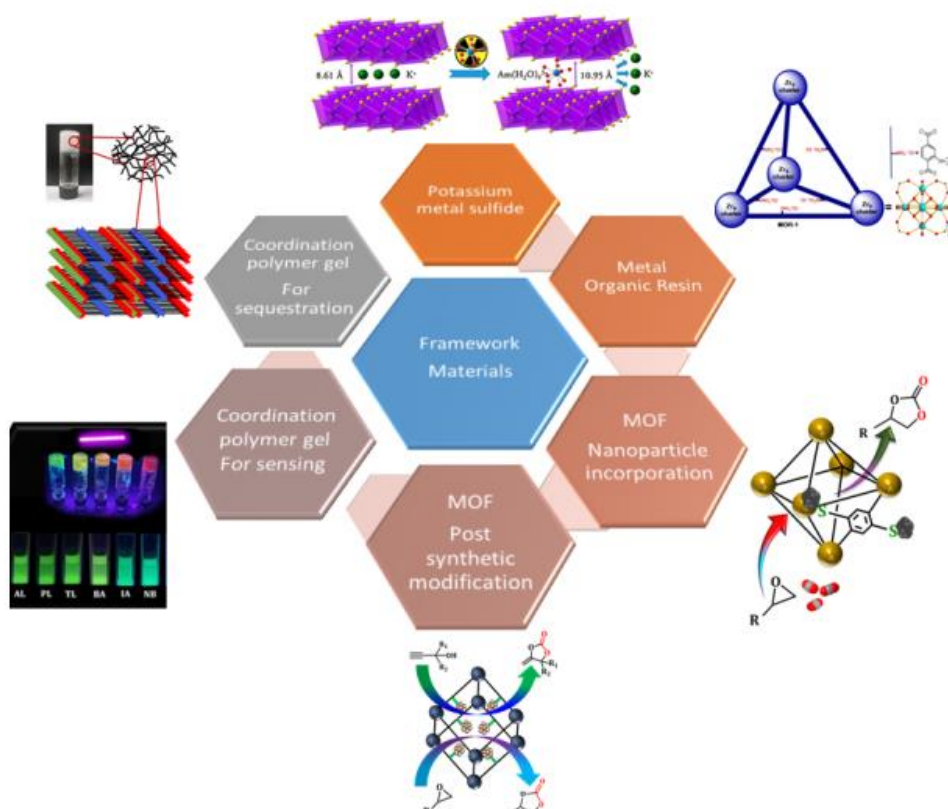


Fig. 1: Schematic representation of the framework materials for multifaceted applications

References:

- [1] J. Am. Chem. Soc., 140 (2018) 11133.
- [2] J. Am. Chem. Soc., 139 (2017) 16494.
- [3] J. Am. Chem. Soc., 138 (2016) 12578.
- [4] J. Am. Chem. Soc., 137 (2015) 13943.
- [5] Chem. Mater., 28 (2016) 3976.
- [6] Chem. Mater., 31 (2019) 1628.
- [7] Chem. Mater., 27 (2015) 2619.
- [8] Chem. Sci., 7 (2016) 1121.



Dr. Debajit Sarma is an Associate Professor in the Department of Chemistry at IIT Patna. He earned his PhD from the Indian Institute of Science (IISc) in 2012, followed by postdoctoral research at Northwestern University, USA (2013–2016), under the mentorship of Prof. Mercouri G. Kanatzidis. His research focuses on solid-state and inorganic materials, particularly coordination polymers, metallogels, metal chalcogenides, and cluster-based systems. He has made notable contributions to the development of advanced materials for the selective capture and removal of radionuclides, with broader applications in nuclear waste management, catalysis, energy, electronics, and environmental remediation. A key aspect of his work is to understand the synthesis–structure–function relationship to bridge fundamental research and practical applications. Dr. Sarma has authored over 50 publications in leading international journals, including multiple articles in JACS. His work has received more than 3,600 citations, with an h-index of 29, and he holds two U.S. patents. He is a recipient of the SERB Early Career Research Award and continues to lead impactful research in materials innovation for energy and environmental challenges.

Research and Development of Molten Salt Fuels

S. C. Parida

*Product Development Division, Radiochemistry and Isotope Group
Bhabha Atomic Research Centre, Mumbai 400094, India*

Email: sureshp@barc.gov.in

The third stage of Indian nuclear power programme envisages use ^{232}Th - ^{233}U fuel cycle using suitable reactors. The required amount of ^{233}U would be obtained from operation of Pu/Th based fast reactors in the later part of the second stage utilising the fast breeder reactors. The thorium fuel cycle has ^{233}Pa as an intermediate isotope in the chain of nuclear reactions, which results in conversion of ^{232}Th to ^{233}U . However, in a reactor core, ^{233}Pa is always subjected to the presence of fission neutrons, which if absorbed, and hence is a parasitic loss. This is unavoidable in case of solid fuelled reactors, since the fuel pins need to be exposed to certain burnups before being extracted for reprocessing.

This problem can be circumvented in a molten salt-fuelled reactor, where the fuel in the fluid form can be configured to give significant breeding ratio. The ^{233}Pa can be separated online as soon as it is produced and allowed to decay to ^{233}U out of core. Therefore, the molten salt breeder reactor (MSBR) seems to be the most attractive option for thorium utilisation and is being proposed for the third stage of Indian nuclear power programme.

To keep the fissile and fertile materials in the molten state, mostly fluoride-based salt systems having low eutectic melting points are the ultimate choice due to several advantages over other type of salts. Hence, considerable R&D effort is being pursued worldwide to develop suitable fluoride-salt based fuels. Various R&D efforts made in this direction in India as well as globally will be discussed in this paper.



Dr. S. C. Parida is currently the Head, Product Development Division of Bhabha Atomic Research Centre, Mumbai, India. His areas of expertise include thermodynamics of materials, actinide chemistry and hydrogen storage materials. He is a professor at Homi Bhabha National Institute. He has more than 90 publications to his credit. Dr. Parida is the Vice-president of Indian Association of Nuclear Chemists and Allied Scientists.

Regulatory Clearance and Hot Commissioning Experience of DFRP

K. Rajan

Director, Reprocessing Group

Indira Gandhi Centre for Atomic Research, Kalpakkam, Tamil Nadu, India

Email: krajan@igcar.gov.in

The Demonstration Fast reactor fuel Reprocessing Plant (DFRP), at IGCAR, Kalpakkam, was dedicated to the nation in January 2024 and subsequently it was hot commissioned in April 2024. The main objective of DFRP is to reprocess the spent fuel discharged from Fast Breeder Test Reactor and to demonstrate the reprocessing of spent fuel from PFBR. Towards meeting this objective, a number of advanced equipment have been designed, validated and installed at DFRP based on the wealth of operating experience gained from CORAL (COmpact Reprocessing of Advanced fuels in Lead cells) facility. The commissioning of this facility was carried out in stages as per regulatory requirements such as pre-commissioning checks and tests, water-acid run, acid-TBP run, uranium run and hot run. In this talk, it is proposed to discuss the challenges in fast reactor fuel reprocessing, strategies followed during various stages of commissioning, the corresponding regulatory aspects for obtaining the clearances and the experience gained during hot commissioning of DFRP.



Dr. K. Rajan, currently, mentoring the Reprocessing Group, IGCAR, Kalpakkam as Director of the group in the field of “Fast Reactor Fuel Reprocessing”. His major achievements are: Commissioning and operation of facility for the recovery of U^{233} ; design and development of remote sampling system for High Pu bearing solution; design, commissioning and operation of CORAL pilot facility; design, construction and hot Commissioning of DFRP for reprocessing of FBTR fuel.

Direct Solid Sampling of Nuclear Materials for Chemical Quality Assurance – An Advanced ETV-ICP-OES Application

S. B. Deb[§] and Abhijit Saha

Radioanalytical Chemistry Division, Bhabha Atomic Research Centre, Mumbai 400085

[§]Email: sbdeb@barc.gov.in (S.B. Deb)

The chemical quality assurance (CQA) of nuclear materials with respect to trace impurities involves various analytical techniques. However, most of the analytical methods require digestion of the material and separation of the matrix element(s) for precise and accurate results. Due to the diverse types of nuclear materials, cumbersome digestion procedures need to be developed specially for the refractory ones. At the same time the matrix separation makes the process tedious and in most of the cases generates significant liquid organic waste. In order to overcome these shortcomings, we had started working on a direct solid sampling method employing electrothermal vapourization coupled inductively coupled plasma optical emission spectroscopy (ETV-ICP-OES) for the CQA of nuclear materials with respect to trace impurities. The application is highlighted below by taking the example of two different nuclear materials:

Gadolinium zirconate ($Gd_2Zr_2O_7$) is a burnable absorber (BA) material that has been proposed as the BA rod in Indian compact high-temperature reactors (CHTR) [1]. In this refractory material, characterization of inseparable trace impurities like Sm, Eu, Tb, Dy, Hf and Y with high neutron absorption cross sections (σ_a) is indispensable. The heating profile in the ETV was optimized to get maximum sensitivity of the analytes. Various combinations like heating at 2500°C in a flow of Ar + CF₄, in-situ fusion with NH₄HF₂ at 230°C followed by heating at 2500°C in a flow of only Ar or Ar + CF₄ were performed. It was found that the in-situ fusion mechanism followed by heating at 2500°C in a flow of Ar + CF₄ easily evaporates maximum amount of analytes as their fluorides. Using this vapourization step the results obtained were validated by a reported ICP-OES procedure and the values are found to be the same at 95% confidence interval [1].

Uranium compounds are the most commonly used fuel materials in various types of nuclear reactors. Although the UO₂ fuel in PHWRs has no specification limit for thorium but the fast reactor fuels have stringent specification [2]. The ETV parameters like gradient heating, flow of the auxiliary gas (argon), mixed flow of the carrier and reactive gas (CF₄), etc. were optimized to get an online separation of the uranium matrix and thorium trace impurity. The noticeable difference between the boiling points of UF₄ (~1417°C) and ThF₄ (~1680°C) leads to their online separation. The gas flows were optimized to get maximum sensitivity for Th without any interference from U emission lines. A 0.4 L min⁻¹ flow of auxiliary Ar gas and a mixed flow of 0.13 L min⁻¹ Ar + 2.5 mL min⁻¹ CF₄ was found to provide the maximum sensitivity for Th. The values determined by the proposed ETV-ICP-OES procedure were validated using a reported procedure and they are found to be the same in 95% confidence interval [2].

References:

- [1] A. Saha et.al., RSC Adv, **14** (2024) 31422.
- [2] S.B. Deb et.al., *At. Spectrosc.*, **29** (2008) 39.



Dr. Sadhan Deb has over 25 years of experience in the field of analytical chemistry, with a particular focus on the development and optimization of techniques for the characterization of nuclear materials. Throughout his career, he has contributed significantly to the advancement of robust analytical methodologies, several of which are now routinely employed in chemical quality assurance of nuclear components. He has extensively worked on optimizing microwave-assisted digestion protocols to ensure the complete dissolution of a wide range of ceramic and alloy materials. This has paved the way for more accurate and efficient analysis of complex matrices. His primary area of specialization lies in the quantification of trace metallic elements using spectrometric techniques, including inductively coupled plasma mass spectrometry (ICP-MS) and inductively coupled plasma optical emission spectrometry (ICP-OES). His research has addressed challenges in sensitivity, matrix effects, and method validation, contributing to enhanced accuracy in trace element determination. Currently, Dr. Sadhan Deb is engaged in the development and application of direct solid sampling methods using Electrothermal Vaporisation Inductively Coupled Plasma Optical Emission Spectroscopy (ETV-ICP-OES), aiming to further streamline and improve the analysis of solid materials without the need for extensive sample preparation. He has more than 30 publications in peer reviewed international journals.

Development of Ion Chromatography as an Analytical Tool in the Nuclear Material Fabrication process at Nuclear Fuel Complex

Shehanaz Bano^{1, §}, A.K. Nayak¹ and Y. Balaji Rao¹

¹Nuclear Fuel Complex, ECIL (PO), Hyderabad, India

[§]Email: shehanaz@nfc.gov.in

Nuclear Fuel Complex (NFC) is a pioneer in fabricating nuclear fuel assemblies and reactor components, where ensuring material purity and process efficiency is paramount. To address the stringent quality requirements, a suite of advanced applications based on ion chromatography (IC) has been developed and integrated into the NFC analytical workflow, providing robust, sensitive, and rapid detection of trace impurities across various process streams.

A novel pyrohydrolysis–ion chromatographic method with conductivity detection has been developed for the quantification of trace chlorine in coolant tubes. This technique enables the precise monitoring of chlorine levels, which is critical for maintaining the mechanical integrity of structural components. The approach was further refined with spectrophotometric detection instead of conductivity detection for enhanced specificity and reduced time of analysis. Complementing this, reversed-phase liquid chromatography (RPLC) has been developed for the measurement of uranium in process stream solutions and liquid waste, thereby ensuring process control. Ion-interaction chromatography (IIC) has been extended to determine trace rare earth elements (REEs) in uranium process streams. By utilizing a C18 column combined with a pre-concentration column, this method selectively quantifies REEs at trace level, providing essential data for maintaining neutron economy in nuclear fuels. Additionally, IC has been tailored for the determination of carbon in zirconium alloys. Pyrolysis enhanced with accelerator ensures complete oxidation of carbon, yielding results that correlate with conventional carbon analyzers. This method is useful in the analysis of scrap material associated with high volatiles, where the conventional carbon analyzer could not meet the requirement. Furthermore, the development of an IC method for boron determination in process water addresses the critical need to maintain trace-level boron concentrations in nuclear materials. The versatility of IC is further underscored by its application in determining Gd₂O₃ content in uranium–gadolinia mixed oxide pellets, a key parameter in controlling burnable poison levels in nuclear fuel, and by its use in evaluating the efficiency of ammonia cracker units. Collectively, these advancements in ion chromatographic methods not only streamline the NFC's quality assurance protocols, but also provide a comprehensive analytical platform that supports the safe, efficient, and economically viable production of nuclear materials.



Smt. Shehanaz Bano holds M.Sc. in Chemistry from the National Institute of Technology (NIT), Warangal, where she was awarded the Gold Medal. She began her career in the R&D department of Dr. Reddy's Laboratories, Hyderabad. In 2011, she joined IGCAR after completing training as part of the 54th batch of the BARC Training School at the IGCAR campus, where she received the Homi Jehangir Bhabha Gold Medal for securing the highest rank in the Chemistry discipline. At IGCAR, she worked in the Radiochemistry Laboratory (RCL), focusing on the synthesis of europium hexaboride and nanocrystalline yttria. In 2012, she was transferred to the Nuclear Fuel Complex (NFC), Hyderabad, where she has specialized in the chemical characterization of nuclear materials

Invited Short Presentation

using ion chromatography. She played a key role in the establishment of the Control Laboratory at NFC-Kota and is currently serving as Additional Manager, overseeing the Instrumental Analysis Group of the Control Laboratory at NFC. Her research contributions include three international publications and twelve conference papers in the fields of analytical chemistry and nuclear material characterization.

Radiation Detection using Scintillators for Multiple Applications

Liviu Matei[§] and Arnold Burger

MSAG, Fisk University, Nashville, TN, USA

[§]Email: lmatei@fisk.edu

The increase in research on semiconductor detectors and scintillators has led to significant progress in performance and a greater choice of the radiation detection devices for many applications. Semiconductor detectors are used in many applications. Significant advances in photo-detector development have led to increase in use of scintillators for certain applications with great success.

While gamma ray sensor instrumentation is quite mature, developments in other fields have rendered parts of the technology used for biological applications obsolete. The technology gap is the largest for scintillators, which fill a vital niche for biological applications that require compact, low-power and low-cost sensors operated at ambient temperature. In our interdisciplinary project, the team focuses on the demonstration and optimization of sensors that display superior energy resolution, spatial resolution, compactness, low-power consumption, better signal-to-noise ratio, and smart, lower-cost operation. The project provides numerous applications for studying fundamental biological processes and provides an exciting platform for training of undergraduate, graduate, and postdoctoral researchers pursuing careers in applied physics and engineering.

Our work focuses on various applications of scintillator radiation detectors coupled SiPM photo detectors. This approach of packaging the scintillator and the photo detector together improve conversion of radiation energy into an electrical signal for further processing.

We developed a prototype of a handheld device with multiple applications. It can be used for measurements of bone mineral density (DEXA), high density material identification, spectroscopy acquisition for cancer diagnostic, and biogenic condition identification. The proto type also offers improved directionality of the probe, by including a 2x2 array of scintillators coupled with a 2x2 array of SiPM. An expansion of the array's size may offer the possibility of imaging for most of the mentioned applications.

Preliminary results show an improved performance for Bone mineral density (BMD) measurements using DEXA approach. The calibration of BMD measurements demonstrates an improved accuracy of BMD determination compared to commercially available systems.



Dr. Liviu Matei holds a Ph.D. in Electrical Engineering from the Technical University of Iasi, Romania, where he also pursued his undergraduate and master's studies. He is currently a Postdoctoral Research Fellow at Fisk University, Nashville, Tennessee (since 2009), and serves as a Professor of Physics at Welch College, Gallatin, Tennessee (since 2018). His research expertise spans the development and characterization of scintillators, neutron detection materials, and radiation detectors. Dr. Matei has authored numerous peer-reviewed publications in high-impact journals, contributing significantly to advancements in nuclear instrumentation and materials science. His work has garnered 977 citations with an h-index of 12.

Calibration free Laser ablation Molecular Isotopic Spectrometry –A New Outlook to the Isotopic Composition Determination of Boron

Arnab Sarkar^{1,2,§}, Anandhu Mohan² and Anannya Banerjee¹

¹Fuel Chemistry Division, Bhabha Atomic Research Centre, Mumbai, India

²Homi Bhabha National Institute, Anushaktinagar, Mumbai, India

§ Email: arnab@barc.gov.in, asarkar@ymail.com

Laser-Induced Plasma (LIP) techniques are powerful analytical tools known for their speed, reliability, and cost efficiency. A widely used LIP-based technique, Laser-Induced Breakdown Spectroscopy (LIBS), primarily analyzes atomic and ionic species. However, LIBS struggles to detect small spectral shifts, especially isotopic emissions. Nearly three decades ago, Hornkohl et al. identified transient molecular emissions in LIP, exhibiting unique spectral patterns with pronounced isotopic shifts. Initially overlooked as background noise, these emissions depend on plasma temperature, laser energy, and surrounding atmosphere. Studies later confirmed that triatomic molecules like BO_2 form in LIP, showing more intense and complex signatures than diatomic molecules.

Two decades later, Russo et al. introduced Laser Ablated Molecular Isotopic Spectrometry (LAMIS), leveraging molecular emissions for isotopic analysis. LAMIS has since been used for elements like boron, carbon, oxygen, strontium, and cerium. Chemometric integration further improved isotopic abundance determination. However, a key challenge is the limited availability of enriched isotopic reference materials. To overcome this, a calibration-free approach was developed, maximizing molecular emission signatures.

A custom algorithm, MAHADEV, was designed for calibration-free LAMIS in boron isotopic analysis. Using anharmonic oscillator and non-rigid rotor models, it generated molecular emission signatures for comparison with experimental spectra. The simulated spectra closely matched experimental data, achieving accuracy below 3% across various samples.

To improve precision, a noise model—Additive White Gaussian Noise (AWGN)—was incorporated, refining accuracy to below 1%. The CF-LAMIS technique eliminates the need for standard reference materials, enhancing efficiency. Addressing spectral interferences and the formation of molecular species can further advance this method. A deeper understanding of molecular emission dynamics underscores the significance of these techniques in analytical and physical chemistry.

References:

- [1] A. Sarkar, X. Mao, R.E. Russo, Spectrochim. Acta B: Atom Spectro 92 (2014) 42-50
- [2] A. Mohan, A. Banerjee, A. Sarkar, J. Anal. At. Spectro 38(8) (2023) 1579-1591.

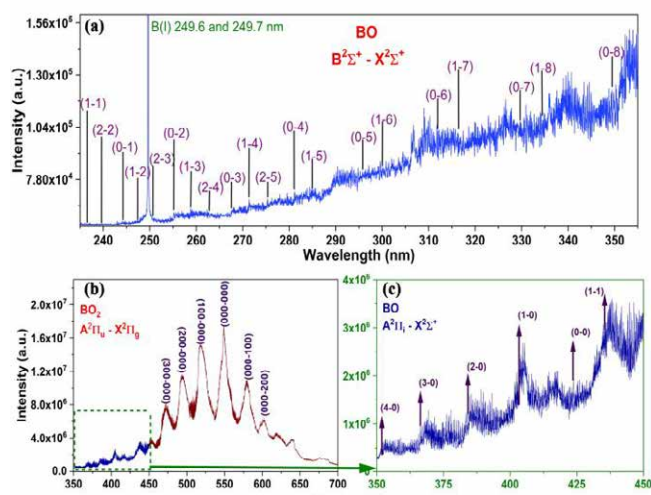


Fig. 1: Recorded Molecular emissions of (a) $\text{BO}:\text{B-X}$, (b) $\text{BO}_2 \text{ A-X}$ and (c) $\text{BO}:\text{A-X}$ transitions



Dr. Arnab Sarkar is a distinguished scientist specializing in laser spectroscopy, chemometrics, and radiation measurements. He earned his M.Sc. in Chemistry from North Bengal University in 2003 and completed his Ph.D. from the Homi Bhabha National Institute (HBNI), Mumbai, in 2011, focusing on laser-induced breakdown spectroscopic studies for material characterization. Dr. Sarkar joined the Bhabha Atomic Research Centre (BARC) in 2005 and later pursued postdoctoral research as an IUSSTF scholar at Lawrence Berkeley National Laboratory (LBNL), USA, during 2012–2013. His research expertise extends to plasma diagnostics, gamma spectroscopy, and chemometric applications in nuclear science and plasma spectroscopy. He has authored over 50 peer-reviewed journal papers, 75 conference reports, and numerous technical reports. His contributions have been recognized with prestigious awards, including the Prof. H. J. Arnikar Best Thesis Award (2012) and the DAE-ESET Group Achievement Award (2010). Beyond research, Dr. Sarkar has held key administrative roles such as Head of Section and Project Coordinator. He has also contributed to academia through his role at HBNI, mentoring students and supervising doctoral research. He actively collaborates with leading organizations and is a member of ISMAS, IANCAS, and ILA.

Dynamics of Neck-rupture in Nuclear Fission using Particle Emission as a Probe

Y. K. Gupta

Nuclear Physics Division, Bhabha Atomic Research Centre, Mumbai, India

Email: ykgupta@barc.gov.in

Despite intense research efforts since the discovery of nuclear fission, the last stage of the process, i.e., the neck-rupture is not clearly understood yet. This stage holds the key to a fundamental property of finite nuclear matter: nuclear viscosity. Several important questions regarding nuclear viscosity are still un-answered. Particle emission during the fission process offers a promising probe to gain insights into the neck rupture. In a recent study conducted as part of an ongoing fission dynamics programme at the BARC-TIFR Pelletron facility, novel observations have been made that shed light on this elusive phenomenon. The talk will begin with a brief overview of the topic, followed by a discussion of these recent experimental results and the future outlook of the research.



Dr. Y.K. Gupta joined the Nuclear Physics Division after graduating from the BARC Training School in 2004. He acquired his PhD degree in 2013 from the Homi Bhabha National Institute, Mumbai. Dr. Gupta spent two years as a postdoctoral fellow at the University of Notre Dame, USA, during 2014–2016. He has been awarded the Ashwini Kumar Rath Memorial Award of the IPA in 2014, and was conferred with the Scientific & Technical Excellence Award in 2020. His interests lie in low-energy nuclear physics and nuclear instrumentation.

Nuclear Instrumentation and Application of AI

P.P. Shete

Computer Division, Bhabha Atomic Research Centre, Mumbai, India

Email: ppshte@barc.gov.in

Machine learning (ML) is a branch of artificial intelligence (AI) that enables systems to learn from data and improve performance without explicit programming. ML techniques are broadly classified into supervised, unsupervised, semi-supervised, self-supervised, and reinforcement learning. Supervised learning uses labeled data, where each input is paired with a known output, allowing the model to learn relationships and patterns. It is widely used for classification and regression tasks. Unsupervised learning identifies patterns and structures in unlabeled data, making it useful for tasks like feature engineering, clustering, and anomaly detection. In nuclear instrumentation, unsupervised learning is effective for anomaly detection by identifying data points that deviate from normal patterns without requiring labeled data. Reinforcement learning trains an agent to make decisions by interacting with its environment and receiving feedback through rewards or penalties. It is well suited for optimizing control systems, robotics, and adaptive decision-making tasks. Semi-supervised learning combines a small amount of labeled data with a large amount of unlabeled data to improve the model performance, bridging the gap between supervised and unsupervised learning. In self-supervised learning, the model generates its own labels from input data, enabling it to learn meaningful patterns without relying on manually labeled datasets. This approach is key in training Large Language Models (LLM), where the model learns to predict missing or next words in text, helping it to understand language structure and syntax. Predictive maintenance uses ML techniques such as regression, classification, and anomaly detection to analyze sensor data, predict equipment failures, and enable timely maintenance to reduce downtime. In nuclear instrumentation, ML enhances safety and reliability by enabling early detection of potential issues in complex nuclear systems.



Mr. Pritam Prakash Shete holds a B.E. in Computer Science from Mumbai University and joined the BARC through 48th OCES batch, where he received the prestigious Homi Bhabha Award for securing the top rank in Computer Science. He has over two decades of experience in the Computer Graphics & Visualization with contributions spanning computer vision, computer graphics, deep learning, and generative AI. He received the Group Achievement Award (2007) for the successful installation of a 51-megapixel 6x6 data wall system, and the Young Applied Scientist/Technologist Award (2014) for his work on stereoscopic visualization systems used in autonomous telerobotics and neurosurgical applications at AIIMS, New Delhi. His notable AI-driven innovations include Anuvaadak – an in-house machine translation system; Talaash – an image search and retrieval system using visual and natural language queries; Sahaayak – a Q&A system tailored for the BARC dataset; and Pehchaan – a large-scale, edge-deployed face recognition system. He is currently working on Sanjeevani, an AI-assisted virtual screening pipeline for novel drug discovery. Mr. Shete has authored over 20 papers in IEEE international conferences and journals, and has received best paper awards for his contributions to data-centric AI and vision-language models. He also secured first place internationally for image captioning with state-of-the-art performance on the FACAD dataset.

Molten Salt-based Electrochemical De-oxidation of Uranium and Thorium Oxides

R. Kumaresan^{1,2,§}

¹*Metal Fuel and Pyroprocessing Division, Materials & Metal Fuel Cycle Group, Indira Gandhi Centre for Atomic Research, Kalpakkam, India*

²*Homi Bhabha National Institute, Kalpakkam, India*

[§]Email: rkum@igcar.gov.in, rkum79@gmail.com

Metals and alloys have played a prominent role in humankind since time immemorial. Most metals exist in the Earth's crust as oxides, and chemical metallurgy is needed to extract them from their oxide precursors. Electrometallurgy facilitated the production of many metals that were difficult to produce by the conventional chemical reduction methods due to the high stability of the metal compounds. Reactive metals like sodium, potassium, lithium, magnesium and calcium have been produced by electrolysis of their fused chlorides. In this context, molten salt electrolysis has evolved as an efficient and economical method for producing metals from highly stable metal compounds.

Electrochemical de-oxidation of solid metal oxides to metals in a high-temperature molten salt medium by electrons and by in-situ generated electro-positive metals like lithium and calcium (an electro-metallothermic reduction process) has been a recent development in electrometallurgy for the production of metals and alloys. These processes utilize chloride-based melts as the electrolyte because of their high solubility for oxide ions. High-density carbon (graphite) or platinum can be used as the anode materials in these processes. The process involves direct electrochemical reduction of metal oxides by either electrons or reductant metals like lithium or calcium. The liberated oxide ion transfers through the melt and reacts with Pt or graphite anodes, producing oxygen or a mixture of CO and CO₂ gases.

The presentation will cover our research on the electro-deoxidation of solid UO₂ (electro-lithotomic process), and ThO₂ (electro-calciothermic process) in LiCl and CaCl₂ melts at 650°C and 900°C, respectively. In this context, a new facility with a 2 kg/batch capacity has been commissioned for direct electrochemical de-oxidation of UO₂. Recently, two batches (500 g/batch) of UO₂ pellets were converted into U metal in this facility with a conversion efficiency of >98%. In addition, the presentation discusses the feasibility of preparing uranium and thorium-based alloys from constituent metal oxides.



Dr. R. Kumaresan earned his master's degree from Madurai Kamaraj University in 2002 and later obtained a Ph.D. in separation science from the University of Madras. In 2009, he joined IGCAR and currently heads the Pyrochemical Processing Studies Section. His research focuses on the direct electrochemical reduction of metal oxides and the pyrochemical reprocessing of spent metallic fuels. His primary areas of interest include molten salt electrochemistry, electrometallurgy, solvent extraction, and ion exchange. He has authored approximately 50 papers in peer-reviewed journals and contributed to around 50 national and international conference proceedings. In recognition of his work, he received the DAE Group Achievement Award in 2011. Dr. Kumaresan is a life member of the Indian Association of Nuclear Chemists and Allied Scientists (IANCAS) and the Society for the Advancement of Chemical Sciences and Education (SACSE). He also plays an active role in organizing radiochemistry workshops in schools and colleges.

Fissile Zone Identification System (FIZIDS)

K. Sundararajan

ACSD, MC&MFCG, IGCAR, Kalpakkam, India

Email: sundar@igcar.gov.in

The Prototype Fast Breeder Reactor (PFBR) uses mixed uranium-plutonium oxide fuel containing 20.7% PuO₂ in the inner core (Core-1) and 27.7% PuO₂ in the outer core (Core-2) to ensure uniform radial flux profile across the core. Fissile Zone Identification System (FIZIDS) using LaBr₃(Ce) detector, which detects the 414 keV peak of ²³⁹Pu in FSAs was proposed in BHAVINI to differentiate the Core-1 and Core-2 FSAs. The experiments using LaBr₃(Ce) detector in FIZIDS concluded that identification of FSAs was not feasible due to the inadequate detector energy resolution and higher ²⁴¹Am activities. Therefore, Cadmium-Zinc-Telluride (CZT), a room-temperature semiconductor detector with better energy resolution was used in FIZIDS to differentiate Core-1 and Core-2 FSAs. The design of the Pb shielding was accordingly modified to accommodate the CZT detector and experiments were carried out with Core-1 and Core-2 FSAs, successfully identifying them without any uncertainty.

Initially, the entire exercise using CZT detector was carried out in manual mode for both fuel calibration and identification. Several features in the old FIZIDS MCA software needed modifications like (1) Auto-saving of files during calibration and recalling them at any time during or after completion of calibration, (2) Calibration with multiple subassemblies in any orientation, (3) Access to fuel subassembly database, and (4) Recalling the incomplete calibration files during abrupt closure of software due to power interruption or accidental closure. Even the detector used for testing was old and lacked back-up in case of its failure. Hence, three new CZT detectors with internal preamplifier were procured for the application of FIZIDS in PFBR.

The FIZIDS software was modified accordingly by Electronics Division, BARC and tested in the laboratory with the new CZT detectors. One CZT detector and modified FIZIDS software were installed in the FIZIDS set-up and tested with standard gamma sources. Both the detector and the modified MCA software functioned satisfactorily. A calibration was obtained to get the limits of Core-1 and Core-2 FSAs with the new CZT detector installed in FIZIDS. The Core-1 and Core-2 subassemblies were identified using this calibration.

This talk will highlight the need for identifying the Core-1 and Core-2 FSAs, the detector assembly configuration, choice of detectors, drawbacks of the LaBr₃(Ce) over CZT detector, the modifications made on the FIZIDS software and the identification of fuel subassemblies, Control rod and Driver subassemblies.



Dr. K. Sundararajan obtained his B.Sc. in Chemistry from Madras University, followed by M.Sc. in Physical Chemistry from Pune University. He subsequently joined the 34th batch of the BARC Training School. He earned his Ph.D. in Chemistry from Madras University in 2003 and later undertook a postdoctoral fellowship at National Chiao Tung University, Taiwan. His areas of specialization include low-temperature matrix isolation infrared spectroscopy, fluorescence spectroscopy, computational chemistry, and radioanalytical chemistry. Dr. Sundararajan has authored over 100 publications in international journals and has guided four doctoral students under the Homi Bhabha National Institute (HBNI). He currently serves as the Head of the Analytical and Spectroscopy Division, MC&MFCG, BARC.

Development of Potentiometric Sensors for Lanthanides and Actinides

Bholanath Mahanty

Radiochemistry Division, Bhabha Atomic Research Centre, Mumbai, India

Email: bmahanty@barc.gov.in

Accurate determination of lanthanides and actinide ions is required at different stages of nuclear fuel cycle (NFC). Therefore, it is important to develop a simple, fast and low-cost analytical method that will have desired precision and accuracy. Although, potentiometric sensors for lanthanide and actinide present several challenges like poor Nernstian sensitivity, low selectivity, and hydrolysis at higher pH, still they have not lost their importance due to their simplicity, speed, and cost-effectiveness [1]. We have developed several potentiometric sensors for trivalent lanthanide ions, such as Eu^{3+} , Gd^{3+} as well as tetravalent ions, Th^{4+} using different diglycolamide (DGA) or tripodal amides as ionophores, polyvinyl chloride (PVC) as the polymer and 2-nitrophenyl octyl ether as the plasticizer. All the components of the membranes, such as polymer, plasticizer, ionic additive and the ionophore together were dissolved in tetrahydrofuran (THF) and casted on one side of a small diameter hollow glass tube. The membranes were characterized using different techniques, such as thermogravimetric (TG), atomic force microscopy (AFM), Fourier transform infrared (FTIR) spectroscopy, photoluminescence (PL) spectroscopy, and small angle x ray scattering (SAXS). The membrane sensors demonstrated good sensitivity toward the analyte ions, offering a wide linear dynamic range and low detection limits. They also exhibited a fast response time and stability of over more than two months. The effect of different monovalent, divalent, trivalent and tetravalent interfering metal ions on the potentiometric response was also tested in the presence of analyte ions. Finally, the membrane sensors were employed for direct potentiometric determination of analyte ions in various samples.

References:

[1] B. Mahanty et al., *J. Electroanal. Chem.*, **808** (2018) 340.



Dr. Bholanath Mahanty graduated from the BARC Training School in 2005 and is currently working in the Radiochemistry Division, BARC, Mumbai. He completed his PhD from the Homi Bhabha National Institute (HBNI) in 2018. His areas of research include potentiometric sensor development for lanthanides and actinides, solvent extraction and liquid membrane studies of actinides and lanthanides, and the synthesis of composite polyoxometalates (POMs) for actinide extraction and sensor development. He is a recognized

PhD guide at the Homi Bhabha National Institute (HBNI) (capitalization corrected). He is the recipient of the Prof. H.J. Arnika Best PhD Thesis Award from IANCAS (2018). He has authored more than 50 publications in peer-reviewed international journals.

Recent Advances in Industrial Applications of Radiotracers for Process Optimization in Glass Production and Waste Water Treatment

Jayashree Biswal^{1,2}

¹Isotope and Radiation Application Division, BARC, Mumbai, India

²Homi Bhabha National Institute, Mumbai, India

Email: jbiswal@barc.gov.in

Industrial plants are used for continuous, large-scale manufacturing of various chemical and pharmaceutical products, catalysts, and food products. It is imperative to understand the material flow profile and evaluate the design of the plants in order to achieve the desired product quality, save energy, and ensure efficient plant operation. On the other hand, wastewater treatment plants are essential for removing contaminants from wastewater, making it safe for discharge back into the environment or for reuse in irrigation, cooling water, and other applications. Radiotracer technique is a unique tool used to obtain hydrodynamic information about industrial and water treatment plants that cannot be acquired by any other means. Two recently conducted large-scale radiotracer applications are discussed in this talk.

First application is study of wastewater hydrodynamics in a constructed wetland using radiotracer technique. Engineered subsurface constructed wetlands (CWs) have been proven to be reliable, cost-effective and long-term solutions for wastewater treatment. The optimal design and efficient operation of the CWs depends on their hydraulic efficacy. Residence time distribution (RTD) measurement is an experimental tool to measure the hydraulic efficacy of CWs in terms of wastewater hydrodynamic parameters. Radiotracer investigation was conducted in a constructed wet land using ^{99m}Tc radiotracer to evaluate the design of the CW. From the measured experimental curves different parameters, such as flow distribution, mean residence time, and effective volume fraction of the wastewater in CW were estimated. Based on the results, it was concluded that no flow abnormalities were present in the system, and the flow behaviour was close to the plug flow.

The second application is radiotracer investigation in solar glass production units. Radiotracer investigations were conducted in two different solar glass production units (SG1, SG2) at Bharuch, Gujarat, to characterize the molten glass flow in the units and identify the cause of inhomogeneity in the product glass sheets. ¹⁴⁰La was used as radiotracer in these studies. The first phase of the study suggested presence of flow abnormalities in SG1 and based on the results the SG1 was modified. The second phase of studies were conducted in modified SG1 and a newly installed SG2. Each glass production unit consists of furnace, forehearth, annealing, cooling and cutting sections. The processing capacity of furnaces of SG1 and SG2 units were 432 and 520 tonnes, respectively. The injected radiotracer was measured at 20 different locations in the units. Based on the analysis, mean residence time (MRT), dead volume, and homogenization time in SG1 unit were found to be 42.5 hr, 34%, and 18.5 h, respectively. In addition to this, recirculation of molten glass was observed in furnace section of SG1. The MRT, dead volume, and homogenization time in SG2 unit were found to be 47.5 hr, 15%, and 22 h, respectively. No major flow abnormality was observed in SG2 unit. Suitable flow models were proposed to describe the flow dynamics of molten glass in each section of the units. The radiotracer investigation helped the glass industry to evaluate the design of the glass production units, optimize the operation of the plant, and improve the quality of the glass sheets produced.

Acknowledgements: The author acknowledges the contributions of Dr. Sunil Goswami, Mr. V. K. Sharma and Dr. R. Acharya for conducting the experiments, data analysis and interpretation of the results of the studies presented in the talk. The author would also like to thank Mr. J. S. Samantray and Mr. S.A. Patil for providing necessary help for conducting the experiments.



Dr. Jayashree Biswal is Scientific Officer at Bhabha Atomic Research Centre and Associate Professor at Homi Bhabha National Institute (HBNI), Mumbai. She received her Ph.D. in Chemistry from HBNI in 2013. Her research interests includes process optimization and evaluation of design of industrial chemical reactors by employing radioisotope techniques, development and application of various radiotracer techniques for flow measurement and troubleshooting in industrial systems; and wear and corrosion rate measurements of industrial components by ion beam technique. She has published about 38 papers in international journals.

Medical Cyclotrons: An Essential Need for Cancer Management

M.R.A. Pillai

Molecular Group, Puthuvype, Ernakulam, India

Email: pillai.m.r.a@gmail.com

PET-CT imaging plays a crucial role in the diagnosis, staging as well evaluation of therapy response and regression of cancer. Radiopharmaceuticals based on fluorine-18 and gallium-68, both produced in cyclotron, are used for PET-CT imaging. Though, there are 28 medical cyclotrons in India, only eleven states out of the 35 states and union territories have medical cyclotron. The patients from majority of the states need to travel long distances to get PET-CT imaging, making it a painful and costly affair. As per IAEA, at least one PET-CT machine per million population is needed, while the availability of PET-CT machines in developed nations far exceeds this figure. In India, there are less than 500 PET-CT machines and majority of them are sourcing radiopharmaceuticals from privately operated cyclotrons.

A medical cyclotron is a profitable business opportunity, however, it needs very high levels of technical expertise for setting up the facility as well as maintaining and operating it on daily basis. Radiation safety as stipulated by AERB guidelines is to be followed during operation of the facility. The lack of trained manpower for the operation and maintenance of the facility remains a major constraint in the expansion of this essential field. A new stand-alone medical cyclotron project costs Rs. 45-50 Crores, depending on the configuration of the cyclotron, hot cells, quality control, and radiation safety equipment selected. Major hospitals are willing to invest in PET-CT machines, provided there is an assured availability of radiopharmaceuticals. For example, within a radius of 15 km, Ernakulam city has seven hospitals offering PET-CT imaging, thanks to the presence of medical cyclotron. However, few business groups are currently willing to step forward to set up cyclotron projects. This needs to change in order to ensure evidence-based cancer treatment to cancer patients across the country.



Dr. M.R.A. Pillai, Ph.D., D.Sc., is currently serving as the Group Director of the Molecular Group in Cochin, Kerala. He retired in 2013 as the Head of the Radiopharmaceuticals Division at Bhabha Atomic Research Centre (BARC). Dr. Pillai worked as a Postdoctoral Research Associate at the University of Missouri-Columbia (1987–1989) and as a Visiting Professor there in 1992 and 1994. From 2003 to 2010, he served as a Technical Officer at the International Atomic Energy Agency (IAEA). He currently serves as the Associate Editor of Cancer Biotherapy and Radiopharmaceuticals. He is also on the editorial boards of four other international journals, including EJNMMI: Radiopharmacy and Chemistry.

Radiolabeled Somatostatin Analogs for Diagnosis and Therapy of Neuroendocrine Cancers: In house synthesis, quality control and preliminary clinical investigation

V. Kusum Vats^{1,2}

¹Radiopharmaceuticals Division, Bhabha Atomic Research Centre, Mumbai, India

²Homi Bhabha National Institute, Mumbai-400094, India

Email: vkusum@barc.gov.in

Peptides, in their radiolabeled form, hold significant promise for both diagnostic imaging and targeted radionuclide therapy due to their high affinity and specificity for receptors over-expressed on cancer cells. Among them, radiolabeled somatostatin analogs have emerged as the most successful peptide-based radiopharmaceuticals for the imaging and treatment of neuroendocrine cancers. ⁶⁸Ga-DOTA-TATE/TOC [DOTA coupled Tyr³-octreotate/Tyr³-octreotide, cyclic 8 amino acid containing peptides] and ^{99m}Tc-HYNIC-TATE/TOC [6-hydrazinonicotinic acid coupled Tyr³-octreotate/Tyr³-octreotide] enable precise tumor detection using PET/CT and SPECT/CT imaging, respectively, while ¹⁷⁷Lu-DOTA-TATE serves as a potent agent for peptide receptor radionuclide therapy (PRRT). However, the high cost and reliance on commercial suppliers limit the affordability and accessibility of these radiopharmaceuticals to a broader patient population. In-house synthesis of peptide ligands and the development of freeze-dried kits for radiopharmaceutical preparation offer a cost-effective and sustainable alternative. The talk will highlight the efforts undertaken at the Radiopharmaceuticals Division, BARC to synthesize peptide ligands (HYNIC-TATE/TOC, DOTA-TATE), develop freeze-dried kits for the convenient preparation of patient doses at nuclear medicine centers, and conduct limited clinical trials of these indigenously developed peptide radiopharmaceuticals in neuroendocrine cancer patients, in collaboration with leading nuclear medicine hospitals of our country. Comprehensive analysis demonstrated that radiopharmaceuticals prepared using in-house synthesized peptides are equivalent to commercial counterparts in terms of purity, stability, and efficacy. These findings highlight the potential of radiopharmaceuticals prepared using the in-house synthesized peptides for imaging and therapy of neuroendocrine cancers, offering a cost-effective and sustainable alternative to commercially available options.



Dr.(Smt.) V. Kusum Vats received her M.Sc. degree in Chemistry from Utkal University, Bhubaneswar. She joined BARC from 54th batch of Training School. She was awarded her PhD in 2018 from HBNI, Mumbai. Her research focuses on the synthesis and functionalization of tumor-targeting peptides. She has experience in radio-metal complexation of functionally modified ligands using various radionuclides with nuclear diagnostic and therapeutic significance, along with their evaluation in animal models. Dr. Vats has authored approximately 26 research articles in peer-reviewed international journals and has made significant contributions towards the development of diagnostic and therapeutic radiopharmaceuticals for the treatment of cancer patients (developed freeze-dried kits of HYNIC-TATE and DOTA-TATE for the formulation of ^{99m}Tc-HYNIC-TATE and ¹⁷⁷Lu-DOTA-TATE, respectively).

To Investigate the Fission Timescale of $^{206}\text{Rn}^*$ Utilizing Neutron Multiplicity as a Probe

Punit Dubey^{1,§}, Mahima Upadhyay¹, Mahesh Choudhary¹, Namrata Singh¹, Shweta Singh¹, Sriya Paul¹, Utkarsha Mishra¹, N. Saneesh², Mohit Kumar², Rishabh Prajapati², K. S. Golda², Akhil Jhingan², P. Sugathan², Jhilmam Sadhukhan³, Raghav Agarwal⁴, Kiran⁴, Ajay Kumar¹

¹ Department of Physics, Banaras Hindu University, Varanasi 221 005, India

² Inter University Accelerator Centre (IUAC), New Delhi 110 067, India

³ Variable Energy Cyclotron Centre (VECC), Kolkata 700 064, India

⁴ Department of Physics, Panjab University, Chandigarh 160 014, India

§ Email: punitdubey@bhu.ac.in

Recently, there has been a notable rise in the study of the effects of nuclear dissipation on heavy ion fusion-fission (HIFF) dynamics. The fission phenomena are more probable in the compound nucleus, impacted by various factors, including entrance channel mass asymmetry (α), $Z_p Z_t$, and excitation energy (E^*) [1]. In the current study, we have computed the neutron multiplicities of the compound nucleus (CN) of ^{206}Rn .

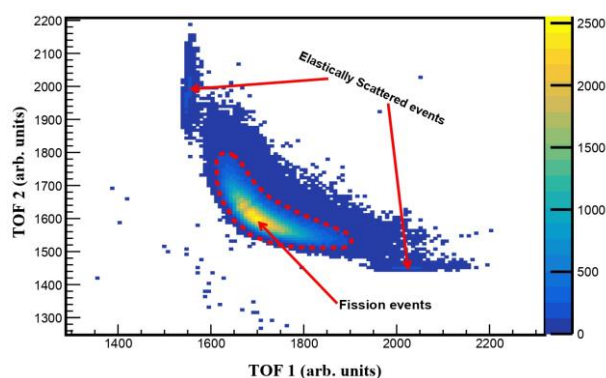


Fig. 1: Time correlation spectrum of complementary fission fragments detected in the two MWPCs.

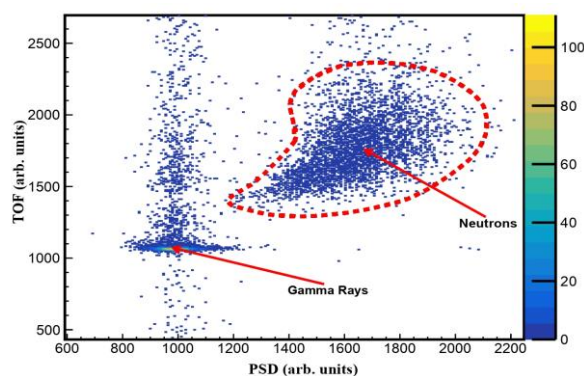


Fig. 2: 2-D plot of PSD vs TOF spectra of one of the neutron detectors. The dashed line clearly separates the neutrons from γ rays.

The experiment was carried out at the 15 UD Pelletron + LINAC accelerator facility of IUAC, New Delhi, where a pulsed beam of ^{28}Si with an energy range of 145-180 MeV was bombarded on ^{178}Hf targets, resulting in the production of the compound nucleus ^{206}Rn . This study investigates the impact of excitation energy on the fission timescale using the theoretical model code VECLAN, based on Langevin dynamics, alongside the analysed experimental data. From the present study, we have observed that with an increase in excitation energy fission timescale decreases. More details regarding the present work will be presented during the conference.

Acknowledgement: The author (Punit Dubey) would like to thank the Prime Minister's Research Fellowship (PMRF) for the financial support for this work.

References:

- [1] Punit Dubey et al., *J. Radioanal. Nucl. Chem.*, **333** (2024) 5363.
- [2] M.T. Senthil Kannan et al., *Phys. Rev. C*, **98** (R) (2018) 021601.

Positron Annihilation Lifetime Spectroscopic (PALS) Study on SBA-15 Nano-pores Under High CO₂ Gas Pressure in Presence of [BmIm][NTf₂] Ionic Liquid

Shapath Bhandari¹, Dhanadeep Dutta^{1,2,§}

¹ Radiochemistry Division, Bhabha Atomic Research Centre, Mumbai 400 085, India

² Homi Bhabha National Institute, Mumbai 400 094, India

§Email: deep@barc.gov.in

SBA-15 is a well-known crystalline meso-porous material having widespread applications in gas adsorption and storage. On the other hand, few ionic liquids (IL) such as 1-butyl-3-methylimidazolium bis(trifluoromethylsulfonyl)imide ([BmIm][NTf₂]) has high affinity towards CO₂ due to the Lewis acid-base interaction of the anion TFSI with CO₂ molecule [1]. In order to observe the change in nano-pore morphology of SBA-15 during CO₂ gas adsorption in presence of confined IL, *in situ* PALS measurements have been carried out in [BmIm][NTf₂] (IL) loaded SBA-15. The [BmIm][NTf₂] (IL) was incorporated in SBA-15 nano-pores using the incipient method for impregnation. The details of the CO₂ adsorption set up are described elsewhere [2]. In the pristine SBA-15, the two ortho-positronium (o-Ps) lifetime components (τ_3 and τ_4) correspond to o-Ps annihilation in micropores and mesopores, respectively. In the IL+SBA-15, the τ_4 component disappeared indicating complete filling of meso-pores with IL. Only the τ_3 component corresponding to o-Ps annihilation in the confined IL and empty micropores in IL+SBA-15 was present. Interestingly, an “expansion” of micropores size (increase in τ_3) both in pristine and IL+SBA-15 was observed up to the CO₂ pressure around 100 psi (Fig. 1), above which the τ_3 gradually decreased in pristine SBA-15 as CO₂ molecules fill up the pore volume, but in IL+SBA-15 at higher pressure, the τ_3 gets saturated at ~3-3.5 ns indicating the availability of space for more CO₂ adsorption in IL+SBA-15 even at high pressure.

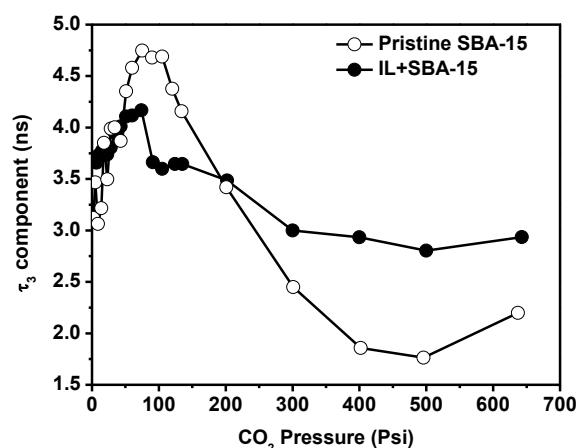


Fig. 1: o-Ps lifetime profile in micropore under CO₂ pressure

Acknowledgement: Authors thankfully acknowledge the contribution of Dr. Seraj Ansari, RCD, BARC in preparing the samples.

References:

- [1] M. Mohamedali et al., *Micropor. Mesopor Mat.*, **284** (2019), 98.
 [2] J. Mor et al., *J. Phys. Chem. C*, **127** (2023), 2160.

Compression Induced Crystalline to Porous Glass Transformation of Zeolitic Imidazolate Framework-62: A Positron Annihilation Spectroscopy Study

J. Mor^{1,2}, Renjith B. Nelliyl^{1,2}, S. K. Sharma^{1,2,§}

¹ Radiochemistry Division, Bhabha Atomic Research Centre, Mumbai, India

² Homi Bhabha National Institute, Mumbai, India

§ Email: skumars@barc.gov.in

Zeolitic Imidazolate Frameworks (ZIFs) are crystalline porous materials composed of divalent metal ions (Zn^{2+} , Co^{2+}) tetrahedrally bonded with imidazole-based linkers [1]. They exhibit high porosity, tunable pore architecture, and excellent thermal and chemical stability. Due to these properties, ZIFs are widely explored for applications in gas storage, separation, catalysis, sensing, and drug delivery [2]. Some ZIFs exhibit high glass-forming ability due to a higher ratio of glass transition temperature (T_g) to melting temperature (T_m), allowing them to melt before decomposition temperature (T_d). Quenching of their molten-state forms porous glasses, distinct from conventional non-porous glasses. Their inherent porosity makes them promising for applications in gas separation, optical materials, and electrolytes. Among ZIFs, ZIF-62 [$Zn(Im)_{2-x}(bIm)_x$; Im: imidazole and bIm: benzimidazole] is extensively studied for its glass-forming ability due to its wide T_m - T_d gap, enabling efficient melt-quenching [3]. Various alternative methods for amorphisation of ZIFs include heating, ball milling, pressurization, irradiation, and plasma discharge are being explored [4]. Among these, non-hydrostatic compression using a pelletizer is the most suitable due to its simplicity, scalability, and cost-effectiveness. Here, we report for the first time the compression-induced formation of a fully amorphous and glassy phase of ZIF-62 ($a_{gp}ZIF-62$), exhibiting a characteristic T_g and inherent porosity similar to melt-quenched glass ($a_gZIF-62$). The crystalline ZIF-62 was compressed in a pelletizer at various pressures from 0.17 to 0.57 GPa. At the highest pressure, $a_{gp}ZIF-62$ exhibits a broad hump in X-ray diffraction pattern showing its amorphous nature. Differential scanning calorimetry measurements show a characteristic T_g confirming the glassy nature of amorphous ZIF-62. Positron annihilation lifetime spectroscopy was used for porosity characterization of $a_gZIF-62$ and $a_{gp}ZIF-62$. $a_gZIF-62$ exhibits a larger average pore size (~ 6.73 Å) with a narrower pore size distribution (FWHM ~ 1.4 Å) compared to $a_{gp}ZIF-62$ (average pore size ~ 5.63 Å, FWHM ~ 2.6 Å) (see Fig.1). Additionally, the o -Ps intensity is lower for $a_gZIF-62$ ($\sim 17\%$) than for $a_{gp}ZIF-62$ ($\sim 23\%$). These observations suggest that $a_{gp}ZIF-62$ has a higher pore density, smaller pore sizes, and greater heterogeneity in pore distribution compared to $a_gZIF-62$.

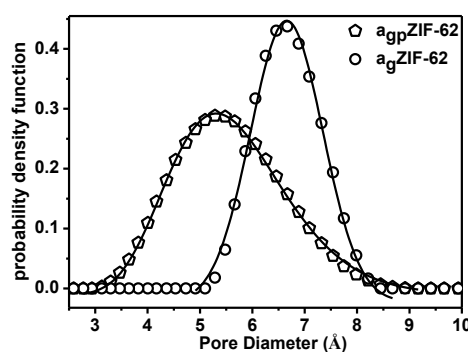


Fig. 1: Pore size distribution of $a_{gp}ZIF-62$ and $a_gZIF-62$ obtained using positron annihilation lifetime

References:

- [1] K.S. Park et al., *Proc. Nat. Acad. Sci., U.S.A.*, **103** (2006) 10186.
- [2] M.Rubio-Martinez et al., *Chem. Soc. Rev.*, **46** (2017) 3453.
- [3] A. Qiao et al., *Sci. Adv.*, **4** (2018) eaao6827.
- [4] T. D. Bennett et al., *Chem. Eur. J.*, **19** (2013) 7049.

CO₂ Pressure Induced Flexibility of Pure and Hybrid ZIF-7: An *in-situ* PALS Study

R. B. Nellyil^{1,2}, J. Mor^{1,2}, S. K. Sharma^{1,2, §}

¹ Radiochemistry Division, Bhabha Atomic Research Centre, Mumbai 400 085, India

² Homi Bhabha National Institute, Anushaktinagar, Mumbai 400 094, India

§Email: skumars@barc.gov.in

Zeolitic Imidazolate Frameworks (ZIFs) are a subclass of Metal Organic Frameworks (MOFs), consists of imidazole-based organic linkers tetrahedrally connected through metal nodes. ZIF-7, [Zn(bIm)₂], exhibits exceptional flexibility, where even complete desolvation can induce a porous to dense phase transition. This transition causes drastic reduction in porosity which results significant reduction in gas capture efficiency of the material. To improve the applicability of ZIF-7 in gas separation and storage, tuning of the flexibility and its pore architecture is required.

In the present study, we used mixed-linker approach for tuning the flexibility and pore architecture of ZIF-7. 4, 5-dichloroimidazole (dcIm) was used as the auxiliary linker. We have synthesized a series of mixed linker ZIF-7 with varying linker ratio along with pure ZIF-7. X-ray diffraction and ¹H NMR measurements confirm that up to 62% of dcIm can be incorporated into ZIF-7 without altering its topology or lattice structure. N₂ adsorption measurements show significant variations in the microporosity of ZIF-7 on linker mixing. PALS measurements confirmed that with incorporation of dcIm, the pore-architecture is altered due to crowding of the linkers within the pore network. Variations in vacant volume at pore sites with increasing CO₂ pressure determined using *in-situ* PALS were distinctly different for pure and hybrid ZIF-7. Fig. 1. shows the comparison of flexibility of ZIF-7 and 46% dcIm incorporated ZIF-7, where the flexibility parameter, f , is defined as the ratio of *ortho*-Positronium lifetime under CO₂ pressure and under vacuum. The f parameter clearly indicates a significant reduction in flexibility for dcIm-incorporated ZIF-7 compared to pristine ZIF-7. The study confirms that mixed-linker approach is an efficient strategy for tuning the pore architecture and flexibility of ZIF-7, which is required for higher separation selectivity of gas mixtures.

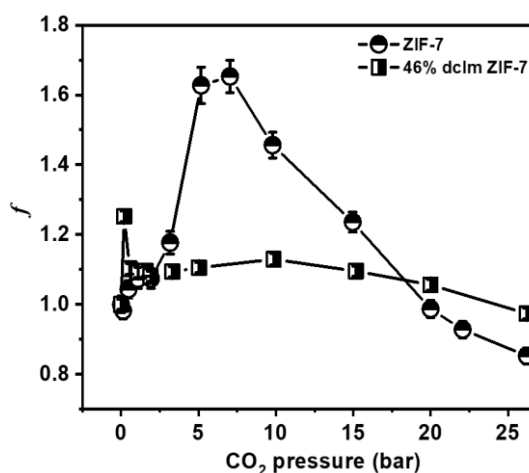


Fig. 1: Flexibility parameter (f) with increasing CO₂ pressure for pure and 0.46% dcIm(ZIF-7).

References:

- [1] K. S. Park et.al., *Proc. Natl. Acad. Sci. U. S. A.*, **103** (2006) 10186.
- [2] L. Xiang et.al., *Adv. Mater.*, **29** (2017) No. 1606999.
- [3] J. Mor et.al., *Micropor. Mesopor. Mater.* **348** (2023) 11238.

Role of Defects in Light Emission of $\text{Zn}_2\text{Ge}_{1-x}\text{Sn}_x\text{O}_4$: A Combined Positron Annihilation Lifetime and Photoluminescence Spectroscopic Study

Bhavana Bharti^{1,2}, Annu Balhara^{1,2}, Santosh K. Gupta^{1,2}, K. Sudarshan^{1,2,§}

¹ Radiochemistry Division, Bhabha Atomic Research Centre, Trombay, Mumbai-400085, India

² Homi Bhabha National Institute, Mumbai-400094

§ Email: kathis@barc.gov.in

Defect-induced light emission occurs when electrons and holes, generated by external excitation (such as ultraviolet or X-ray irradiation), recombine at defect sites in the material. The energy and wavelength of the emitted light are strongly dependent on the type, concentration, and distribution of defects present in the material. By controlling these defects, it is possible to manipulate the emission spectra, ranging from ultraviolet to visible to infrared regions, making these materials valuable for applications in lasers, light-emitting diodes (LEDs), phosphors, and display technologies. In the context of transition metal oxide semiconductors, such as $\text{Zn}_2\text{Ge}_{1-x}\text{Sn}_x\text{O}_4$, defects play a crucial role in determining their light emission characteristics. The incorporation of elements such as tin (Sn) in the zinc germanate matrix, for instance, can introduce a variety of defect sites that can shift the light emission from the visible to the near-infrared region. Understanding how defects contribute to these changes is key to advancing the design of next-generation optoelectronic materials [1, 2].

To explore the role of defects in the light emission process/photoluminescence (PL), positron annihilation lifetime spectroscopy (PALS) was employed to probe the defect structure. X-ray diffraction results confirm the formation of the spinel phase of Zn_2GeO_4 and Zn_2SnO_4 at the end compositions, with mixed-phase structures observed at intermediate compositions. Field Emission scanning electron microscopic (FESEM) images reveal the formation of microcrystals with sizes ranging from 2-3 microns. Raman spectroscopy further corroborates the structure of these compounds, confirming their crystalline phases. The typical PALS spectra are shown in Fig. 1. This figure illustrates the variation in defect concentration as Sn is incorporated in place of Ge. PL studies revealed that Zn_2GeO_4 exhibits strong green light emission. However, as the composition transitions to mixed phases and ultimately to Zn_2SnO_4 , a significant shift in the PL band was observed, moving from green to the red and near-infrared (NIR) regions. This shift is attributed to the variation in the defect density and the alteration of the local bonding environment as a function of composition, which directly impacts the material's light emission properties.

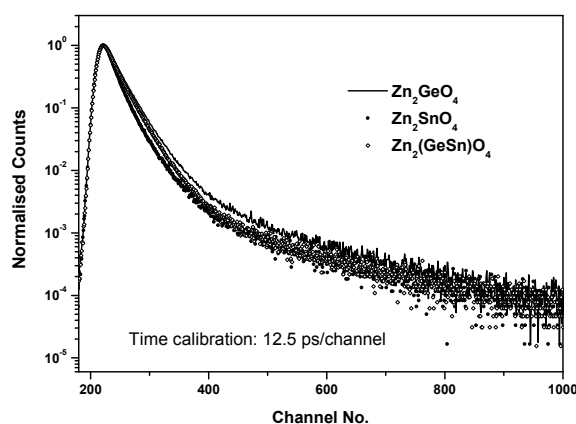


Fig. 1: Typical positron annihilation lifetime spectra from the samples.

References

- [1] S.K. Gupta et al., *J. Mater. Chem. C*, **4** (2016) 4988.
 [2] K. Sudarshan et al., *J. Luminescence*, **212** (2019) 293.

Study of Fission Product Mass Distribution in $^{11}\text{B}+^{237}\text{Np}$ Reaction to Investigate the Role of Shell Closure

S. Kumar^{1,§}, S. Patra¹, A. Mhatre, A. Kumar¹, K. Ramachandran², R. Tripathi^{1,3}

¹ Radiochemistry Division, Bhabha Atomic Research Centre, Mumbai – 400 085, India

² Nuclear Physics Division, Bhabha Atomic Research Centre, Mumbai – 400 085, India

³ Homi Bhabha National Institute, Mumbai – 400 094, India

§Email: ksatyam@barc.gov.in

In the low to medium energy fission of heavy nuclei, fission product (FP) mass distribution may exhibit distinct deviations from the Liquid drop model predictions. These deviations can be explained on the basis of contribution from the three independent fission modes proposed by Brosa et al. [1], symmetric (S); two asymmetric, S1 and S2; and Superasymmetric (S3) arising mainly due to different closed proton and neutron shells in the actinide region. Mass distribution observed in $^{16}\text{O}+^{232}\text{Th}\rightarrow^{248}\text{Cf}^*$ reaction by Goswami *et al.* at $E^* = 49.5$ MeV [2] and Gikal et al. at $E^* = 40-45$ MeV [3] showed a broad Gaussian mass distribution. However, the mass distribution of ^{248}Cf at $E^* = 45$ MeV calculated by Pasca *et al.* showed a double-humped mass distribution having peak to valley ratio of 0.9 [4]. The present article reports the FP mass distribution in $^{11}\text{B}+^{237}\text{Np}$ reaction at $E^* = 49.3$ MeV carried out at BARC-TIFR Pelletron-LINAC facility using recoil catcher technique followed by offline γ -ray spectrometry in order to investigate the role of specific neutron and proton shells and contribution from transfer induced fission. The ^{237}Np target (~ 0.25 mg/cm²) electrodeposited on the Al backing (~ 6.75 mg/cm²) was placed with ~ 6.75 mg/cm² Al as backward catcher mounted on a conical support having a hole for beam to pass through. The target was irradiated with ^{11}B beam of 66 MeV energy (~ 34 hours). The end of irradiation activity of the fission products was calculated using acquired γ -ray spectra and was used to obtain their respective yields. The charge distribution parameters, Z_P was obtained using UCD hypothesis taking v_T into account and σ_Z was obtained by the best fit of the theoretical and experimental yield ratio of the $^{95}\text{Zr}-^{95}\text{Nb}^g$, $^{97}\text{Zr}-^{97}\text{Nb}^g$, $^{112}\text{Pd}-^{112}\text{Ag}$ and $^{140}\text{Ba}-^{140}\text{La}$ parent-daughter pairs. The fission product yields were corrected using these parameters to obtain the respective mass yields. As seen from Fig. 1, the obtained mass distribution shows deviations from the GEF calculations [5] which predicts dominant symmetric contribution along with $\sim 10\%$ contribution from S2 asymmetric mode. Deviations from GEF calculations specially in the mass region around ~ 136 indicates significant contribution from transfer fission channels and possibly, larger contribution from asymmetric fission compared to the GEF. A systematic study of the contribution from various fission channels will help to understand the role of shell closure as well as transfer fission contribution in actinide region.

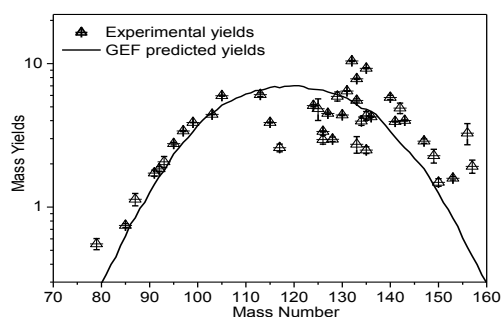


Fig. 1: Mass yield distribution of $^{11}\text{B}+^{237}\text{Np}$ reaction at $E_{\text{lab}} = 66$ MeV.

References:

- [1] U. Brosa et al., *Phys. Rep.*, **197(4)** (1990) 167.
- [2] A. Goswami et al., *Radiochim. Acta.*, **62** (1993) 173.
- [3] K. B. Gikal et al., *Bull. Russ. Academy of Sciences: Physics*, **82** (2018) 716.
- [4] H. Pasca et al., *Phys. Rev. C*, **99** (2019) 064611.
- [5] K.-H. Schmidt et al., *Nucl. Data Sheets*, **131** (2016) 107.

Neutron Capture Cross Section of ^{68}Zn : Uncertainty Analysis and Comparison with γ -Ray Strength Functions

Monika^{1,§}, Sumit Bamal¹, A. Gandhi^{1,2}, S. Lawitlang³, B. Lalremruata³,
A. Kumar¹, Rajeev Kumar^{4,5}, K. Umasankari⁴, L. S. Danu⁶, S. Santra^{5,6},
B. K. Nayak⁵, Rebecca Lalnuntluangi^{1,§}

¹ Department of Physics, Banaras Hindu university, Varanasi-221005, India

² Horia Hulubei National Institute of Physics and Nuclear Engineering - IFIN-HH,
Bucharest-077125, Romania

³ Department of Physics, Mizoram University, Tanhril, Aizawl-796004, India

⁴ Reactor Physics Design Division, Bhabha Atomic Research Centre, Mumbai-400085, India

⁵ Homi Bhabha National Institute, Anushaktinagar, Mumbai-400094, India

⁶ Nuclear Physics Division, Bhabha Atomic Research Centre, Mumbai-400085, India

§ Email: monika.007@bhu.ac.in, rebecca24@bhu.ac.in

The $^{68}\text{Zn}(n,\gamma)^{69}\text{Zn}^m$ reaction cross section has been measured at 1.12 ± 0.13 , 1.40 ± 0.12 and 2.42 ± 0.10 MeV using $^7\text{Li}(p, n)^7\text{Be}$ reaction as neutron source. Zinc is important in nuclear reactor to decrease the radiation fields and primary water stress corrosion cracking [1]. The irradiation was followed by offline γ -ray counting of activated samples using HPGe detector having 50% relative efficiency is shown in Fig. 1. along with its fitted curve. The spectrum averaged neutron energy was calculated using the neutron energy spectrum code EPEN [2] is shown in Fig. 2. The neutron flux was normalized using $^{115}\text{In}(n,n')^{115m}\text{In}$ monitor reaction. The analysis used the latest decay data, with corrections for low energy background neutrons and γ -ray self-attenuation. The total uncertainty in the measured cross section is under 6%.

Detailed uncertainty propagation has been performed. The newly measured cross sections are compared with the earlier reported data available in the EXFOR database. The data show good agreement with A.G. Dovbenko. However, the reported data by Yu. N. Trofimov is much lower. The theoretical model prediction using TALYS-2.0 [3] with various level density models and gamma strength functions is shown in Fig. 3. The prediction agrees with ldmodel-3 including four gamma strength functions (strength 2, 3, 8 and 9). This work will also be helpful for the verification of nuclear reaction codes.

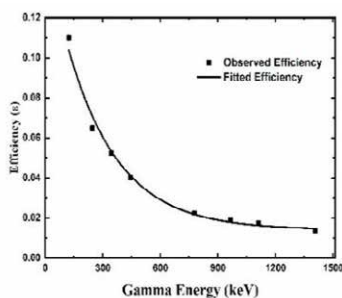


Fig. 1. HPGe detector efficiency data points and its fitted curve.

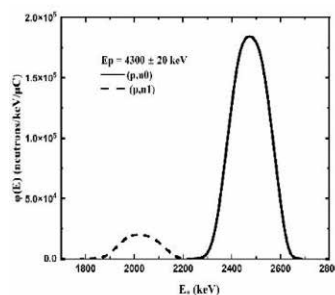


Fig. 2. Neutron flux energy spectra obtained from EPEN
 $E_p = 4300 \pm 20$ keV.

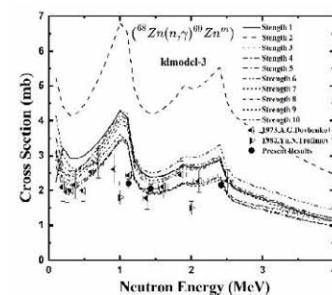


Fig. 3. Comparison of the measured $^{68}\text{Zn}(n,\gamma)^{69}\text{Zn}^m$ reaction cross section with literature data and theoretical model TALYS-2.0.

References:

- [1] J. S. et al., *Natural Science* **5**, (2013) 173.
- [2] R. et al., *Nuclear Science and Engineering* **187** (2017) 70.
- [3] A. J. Koning and D. Rochman, *Nuclear data sheets* **113** (2012) 2841.

Neutron Yield from Stable Heavy Ion on High Z Beam Dump

Vitisha Suman[§], Biju K.

Health Physics Division, BARC, Mumbai, India

[§] Email: vitisha@barc.gov.in

Interaction of energetic and charged heavy ions in thick targets is a source of neutrons in positive ion accelerators. The emitted neutrons along with gammas may have wide energy range depending on the target, projectile, and its energy. Neutrons are of primary concern due to their high penetrability and higher biological damage causing characteristics. The radiological safety aspect requires estimation of the radiation field in the accelerator environment. The information of the energy and the angular distribution of neutrons in an accelerator environment are important as the corresponding neutron dose has an energy dependence and also have directional dependence with respect to the particle beam direction. The radiation yield so estimated is referred to as source term and is applied for estimation of variety of important parameter like the design of accelerator shielding, prediction of induced activity and radiation damage. The effective dose or equivalent dose can also be estimated from such data using appropriate conversion factors (ICRP, 1996) [1].

A Monte Carlo simulation study using a versatile code Fluka (Version 4.3.2.) [2] is carried out to estimate neutron source term from a typical heavy ion reaction. The heavy ion studied are ^{209}Bi and ^{56}Fe absorbed on beam dump material taken as copper and tantalum of thickness 10 mm and 20 mm diameter. Pencil beam of 10 MeV/u energy heavy ion beam having flat distribution and annular size of 2 mm is made to fall on thick dump. The dump is placed at a distance of 300 cm from the target at the end of the beam line. The total neutron yield and energy distribution of neutron are scored using USRBDX scoring option in the Fluka simulation.

During accelerator operation, high energetic projectile falling on thick target will produce neutrons from nuclear reaction, mostly from the nuclear evaporation of the compound nucleus. The total neutron yield from the system is estimated to be $1.31\text{E}+7 \text{ ns}^{-1}\text{nA}^{-1}$ and $2.33\text{E}+7 \text{ ns}^{-1}\text{nA}^{-1}$ from the projectile and target combination of ^{56}Fe on copper (Cu) and ^{209}Bi on Cu respectively. The neutron yield is $1.40\text{E}7 \text{ ns}^{-1}\text{nA}^{-1}$ and $2.75\text{E}7 \text{ ns}^{-1}\text{nA}^{-1}$ for ^{56}Fe on tantalum (Ta) and ^{209}Bi on Ta respectively. It is found that the neutron yield and hence the dose is more for the reactions involving ^{209}Bi ion. The neutron dose rate at 1 m distance from the target estimated is $2.6 \text{ mSv h}^{-1} \text{ nA}^{-1}$ for the reaction ^{209}Bi on copper. The neutron spectra obtained is a hard spectrum as more than 90% neutrons obtained are above 1 MeV. The dose and energy distribution will govern the estimation of shielding and quantifying the induced activity in the air inside the beam hall and the structural material.

References:

- [1] ICRP Publication 74, *Ann. ICRP*, **26** (3/4) (1996).
- [2] G. Battistoni, et al. *Ann. Nuclear Energy* **82** (2015)10.

Investigation of Site-Selective Doping Induced Defects in CaSnO_3 Perovskite: A Positron Annihilation Spectroscopic Study

D. Das^{1,2}, S.K. Gupta^{1,2}, K. Sudarshan^{1,2,§}

¹ Radiochemistry Division, Bhabha Atomic Research Centre, Mumbai-400085, India

² Homi Bhabha National Institute, Anushaktinagar, Mumbai-400094, India

§ Email: kathis@barc.gov.in

Inorganic perovskite material such as CaSnO_3 has many technological applications, like in light-emitting devices, radiation detectors, solar cells, sensors, and catalysts [1]. Its multifunctional applications can be tuned by judicious choice of dopant ions and processing conditions. There are two different sites available for doping in CaSnO_3 and the properties will depend on the site where the dopant ion is incorporated. In literature, there are reports showing enhancement in catalytic and optical properties of CaSnO_3 upon doping and changing processing conditions, however a consolidated picture of the defects evolved at the atomistic level is relatively scarce [1, 2]. Positron Annihilation Lifetime Spectroscopy (PALS) is an efficient, sensitive, and non-destructive technique to probe the nature and concentration of defects at the atomistic level. Therefore, the objective of the present study is to investigate defect evolution in aliovalent Bi^{3+} ion doped CaSnO_3 perovskite employing PALS along with the support of theoretically calculated positron lifetime. Here site-selective doping of Bi^{3+} is envisaged by modulating the initial stoichiometry of the precursors. Undoped and Bi^{3+} doped CaSnO_3 samples are prepared using a solid-state synthesis method, starting with a homogeneous mixture of CaCO_3 , SnO_2 , and the appropriate amount of Bi_2O_3 . Bi doping is performed at concentrations of 1%, 2%, and 5% relative to Ca and Sn sites. Heat treatment at 900°C for five hours and final annealing at 1200°C for five hours are carried out involving intermittent grinding. Finally, the annealed samples are ground once more and characterized using powder XRD technique. All the powder XRD patterns are found to be in well-agreement with the standard pattern. Peak shifts in doped samples are observed corresponding to site-specific doping. PAL spectra could be fitted as a sum of three lifetime components where the third lifetime component is of negligible intensity corresponding to *o*-Ps pick-off annihilation. Typical fitted PAL spectrum of 1% Bi doped at Sn site of CaSnO_3 is shown in Fig. 1. The first lifetime component (τ_1) corresponds to free positron annihilation inside bulk along with some contribution from shallow positron traps. The second longer lifetime component (τ_2) is attributed to the annihilation at defect sites which are presumed to be mostly located at the surface. Doping of Bi at Ca site can either lead to cation vacancy or oxygen interstitial formation, whereas doping at Sn site will lead to oxygen vacancy creation (V_O) for charge compensation. Here, doping at both Ca and Sn sites has led to oxygen vacancy creation. τ_2 is found to increase in all doped samples and the enhancement is higher when Bi is present at Ca site. This indicates creation of large vacancy associates with Ca site-specific doping.

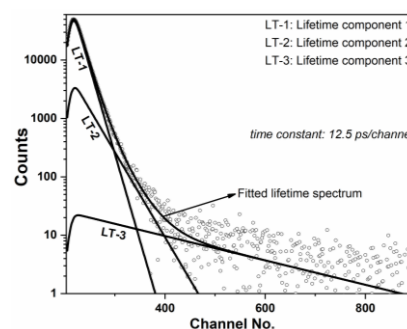


Fig. 1: Fitted PAL spectrum of 1% Bi^{3+} doped (at Sn site)

References:

[1] H Shalil et. al, *ACS Omega*, **6** (2021) 32537.

[2] T. Kang et al., *ACS Sustain. Chem. Eng.*, **8** (2020) 15005.

Simulations for Proton Induced Positron Annihilation Facility

K. Dhankar¹, S. Kulkarni¹, K. Shastry^{1,§}, S. Mukherjee²,

¹ RV College of Engineering, Bengaluru, India

² Radiochemistry Division, BARC, Mumbai, India

§ Email: karthikshastry@rvce.edu.in

In-situ positron generation in samples by pair-production process and the subsequent matter-antimatter annihilation provides an effective alternative to probe materials in comparison to conventional isotope-based positron sources [1]. The advantages of such techniques are- (a) absence of annihilation signals from radioactive source itself [1] and (b) possibility of probing large engineering samples. One of the methods to generate positrons in-situ is to have a beam of proton incident on a teflon or aluminum target to produce proton induced gamma emission. These gamma rays will fly down a collimator and will be incident on a sample where pair production process will be initiated. In this paper, we present the first ever FLUKA monte-carlo simulations [2-4] of proton induced positron annihilation (PIPA) setup [5]. The various processes that were simulated are- proton induced gamma ray production, transport of gamma ray through collimator, pair production in sample and the ensuing detection of annihilation signals from a sample. The first step was to simulate the emission of gamma rays due to the proton beam (from the Folded Tandem Ion Accelerator FOTIA [6]) hitting a Teflon plate. These gamma photons are transported through a collimator and are incident on a sample to generate positron-electron pairs through pair production mechanism. The ensuing annihilation gamma rays are detected by shielded HPGe and NaI detectors in singles or coincidence mode. The simulated 511 keV annihilation peak, as recorded by the gamma detectors, includes contributions from various factors - (a) positron production and annihilation in the sample, (b) positron production and annihilation in the collimator and (c) the scattered gamma rays. The simulated setup has been designed to suppress the last two contributions. We have also simulated the effect of background in measuring the 'sharpness' of the 511 keV peak. The results will be applicable in building a PIPA setup with high sensitivity as well as providing a threshold of acceptable background counts that will be present in any similar setup.

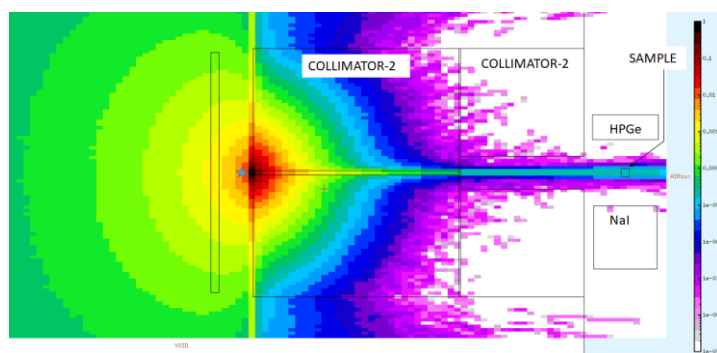


Fig. 1: Heat Map showing 6 MeV gamma ray intensity variation as they transverse a 40 cm lead collimator. 'Star' marks the position of photon emission.

References:

- [1] F. A. Selim, et. al., *Rev. Sci. Instrum.*, **76**, (2005) 033905.
- [2] C. Ahdida, et al. *Frontiers in Physics*, (2022) 705.
- [3] G. Battistoni, et al. *Annals of Nuclear Energy* **82** (2015) 10.
- [4] V. Vlachoudis, *Proc. Int. Conf. on Mathematics, Comp. Methods & Reactor Physics (M&C 2009)*, **176** (2009).
- [5] P. K. Pujari, *NIMB*, **270** (2012).
- [6] S. Santra, *Pramana*, **59** (2002) 53.

Influence of Electron Beam Irradiation on Free Volume of LLDPE/POE Blends: A Positron Annihilation Lifetime Spectroscopic Study

M. Singh¹, R. Agarwal¹, D. Dutta², S. Ray Chowdhury^{1,§}

¹ Electron Beam Processing Section, Radiation Technology Development Division, Bhabha Atomic Research Centre, Mumbai, India

² Radiochemistry Division, Bhabha Atomic Research Centre, Mumbai, India

§ Email: rcsubhen@barc.gov.in, manjeets@barc.gov.in

During electron beam (EB) irradiation of polymers, crosslinking and chain scission compete [1]. Crosslinking increases molecular weight by forming new chemical bonds, while scission decreases it. However, few probes are available to characterize free-volume properties in irradiated polymers. Positron annihilation lifetime spectroscopy (PALS) effectively detects free-volume holes at the atomic scale [2]. In this study, thermoplastic elastomeric blends of LLDPE (LL) and polyolefin elastomer (POE) are prepared in varying ratios (LL/POE 80/20, 60/40, 40/60, 20/80 wt%). The prepared blends are irradiated by electron beam (EB) at 50–250 kGy. These samples including pure LL, pure POE, non-irradiated LL/POE blends and irradiated blends are studied using PALS for fractional free volume (FFV) measurements.

The four-component fitting provides better variance in PALSFit analysis compared to the three-component fitting. The first two components offer no information about polymer phases. The third component represents the crystalline phase, reflecting ortho positronium (o-Ps) pick-off annihilation, with τ_3 and I_3 indicating its lifetime and intensity, respectively. The fourth component corresponds to the amorphous phase, with τ_4 and I_4 representing the lifetime and intensity of o-Ps pick-off annihilation in this phase. LLDPE exhibits highest crystallinity and POE has the lowest crystallinity. Prepared blends have intermediate crystallinity of LLDPE and ENGAGE. Crystalline phase intensity (I_3) and amorphous phase intensity (I_4) for prepared blends is shown in Fig. 1.

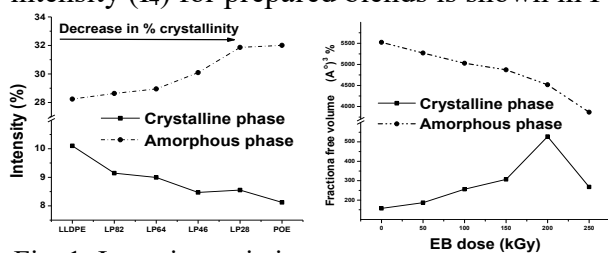


Fig. 1: Intensity variation Fig. 2: FFV variation

The o-Ps mimicking the crystalline phase shows increasing trends of τ_3 and FFV with increase in EB dose (Fig. 2). With increase in EB dose, cross-linkage portion increases, which gives coherent 3-D network that may be the reason of observed increasing trend. τ_4 and corresponding FFV show slow and regular decreasing trend of

with EB dose (Fig. 2). This is attributed to the fact that crosslinking occurs predominantly in amorphous phase, which increases with radiation dose and results in decreases of τ_4 and FFV of the amorphous phase. Both intensities, I_3 and I_4 shows decreasing trend with EB radiation dose indicating formation of new bonds as a result of crosslinking on irradiation. This may reduce the abundance of amorphous and crystalline phase, consequently decreasing the intensity. Degree of crosslinking in polymeric chains is determined by calculating the gel fraction, which is found to increase with increase in EB radiation dose supporting the PALS observations.

References:

- [1] M. Singh et.al. *J. Reinf. Plast.*, <https://doi.org/10.1177/07316844241266649>.
 [2] I. Y. Al-Qaradawi et. al., *Radiat. Phys. Chem.*, **68** (2003) 457.

Measurement of Activation Cross Sections of Alpha Induced Reactions on ^{nat}Ta up to 40 MeV

Sk Wasim Raja^{1, 2, §}

¹ RCD (BARC), Variable Energy Cyclotron Centre, Kolkata-700064, India

² Homi Bhabha National Institute, Mumbai-400094, India

§ Email: sw.raja@vecc.gov.in

Ta is used as a structural material in accelerator industry and is one of the candidate materials for the first wall of a fusion reactor chamber [1, 2]. High stopping power, low neutron yield, high melting point and thermal conductivity make it a choice for making irradiation chambers. Hence, accurate knowledge of the activation cross sections of the produced radionuclides via charged particle induced reactions will be helpful for dose estimation [2]. Alpha induced reactions on Ta gives several long-lived isomeric pairs, hence isomeric ratio measurements will provide insights about angular momentum distribution of the de-excited nuclei. There are few data available on the detailed activation cross section measurements of $^{nat}\text{Ta}(\alpha, x)$ reactions and there are obvious discrepancies among them [1, 2].

In this work, activation cross sections of $^{nat}\text{Ta}(\alpha, x)^{181, 182m, 182g, 183, 184m, 184g}\text{Re}$ reactions from their respective threshold energy up to 40 MeV were measured using alpha beam (Fig. 1) from K130 cyclotron of VECC, Kolkata. The standard stacked foil activation method was used for irradiation and induced activity was measured by high-resolution gamma spectrometry for activation cross section measurements [3]. Targets were 25.4 μm thick Ta and beam current was monitored using Cu foil.

The present activation cross sections data of $^{nat}\text{Ta}(\alpha, x)$ reactions will be helpful for improvement of theoretical model codes to study the reaction mechanism at higher mass region, investigation of the fusion–evaporation process at near Coulomb barrier energies, in thin layer activation (TLA) to study wear, corrosion and erosion of Ta, for determination of thermonuclear reaction rate etc. [1-3] Experimentally obtained cross section data for the radioisotopes will be compared with the earlier reported literature data wherever available and theoretical data from TENDL-2024 nuclear data library based on the TALYS-2.2 code.

Acknowledgement: Dr. R. Tripathi, Head, NCS, RCD, BARC is acknowledged for the fruitful discussion in preparing of this abstract.

References:

- [1] S. Takacs et al., *Nucl. Instru. Methods B*, **545** (2023) 165127.
- [2] F. Tarkanyi et al., *Nucl. Instru. Methods B*, **211** (2003) 22.
- [3] Sk Wasim Raja and R. Acharya, *Eur. Phys. J A*, **59** (9) (2023) 214.

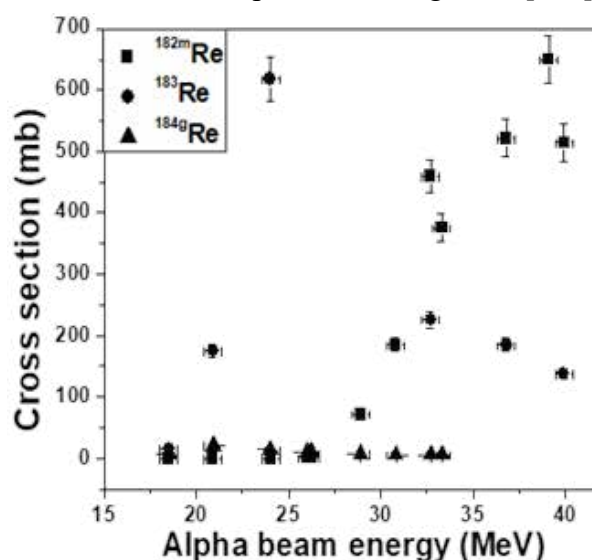


Fig.1: Excitation functions of $^{nat}\text{Ta}(\alpha, x)^{182m, 183, 184g}\text{Re}$ reactions.

Quark-Gluon Interactions and Color Confinement: An Algebraic Approach to Theoretical Modeling

B. C. Chanyal^{1,§}, V. K. Sharma², Neeraj Bisht³

¹ Department of Physics, G. B. Pant University of Agriculture and Technology, Pantnagar, Uttarakhand, India

² Department of Physics, Uttarakhand Open University, Haldwani, Uttarakhand, India

³ Department of Mechanical Engineering, G. B. Pant University of Agriculture and Technology, Pantnagar, Uttarakhand, India

§ Email: bcchanyal@gmail.com

The strong interaction is one of the four fundamental forces of nature that governs the behavior of the smallest building blocks of matter (i.e., quarks and gluons) and helps to understand the structure of the universe at subatomic scale. In this way, the present study explores the algebraic-based color charge theory which shows that the theory of strong interactions can be explained beautifully in terms of hypercomplex octonion algebra. Consequently, in this model, we have constructed the algebraic-based isospin multiplets corresponding to I, V, U-spin planes. The color-quark interactions and gluon-gluon interactions are also studied in octonion quantum chromodynamics (QCD). We proposed the condition for octonion color confinement of hadrons and established the glueballs formation in the generalized octonionic color field. It has been emphasized that for the formation of octonion glueballs, only eight combinations that associated with gluons in pairs, are possible to provide the colorless states of hadrons.

Meanwhile, the octonion color wavefunctions for a baryon particle are obtained in terms of octonion operators with their different pairs. Accordingly, the octonionic version of QCD Lagrangian is also discussed along with non-associative division algebra that can be described the interesting consequences of QCD like asymptotic freedom, hierarchy problem etc. In experiment point of view, particle accelerator experiments have found several particles that have been considered viable candidates for glueballs, but there is no scientific consensus on whether one of these signals may actually be a mysterious particle composed of pure force. Because of the very short life-time of glueballs, it cannot be detected directly in laboratory.

In mathematical terms, the octonion is important to represent the SU(3) symmetry group that is connected with the strong interaction. The crucial point is that the antisymmetric structure constant for both the SU(3) symmetry and the octonion algebra, which are isomorphic. Here, one may write [1,2]:

$$\begin{aligned}
 F^{\alpha\beta\gamma} &= f^{\alpha\beta\gamma}; \leftrightarrow [e_\alpha, e_\beta] = i[\lambda_\alpha, \lambda_\beta], & (\forall \alpha\beta\gamma = 123) \\
 &= \frac{1}{2} f^{\alpha\beta\gamma}; \leftrightarrow [e_\alpha, e_\beta] = \frac{i}{2}[\lambda_\alpha, \lambda_\beta], & (\forall \alpha\beta\gamma = 147, 246, 257, 435, 516, 673) \\
 &= \frac{\sqrt{3}}{2} f^{\alpha\beta\gamma}; \leftrightarrow [e_\alpha, e_\beta] = \frac{i\sqrt{3}}{2}[\lambda_\alpha, \lambda_\beta], & (\forall \alpha\beta\gamma = 458, 678)
 \end{aligned} \tag{1}$$

where $F^{\alpha\beta\gamma}$ and $f^{\alpha\beta\gamma}$ are the structure constants respectively for SU(3) group symmetry and octonionic symmetry. Here, λ 's show the SU(3) generators while e 's show the octonion basis elements.

References:

- [1] M. Günaydin and F. Gürsey, *Phys. Rev.*, **D9** (1974) 3387.
 [2] B.C. Chanyal, *Mod. Phys. Lett.*, **A36** (2021) 2150264.

Measurement of Production Cross Sections of ^{196}Au Produced from $^{197}\text{Au} + ^{20}\text{Ne}$ Reactions from 108 to 171 MeV Projectile Energy

S. Mukherjee¹, S. Lahiri^{1,2,§}, C. Barman¹, S. Bhattacharyya³, S. Chatterjee⁴,
S. Dasgupta⁵, J. Datta⁵, G. Mukherjee³

¹ Department of Physics, Sidho-Kanho-Birsha University, Purulia, India

² Department of Chemistry, Diamond Harbour Women's University, South 24 Pargana, India

³ Experimental Nuclear Physics Division, ⁴ TLD unit, VECC, Kolkata, India

⁵ Analytical Chemistry Division, BARC, VECC, Kolkata, India

§ Email: susanta.lahiri.sinp@gmail.com

The heavy ion (HI) induced nuclear reactions are of interest due to their ability to produce neutron deficient radioisotopes. Earlier, ^{20}Ne induced reactions on gold target were studied at different energy range, 172–252 MeV [1], 8 GeV [2], etc. In this paper, we have reported production cross section of ^{196}Au , measured by off-line γ -spectrometry, through the interaction of 108.5–171.2 MeV ^{20}Ne on natural gold target. For this purpose, five gold targets (3–4.8 mg cm⁻²) were bombarded with $^{20}\text{Ne}^{7+}$ beam of incident energy 114–174 MeV. The offline gamma spectra from ~1 h to 55 d after the end of bombardment (EOB) were taken.

Fig. 1 shows the production cross section of ^{196}Au at projectile energy. The combined uncertainty of measured cross section was estimated ~10%. A comparative study was carried out using two simulation techniques, PACE4 and FLUKA4-3.3. The number of cascades taken in PACE4 and FLUKA were 9.9×10^5 and 2.0×10^9 respectively. All other parameters were same as experiment. PACE4 did not predicted production of ^{196}Au , while FLUKA4-3.3 predicted the same above 157 MeV, though the cross sections were grossly underpredicted compared with experimental data. Probably ^{196}Au has been produced by direct reaction mechanism, i.e., HI knocked out a spin $\frac{1}{2}$ particle from target. PACE4 considers only equilibrium (EQ) reactions and therefore is silent about the production of ^{196}Au . In future cross sections of each produced radioisotopes will be compared with theoretical codes.

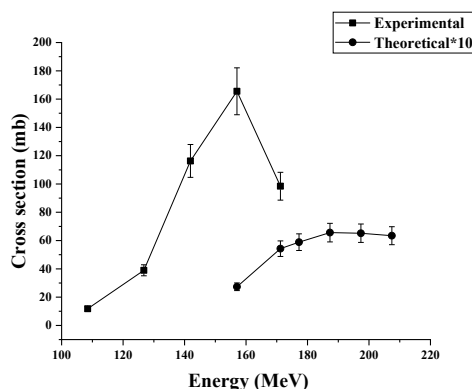


Fig. 1: Excitation function of ^{196}Au (the projectile energy is the average of incident and exit energy)

Acknowledgement: Authors acknowledge target laboratory and cyclotron crew of VECC; S. Show and S. Ghose of DHWU for their cooperation. SM is grateful to DST for INSPIRE Fellowship; SL acknowledges CSIR-ES Scheme; CB acknowledges UGC-DAE CSR project.

References:

- [1] G. J. Mathews et al., *Phys. Rev. C*, **25**(1) (1982) 300.
- [2] D. J. Morrissey et al., *Phys. Rev. C*, **21** (1980) 1783.

Spectroscopic Investigation of Defects in Natural Zircon Irradiated with 10 MeV Electron Beam

Rumu H Banerjee^{1,§}, Nishant Chaudhary², Rajath Alexander³,
Kulwant Singh¹, Pranesh Sengupta¹

¹ Materials Science Division, ² Applied Pulse and Power Division, ³ Glass and Advanced Materials Division, Bhabha Atomic Research Centre, Mumbai-400 085, India

§ Email: rumu@barc.gov.on

Zircon is a slag host matrix associated with the metallic waste form. The long-term performance of these matrices can be assessed through the natural analogue study. Naturally occurring zircon embodies the cumulative effects of α -particle radiation damage over geologically significant periods. Hence, studying the irradiation and annealing effects in natural zircon can provide insights on the defect formation. This study examines the impact of 10 MeV electron irradiation on the defect structure of self-irradiated natural zircon, which is of interest for its potential application in nuclear waste storage as a slag host matrix [1]. Natural zircon crystals with a reddish-brown hue, sourced from Tamil Nadu, India, were ground into powder and annealed at 1673 K for 96 hours. Both the as-received and annealed specimens were then subjected to 10 MeV electron beam irradiation up to a total dose of 20 MGy. The estimated collision and radiative stopping powers were 0.71 keV/ μm and 0.22 keV/ μm , respectively, while the nuclear stopping power was calculated as 2.45×10^{-5} keV/ μm , indicating that energy loss primarily occurs through collisions.

X-ray diffraction confirmed the tetragonal crystal structure of zircon, with minor peak shifts attributed to the presence of trace elements and radiation-induced effects. Photoluminescence analysis revealed a significant reduction in PL intensity in both as-received and annealed samples following irradiation. Raman spectroscopy showed slight peak shifts, intensity variations, and a consistent decrease in the full width at half maximum (FWHM) of the silicate band for both sample types after irradiation. These findings suggest that electron irradiation induces a non-thermal annealing effect on pre-existing defects in natural zircon. Overall, the results confirm that zircon maintains good radiation stability under electron beam exposure.

Acknowledgements: The authors are thankful to Dr. A. Biswas, Head, MSD and Dr. R. Tewari, Director, Materials Group for their constant support and encouragement.

References:

- [1] Rumu H. Banerjee, et. al., *Spectrochim. Acta Part A: Molecular and Biomolecular Spectroscopy*, **326** (2025) 125159.

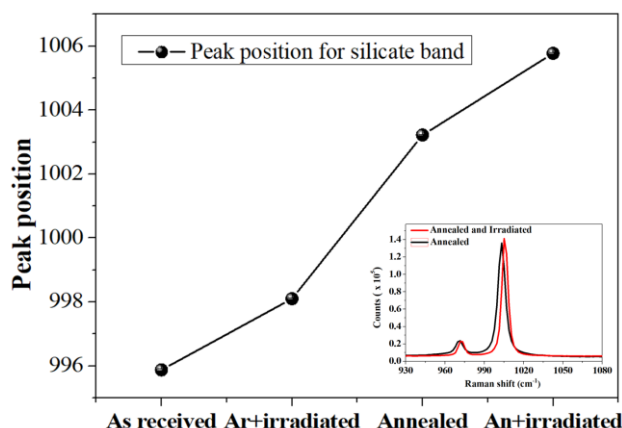


Fig. 1: Variation of peak position for silicate band for Zircon specimens. The inset compares the intensity of silicate band for annealed specimen before and after irradiation.

Study of Uncertainty Propagation of $^{58}\text{Ni}(n,p)^{58}\text{Co}$ Reaction

Namrata Singh^{1,§}, Mahesh Choudhary¹, Mahima Upadhyay¹, Punit Dubey¹, Shweta Singh¹, Sriya Paul¹, G. Mishra², Sukanya De², L. S. Danu², Ajay Kumar², R. G. Thomas², A. Kumar¹

¹ Department of Physics, Banaras Hindu University, Varanasi 221005, India

² Nuclear Physics Division Bhabha Atomic Research Centre, Mumbai 400085, India

§ Email: namratasingh.jwala@gmail.com

The $^{58}\text{Ni}(n,p)^{58}\text{Co}$ reaction is a key neutron-induced process with significant applications in nuclear science, including reactor design, astrophysics, and radiation shielding [1,2,3]. In this study, we examine the impact of uncertainties in nuclear input parameters that affect the reaction cross-section using the Monte Carlo method. By exploring a range of parameter values within their respective uncertainty limits, we can generate a distribution of cross-sections, offering insights into result variability due to theoretical model uncertainties. This approach involves randomly sampling input model parameters and conducting simulations with the TALYS-1.95 code [4]. As initial parameters, we utilized the global-level density parameters proposed by Koning et al. and the optical model parameters recommended by Koning and Delaroche [5]. The present experiment was performed at the Folded Tandem Ion Accelerator (FOTIA) facility at Bhabha Atomic Research Centre (BARC), Mumbai, India.

In this experiment, neutrons were produced via the $^7\text{Li}(p, n)^7\text{Be}$ reaction, and the $^{58}\text{Ni}(n,p)^{58}\text{Co}$ reaction [6,7] cross-sections were measured relative to the $^{115}\text{In}(n, n, \gamma)^{115\text{m}}\text{In}$ monitor reaction cross-section. We performed this experiment at different neutron energies 1.27, 1.47, 1.87, 2.26, 2.46 and 3.06 MeV because no data is available in EXFOR. Also, we are doing the uncertainty quantification associated with covariance analysis which is valuable

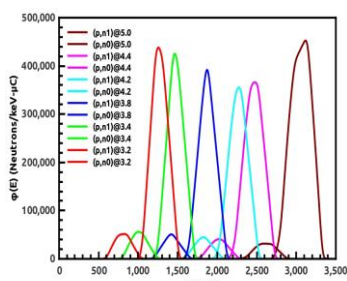


Fig.1: Neutron flux spectra at proton energies obtained from EPEN.

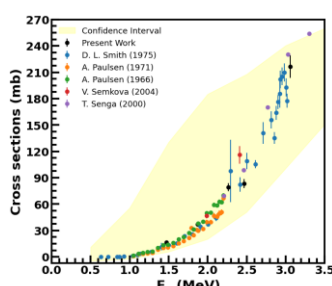


Fig.2: Measured reaction cross-section of $^{58}\text{Ni}(n,p)^{58}\text{Co}$.

in reactor design, astrophysics, and radiation shielding studies. The study systematically analyzed the influence of uncertainties in optical model parameters and level density parameters on cross-section predictions using the Monte Carlo method.

Acknowledgements: Namrata Singh expresses gratitude for the financial support provided by the UGC Non-NET Fellowship. The authors would like to thank the FOTIA facility staff

for their accelerator operation and assistance during the experiment.

References:

- [1] A. L. Cole et.al., *Physical Review C* **74** (2006) 034333.
- [2] M. Aygun et.al., *Iranian Journal of Science* **49** (2024) 559.
- [3] J. J. G. Kelly et.al., *In Reactor Dosimetry. ASTM International* (1994).
- [4] A. J. Koning, S. Hilaire and M. C. Duijvestijn, TALYS-1.0, *Proceedings of the International Conference on Nuclear Data for Science and Technology*, April 22-27, 2007, Nice, France, EDP Sciences, (2008) 211.
- [5] A.J. Koning, S. Hilaire, S. Goriely, *Nuclear Physics A* **810**, (2008) 13.
- [6] A. Hingu et. al., *Chinese Physics C* **48**, (2024) 024001.
- [7] M. Choudhary et.al., *Chinese Physics C* **48**, (2024) 1.

Induced Air Activity Studies in a Photo-Fission Experimental Vault

K. Biju[§], V. S. Dagle, P. Srinivasan

Health Physics Division, Bhabha Atomic Research Centre, Mumbai, India

[§] Email: bijuk@barc.gov.in

Photo fissions studies are found useful for detecting and quantifying fissile materials in cargo [1]. As the photo fission cross sections are much lower than that of the neutron cross sections, high intense beam is required to get the desired fission rates. The bremsstrahlung produced by high energy accelerators can produce considerably large number of fissions as compared to photons produced by nuclear reactions. These fissions sources are also used for producing rare ion beams for basic research [2]. This paper presents the Monte Carlo studies carried out to estimate the radionuclides produced in the air from neutron activation of the air due to the neutrons emitted by photons. The neutron yield and spectra are also reported. These results are important to assess the radiological safety aspects such as shielding and the environmental releases of the facility.

The studies were done using Fluka (Version 4.3.2.) Monte Carlo simulations [3]. A pencil beam of energy 50 MeV electrons falling on a thick tungsten target of 4.5 mm thick is simulated. The geometry of the simulation is as follows. The tungsten target is followed by a graphite block of thickness 30 mm to stop the transmitted electrons and falls on a natural uranium fission target. The inner vault dimension considered is 5 m x 6 m x 5 m and the thickness of the shielding walls are assumed as 200 cm. The length of the photo-fission target used in the simulation study is 10 cm. The bremsstrahlung produced from the tungsten target induces the fission reactions in the uranium target. The energy angle integrated neutron yield is estimated as 1.73E-2 per incident electron. This includes both photo neutrons as well as fission neutrons.

The neutron yield and spectra are scored using USRBDX option of the Fluka code. The build up and decay of the radio nuclides produced in the air is estimated using the RESNUCLEi option of the Code. Fig. 1 presents the build up and decay of the radionuclide activity produced in air inside the vault irradiated for 8 hrs and further 2 hours of cooling. It is found that the saturated concentration of Ar-41 produced 30 Bq/cm³ per mA of electron current. 99% of the activity induced in air by the neutrons is Ar-41. The other radionuclides produced are Ar-37, N-13, C-14 and H-3 whose concentrations are 2 to 6 orders less.

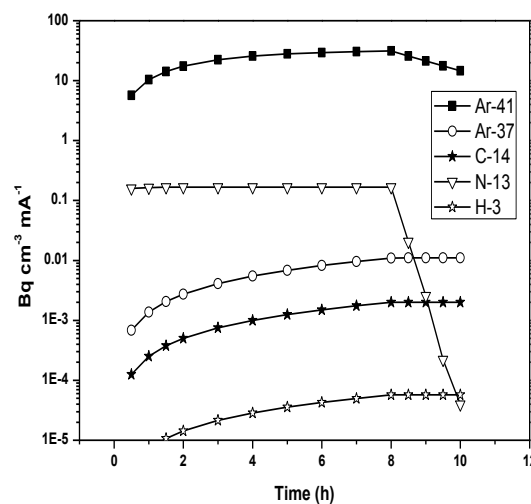


Fig.1 Build up and decay of radio nuclides produced in air.

References:

- [1] Priyamvada M. Dighe et al. *Nucl. Inst. Methods Phys. Res. A*, **946** (2019), 162624.
- [2] S. Essabaa et al. *Nucl. Inst. Methods Phys. Res. B*, **204** (2003), 780.
- [3] G. Battistoni, et al. *Ann. Nucl. Energy*, **82** (2015)10.

Effect of Ions and Oxides on Hydrogen Peroxide Yield

Muniasamy. L.^{1,2,§}, Puspallata Rajesh^{2,3}, R. Ramakrishnan¹,
S. Bera^{2,3}, I.V.N.S. Kamaraju¹, T.V. Krishna Mohan³

¹ PRPD, Bhabha Atomic Research Centre Facilities, Kalpakkam, India

² Homi Bhabha National Institute, Mumbai, India

³ WSCD, Bhabha Atomic Research Centre Facilities, Kalpakkam, India

§Email: munish20680@igcar.gov.in

In nuclear reactors, the generation of oxidizing H_2O_2 from coolant radiolysis is the key factor affecting the corrosion of structural materials. H_2O_2 undergoes hetero-catalytic decomposition [1] on the oxide-covered structural material surfaces at the reactor operating temperatures, generating O_2 and shifting the electrochemical potential to a more corroding region. The typical oxides present in the pressurized water reactors are mainly Fe_3O_4 , $NiCrFeO_4$ and ZrO_2 on carbon steel, SS and zirconium alloys, respectively. The presence of any ionic impurities and pH will affect the yield of H_2O_2 . Hence, it is important to understand the dependence of H_2O_2 concentration on these factors to assess the water chemistry conditions prevailing in the reactors and arrive at the critical H_2 concentration necessary to suppress radiolysis.

In this study, experiments were conducted to understand the effect of a few probable ions (cations: K^+ , Na^+ , Li^+ , Cu^{2+} and Fe^{3+} ; anions: Cl^- , SO_4^{2-} , CO_3^- and NO_3^-) in 0-100 ppm range and oxides, on the radiolytic yield of H_2O_2 by irradiating aerated solutions to varying gamma doses. Further experiments were carried out to evaluate the extent of H_2O_2 thermal decomposition on the oxide-coated structural material surfaces. The initial $G(H_2O_2)$ values were determined from the concentration vs. dose plot slopes of at lower doses. The H_2O_2 concentration decreased slightly in the presence of CO_3^- ion and increased ~ 2.5 times with NO_3^- . Unlike anions, the alkali metal ions (K^+ , Na^+ and Li^+) did not affect the radiolytic H_2O_2 formation. The H_2O_2 concentration increased slowly with dose and reached steady-state condition after ~ 20 kGy. The yield was slightly lower than pure water radiolysis steady-state concentration in the presence of Fe_3O_4 and ZrO_2 .

To predict the accurate H_2O_2 concentrations in nuclear reactors, the thermal decomposition of radiolytically generated H_2O_2 on the oxide-covered structural material surfaces has to be accounted for. The extent of interaction and thermal decomposition was measured by keeping the amount of oxide powders (Fe_3O_4 , $NiCrFeO_4$ and ZrO_2) and H_2O_2 concentration the same (0.2% wt vol⁻¹) and varying the temperature from 295-353 K. The decomposition kinetics was measured by analyzing the H_2O_2 concentration with time. From the decomposition kinetics, the activation energy (E_a) was calculated from the plot of the pseudo first-order rate constants with the inverse temperature. The change in rate constants in the presence and absence of Fe_3O_4 , $NiCrFeO_4$ and ZrO_2 at different pHs are shown in Fig. 1. The E_a for H_2O_2 decomposition was minimum with $NiCrFeO_4$ (20 kJ mol^{-1}) among the oxides evaluated.

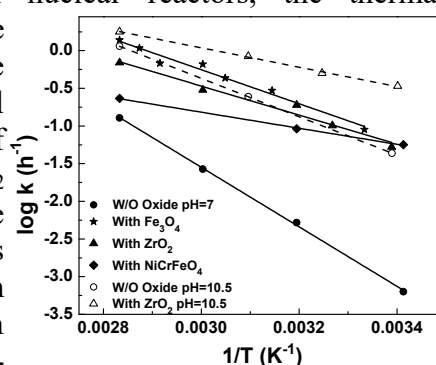


Fig. 1: Activation energy for H_2O_2 decomposition at pH=7 & 10.5.

Reference:

[1] A. Hiroki and J.A. LaVerne, *J. Phys. Chem. B*, **109** (2005) 3364.

Electrochemical Conversion of $\text{UO}_2\text{-ZrO}_2$ Mixture to U and Zr by Direct Oxide Electrochemical Reduction (DOER)

N. Sanil^{1,§}, L. Shakila¹, V. Arunkumar¹, R. Kumaresan^{1,2}

¹Materials Chemistry & Metal Fuel Cycle Group, IGCAR, Kalpakkam, India.

²Homi Bhabha National Institute, IGCAR, Kalpakkam, India.

§ Email: sanil@igcar.gov.in

In the recent past, U-Zr binary metal system has gained more attention due to focus on the importance of metallic fuel programme. Generally, U-Zr alloys are prepared by arc melting or by vacuum induction melting of individual metals. This paper presents the results of investigations conducted to convert a mixture of solid $\text{UO}_2\text{-ZrO}_2$ to U and Zr by a novel method namely Direct Oxide Electrochemical Reduction (DOER). Herein, the sintered pellet of mixture of the oxides are converted to corresponding metals by in-situ generated lithium metal during its electrolysis as cathode in $\text{LSiCl-Li}_2\text{O}$ molten salt. XRD of the sintered product of the mixture of oxides showed existence of UO_2 and ZrO_2 as separate phases (fig.1). CV with blank Metallic Cavity Electrode (MCE) and precursor oxides conducted in LiCl melt identified the reduction potentials of ZrO_2 and UO_2 at -2.0V and -2.16V w.r.t. a Ni/NiO reference electrode (Fig. 2). Constant current electrolysis of different compositions of the oxides ($\text{UO}_2 - 6$ to 50% ZrO_2) was conducted at 650°C and XRD of the products indicated the formation of U and Zr as separate phases (Fig. 3). The reduction efficiency or kinetics was not observed to be influenced by varying concentrations of ZrO_2 .

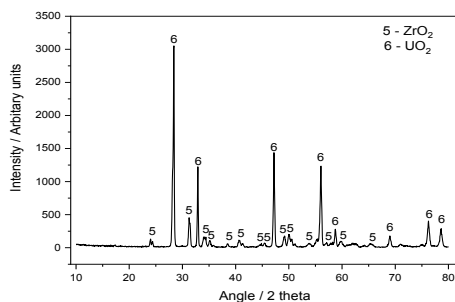


Fig. 1: XRD of the powder of sintered $\text{UO}_2\text{-}50\%$ ZrO_2

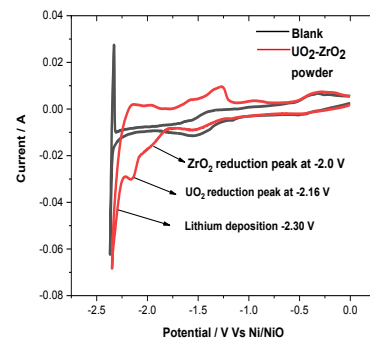


Fig. 2: CVs of blank MCE, $\text{UO}_2\text{-ZrO}_2$ MCE WEs in LiCl melt at 650°C . 100 mV/s .

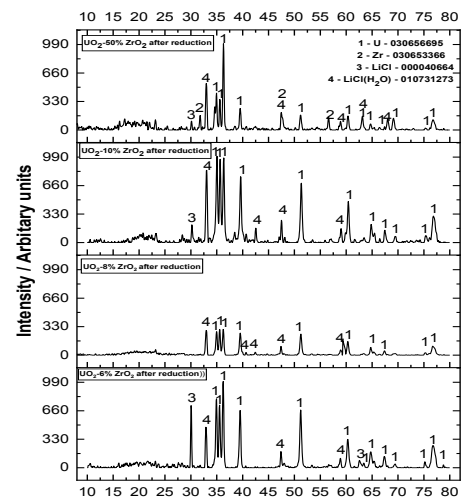


Fig. 3: XRD of the product of electrolysis of different $\text{UO}_2\text{-ZrO}_2$ sintered mixtures.

References:

[1] Yi Xie et al., *Journal of Nuclear Materials*, **564** (2022) 153681

Electrochemical Behavior of Gd^{+3} in LiCl-KCl at W and Fe Electrodes

Suvra Sil, S. Nedumaran, Patoju Sai Dilip, Anwasha Mukherjee,
Gurudas Pakhui, R. Kumaresan[§]

Indira Gandhi Center for Atomic Research, Kalpakkam, India

[§] Email: rkum@igcar.gov.in

Molten salt electrorefining is the most suitable pyrochemical process for separating actinides (uranium, plutonium, and minor actinides) from lanthanides and other fission products in spent metallic fuel. In this process, uranium is electrochemically deposited onto a solid steel cathode, while uranium, plutonium, and minor actinides are collectively recovered on a liquid cadmium cathode. This leaves behind the other fission products in the molten salt and in the anode residue. Monitoring lanthanides' concentration and their electrochemical behaviour during the electrorefining process is essential, as lanthanides may co-deposit with minor actinides.

In this context, the electrochemical behaviour of gadolinium ions (Gd^{3+}) in a LiCl-KCl molten salt eutectic has been studied using tungsten (W) and iron (Fe) cathodes, along with a graphite counter electrode and an Ag|(1wt% AgCl-LiCl-KCl) reference electrode. Various electrochemical techniques, including cyclic voltammetry (CV), chronopotentiometry (CP), square wave voltammetry (SWV), and open-circuit chronopotentiometry (OCP), were employed. CV measurements were conducted at the tungsten electrode from 698 K to 798 K, with scan rates (v) increasing from 10 mV/s to 125 mV/s. The number of electrons transferred (n) was determined to be 2.57 from square wave voltammetry at the tungsten electrode.

Additionally, the diffusion coefficient (D) for Gd^{3+} and other parameters were calculated using Sand's equation based on the CP data. Diffusion coefficient of Gd^{3+} is $1.028 \times 10^{-5} \text{ cm}^2 \cdot \text{s}^{-1}$ at 773K and temperature dependence expression of D in temperature range of 698-798 K is given by following equation.

$$\ln(D/\text{cm}^2\text{s}^{-1}) = (-5.466 \pm 1.127) + (-4683.922 \pm 840.491)/T \text{ (K)}$$

The cyclic voltammetry (CV) recorded at the Fe working electrode (Figure 1) displayed cathodic peaks at -1.55 V and -2.02 V, which are attributed to the formation of Gd-Fe alloys and the deposition of Gd, respectively. Additionally, several anodic peaks observed at the Fe electrode indicated the anodic dissolution of various Gd-Fe species. The open circuit potential (OCP) measurements at the Fe electrode also suggested the formation of different Gd-Fe alloys.

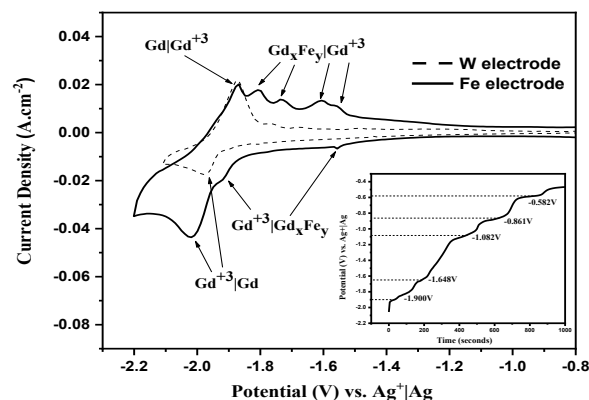


Fig. 1: Cyclic Voltammetry of $GdCl_3$ in LiCl-KCl melt at W and Fe electrodes, Scan rate: 100mV/s, Temperature: 798K; Inset: OCP at Fe electrode, -2.1V for 30s

References:

[1] S. Vandarkuzhali et al., *Electrochimica Acta*, **59** (2012) 245.

Ion Chromatographic Determination of Phosphorous in Stainless Steel

U. K. Thakur¹, Poonam Verma^{1,§}, S. Jeyakumar²

¹Radioanalytical Chemistry Division, BARC, Trombay, Mumbai – 400085.

²Radiochemistry Division, BARC, Trombay, Mumbai – 400085.

§ Email: poonamv@barc.gov.in

Phosphorus is a vital alloying component in steel as it improves strength, hardness, and machinability and corrosion resistance. However, P decreases ductility and can cause embrittlement of steels [1,2]. Therefore, phosphorus determination in steel is of the utmost importance. Stainless Steel samples of TAPS1, KKNPP1, and TAPS3 were received for P analysis as a part of failure analysis. Hence, an ion chromatographic (IC) method was developed for phosphorous determination in stainless steel. Samples were cut, washed and then dissolved in aqua regia. As NaOH is used as the mobile phase in IC, matrix cations in steel would hydrolyze and precipitate, causing irreversible damage to the column. To prevent this adverse situation, matrix cations in the dissolved steel were separated with a cation exchange cartridge. Acid medium anions (nitrate and chloride) were evaporated off and sample solution was made with high purity deionised water. Recovery of P from cartridge was better than 96%. P, as phosphate anion, was then determined by IC employing anion exchange column (Dionex IonPac AS16) in suppressed conductivity mode. IC parameters were optimized (eluent of 26 mM NaOH at a flow rate of 1 mL/min) to get distinct phosphate peak without interference in the minimum run time as shown in Fig. 1. Retention time obtained for phosphate peak is at 10.4 minutes in run time of 12 minutes. Calibration is linear in 0.3 to 3.3 ppm range of P with R^2 better than 0.998 (Inset of figure 1). LOD is 0.04 ppm. Developed method was validated by studying the recovery (better than 94% at 1 ppm level) of P in stainless steel matrix. Results obtained by the developed IC method are shown in Table 1. Additionally, P determination was carried out by alternate established molybdenum spectrophotometric method (Table 1) to further authenticate the developed IC method.

Table 1: Results obtained for P in stainless steel by the developed IC and photometry

Sam ple	Phosphorus (ppm)		
		IC	Photometry
1	KKNPP-1	78 ± 8	81 ± 7
2	KKNPP-2	139 ± 14	146 ± 16
3	KKNPP-3	620 ± 62	609 ± 31
4	TAPS1-1	484 ± 14	469 ± 17
5	TAPS1-2	349 ± 14	355 ± 11
6	TAPS3-1	88 ± 9	84 ± 6
7	TAPS3-2	91 ± 9	96 ± 9

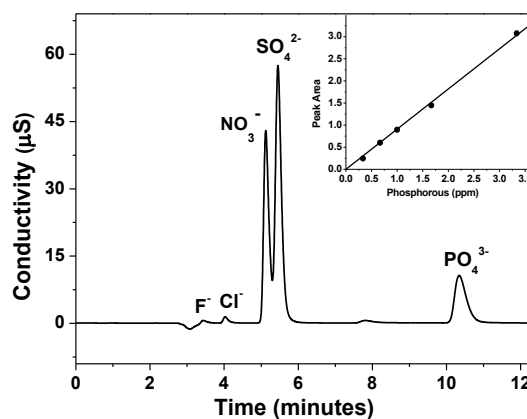


Fig. 1: Chromatogram of phosphate. Inset: calibration plot

Acknowledgement: Authors are thankful to Head, RACD and AD, RC&IG for their kind support. Authors are grateful to Smt. V. V. Raut for providing cation exchange cartridge.

References:

- [1] Yu Guo et al., *Journal of Materials Research and Technology*, **18** (2022) 2240.
 [2] R. R Hussain et al., *Sci Rep*, **12** (2022) 12449.

Analysis of Gases in Sodium-Limestone Concrete Interactions by Gas Chromatography

Venkat Reddy G^{1, §}, Arjun Pradeep^{1,2}, Malarvizhi B¹,
Sanjay Kumar Das¹, Sreedhar B. K^{1,2}

¹ Indira Gandhi Centre for Atomic Research, Kalpakkam, India

² Homi Bhabha National Institute, Mumbai, India

§ Email: gvenkat@igcar.gov.in

In secondary circuit of sodium cooled fast reactor, accidental sodium leak at high temperatures (525°C) pose significant safety concerns due to thermochemical interactions with structural concrete [1]. To mitigate the thermochemical effects, a 50 mm sacrificial layer of sodium fire-resistant limestone concrete is used for protection of concrete. Limestone Concrete (LC) comprises carbonate based lime stone aggregate (60-75%), water (14-21%) and cement (7-15%). The analysis of hazardous and toxic gases evolving during sodium-limestone concrete interactions is essential for safety assessment. This study utilized gas chromatography-thermal conductivity detector (GC-TCD) method to identify gases evolved during sodium-LC interactions. The GC system (YL6500 GC) operating conditions for analysis of gases are oven temperature of 70°C, injector temperature of 250°C, detector temperature of 250°C and nitrogen carrier gas flow rate of 20 L/min. A molecular sieve 5Å column (7.62 m length, 1/8" OD, 2 mm ID, 60/80 mesh size) is used as packed column stationary phase. 500µL gas samples are injected into injector using gas sampling valve. Real-time analysis of gases by GC-TCD provides superior accuracy and repeatability across a wide dynamic range (trace level to percentage) of gases.

In the experimental setup (Fig. 1), 200 g of sodium was heated to 525°C in a reaction vessel. After that, limestone concrete disc specimen was introduced into the liquid sodium. The GC chromatogram (Fig. 2) shows hydrogen peak at 2.55 min, indicating hydrogen gas with no detection of other toxic gases. These preliminary results confirm that sodium-limestone concrete interaction does not produce toxic gaseous emissions. Real-time analysis of gases in sodium-LC interactions by GC-TCD is useful for safety assessment in sodium cooled fast breeder reactors, solar thermal power plants and sodium production facilities.



Fig.1: Sodium-LC interaction Exp. Set up

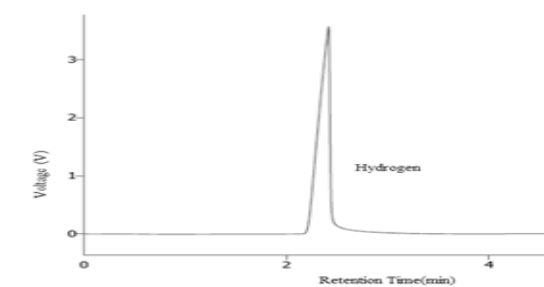


Fig. 2: Chromatogram of Sodium-LC interaction

Authors are thankful to Smt. R. Preetha, Head, CM&QCD, and Shri. J. Ashok Kumar, QCS, CM&QCD, for providing LC specimens for this study.

References:

[1] K. M. Haneefa *et al.*, *Nuclear Engineering and Design*, **258** (2013) 76.

Electrical Conductivity Measurement of LiCl-Li₂O Molten Salts

N. Sanil^{1,§}, V. Arunkumar¹, R. Kumaresan^{1,2}

¹Materials Chemistry & Metal Fuel Cycle Group, IGCAR, Kalpakkam, India

²Homi Bhabha National Institute, Kalpakkam, India

§ Email: sanil@igcar.gov.in

Preparation of uranium metal by a novel method namely Direct Oxide Electrochemical Reduction (DOER) involves the electrolysis of UO₂ pellets in LiCl-Li₂O melt at 650°C, using platinum anode. Generally 1-2 wt % Li₂O is added to the LiCl melt for effective oxygen transport in the melt and also to prevent anodic dissolution of Pt anode during electrolysis. However, the electrical conductivity of LiCl-Li₂O melts, which is an important parameter of an electrolytic cell, was not yet reported in the open literature. The present paper describes the results of the preliminary experiments conducted to measure the electrical conductivity of LiCl-(0-1.0%) Li₂O melts at different temperatures 650°C, 675°C and 700°C. A new dip-type conductivity cell was designed and was calibrated using standard 0.1N KCl solution at 25°C and also by using molten LiCl at 650°C. Using the calibrated conductivity cell, electrical conductivity of molten LiCl and LiCl-(0.5-1.0%) Li₂O was calculated from the resistance of the melts measured employing impedance spectroscopy. Typical impedance spectrum obtained in LiCl-1% Li₂O melt at 650°C is given in Fig. 1. The measured values of conductivity of LiCl (5.645, 6.084, 6.510 Scm⁻¹, at 650, 675, 700°C respectively) agreed well with that of reported value within 5% and conductivity of melts were found to be enhanced on addition of Li₂O to LiCl melt (Fig. 2). The enhanced conductivity may be attributed to the increased ionic mobility due to the higher charge and smaller size of oxide ion compared to that of chloride ion.

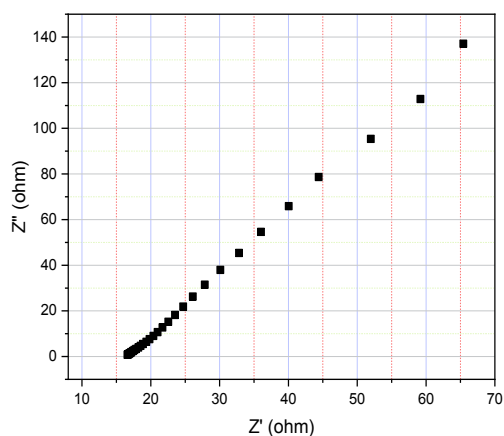


Fig. 1: Impedance spectrum of molten LiCl-1% Li₂O at 650°C

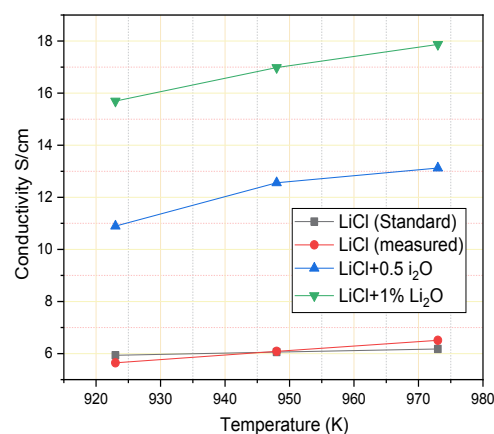


Fig. 2: Variation of electrical conductivity with temperature for LiCl and LiCl-(0.5-1.0%) Li₂O melts.

References:

[1] Elena V. Nikolaeva et al., *Journal of The Electrochemical Society*, **169** (2022) 036511

Measurement of Dielectric Constant and Loss Tangent of Uranium Compounds at 2.45 GHz by Rectangular Waveguide Cavity Resonator

Pasupuleti Kalpana^{1,3,§}, Jayanta Mondal², A.N.Patil¹, S.K.Satpati^{1,3} Rishi Verma^{2,3}

¹ Uranium Extraction Division, B.A.R.C., Mumbai, India

² Accelerator and Pulse Power Division, B.A.R.C., Mumbai, India

³Homi Bhabha National Institute, Mumbai, India

§ Email: pkalpana@barc.gov.in

This paper presents the design and development of a resonant cavity tuned at 2.45 GHz microwave frequency for measurement of dielectric coefficient of different uranium compounds. Depending on the behavior of the material at 2.45 GHz microwave field, it absorbs, reflects or conducts the microwave power. This eventually gets reflected in the Scattering parameters or S-parameters of the cavity. In this experiment, cavity is connected to VNA (Vector Network Analyzer) and S21 parameter is measured in presence and absence of sample uranium compound. Dielectric coefficient of the sample compound can be calculated from the shift in S-parameters, resonance frequency and Q-factor of the cavity.

Resonant cavity perturbation method is suitable for wide range of dielectric properties of materials. The measurements can be done for single frequency and it is suitable for all types of samples i.e. solid, liquid and powder. Guiding equation for finding the dimensions of the cavity is [1]

$$f_{mnl} = \frac{c}{2\pi\sqrt{\mu_r\epsilon_r}} \sqrt{\left[\left(\frac{m\pi}{a}\right)^2 + \left(\frac{n\pi}{b}\right)^2 + \left(\frac{l\pi}{c}\right)^2\right]} \quad (1)$$

From the above calculations cavity dimensions are estimated as 352.6 mm x 72.1 mm x 34.0 mm. WR284 is connected with the cavity for feeding the microwave power. Fig. 1 shows the cavity. The guiding equations for calculation of dielectric coefficients are as follows and the results have been tabulated in Table 1.

$$\epsilon' = 1 + 0.5 \frac{V_c}{V_s} \left(1 - \frac{f_s}{f_0}\right)$$

$$\epsilon'' = 0.25 \frac{V_c}{V_s} (1/Q_c - 1/Q_s)$$

V_c = volume of the cavity resonator.

V_s = volume of the under test dielectric sample

f_0 = Resonant frequency of empty cavity

f_s = shifted Resonant frequency

Q_c = Q value with the sample inside the resonator

Q_s = Q value of the empty resonator.

Material	Resonant frequency	Loss tangent
ADU	2.4480	0.027
U ₃ O ₈	2.4495	0.100
UF ₄	2.4498	0.028
UO ₂	2.4486	0.120

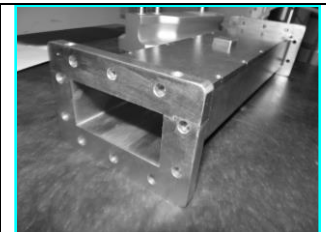


Table 1: Experimental results for different materials

Fig 1 : Resonant Cavity

References:

1. C.K. Kim, et al. 2015 International Symposium on Antennas and Propagation (ISAP), (2015) 1-3.

Determination of Trace Thorium in Uranium Oxide via Direct Solid Sampling in Electrothermal Vapourization Coupled ICP-OES

Abhijit Saha[§], S.B. Deb[§], Khushboo Kumari

Radioanalytical Chemistry Division, BARC, Mumbai, India

[§] Email: asaha@barc.gov.in and sbdeb@barc.gov.in

Uranium compounds are the most commonly used fuel materials in various types of nuclear reactors. The tolerable amounts of various trace impurities in different fuels have stringent specifications. Although the UO₂ fuel in PHWRs has no specification limit for thorium but the fast reactor fuels have stringent specification [1]. This is because the fast neutrons convert ²³²Th into ²³²U which causes high radiation hazard during reprocessing of the burnt fuel as well as in the reprocessed fuels. The analytical procedures available till date involve dissolution of the fuel material followed by separation of Th(IV) from the U(VI) matrix. In order to overcome these cumbersome procedures we had gone for direct solid analysis by ETV-ICP-OES. The solid sampling methodologies generally need matrix matched reference materials for standardization of the process. However, in this work we have controlled the evaporation of the matrix element and the analyte of interest to get rid of the dependence on matrix matched reference material. The ETV parameters like gradient heating, flow of the auxiliary gas (argon), mixed flow of the carrier and reactive gas (CF₄), etc. were optimized to get an online separation of the uranium matrix and thorium trace impurity. The high melting and boiling points of the oxides of U and Th led us to the choice of using a react gas in the ETV chamber which converts them into respective fluorides. The noticeable difference between the boiling points of UF₄ (~1417°C) and ThF₄ (~1680°C) leads to their online separation. The gas flows were optimized to get maximum sensitivity for Th without any interference from U emission lines. A 0.4 L min⁻¹ flow of auxiliary Ar gas and a mixed flow of 0.13 L min⁻¹ Ar + 2.5 mL min⁻¹ CF₄ was found to provide the maximum sensitivity for Th. Using these parameters standard Th solution was drop casted on graphite boats and heated in the ETV to construct the calibration spectrum (R² > 0.99) and using this calibration two UO₂ samples were analyzed. The values were validated using a reported procedure and they are found to be the same in 95% confidence interval [1].

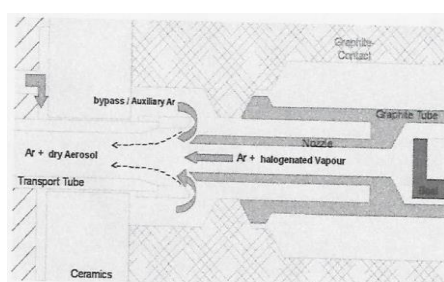


Fig.1: Schematic diagram of ETV

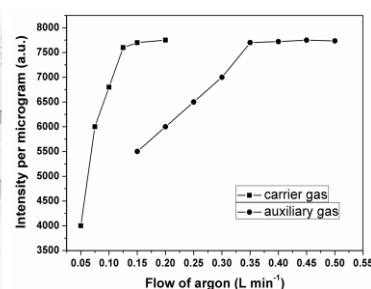


Fig.2: Optimization of Ar

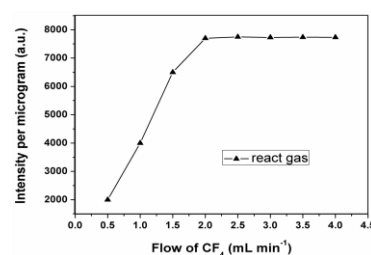


Fig.3: Optimization of react gas flow

Table 1: Analysis of real UO₂ samples (N=5)

Sample name	ETV-ICP-OES (µg g ⁻¹)	ICP-OES (µg g ⁻¹)
UO2-1S	12.4±0.3	12.2±0.2
UO2-2S	7.6±0.3	7.7±0.2

References:

[1] S.B. Deb et al., *At. Spectrosc.*, **29** (2008) 39.

Addictive White Gaussian Noise (AWGN) Incorporated Calibration-Free LAMIS for Improved Direct Boron Isotopic Analysis

Anandhu Mohan^{1,2}, Anannya Banerjee², Arnab Sarkar^{1,2,§}

¹Homi Bhabha National Institute, Mumbai-400094, India

²Fuel Chemistry Division, Bhabha Atomic Research Centre, Mumbai-400085, India

§Email: arnab@barc.gov.in

In recent times calibration-free methodologies have emerged as a promising analytical tool [1]. Calibration-free laser ablated molecular isotopic spectroscopy (CF-LAMIS) is a laser-based spectroscopic technique used for isotopic composition analysis which provides substantial benefits in portability, rapid analysis, and cost-efficiency. Our group has developed a CF-LAMIS methodology that offers reliable accuracy and precision for determining boron isotopic composition [2]. However, the fitting between the simulated and experimental spectra was inadequate due to inherent random noise in the experimental spectra. This study focuses on profiling various detector noises using a photon transfer curve (PTC) and introducing the random noises to the simulated spectra to minimize the fitting error.

Natural boric acid crystals, natural B₄C and ¹⁰B enriched B₄C are used in the present study. The boric acid samples yielded an accuracy and precision consistent with previous studies, whereas the B₄C samples initially proved difficult due to atomic and ionic interference. But the use of BO:B-X (0-1) RVB, in a longer acquisition delay time, minimized these interferences and provided a clearer signal. This approach enabled to achieve reasonable accuracy and precision (~3%) comparable to that of pure boric acid samples and previous studies. These results highlight the effectiveness of the CF-LAMIS method in analyzing complex matrices.

Various noises in the spectrometer-iCCD detector system were profiled (Fig. 1a) and correlated with the recorded signal. This relation was used to generate an additive white gaussian noise (AWGN) model. The introduction of the AWGN model to the simulated spectra led to a significant improvement in precision while maintaining comparable accuracy (Fig. 1b). By applying the AWGN-CF-LAMIS methodology, boric acid samples achieved an accuracy of 0.34% and a precision of 0.83%. Meanwhile, natural B₄C and ¹⁰B-enriched B₄C samples attained accuracies of 0.65% and 0.2%, with corresponding precisions of 0.92% and 0.63%, respectively. This study highlights the new possibilities for advancing the calibration-free methodologies by integrating AWGN for improved accurate and precise measurements.

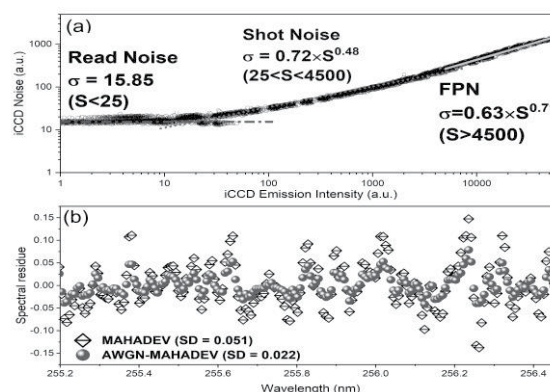


Fig. 1: (a) Relation between noise and recorded signal (b) Spectral residue before and after the addition of AWGN

References:

- [1] Zhang et al., *Frontiers in Physics*, **10** (2022) 446.
- [2] Mohan et al., *Journal of Analytical Atomic Spectrometry*, **38** (2023) 1579.

Application of Electrothermal Vapourization Coupled ICP-OES for Preparing In-house Reference Materials of $Gd_2Zr_2O_7$

S.B. Deb[§], Khushboo Kumari, Abhijit Saha[§]

Radioanalytical Chemistry Division, BARC, Mumbai, India

[§]Email: asaha@barc.gov.in (A. Saha) and sbdeb@barc.gov.in (S.B. Deb)

Gadolinium zirconate ($Gd_2Zr_2O_7$) is a burnable absorber (BA) material which has been proposed as the BA rod in Indian compact high-temperature reactors (CHTR) [1]. The BA rods control the excess reactivity at the beginning of the reactor cycle. In this material, characterization of inseparable trace impurities like Sm, Eu, Tb, Dy, Hf and Y with high neutron absorption cross sections (σ_a) is indispensable. The pyrochlore structure of $Gd_2Zr_2O_7$ makes it highly refractory in nature and requires cumbersome microwave assisted dissolution for analytical measurements. Direct solid analysis of this material needs certified reference material (CRM) which is commercially unavailable. Hence we synthesized six $Gd_2Zr_2O_7$ standard samples by mixing pure and impure lots of starting materials viz., Gd_2O_3 and ZrO_2 . The resulted crystalline powder samples were analyzed in XRD for phase conformation (Fig. 1). In order to characterize these samples we have used electrothermal vapourization coupled ICP-OES (ETV-ICP-OES) (Fig. 2). Appropriate volumes of MERCK made 10000 $mg.L^{-1}$ solutions of Gd and Zr were mixed with 1000 $mg.L^{-1}$ analyte solutions to prepare synthetic standard solutions. These solutions were dried and heated in a Muffle furnace at 1000°C and then taken on the graphite boat to inject into the ETV. The heating profile in the ETV was optimized to get maximum sensitivity of the analytes. Various combinations like heating at 2500°C in a flow of Ar + CF_4 , in-situ fusion with NH_4HF_2 at 230°C followed by heating at 2500°C in a flow of only Ar or Ar + CF_4 were performed. It was found that the in-situ fusion mechanism followed by heating at 2500°C in a flow of Ar + CF_4 easily evaporates maximum amount of analytes as their fluorides (Fig. 3a & 3b). Using this vapourization step external calibration of all the analytes were carried out ($R^2 > 0.99$) and the six in-house made standard samples were analyzed. These results were validated by analyzing those standard samples by a reported ICP-OES procedure and the values are found to be the same at 95% confidence interval [1].

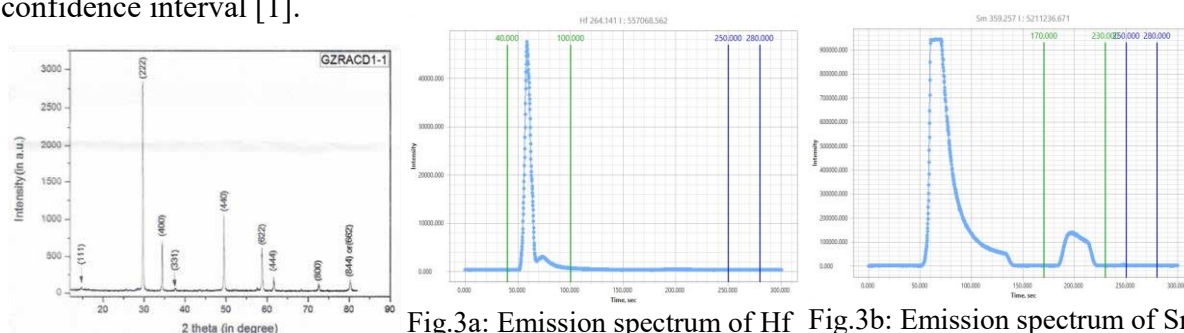


Fig.1: XRD spectrum of synthesized $Gd_2Zr_2O_7$

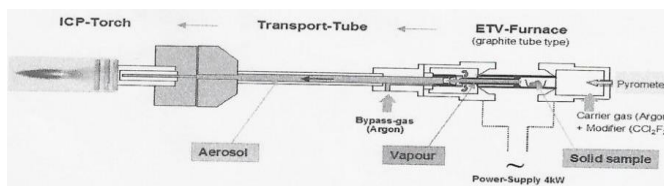


Fig.2: Schematic diagram of ETV-ICP-OES

References:

[1] A. Saha et al., *RSC Adv.*, **14** (2024) 31422.

Characterizing Isotopic Fractionation in Boron Plasma Plume Produced by Laser Ablation

Anandhu Mohan^{1,2}, Anannya Banerjee², Arnab Sarkar^{1,2,§}

¹Homi Bhabha National Institute, Mumbai -400094, India

²Fuel Chemistry Division, Bhabha Atomic Research Centre, Mumbai-400085, India

[§]E-mail: arnab@barc.gov.in

The formation of laser-induced plasma (LIP) involves multiple complex mechanisms initiated by laser-matter interactions. During laser ablation, preferential excitation or removal of specific isotopes can alter their relative abundances in the plasma, leading to isotopic fractionation [1]. Understanding this fractionation within the LIP plume is essential for improving analytical techniques such as Laser Ablation Molecular Isotopic Spectrometry (LAMIS). In this study, boron was selected as a model element to investigate the isotopic fractionation process. The insights gained from this work contribute to optimizing LIP-based methods, enhancing measurement accuracy, and improving the reliability of both qualitative and quantitative analyses.

The emissions from the laser-ablated plasma were recorded using a Czerny–Turner spectrograph coupled with an iCCD detector. The isotopic composition was calculated using CF-LAMIS methodology coupled with an in-house written MAHADEV algorithm [2]. The distinct band-head appearance of ¹¹BO and ¹⁰BO rotational-vibrational bands (RVB) observed at different spatial locations provided initial evidence of isotopic fractionation. The calculated isotopic composition of ¹⁰B showed a deviation from the natural isotopic ratio near the ablation point, which progressively increased toward the periphery of the LIP (Fig. 1).

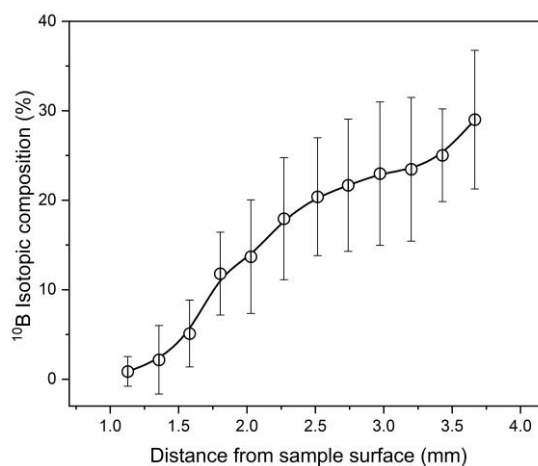


Fig. 1: ¹⁰B isotopic composition variation with respect to distance from sample surface

The vertical and horizontal spatial profile of LIP indicates that the ¹⁰B isotopic composition is significantly lower near the ablation point. As the LIP expands horizontally and vertically, the ¹⁰B isotopic composition increases in a uniform scale. The lighter isotopes preferentially migrate with the expanding plasma, likely driven by shockwave-induced expansion mechanisms within the LIP. Further investigation into fractionation trends under different atmospheric conditions suggests that plasma temperature gradients play a significant role in governing isotopic fractionation within the plume. These findings provide valuable insights into the spatial orientation of particles within plasma, helping to optimize different analysis methodologies for achieving better accuracy and precision.

References:

[1] Kuhn et al., *Journal of Analytical Atomic Spectrometry*, **22** (2007), 547.

High-Precision Measurement of ${}^6\text{Li}/{}^7\text{Li}$ Isotopic Abundance in Highly Depleted ${}^6\text{LiF}$ for Molten Salt Reactor

Preeti Goswami¹, K. Sasi Bhushan^{1,§}, P. G. Jaison²

¹ Fuel Chemistry Division, Bhabha Atomic Research Centre, Mumbai, India

² Radioanalytical Division, Bhabha Atomic Research Centre, Mumbai, India

§ Email: sashi@barc.gov.in

Lithium Fluoride (LiF) is an essential component of the fuel as well as of the coolant in the molten salt reactors. However, ${}^6\text{Li}$ has a higher neutron capture cross-section (~ 940 b) compared to ${}^7\text{Li}$ (~ 0.003 b), hence the large coolant volume in MSR necessitates the use of LiF, having extremely low ${}^6\text{Li}$ abundance ($<0.01\%$), to maintain the neutron economy. ${}^6\text{Li}/{}^7\text{Li}$ ratio measurement in this highly depleted ${}^6\text{LiF}$ is essential for the chemical quality assurance. Precise measurement of atom ratio of such low abundant isotopes is a challenging task. Due to the significant relative mass difference ($\sim 13\%$), lithium isotopes exhibit severe isotopic fractionation in the Thermal Ionization Mass Spectrometric analysis using atomic ions.

Recently, our laboratory developed a precise and accurate TIMS method for the measurement of lithium isotopic ratio by adding sodium borate and monitoring the resultant NaLiBO_2^+ ions (m/z 71 – 73) and Na_2BO_2^+ (m/z 88 & 89), in which ${}^6\text{Li}/{}^7\text{Li}$ isotope ratio can be obtained from either of the two polyatomic ion abundance ratios ${}^{71}\text{I}/{}^{73}\text{I}$ and ${}^{72}\text{I}/{}^{73}\text{I}$ [1]. This ${}^{71}\text{I}/{}^{73}\text{I}$ ratio offers good accuracy and precision for highly enriched ${}^6\text{Li}$ but is not suitable for samples with low ${}^6\text{Li}$ abundance. The other ratio, ${}^{72}\text{I}/{}^{73}\text{I}$, necessitates a correction for boron isotope contributions. This correction is achieved by subtracting the ${}^{10}\text{B}/{}^{11}\text{B}$ ratio obtained from the ${}^{88}\text{I}/{}^{89}\text{I}$ measurement as given in the equation, ${}^6\text{Li}/{}^7\text{Li} = {}^{72}\text{I}/{}^{73}\text{I} - {}^{88}\text{I}/{}^{89}\text{I}$. As shown in the table 1, when sodium borate with natural boron, added to natural lithium sample, it results in 25% relative difference between ${}^{72}\text{I}/{}^{73}\text{I}$ and ${}^{88}\text{I}/{}^{89}\text{I}$ isotope ratios. This large difference helps in achieving the precise and accurate isotope ratio of ${}^6\text{Li}/{}^7\text{Li}$. However, when natural boron is added to depleted ${}^6\text{Li}$ (typically 0.003%), this difference between the ratios diminishes to 0.012%. Thus, a slight deviation in the measurement of either ${}^{72}\text{I}/{}^{73}\text{I}$ or ${}^{88}\text{I}/{}^{89}\text{I}$ isotope ratio can potentially cause significant error in the determination of ${}^6\text{Li}/{}^7\text{Li}$.

Table 1: Isotopic abundances and polyatomic ion ratios

${}^6\text{Li}$ (abundance in %)	Natural	0.003		
${}^{10}\text{B}$ (abundance in %)	Natural	0.1	0.01	
$R = {}^{72}\text{I}/{}^{73}\text{I}$	0.3294	0.25003	0.001030	0.00013
$B = {}^{88}\text{I}/{}^{89}\text{I}$	0.2844	0.25000	0.001001	0.00010
% Difference in R & B	25	0.012	3	23

In order to circumvent this difficulty, we added sodium borate solution with ${}^{10}\text{B}$ abundance $\sim 0.01\%$ to the lithium samples with ${}^6\text{Li}$ abundance $\sim 0.15\%$ (which is the least abundant ${}^6\text{Li}$ available at present), in such a way that the mole ratio of Li/Na ~ 1 and B/Na ~ 10 . As the % difference between ${}^{72}\text{I}/{}^{73}\text{I}$ and ${}^{88}\text{I}/{}^{89}\text{I}$ isotope ratios is ~ 23 , an external precision of better than 0.15% was achieved for ${}^6\text{Li}/{}^7\text{Li}$ when faraday cups were employed. Future studies will be carried out by employing ion counters like Secondary Electron Multiplier, to improve the precision and accuracy of the measurement of ${}^6\text{Li}$ at still lower isotopic abundances.

References:

[1] K. Sasi Bhushan, et. al., *J. Radioanal. Nucl. Chem.*, **326** (2020)1009.

Trace Boron Determination in Graphite by Isotope Dilution-Thermal Ionization Mass Spectrometry

K. Sasi Bhushan^{1,§}, Preeti Goswami¹, P. G. Jaison²

¹ Fuel Chemistry Division, Bhabha Atomic Research Centre, Mumbai, India

² Radioanalytical Division, Bhabha Atomic Research Centre, Mumbai, India

§ Email: sashi@barc.gov.in

Nuclear-grade graphite, essential for use as a moderator, reflector, and structural material, requires precise control of boron impurity (0.06-0.4 mg/kg) due to the significant impact of ¹⁰B (having a large neutron capture cross-section) on neutron economy. Analytical methods for determining boron usually involve extensive sample preparation, including alkali fusion with barium or sodium hydroxide at ~800°C, followed by acid dissolution [1,2].

The present study aims at developing an Isotope Dilution-Thermal Ionization Mass Spectrometry (ID-TIMS) method for the determination of boron in graphite matrix with minimal sample preparation. This involves adding a ¹⁰B-enriched spike to the graphite powder, along with sodium carbonate (B/Na mole ratio ~0.1) and mannitol (40 times to the boron amount) in an acid leached quartz beaker. It is reported in the literature that the boron-mannitol complex resists vaporization losses and isotopic fractionation during high-temperature processes, and thus has been employed in ETV-ICP-MS, TIMS etc. Moreover, in the acidic medium, mannitol is deliberately added to the boron compound to prevent boron loss during evaporation [3-5]. This mixture is heated to dryness on the hot plate and further heated to 650°C for 3 hours in a muffle-furnace. The residue, then dissolved in high purity water and loaded onto a rhenium single filament for TIMS analysis. A graphite coating was done on the Re-filament for the enhancement in the signal intensity. Boron isotope ratio measurement was carried out by monitoring sodium metaborate (Na₂BO₂⁺) ions. In the present work, a reference material with a boron concentration of 7.8 ppm, significantly higher than anticipated in actual samples was used for the initial trials [2]. A higher boron level is desirable during method development to monitor potential losses and fractionation. Future validation of the method will involve analyzing samples with sub-ppm boron levels. Though the present methodology requires minimal sample preparation, a precision of ~6% was obtained for the determination of boron concentration, as shown in the Table 1. Further studies are in progress to improve the precision and the bias of the measurement.

Table 1: Analytical results

Experimental parameters	Boron concentration in graphite IRM (in µg/gm)	
	Assigned value	Measured value (present study)
Mole ratio of B/Na ~ 0.1; Mannitol added: 40 times to boron; Heating conditions: 650°C for 3 hours.	7.30 ± 0.46	8.1 ± 0.5

References:

- [1] S. Dasgupta, et. al., *J. Radioanal. Nucl. Chem.* **328** (2021) 33.
- [2] Sanjukta A. Kumar et. al., *BARC REPORT*, BARC/2016/E/005.
- [3] W.C. Wei, C.J. Chen, M.H. Yang, *JAAS* **10** (1995) 955.
- [4] E. Nakamura, et. al., *Chemical Geology*, **94** (1992) 193.
- [5] R. M. Rao, et. al., *Int. J. Mass Spectr.* **273** (2008) 105.

Determination of Impurities in Helium Bond Gas of FBTR Fuel Pins

M. Phanindra Kumar, P.S. Ramanjaneyulu[§], Sunil Kumar,
A.S. Kulkarni, B.K. Nagar, M.K. Saxena

Radioanalytical Chemistry Division, Bhabha Atomic Research Centre, Mumbai, India

[§] Email: psr@barc.gov.in

Due to its high thermal conductivity and radiation stability, helium gas is being used as a bond gas in FBTR nuclear fuel pins for effective heat transfer from fuel pellets to the clad material. It requires impurity analysis as part of chemical quality control. The Radiochemistry & Isotope Group has been conducting this analysis for four decades [1]. However, the current setup cannot detect impurities in high-purity helium gas due to low sensitivity and poor vacuum sustainability. This data is crucial for identifying contamination sources in the bond gas of nuclear fuel pins. Therefore, a new gas collection chamber was designed and fabricated and then coupled with a gas chromatograph equipped with highly sensitive detector i.e. helium discharge pulse ionization detector (HDPID) as well as puncturing unit located inside the glove box. After optimizing all analytical parameters, calibration plot was constructed between peak area in the chromatogram and pressure of the helium based gas standard having 5000 ppm of H₂ and 100 ppm of O₂, N₂, CH₄, CO. Calibration plot is given in Figure 1. An FBTR nuclear fuel pin was punctured; gases were extracted into pre-evacuated collection chamber; pressure of the gas was monitored and then gas sample was fed into the GC for obtaining chromatogram. Using the observed peak areas, gas pressure and the calibration data, the concentration of all impurities was calculated. Typical results are shown in Table 1. The results indicate that the contribution of impurities from the starting filling gas is negligible. However, a significant amount of hydrogen (H₂) was observed in the analysis of the dummy fuel pin, where only the fuel pellets differ from the actual fuel pin configuration. This may be due to the adsorption of moisture on the surface of the clad tube from the atmosphere, which could decompose during the welding process, releasing H₂ into the gas. In actual pins, this adsorbed moisture may further react with the carbide fuel pellets [2], releasing CH₄ and H₂ into the helium bond gas. The presence of nitrogen in the bond gas may be attributed to contamination from the glove box atmosphere.

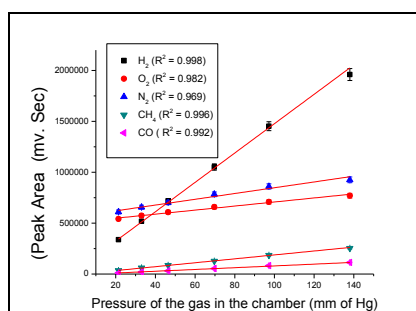


Fig.1. Calibration plot obtained using He based gas standard.

Table 1. Typical results of impurity analysis in various gases

Type of the gas sample	Hydrogen (%)	Oxygen (ppm)	Nitrogen (%)	Methane (ppm)	Carbon monoxide (ppm)
H.P. He gas Cylinder	0.0005 ± 0.0001	20 ± 2	0.0030 ± 0.0003	BDL	BDL
Dummy Pin-1	0.78 ± 0.08	210 ± 20	0.22 ± 0.02	50 ± 5	70 ± 10
FBTR Fuel Pin	2.53 ± 0.25	190 ± 20	0.16 ± 0.02	1060 ± 100	70 ± 10

BDL: Below detection limit of the method i.e. 0.5 ppm of impurity

Acknowledgements: Authors are thankful to Dr. P.G. Jaison, Head, RACD for his keen interest in this work.

References:

- [1] S.G. Kulkarni et al., *J. of Chromatographic Science*, **23** (1985) 68.
- [2] M.J. Bradely et al., *Inorganic Chemistry*, **1** (1962) 683.

Studies on the Kinetic Effect of Hydrogen Isotope Oxidation using Copper Oxide Beads

Jitendra Singh[§], Sandeep K C, Kalyan Bhanja

Heavy Water Division, Bhabha Atomic Research Centre, Trombay, Mumbai, India

[§] E-mails: jitendras@barc.gov.in

Hydrogen isotopes are the fuel for nuclear fusion reactor such as ITER. Hydrogen can permeate from three barriers of containments, of its handling systems viz. subsystems of fusion reactor systems, isotope separation system and enrichment facilities. Removal of hydrogen isotopes from inert gas in gloveboxes is necessary to minimise its exposure to operational and maintenance personnel. Hydrogen isotope oxidation using copper oxide as per equation (1) is one of the approaches to extract hydrogen isotopes from inert gas.



Subsequently, effluent oxides of H₂ isotopes from packed bed reactor are captured from inert gas using molecular sieves or silica gel beds. Even there are multiple reaction kinetics studies in literature, it is observed in the present study that gas-solid reaction (1) using CuO on Al₂O₃ spheres of diameters more than 0.5mm is in internal diffusion-controlled regime [1]. In the present study, the breakthrough data for hydrogen and deuterium oxidation using 10% copper oxide loaded on alumina beads have been generated at different temperatures up to 350°C using known feed gas mixture of H₂ in N₂ and D₂ in N₂. Process flow diagram of experimental system and typical breakthrough curve of hydrogen and deuterium conversion versus time are shown in Fig. 1 and Fig. 2 respectively.

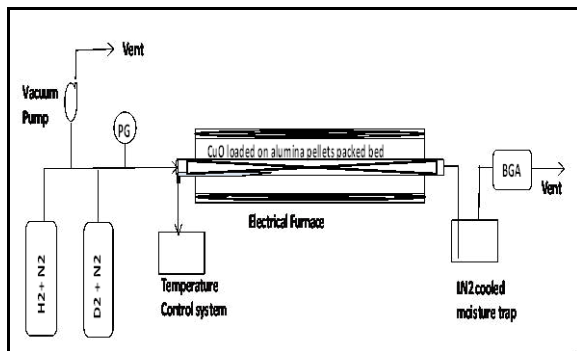


Fig. 1: Process flow diagram of experimental system

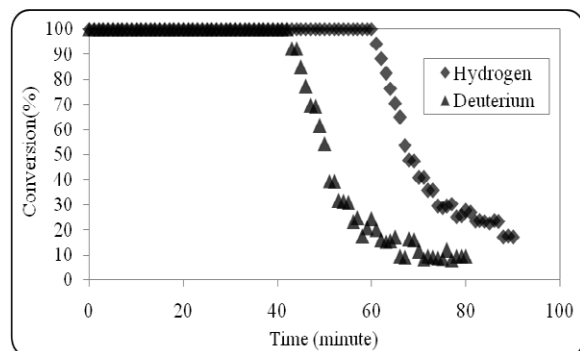


Fig. 2: Breakthrough curve for H₂ and D₂

It is observed from different experimental data that there is significant isotopic effect on gas-solid reaction kinetics on CuO in the present operating regime. These findings will be useful for design and scale up of CuO packed bed reactor for removal of radioactive hydrogen isotopes from nitrogen and helium inert gases.

References:

- [1] R. Bhattacharyya, K. Bhanja, S. Mohan, *Fusion Engineering and Design*, **100** (2015) 560.

Application of Fluoro-Phosphate Salts for Uranium Determination in Tin Slag, Zircon and Sillimanite Minerals via LED Fluorimetry

C. Santosh Reddy, V. V. Hanuman[§]

Chemistry Lab, Atomic Minerals Directorate for Exploration and Research, NER, Shillong.

[§] Email: vvhanuman.amd@gov.in

Determination of uranium in tin slag, zircon and sillimanite is crucial for nuclear industry (secondary resource utilization), geological research, and enhancing the value of these materials. Of the many techniques available for uranium determination, Light Emitting Diode (LED) fluorimetry is a simple, accurate, fast, and cost-effective technique. It requires the addition of fluorescence enhancing reagents (FERs) for uranium determination. The commonly used salts for fluorescence enhancement of uranium are phosphates and fluorides. Various phosphate fluxes are used to decompose the non-silicate minerals and act as FERs at the same time [1]. But these salts have limitations in decomposing silicate minerals, and can't be applied on tin slag, zircon and sillimanite, which are silicate minerals. These minerals, also being refractive, are resistant to standard acid digestion. The methods in literature for decomposition of these minerals are based on fusion with fluxes like NaF-KHF₂, Na₂O₂, KHSO₄. These methods again require acids for dissolution, have stability issues, and require addition of FER for uranium determination by LED fluorimetry. Hence, authors attempted to digest these minerals utilizing a mixture of fluoride and phosphate salts to develop a rapid and environmentally friendly method for uranium determination, which does not require addition of FER externally.

A 0.1-0.2g mineral sample was weighed in a platinum crucible and was treated with 4g flux of mixed fluoride (1:3 NaF-KHF₂) and NaH₂PO₄ in 1:3 ratio for half an hour at 800 °C in a muffle furnace. The fused mass was dissolved in distilled water in a polypropylene beaker heated on a water bath. The solution obtained was made up to 100 ml in a polypropylene volumetric flask. A suitable aliquot was taken for uranium fluorescence measurements using LED Fluorimeter (M/s Quantalase make, Uranium Analyser UA-2) without external FER. The fluoro-phosphate flux combination used in this method has completely decomposed tin slag, zircon and sillimanite mineral samples in a shorter time compared to the other fusion methods; fluoride removes silica, and the rest of the elements dissolved as phosphates in distilled water medium. The dissolution step avoids hazardous acids, and the solutions have more stability (over one month), making the method user and environment friendly. Also, this combination of flux has lower process blank values and higher signal to blank ratio, comparatively [2]. The present method, developed by integrating advanced flux chemistry with latest fluorescence detection technique was validated with conventional pellet fluorometry procedure, due to non-availability of certified reference materials and the results are given in table-1. The results are in close agreement and the relative standard deviation of the present method is ± 5%.

Table 1: Comparison of uranium values in mineral samples

Name of mineral	U (ppm) by present method	U (ppm) by Pellet Fluorimetry
Tin Slag-1	332	346
Tin Slag-2	364	353
Zircon	245	261
Sillimanite-1	17	15
Sillimanite-2	3	<10

References:

- [1] R. Radhamani et.al. *J Radio analytical and Nuclear Chemistry*, **285** (2010), 287.
 [2] C. Santosh Reddy et.al. *Proceedings of CAMC-2024*, 55.

Effect of Annealing Conditions on Diffusion of Deuterium in Zircaloy-4 Clad Material

Sunil Kumar^{1,2}, P.S. Ramanjaneyulu^{1,2,§}, M. Phanindra Kumar¹,
A.S. Kulkarni¹, B.K. Nagar¹, M.K. Saxena¹

¹ Radioanalytical Chemistry Division, B.A.R.C., Mumbai-85.

² Homi Bhabha National Institute, Anushaktinagar, Mumbai-94

§ Email: psr@barc.gov.in

Zircaloy-4 (Zry-4) is used as a cladding material in IPHWRs. Hydrogen (H) embrittlement can deteriorate the mechanical properties of this structural material. Hydrogen migration plays a crucial role in understanding hydrogen embrittlement. Therefore, studies were initiated to investigate the effect of annealing conditions on the diffusion of deuterium (D) in Zircaloy-4. Deuterium was chosen to eliminate background H interference. It is well known that the diffusion coefficient is not influenced by other solute atoms in the matrix for dilute solutions (at low concentration) [1]. Therefore, it could be assumed that D diffusion is independent of dissolved H present in the matrix as an impurity. For the present studies, the time and temperature of annealing were optimized, and a temperature of 1073 K with varying annealing times was selected to grow the grain size. Samples were vacuum-sealed in quartz tubes for annealing to prevent oxidation of samples and then annealed for 48 h and 326 h. One end of sample clad tube (~10 cm) was polished and then D was charged electrochemically. These charged pieces were again vacuum-sealed and then annealed at 523 K for 241 h to diffuse deuterium from charged end to the rest of the matrix. From these samples, 1 mm slices were cut along the axial direction and then D content was determined employing Hot Vacuum Extraction Quadruple Mass Spectrometry (HVE-QMS) technique. The deuterium diffusion coefficient (D_D) was estimated by non-linear fitting of the data to the equation obtained by solving Fick's second law of diffusion for a semi-infinite medium with an infinite source as boundary conditions. Experimental data with fitted curve along with diffusion coefficients values is shown in Fig. 1.

$$(C_x - C_0) = (C_s - C_0) \times \operatorname{erfc}\left(\frac{x}{2\sqrt{Dt}}\right) \dots (1)$$

From the figure, it could be observed that the D_D value is increased with time of annealing. It is well known that grain size increases with time of annealing at 1073 K. A similar trend was observed in our previous studies where effect of grain size on D_D in Zry-4 was studied at 623K [2]. For a unit volume of the matrix, grain boundary fraction increases with decrease in grain size which decreases D_D value. Therefore, it could be concluded that grain boundaries act as trapping sites for D, which retard its diffusion in Zry-4.

Acknowledgements: Authors are thankful to Dr. P.G. Jaison, Head, RACD for his keen interest in this work.

References:

1. Crank, J. *The Mathematics of Diffusion*. 2nd edition, Oxford University Press, London, (1975) 2.

where, C_x =conc. at distance x ,
 C_s =interface conc. (M-MH),
 C_0 =background conc., D =
Diffusion Coefficient, t = time.

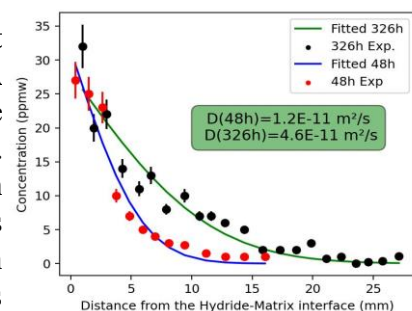


Fig. 1: Deuterium concentration profile with D_D values.

Thermophysical Properties of Intermediate Ternary Compounds Relevant to LiF-ThF₄-UF₄ System

Abhishek Kumar Rai^{1,3,§}, M.K. Sharma^{2,3}, S.K. Rakshit¹

¹ Product Development Division, RC&IG, BARC, Mumbai, India

² Fuel Chemistry Division, RC&IG, BARC, Mumbai, India

³ Homi Bhabha National Institute, Anushaktinagar, Mumbai, India

§ Email: abhirai@barc.gov.in

Heat transport properties like thermal diffusivity and thermal conductivity of the fuel and coolant salts directly influence the energetics of the fuel during heating/cooling cycles as well as the heat transfer. Specific heat capacities, thermal diffusivities and thermal conductivities of various intermediate ternary compounds related to LiF-ThF₄ and LiF-UF₄ systems were measured experimentally by *HF-DSC* (*DSC-131*) and laser flash techniques (*LFA-1000*), respectively. Thermal diffusivities and thermal conductivities of these compounds have been measured for the first time.

Li₃ThF₇, Li₇Th₆F₃₁, LiTh₂F₉, LiTh₄F₁₇, LiUF₅ and LiU₄F₁₇ were synthesized by solid-state reaction route using LiF, ThF₄ and UF₄ as starting materials. ThF₄ was prepared by hydro fluorination of ThO₂ by NH₄HF₂ [1]. All the prepared compounds were characterized by *XRD* and *DTA* techniques. The upper stability temperatures of the compounds were determined by indigenously designed *DTA*. Specific heat capacity measurements were carried out by standard three step method in continuous mode with a heating rate of 5 K.min⁻¹ using α -Al₂O₃ (*SRM 720*) as reference material. For measurement of thermal diffusivities, the samples (disc shape) were coated with graphite spray to enhance the emission/absorption properties of the sample. All experiments were done under *HP-Ar* atmosphere below the upper stability points.

Thermal diffusivity (α) is related to the thickness of sample (l) and time required for attaining the maximum temperature rise at the other surface of sample ($t_{1/2}$) as follows [2]:

$$\alpha = 0.13879 \times l^2 / t_{1/2} \quad (1)$$

Thermal conductivity (λ) was calculated from thermal diffusivity (α), specific heat capacity (C_p) and geometrically determined density (ρ) of the sample as $\lambda = \alpha \times C_p \times \rho$.

Specific heat capacities, thermal diffusivities and thermal conductivities determined in this work are tabulated in Table 1.

Table 1. Upper stability points, specific heat capacities, thermal diffusivities and thermal conductivities of Li₃ThF₇, Li₇Th₆F₃₁, LiTh₂F₉, LiTh₄F₁₇, LiUF₅ and LiU₄F₁₇

Compound	Upper Stability Point	C_p (Jg ⁻¹ K ⁻¹)	α (cm ² s ⁻¹)	λ (Wm ⁻¹ K ⁻¹)	Temp. Range
Li ₃ ThF ₇	823 K	$0.649 + 1.57 \times 10^{-5} \times T - 7374.42/T^2$	$0.0040 + 1.28/T$	$1.35 + 139.1/T$	300-700 K
Li ₇ Th ₆ F ₃₁	870 K	$0.508 + 8.48 \times 10^{-5} \times T - 5538.83/T^2$	$0.0042 + 1.54/T$	$1.27 + 192.1/T$	300-700 K
LiTh ₂ F ₉	1038 K	$0.447 + 5.32 \times 10^{-5} \times T - 4736.93/T^2$	$0.0045 + 1.14/T$	$1.33 + 249.7/T$	300-900 K
LiTh ₄ F ₁₇	1176 K	$0.422 + 4.05 \times 10^{-5} \times T - 4413.36/T^2$	$0.0046 + 1.88/T$	$1.38 + 294.9/T$	300-1000 K
LiUF ₅	880 K	$0.489 + 7.95 \times 10^{-5} \times T - 4278.77/T^2$	$0.0036 + 1.47/T$	$1.11 + 220.9/T$	300-700 K
LiU ₄ F ₁₇	1045 K	$0.419 + 4.36 \times 10^{-5} \times T - 3298.36/T^2$	$0.0036 + 1.70/T$	$1.13 + 311.7/T$	300-900 K

References:

[1] Wani et al., *Journal of Fluorine Chemistry*, **44** (1989) 177.

[2] Parker et al., *J. Appl. Phys.*, **32** (1961) 1679.

Liquid Chromatography Separation of Rare Earths Impurities in Gadolinium Zirconate, a Burnable Poison Material

Vaibhavi V. Raut¹, S. Jeyakumar^{2,3,§}, M.K. Saxena¹

¹ Radioanalytical Chemistry Division, Bhabha Atomic Research Centre, Mumbai, India

² Radiochemistry Division, Bhabha Atomic Research Centre, Mumbai, India

³ Homi Bhabha National Institute, Mumbai, India

§ Email: sjkumar@barc.gov.in

Gadolinium zirconate ($Gd_2Zr_2O_7$) is used as a burnable poison in nuclear reactors. Determination of rare earth impurities in $Gd_2Zr_2O_7$ is essential in order to ascertain the performance of the material. However, this poses analytical challenges including the difficulty in separating trace rare earths from a rare earth element (Gd) matrix and difficult to digest in acid media due to the highly refractive nature of $Gd_2Zr_2O_7$. The present study is aimed at exploring the feasibility of separating all the rare earth elements in $Gd_2Zr_2O_7$ using HPLC. A microwave-assisted method was followed to digest $Gd_2Zr_2O_7$ and taken in appropriate nitric acid medium (1% HNO_3) prior to separation of rare earths [1].

An HPLC method was developed with a view to inject the dissolved solution of $Gd_2Zr_2O_7$ directly into the separation column. The separation method was developed by using a RP-column (C18, ODS) dynamically modified with camphor-10-sulphonic acid (CSA), an ion-pairing agent and α -HIBA as complexing agent. A gradient elution profile was devised in which the concentration of α -HIBA was varied from 0.03M to 0.25M (pH4) for separating all the lanthanides. With this gradient elution, it was seen that Zr appeared along with Lu. Further modifications were incorporated in the initial concentration of α -HIBA to elute Zr prior to Lu. Owing to the high detection limit of lanthanide-Arsenazo III complexes in UV-VIS detector, we could not detect the rare earth impurities in HPLC. Hence, during the method development, sample solutions were spiked with rare earth standards and explored the feasibility of separating all lanthanides from the matrix Gd. The method enables the fraction collection of separated fractions of rare earths, which can be further analysed by ICP-MS for their quantification.

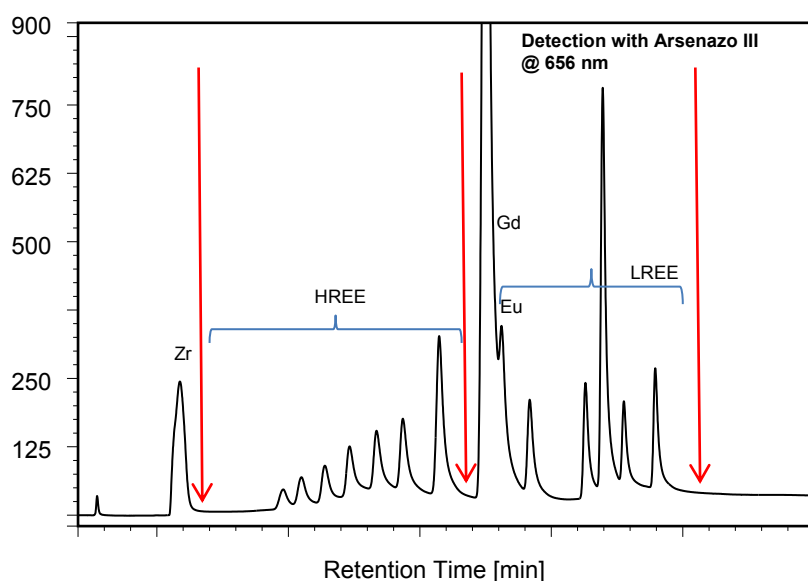


Fig 1: Chromatogram obtained for the $Gd_2Zr_2O_7$ sample spiked with 1 ppm REE. Column: ODS-2 RP Column; Eluent: concentration gradient of α -HIBA (pH 4).

Reference:

[1]. Abhijit Saha, et. al., *RSC Adv.*, **14** (2024) 31422.

Solubility of Nickel in Molten Sodium Hydroxide

S.M. Bhojane^{1, §}, V. Chandanshive¹, E.D Shiny Sam¹, H.V. Khadilkar¹, P. Ginish Kumar¹,
B.D.Thakur¹, P. Samui¹, A. Saha², S.K. Rakshit¹, S.C. Parida¹

¹ Product Development Division, Bhabha Atomic Research Centre, Mumbai, India

² Radioanalytical Chemistry Division, Bhabha Atomic Research Centre, Mumbai, India

§ Email: santoshm@barc.gov.in

The solubility of nickel in molten NaOH was determined in the temperature range of 723 to 903 K. Nickel and nickel-based alloys are used for structural materials for high temperature molten salt reactor. The solubility data on fuel, fission products and structural materials in molten salts is prime requirement for choosing these as structural materials in a conceptual design of Indian molten salt reactor. The experimental assembly is designed and set up in our laboratory for generating the solubility data of fluoride system relevant to molten salt reactor [1] and the schematic diagram is shown in Fig. 1. The assembly set up was first tested and validated by studying the solubility of TiO₂ in molten NaOH. In the experimental set up, sample container used, was made of Nickel. Hence, the experiment was carried out to study the solubility of Nickel in molten NaOH [2-3]. The analytical grade solid NaOH (Purity: 99%) and metallic Ni ring (dia: 12.6 mm, thickness: 1.2 mm) were used for the experiments. Each experiment was carried out at constant temperature for an half an hour under high pure argon atmosphere. The solubility of nickel was found out by weighing the metallic Ni piece before and after the experiments. The solubility data obtained is tabulated in Table -1 and the variation as a function of temperature is shown in Fig. 2. The result of this study indicates a very low solubility of Ni in molten NaOH and increases as a function of temperature.

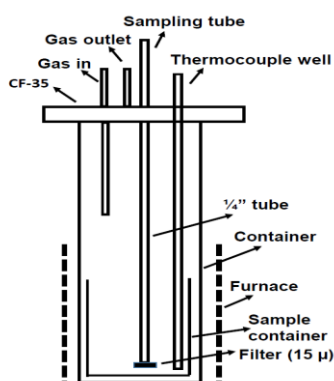


Fig. 1: Assembly sketch

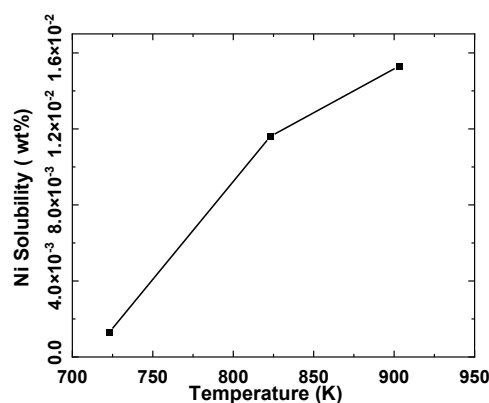


Fig. 2: Temperature dependence of Ni solubility

Table 1: Solubility of Ni against Temperature

Temperature (K)	Wt. of NaOH (g)	Wt. of Ni ring before expt. (mg)	Wt. of Ni ring after expt. (mg)	Ni Solubility in NaOH (wt.%)
723	100.2	325.14	323.83	0.0013 (± 7.1%)
823	98.7	318.24	306.79	0.0116 (± 0.8%)
903	99.5	310.54	295.31	0.0153 (± 0.6%)

References:

- [1] D.D. Sood et al, *Nuclear Technology*, **27** (1975) 411.
- [2] M. Komath, *Materials Chemistry and Physics*, **45** (1996) 171.
- [3] Birgitte Stoffersen et al, *Heliyon*, **10** (2024) e31995.

Quality Control of Materials for Reactor Applications

S. Sriram^{1,§}, Manisankar Palai¹, V. Hemalatha¹, S Maji¹, K. Sundararajan^{1,2}

¹ Materials Chemistry & Metal Fuel Cycle Group, IGCAR, Kalpakkam, 603 102, India

² Homi Bhabha National Institute (HBNI), IGCAR, Kalpakkam, 603 102, India

§ Email: sram@igcar.gov.in

Tungsten carbide (WC) and Ferro boron (FB) are envisaged as candidate materials for their application as lower axial shield in nuclear reactors. Hydraulic relief pots are used as passive safety relief device in the gas systems of fast breeder reactors. Pressure in the upstream side of the relief pot is relieved by bubbling the gas against a liquid column. Mercury is used as the liquid column in many relief pots in various gas circuits. Galinstan is an alternate to mercury due to its non-toxicity. Binary eutectic Tin-Bismuth alloy is used in rotating plugs meant for fuel handling in the reactor vessel due to its low melting point property. It is important that the sealant is free from poison elements apart from the elements that are meant to cause corrosion during its prolonged operation. The current work explores the quality control in these materials that have applications in nuclear reactors using ICP-OES after microwave assisted dissolution.

For WC samples, in order to improve the detection limit, removal of W matrix as tungstic acid was attempted and WC was dissolved without HF by using nitric acid and hydrogen peroxide in microwave digestion. Standard addition studies indicated the precipitation of Fe and the extent of precipitation was found to vary with the concentration of Fe. Percentage recovery in standard addition studies was used to calculate the detection limit of Fe. When B₄C containing W was analysed for Fe by following fusion method, precipitation of tungstic oxide on dissolution was found to result in lower Fe concentration when compared with MW dissolution, indicating the co-precipitation of Fe. For ferro-boron samples, a separate study on co-precipitation of impurity elements along with matrix element was carried out. Spectral interference study for the analysis of boron in Ferro-boron by ICP-OES was carried out and highly sensitive B 249.773 nm line was found to have wing overlap from Fe matrix (249.782 nm). Hence, use of 182.641nm for B was recommended and use in the analysis of boron in the sample. Similar microwave digestion procedure was carried out on galinstan alloy and liquid metal sealant the results of composition characterization achieved using ICP-OES are tabulated in Table 1.

Table 1. Impurities present in Galinstan alloy and binary eutectic Tin-Bismuth alloy liquid metal seal analysed by ICP-OES following microwave digestion.

Gallinstan alloy		Binary eutectic Tin-Bismuth alloy	
Elements	Conc. (%)	Elements	Conc. (%)
Ge	0.0064	Sn	40.84 %
Zn	0.0020	Bi	58.53 %
Fe	0.0010	Pb	0.10 %
Cr, Ni, Mo, Cd, Ag, Cu, Bi, Pb, Ca, P, Si, Al, Mg	<0.0010	Fe and Zn (individually)	<0.006 %

Overall, in the present work, the role of ICP-OES following microwave digestion for the quality control is distinctly highlighted for materials of importance to reactors.

A Single Method Approach for Chemical Characterization of PHWR Steam Generator Tube Material using RF GDOES

Y. Balaji Rao¹, S.N.V.M.S. Gupta¹, P.V. Nagendra Kumar^{2,§}, Dinesh Srivastava¹

¹ Nuclear Fuel Complex, Dept. of Atomic Energy, ECIL post, Hyderabad, India

² Dept of Chemistry, GITAM University, Hyderabad, India

§ Email: vputta@gitam.edu/ pvenkatanagendrakumar@gmail.com

Steam Generator (SG) tubes are one of the important structural materials for Pressurized Heavy Water Reactors (PHWRs) reactors operating in India. SG tube is manufactured using Incaloy 800 which is a nickel-iron-chromium alloy with a composition of Ni (32%-35%), Cr (20%-23%), Mn (0.4%-1.0%) Si (0.3%-0.7%), Al(0.15%-0.45%), Ti (0.6% with Ti/C ratio minimum 12) and Fe as balance. Chemical composition of this alloy plays significant role in imparting beneficial properties to SG tubes as Ni enhances corrosion resistance and high temperature strength, Cr provides excellent resistance to oxidation, carburization and sulfidation, Mn improves workability of the material and Fe increases the strength of the material. Nuclear Fuel Complex (NFC) is engaged in manufacture and supply of SG tubes to all PHWRs operating in India. In view of the critical application of this material in PHWRs, chemical characterization of the same has become integral part of QA/QC program. Multiple techniques like Gravimetry, Spectrophotometry, AAS, ICP-OES are being regularly used for the analysis of SG tube material. However, these techniques have limitations like cumbersome sample preparation procedures, generation of liquid analytical waste etc. In view of this a successful attempt has been made to analyze direct solid samples of Incaloy 800 based SG tubes for Al, Ni, Cr, Mn, Cu, Si, Ti using Radio Frequency Glow Discharge Optical Emission Spectrometer (RF GD-OES). Important analytical conditions like Pre integration time, Integration time, Ar Pressure inside GD source, RF power applied to GD Source are optimized in this method. Set of Certified Reference Materials (CRMs) from MBH Analytical, UK are used for calibrating the equipment. All the calibration curves have been found to be linear with co-relation coefficient (R^2) ≥ 0.99 . The developed method is compared with regularly employed methods as shown in Table 1. % RSD of the developed method found to be less than 3% for most of the elements.

Table 1: Comparison of results obtained for a typical sample using the developed method with the regularly employed methods

Element	Developed method	Regularly employed methods*
Al (%)	0.354 \pm 0.006	0.36
Ni (%)	33.8 \pm 0.3	34.1
Cr (%)	22.2 \pm 0.2	21.90
Mn (%)	0.785 \pm 0.021	0.77
Cu (%)	0.0125 \pm 0.0005	0.012
Si (%)	0.502 \pm 0.009	0.49
Ti (%)	0.453 \pm 0.008	0.45

*Regularly employed methods: Al, Mn, Cu, Si - AAS, Ti-ICP-OES, Ni-Gravimetry and Cr-Spectrophotometry.

References:

[1] R. S. Dutta, *Journal of Nuclear Materials*, **393** (2009) 343.

Evaluation of Hydrodynamic Properties of Phosphate and Phosphonate Ligands

K.N. Bikash¹, S. Rajeswari¹, B. Sreenivasulu^{1,2} §, C.V.S. Brahmmananda Rao^{1,2}

¹Materials Chemistry and Metal Fuel Cycle Group, IGCAR, Kalpakkam, India

²HBNI, IGCAR, Kalpakkam, India

§ E-mail: bsrinu@igcar.gov.in

Third phase formation is major concern during the extraction of tetravalent metal ion such as Pu(IV), Th(IV), and Zr(IV) with tri-n-butyl phosphate (TBP) based solvent extraction process. Our earlier studies on development of alternative extractant to TBP revealed that phosphonate based solvent such as dibutylbutyl phosphonate (DBBP) and diamylamyl phosphonate (DAAP) exhibit lower third phase forming tendency than TBP [1]. For fast reactor fuel reprocessing, where plutonium concentrations are high, limitations of TBP make phosphonates a promising alternative due to their reduced third phase tendency and superior actinide extraction efficiency, attributed to higher basicity of phosphoryl oxygen [2]. Physical properties like density, viscosity, and interfacial tension (IFT) plays an important role while choosing a solvent. During spent nuclear fuel reprocessing, solvent's physicochemical property as well complexation properties undergoes significant alteration. To simulate the reprocessing condition, 0.37, 0.75, 1.1, 1.47, and 1.85 M of TBP, DBBP, and DAAP in n-DD were exposed to gamma irradiation upto 500 kGy using a ⁶⁰Co source. The density, viscosity, and IFT were experimentally determined for irradiated and unirradiated solvents and values were compared. For a particular solvent both density and viscosity decreases with temperature and for a particular solvent concentration TBP possess higher density and viscosity as compared to DBBP and DAAP. Density and viscosity is higher for gamma irradiated solvents as compared to unirradiated one where as IFT decreases upon irradiation due to the formation of surface active compounds. Upon irradiation, the magnitude of decrease in IFT is more in the case of TBP as compared to DBBP and DAAP which make phase separation difficult in the case of TBP. For a particular solvent concentration, the IFT value is higher for TBP followed by DAAP and least for DBBP and after irradiation, DAAP has higher IFT values followed by TBP and least for DBBP.

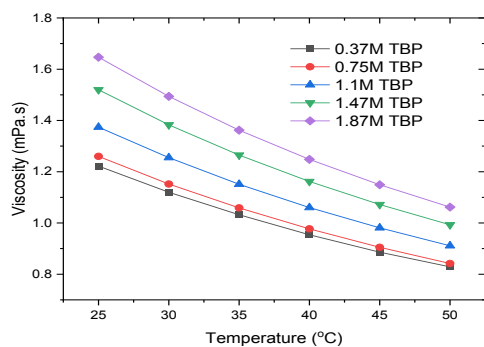


Fig. 1: Variation of viscosity with temperature for unirradiated TBP of various concentration

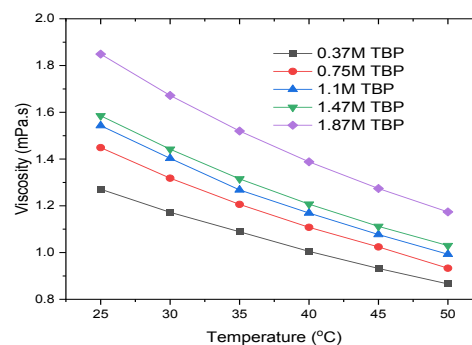


Fig. 2: Variation of viscosity with temperature for irradiated TBP of various concentration

References:

[1] C.V.S. B. Rao et al., *Solvent Extr. Ion Exch.*, **25** (2007) 771.

Acid Free, Ligand Free, Selective, Room Temperature Dissolution of UO_3 into Ionic Liquid with Subsequent Electro-Deposition

D. Karmakar^{1,2}, A. Nagar,³ A. Srivastava,¹ R.M.R Dumpala,¹ A. Sengupta,^{§, 1,2}

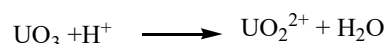
¹ Radiochemistry Division, Bhabha Atomic Research Centre, Mumbai, India

²Homi Bhabha National Institute, Mumbai, India

³UM-DAE Centre for Excellence in Basic Sciences, Mumbai, India

[§] Email: arijita@barc.gov.in

Room temperature ionic liquids have been chosen as the potential 'green' alternatives to the volatile organic diluents. In recent years, the use of ionic liquid as a suitable medium for selective dissolution followed by electro-deposition has been recognized as potential alternative to non-aqueous reprocessing involving high temperature operation and chemically drastic environment [1]. In this paper, UO_3 has been dissolved into $\text{C}_4\text{mim.PF}_6$, ionic liquid at room temperature within 2 hours of equilibration without application of any ligand, mineral acid or water from outside into ionic liquid phase [Fig. 1 (a)]. The extent of dissolution as estimated from the UV–Vis absorption spectra, increases with time of equilibration [Fig. 1 (b)]. At higher temperature, the extent of dissolution enhanced [Fig. 1 (c)]. The probable selective dissolution mechanism of UO_3 in $\text{C}_4\text{mim.PF}_6$ can be represented as:



This endothermic nature of UO_3 dissolution was confirmed by calorimetric study. The quantitative dissolution required 2 hours for 5 mg/mL loading; while 10 mg/mL, 20 mg/mL, and 50 mg/mL loading required 4h, 6h, and 8 h, respectively. Nd_2O_3 , Pr_6O_{11} , Yb_2O_3 , CuO , MnO_2 , CeO_2 , Fe_2O_3 were also subjected to dissolution into $\text{C}_4\text{mim.PF}_6$. However, except for Nd_2O_3 , no other oxide was dissolved into ionic liquid. This was attributed to their higher lattice energies compared to UO_3 . In same experimental conditions ~15-20 % of UO_2 and U_3O_8 were dissolved. The extent of UO_3 dissolution in $\text{C}_6\text{mim.PF}_6$ and $\text{C}_8\text{mim.PF}_6$ was below 25%; ascribed to the absence of in situ fluoride ion generation.

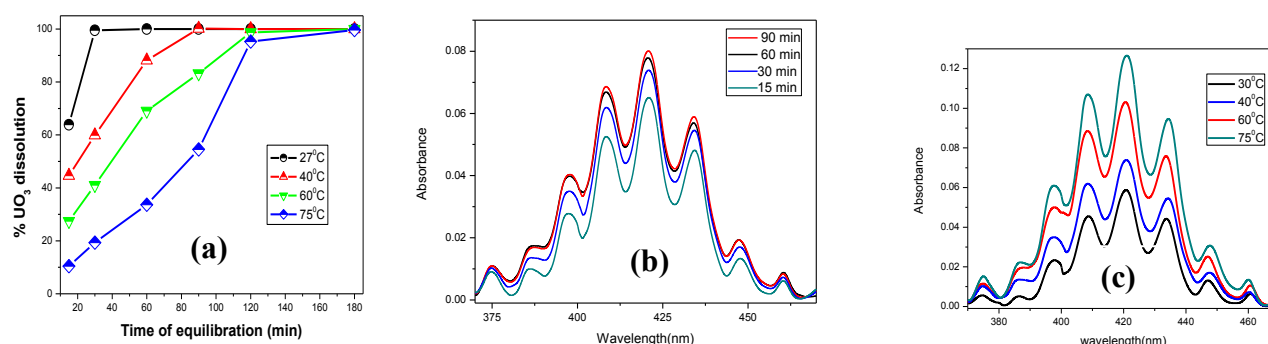


Fig. 1: (a) % of UO_3 dissolution at different equilibration time and at different temperatures; UV-Vis spectra for dissolved U in ionic liquid phase at various (b) Time; and (c) Temperature

Acknowledgements: The author wish to acknowledge Dr. S. Jeyakumar, Head, RCD, BARC and Dr. A. Bhattacharyya, Head, ACS, RCD, BARC for their constant support

References:

[1] P. Goyal, et. al., *Inorg Chem*, **63** (2024) 7161.

Evaluation of Electrocatalytic Performance of RGO-Pt Catalyst for U(IV) Generation

Kuntal Kumar Pal^{1,2§}, Chanchal Ghosh^{1,2}, Sandip Kumar Dhara^{1,2}

¹ Homi Bhabha National Institute, IGCAR, Kalpakkam, India

² Indira Gandhi Centre for Atomic Research, Kalpakkam, India

Reprocessing Group, Indira Gandhi Centre for Atomic Research, Kalpakkam, India

§ Email: kuntal@igcar.gov.in

In a spent fuel reprocessing plant, U(IV) is used as a key reagent in the partitioning cycle to separate the Pu from U-Pu stream. However, the current method for electrochemical U(IV) generation suffers from poor kinetics, associated with very high over potential. In this context, we have synthesized reduced graphene oxide supported Pt (RGO-Pt) by in situ ethylene glycol reduction method. The as-synthesized sample was characterized by XRD, FT-IR, FESEM, and STEM-HAADF studies. The characterized material was used as electrocatalysts for the reduction of U(VI) to U(IV). For this purpose, 4 mg of the catalyst's material was dispersed in 1 ml H₂O with 160 μ l of 5% Nafion solution and sonicated for 1 h to get a homogeneous catalyst ink. A 5 μ l of the catalysts ink solution was coated over a 3 mm dia glassy carbon (GC) electrode. Finally, this RGO-Pt coated GC electrode was used as a working electrode in a three-electrode setup with U(VI) in HNO₃ as an electrolyte solution to record the polarization curves and cyclic voltammetry (CV) studies. The polarization curve for U(VI) reduction over RGO-Pt was compared with Pt rod electrode, and \sim 50 mV reduction of over potential was obtained in the case of RGO-Pt catalysts as compared to Pt rod. Corresponding Tafel slope analysis also shows that the Tafel slope for U(VI) reduction over RGO-Pt has come down to \sim 100 mV/dec from 147 mV/dec for Pt rod at low HNO₃ concentration (\sim 0.05 to 0.1 M HNO₃) indicating a different more efficient electron transfer kinetics in case of RGO-Pt coated GC electrode (Fig. 1). It could be due to strong electronic interaction between RGO and Pt nanoparticles can modify the electronic structure of the Pt, optimizing its catalytic activity for the U(VI) reduction. Moreover, high electrochemically active surface area in the case of RGO-Pt could also decreased over potential. The corresponding CV study at low acid concentration has indicated a 1 electron transfer reaction for the corresponding Tafel slope with two cathodic reduction peak and one anodic oxidation peak, indicating a two-step electron transfer for U(VI) to U(IV) reduction at low acidity [1]. The study at high acid concentration (0.5-1.5 M HNO₃ with 0.25 M N₂H₄) also showed improved performance with a single-step proton-coupled two electron transfer reduction to U(IV), which indicates that RGO-Pt can be used as a cathode material in a spent fuel reprocessing plant for the generation of U(IV) in a more facial and power efficient manner via an electrochemical process.

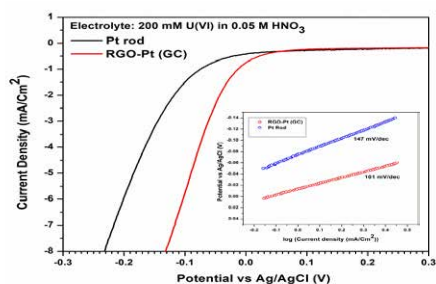


Fig. 1: Polarization curve for U(VI) over Pt rod and RGO-Pt (GC) electrode. Inset shows the corresponding Tafel plots

Acknowledgements: The authors are thankful to Mr. Ravi Kumar Yadav and Dr. R. Pandian for their support in XRD and FESEM studies of the sample, respectively.

References:

[1] S. Mishra et al., *Journal of Electroanalytical Chemistry*, **776** (2016) 127.

Green Route for Uranium Recovery from Solid Analytical Waste using Supercritical Carbon Dioxide Extraction

A.S. Kanekar¹, A. Rao^{1,2, §}, S. S. Kumar¹, S. Dhara^{2,3}

¹ Radiochemistry Division, Bhabha Atomic Research Centre, Mumbai, India

² Homi Bhabha National Institute, Mumbai, India

³ Fuel Chemistry Division, Bhabha Atomic Research Centre, Mumbai, India

§ Email: ankita@barc.gov.in

Supercritical carbon dioxide (SC CO₂) extraction [1] is an attractive candidate for direct extraction and purification of uranium from secondary sources (scraps, waste matrices), thus minimising corrosive acid and organic chemical usage as well as simplifying the overall process. Adducts of incinerable N, N-dialkyl amides viz. N, N-dibutyl octanamide (DBOA), N, N-dihexyl octanamide (DHOA), and N, N-dibutyl-2-ethyl hexanamide (DBEHA) were employed for direct dissolution and extraction of uranium from two lots of analytical solid waste (W1 and W2, having different contents of major impurities Fe, Ni, Ti, Cr), containing uranium along with other metal impurities. SC CO₂ parameters (viz. pressure, temperature, flow rate, adduct amount) were optimized for maximizing U extraction efficiency and purity, assayed by Total Reflection X-ray Fluorescence. Structure of amides as well as temperature and pressure influenced solubility of U-amide complex. Chemical compositions (acid and water content) decided overall efficiency. DBOA adduct yielded highest uranium extraction (88 ± 4 %) owing to higher amide content and SC CO₂ solubility. DBOA adduct also yielded highest purification (separation factors for impurities) due to least acid content. Pure ammonium diuranate was precipitated from the collected compact SC CO₂ extract. Hence, crude solid wastes (<30 % U content) to purified ADU (~ stoichiometric U content) conversion was demonstrated with less process steps and minimised chemical inventory.

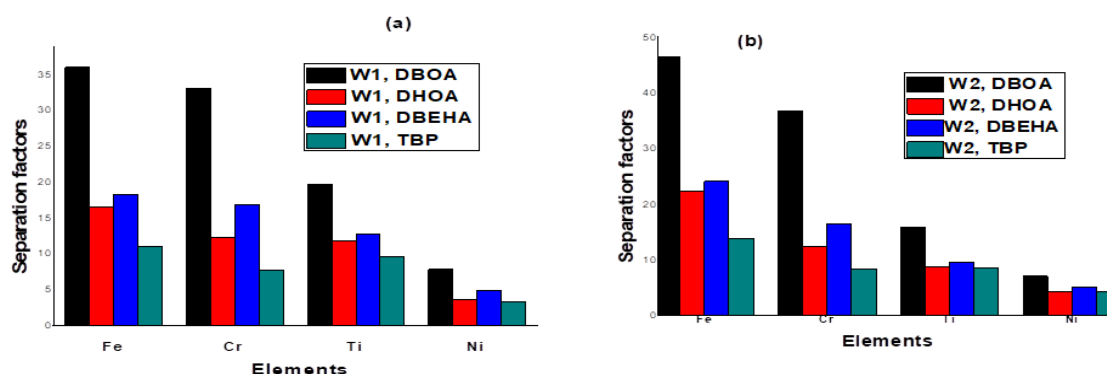


Fig.1. Separation factors for SC CO₂ extraction of uranium using different adducts for (a)W1 and (b)W2 (Results are average of triplicate runs with avg. std. deviation ± 4 %)

Acknowledgements: Authors acknowledge constant support from Dr. P.K. Mohapatra, Former Director, RC&IG and Dr. Arunasis Bahttacharya, Head, ACS, RCD.

References:

- [1] M. A. Mehugh and V. J. Krukonsis, *Supercritical Fluid Extraction Principles and Practice*, Butterworth-Heinmann (1994).

Electrodeposition Study of Uranium from Non-Aqueous Methane Sulphonic Acid Medium

A. Srivastav¹, A. Rao^{1,2, §}, S. S. Kumar¹, P. Agarkar¹

¹ Radiochemistry Division, Bhabha Atomic Research Centre, Mumbai

²Homi Bhabha National Institute, Mumbai

§ Email: ankita@barc.gov.in

Dissolution of fuel matrices and reagent-free, U determination has been demonstrated in biodegradable organic solvent, methane sulphonic acid by our group [1]. Towards our continued efforts to explore green, non-aqueous routes for actinide separation, electro-recovery of uranium was attempted from non-aqueous medium. Uranium electrodeposition from pure MSA was not feasible due to its highly complexing nature. Hence, uranium solution ($\sim 39 \text{ mg g}^{-1} \text{ U}$) in MSA, with propylene glycol (PG), as inert diluent, was subjected to constant voltage mode (-0.6 V) of electrodeposition on a Cu strip at room temperature. Further enhancement of voltage led to H_2 evolution. $\sim 49 \%$ recovery was achievable in 15 hrs., as assayed by biamprometry. Effect of increase of deposition time and temperature are being probed. U(IV) formation, as intermediate in solution was confirmed electrochemically and by UV-Vis spectrophotometry (Fig. 1a). Two peaks were observed in the cyclic voltammetry signifying stepwise U(VI) to U(IV) reduction. From scan rate variation, diffusion coefficient for U(IV), D_0 was determined to be $6.3 \times 10^{-7} \text{ cm}^2 \text{ s}^{-1}$. U deposited on Cu strip was characterized by Energy Dispersive X-ray spectra (Fig.1b) and X-ray diffraction.

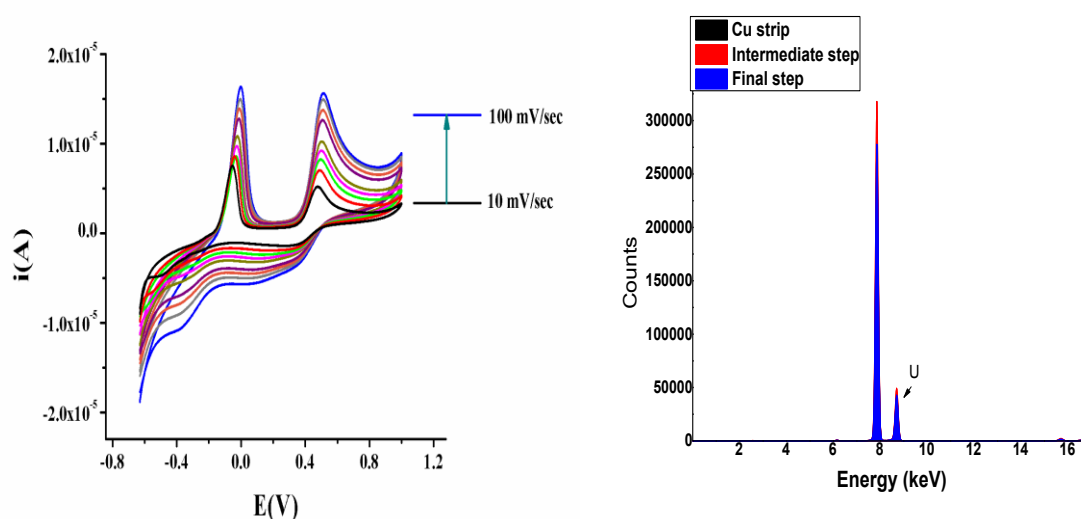


Fig.1: (a) Scan rate variation study for U(IV) in non-aqueous medium; (b) EDX spectra

Acknowledgements: Authors thank Dr. S. Dhara and Dr. B.G. Vats for EDX and XRD, respectively.

References:

[1] A. Srivastava, et. al., *Anal. Chem.*, **96** (2024) 14891.

Complexation of UO_2^{2+} Ion with DGA & CMPO Functionalized Ionic Liquids

Priya Goyal, A. Sengupta[§], P. K. Mohapatra

Radiochemistry Division, Bhabha Atomic Research Centre, Mumbai - 400 085

[§]Email: arijita@barc.gov.in

DGA and CMPO functionalized ILs (Fig. 1 (a and b)) exhibited efficient extraction efficiency for UO_2^{2+} from aqueous acidic feed streams [1]. Therefore, it is imperative to understand the complexation behaviour of UO_2^{2+} ion with them into $\text{C}_4\text{mim.NTf}_2$. Fig. 1 (c) and (d) are depicting the changes in the UV-Vis absorption of uranyl ion [$\text{UO}_2(\text{NTf}_2)_2$ as precursor] on incremental addition of the TSILs. On incremental addition of DGA-TSIL, not only there is an enhancement in the intensity; the peak shifts associated with changes in spectral characteristics have been observed. The fitting of the data revealed the formation of ML_1 and ML_2 stoichiometric complexes [Fig. 1 (e)]. Similar speciation has also been reported for biphasic extraction of uranyl ion from aqueous acidic feed solution. In case of CMPO functionalized ionic liquid, apart from the evidences of uranyl complexation by enhancement in peak intensity and shifting in peak positions, the overall background was found to enhance (possibly due to the fact that, the CMPO-TSIL is a coloured compound). It revealed the predominance formation of 1:1 and 1:2 species (Fig. 1 (f)). The complexation with DGA-IL was found to be stronger compared to CMPO-IL. For both the cases as L/M ratio was enhanced, the equilibrium were found to be shifted towards ML_2 species.

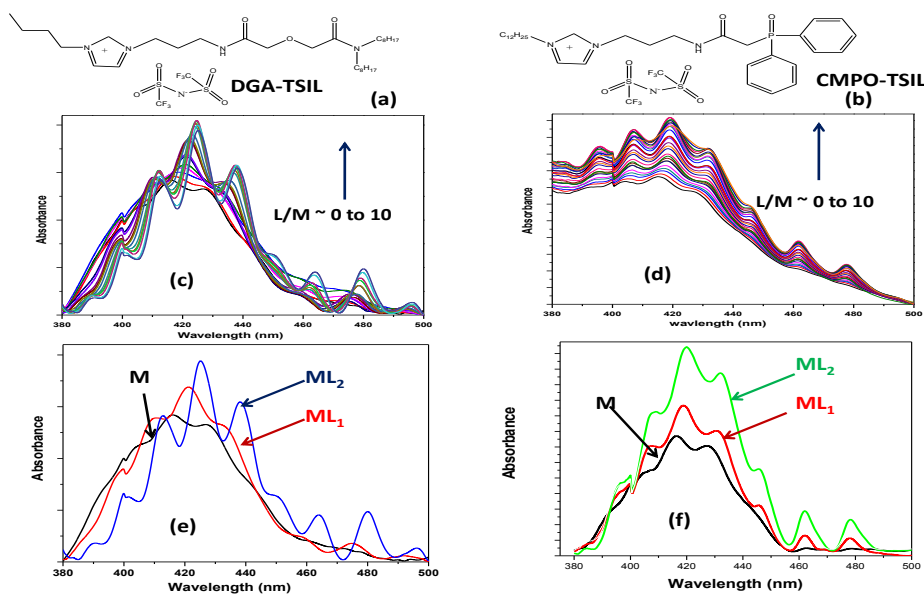


Fig. 1: (a) Chemical Structures of DGA-TSIL and (b) CMPO-TSIL. UV-Vis titration of UO_2^{2+} with (c) DGA-TSIL and (d) CMPO-TSIL in $\text{C}_4\text{mimNTf}_2$; Deconvoluted absorption spectra for ML_1 and ML_2 species for (e) U-DGA, (f) U-CMPO TSIL complexation.

Acknowledgements: The author wish to acknowledge Dr. S. Jeyakumar, Head, RCD, BARC and Dr. A. Bhattacharyya, Head, ACS, RCD, BARC for their constant support

References:

[1] A. Sengupta, et. al., *Sep Purif Technol.*, **118** (2013) 264

Speciation of Uranium in K_2MgGeO_4 and its Implication on Photochemistry

Annu Balhara^{1,2}, J. Balasurendran¹, B. Modak³, A.K. Yadav⁴, Santosh K. Gupta^{1,2, §}

¹Radiochemistry Division, BARC, Trombay, Mumbai, India

²Homi Bhabha National Institute, Mumbai

³Chemistry Division, BARC, Trombay, Mumbai, India

⁴Atomic & Molecular Physics Division, BARC, Mumbai, India

§ Email: santoshg@barc.gov.in

The photophysical properties of actinides are both intriguing and enriching, primarily due to the distinct behaviour of their 5f electrons in comparison to the 4f electrons of lanthanides. Actinide ions are characterized by large spin-orbit coupling and closely spaced J-levels, which differentiate them from lanthanides and result in a significant number of non-radiative decay channels. Uranium, in particular, stands out within the actinide series, offering numerous applications beneficial to humanity due to its unique redox chemistry and distinctive physicochemical properties. In recent years, uranium chemistry has gained renewed attention, fuelled by advances in synthetic chemistry, novel photochemical characteristics, intriguing coordination chemistry, and its pivotal role in nuclear energy production.

To explore the unique potential of uranium, we have selected a new class of materials, $KMgGeO_4$ (KMGO), as a luminescent host. KMGO crystallizes in an orthorhombic structure, where K^+ ions exhibit multiple coordination in a rigid framework. XANES measurements confirm the stabilization of uranium in its +6 oxidation state. EXAFS data reveal two distinct U-O bond distances within KMGO doped with uranium ions. The shorter U-O bond distances, around 1.8 Å, correspond to uranium-axial oxygen bonds, while the longer U-O distances, approximately 2.30 Å, are indicative of uranium-equatorial oxygen bonds. These two coordination shells support the presence of uranyl polyhedra, with a coordination number of around 2 for the first shell, suggesting uranyl speciation (UO_2^{2+}) within the KMGO lattice.

Fig. 1 illustrates the photoluminescence spectrum of KMGO: 0.5%U under X-ray excitation. KMGO-U demonstrates efficient conversion UV to green light down conversion luminescence conversion which is attributed to the HOMO-LUMO transition in hexavalent uranyl ions (UO_2^{2+}), involving radiative de-excitation from the non-bonding 5f orbitals of uranium to the bonding 2p orbitals of oxygen atoms. The photoluminescence (PL) emission intensity was found to be maximal at a 0.5 mol% uranium ion doping concentration. Beyond this concentration, a phenomenon known as concentration quenching occurs, likely due to the decreased distance between uranyl ions at higher doping levels, leading to non-radiative energy transfer. The photoluminescence decay curve can be fitted using a tri-exponential function, with the multi-exponential decay attributed to the inhomogeneous distribution of uranyl ions in the KMGO host matrix. This distribution is primarily due to the stabilization of uranyl ions at both Mg and Ge sites.

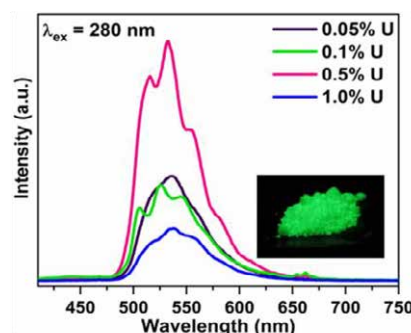


Fig. 1: Radioluminescence spectrum of KMGO: 0.5%U

Demonstration of Mixer-Settler Runs for the Processing of U-Pu-Zr Feed Solutions using Tri-iso-Amyl Phosphate

B. Sreenivasulu^{1,2,§}, P. Amarendiran¹, A. Suresh^{1,2}, C.V.S. Brahmananda Rao^{1,2}

¹Materials Chemistry and Metal Fuel Cycle Group, IGCAR, Kalpakkam-603102

²Homi Bhabha National Institute, IGCAR, Kalpakkam – 603102

[§]E-mail: bsrinu@igcar.gov.in

Metallic alloy fuels, U-Pu-Zr can be reprocessed by aqueous based PUREX process [1]. Tri-n-butyl phosphate is being used as an extractant for reprocessing of spent nuclear fuels for last seven decades. In the recent past, Tri-iso-amyl phosphate(TiAP) has been examined as an alternate solvent to TBP for the aqueous reprocessing of metallic alloy fuels[2], U-Pu-Zr. TiAP was synthesized in our laboratory and liquid-liquid solvent extraction runs were performed with U-Pu-Zr feed solutions using 1.1 M TiAP/n-Dodecane(n-DD) with ejector mixer-settler facility. A feed solution containing U, Pu and Zr about 76.8, 20.4, and 5 g/L in 4.33 M HNO₃ was prepared. Mixer-settler runs were carried out with U-Pu-Zr solution to understand the extraction and stripping behavior of U, Pu, and Zr with TiAP in nitric acid media. Extraction profiles for U and Pu are shown in Fig. 1 and 2, respectively. Results indicate that quantitative extraction (>99%) of U and Pu was achieved with negligible extraction of Zr using 1.1 M TiAP/n-DD in mixer-settler runs. Subsequently, stripping of U and Pu from the loaded organic phase was carried out with dual stripping agents such as 2 M and 0.01M HNO₃ with suitable flow rates in a counter-current manner. Results indicate that quantitative stripping of Pu(>99%) was achieved in 7 stages whereas stripping of U was found to be about 81% indicating that more number of stages required for the quantitative stripping of uranium from loaded 1.1 M TiAP /n-DD. The present study demonstrates the feasibility of using TiAP as the extractant for reprocessing of metallic alloy fuels.

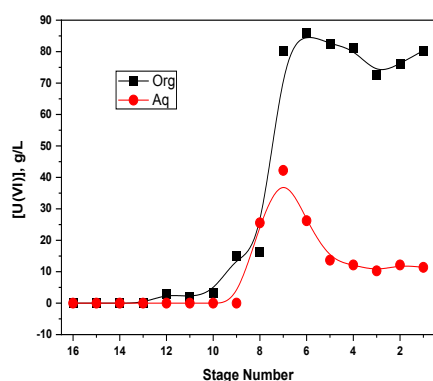


Fig. 1: Organic and aqueous stage profiles for U the extraction run with U-Pu-Zr feed solutions using 1.1M TiAP/n-DD system.

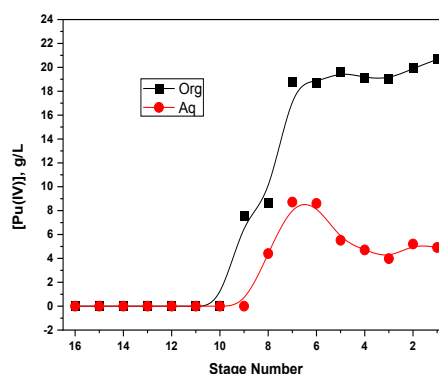


Fig. 2: Organic and aqueous stage profiles for Pu the extraction run with U-Pu-Zr feed solutions using 1.1M TiAP/n-DD system.

References:

- [1] B. Sreenivasulu et al., *J. Radioanal. Nucl. Chem.*, **311** (2017) 789.
 [2] B. Sreenivasulu, *Solvent Extr. Ion Exch.*, **33** (2015) 120.

Nitridation and Dissolution Behavior of U-Zr Alloy with Different wt % of Zirconium

M. Bootharajan^{1,§}, Suranjan Bera¹, B. Sreenivasulu^{1,2,§},
K. Sundararajan^{1,2}, C.V.S. Brahmananda Rao^{1,2}

¹Materials Chemistry and Metal Fuel Cycle Group, IGCAR, Kalpakkam-603102

²Homi Bhabha National Institute, IGCAR, Kalpakkam – 603102

[§]E-mail: bsrinu@igcar.gov.in, mbrajan@igcar.gov.in

Pyro-reprocessing is the best method for reprocessing of metallic fuels. An alternate method is aqueous reprocessing which involves, the conversion of metallic fuel into respective oxides or nitrides followed by dissolution. This study is aimed to convert metallic fuel by nitridation of the U-Zr alloy followed by dissolving the nitrides in 12 M HNO₃ acid medium. In addition the effect of Zr in U-Zr (1-50 wt %) metallic alloys on nitridation and dissolution behaviour also investigated. Initially the U-Zr_x(x=10-50 wt%) with varying Zr composition was prepared by arc melting method. The XRD analysis was carried out for the U-Zr_x(x=10-50 wt%) as shown in Fig.1. Initially U-10wt%Zr was converted into hydrides at 400-500°C using hydrogen getters followed by dehydriding at 700°C. Nitridation was initiated in N₂ atmosphere at 400°C. To ensure the complete reaction the temperature was gradually raised to 1100°C with rate a of 10-12°C/min. The formation of nitride was confirmed by comparing the XRD pattern with standard JCPDF as shown in Fig. 2. Similar procedure was adopted for nitridation of 20 and 30 wt% of Zr in U-Zr alloys. The nitridation was found to be difficult owing to the poor kinetics for high Zr content (40 & 50 wt% of Zr in UZr) and demands a temperature more than >1100°C to carry out nitridation. Furthermore, the metallic nitrides were dissolved in nitric acid by refluxing in 12 M HNO₃ at 120°C for 8 h. The dissolution of U was found to be >99.9% in all the cases and the dissolution of Zr decreases with increase in Zr content in U-Zr alloys. These studies may pave way for the development of flow sheets for the aqueous reprocessing of metallic fuels by nitridation route.

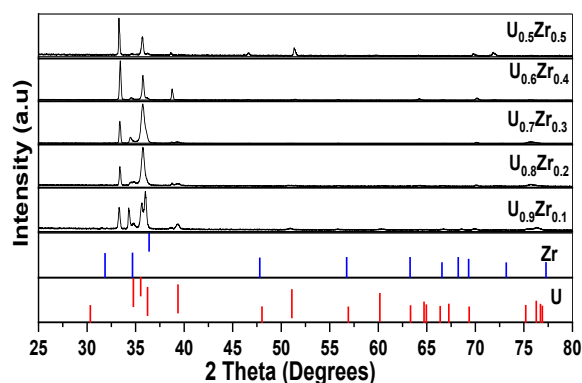


Fig. 1: XRD pattern of U, Zr, (U_{0.9}Zr_{0.1}) (U_{0.8}Zr_{0.2}), (U_{0.7}Zr_{0.3}), (U_{0.6}Zr_{0.4}) and (U_{0.5}Zr_{0.5})

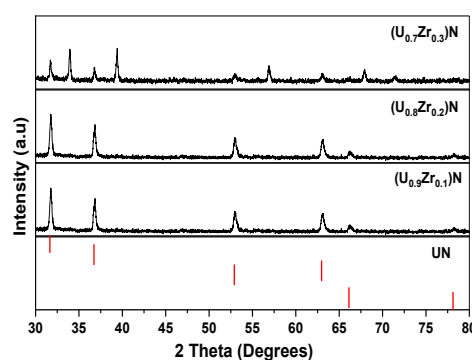


Fig. 2: XRD pattern of UN, (U_{0.9}Zr_{0.1})N (U_{0.8}Zr_{0.2})N and (U_{0.7}Zr_{0.3})N

References:

- [1] B. Sreenivasulu et al., *J. Radioanal. Nucl. Chem.*, **311** (2017) 789.
- [2] Hadi Suwarno, *Advanced Materials Research*, **789** (2013) 360-366

Separation of Uranium, Thorium and Lanthanides for the Processing of Monazite feed Solutions using Tri-iso-amyl Phosphate

B. Sreenivasulu^{1,2,§}, N. Navamani¹, A. Suresh^{1,2}, C.V.S. Brahmananda Rao^{1,2}

¹Materials Chemistry and Metal Fuel Cycle Group, IGCAR, Kalpakkam-603102

²Homi Bhabha National Institute, IGCAR, Kalpakkam – 603102

[§]E-mail: bsrinu@igcar.gov.in

Monazite ore contains phosphates of thorium and rare earths with significant quantity of uranium [1]. At present TBP based solvent is being used for the separation of uranium and thorium from each other and from rare earths. However, TBP has some limitations, especially third phase formation with Th(IV). An alternate extractant TiAP has been examined in our laboratory for processing of Th(IV) containing solutions [2]. In this context, the extraction and stripping behavior of U(VI), Th(IV), and rare earths(REs) with TiAP in nitric acid medium has been investigated in cross-current mode. A feed solution containing U, Th and REs about 8.3, 203, and 207 g/L in 4M HNO₃ was prepared. Cross-current experiments were carried out for the separation of U and Th from REs using 0.183M and 1.47M TiAP/n-DD, respectively. Experiments were also performed with 0.183M and 1.47M TBP/n-DD; results indicate that TBP based solvent forms third phase with Th under identical conditions. However, third phase was not observed with Th in the case of TiAP based solvent. TiAP require 4 stages for quantitative extraction of U(VI) with partial extraction of Th(IV). The concentration of U(VI) in the aqueous phase (raffinate) in the 4th stage was found to be below detection limit (BDL) which is less than 1 mg/L, whereas Th(IV) and RE(III) concentrations were found to be about 154 and 157 g/L (Fig. 1). The raffinate was employed as such for the separation of Th(IV) from RE(III) using 1.47M TiAP/n-DD. The extraction of Th was found to be >98% in 4 stages with partial extraction of RE(III). The extraction of RE(III) was found to be about 4.2%. The concentration of Th(IV) in the aqueous phase (raffinate) in the 4th stage was about 1.9 g/L. Subsequently, stripping of the metal ions from the loaded organic phase was carried out using 0.01M HNO₃ and quantitative stripping of U(VI) and Th(IV) is achieved within 2 stages, respectively. The present study provides an opportunity for the development of new process flow sheets for monazite ore processing using TiAP based solvents.

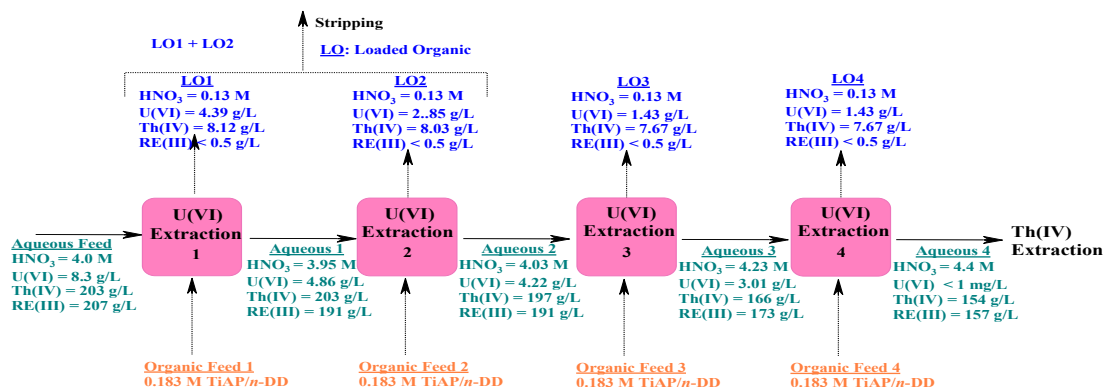


Fig. 1: Separation of U(VI) from Th(IV) and RE(III) from 4 M HNO₃ by 0.183 M TiAP/n DD

References:

- [1] T.K. Mukherjee et al., Characterisation and quality control of nuclear fuels, (2004).
- [2] B. Sreenivasulu et al., *Solvent Extr. and Ion Exch.*, **33** (2015) 120.

Trap Level Spectroscopic Properties of Uranium Incorporated $\text{Li}_2\text{B}_4\text{O}_7$

Hemachandar V¹, Saparya Chattaraj^{1,3}, D.K. Patre¹, D.P. Rath¹,
Ashokkumar P.¹, M. Mohapatra^{2,3,§}

¹Health Physics Division, Bhabha Atomic Research Centre, Trombay, Mumbai – 400 085

²Radiochemistry Division, Bhabha Atomic Research Centre, Trombay, Mumbai – 400 085

³Homi Bhabha National Institute, Mumbai – 400 085

[§] E-mail: manojm@barc.gov.in

Lithium tetraborate ($\text{Li}_2\text{B}_4\text{O}_7 = \text{LTB}$) with $Z_{\text{eff}} \approx 7.2$ has been investigated for its valuable spectroscopic properties. Like lanthanides, the actinide element, uranium is known to have variable oxidation states that can be stabilized in a particular host. In this regard, luminescence and optical properties of different oxidation states of uranium namely VI, V, IV and III and the radiation-induced changes have been reported [1]. Hence, in this study, uranium with nominal doping concentration was chosen as the activator material for wavelength shifting and optimum luminescence in LTB matrix. The choice of uranium was also due to its allowed electronic transition that results in improved absorption and emission cross sections. The uranium concentration was earlier optimised to 2 mol% for maximum photoluminescence output [2]. Presently, thermally stimulated luminescence (TSL) experiments were carried out on the system to get an idea about the trap parameters, such as activation energy (E_a) and frequency factor (s) of the system that affect the dosimetric properties of a material. The system was optimised for the dose range of 1 kGy to 15 kGy with maximum output at 2 kGy of gamma dose upon irradiation with ^{60}Co source. Two glow peaks at around 405 and 515 K were obtained for the dose with the former being the more intense.

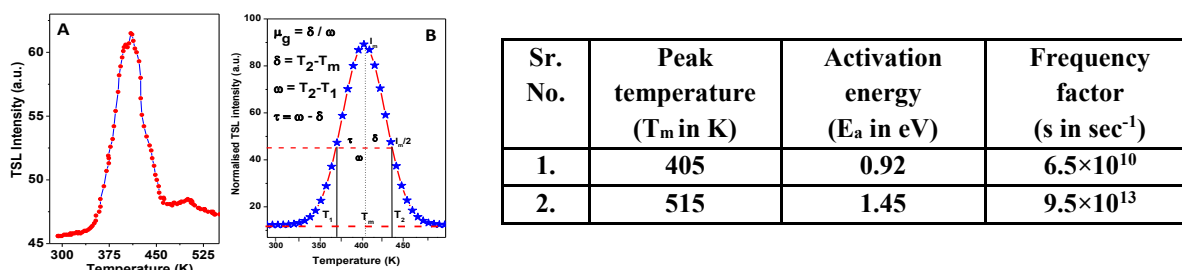


Fig. 1 (A): TL glow curve (B) TL Kinetics plot for LTB doped with 2% U; The table shows the trap parameters for the two glow peaks

Figure 1A and 1B shows the TSL glow curve and the kinetics plot for the LTB-U system and the adjacent table lists the trap parameters. No TSL signal was observed for the unirradiated or the undoped system confirming the role of the dopant ion in the overall TSL process.

Acknowledgements:

Authors thank Head RCD, Head HPD, and Director HS&EG for their unconditional help and support during the work.

References:

- [1] O.M. Pop et al., *Opt. Mater.*, **132** (2022) 112791
[2] Hemachandar V. et al., *Proceedings in SESTEC-2024*, 2024.

Direct Uranium Extraction from Solid Oxides Employing Novel Supercritical CO₂-Philic Extractants

N. Nayak¹, A.S. Kanekar², Shiny S.², P. Agarkar², A. Rao^{2,3,§}, S. Jeyakumar^{2,3}

¹ Mithibai College of Arts, Chauhan Institute of Science
& Amrutben Jivanlal College of Commerce and Economics, Mumbai
² Radiochemistry Division, Bhabha Atomic Research Centre, Mumbai
³ Homi Bhabha National Institute, Mumbai
§ Email: ankita@barc.gov.in

To exploit the advantage of direct dissolution-uranium extraction from solid matrices by SC CO₂, novel solvents were prepared employing solid trioctyl phosphine oxide (TOPO) and penta decafluoro n-octanoic acid (HPFOA). TOPO is a popular extractant for uranium and HPFOA aids SFE of metal ions due to multiple SC CO₂-philic C-F bonds. Hydrophilic eutectic solvent had been used by us for SC CO₂ extraction of uranium, but with less efficiency [1]. Different mole ratios were mechanically mixed followed by warming at 313 K to obtain TH1 and TH2. They were characterized with respect to relevant properties viz. viscosity and density (Fig.1), which were found to decrease slightly with temperature under atmospheric pressure. Subsequently, feasibility of mineral acid-free direct dissolution and SC CO₂ extraction of uranium from solid oxide matrices was explored under various conditions of pressure, temperature, extraction time and extractant amount. Uranium, in extract was analysed by Ti(III) reduction, with biamperometric end-point determination. Pressure and temperature were found to influence uranium extraction significantly by affecting the density of SC CO₂. TH2, having TOPO: HPFOA mole ratio of 1:2, yielded better extraction. Under optimised conditions (200 atm., 323 K, 60 min. static and dynamic extraction time, 0.5 mL TH2), U extraction efficiency followed the order UO₃ (87%) ~ U₃O₈ (86%) > UO₂ (68%). The extracts were characterised by electrometry, UV-Vis spectrophotometry and IR spectroscopy (Fig.2), revealing presence of U(VI), independent of initial matrix.

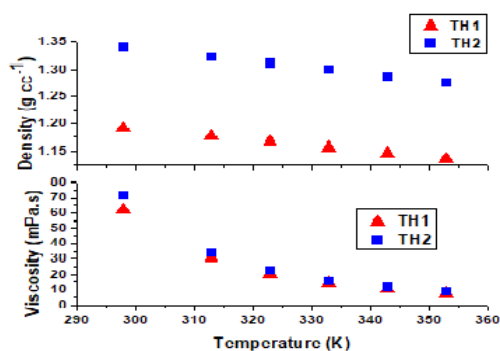


Fig.1: Density & Viscosity variation with temperature

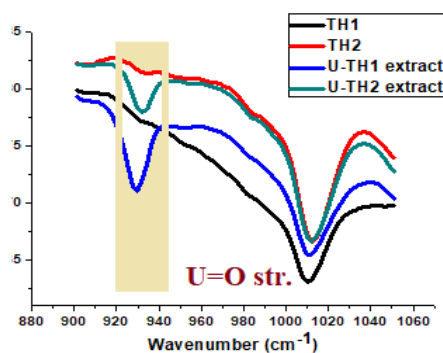


Fig.2: IR Spectra of extractant and U-extract

References:

[1] A. Rao, A. Srivastav, *Sep. Purif. Technol.*, **257** (2021) 117950.

Understanding the Plutonium Transient Profiles in the Stripping Bank for Minimizing the Retention of Plutonium in Lean Organic Phase

S. Balasubramonian^{1,2,§}, N. Desigan^{1,2}, K. A. Venkatesan^{1,2}

¹ Reprocessing Group, IGCAR, Kalpakkam, India

² Homi Bhabha National Institute, Mumbai, India

§ Email: balasubramanian@igcar.gov.in

The presence of dibutyl phosphate (HDBP) in PUREX solvent is the major reason for the incomplete stripping of Pu(IV) in fast reactor fuel reprocessing. In this work, the simulation of plutonium transient profiles in the lean organic phase after the startup procedure of the stripping bank and the possibility of minimizing the Pu(IV) retention by pumping of U(VI) solution in the bank are presented. The co-stripping bank consisted of 20 mass transfer stages. The loaded organic enters in the 1st stage and exits at 20th stage. Dual stripping procedure has adopted for the recovery of U(VI) and Pu(IV) from the loaded organic phase using 0.01 M and 0.45 M acid concentration, respectively. In this procedure, the first aqueous strip solution-1 (0.01 M HNO₃) enters from the 20th stage and undergoes mixing with the second aqueous strip solution-2 (4 M nitric acid) at 11th stage, and exits at 1st stage. The resultant concentration of nitric acid after mixing of 0.01 M and 4 M nitric acid is 0.45 M, which is suitable avoiding polymerization of Pu(IV).

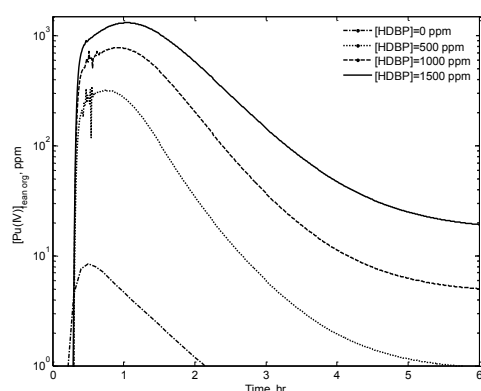


Fig 1: The transient profile of $[Pu(IV)]_{org}$ in various stages

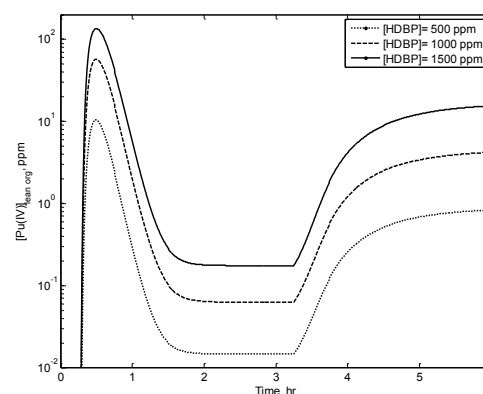


Fig 2: The transient profile of $[U(VI)]_{org}$ in various stages

The simulation of DFRP HC cycle flow sheet is carried out using the indigenous SEESPEC code. The simulation was carried out for the typical FBTR spent fuel composition with total metal ion concentration in the organic phase is 14 g/L. After the startup of the stripping bank (Fig 1), the Pu(IV) concentration in the organic phase reaches maximum within 1 hr and reduces gradually to less than 5 ppm after 3 hr depending on the concentration of HDBP. This results in the cumulative Pu(IV) concentration of 15, 51, and 111 ppm respectively for HDBP concentration of 0.5, 1 and 1.5 g/L in the lean organic tank (HCW) for the typical operation of 20 hr. To minimize the plutonium in HCW, U(VI) solution (100 g/L) has been added at 11th stage for the first 3 hr of the startup procedure, and the Pu(IV) retention in the lean organic phase is reduced to a significant extent (for instance < 5 ppm for 1 g/L HDBP), as shown in fig 2. This is due to the high concentration of U(VI) in the organic phase leading to the stripping of Pu(IV) in to the aqueous phase due to the competitive equilibrium. The same was confirmed by selective batch equilibrium studies done at the 11th stage condition as predicted by simulation.

Application of Tetra Alkyl Ammonium Hydrogen Phthalate Ionic Liquid for the Extraction of Pu⁴⁺ and UO₂²⁺ from Aqueous Hydrochloric Acid

S. D. Chowta¹, A. Sengupta,^{2,§} S. Biswas,³ K.K.Gupta,¹ G. Sugilal¹, P.K.Mohapatra^{2,§}

¹ Fuel Reprocessing Division, BARC Mumbai, India

² Radiochemistry Division, BARC Mumbai, India

³ Mineral Processing Division, BARC, India

§Email: arijita@barc.gov.in; mpatra64@gmail.com

Tri octyl-methyl ammonium hydrogenphthalate¹ [Fig 1 (a)], ionic liquid has been used for the extraction of plutonium and U from aqueous HCl feed solution with preferential extraction of Pu. Though HCl is corrosive in nature, this kind of solutions can be generated as analytical waste. The D_{Pu} were found to enhance with enhancement in the feed acidity [Fig. 1 (b)]. The formation of anionic $PuCl_6^{2-}$ species, might be responsible for the predominance of 'anion exchange' mechanism. The formation of $UO_2Cl_4^{2-}$ might also be responsible for the extraction of U from higher feed acidity. However, at 7 M HCl, the D_U was ~ 1.5 ; whereas D_{Pu} was ~ 22 (in 7 M HNO₃, $D_U \sim 2.6$; $D_{Pu} \sim 34$). In HNO₃ medium, there might be predominance of 'anion exchange' mechanism involving $Pu(NO_3)_6^{2-}$ species. However, for UO_2^{2+} , 'solvation mechanism' involving $UO_2(NO_3)_2 \cdot 2[R_4N^+Phthalate^-]$ might be predominating. The radiolytic stability study revealed that there was a continuous reduction in D values for Pu and U upon increase in gamma exposure [Fig. 1 (c)]. After 100 kGy exposure, the D_{Pu} was found to be 12, while D_U became 0.8. The back extraction study revealed that, 10 mM oxalic acid was suitable for Pu, while 10 mM Na₂CO₃ was effective for U [Fig. 1 (d)]. However, multiple contacts were necessary for having quantitative back extraction (more than 99.9 %).

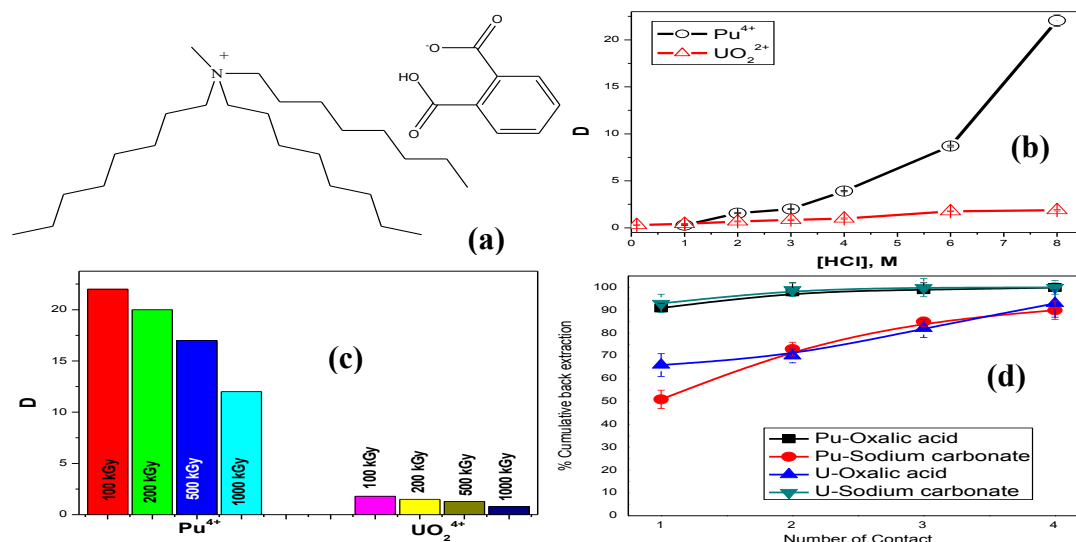


Fig.1: (a) Structure for TSIL; (b) variation in D vs feed acidity; (c) Radiation stability; (d) Back extraction

Acknowledgements: The author wish to acknowledge Dr. S. Jeyakumar, Head, RCD, BARC and Dr. A. Bhattacharyya, Head, ACS, RCD, BARC for their constant support.

References:

[1] S. Pathak, S. Biswas, A. Sengupta, *J Mol Liquids*, **338** (2021) 116616.

Feasibility Study on Simultaneous Acid Killing cum Catalytic Oxalate Destruction cum Volume Reduction in the RA Cycle Evaporator

Arvind Prasad^{1,2}, Satyabrata Mishra¹, N. Desigan, P. Sivakumar¹, K. A. Venkatesan^{1,2,§}

¹Reprocessing Group, IGCAR, Kalpakkam, India

²HBNI, Mumbai, India

§ Email: kavenkat@igcar.gov.in

The Pu-oxalate filtrate stream of DFRP contains about 20–100 ppm of Pu(IV), along with oxalic acid and nitric acid in the ranges 0.1–0.15 M and 2.5–3.5 M respectively. In DFRP, Pu recovery from the filtrate is planned in the recovery cycle (RA cycle), using 15% TBP/n-DD. The presence of oxalic acid in the aqueous phase hinders the extraction of Pu(IV). Therefore, the destruction of oxalic acid in the filtrate is necessary in the RA cycle. The traditional method for removing oxalate ions from the filtrate stream involves addition of an excess of KMnO₄. Implementing this method in fast reactor fuel reprocessing (FRP) plants presents significant challenges due to the use of comparatively dilute flow sheet and high Pu content. This method being a chemical method need stoichiometric amount of KMnO₄ and leads to substantial secondary solid waste generation. But, catalytic amount of Mn²⁺ can destroy same quantity of oxalate in nitric acid medium at elevated temperature and can reduce the secondary solid waste by 80-90% [1]. Simultaneous acid killing cum oxalate destruction using Mn²⁺ along with volume reduction, using an evaporator can be a viable option for implementing in reprocessing plant to minimize the waste generation in RA cycle. A series of preliminary studies were conducted to determine the evaporation rate that can be achieved during acid killing by varying the parameters such as temperature (371 K – 377 K), negative pressure (-125 mm WC to -275 mm WC), and flow rate of formaldehyde (0.2 mL/min – 0.6 mL/min). The one-factor-at-a-time (OFAT) method was used to isolate the effect of each variable. The experimental results are given in Table 1.

Table 1: Effect of process parameters on evaporation rate.

Parameters	Temperature /K	-Ve pressure/ mm of WC	HCHO flow rate/mL.min ⁻¹	Evaporation rate/mL.min ⁻¹	Final [HNO ₃]/M
Temperature effect	371	200	0.2	0.62	1.8
	373	200	0.2	1.21	2.24
	375	200	0.2	1.63	2.8
	377	200	0.2	2	5.2
Negative pressure effect	373	125	0.2	1.5	2.96
	373	200	0.2	1.57	2.62
	373	275	0.2	1.81	3.65
HCHO flow rate effect	375	200	0.2	1.63	2.8
	375	200	0.3	1.59	2.85
	375	200	0.6	1.61	3.03

Based on the experimental results, operating temperature of 375 K and -200 mm of WC with flow rates of HNO₃ and HCHO as 1.4 mL.min⁻¹ and 0.2 mL.min⁻¹ respectively could achieve an optimal evaporation rate.

Reference:

[1] Arvind Prasad et al., *Radiochim. Acta*, **112** (2024) 471.

Conditions Prior to Acidification of Carbonate Waste Generated During Clean-up of Degraded PUREX Solvent for Metal Recovery

Satyabrata Mishra[§], Rudrashis Bhattacharja,
N. Desigan, J. Kodandaraman, K.A. Venkatesan

Reprocessing Group, Indira Gandhi Centre for Atomic Research, Tamil Nadu, India

[§]Email: sbmishra@igcar.gov.in

Reprocessing of high plutonium content spent nuclear fuel (SNF), leads to severe degradation of the solvent (1.1 M TBP/n-DD). A considerably high amount of di-butyl phosphate (HDBP) higher than the quantity required for recycling is generated in the lean solvent. Accordingly, the lean organic is treated with sodium carbonate (SC) or hydrazine carbonate (HC) for the primary clean-up. The management of this aqueous waste demands near quantitative removal or destruction of DBP followed by acidification, evaporation, and solvent extraction (for the recovery of metal ions) for further processing and disposal. The retained metal content in the lean organic varied in the range 100-750 ppm during various reprocessing campaigns at CORAL during reprocessing of SNF from FBTR. Accordingly, the DBP content in the carbonate wash solution after clean-up of lean solvent will vary depending on the aging of the solution prior to processing.

Acidification of the carbonate solution containing DBP and metal ion leads to formation of precipitate. Ozonolysis, a comparatively slow process reduces the DBP content in carbonate waste to a significant extent. In this context, simulated studies were carried out to find out the minimum DBP content that should be achieved during ozonolysis such that acidification process will not lead to floating mass formation. The DBP content was analyzed by ion chromatography. Two sets of solutions (1.5 M HC and 0.5 M SC) containing U (VI) as a representative of heavy metal in the range 100-750 mgL⁻¹ were taken. For each U(VI) concentration, the DBP concentration in the solution varied and acidification was carried out by adding equal volume of nitric acid of different concentrations to a final acidity of 2M. Based on the results, it was observed that, the DBP concentration should be reduced to below 200 and 250 mgL⁻¹ respectively, when the U(VI) concentration in carbonate medium is up to 250 and 750 mgL⁻¹ respectively. Under similar conditions, for 0.5 SC, the DBP concentration should be reduced to below 500, 1500, and 2000 mgL⁻¹ respectively when the U(VI) concentration in carbonate medium is up to 100, 250, and 500-750 mg. L⁻¹ respectively. The result is compared in figure 1. The study suggests that the solubility of HDBP-metal complex in HNO₃ medium is mostly dependent on the U(VI) rather than DBP concentration.

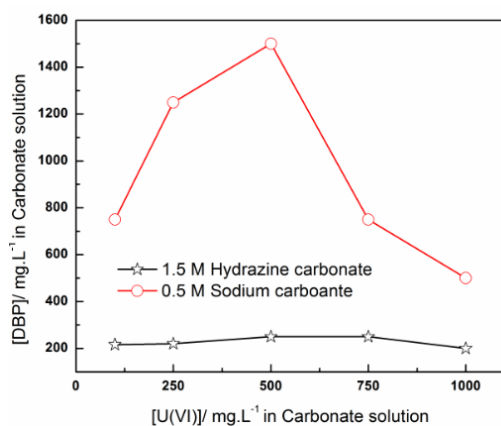


Fig1. Minimum DBP concentration to be achieved in carbonate medium under different concentrations of U(VI) to avoid precipitation prior to acidification.

Plutonium Estimation by Spectrophotometry Using 2-(5-Bromo-2-pyridylazo)-5-(diethylamino) Phenol

P. Chakraborty^{1,§}, V. K. M. Kutty¹, G. Srinivasa Rao¹, J. Mohandas¹, D. Gogoi¹, A. Das²

¹INRPK Lab, NRB, Bhabha Atomic Research Centre, Kalpakkam- 603102, India

²MSG, Indira Gandhi Centre for Atomic Research, Kalpakkam- 603102, India

§ Email: parichay@igcar.gov.in

Accurate estimation of important nuclear materials like uranium and plutonium is of immense importance in a spent nuclear fuel reprocessing plant. In order to accomplish it, analytical methods such as spectrophotometry using 2-(5-bromo-2-pyridylazo)-5-(diethylamino) phenol (Bromo- PADAP) is reliably used for U(VI) analysis [1]. The present report focuses on the usage of the same chromogenic reagent for the estimation of Pu.

The reagents used were: 0.5 g/l Bromo-PADAP in pure ethanol, triethanolamine (TEA) buffer with pH 7.8, complexing solution containing CYDTA, NaF and sulphosalicylic acid with pH adjusted to 7.8 [1]. Pu in solution remains mainly in three different oxidation states as Pu(III), Pu(IV), and Pu(VI). Here, all the Pu in a suitable aliquot is oxidized to Pu(VI) using 0.05 M ceric ammonium nitrate in 1 M HNO₃. Suitable sample of Pu(VI) is mixed with 1 ml of complexing agent, 1 ml of buffer, 4 ml of ethanol, 0.5 ml of Bromo-PADAP solution and this mixture is diluted with DI water to total volume of 10 ml. Pu(VI) makes complex with Bromo-PADAP which has UV-Visible absorbance maxima at 566.8 nm at pH 7.8.

To explore the viability of the method of Pu-estimation, total five standards were prepared and the absorption spectrums were recorded (see Fig. 1). The absorbances observed at 566.8 nm for all known concentrations are plotted in Fig. 2. The linear fitting allows estimation of the molar absorption coefficient as 26309 Lmol⁻¹cm⁻¹. Pu can be quantified with the precision & accuracy of ±5% for the range of 9-80 µg per aliquot with a detection limit of for Pu being 2.7 µg. This method is more sensitive compared to conventional Pu estimation based on oxidation of Pu to Pu(VI) by Ce(IV). No significant interference is observed for Ca(II), Ba(II), Sn(II), Ce(IV), Fe(III) for a concentration up to 2 mg/L. U can interfere in the estimation of Pu and thus this method is primarily applicable for pure Pu samples. However, nominal contamination of U up to 0.4% in Pu can be deduced with a 1% tolerance of the absorbance.

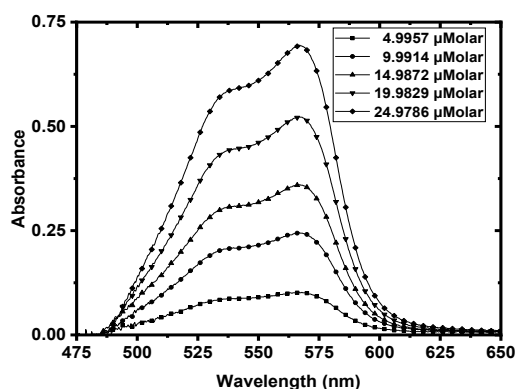


Fig. 1: Absorption spectrum of Pu(VI)-Bromo-PADAP complex

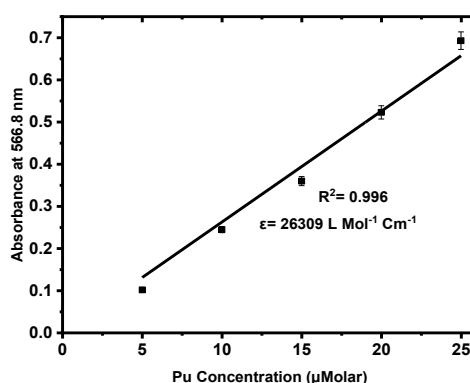


Fig. 2: Calibration plot: Abs. at 566.8 nm w.r.t. Pu conc. (µM)

References:

[1] S. K. Das et al., *J. Radioanal. Nucl. Chem.*, **285** (2010) 675–681.

Spectrophotometric Determination of Plutonium Using KMnO_4

Parichay Chakraborty^{1,§}, V. K. M. Kuty¹, Jaya Mohandas¹,
C. Krishna Kumar¹, G. Srinivasa Rao¹, Arindam Das²

¹INRPK Lab, NRB, Bhabha Atomic Research Centre, Kalpakkam- 603102, India

²MSG, Indira Gandhi Centre for Atomic Research, Kalpakkam – 603102, India

§ Email: parichay@igcar.gov.in

Plutonium(VI) shows sharp UV-Visible absorption peak at 830 nm. Pu can be oxidized quantitatively to Pu(VI) using cerium (IV) and the assay of Pu can be determined from its absorbance [1]. There has been a lookout for inexpensive, readily available, environment friendly and yet strong oxidant for Pu against the current usage of Ce(IV). Potassium permanganate with standard reduction potential of +1.68 V is a well utilized oxidant in industry and stands to be an excellent alternative. We report here the usefulness of KMnO_4 as an alternative oxidant for quantitative estimation of Pu by Spectrophotometry.

Standard plutonium nitrate solution (10.8381 g/Kg) was used for generating calibration plot. 0.025 (N) KMnO_4 in 1 (N) HNO_3 was used as oxidizing medium.

The oxidation of Pu to Pu (VI) in 0.025 (N) KMnO_4 medium in 1 (N) HNO_3 is completed within 30 minutes and the Pu(VI) so formed is stable in this medium (see inset of fig. 2). The constant background in the absorption-spectrum may be due to formation of MnO_2 and corrected in the range 820 nm to 840 nm using equation (1) (alternately, centrifugation is done prior to absorbance measurements) and the results for five different standards are shown in figure 1.

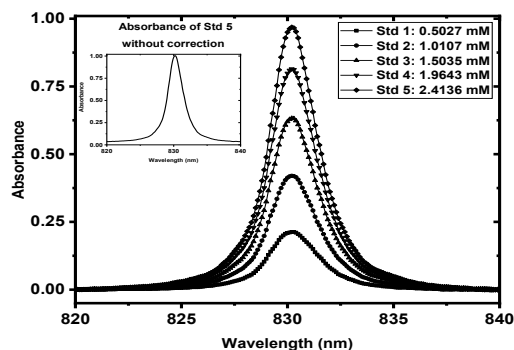


Fig. 1: UV-Visible Absorption spectrum of Pu(VI) in 0.025 (N) KMnO_4 and 1 (N) HNO_3 medium.

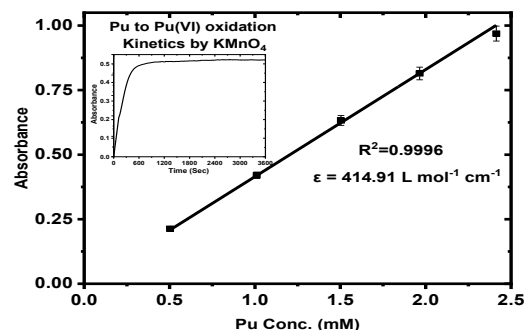


Fig. 2: Plot of absorbance at 830.2 nm vs Pu(VI) concentration (mM)

Absorbance maxima (λ_{max}) was obtained at 830.2 nm for different standard concentrations. The absorbance values hold good linearity with R^2 value 0.9996 (figure 2). Pu concentration of unknown samples can be found to be within 0.7% of the reported values. The method is highly precise in Pu conc. range of 0.4 – 2.0 mM & the analytical waste can be recycled which avoids generation of secondary waste.

$$A_{\text{Wavelength,Corrected}} = A_{\text{Wavelength}} - \frac{A_{820} + A_{840}}{2} \quad (1)$$

References:

- [1] L. F. Walker et al., Los Alamos National Lab, Procedure for Plutonium Determination using Pu(VI) spectra (1996).

Estimation of Plutonium (IV) by Spectrophotometric Methods to Explore an Alternative Method for Online Determination of Plutonium in Oxalate Supernatant

Suman Panja[§], S K Gupta, N S Rathore, A Kelkar, D B Sathe, R B Bhatt

Fuel Fabrication, Nuclear Recycle Board, BARC, Tarapur-401501

[§]Email: sumanp@barc.gov.in

Estimating the amount of Pu(IV) in the oxalate supernatant at regular intervals is crucial for monitoring and reducing plutonium loss in the oxalate supernatant during the precipitation of plutonium (IV) nitrate using oxalic acid. Regular analysis is particularly difficult since it requires frequent sampling, sample sealing, and sample delivery for analysis. These steps take time, more manpower, and expose workers to additional radiation. Currently, the traditional radiometry is used to analyze Pu(IV) in oxalate supernatant, which has a significant analytical error. Hence, an online system is required as part of automation, which can give a very fast estimation of Pu(IV) in regular intervals. It is well-established to use a spectrophotometer to determine Pu(VI) by measuring the absorption at 830 nm. Nevertheless, because of its extremely low molar absorptivity at its distinctive absorption peak of 477 nm, there is currently no method for determining Pu(IV) by spectrophotometry. The current work explores the estimation of Pu(IV) by spectrophotometry as a substitute method for online plutonium determination. This method is very helpful for quick estimation of Pu throughout the process and lowering exposure.

Different Pu(IV) stock solution concentrations, ranging from roughly 50 ppm to 250 ppm, were made by controlling the acidity, uranium concentration, and oxalic acid concentration, which were comparable to the oxalate solution obtained after precipitation. Using Orion™ Aqua Mate Vis and UV-Vis Spectrophotometers, a full spectrum scan of each solution was performed from wave length 400 nm to 650 nm. To guarantee quantitative plutonium precipitation, an excess of 0.1 M oxalic acid over the stoichiometric was supplied during the precipitation step. The original Pu(IV) spectra peak moved from 477 nm to 490 nm because of the excess oxalic acid's assistance in creating a soluble complex with Pu(IV). Each plutonium solution's absorbance at 490 nm was measured and plotted against the solution's concentration. If absorbance is known, the conc. of an unknown sample can be computed using this plot. To avoid the interference of the U(VI) 375 nm peak in the spectra, the uranium concentration was kept below 500 ppm in the study mentioned above (the uranium concentration in the oxalate solution is approximately 250 ppm). The amount of Pu(IV) can therefore be determined from the calibration plot by dipping the spectrometer's optical probe in the supernatant tank, which will yield an absorbance at 490 nm that can be measured online without withdrawing samples. This approach will minimize radiation exposure by cutting down on analysis time.

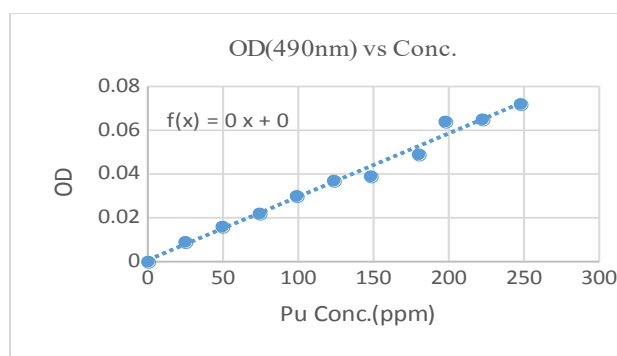


Fig. 1: OD of Pu at 490 nm vs. conc of Pu plot

References:

[1] *Anal. Chem.*, **89** (2017) 9354.

Computational Studies of U(VI) and Th (IV) Metal Complexes with TAP and DAAP Ligands

Vemuri Lakshmi Ganesh^{1, 2, §}, T. Revathy^{1, 2}, B. Sreenivasulu^{1, 2},
C V S Brahmananda Rao^{1, 2}, Gopinadhanpillai Gopakumar^{1, 2}

¹Indira Gandhi Centre for Atomic Research, Kalpakkam – 603102, Tamil Nadu, India.

²Homi Bhabha National Institute, IGCAR Campus, Kalpakkam – 603102, Tamil Nadu, India.

§ Email: vemurilakshmganesh720@gmail.com

Tri-*n*-butyl phosphate (TBP) is key in nuclear fuel reprocessing but has limitations like high solubility, third-phase formation, etc., necessitating more stable alternatives. In this context, we have investigated the coordination behavior of tri-*n*-amyl phosphate (TAP) and diamyl amyl phosphonate (DAAP) with U(VI), Th(IV) metal ions. Since the conformational studies of these ligands have not been extensively explored through experimental methods, we were motivated to examine them computationally using the Conformer and Rotamer Ensemble Sampling Tool (CREST) [1]. The 100 lowest-energy conformers derived from CREST were considered as starting geometries for DFT calculations and the lowest-energy conformer was selected for further analysis. On the other hand, the geometries of the complexes were established using the BP86 density functional in conjunction with SARC-ZORA basis sets for U and Th atoms (cf. Figure 1). CREST analysis indicates that TAP had 12,736 conformers under 5 kcal/mol, whereas DAAP has 15,421 conformers. NBO analysis reveals that the net charge of the phosphoryl group in DAAP is lower (ca. +1.21e) compared to TAP (ca. +1.36e), indicating a slightly stronger donor character of the former. All calculations were performed using the ORCA quantum chemistry program package [2], NBO version 6 [3], and CREST [1] program packages.

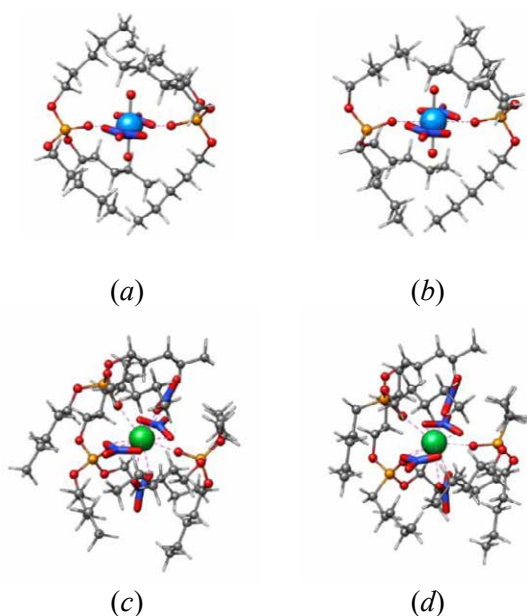


Fig. 1: DFT optimized geometries of (a) $\text{UO}_2(\text{NO}_3)_2 \cdot 2\text{TAP}$, (b) $\text{UO}_2(\text{NO}_3)_2 \cdot 2\text{DAAP}$, (c) $\text{Th}(\text{NO}_3)_4 \cdot 3\text{TAP}$ and (d) $\text{Th}(\text{NO}_3)_4 \cdot 3\text{DAAP}$.

References:

- [1] P. Pracht; F. Bohle; S. Grimme, *Phys. Chem. Chem. Phys.*, **22** (2020) 7169-7192.
[2] Neese, F. F. Neese, *Wiley Interdiscip. Rev. Comput. Mol. Sci.*, **8** (2017) e1327.
[3] NBO version 6.0. E. D. Glendening et al., Theoret. Chem. Inst., Univ. Wisconsin, Madison (2013).

Solvent Extraction Study of Irradiated U-Zr Feed Solution using Phosphate and Phosphonate Based Solvents

K.N. Bikash¹, B. Sreenivasulu^{1,2,§}, C.V.S. Brahmmananda Rao^{1,2}

¹Materials Chemistry and Metal Fuel Cycle Group, IGCAR, Kalpakkam – 603102.

²HBNI, IGCAR, Kalpakkam – 603102

§ E-mail: bsrinu@igcar.gov.in

Metallic alloys are recognized as promising candidate fuels for fast reactors due to high thermal conductivity, high breeding ratio, lower doubling time and higher fissile atom density [1]. The U-Zr binary alloy is an important subsystem of U-Pu-Zr alloy and has also been proposed as the blanket material for the sodium bonded U-Pu-Zr fuel. Due to third phase formation problem with tri-n-butyl phosphate(TBP), there is need to develop alternative solvent for the aqueous reprocessing of metallic fuel. It is interesting to note that phosphonate based solvents such as dibutylbutyl phosphonate(DBBP), diamylamyl phosphonate(DAAP) have lower tendency to form third phase as compared to phosphate with same number of carbon atoms which makes phosphonate based solvents a potential candidate for further studies for metallic fuel reprocessing [2]. U-6%Zr fuel irradiated in FBTR was dissolved in 12M HNO₃ in the presence of small amount of HF. The acidity of the dissolver solution was maintained at 4M and given a contact with 1.1M solvent of TBP, DBBP and DAAP in n-DD maintaining organic to aqueous ratio of 1. The extraction mechanism is similar to that of uranium TBP extraction. Stripping study was also carried out on loaded organic sample by using 0.01M HNO₃. Analysis of U, Pu, Zr, and fission product were measured by suitable analytical techniques. The extraction study shows that phosphonate based solvents possess higher extraction efficiency for U and Pu as compared to TBP which indicate that phosphonate can be employed for extraction of U and Pu from spent fuel dissolver solution (Fig.1). Stripping study data shows stripping efficiency of all the three solvents are identical. Stripping study also reveals that decontamination factor with respect to ¹⁰⁶Ru, ¹³⁷Cs, ¹⁵⁴Eu is higher for DBBP and DAAP as compared to TBP which is a desirable property for any solvent to be employed in the nuclear industry.

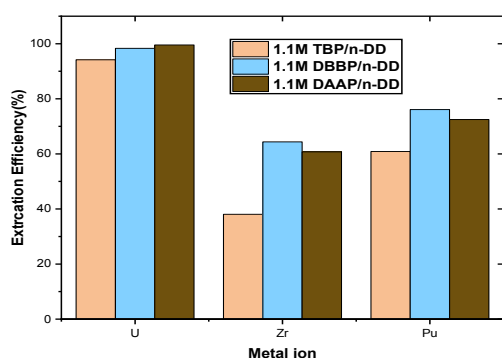


Fig. 1: Extraction study with 1.1M solvent/n-DD with irradiated U-Zr fuel solution at 4M acidity

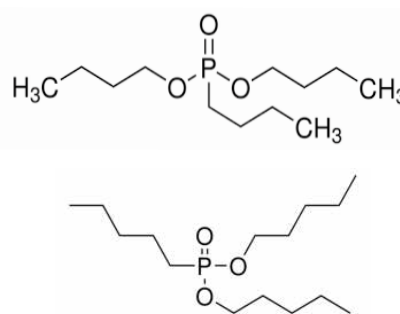


Fig. 2: Structure of DBBP and DAAP respectively

References:

- [1] H.S. Kamath et al., *Energy procedia*, **7** (2011) 110-119.

Aggregate Size Based Evaluation of Nature of Gel Formed During the Reaction Between Citric Acid and Uranyl Nitrate

G. Jogeswara Rao^{1,2}, A.S. Suneesh^{1,2}, S. Balakrishnan^{1,§}, Rajesh Ganesan^{1,2}

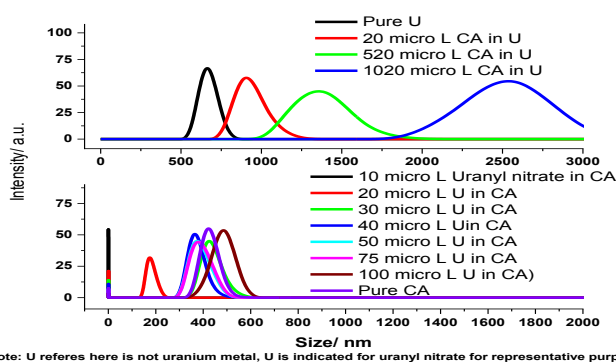
¹Fuel Chemistry Division, Indira Gandhi Centre for Atomic Research, Kalpakkam, India

²Homi Bhabha National Institute, Kalpakkam, India

§Email: balakrish@igcar.gov.in

The citrate-assisted gel combustion method, one of the well-known procedures for the preparation of nanocrystalline powders, utilizes an exothermic reaction between uranyl nitrate (known as fuel) and a complexing agent (known as an oxidizer) to produce a gel, which upon heating to around 250°C, generates nanocrystalline urania powder. This study is particularly interesting in nuclear technology due to the superior properties of the resultant urania powder. This paper explores a preliminary understanding of the influence of varying the concentration of citric acid (CA) and uranyl nitrate on the uranyl nitrate-CA gel formed by critically analyzing the sizes of the gels produced during the mixing of citric acid and uranyl nitrate at different compositions with the help of Dynamic Light Scattering (DLS).

The addition of citric acid to uranyl nitrate leads to the formation of complex before gelation in the combustion method. For understanding the variation of the aggregate size of the gels formed during the addition of CA to uranyl nitrate, two different experiments were performed at room temperature in the first experiment 20 µL, 500 µL and 1000 µL of citric acid [1.5M] solution was introduced into the 6×10^{-3} moles of uranyl nitrate. In the second set experiment, around 50 µL with increment of 10 µL was injected initially and further 75 and 100 µL of $\text{UO}_2(\text{NO}_3)_3$ [3 M] were introduced into the 3×10^{-3} moles of citric acid. The aggregate size of the colloidal gel formed during the interaction was analyzed by DLS (Malvern Pan analytical, Zeta Sizer Lab) was shown in the Fig. 1. The size of gels pure uranyl nitrate and citric acid corresponding to 0.7 nm and 533 nm respectively. In order to



Note: U refers here is not uranium metal, U is indicated for uranyl nitrate for representative purpose

Fig. 1: Aggregate sizes on addition of CA to U and vice versa

understand the mutual role of uranyl nitrate and citric acid, two different studies were performed: varying the composition of CA in uranyl nitrate (see top figure of Fig. 1), varying the composition of uranyl nitrate in CA. It was seen that addition of CA caused an increase in size of the uranyl nitrate (top Fig. 1), possibly due to the formation of a larger sized colloid of uranyl nitrate and CA. Whereas the reverse case while adding the uranium metal ion to citric acid not much change was observed due to the lack of complexing molecules surrounded by metal ion. The studies conclude that the addition of citric acid to uranyl nitrate causes an increase in the size of the uranyl nitrate-citric acid colloidal gel. Concentration of uranium also has a significant role in uranyl nitrate-CA gel size which increases with uranyl nitrate.

References:

[1] Gong, B. et al., *J. Nucl. Mater.*, **516** (2019) 169.

Effect of Aqueous Phase Acidity on Gamma Radiolysis of TBP/N-DD System

Chandan Mukhopadhyay^{1,4}, Satyabrata Mishra¹, R. Karthick¹, Debasish Saha², Pabitra Ghosh²
Pushpalata Rajesh^{3,4}, K. Dhamodharan¹, K. A. Venkatesan^{1,4,§}

¹Reprocessing Group, IGCAR, Kalpakkam

²MCMFCG, IGCAR, Kalpakkam, ³BARC(F), IGCAR, Kalpakkam, ⁴HBNI, Mumbai

§ Email: kavenkat@igcar.gov.in

PUREX process using TBP/n-DD as solvent is adopted worldwide for the separation and recovery of valuable materials like U & Pu from dissolver spent nuclear fuel solution. During extraction, the aqueous phase acidity is maintained at certain values to achieve a better separation of U and Pu over the other fission products and to avoid hydrolytic degradation of solvent. Accordingly, a low acid (~ 3 M) extraction flow sheet or a high acid extraction flow sheet (~ 5.5 M) is maintained during thermal and fast reactor fuel reprocessing to get better DF w.r.t. Zr and Ru respectively. In our earlier study, we observed that upon α -radiolysis, the degree of degradation of TBP/n-DD system is more under low acid loading condition compared to high acid loading condition, the reason for which was not clear [1]. The present study deals with the effect of aqueous phase acidity on gamma radiolysis behavior of TBP/n-DD system.

1.1 M TBP/n-DD was prepared and was subjected to multiple alkali wash followed by dilute nitric acid wash to ensure the solvent to be free from any acidic impurity. Prior to gamma radiolysis, the washed TBP/n-DD was equilibrated with 1-6M HNO₃ in 1:1 (v/v) ratio. The acid loaded organic phase was analyzed for its moisture content by KF titration method and the result is plotted in Fig. 1. Four sets of organic solutions [1.1 M TBP/n-DD, 1.1 M TBP/n-DD with 0.88 M HNO₃, 1.1 M TBP/n-DD with 11 g.L⁻¹ U(VI) -0.74 M HNO₃, 1.1 M TBP/n-DD with 11 g.L⁻¹ U(VI) -0.01 M HNO₃] were subjected to gamma irradiation up to 400 kGy absorbed dose using ⁶⁰Co gamma chamber to simulate plant operation condition. Samples were withdrawn at regular intervals of 100 kGy to access the extent of degradation in terms of Pu metal retention behavior. As observed earlier, the extent of degradation in the organic phase with low acid content was more in terms of metal retention compared to high acid loading condition as plotted in Fig. 2. This could be due to the presence of high moisture content under low acid loading condition which upon radiolysis forms highly interactive radical species like hydroxyl radical, H₂O₂, [O], H[•] and e_{aq}⁻ etc.

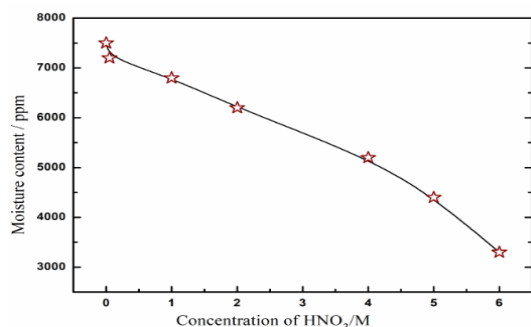


Fig. 1: Moisture content in 1.1 M TBP/n-DD upon equilibration with HNO₃

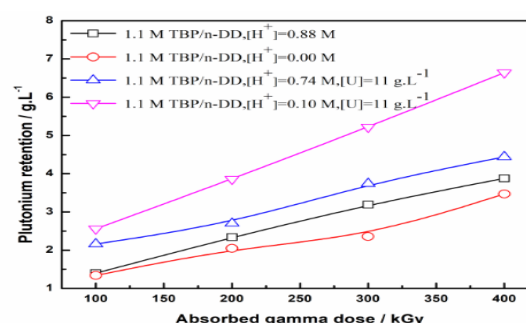


Fig 2: Effect of organic phase acidity on Pu retention in gamma radiolyzed solvent. % RSD: \pm 5%

References:

[1] Chandan Mukhopadhyay et al., NUCAR-2023, E-40.

Speciation of Uranium in Barium Molybdate Host through Time Resolved Photoluminescence Spectroscopy

Ritu Singh^{1,2,§}, T. P. Reshmi^{1,2}, M. Mohapatra^{1,2}

¹ Radiochemistry Division, BARC, Trombay, Mumbai-400085

² Homi Bhabha National Institute, Anushakti Nagar, Mumbai-400094

§ Email: ritusing@barc.gov.in

Among the actinide ions, Uranium has a special place not only due to its nuclear but also optical properties. Uranium in its VI and IV oxidation states are among the few actinide ions that show efficient radiative emission in the visible region. Though, in aqueous solution, the predominant uranium species is the oxo-cation uranyl ion UO_2^{2+} , in solids, the tetravalent/hexavalent uranium may take either tetrahedral or octahedral oxide forms such as UO_2 , UO_3 , UO_4^{4-} , UO_6^{6-} , UO_9^{12-} , U_4O_{12} or the usual UO_2^{2+} depending on the host lattice [1]. In view of this, the speciation studies of uranium in a solid host proposes an interesting challenge.

Among the many hosts, barium molybdate (BaMoO_4 , BMO) is a well-known host

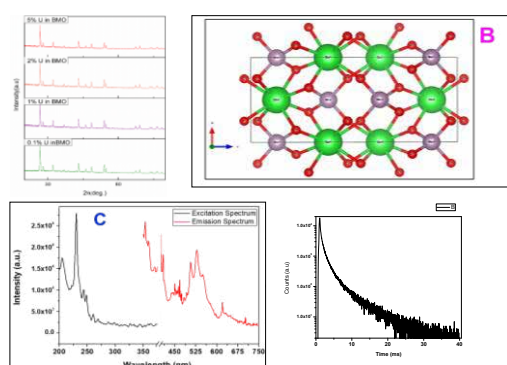


Fig. 1: A- XRD, B-Crystal structure, C- Excitation and emission, D - PL decay time of the 1%U doped BMO system

material for rare earth as well as transition metal ions that has a wide range of applications. The scheelite type crystal structure of this matrix provides suitable environment for the incoming activator ion to substitute the barium ion. Further, BMO exhibits good thermal and chemical stability making this a good candidate for luminescent host materials capable of operation in variety of conditions. The presents work focuses on understanding of the speciation and radiative properties of uranium in this BMO host. The samples for the study were prepared through the conventional solid-state reaction route and X-ray diffraction studies were done for the phase characterization. It was observed that, after

annealing at 600°C for 4 hours, a single-phase BMO was obtained. The dopant ion concentration was varied from 0.5 to 5%. Photoluminescence excitation, emission, and decay time data suggested the stabilization of a hexavalent uranium species in the BMO matrix with maximum luminescence output from the 1% doped sample. Higher concentration doped samples showed concentration quenching reducing the radiative output from the system. Figure 1 shows the XRD, photo luminescence excitation, mission, decay time results along with the crystal structure of the 1% Uranium doped BMO system. The excitation spectra for all the samples showed prominent peak at 230 nm while the emission data showed five-line finger like structure due to U(VI) with the most intense peak at 530 nm. The life time data showed a bi-exponential decay of 10 and 40 micro seconds with relative distribution of 40% and 60% respectively. From these data, it was inferred that the actinide ion was present as the Octedhral uranate species $(\text{UO}_6)^{6-}$ in the BMO host.

References:

[1] M. Mohapatra, V. Natarajan, *J. Radioanal. Nucl. Chem.*, **302** (2014) 1327

Highly Efficient Pertraction of Np(IV) and Pu(IV) using Two Alkyl Substituted Diglycolamides in Octanol Medium

R.B. Gujar¹, B. Mahanty^{1,2,§}, P.K. Mohapatra², W. Verboom³

¹Actinide Chemistry Section, Radio Chemistry Division, BARC, Trombay

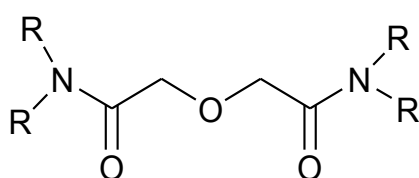
²Homi Bhabha National Institute, Mumbai

³Laboratory of Molecular Nanofabrication,

University of Twente, P.O. Box 217, 7500 AE Enschede, the Netherlands

§ Email: bmahanty@barc.gov.in

²³⁷Np is a long-lived activation product which is present in the pressurized water reactor (PWR) spent fuel dissolver solution at quite significant concentration. The presence of multiple oxidation state and autocatalytically generated HNO₂ in the dissolver solution complicates the extraction of Np in the TBP containing organic phase. Diglycolamides (DGA) based extractant can extract tri and tetravalent actinide ions very efficiently from nitric acid medium. Supported liquid membrane (SLM) based extraction have many advantages over solvent extraction [1]. In the present study, we have carried out a systematic study on the separation of tetravalent Np and Pu using SLM containing *n*-butyl and isobutyl substituted DGA (Fig. 1) in octanol medium. The oxidation states of Np and Pu were adjusted to +4 by using ferrous sulfamate/hydroxyl amine mixture and NaNO₂ respectively. The kinetics of extraction and stripping (strippant: 0.5 M HNO₃ + 0.5 M oxalic acid) was found to be fast (~10 minutes). The transport study was done in a 20 mL transport cell with the PTFE membrane soaked with the extractant solution and sandwich between the two transport cells. The cumulative transport efficiency of the metal ions at 3 M HNO₃ was shown in Fig. 2. The transport efficiency follow the trend among actinide, Pu(IV)>Np(IV) and *n*-butyl>iso-butyl among the DGA. The transport efficiency increases with the increase of nitric acid. The study showed highly promising results for the transport of the tetravalent actinides at 3 M HNO₃.



R= *n*-butyl / iso-butyl

Fig. 1: Structure of DGA

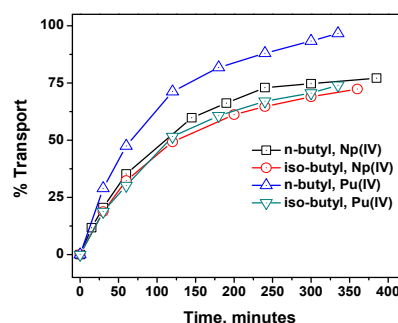


Fig. 2: Transport of actinide through SLM, [L]: 20 mM in octanol, Feed: 3 M HNO₃, strip: 0.5 M oxalic acid+0.5 M HNO₃

References:

[1] P. K. Parhi, *J. Chemistry.*, **1** (2013) 6182361.

Routing Behaviour of Neptunium in PUREX Process Streams During Reprocessing of Fast Reactor Spent Nuclear Fuel at DFRP

K. Dhamodharan[§], T. Aneesh, K. A. Venkatesan, K. Rajan

Reprocessing Group, IGCAR, Kalpakkam, Tamilnadu-603102

[§] Email: kdn@igcar.gov.in

Neptunium (^{237}Np) is considered as an important minor actinide (MAs) among the other MAs, americium and curium, present in the spent fuel discharged from nuclear reactor. Due to the alpha radioactivity of ^{237}Np ($t_{1/2} \sim 10^6$ years), variable valency, and being employed as the target nuclide for the production of ^{238}Pu , understanding the route of neptunium in PUREX process stream is essential for the recovery and nuclear waste management aspects. Since Np exists in different oxidation states mainly Np (IV), Np(V) and Np (VI) and their concentration varies in HNO_3 in presence of HNO_2 , its extraction chemistry is very complex. The direct UV-Visible absorption spectrophotometric method is promising technique for finding the concentration of Np in various oxidation states. But this method is not suitable for the determining the relative % of Np in different oxidation state due to its lower concentration. The presence of nitrite ion in feed solution stabilizes the Pu in +4 oxidation state which enables the quantitative recovery of Pu into organic phase minimizing the loss of Pu in high level waste (HLW). At the same time, the presence of nitrite ion (NO_2^- concentration $> 10^{-3}$ M) partially reduces Np from its hexavalent to pentavalent oxidation state diverting Np present in dissolver solution to high level waste stream [1]. Therefore, experiments have been performed to determine the route of Np in PUREX process streams during reprocessing of spent nuclear fuel discharged from Fast Breeder Test Reactor at DFRP. Extractive alpha spectrometry was employed for the qualitative as well as quantitative analysis of Np in all the streams. The reaction mixture consisting ascorbic acid and hydrazine nitrate was employed for converting the valence of Np to Np (IV) and thenoyltrifluoroacetone (TTA) as a selective extractant for Np (IV). The selective extraction of Np (IV) step was performed inside the hot cell in aqueous sample consisting fission products. Then, the loaded organic extract was delivered to lab for further analysis. The concentration of Np in product and organic samples were performed inside fume hood. In case of U_3O_8 , a weighed quantity of uranium oxide was dissolved in HNO_3 (5.0 M) at 45-50°C in a 50 mL Teflon beaker inside glove box & made up to known volume. The Np concentration in dissolved product was analysed after separation of Np into organic phase (TTA) leaving bulk of U & associated Pu in aqueous phase. The results are shown in table 1 and figure 1.

Table 1. Concentration of Np in DFRP PUREX process streams

Sr. No	Sample Id	[Np], mg/L	% Distribution
1	Dissolver	23.0 - 24.1	99 ± 1.3
2	Loaded org-HAP	6.35 - 6.81	90 ± 3.0
3	U strip pdt-2CP	4.8 - 5.12	70 ± 1.8
4	Lean org.-HCW	< 0.50	≈ 10
5	HLW	< 0.30	≈ 10
6	U_3O_8	250 mg/Kg	60 ± 1.8

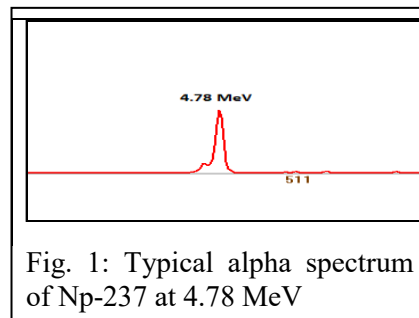


Fig. 1: Typical alpha spectrum of Np-237 at 4.78 MeV

References:

[1] Rawat et al., "Neptunium determination in PUREX process streams". BARC/2016/E/012.

Tailored Polyethersulfone Beads with TiAP/DEHPA for Enhanced Plutonium (IV) Separation from Aqueous Acidic Feed

S.R. Guchhait^{1,2,§}, P.J. Wagh¹, Partha Sarathi¹, A. Kelkar¹, D.B. Sathe¹,
R.B. Bhatt¹, Kartikey K. Yadav^{2,3}, D.K. Singh^{2,3}

¹ Nuclear Recycle Board, BARC, Tarapur - 402502, India

² Homi Bhabha National Institute, Anushaktinagar, Mumbai - 400094, India

³ REDS, Materials Group, BARC, Mumbai, India

§ Email: srguchhait@barc.gov.in

This research demonstrates a method for sequestration of plutonium (IV) from aqueous acidic feed using polyethersulfone (PES) beads impregnated with two extractants, TiAP and DEHPA. PES polymer is renowned for its exceptional chemical and thermal stability, mechanical strength, and versatility in fabrication, provides an ideal platform for immobilizing these extractants. By incorporating TiAP and DEHPA into the PES matrix, we aim to create a robust solid-phase extractant that combines the desirable extraction properties of both compounds while minimizing the limitations associated with liquid-liquid systems. This approach offers the potential for enhanced extraction efficiency, reduced solvent consumption, minimized waste generation, and simplified process operation. This study delves into the meticulous fabrication and comprehensive characterization of these PES composite beads, employing advanced techniques like FTIR, TGA and SEM to elucidate their morphology, porosity, and extractant distribution. The research systematically investigates the synergistic effects of TiAP and DEHPA on plutonium (IV) extraction, examining the influence of key parameters such as solution acidity, extractant concentration, and temperature on the extraction process. The distribution coefficient (K_d) for plutonium (IV) exhibited a peak at 1M HNO_3 , followed by a subsequent decrease. Kinetic analysis reveals remarkably rapid plutonium (IV) sorption, achieving equilibrium within 35 minutes, with adherence to pseudo-second-order kinetics, strongly indicative of chemisorptive mechanisms. Efficient desorption of the sequestered plutonium (IV) was achieved using oxalic acid, and the beads demonstrated commendable reusability and structural integrity over multiple cycles of sorption-desorption. This study comprehensively demonstrates the potential of these TiAP/DEHPA-PES composite beads for the expeditious and sustainable sequestration of plutonium (IV) from acidic aqueous media, offering a promising avenue for advancements in nuclear waste management and environmental remediation strategies.

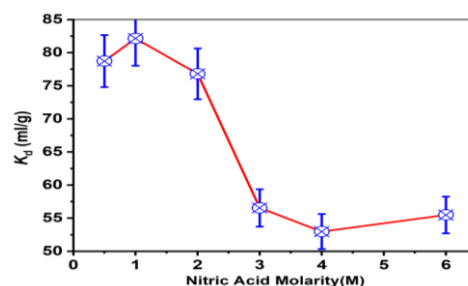


Fig. 1: Plot of K_d vs. Acidity

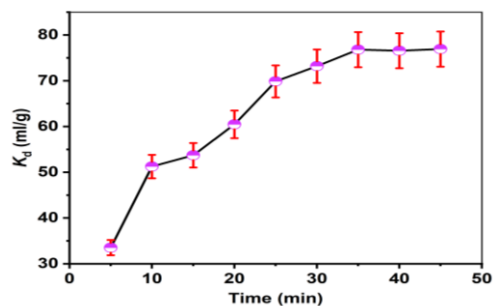


Fig. 2: Plot of K_d vs. Time

References:

[1] R.B. Gujar et al., *Journal of Chromatography A*, **1422** (2015) 206.

An Offline Conjugation of Cloud Point Extraction with Inductively Coupled Plasma Optical Emission Spectrometry for Determination of Trace Lanthanides in Uranium Matrix

Khushboo Kumari, Abhijit Saha[§], S.B. Deb[§]

Radioanalytical Chemistry Division, BARC, Mumbai 400085

[§]Email: asaha@barc.gov.in, sbdeb@barc.gov.in

Determination of trace impurities in nuclear materials is an integral part of their chemical quality assurance (CQA) program. The separation of matrix element(s) and the desired analytes is a pre-requisite step for such precise determination. The age-old liquid-liquid extraction procedure, employing various ligands, specific to the matrix element or analyte(s), is cumbersome and generates a lot of organic waste. In order to overcome such problems, we have explored an environmentally benign cloud point extraction (CPE) [1] for separation and determination of trace rare earth impurities in uranium matrix. CPE has never been used in such separation since high acidity of the solution (which is required to dissolve nuclear materials) disrupts the micelles [1]. A synergistic mixture of a hydrogen bond donor (here di-(2-ethylhexyl) phosphoric acid) and an acceptor (here trioctylphosphine oxide) was explored to be used as ligand in the CPE process using the nonionic detergent Triton X-114. The 1:2, 1:1 and 2:1 mixtures of TOPO and D2EHPA respectively were found to be liquid at RT and their FTIR spectra (Fig. 1) confirm the H-bonding between the P=O group of TOPO and O-H group of D2EHPA. Thus, the synergistic mixture is thought to behave as a tripodal ligand like TODGA, being selective for lanthanides [2]. An inductively coupled plasma optical emission spectrometer (ICP-OES) was used for analysis of the surfactant rich phase (SRP) after dilution with HNO₃ solution + methanol. The 1:1 synergistic mixture was found to recover > 90% of all lanthanides from uranium matrix in 1.0 mol L⁻¹ H₃PO₄ medium to the SRP. By adding oxalic acid to the solution, the recovery of lanthanides is not affected even in presence of 10⁶ times more uranium. A high purity U metal (99.9%, UED/BARC) was dissolved in conc. HNO₃ and then converted to 1.0 mol L⁻¹ H₃PO₄ medium by evaporation for conducting the proposed CPE process via spike addition. The results of the study are given in Table 1.

Table 1: CPE assisted ICP-OES determination of Ln in a matrix of 1.0 g high purity uranium metal

Element	Amount added (μg g ⁻¹)	Amount found (μg g ⁻¹)	Recovery (%)
Nd	1.0	0.95±0.05	95
Sm		0.92±0.06	92
Eu		0.98±0.04	98
Gd		0.98±0.04	98
Tb		0.93±0.05	93
Dy		0.95±0.04	95
Ho		0.91±0.04	91

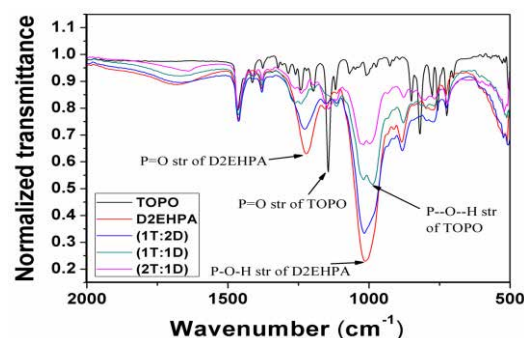


Fig. 1: FTIR spectra of TOPO, D2EHPA and the three synergistic mixtures

References:

[1] A. Saha et al., *RSC Adv*, **6** (2016) 20109.

An Accurate and Precise Isotope Dilution Mass Spectrometry Method for the Determination of U in High Active Liquid Sample

Ananda Karak^{1,§}, A. K. Tiwari¹, M. A. Kesarkar¹, P. Banerjee¹, P. S. Mukherjee¹, A. Kelkar¹, D. B. Sathe¹, R. B. Bhatt¹

¹Nuclear Recycles Board, INRPO, BARC, Tarapur, Maharashtra – 401 502, India

[§]E-mail: akarak@barc.gov.in

In this work, we report development of an isotope dilution mass spectrometric (IDMS) method for precise and accurate determination of uranium (U) in high level radio-active liquid waste (HLW), which is raffinate of PUREX process. The conventional methods used for determination of U in HLW have relatively poor accuracy and precision. Moreover, spectrophotometric based thiocyanate method suffers from corrosion issues [1], and ICP-AES based method, installed inside glove box, is prone to enhance background radiation levels due to residual activity present inside glove box. Redox titrimetric method is highly accurate and precise ($\pm 0.2\%$), where uranyl is reduced to uranous using ferrous solution and after treating the excess ferrous with ammonium molybdate, uranium was estimated by the titration with $K_2Cr_2O_7$ in H_2SO_4 . This method requires minimum 3-4 ml HLW sample, which restricts its analysis in hot cell due to high gamma radiation. In the proposed method, the sample (0.02-0.03 g) was mixed directly (without dilution) with spike (containing ^{233}U) on weight basis followed by addition of 3.5 M HNO_3 and 30% tri-n-butyl phosphate (TBP). After washing the organic phase, U was stripped using 0.01 M HNO_3 and analysed in thermal ionisation mass spectrometer (TIMS 3090). Moreover, there are several advantages of the proposed IDMS method: a) In IDMS analysis, sample aliquots containing microgram sample elements are sufficient to provide good sensitivity and highly precise isotopic ratios in mass spectrometry analysis. b) The separation of U was carried out using only nitric acid and 30% TBP in *n*-dodecane. Therefore, the wastes generated are compatible with plant process. c) In IDMS method, quantitative separation is not required after thorough mixing of sample and spike.

IDMS method and redox titrimetry method are compared with potentiometric end point (Metrohm 800 Dosino) and both the results were found in good agreement. The method was validated with laboratory standard solution. Moreover, simulated solutions (2.52, 3.66, 4.89, 6.96 and 9.49 mg/g) were prepared, and no significant change in accuracy and precision of the

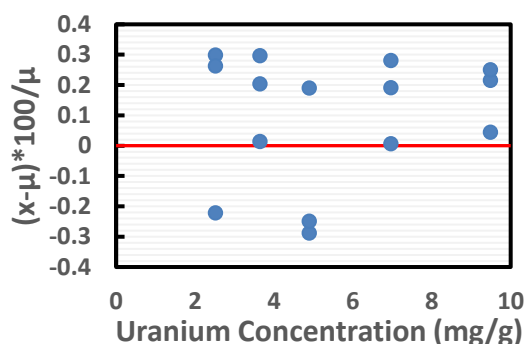


Fig. 1: Deviation of analysis data (x) from true value (μ) using simulated solutions.

measurement was observed. Using the proposed method, real field HLW (U conc. <10 mg/g) from PHWR fuel ($\sim 99.6\%$ U is ^{238}U) reprocessing was analysed for U concentration, where no significant interference of low concentration of plutonium was seen, and the gamma activity of the separated sample was >1000 times reduced. The accuracy and precision of the measurements were found to be better than $\pm 0.3\%$. This method is highly reproducible and are free from the limitations of spectrophotometric and ICP-AES methods. As no

conventional method gives accuracy and precision better than $\pm 0.3\%$ for U analysis in HLW sample, this method can be applied to get a precise and accurate result of U in HLW.

References:

[1] R.K. Dinnappa, H.B. Rudresh, S.M. Mayanna, *Surface Technology*, **10** (1980) 363.

Electrochemical Study of Uranium at Bimetallic Ni Zn Based MOFs Modified Electrode

Nitin Gumber^{1,2}, Apeksha Kadam³, Ashutosh Srivastava⁴, Rajesh V. Pai^{1,2,§}

¹ Fuel Chemistry Division, Bhabha Atomic Research Centre, Mumbai

² Homi Bhabha National Institute, Anushakti Nagar, Mumbai

³ Vivekanand Education Society's College of Arts Science & Commerce, Mumbai

⁴ Radiochemistry Division, Bhabha Atomic Research Centre, Mumbai

§Email: rajeshvp@barc.gov.in

The redox speciation of uranium at tracer level concentration in aqueous medium using conventional electrodes is highly challenging due to its sluggish redox kinetics and lower potential window. Therefore, the advancement of electrodic materials is essential for understanding the speciation of uranium at low concentration levels to predict its mobility and reactivity in the environment. Because of high chemical and thermal stability and high adsorption efficiency, the Metal Organic Framework (MOF) would be a fascinating material for speciation studies of uranium in an aqueous medium at the tracer level.

Two bimetallic MOFs based on Ni and Zn metallic clusters were synthesized using solvothermal approach. MOF-2 consists of Ni and Zn as the metal centers and 1,3,5-tricarboxylic acid (BTC) as the linker whereas MOF-1 consists of same metals however 10 % of BTC is now substituted with phthalic acid (PA) to induce defects into the structure and the corresponding XRD is shown in Fig. 1. Since defects would not change the crystal structure, similar XRD is observed for both the MOFs. Further the defective structure was confirmed by observing the increase in surface area of substituted MOF ($652 \text{ m}^2\text{g}^{-1}$) compared to bare MOF ($288 \text{ m}^2\text{g}^{-1}$).

In the present work, the efficacy of MOFs (1 and 2) was examined for the speciation of uranium by cyclic and differential pulse voltammetry. The CV plots of uranium at bare GC and MOF/GC are shown in Fig. 2, which indicates the peak current enhancement at MOFs/GC than the bare GC. This current enhancement may be due to the pre-concentration of uranium at the electrode surface by the present MOF. This is because of their high adsorption capacity ($\sim 400 \text{ mg/g}$). Furthermore, due to their peak current enhancement at MOFs/GC, the detection limit for the speciation of uranium is 10^{-8} M , which is quite higher than the conventional electrode. The diffusion coefficient of uranyl at the MOFs/GC was found to be in the order of $10^{-6} \text{ cm}^2/\text{sec}$. The result indicates that both MOF-1 and 2 are efficient for sensing of uranium at low concentration level.

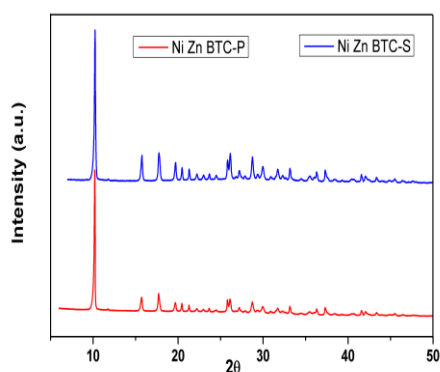


Fig. 1: XRD patterns of MOF-1 and MOF-2.

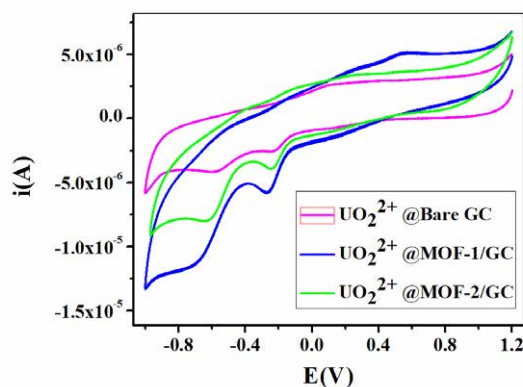


Fig. 2: CV plots of Uranium (10^{-4} M , pH 3) at bare GC and Modified GC.

Speciation and Decorporation of Uranium with Pyrazine-2-Amidoxime Chelate

Ashutosh Srivastava¹, Manjoor Ali², Shikha Sharma¹, Pranaw Kumar, Rama Mohan Rao Dumpala^{1, §}, Amit Kumar^{2, §}

¹Radiochemistry Division, BARC-Mumbai, India

²Radiation Biology and Health Services Division, BARC-Mumbai, India

§Email: rammohan@barc.gov.in; amitk@barc.gov.in

Uranium is the most important naturally-occurring actinide and a crucial resource for nuclear power, which is also recognized as a global environmental contaminant due to its combined radio- and chemo-toxicities [1, 2]. Although different routes that introduce uranium into the human body exist, e.g., through ingestion, inhalation, and wound related absorption, approximately two-thirds of uranium is subsequently eliminated from plasma and excreted through the kidney. However, the portion of uranium that remains is retained in deposits found in kidneys and bone tissues in the form of the hexavalent uranyl ion (UO_2^{2+}), leading to both acute and chronic renal damage, as well as a heightened risk of osteosarcoma and osteogenesis [1-2]. A decorporation agent which can effectively remove uranium from these parts in humans is highly desirable. Amidoxime based chelators are well known for their strong binding ability for metal cations and with many metal cations and its redox capability in adjusting/controlling the oxidation states of metal ions. Amidoxime based chelators have been intensively studied for its applications in separation processes such as the sequestration of uranium from seawater and actinide separations in spent nuclear fuel cycle. In this work, we have taken a redox active amidoxime ligand i.e., Pyrazine-2-Amidoxime (PyAm) to understand the speciation and decorporation efficiency of uranium. The speciation information such as redox behaviour, coordination modes, and stoichiometry for the uranyl-PyAm complex are obtained by cyclic voltammetry, UV-visible spectroscopy, and ESI-MS. PyAm (5-200 μM) did not cause any significant hemolysis, suggesting biocompatibility of ligand. Also, PyAm at 200 μM decreased U content by $\sim 40\%$, as compared to only U-treated erythrocytes. Results indicates that PyAm showed prominent decorporation efficacy for removal of uranium.

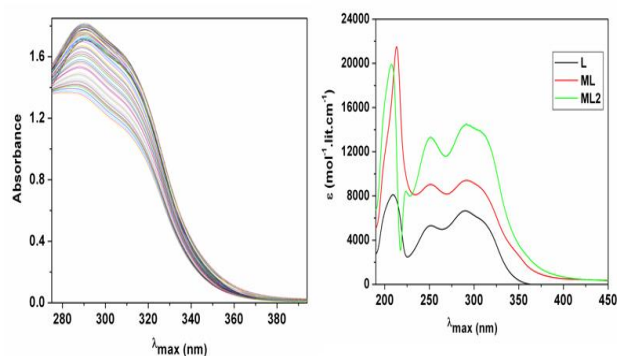


Fig. 1: UV-Visible spectra of uranyl with increasing concentration of PyAm ligand.

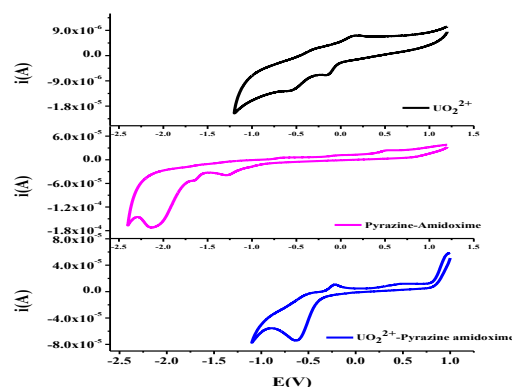


Fig. 2: Cyclic voltammetry of uranyl, PyAm, and Uranyl-PyAm.

References:

- [1] Ashutosh Srivastava et al., *Inorganic Chemistry*, **61** (2022)15452.
- [2] Z Qin et al, *Dalton Transactions*, **45** (2016) 16413.

A Sensitive Differential Pulse Voltammetry Method for Dissolution and Destructive Assay of Uranium Oxide in Acidic Media

Shiny S. Kumar, Pooja Agarkar, Ashutosh Srivastava[§], S. Jeyakumar[§]

Radiochemistry Division, BARC-Mumbai, India

[§] Email: sriashu@barc.gov.in; sjkumar@barc.gov.in

Exploration of sensitive method for understanding the dissolution and subsequent destructive analysis of Uranium oxides is essential for routine chemical quality control and physical inventory verification exercise for nuclear material accounting purposes of fuel matrices and waste management [1-2]. The kinetics of dissolution of uranium oxide in aqueous solution is significant for a better knowledge of mechanism and to enable the prediction of factors which contribute to faster dissolution. Particularly intriguing is the dissolving of uranium oxide in nitric acid since it is the initial step in the reprocessing of nuclear fuels. Despite the development of numerous processes [1-2] on nitric acid dissolution and assay by spectrophotometry and redox titrimetric methods, there is lack of reagent free sensitive method which can provide the information about the dissolution mechanism and destructive assay at one place and time (i.e., in-situ mode). In this context, our aim is to develop reagent free differential pulse voltammetry (DPV) method for understanding the dissolution mechanism and destructive assay of uranium oxide (U_3O_8) with varying molarity of nitric acid medium. Approximately 50 mg of U_3O_8 was taken in 4 ml of 0.1 M nitric acid medium and dissolution was carried out at room temperature as well as 50°C using DPV in-situ approach. The equilibration time for dissolution was found to be 60 minutes. The DPV was also recorded with increasing concentration of uranium in 0.1 M nitric acid and the corresponding plot is shown in Fig. 1. Related to it the calibration plot is shown in Fig. 2, which shows the linearity between peak current and concentration of uranium. Using the calibration plot, the concentration of dissolved uranium oxide was determined and validated by biamperometry end point detection method. The detection limit of calibration plot was found to be 2×10^{-3} mg/g, which is better than the redox titrimetry biamperometry method.

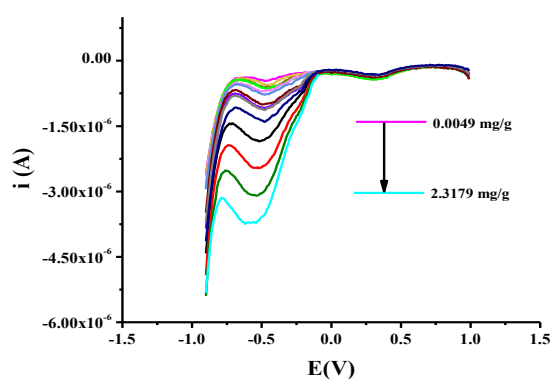


Fig. 1: Differential pulse voltammetry plot with increasing concentration of uranium

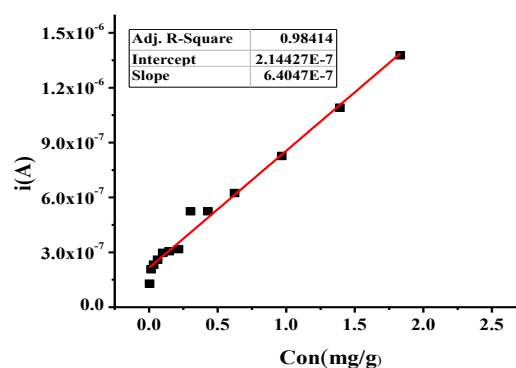


Fig. 2: Calibration plot of Uranium in 0.1 M Nitric acid medium

References:

- [1] A. Srivastava et al., *Analytical Chemistry*, **96** (2024) 14891.
- [2] T. Li et al., *ACS omega*, **9** (2024) 46851.

Development of Amide-Based Resin for Rapid Uranium Sorption

Vinita Kumari^{1,3}, Ritesh Ruhela^{1,3,§}, Mahesh Tiwari^{2,3}, S.K. Sahu^{2,3}

¹ Materials Processing & Corrosion Engineering Division,

² Environmental Monitoring & Assessment Division
Bhabha Atomic Research Centre, Mumbai, India

³ Homi Bhabha National Institute, Mumbai, India

§ Email: riteshr@barc.gov.in

The recovery of low-concentration uranium-bearing effluents has gained significant importance due to their adverse environmental impact. The ion exchange method has been widely used for the recovery of hazardous metal ions from dilute aqueous solutions containing metal ions at sub ppm levels. Amide extractants offer several advantages, including radiation resistance, resistance to hydrolysis and radiolysis, easy removal of decomposition products without affecting the extraction and separation process, complete combustion without generating solid waste, and ease of synthesis.

In this study, a novel solid sorbent, namely, BM PPSD resin was synthesized by grafting butyryl diamide onto a resin. The introduction of ionic core functionality into the polymer backbone enhanced the kinetics of uranium sorption. The functional groups incorporated into the resin were characterized using FTIR and SEM-EDS. The maximum uranium uptake was achieved at a 2 M ammonium nitrate concentration under dilute acidic conditions (pH 2-3). Within the first 5 minutes of contact, the resin exhibited an impressive uranium uptake of 50-60%, with approximately 80% being absorbed within 15–20 minutes. The loading capacity of resin was determined to be 40 mg/g. The sorption mechanism followed a pseudo-second-order model, confirmed by fitting the uranium uptake data in kinetic models, which can be attributed to the interaction of uranyl ions with the amide groups of the resin. The sorption isotherm data were well-fitted to both the Langmuir and Freundlich isotherm models.

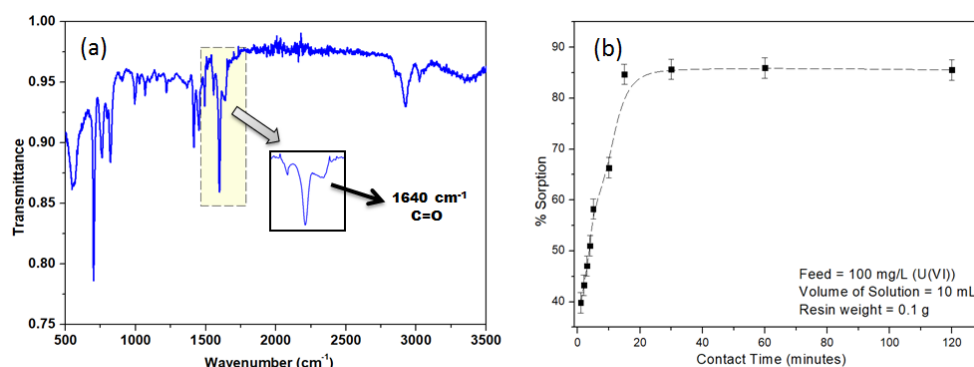


Fig. 1: (a) FT-IR of BM-PPSD resin (b) Sorption behavior of U(VI) onto BM-PPSD.

References:

- [1] Xiujing Peng, Xiaolei Liu et. al., *Journal of Radioanalytical and Nuclear Chemistry*, **327** (2021) 395.
- [2] Lidan Zonga, Fuqiang Liu et.al., *Chemical Engineering Journal*, **334** (2018) 995.

Separation of Plutonium, Thorium and Uranium in MSBR Fuel Using HPLC

Vijay M. Telmore^{1,§}, Raju V. Shah¹, Pranaw Kumar¹, P.G. Jaison²

¹ Fuel chemistry Division, Bhabha Atomic Research Centre, Trombay, Mumbai

² Radioanalytical Chemistry Division Bhabha Atomic Research Centre, Trombay, Mumbai

§ E-mail: telmorev@barc.gov.in

Molten Salt Breeder Reactor (MSBR) is a fourth-generation reactor which has many advantages like inherent safety, excellent neutron economy, no fuel assembly fabrication and amenable to online reprocessing and refilling [1]. MSBR utilizes fuel in molten form, typically consisting of fissile (such as PuF₃ and UF₄) and fertile (ThF₄) elements dissolved in a fluoride medium of alkali and alkaline earth metal fluorides. The most important challenge while developing the separation methodology for this fuel is due to corrosive nature of fluoride salts.

The present paper discusses the development of a method for the separation of actinides like U, Pu and Thorium using high performance liquid chromatography. A C₁₈ reversed phase column (4.6 mm x 250 mm, Chromolith) was used as the stationary phase. Mandelic acid and acetonitrile were used as eluent. The eluted fraction was monitored using Arsenazo (III) as a post column-derivatizing reagent at 653 nm. The UF₄-LiF sample was dissolved and then treated with nitric acid. This sample was then spiked with thorium and plutonium (IV). The sample was evaporated to near dryness and then made up with mobile phase before injection. Different chromatographic conditions such as concentration of eluent, pH and composition of acetonitrile were studied systematically and optimized. Under the optimized conditions, Pu, Th and U spiked in to the dissolved MSBR fuel, were found to be separated. Under the developed conditions, Pu(IV) and Th were found to elute prior to uranium, as seen in the Fig.1.

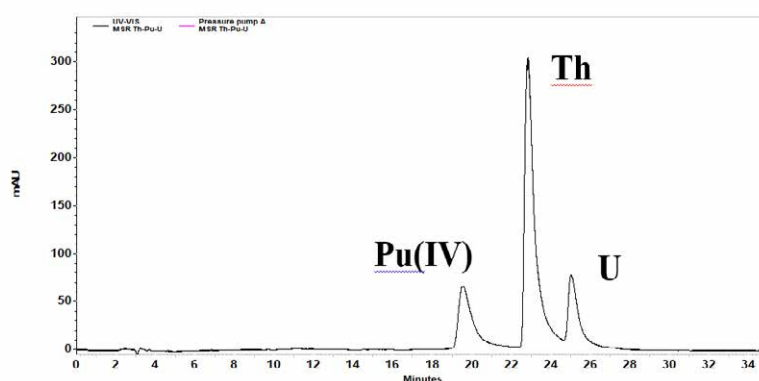


Fig.1 Chromatogram obtained for the dissolved MSR fuel salt spiked with Pu and Th (HPLC conditions: Mandelic acid (pH = 6.0) = 30 % , pH = 2.0 (8 %) , ACN = 10% to 30 % in 10 mins.)

References:

- [1] U.S. DOE. A technology roadmap for generation IV nuclear energy systems. In Nuclear Energy Research Advisory Committee and the Generation IV International Forum; USDOE Office of Nuclear Energy, Science and Technology (NE): Washington, DC, USA, (2002).

Development of Functionalized Aluminosilicate Composites from Fly Ash for Efficient Sorption of Am(III)

Atanu Das¹, Ranjeet Saket³, Aishwarya S. Kar^{1,2,§}

¹Radioanalytical Chemistry Division, ²Homi Bhabha National Institute, Mumbai, India

³K J Somaiya College of Science and Commerce, Mumbai

§ Email: aishj@barc.gov.in

Fly ash, a byproduct of thermal power plants, is rich in alumina and silica, making it a promising candidate for the synthesis of aluminosilicate-based composites with notable sorption properties. In this study, we report a novel approach for synthesizing aluminosilicate composites from fly ash, followed by its functionalization with 3-aminopropyl trimethoxy silane to further enhance its sorption capabilities. The composites were characterized using FTIR, SEM, and XRD to gain comprehensive structural insights. The primary objective was to evaluate the sorption efficiency of these composites for Am(III), a long-lived minor actinide found in nuclear waste, for its effective removal from waste streams to minimize environmental and health risks. The FTIR spectrum of functionalized composites exhibited characteristic bands at ~ 1500 and 2900 cm^{-1} which are assigned to C-C and C-H stretching, respectively. The stretching associated with $-\text{NH}_2$ group could not be clearly identified due to the overlap with $-\text{OH}$ stretching in the functionalized composite (Fig. 1). Initial results demonstrated that the functionalized aluminosilicates (98% sorption) exhibited better sorption efficiency as compared to pristine; therefore, our focus was to study the functionalized composite in detail. The enhanced sorption capacity suggests that the enhanced sorption is due to the grafted alkyl amine sites on the composite. Sorption studies were carried out using ^{241}Am as a radiotracer. Kinetics experiment of Am(III) sorption on functionalized aluminosilicate showed that sorption equilibrium was attained within 2 h and obtained data were best explained by pseudo second-order kinetic model. The pH dependent sorption of Am(III) on functionalized composite shows an S-shape curve wherein Am(III) sorption capacity initially increases with pH thereafter attaining saturation at $\text{pH} > 5$ (Fig. 2). This can be explained in terms of deprotonation of aluminol, silanol sites as well as complexation of Am(III) with $-\text{NH}_2$ group present in functionalized composite. Furthermore, isotherm studies conducted at 25, 40, and 55°C , revealed an increase in Am(III) sorption with temperature (Fig. 3). These findings underline the potential of functionalized aluminosilicate composites as highly efficient materials for the removal of Am(III) from aqueous solutions, offering a promising approach for environmental cleanup in radioactive contamination scenarios.

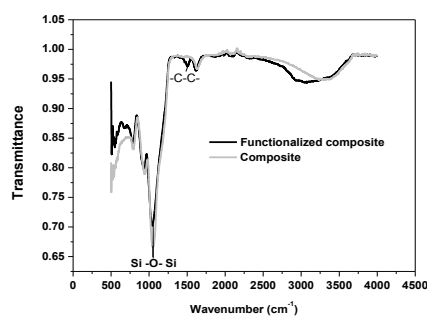


Fig. 1. FTIR of aluminosilicate composites

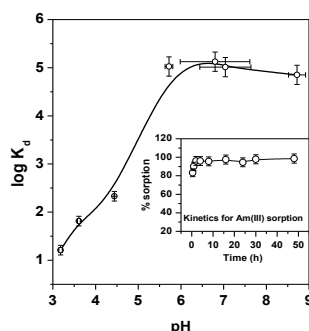


Fig. 2 Am(III) sorption kinetics (Inset) & effect of pH. Solid to liquid ratio: 1 g L^{-1} ; Am(III) = $6.5 \times 10^{-9}\text{ M}$.

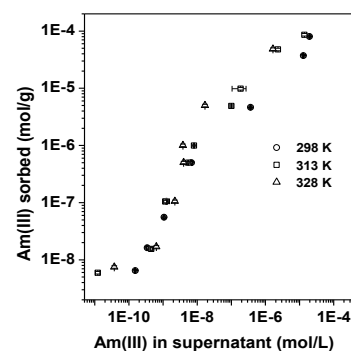


Fig. 3 Am(III) adsorption isotherm. Solid to liquid ratio: 1 g L^{-1} ; Am(III) = $6.5 \times 10^{-9}\text{ M}$.

Sorption Properties of Eco-friendly Fly Ash-based Geopolymer for Am(III) Ion Removal in Nuclear Waste Management

Atanu Das¹, Aishwarya S Kar^{1,2,§}, M. K. Saxena¹

¹Radioanalytical Chemistry Division, B.A.R.C., Mumbai, India

²Homi Bhabha National Institute, Mumbai, India

§Email: aishj@barc.gov.in

Geopolymers (GP's) have emerged as one of the most promising sorbents for the removal of heavy metals from contaminated waters [1]. However, GP's have not been extensively explored for the removal of radionuclides [2]. Americium is one of the long-lived minor actinides present in nuclear waste streams. Though conventional methods are employed for its effective removal, the present study aims to evaluate the sorption characteristics of an eco-friendly GP, synthesized from coal fly ash, a byproduct of thermal power plants and aluminum source, derived from aluminum foil- a house hold waste, using alkaline solutions of sodium metasilicate and sodium hydroxide. Comprehensive characterization of the synthesized GP's was carried out using X-ray diffraction (XRD) Energy-dispersive X-ray fluorescence (ED-XRF), Scanning electron microscopy (SEM), and Fourier-transform infrared spectroscopy (FTIR), prior to the evaluation of its sorption characteristics. The XRD of synthesized GP's showed mullite, quartz, rutile and anatase as major phases, whereas in the FTIR spectra a major shift ($\sim 50 \text{ cm}^{-1}$) in Si-O-Si band was observed in GP as compared, to precursor (Fig. 1). The sorption behavior of GP was evaluated for Am(III), using ^{241}Am as a radiotracer, where the sorption equilibrium was achieved within 0.5 h (Fig. 2) and the sorption kinetics followed a pseudo-second-order model. The pH dependent sorption experiments indicated quantitative Am(III) sorption above pH 4 thereby that exhibiting that GP possesses excellent sorption capabilities with regard to Am(III) (Fig. 3). Thus, the eco-friendly GP offers a promising, cost-effective, and environmentally sustainable alternative for nuclear waste management.

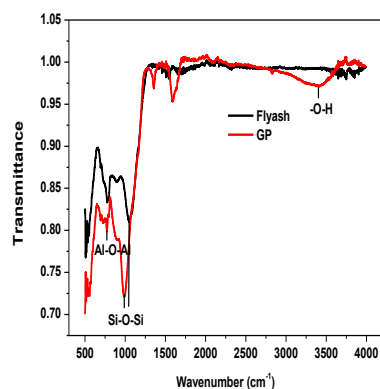


Fig.1 FTIR of fly-ash and GP

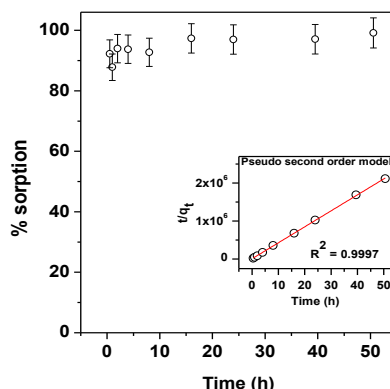


Fig. 2 Kinetics of Am(III) sorption on GP. Solid to liquid ratio: 1 g L^{-1} ; Am(III) = $1 \times 10^{-5} \text{ M}$.

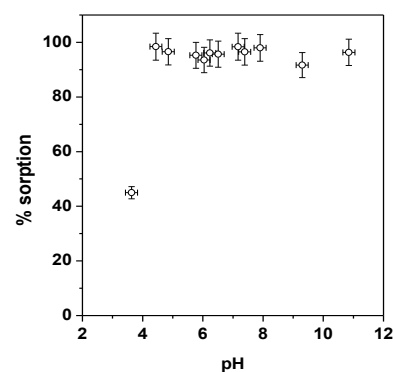


Fig. 3 Am(III) sorption on GP at varying pH. Solid to liquid ratio: 1 g L^{-1} ; Am(III) = $1 \times 10^{-5} \text{ M}$.

References:

- [1] K. Al-Zboon, M.S. Al-Harashsheh, F.B. Hani, *J. Hazard. Mater.*, **188** (2011) 414.
 [2] X. Niu et al., *J. Hazard. Mater.*, **429** (2022) 128373.

Complexation Thermodynamics Studies of UO_2^{2+} /DGA Complexes by Optical Spectroscopy and Microcalorimetry: Effect of Alkyl Chain Branching

D.B. Sharma^{1,§}, A.P. Wadawale², S.A. Ansari¹, A. Bhattacharyya¹

¹ Radiochemistry Division, BARC, Mumbai – 400 85, India

² Chemistry Division, BARC, Mumbai – 400 085, India

§ Email: dbsharma@barc.gov.in

Diglycolamide (DGA) ligands have been extensively studied for actinide partitioning as the ligands show excellent complexation ability with trivalent actinides over hexavalent actinyl ions [1]. Though the DGA ligands show poor extraction for UO_2^{2+} ions, their fundamental complexation studies with this ligand has been also well studied. Previous studies have shown that formation constants of DGA/ UO_2^{2+} complexes increase linearly with increasing the alkyl chain length of DGAs [2]. In this paper, we report the complexation of UO_2^{2+} ion with a series of DGA ligands having branched alkyl chains, but the same number of carbon atoms. In order to investigate the effect of alkyl chain branching on UO_2^{2+} cation, the chosen DGA ligands in this study were *n*-butyl DGA, *sec*-butyl DGA and *iso*-butyl DGA (Fig 1).

Initial spectrophotometric titration of UO_2^{2+} ions with DGAs (in methanol) could be succeeded with *n*-butyl and *sec*-butyl derivatives, but *iso*-butyl DGA formed precipitate during the titration. As shown in Fig 2, as the titration of UO_2^{2+} ions proceeded with the DGA ligands, the changes in the absorption spectra indicated the complexation of the uranyl ion with the ligands. The incremental changes in the spectra were higher for *n*-butyl DGA, indicating that the interaction of normal DGA is stronger than the branched one. The analysis of the spectra indicated the formation of two successive complexes, $(\text{UO}_2\text{L})^{2+}$ and $(\text{UO}_2\text{L}_2)^{2+}$ for both the ligands. The stability constant values were calculated as: *n*-butyl DGA: $\log\beta_1 = 3.29 \pm 0.03$, $\log\beta_{1,2} = 6.21 \pm 0.07$; *sec*-butyl DGA: $\log\beta_1 = 2.50 \pm 0.04$, $\log\beta_{1,2} = 4.42 \pm 0.06$. The $\log\beta$ values for *iso*-butyl DGA could not be determined due to formation of precipitate during the titration. In order to look into the complexation insight with the *iso*-butyl DGA, DFT calculations were done for all the three ligands given above. The DFT calculations indicated the strength of complexes in the order: *n*-butyl DGA \sim *iso*-butyl DGA $>$ *sec*-butyl DGA. The calorimetric titration studies indicated the complexation of uranyl cation with both the ligands (*n*-butyl DGA and *sec*-butyl DGA) was endothermic. Detail results of complexation thermodynamics will be presented in this paper.

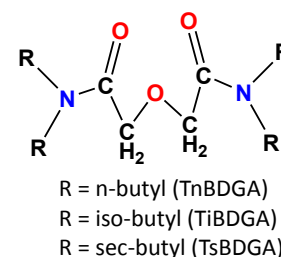


Fig 1. Structure of DGA

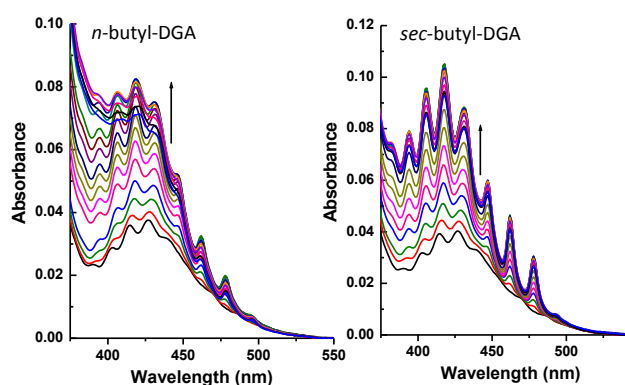


Fig 2. Spectrophotometric titration of UO_2^{2+} with DGA in methanol. Cuvette: 5 mM $\text{UO}_2(\text{ClO}_4)_2$. Ligand: 25 mmol/L.

indicated the formation of two successive complexes, $(\text{UO}_2\text{L})^{2+}$ and $(\text{UO}_2\text{L}_2)^{2+}$ for both the ligands. The stability constant values were calculated as: *n*-butyl DGA: $\log\beta_1 = 3.29 \pm 0.03$, $\log\beta_{1,2} = 6.21 \pm 0.07$; *sec*-butyl DGA: $\log\beta_1 = 2.50 \pm 0.04$, $\log\beta_{1,2} = 4.42 \pm 0.06$. The $\log\beta$ values for *iso*-butyl DGA could not be determined due to formation of precipitate during the titration. In order to look into the complexation insight with the *iso*-butyl DGA, DFT calculations were done for all the three ligands given above. The DFT calculations indicated the strength of complexes in the order: *n*-butyl DGA \sim *iso*-butyl DGA $>$ *sec*-butyl DGA. The calorimetric titration studies indicated the complexation of uranyl cation with both the ligands (*n*-butyl DGA and *sec*-butyl DGA) was endothermic. Detail results of complexation thermodynamics will be presented in this paper.

References:

- [1] S.A. Ansari, et. al., *Chem. Rev.* 112 (2012) 1751.
- [2] S.A. Ansari, et. al., *Polyhedron*, 220 (2022) 115820.

Diluent Free Solvent Extraction of Uranium with Higher Analogue of TOPO-DEHPA Eutectic

M. Sharathbabu¹, Prashant Patil¹, Sachin Pathak¹, Ashutosh Srivastava^{2,§}, S.K. Rakshit¹

¹Product Development Division, ²Radiochemistry Division, BARC-Mumbai, India-400085

§Email: sriashu@barc.gov.in

Liquid-liquid extraction (LLE) is effective for separating actinides in nuclear reprocessing but involves challenges associated with large volumes of volatile organic solvents (VOCs). Advancements in extraction methods are sought to improve efficiency and environmental sustainability. Hydrophobic deep eutectic solvents (DESs) are emerging as suitable alternatives due to their promising solvent properties and tunable characteristics, with applications in solvent extraction. The properties of DES such as non-toxicity and biodegradability and ease of synthesis makes DESs a better option in the extraction of metal ions. DES are composed of primarily a hydrogen bond donor (HBD) and hydrogen bond acceptor (HBA) in appropriate ratio, which results in a liquid at room temperature with melting point lower than either of the components.

Usually, TOPO or DEHPA in organic diluents or in ionic liquid diluents were used for the extraction of Uranium. In the present work, the DES was prepared by combining 1:3 mole ratio of TOPO and DEHPA. This solvent was directly employed for liquid-liquid extraction of Uranium from nitric acid medium. The stock solution of ²³³U tracer (~15µg/ml) in nitric acid was used in extraction studies. The extraction experiments were carried out by equilibrating aqueous phase containing ²³³U tracer in required nitric acid molarity with hydrophobic TOPO-DEHPA [1:3] solvent keeping DES:Aqueous phase ratio 1:2. The solutions were centrifuged and the assay of ²³³U in both the phases was carried out by using alpha liquid scintillation counting. About 15-20 minutes was found to be sufficient for equilibration. Fig.1 depicts that the extraction increases with increase in nitric acid concentration upto 4M thereafter, it was found to be decrease at higher concentrations. Phase ratio variation studies indicate more than 90% extraction could be achieved with the phase ratio of [1:10] as shown in Fig. 2 signifies even small amount of DES phase could efficiently extract Uranium from 1M nitric acid medium.

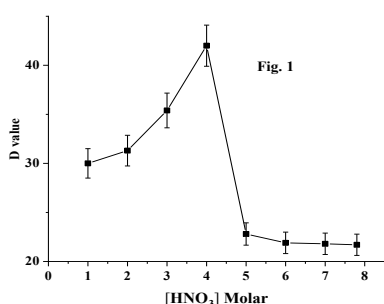


Fig. 1: D value of U with varying acidity

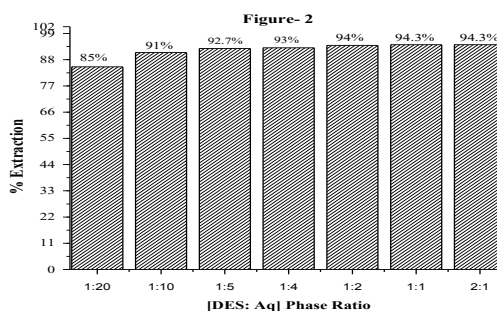


Fig. 2: % extraction of U with phase ratio

Acknowledgements: Authors would like to acknowledge Dr. S.C. Parida, Head, PDD and Dr. S. Jeyakumar, Head, RCD, BARC for their support during the course of this work.

References:

- [1] M Gilmore et al. *ACS Sustainable Chem. Eng.*, **6** (2018) 17323.
- [2] S.K.Patil and V. V. Ramakrishna, *Sep. Sci. Technol.*, **15** (1980) 1459.

Extraction Behaviour of Pu(IV) into Hydrophobic DES of TBACl:DA

Prashant Patil¹, Sachin Pathak¹, M. Sharathbabu¹, Ashutosh Srivastava^{2,§}, S.K. Rakshit¹

¹Product Development Division, B.A.R.C., Mumbai

²Radiochemistry Division, B.A.R.C., Mumbai

§ Email: sriashu@barc.gov.in

Deep eutectic solvents (DESs) are emerging as a promising alternative to conventional volatile organic solvents in several fields including extraction and separation due to their non-volatile and non-flammable nature. Composed of a hydrogen bond donor and acceptor, DESs form eutectic mixtures with a large depression in freezing point than the individual components due to hydrogen bonding interaction. They share similar properties with ionic liquids (ILs) but offer advantages like fast synthesis, easy handling, biodegradability, and non-toxicity, making them ideal for replacing ILs in liquid-liquid extraction (LLE) process of actinides.

In the present work synthesis of DES was prepared by mixing 1:1 mole ratio of tetra butyl ammonium chloride (TBACl) and decanoic acid (DA). This mixture was kept at 60°C in an oven for about 40 minutes. This formed homogeneous hydrophobic eutectic solvent at room temperature. The DES thus prepared was employed for the extraction of Pu(IV) from nitric acid medium. Solution containing ²³⁹Pu tracer in nitric acid was purified by TTA extraction to ensure purity of Pu(IV) stock before using into extraction experiments. The extraction studies were carried out by equilibrating equal volumes of acidic phase of required molarity containing Pu(IV) with (TBACl:DA) DES for 30 minutes in temperature controller shaker bath. The solution was centrifuged to allow proper phase separation. Assay of ²³⁹Pu in aqueous and organic phase was carried out by alpha liquid scintillation counting for the evaluation of D value. Fig. 1 illustrates extraction kinetics of Pu(IV) from 1M HNO₃. It was observed that about 20-30 minutes are required to reach a constant D value. Figure 2 depicts the effect of nitric acid concentration on the extraction of Pu(IV). Steep increase in the D value was noticed between 1M (60%)-3M (96.5%) range. Afterwards the D value increased steadily upto 7.8M.

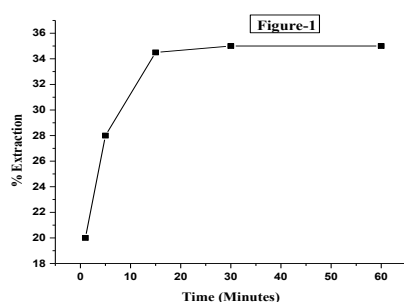


Fig. 1: Extraction of Pu with Time

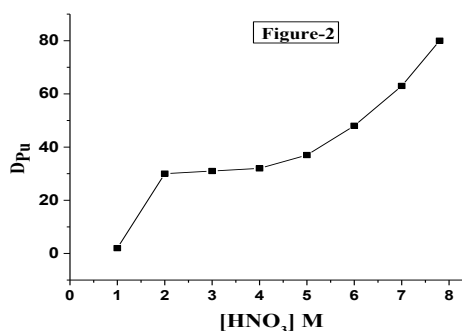


Fig. 2: D value of Pu with acidity

Acknowledgement: Authors grateful to acknowledge Dr S. C. Parida, Head PDD and Dr. S. Jeyakumar, Head, RCD, BARC for their support during the course of this work.

References:

- [1] G. Zante and M. Boltoeva, *Sustainable Chemistry*, **1** (2020) 238.
- [2] A. Kshirsagar et al., *J. Radio. Nucl. Chemistry*, **330** (2021) 1053.
- [3] M. Gilmore et al., *ACS Sustain. Chemistry & Eng.*, **6** (2018) 17323.

XAFS Study of Isostructural Sulphate Salts of Tetravalent Actinides and Lanthanides

Sumit Kumar^{1,2,§}, Meera Keskar³¹ Radioanalytical Chemistry Division, Bhabha Atomic Research Centre, Mumbai, India² Homi Bhabha National Institute, Anushaktinagar, Mumbai, India³ Fuel Chemistry Division, Bhabha Atomic Research Centre, Mumbai, India

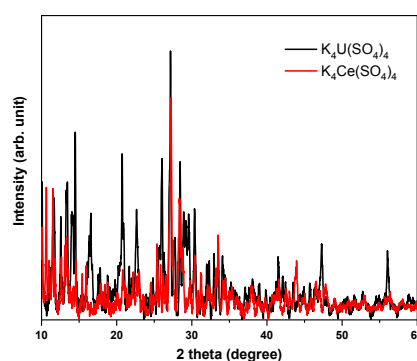
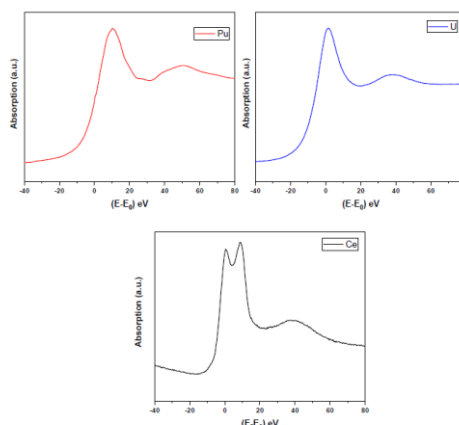
§ Email: sumitk@barc.gov.in

Actinide ions complex with ground water anions and thereby alter their chemical behaviour in environment [1]. Further, investigation of the chemical properties of their salts is important in view of potential applicability in nuclear energy program [2]. In the present work, Uranium and Ce^{IV} isostructural analogues of Potassium Plutonium sulphate salt (K₄M(SO₄)₄: M = U, Ce^{IV}, Pu) were prepared using solid synthesis route and investigated using X-ray absorption fine structure (XAFS) spectroscopy. Aim is to correlate the local-level structural change on varying metal ions with the associated electronic characteristics of the solids. Formation of the solids in the isostructural geometry was ensured using room temperature powder X-Ray Diffraction (XRD) measurement (Figure 1). Lattice constants of the synthesized salts were found matching the literature reported values [3]. The extended XAFS of the three salts measured at their L₃ edge showed M-O bond distance in the order Pu-O < U-O < Ce-O. In the near edge part of XAFS spectra, U and Pu spectra are similar near the edge region while the higher energy feature at $\Delta E \sim 40$ eV beyond the white line position of absorption edge splitted in doublet for Pu case. White line in the edge region was found more intense for uranium salt compared to that of Pu salt. Any fine structure was absent in the pre-edge and edge region. In cerium salt, the edge region splitted in doublet while higher energy feature was similar to the Uranium case. Probe atoms, for which d and f orbital mixing have been observed in previous studies, differ in f orbital population (Pu⁴⁺: 6d⁰5f⁴; U⁴⁺: 6d⁰5f² and Ce⁴⁺: 5d⁰4f⁰). As spectra (Fig. 2) represent excitation of metal ion 3p_{3/2} electron to nd orbital, variation in the spectral feature for edge region clearly indicates that d orbital participation differs in its hybridization with oxygen 2p orbital (for M – O bonding). Spectra simulation is being pursued to understand the effect of bond covalency in defining these spectra.

Acknowledgements: Authors acknowledge the support and encouragement of Head, RACD.

References:

- [1] M. Altmaier et al. *Chem. Rev.*, **424** (2022) 127603.
- [2] K. D. Singh Mudher et al., *BARC Report.*, **1496** (1990).
- [3] Meera Keskar, et al., *J. Nucl. Mat.*, **334** (2004) 207.

Fig. 1: XRD profile of K₄M(SO₄)₄ salts.Fig. 2: XANES spectra of K₄M(SO₄)₄ salts.

Uranyl Complexation by Hydroxy-Pyridine Dicarboxylic Acid: Thermodynamic and Theoretical Studies

Diksha P Dalvi¹, Shiny S Kumar², Rama Mohana Rao Dumpala^{2,§}, S. Jeyakumar²

¹Department of Chemistry, K. J. Somaiya College of Science and Commerce, Vidyavihar, Mumbai University, Mumbai, India

²Radiochemistry Division, Bhabha Atomic Research Centre, Mumbai, India

§ Email: rammohan@barc.gov.in

Uranyl (UO_2^{2+}) complexation by ligands of biogeo relevance is a key input to predict and model the uranium mobility and transportation in various geological confinements [1]. Organic moieties existing naturally can modify the speciation of uranyl in aquifers. Hydroxy-pyridine dicarboxylic acid capable of forming tridentate chelate complexes with many metal ions, is one such naturally occurring pyridine skeleton moiety [2]. Determination of thermodynamic parameters is a preliminary necessity to estimate solution speciation. The present studies focused on determining the stability, enthalpy of complex formation by uranyl with hydroxy-pyridine dicarboxylic acid. Absorption spectroscopy and isothermal titration calorimetry were employed to determine the stability and enthalpy of complex formation respectively. The present studies involve the titration mode of absorption measurement in which to a fix volume of uranyl solution, the ligand solutions are added in increments and the spectra was collected for each addition of ligand in the range 370-520 nm with an interval of 1 nm in data collection. The variation in absorption intensities (Fig. 1) was used to analyse by HypSpec code to obtain the stability and speciation, while the raw calorimetric data was analysed to know the complex formation enthalpies.

Uranyl found to form ML and ML_2 kind of species with decrease in stability on successive complexation for both the ligands and the determined $\log \beta$ values for the complex formation are 11.92 ± 0.09 , and 21.56 ± 0.20 , while the complexation enthalpies were found to be -11.09 ± 0.09 and, -29.20 ± 0.45 respectively. Both the complex formations are favoured enthalpically though the majority contribution to free energy originated from entropy changes. Density functional calculations employed to estimate the energetics, bond distance and partial charges on key atoms on either side of reaction (for bare and complexes species). The estimated binding energies for ML and ML_2 were found to be -188.0 and -280.4 kJ/mol respectively and are in line with the experimentally determined trends in complex stabilities. The results helped to understand the speciation uranyl by hydroxy-pyridine dicarboxylic acid.

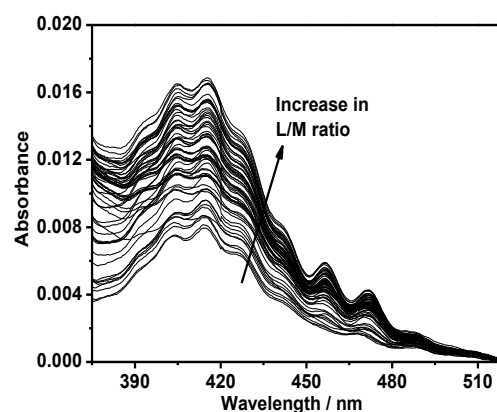


Fig. 1: Absorption spectra of Uranyl (UO_2^{2+}) on changing L/M ratio with addition of hydroxy-pyridine dicarboxylic acid to Uranyl solution.

References:

- [1] K. J. Pastoor et al., *Inorg. Chem.*, **60** (2021) 8347.
 [2] S. Abdolmaleki, M. Ghadermazi, A. Aliabadi, *Sci. Rep.*, **11** (2021) 15699.

Novel Tri-Copolymerized Pyridinium Functionalized Polymeric Resins for Removal of Pb from Lanthanum Chloride Solution

Nikhilesh Nav Vigyan^{1,2}, Ritesh Ruhela^{1,2,§}

¹Materials Processing & Corrosion Engineering Division, B.A.R.C., Mumbai, India

²Homi Bhabha National Institute, Mumbai, India

§Email: riteshr@barc.gov.in

Lead, a toxic metal, is found in rare earth process streams originating from monazite origin. One of the hazards associated with lead is owing to radioactivity associated with one of its isotopes, ²¹⁰Pb, with half-life ~22 years and low energy β ~63.5 keV. Currently, removal of lead from the rare earth leach liquor is achieved using sodium sulphide. However, it has been observed that a very small fraction of lead remains in lanthanum bearing stream. Therefore, there is a need to develop process for its removal from La process stream before discharge [1].

In this work, a novel resin, namely HPMP resin was synthesized by suspension co-polymerisation and characterized using TGA and FTIR. Synthetic feed solution was prepared by dissolving lanthanum carbonate in HCl media along with addition of PbCl₂ and NaCl to promote formation of Pb-anionic complexes [2,3]. Final composition of synthetic solution was Pb ~80 mg/L, La ~ 3550 mg/L in 0.5 M HCl and 1.0 M NaCl. Batch sorption studies showed high selectivity for Pb over La with distribution coefficient (k_d, Pb) ~ 17. Column studies carried out using 60 ml resin, 3 columns of 20 ml each, at flow rate of 3 ml/min, could generate 780 ml of lead free La solution and the loaded Pb could be removed using 0.5 M Thiourea solution for making the resins ready for next cycle of loading.

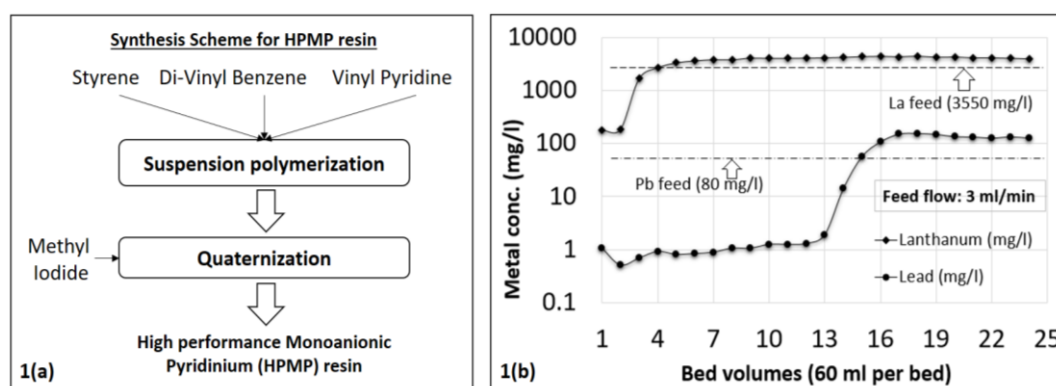


Fig. 1(a): Scheme for HPMP resin synthesis 1, (b) Column runs for Pb-La separation

References:

- [1] D. Pittauerová, B. Hettwig and H.W. Fischer, *Radioprotection*, **46**, 6 (2011) S277.
- [2] Ryan J. Woosley, Frank J. Millero, *Marine Chemistry*, **149**, 20 (2013) 1.
- [3] Aleksandra Wojciechowska, et. al., *Sep. Purif. Technol.* **177**, 28 (2017) 239.

Reverse Phase Liquid Chromatographic Method with Online Pre-Concentrator for Trace Level Uranium Determination in Active Liquid Waste Generated from Uranium Production Facility

Y. Balaji Rao^{1,§}, Shehanaz Bano¹, P.V. Nagendra Kumar², Dinesh Srivastava¹

¹Nuclear Fuel Complex, Dept. of Atomic Energy, ECIL post, Hyderabad- 500062

²Asst Professor, Dept of Chemistry, GITAM University, Hyderabad-502329

[§]Email: ybrclabnfc@gmail.com

Nuclear fuel complex (NFC) is involved in the production of natural UO₂ pellets for pressurized heavy water reactors (PHWR) from different raw materials such as sodium diuranate (SDU), heat treated uranium peroxide (HTUP) and uranium ore concentrate (UOC). During the production of UO₂ pellets, Active liquid wastes are generated from the production plants such as hand wash water and floor clean water. All of these active liquid wastes are collected and treated using electrocoagulation before using as gardening water. The specification for uranium in gardening water is 0.12 µg/mL. Before and after treatment liquid waste is analysed for uranium content.

Laser fluorimetry and ICP-MS are the only known techniques which can cater to low uranium concentration, however laser fluorimetry is the only cost-effective method. RPLC is also a simple, cost effective and interference free technique for uranium determination but found to be suitable at uranium concentration > 0.5 µg/mL [1]. Therefore, for first time a successful effort has been made to develop a simple method to analyze low concentration of uranium in active liquid waste by RPLC method using an online pre-concentrator.

In the developed methodology, C18 column was used as stationary phase and mixture of HIBA and methanol was used as eluent and on online pre-concentration column (PCC) consisting weak acid cation exchanger was used in place of loop and measurement was carried out using spectrophotometer detector. The effect of different parameters like pH and sample medium were studied in trapping of uranium by PCC during the development of the method. A linear calibration graph was obtained in the range 0.01 to 0.1 µg/mL with R² value >0.99. Active liquid waste samples analysed using developed method were compared with other method and found to be in agreement. A typical chromatogram of active liquid waste sample with the developed method is shown in Fig. 1.

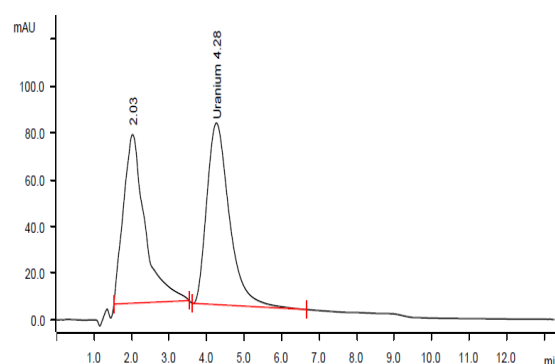


Fig. 1: A typical chromatogram of Liquid active waste sample (eluent 0.1M α -HIBA+10% methanol, pH 4, $\lambda_{652\text{nm}}$)

References:

- [1] Y. Balaji Rao, Shehanaz Bano, P. V. Nagendra Kumar and Dinesh Srivastava, *Radiochim. Acta*, **112** (2024) 221.

Complexation Behavior of Terpyridine Ligands with Am(III) and Eu(III)

FN Femina^{1, 2, §}, Vemuri Lakshmi Ganesh^{1, 2}, C V S Brahmananda Rao^{1, 2},
Gopinadhanpillai Gopakumar^{1, 2}

¹Indira Gandhi Centre for Atomic Research, Kalpakkam – 603102, Tamil Nadu, India.

²Homi Bhabha National Institute, IGCAR Campus, Kalpakkam – 603102, Tamil Nadu, India.

§Email: feminanoushad98@gmail.com

Late 90s have proven the use of *N*-donor ligands to stabilize actinide complexes over lanthanide ones due to their greater polarizability and softer nature. This result arises from the stronger covalent interactions between the ligands and the *5f* orbitals of the actinides compared to the *4f* orbitals of the lanthanides. To illustrate their behaviour, we used terpyridine as a representative ligand to probe the complexation behaviour with Am(III) and Eu(III) metal ions. As a first step, we explored the conformational landscape of the terpyridine ligand to identify the most stable conformer (see Figure 1a). During this step, the corresponding transition-state structures for conformational interconversion were also characterized, and the molecular orbitals responsible for coordination with the metal atom were identified. In the subsequent step, the lowest-energy structures of the corresponding complexes with Am(III) and Eu(III) were derived using density functional theory (DFT) methodologies (see Figure 1b and 1c). Geometry optimizations were performed with and without including dispersion corrections. In the case of Am(III), the dispersion parameters for Eu(III) were used during geometry optimization. All calculations were performed using Turbomole [1], NBO version 6.0 [2], and ORCA version 4.2.1 [3] program packages. It was found that the terpyridine (terpy) ligand exhibits stronger complexation with Am(III) than Eu(III), suggesting that it has a higher affinity for americium. This enhanced selectivity suggests that other terpy ligand derivatives might also be effective in selectively extracting Am(III), potentially offering improvements in nuclear fuel reprocessing.

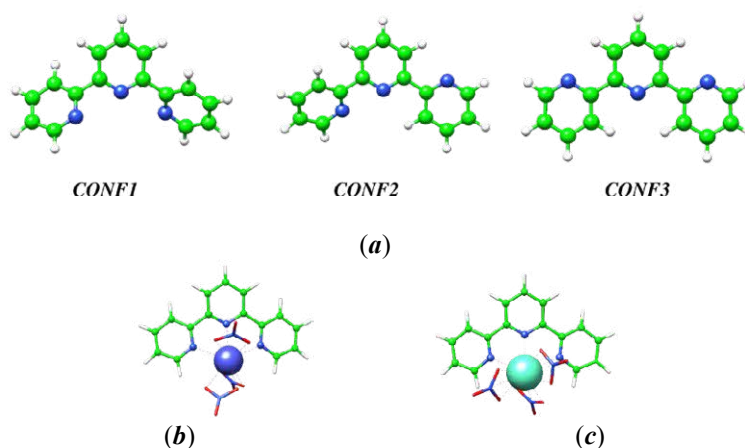


Figure 1. The optimized geometries of (a) 2,2';6',2''-terpyridine conformers and (b) Am(NO₃)₃(terpy) and (c) Eu(NO₃)₃(terpy) complexes at RI-BP86-D3BJ/TZVP level.

References:

- [1] *Turbomole V7.3*; TURBOMOLE GmbH, Karlsruhe, <http://www.turbomole.com>.
- [2] NBO version 6.0. E. D. Glendening et al., Theoretical Chemistry Institute, University of Wisconsin, Madison (2013).
- [3] F. Neese, *Wiley Interdiscip. Rev. Comput. Mol. Sci.*, **8** (2017) 1327.

Computational Prediction of Enthalpy of Extraction for Zr Complexes with Tri-Amyl Phosphate and Diamyl Amyl Phosphonate

Gopinadhanpillai Gopakumar^{1,2,§}, T. Revathy², B. Sreenivasulu^{1,2},
Vemuri Lakshmi Ganesh^{1,2}, C. V. S. Brahmananda Rao^{1,2}

¹Indira Gandhi Centre for Atomic Research, Kalpakkam – 603102, Tamil Nadu, India.

²Homi Bhabha National Institute, IGCAR Campus, Kalpakkam – 603102, Tamil Nadu, India.

§Email: gopakumar@igcar.gov.in

During nuclear fuel reprocessing [1,2], the fission product Zr, produced as a major element during U/Pu fission, can potentially be co-extracted by the degradation products of TBP. This decreases the decontamination factor for U/Pu products and underscores the importance of zirconium chemistry in nuclear fuel reprocessing [3]. In this regard, quantum chemical calculations were performed to predict the enthalpy of extraction for Zr complexes with the ligands tri-amyl phosphate (TAP) and diamyl amyl phosphonate (DAAP) (see Figure 1a & 1b, respectively). Geometry optimizations were carried out using the BP86 density functional in conjunction with the triple- ζ def2-TZVP basis set. To account for relativistic effects, the zero-order regular approximation (ZORA) approach was applied, employing the segmented all-electron relativistically contracted (SARC) basis sets for the Zr atom [4]. For accurate estimation of enthalpy values, total energies were calculated using the domain-based local pair natural orbital coupled-cluster (DLPNO-CC) method, with thermal and non-thermal corrections evaluated at the DFT level. The effect of the solvent environment was also considered during this step by applying the Polarizable Continuum Model (PCM) implicit solvation approach. All calculations were carried out using ORCA version 4.2.1 [5]. The results indicate that the enthalpy of extraction for both TAP and DAAP complexes is comparable, with a marginal preference observed for the former [*i.e.*, $\text{Zr}(\text{NO}_3)_4 \cdot 2\text{TAP}$: 44 kcal/mol vs. $\text{Zr}(\text{NO}_3)_4 \cdot 2\text{DAAP}$: 43.2 kcal/mol]. The results are also compared with those of actinides.

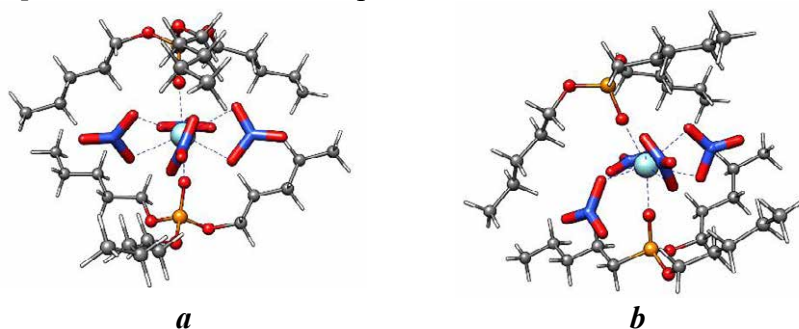


Figure 1. Optimized geometries of (a) $\text{Zr}(\text{NO}_3)_4 \cdot 2\text{TAP}$ and (b) $\text{Zr}(\text{NO}_3)_4 \cdot 2\text{DAAP}$ complexes at RI-BP86-D3BJ/def2-TZVP-ZORA level.

Acknowledgements: The authors gratefully acknowledge the computing time on IVY-Cluster, the High-Performance Computing facility at IGCAR, India.

References:

- [1] D. D. Sood and S. K. Patil, *J. Radioanal. Nucl. Chem.*, **203** (1996) 547.
- [2] C. F. Coleman and R. E. Leuze, *J. Tenn. Acad. Sci.*, **53** (1978) 102.
- [3] S. Tachimori, et al. *Ion Exch. and Sol. Extr. A Series of Advances*, **19** (2009), 1.
- [4] G. Gopakumar et al., *J. Phys. Chem. A*, **120** (2016), 4201.
- [5] F. Neese, *Wiley Interdiscip. Rev. Comput. Mol. Sci.*, **8** (2017) 1327.

Spectroscopic Studies on Irradiated La₂O₃ and BaO-Doped Sodium Borosilicate (NBS) Glass for Application in Radioactive Waste Immobilization

Nimai Pathak^{1,2,§}, Prithwish Sinharoy³, Dayamoy Banerjee^{2,3}, Manoj Mohapatra^{1,2}

¹Radiochemistry Division, Bhabha Atomic Research Centre, Mumbai, 400085, India

²Homi Bhabha National Institute, Mumbai, 400094, India

³Process Development Division, Bhabha Atomic Research Centre, Mumbai, 400085, India

§Email: nimai@barc.gov.in

Borosilicate glasses are well-regarded for their mechanical and chemical resilience, making them promising candidates for the safe disposal of High-Level Radioactive Waste (HLW) [1-2]. Understanding the long-term stability and performance of these vitrified waste forms is crucial for ensuring the development of reliable safety cases for disposal, addressing both regulatory requirements and public safety concerns. It is essential to study how actinides interact with borosilicate glass matrices to ensure their stability for waste containment. BaO-doped sodium borosilicate (NBS) glass has been shown to significantly improve the chemical durability of the material [3]. This enhancement occurs due to the incorporation of BaO, which strengthens the glass network, making it more resistant to degradation when exposed to harsh environmental conditions. Additionally, the ability of this doped glass to incorporate actinides, such as americium (Am³⁺) and curium (Cm³⁺), has been explored by using surrogate ions like lanthanum (La³⁺) and europium (Eu³⁺) to represent the behavior of these radioactive elements within the glass matrix. The study revealed that La³⁺ ions can be incorporated into the glass network at concentrations up to 14 wt%, without significantly altering the structural integrity of the glass. This finding is important for the development of glass materials that can store radioactive isotopes, ensuring the material remains stable even under high concentrations of these elements.

Furthermore, the radiation stability of BaO-doped sodium borosilicate glass was extensively studied by using Eu³⁺ ions as a photoluminescence (PL) probe. The glass samples were irradiated with varying doses of gamma radiation, ranging from 5 kGy to as high as 1000 kGy. The PL emission and lifetime (see Figure 1) results showed that the glass network remained remarkably intact, without significant changes in its structural or optical properties, even after exposure to high levels of gamma radiation. This suggests that the La₂O₃ and BaO-doped sodium borosilicate glass exhibits excellent radiation stability, making it a promising candidate for long-term storage of HLW.

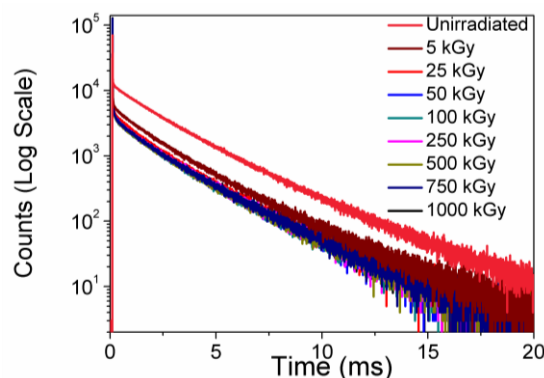


Figure 1: PL decay profile of La₂O₃ and BaO-doped NBS

References:

- [1] K. S. Chun, S. S. Kim and C. H. Kang. *J. Nucl. Mat.* **298** (2001)150.
- [2] S. V. Stefanovsky, A. A. Shiryaev, J. V. Zubavitchus, A. A. Veligjanin and J. C. Marra, *Glass Phys. Chem.* **35** (2009) 141.
- [3] P. Sahu and Sk. Musharaf Ali, *Mol. Syst. Des. Eng.*, **7** (2022) 1477.

Synthesis, Characterization and Phase Transitions in $\text{Ca}_x\text{Th}_x\text{Ce}_{1-2x}\text{PO}_4$

Bal Govind Vats^{1,2,§}, Geeta R. Patkare¹, Muhammed Shafeeq¹

¹Fuel Chemistry Division, Bhabha Atomic Research Centre, Trombay, Mumbai-400085

²Homi Bhabha National Institute, Anushaktinagar, Mumbai-400094

§Email: bgvats@barc.gov.in

The oxidation state of actinides determines how they are incorporated into the monazite structure. The direct inclusion of trivalent actinides (such as Pu and Am) was previously reported in relation to the $\text{Ln}_{1-x}\text{AnIII}_x\text{PO}_4$ formula. Interestingly, tetravalent actinides ($\text{An(IV)} = \text{Th, U, Np}$) always require a coupled substitution. Recently, Qin *et al.* has incorporated thorium in Rhabdophane structure by hydrothermal route which can be converted to monazite by heating at 700°C [1, 2]. In this work, we have shown the feasibility of incorporation of Thorium in $\text{CePO}_4 \cdot n\text{H}_2\text{O}$.

Synthesis of $\text{Ca}_x\text{Th}_x\text{Ce}_{1-2x}\text{PO}_4$ (where $x = 0.025, 0.050, 0.075$ and 0.10) was carried out by

taking metal nitrates solution and mixing them in proper stoichiometric ratio (Calcium was taken in 10 times excess). This solution is mixed with H_3PO_4 solution and this mixture is taken in teflon lined autoclave and heated at 110°C for four days to get the white precipitate. The precipitates thus obtained was washed several times with water and dried.

Powder XRD patterns of $\text{Ca}_x\text{Th}_x\text{Ce}_{1-2x}(\text{PO}_4)$ have been shown in Fig. 1. For $x = 0.025$, we get pure phase of Rhabdophane. Impurity lines of thorium phosphate diphosphate observed when x exceeds 0.05. To gain more insight on the structural changes of this Rhabdophane structure we have recorded high temperature XRD of $\text{Ca}_{0.05}\text{Th}_{0.05}\text{Ce}_{0.90}\text{PO}_4$ as shown in Fig. 2. From the figure, it can be clearly seen that at 300°C the XRD pattern changes due to loss of water molecule from the Rhabdophane structure while at 700°C the structure changes to monazite. The same has been confirmed from the thermogravimetric analysis. This study concludes that incorporation of Thorium in cerium based monazite is feasible.

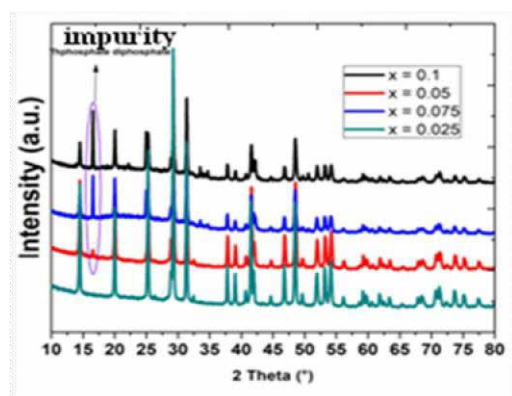


Fig. 1: Powder XRD patterns of $\text{Ca}_x\text{Th}_x\text{Ce}_{1-2x}\text{PO}_4$

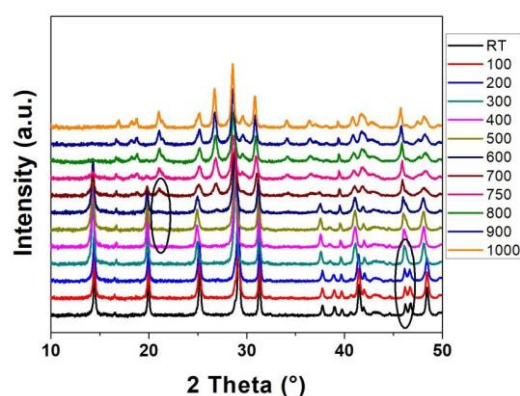


Fig. 2: HT XRD pattern of $\text{Ca}_{0.05}\text{Th}_{0.05}\text{Ce}_{0.90}\text{PO}_4$

References:

- [1] D. Qin, et. al., *J. Nucl. Mat.*, **492** (2017) 88.
 [2] D. Qin, et. al., *J. Crystal Growth and Design*, **19** (2019) 2794.

Synergism in Extraction of ^{241}Am from Acidic Feed using Combined Ligand Polymer Inclusion Membrane

Soumitra Panda^{1,3,§}, Bholanath Mahanty^{2,3}, Smita Thakur¹,
Pramilla D. Sawant¹, A. Bhattacharyya^{2,3}

¹Internal Dosimetry Section, Radiation Safety Systems Division, BARC, Mumbai

²Actinide Chemistry Section, Radio Chemistry Division, BARC, Mumbai

³Homi Bhabha National Institute, Mumbai

§ Email: spanda_ta@barc.gov.in

Recently, membrane-based processes have gained significant attention for metal ion separation. Among these, transport across liquid membranes, particularly Polymer Inclusion Membranes (PIMs), presents a promising alternative to conventional solvent extraction methods due to their high selectivity, operational simplicity, minimal solvent and extractant usage, and the integration of extraction and stripping into a single stage, thereby reducing costs. This paper aims to explore the application of combined ligand formalism in PIMs, a concept well-known in solvent extraction, for the separation of trivalent actinides from acidic feed solution. Three different PIMs were prepared namely D2EHPA PIM (D2EHPA 28.5%, NPOE 23.8%, CTA 47.7%), TODGA PIM (TODGA 26.8%, NPOE 24.4%, CTA 48.8%) and MIX PIM (D2EHPA 21.2%, TODGA 19.6%, NPOE 19.2%, CTA 40%).

The uptake efficiency of ^{241}Am was evaluated for each PIM at varying acidity (0.01 to 2 M HNO_3). The experiment involved placing a small piece of PIM (1 cm x 1 cm) into different acidic solutions (total volume: 10 mL). The

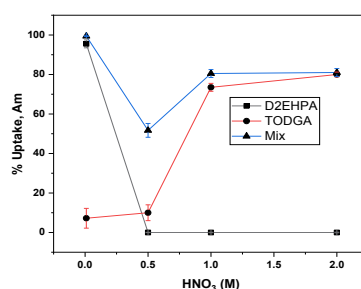


Fig 1: Am(III) uptake at different acidity

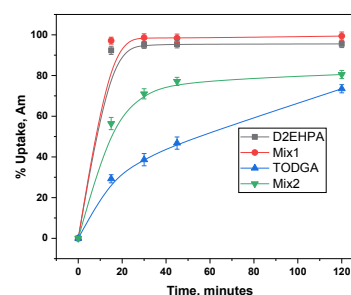


Fig 2: Am(III) uptake kinetics

solutions were continuously stirred at 200 rpm using a high-speed precise magnetic stirrer for 2 hours. Thereafter, the samples were directly analyzed using gamma-ray spectroscopy. The acidic ligand D2EHPA extracts trivalent actinides at lower nitric acid concentration. However, at higher acidity, the competition between H^+ ions and Am^{3+} ions reduce the efficiency of Am extraction. Diglycolamide, on the other hand, can form reverse micelle that can extract metal ions with an ionic radius of approximately 100 pm, regardless of their oxidation state. In the case of the MIX ligand, Am is effectively extracted over a wide range of acidity, indicating a synergistic effect within the MIX membrane shown in figure 1. The uptake kinetics study performed at pH 2 and 1M HNO_3 shows that MIX PIM extracts Am rapidly from feed solution compared to the PIM containing individual ligand as shown in figure 2. The PIMs were characterized using different techniques, e.g., FTIR, SAXS, photoluminescence. Isotherm study shows that the sorption follows the Langmuir isotherm and the maximum uptake capacity was found to be 20 mg/g of the membrane. This work highlights the potential of combined ligand based PIM for the uptake of trivalent actinide ions from dilute solution.

References:

[1] B. Mahanty et. al., *J. Membr. Sci.*, **501** (2016) 134.

Understanding the Complexation of CMPO and DGA Functionalized Task Specific Ionic Liquids (TSILs) with Trivalent *f*-Cations

Adityamani Nagar¹, A. Sengupta^{§2,3}, P. K. Mohapatra²

¹UM-DAE Centre for Excellence in Basic Sciences, Mumbai 400098

²Radiochemistry Division, Bhabha Atomic Research Centre, Mumbai - 400 085

³Homi Bhabha National Institute, Mumbai 400094, India.

§Email: arijita@barc.gov.in

Diglycolamide (DGA) and carbamoyl phosphineoxide (CMPO) are two prominent functionalities known to co-extract trivalent lanthanides and actinides during the first step of actinide partitioning. DGA and CMPO functionalized task specific ionic liquids have demonstrated as potential 'green' media for highly efficient and selective extraction of trivalent lanthanides and actinides (Am^{3+} , Eu^{3+}) from aqueous acidic waste with high degree of radiolytic stability [1]. In view of this, attempt was made to understand the complexation of DGA and CMPO functionalized ionic liquids with trivalent *f*-cations. Nd^{3+} was chosen as UV-vis probe, while Eu^{3+} has utilized as photoluminescence probe. The UV-Vis titration revealed the predominance of ML_1 , ML_2 and ML_3 species for DGA-TSIL; whereas for CMPO-TSIL. ML_2 and ML_4 species were found to be dominant. The exothermic nature of complexation for both the ligands was evidenced. The complexation constant values for any species were found to be more for Eu^{3+} as compared to Nd^{3+} , ascribed to lanthanide contraction. The stability constant values for any species were found to be more for DGA-TSIL compared to CMPO-TSIL, indicating better complexation ability of the former. There was decrease in the stretching frequency of carbonyl C=O bond on complexation as evidenced in FTIR spectra, indicating the interaction between metal and carbonyl oxygen. The decrease in the stretching frequency of N-H bond next to the carbonyl carbon on complexation has also been observed.

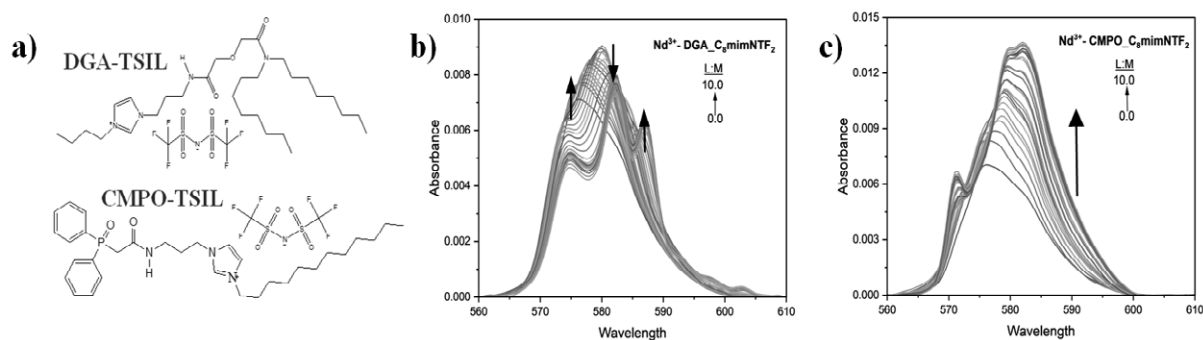


Fig. 1: (a) Chemical Structures of DGA-TSIL and CMPO-TSIL. (b) UV-Vis titration of Nd^{3+} with DGA-TSIL in $\text{C}_8\text{mimNTf}_2$. (c) UV-Vis titration of Nd^{3+} with CMPO-TSIL in $\text{C}_8\text{mimNTf}_2$.

Acknowledgements: The author wish to acknowledge Dr. S. Jeyakumar, Head, RCD, BARC and Dr. A. Bhattacharyya, Head, ACS, RCD, BARC for their constant support

References:

[1] A. Sengupta et.al., *Sep Purif Technol.*, **118** (2013) 264.

Selective Separation of Cesium from a Mixture of Alpha and Beta-Gamma Activities using Ammonium Phosphomolybdate Modified Nafion Membrane

Amol Mhatre, Chhavi Agarwal[§]

¹Radiochemistry Division, Bhabha Atomic Research Centre, Mumbai, India

[§]Email: cagarwal@barc.gov.in

Ion-exchange membranes such as Nafion® are widely used in a variety of applications owing to their high proton conductivity and high temperature chemical stability. However, their lack of ion selectivity, arising from electrostatic interactions between sulfonic acid groups and hydrated cations, limits their applicability. In our previous studies, ammonium phosphomolybdate (AMP) was successfully synthesized in Nafion-117, significantly enhancing the membrane's selectivity for Cs⁺ ions, as indicated by higher partition coefficients compared to unmodified Nafion [1]. Presently, the experimental diffusion exchange rates have been fitted to the membrane-controlled diffusion equations, where the time-dependent tracer concentration at the membrane surface was empirically derived from solution-phase tracer concentration variations [2]. Figure 1 illustrates the fitted diffusion profiles for 10 μmol.L⁻¹ Cs⁺ in different acid concentrations and in water. As seen, a reasonably good fitting could be observed. The AMP-modified membranes were further evaluated for Cs⁺ uptake from a fission product solution at two acid concentrations (2 and 4 mol.L⁻¹ HNO₃). The solution contained fission products such as ⁹⁹Mo, ¹⁴¹Ce, ¹⁴⁰Ba, ¹⁰³Ru and the activation product ²³⁹Np, identified via high-resolution gamma-ray spectrometry. For this study, both the solutions were spiked with ¹³⁷Cs radiotracer. As seen from figure 2, at both the acidities, the Cs⁺ uptake was nearly 100%, whereas the uptake of other ions remained below 12 %. Notably, at 4 mol.L⁻¹ HNO₃, elements such as Ce, Ba, and Ru showed negligible uptake. Additionally, the AMP modified membranes were also tested for Cs⁺ separation from an old legacy waste sample containing Pu, ²⁴¹Am, ¹⁵²Eu and ¹³⁷Cs activities. For studies, the acidity of the solution was first adjusted to 2 mol.L⁻¹ HNO₃. A ¹³⁷Cs uptake of ~94% was observed by the membrane, thereby showing the efficacy of modified membrane for Cs⁺ separation. These findings highlight the potential of AMP-modified membranes for selective Cs⁺ recovery from complex matrices.

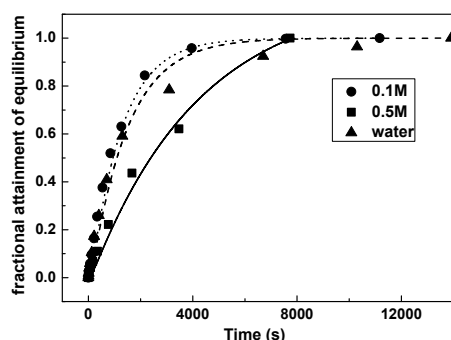


Fig. 1: Experimental points and fitted curves for fractional attainment of Cs⁺ ion in presence of different acid concentration and in water.

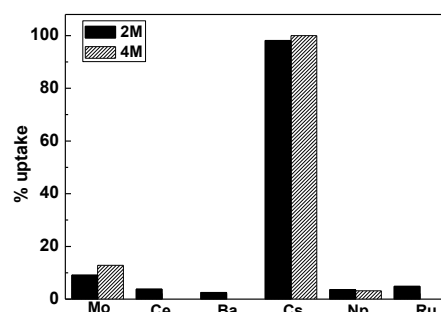


Fig. 2: Uptake (%) of ions by AMP-modified Nafion membrane at two different acid concentrations (2 M and 4 M).

References:

[1] A. Mhatre, C. Agarwal, SESTEC-2024, Page-217.

[2] A. N. Naik, C. Agarwal, S. Chaudhury, A. Goswami, *J. Phys. Chem. B*, **121** (2017) 10081.

Effect of γ - Radiation on Structural and Dissolution Behaviour of Fission Product Doped Chromium Ferrites

B. Padma Shruti¹, V. Balaji² §, P Chandramohan^{2,3}, R. Puspallata^{2,3}, T.V. Krishna Mohan²

¹Indian Institute of Technology Madras, Chennai, India

²Water and Steam Chemistry Division, BARC Facilities, Kalpakkam, India

³Homi Bhabha National Institute, BARC, Mumbai, India

§Email: vbalaji1764@gmail.com

The metal ion passivation (MIP), is one of the long term methods to control radiation field build-up in water cooled nuclear reactors. Zn and Mg injection is particularly being practised as they minimise general corrosion by modifying the oxide structure and also reduce the pick-up of ⁶⁰Co activity on primary heat transport circuits during plant operation [1]. In addition to activated corrosion products (ACPs), deposition of fission isotopes such as Ce / Zr / La on the existing oxide surfaces also contribute towards the overall radioactivity build up in the case of clad failures [2]. High radiation field from these inclusion processes can modify the oxide structure and are usually removed from the structural materials along with the surface oxides using decontamination methods. For better understanding on the effectiveness of a decontamination process one needs to find the dissolution rates of all possible oxides which can be formed. In this regard, a series of fission product doped simulated corrosion products (SCP) $\{Zn_{0.5}Mg_{0.5}Ce_xCrFe_{1-x}O_4$ ($x = 0.0, 0.05$ and 0.1) $\}$ were synthesized using the combustion route. This combustion process has the advantage due to its inexpensive precursors and simple to prepare the desired oxides. The changes in the structural and magnetic properties, dissolution behaviour of these oxides in oxidizing permanganic acid medium before and after gamma irradiation (up to 500 kGy) were measured to simulate the inclusion of radioactivity into the matrix. The changes in structural and magnetic properties were investigated by X-ray diffraction (XRD), Diffuse Reflectance Spectroscopy (DRS) and vibrating sample magnetometer (VSM). XRD of irradiated and un-irradiated $Mg_{0.5}Zn_{0.5}Ce_xCrFe_{1-x}O_4$ samples showed (see Fig. 1) a single-phased cubic spinel structure with small amount of Ce phase. The optical properties of these oxide samples from diffuse reflectance spectroscopy showed no appreciable change in both pristine and 500 kGy gamma irradiated samples. During dissolution in 3.0 mM nitric acid permanganate (NP) at 90°C, the release of divalent metal ions Zn and Mg along with chromium and cerium was observed. Rate constants were evaluated using sinking sphere model (SSM). This study will give insights in optimizing the chemical decontamination processes for modified chromium-iron oxides in nuclear reactors.

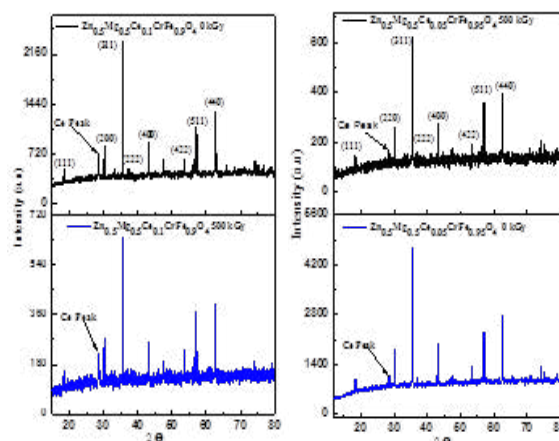


Fig. 1: XRD patterns of $Zn_{0.5}Mg_{0.5}Ce_xCrFe_{1-x}O_4$ before and after Gamma irradiation.

References:

- [1] S. Velmurugan et al., *J Nucl Sci Technol.*, **33** (1996) 641.
- [2] V. Balaji et al., *J. Radioanal. Nucl. Chem.*, **324** (2020)791.

Studies on Selective Separation of Palladium (Pd) from High Level Radioactive Liquid Waste (HLW) using Bis-Triazinyl-Pyridine

Kumari Anshul^{1,2}, Pawan Kumar Cheeta², J. Selvakumar^{1,2,§}, S. Srinivasan²,
G. Srinivasa Rao², J.K. Gayen²

¹Homi Bhabha National Institute, Mumbai 400 085, India

²Integrated Nuclear Recycle Plant, Nuclear Recycle Board, BARC, Kalpakkam, India

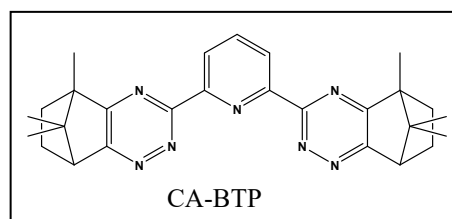
§Email: jselva@hbni.ac.in

Spent nuclear fuel contains valuable noble metals, including palladium (Pd). Fission produces palladium with stable isotopes—¹⁰⁴Pd (17 wt.%), ¹⁰⁵Pd (29 wt.%), ¹⁰⁶Pd (21 wt.%), ¹⁰⁸Pd (12 wt.%), and ¹¹⁰Pd (4 wt.%)—and the radioactive isotope ¹⁰⁷Pd (17 wt.%), which has a half-life of 6.5×10^6 years. Interest in recovering palladium from high-level liquid waste (HLLW) is growing [1]. Theoretical calculations show that HLW from spent PHWR fuel with a burn-up of 6700 MWd/t_{HM} contains 165 mg/L of Pd [2]. Efficiently separating palladium from HLLW is essential to recovering it as a valuable resource and preventing challenges in the vitrification process.

This study evaluated the extraction properties of bis-triazinyl-pyridine (CA-BTP) for Pd recovery from HLLW. Based on Pearson's HSAB principle, CA-BTP, a soft base, forms a stable complex with Pd(II), with its unoccupied p-orbital, a Lewis soft acid, enabling strong extraction. Pd extraction increases with nitric acid up to 0.5 M, then stabilizes above 90% due to phase equilibrium constraints. CA-BTP shows high Pd selectivity over Ru, Rh, and lanthanides. It forms a 1:1 complex with Pd²⁺, similar to CyMe₄-BTBP ligands [3]. Nearly complete Pd back-extraction was achieved in a single step using 0.01 M thiourea in 0.01 M nitric acid. The distribution ratios of metal ions are presented in Table 1.

Table 1: The distribution ratio of metal ions obtained using 0.05M CA-BTP/octanol at 1M HNO₃.

Element	Initial conc (ppm)	D _M	SF _{Pd/M}
Eu	97	<10 ⁻⁴	1.2 × 10 ⁵
Nd	83	<10 ⁻⁴	1.2 × 10 ⁵
Pr	54	<10 ⁻⁴	1.2 × 10 ⁵
Ce	186	<10 ⁻⁴	1.2 × 10 ⁵
Y	22	<10 ⁻⁴	1.2 × 10 ⁵
Ru	194	0.009	1.3 × 10 ³
Rh	57	0.003	4.0 × 10 ³
Pd	87	12	-



References:

- [1] R. Ruhela et. al., *RSC Adv.*, **4** (2014) 24344.
- [2] B. S. Tomar, Internal Report, BARC, 2011; (b) R. Ruhela, Ph.D., Thesis, Homi Bhabha National Institute, 2013.
- [3] E. Aneheim et. al., *Polyhedron*, **50** (2013) 154.

Comparative Adsorption Behavior of Sr²⁺ Ions on Kaolinite and Lizardite Clay Minerals in the Presence of Sulphate Ions using Molecular Dynamics

Shelly Goel^{1,4,§}, Manish Chopra², Niharendu Choudhury^{3,4}

¹Health Physics Division, Bhabha Atomic Research Centre, Mumbai 400085, India,

²Radiation Safety Systems Division, Bhabha Atomic Research Centre, Mumbai 400085, India,

³Chemistry Division, Bhabha Atomic Research Centre, Mumbai 400085, India,

⁴Homi Bhabha National Institute, Anushaktinagar, Mumbai 400094, India

§Email: shellygarg@barc.gov.in

Adsorption behavior of Sr²⁺ ions on two 1:1 layer-type clay minerals, kaolinite (K) and lizardite (L), in the presence of sulphate ions (SO₄²⁻) is investigated using atomistic molecular dynamics (MD) simulations. L is a trioctahedral clay with Mg-O octahedra, while K is dioctahedral having Al-O octahedral sheets. Both L and K have one common siloxane basal surface whereas other basal surface is brucite for L and gibbsite for K. MD simulations were conducted using LAMMPS (Large-scale Atomic/Molecular Massively Parallel Simulator), employing the CLAYFF force field for clay minerals, SPC water model, and appropriate parameters for Sr²⁺ [2] and SO₄²⁻. Aqueous systems were prepared by solvating 15 Sr²⁺ ions and an equivalent number of SO₄²⁻ (15) ions in 2000 water molecules. The systems were equilibrated in NVT ensemble at 300 K for 70 ns and production run of 30 ns was used for analysis. Coordination number (n(r)) for the Sr-O_w (oxygen of water) and Sr-O_s (oxygen of SO₄²⁻) pair was found to be 5.02, 5.85 and 2.98, 2.25 for L and K respectively (Fig. 1(a)), leading to a total n(r) of approximately 8. This indicates that more number of SO₄²⁻ ions are coordinating with Sr²⁺ ions in case of L compared with K. Maximum g(r) (radial distribution function) for both L and K system occurs at 2.51 Å for Sr-O_w and 2.41 Å for Sr-O_s. The peak near siloxane surface (Z ~17 Å) of both K and L in the single-particle atomic density profiles of Sr²⁺ indicates the adsorption of Sr²⁺ ions by forming the outer sphere complex through water molecules, with intensity being higher in case of L. For K, a primary Sr peak is observed near Gibbsite surface (Z ~7 Å) corresponding to the adsorption of negatively charged complexes of Sr²⁺ ion involving SO₄²⁻ ions on to the positively charged surface (Fig 1(b)). It can be concluded that Sr²⁺ preferably adsorbs on siloxane surface in case of L and gibbsite surface in case of K.

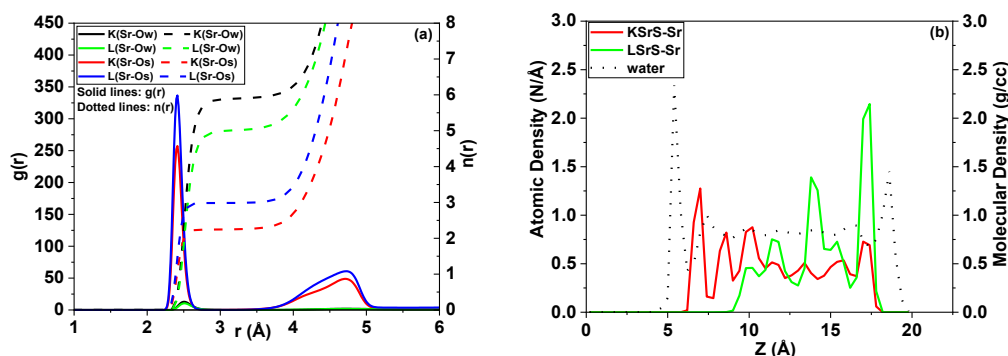


Fig. 1: (a) Radial distribution function (g(r)) and coordination number n(r) of Sr²⁺ w.r.t water (Ow) and oxygen of counter ion (Ox) (b) Density profiles of Sr²⁺ ion and water

References:

- [1] Nikitin and G. D. Frate, *J Comput Chem*, **40** (2019) 2464.
 [2] K. S. Karadima et. al., *Phys. Chem. Chem. Phys.*, **19** (2017) 16681.

Extraordinarily High Mutual Separation of Nd-Pr by Selective Dissolution of Nd into Ionic Liquid Containing Furyl Trifluoroacetone (FTA)

Dipita Karmakar^{1,2}, Adityamani Nagar³, Priya Goyal¹, A. Sengupta^{1,2,§}, P. K. Mohapatra¹

¹Radiochemistry Division, Bhabha Atomic Research Centre, Mumbai - 400 085;

²Homi Bhabha National Institute, Mumbai 400094, India;

³UM-DAE Centre for Excellence in Basic Sciences, Mumbai 400098;

§ Email: arijita@barc.gov.in

Due to the similar size and predominant existence of +3 oxidation state, the Nd and Pr possess similar chemistry and hence, their mutual separation is highly challenging. The present method demonstrated the highly efficient method of separation of Nd and Pr with separation factor of $\sim 10^2$ - 10^3 , which is two orders of magnitude higher than the conventional method by selective dissolution of Nd into ionic liquid phase containing FTA from the physical mixture of Nd_2O_3 and Pr_6O_{11} [1]. This investigation revealed a $\beta_{\text{Nd/Pr}} > 2000$, the highest ever reported. The difference in the lattice energy of these two oxides induced the selectivity in dissolution. However, the preferential complexation of Nd^{3+} with FTA over Pr^{3+} , channelized the equilibrium in the forward direction. Various parameters: structural modification in ionic liquid, water content in ionic liquid, dissolution and sintering temperature were screened to get the optimum conditions. The behaviour of other rare earth fission products (La, Ce, etc) in the selective dissolution into IL depends upon the lattice energy of the oxides. Kinetic analysis revealed the dissolution of Nd predominantly followed pseudo 1st order kinetics. The dissolution was also found to be exothermic in nature [see Fig. 1(a)]. Complexometric titration using UV-Vis spectroscopy was employed to understand the competitive binding of Nd^{3+} and Pr^{3+} with FTA [see Fig. 1(b) and (c)]. The predominance of ML_2 and ML_4 species were evidenced. The enolate form of FTA was found to be responsible in complexation during the dissolution process. The direct dissolution of oxides into the ionic liquid avoids aqueous phase dissolution, hence, the use of corrosive acids. Ionic liquid can be reused by effective stripping of loaded Nd with 0.5M nitric acid.

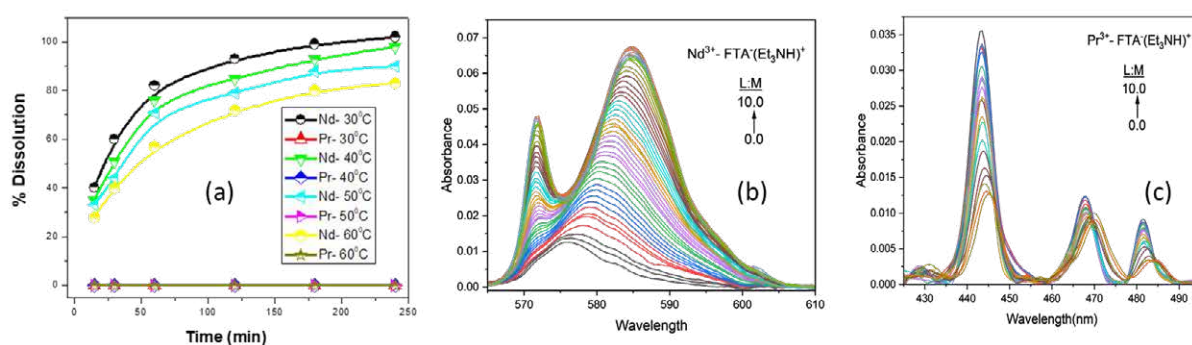


Fig. 1: (a) Dissolution profiles of Nd_2O_3 and Pr_6O_{11} in $\text{C}_4\text{mimNTf}_2$ at different temperatures. (b) UV-Vis titration of Nd^{3+} with $\text{FTA}(\text{Et}_3\text{N})^+$ in $\text{C}_4\text{mimNTf}_2$. (c) UV-Vis titration of Pr^{3+} with $\text{FTA}(\text{Et}_3\text{N})^+$ in $\text{C}_4\text{mimNTf}_2$.

Acknowledgements: The author wish to acknowledge Dr. S. Jeyakumar, Head, RCD, BARC.

References:

[1] Y. Bhat et.al, *Ind Eng Chem Res.*, **63** (2024) 14863.

DFT Approach to Elucidate Eu³⁺ Complexation with TOPO-Decanoic Acid Deep Eutectic Solvent

Pratyasha Panda¹, Bibek Dash², Pratyusha Parida¹, Sujata Mishra^{1,§}

¹Department of Chemistry, Institute of Technical Education and Research (FET) Siksha 'O' Anusandhan Deemed to be University, Bhubaneswar-751030, Odisha, India

²Process Engineering & Instrumentation Department, CSIR - Institute of Minerals & Materials Technology, Bhubaneswar- 751013, Odisha, India

§Email: drsujatamishra97@gmail.com/sujatamishra@soa.ac.in

Nuclear fuel produces lanthanides because of the uranium fission and investigations related to the chemistry of these lanthanides are of great importance to nuclear energy industry. This work presents an investigation based on density functional theory (DFT) calculations of electronic structural parameters of Eu³⁺ extracted complex using TOPO (Tri-n-octyl phosphine oxide)-DecA (Decanoic acid) deep eutectic solvent (DES) from nitrate medium. DFT calculations have been performed with the use of linear combination of atomic orbitals (LCAO) method as executed in the Quantum ATK (Synopsys, USA) package. The exchange-correlation of electrons was encompassed using the Hybrid Generalized Gradient Approximation (Hybrid GGA) of the Becke-Lee-Yang-Parr exchange correlation three-parameter functional. The van der Waals interactions have been carried out using the DFT-D3 of Grimme's method [1,2]. It has been observed from structural optimization that neutral complex of 1:1 (metal/DES) stoichiometry (see Fig.1) is formed where TOPO-DecA primarily coordinates with europium cation through the phosphoryl oxygen atom of TOPO which supports our experimental results reported by our group [3]. The FTIR spectra of TOPO-DecA DES and Eu-loaded DES were studied and it was observed that the P-C and P=O bond frequencies have been shifted from 1464 cm⁻¹ (DES) to 1460 cm⁻¹ and from 1128 cm⁻¹ (DES) to 1124 cm⁻¹, respectively in Eu loaded DES showing complexation. The TOPO-DecA DES concentration variation experimental results revealed formation of Eu(NO₃)₃.TOPO-DecA complex in the loaded DES phase [3]. Eu-O bond length is 2.307 Å. The P=O bond length in TOPO-DecA DES is 1.529 Å while it is 1.558 Å in Eu-DES complex as predicted by DFT calculation. This clearly confirms complexation of europium by DES.

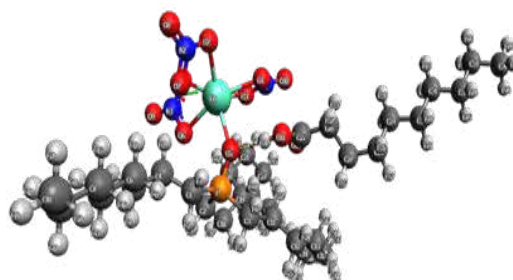


Fig. 1. Optimized structure of Eu nitrate-TOPO-DecA complex

Acknowledgements: The authors (P. Panda, P. Parida and S. Mishra) are thankful to the Siksha 'O' Anusandhan Deemed to be University for the kind support. B.Dash is grateful to IMMT for permission to publish the work.

References:

- [1] T. D. K. Wungu et al., *IOP Conference Series*, **214** (2017) 012004.
- [2] S. Grimme, *Journal of Computational Chemistry*, **27** (2006) 1787.
- [3] P. Panda et.al., *Journal of Molecular Liquids*, **410** (2024) 125629.

Extraction of Platinum Group Metals with Dialkyl H-Phosphonates

Somnath Sengupta^{1,2}, B. Sreenivasulu^{1,2,§}, C.V.S. Brahmananda Rao^{1,2}

¹Fuel Chemistry Division, IGCAR, Kalpakkam, India

²Homi Bhabha National Institute, IGCAR, Kalpakkam, India

§E-mail: bsrinu@igcar.gov.in

Platinum group metals (PGMs) like palladium (Pd), rhodium (Rh), and ruthenium (Ru) are essential for catalysis, electronics, and hydrogen technologies [1]. Their scarcity and increasing demand necessitate efficient recovery methods from secondary sources like spent nuclear fuel (SNF), which not only conserves resources but also reduces nuclear waste radiotoxicity. This study explored the extraction behavior of individual PGMs and their mixture using 1.1 M diheptyl H-phosphonate in *n*-dodecane, beginning with the preparation of 500 ppm solutions of Pd, Ru, and Rh in different nitric acid media, followed by the preparation of a mixed solution with 500 ppm of each metal at varying acidity levels. The extraction behaviour was studied as a function of initial nitric acid concentration and it revealed that extraction is maximum at lower acidity corresponding to 0.5 M nitric acid concentration owing to the fact that H-phosphonates act as acidic extractants at lower acidity. Also, the results indicated that palladium consistently exhibited a significantly higher distribution ratio (D) compared to rhodium and ruthenium in both individual and mixed PGM extraction scenarios. Palladium demonstrated an extraction efficiency exceeding 90% at 0.5 M HNO₃, with extraction efficiency decreasing as nitric acid concentration increased. H-phosphonate is beneficial for palladium extraction due to its ion exchange mechanism, which operates effectively at lower acidity, where palladium predominantly forms cationic complexes. However at higher acidity, palladium will form neutral and anionic complex and extraction will proceed via solvation mode which is less efficient. Rhodium showed marginal extraction with approximately 20% recovery, while ruthenium extraction remained negligible under all tested conditions. These findings highlight the potential of H-phosphonates as effective agents for selective palladium recovery from spent nuclear fuel, though their direct application would require further evaluation. For a viable PGM recovery flowsheet, ligands with higher Rh and Ru affinity should be explored.

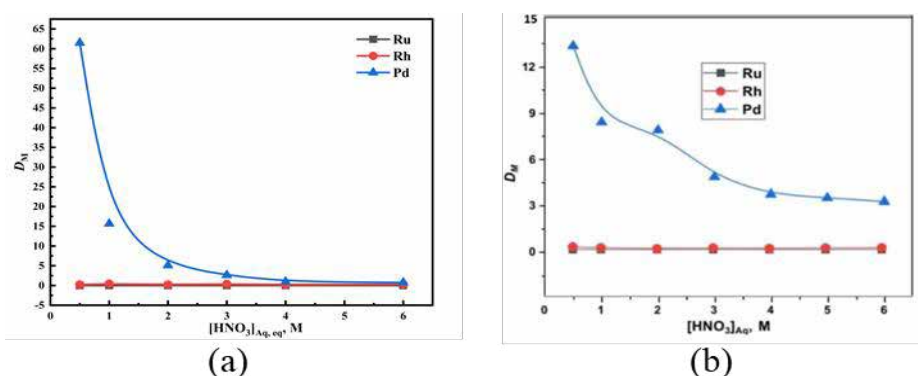


Fig. 1. (a) Variation of distribution ratio of Ru, Rh and Pd from individual solutions as a function of nitric acid concentration (b) Variation of distribution ratio of Ru, Rh and Pd in a mixed solution as a function of nitric acid concentration.

References:

[1] Pianowska Karolina et.al., *Materials*, **16** (2023) 4681.

Comparing the Extraction Behavior of Actinides and Fission Products with Phosphates and Phosphonates

T. Revathy¹, B. Sreenivasulu^{1,2§}, C. V. S. Brahmananda Rao^{1,2}

¹Homi Bhabha National Institute, IGCAR Campus, Kalpakkam – 603102, Tamil Nadu, India.

²Indira Gandhi Centre for Atomic Research, Kalpakkam – 603102, Tamil Nadu, India.

§Email: bsrinu@igcar.gov.in

Spent nuclear fuel (SNF) from thermal and thorium-based reactors contains a variety of metals like U(VI), Th(IV), Zr(IV), Pd(II) and some trivalent lanthanides. Though tri-n-butyl phosphate (TBP) is widely used, the formation of a third phase during the extraction of tetravalent metal ions such as Th(IV), Zr(IV), and Pd(II) poses a significant challenge. Diamylamyl phosphonate (DAAP) and tri-n-amyl phosphate (TAP) were investigated as alternate solvents for the extraction of actinides [1,2]. However, the data on the comparison of phosphates and phosphonates is very scarce. Thus, a preliminary study was performed to evaluate the extraction behavior of various metal ions using alternate solvents like diamylamyl phosphonate (DAAP) and tri-n-amyl phosphate (TAP) in n-dodecane. Metal ions with different oxidation states were chosen to understand the versatility of the solvent. Distribution data for the extraction of U(VI), Th(IV), Zr(IV), Pd(II), and Nd(III) as a function of extractant and nitric acid concentration was generated and compared with the extraction behaviour of these ions by 0.5M TAP in n-dodecane was compared with TBP and TAP based solvents. The extraction efficiency of the solvents at different concentrations of nitric acid was studied. By calculating the distribution ratios, the potential of the extractants used was found to be in the order DAAP>TAP>TBP. The distribution ratios for various metal ions were found to be in the order: U(VI)>Th(IV)>Zr(IV)>Nd(III)>Pd(II) for any extractant at any given concentration of extractant and nitric acid (see Figure 1(a) and (b)). The complexing ability of Th is higher than that of Zr. The extraction of Pd(II) was found to be negligible with 0.5M extractant in n-DD; hence the extraction of Pd(II) was investigated with neat extractants (100%). The present study reveals that phosphonates are superior to phosphates for the extraction of actinides.

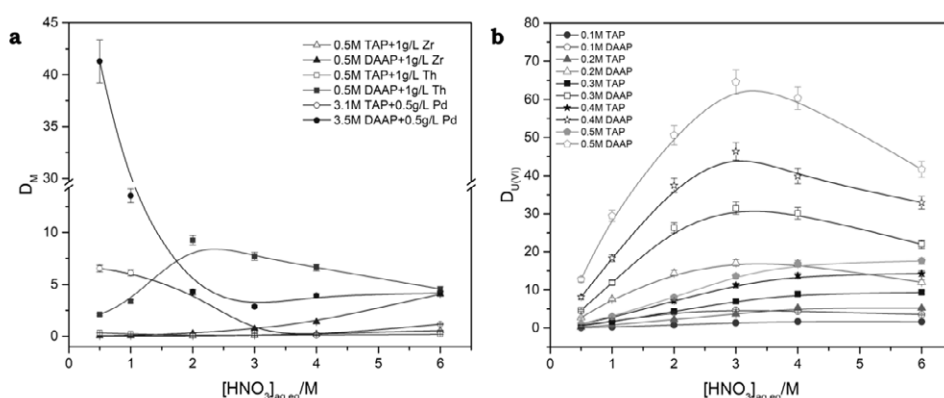


Fig. 1: Distribution ratio of different metals (M) in TAP and DAAP.
(a) M = Zr(IV), Th(IV), Pd(II) (b) M = U(VI)

References:

- [1] A. Suresh et al., *Solvent Extr. Ion Exch.*, **27** (2009) 258
- [2] C.V.S. Brahmananda Rao et al., *Solvent Extr. Ion Exch.*, **25** (2007) 771.

Advanced Separation of Radioactive Pertechnetate (TcO_4^-) from Low Level Waste Using MOF-808(Zr): A Cutting-Edge Approach

Kankan Patra^{1,2,§}, V. K. Mittal¹, Arijit Sengupta², A. K. Sahu²,
Anoop Kelkar¹, D. B. Sathe¹, R. B. Bhatt¹

¹Nuclear Recycle Board, Bhabha Atomic Research Centre, Tarapur 401504, India

²Homi Bhabha National Institute, Anushaktinagar, Mumbai 400 094, India

§Email: kpatra@barc.gov.in

The removal of radioactive pertechnetate (TcO_4^-) from low-level waste is a critical challenge in nuclear waste management. Traditional methods often fall short in terms of efficiency and selectivity. However, the use of Metal-Organic Frameworks (MOFs), particularly MOF-808, offers a revolutionary solution. MOF-808, with its high surface area, tunable structure, and functional groups, has emerged as a promising material for the selective separation and capture of pertechnetate ions. This cutting-edge approach not only enhances the efficiency of TcO_4^- removal but also opens new pathways for safer and more sustainable nuclear waste treatment. Herein, we report the successful synthesis of MOF-808 using the solvothermal method [1]. We have characterized the MOFs using Powder X-ray Diffraction (PXRD) (Fig. 1a), Field Emission Scanning Electron Microscopy (FE-SEM) (Fig. 1a), Energy Dispersive Spectroscopy (EDX). We have studied the ion exchange property of the materials with the TcO_4^- ions in the range of pH 2 to 13. Efforts were made to determine the kinetics of the reaction. Effects of interfering ions like NO_3^- and SO_4^{2-} were studied. The selectivity of MOF-808 was studied in presence of NO_3^- ions. At higher pH, the concentration of negatively charged pertechnetate ions (TcO_4^-) is enhanced due to the deprotonation of HTcO_4 . MOF-808 contains zirconium metal centres, that coordinate negatively charged species effectively. Hence, at higher pH, the better electrostatic interaction between TcO_4^- species and Zr metal centre of MOF-808 resulted higher % removal of Tc (Fig. 1b). The MOF-808 material was tested for the separation of TcO_4^- from low-level waste, and it was observed that 80% removal occurred within 30 minutes in the first cycle. The experiment revealed that, the material shows significant promise for real-time TcO_4^- ion remediation from low level waste.

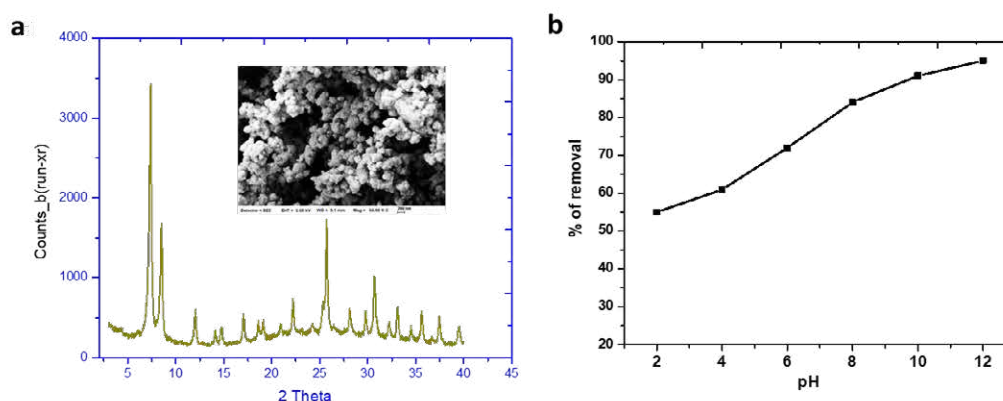


Fig.1 (a) PXRD pattern and SEM image of MOF-808, (b) % removal of Tc from aqueous feed solutions with pH in the range of 2-12 using the MOF-808.

References:

[1] Honghao Su et. al., *Separation and Purification Technology*, **333** (2024) 125957.

Ion Exchange Behavior of Sodium Titanium Phosphate towards Exchanging Cesium

B. Robert Selvan¹, A. S. Suneesh^{1,2}, M. Amutha Suba¹, N. Ramanathan^{1,2}

¹Fuel Chemistry Division, Indira Gandhi Centre for Atomic Research, Kalpakkam, India

²Homi Bhabha National Institute, Kalpakkam, India

Email: suneesh@igcar.gov.in

The separation of cesium (particularly Cs-137) from the intermediate and high level nuclear waste is challenging due to its high radiotoxicity and complicated interference due to the presence of different ions. Cs-137 removal not only reduces the radiotoxicity, the separated Cs-137 also serves as a potential radioactive source that can be used for variety of industrial application as a radioactive source. The development of advanced inorganic ion exchangers enhances nuclear waste management, reducing environmental risks and facilitating safer disposal.

In the present study, the removal of Cs was explored by using an inorganic material, sodium titano phosphate (STP). STP was prepared by precipitation reactions of metatitanic acid in the presence of sodium carbonate and phosphoric acid. STP was characterized by FTIR, Raman, SEM, XRD, TG-DTA and DSC. It can be seen that at 90 minutes of time, approximately 99 % of Cs was exchanged to STP, and therefore, all the subsequent ion exchange studies were performed for 90 minutes, and extraction was higher at all the pH conditions varying from pH 1 to 7 and was higher at pH 7 (Fig. 1). Following equation could represent the exchange of Cs⁺.



Therefore, it can be expected that the exchange of ions are accompanied by release of H⁺ ion. Fig. 1 shows the change in the pH of the aqueous solution after the exchange of Cs⁺.

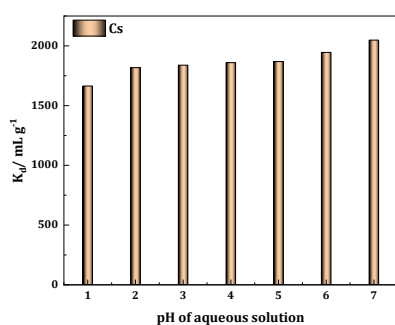


Fig. 1. Ion exchange behaviour of Cs

Table 1. Stripping of Cs using nitric acid.

Stripping agent	% stripping
0.1 M thiourea	5.6
0.1 M citric acid	22.98
0.1 M sodium carbonate	81.66
0.5 M nitric acid	63.05
1.0 M nitric acid	93.66
2.0 M nitric acid	93.62
3.0 M nitric acid	100

Stripping Cs from the STP-loaded phase was also studied using different stripping agents (shown in Table 1), indicated that stripping Cs is extremely difficult with 0.5 M nitric acid and with thiourea, citric acid or sodium carbonate. Stripping of Cs increases with the concentration of nitric acid, and quantitative stripping was observed with 3 M nitric acid. Results of these studies (including competitive ion exchange with other ions) indicated that STP can be effectively used as an ion exchange material for the separation of Cs from the nuclear waste.

Extraction and Stripping Behavior of Nd(III) in TODGA+TBP/*n*-Dodecane Phase in using Six Stage Annular Centrifugal Extractor

Jammu Ravi[§], M. Balamurugan, N. Desigan, R. Rajeev

Plant Design, Research and Hot Cell Systems Division, IGCAR, Kalpakkam, India.

[§] Email: jammuravi@igcar.gov.in

Among the various solvents proposed for the trivalent actinide separation from high-level liquid waste, diglycolamide class of extractants like *N,N,N',N'*-tetraoctyl diglycolamide (TODGA) and *N,N,N',N'*-tetra-2-ethylhexyl diglycolamide (T2EHDGA) received much attention [1]. The annular centrifugal extractor (ACE) is the preferred contactor for the reprocessing of spent nuclear fuel emanating from fast reactors. In view of this, the current study is aimed at verifying the feasibility of employing a multistage ACE for the separation of trivalent f-ions from HLLW of fast reactor origin. In the present study, the extraction of a trivalent f-ion representative, Nd(III), from 4 M nitric acid was carried out into the organic phase consisting of 0.2 M TODGA + 0.5 M tri-*n*-butyl Phosphate/*n*-dodecane using a six-stage ACE having rotating bowl of 40 mm inner diameter. A solution of 0.05 M Nd(III) in 4 M nitric acid was used as the aqueous feed for the extraction. The aqueous and organic phases were fed with equal flow-rates of 100 mL/min in counter-current mode while the bowl was rotating at the speed of 3600 rpm. Both organic and aqueous samples were collected at regular intervals of time during the extraction. Similarly, samples from both aqueous and organic phases were collected from the bowls of each stage at the end of the experiment. The concentration of Nd(III) in both the phases was estimated by the titration against the standard ethylene diamine tetraacetic acid (EDTA) using methylthymol blue indicator in the presence of hexamethylenetetraamine at pH 6. The acidity of each sample was determined by standard acid-base titration using standard sodium hydroxide in the presence of potassium oxalate. The analytical results clearly indicated that the six-stage ACE setup reached steady state condition within five minutes under the operating flow-rate conditions. Data obtained from the stage-wise sample analysis shown that Nd(III) was extracted quantitatively within three stages of extraction. Subsequent to the extraction, the Nd(III) recovery from the loaded organic phase was carried out into dilute (0.01 M to 0.06 M) nitric acid using the same ACE under similar flow-rate conditions. The steady state was reached within 15 minutes of operation. It was also observed that Nd(III) was recovered quantitatively within 3 stages of stripping. However, it is important to mention here that there was a milky white interfacial crud formation during the metal recovery into 0.03 M or lower nitric acid medium after the three stages of contact (4 to 6 stages). This may be due to the inappropriate interfacial tension and other physical properties of the system. However, this challenge did not exist when the acidity of the strippant increased to higher values. It was observed that the stripping was not quantitative whenever the acidity of the strippant increased to more than 0.06 M. Thus, the studies clearly indicate that the quantitative recovery of trivalent f-ions is possible only if the aqueous phase acidity is less than 0.1 M (0.03-0.06 M). Therefore, the stripping was carried out using 0.03 M nitric acid. Thus, the current studies revealed that the ACEs are suitable to carry out the trivalent extraction and stripping by diglycolamide systems like TODGA.

Reference:

[1] S. A. Ansari et. al., *Chemical Reviews*, **112** (2012) 1751.

Assay of Leached Hulls of FBTR Irradiated Fuel for Plutonium at DFRP

J. S. Brahmaji Rao¹, G. V. S. Ashok Kumar^{1,§}, Debasish Saha¹, K. Sundararajan¹, V. Jayaraman¹, V. Anandhanarayanan², S. Sudhagar², P. Sivakumar², N. Desigan², K. Rajan²

¹Materials Chemistry and Metal Fuel Cycle Group, IGCAR, Kalpakkam, India

²Reprocessing Group, IGCAR, Kalpakkam, India

§ Email: gvs@igcar.gov.in

The Demonstration Fast Reactor Fuel Reprocessing Plant (DFRP) was setup to reprocess irradiated fuel from the Fast Breeder Test Reactor (FBTR). Measurement of fissile materials in leached hulls of irradiated fuel is necessary to estimate the plutonium (Pu) content for strategic material accounting and waste disposal point of view. Gamma spectrometric measurement is not feasible due to interference from activation products like ⁶⁰Co and ⁵⁴Mn in SS hulls. Instead, the presence of Pu isotopes in leached hulls is typically measured by detecting ¹⁴⁴Ce-¹⁴⁴Pr, assuming similar dissolution behaviors of cerium and plutonium oxides. As a result, the Pu-to-¹⁴⁴Ce ratio in the dissolver solution (DS) & leached hulls should remain consistent. The dissolver solution is analysed chemically and via gamma spectrometry to determine Pu and ¹⁴⁴Ce levels. The activity of ¹⁴⁴Ce in the hulls can be determined by gamma spectrometry. However, knowledge of full energy peak efficiency (FEPE) is needed to estimate the activity of ¹⁴⁴Ce, for which its high energy gamma at 2185.6 keV was used.

KAMINI irradiated ⁷²Ga source ($t_{1/2} = 14.1$ h, gamma range 600-2508 keV) with activity of 0.6 mCi was used for FEPE calibration studies at DFRP employing a portable 50% HPGe detector. To reduce the radiation dose on the detector during the hull assay, a 50 mm Pb block between the detector and hull assay basket and a 200 mm Pb shielding around the detector assembly were provided (Fig.1). Further to reduce dead-time on the detector, a series of removable lead attenuators are provided in front of the detector having thickness of 15 mm each. The ⁷²Ga source was then employed as a point source for calibration of the HPGe detector at various detector-shielding-source geometries in the Hull assay system. However, the gamma source

geometry in the hull basket was quite different from the point source and therefore, the FEPEs obtained for the ⁷²Ga point source have been converted to hull assay basket geometry using a MCNP based EFFTRAN code (Fig. 2). The converted FEPEs for the hull basket geometry were employed on leached hulls from 20 irradiated FBTR fuel pins in the first DFRP campaign. No 2185 keV photopeak from ¹⁴⁴Ce was observed, likely due to the fuel being cooled for over 5 years, resulting in reduced ¹⁴⁴Ce levels. Hence, the Pu content in the leached hulls was found to be below detection limits and reported as < 3 g, based on the registered background counts in the 2185 keV region & ¹⁴⁴Ce to Pu ratio (14.43 MBq of ¹⁴⁴Ce per g of Pu) in the dissolver solution.

References:

[1] T.D. Reilly, *The measurement of leached hulls*, LA-7784-MS (July 1979).

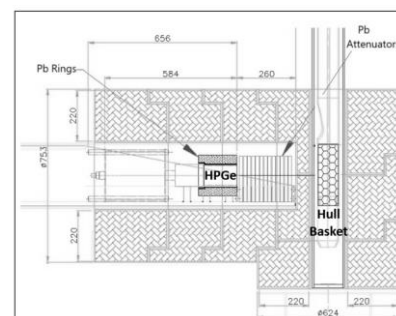


Fig.1: HPGe detector & Hull basket configuration in Hull assay facility

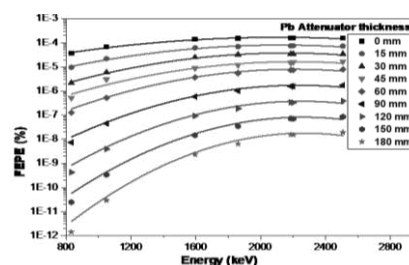


Fig. 2: Variation of FEPEs as a function of gamma energy

Conformational Studies of Tri-Amyl Phosphate (TAP) and its Branched Derivatives

Vemuri Lakshmi Ganesh,^{1, 2, §}

C. V. S. Brahmananda Rao,^{1, 2}, Gopinadhanpillai Gopakumar,^{1, 2}

¹Indira Gandhi Centre for Atomic Research, Kalpakkam, Tamil Nadu, India.

²Homi Bhabha National Institute, IGCAR Campus, Kalpakkam, Tamil Nadu, India.

§Email: vemurilakshmiGANESH720@gmail.com

Tri-*n*-butyl phosphate (TBP) is a key extractant in the closed nuclear fuel cycle, effectively separating uranium and plutonium from spent nuclear fuel and aiding in the extraction of minor actinides from high-level liquid waste (HLW). However, TBP has several drawbacks, including high aqueous solubility, susceptibility to radiation-induced degradation, and the formation of a third phase, which necessitate the development of alternative ligands with enhanced stability and performance. Recent studies have shown that the basicity of the phosphoryl oxygen remains unchanged with increasing alkyl chain length [1]. The conformational studies of these ligands have not been exclusively explored through experimental methods. In this context, we have computationally explored the conformational landscape of tri-amyl phosphate (TAP) and its branched derivatives as a preliminary step to investigate their complexation behaviour. For this step, we used the Conformer and Rotamer Ensemble Sampling Tool (CREST) [2], and the 100 lowest-energy conformers derived were considered as starting geometries for DFT calculations. The resulting lowest-energy structure obtained at the DFT level was selected for further analysis, including NBO and orbital analysis. All calculations were performed using the ORCA quantum chemistry program package [3], NBO version 6 [4], and the CREST [2] program package. CREST analysis shows that for TAP, there are 12,736 conformers within 5 kcal/mol, whereas TiAP, T2MBP, and TsAP form 8,331, 6,605, and 10,878 conformers, respectively. NBO analysis indicates that the charges on P and O do not change upon branching.

Ligands	NBO Charges		
	P	O	Net
TAP	2.42	-1.05	1.36
TiAP	2.43	-1.06	1.37
T2mbP	2.42	-1.05	1.37
TsAP	2.44	-1.07	1.37

Ligands	CREST Energy Window (kcal/mol)		
	< 1	1-5	> 5
TAP	654	12082	1927
TiAP	601	7730	623
T2mbP	569	6036	587
TsAP	437	10441	2163

References:

- [1] P. Rajani et.al., *Chem. Phys. Lett.* **775** (2021) 138641.
- [2] P. Pracht et.al., *Phys. Chem. Chem. Phys.*, **22** (2020) 7169.
- [3] F. F. Neese, *Wiley Interdiscip. Rev. Comput. Mol. Sci.*, **8** (2017) 1327.
- [4] NBO version 6.0. E. D. Glendening et.al., Theoretical Chemistry Institute, University of Wisconsin, Madison (2013).

Synthesis of Ion-Imprinted Polymer Gels for Selective Separation of Strontium Ions

Aditi Chourasia¹, Amol Mhatre², Chhavi Agarwal^{2,§}, R. Tripathi²

¹K. J. Somaiya College of Science and Commerce, University of Mumbai

²Radiochemistry Division, Bhabha Atomic Research Centre, Trombay, Mumbai-400085

§ Email: cagarwal@barc.gov.in

Radiostrontium is an important radionuclide from environment contamination point of view and there is a need to selectively separate/extract radiostrontium from environmental samples in order to prevent its harmful effects [1]. Conventional separation methods such as solvent extraction, ion-exchange etc have been reported, however these techniques involve multiple steps and require hazardous solvents, which can pose environmental and safety concerns [2]. In contrast, polymer gels can be engineered to selectively bind target ions, enhancing separation efficiency. In the present studies, an attempt has been made to synthesize strontium selective polymer gels by imprinting Sr^{2+} ion in the polymer matrix using ion-imprinting technique. For preparing the Sr^{2+} imprinted gel, acrylic acid was chosen as the functional monomer owing to the presence of carboxylic acid moieties in it and the strontium ion was first equilibrated with acrylic acid to allow its binding with the latter's functional moieties. This was followed by synthesis of polymer gel using polyethylene glycol methacrylate (PEGMA) as the monomer, ethylene glycol dimethacrylate (EGDMA) as the cross-linker, and the equilibrated solution. For polymerization, in-situ UV polymerization technique was employed. The strontium ion was then removed from the imprinted sites by hydrogen peroxide treatment. This imprinted gel is referred as gel-1. Along with this, a non-imprinted (gel-2) was also prepared under same conditions. The strontium ion and other fission product (Cs-137, Ba-140, Ce-144, Eu-152) uptake by these gels from aqueous solution ($\sim\text{pH } 7$) was studied. It was observed that though there is only slight increase in uptake of strontium ion upon ion-imprinting (from 36% to 44%) but the selectivity of gel for Sr^{2+} was enhanced > 7 times wrt Ba^{2+} , 5 times wrt Eu^{3+} and ~ 16 times wrt Ru ion. This was observed by negligible uptake of Cs and Ce ion and significantly decreased uptake of other ions in the imprinted gel. This shows successful Sr^{2+} imprinting in the synthesized polymer gel. The Sr^{2+} uptake by these gels was compared with the crown ether impregnated polymer gel (gel-3), prepared by following similar methodology. A Sr^{2+} uptake of 74 % by gel-3 in contrast to only 23% uptake by gel-4 (corresponding non-imprinted gel) was observed from 2 molL^{-1} HNO_3 medium thereby showing successful impregnation of crown ether in the gel-3. However, the uptake of Sr^{2+} was found to decrease significantly ($\sim 19\%$) as the acidity was lowered to pH 1, thereby making this gel usable for only highly acidic conditions. The successful synthesis of strontium-selective ion-imprinted polymer gels highlights their effectiveness in the selective separation of radiostrontium with the future scope of improving the efficiency.

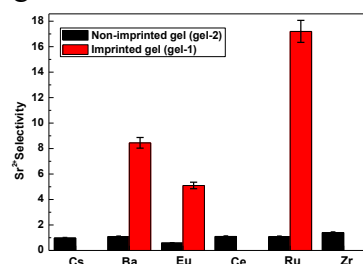


Figure 1. Selectivity of Sr^{2+} imprinted and non-imprinted polymer gel. The selectivity of Cs, Ce and Zr could not be measured due to negligible uptake by the imprinted gel.

References:

- [1] N. Vajda and C. K. Kim, *Appl. Radiat. Isot.* **68** (2010) 2306.
 [2] S. Dai, et. al, *J. Chem. Soc., Dalton Trans.*, **1201** (1999) 1201.

Tailoring the Electrochemical Behavior and Speciation of Eu(III) in Choline Chloride-Based Deep Eutectic Solvents

Arkaprava Layek¹, Kavitha Jayachandran¹, Annu Balhara², Ruma Gupta^{1, §}

¹Fuel Chemistry Division, Bhabha Atomic Research Centre, Mumbai, India

²Radiochemistry Division, Bhabha Atomic Research Centre, Mumbai, India

§Email: rumac@barc.gov.in

The study investigates the electrochemical behavior and speciation of Eu(III) ions in choline chloride (ChCl)-based deep eutectic solvents (DESs), focusing on the role of different hydrogen bond donors (HBDs) in stabilizing europium complexes. Utilizing a combination of electrochemical techniques, spectroscopic analyses, and theoretical methodologies, we explore how hydrogen bonding interactions influence Eu(III) coordination and reactivity. Cyclic voltammetry experiments were conducted in DESs composed of ChCl with urea (U), ethylene glycol (EG), and malonic acid (MA) to assess the impact of Eu³⁺. Based on the CV data (Fig. 1A), it can be concluded that Eu(III) forms the most stable complex with ChCl:1MA DES due to the chelate effect provided by its bidentate carboxyl group, requiring the highest amount of energy to reduce. The viscosity of the three DESs follows the order ChCl:2EG < ChCl:2U < ChCl:1MA at 303 K. Also, DES viscosity, and mass transport properties have significant impact on electron transfer kinetics. The results indicate quasi-reversible redox behavior across all systems, with ChCl:2EG demonstrating the highest charge transfer rate. Photoluminescence studies, further reveal variations in interactions between hydrogen bonds and functional groups such as –NH₂, –COOH, and –OH, enhancing the understanding of Eu³⁺-complexes. Fig 1B shows the emission spectra of Eu(III) in three different DES which clearly indicate the changes in different transitions of Eu³⁺ as an effect of changing the HBD in the DESs. The findings offer critical insights into the modulation of Eu(III) redox properties within DESs, contributing to advancements in lanthanide chemistry. We believe this work paves the way for the rational engineering of Eu(III)-based materials with tailored electronic and optical characteristics, suitable for diverse technological applications in catalysis, sensing, and optoelectronics.

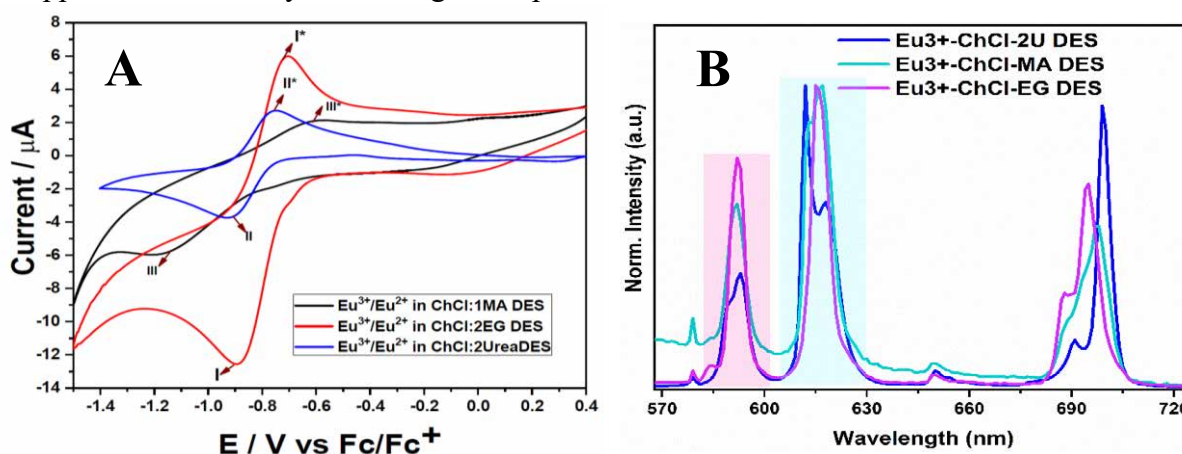


Fig. 1: A) Cyclic voltammogram of Eu³⁺ in three different DESs B) Normalized photoluminescence emission spectra of Eu³⁺-DES complexes

References:

[1] Arkaprava Layek, et. al., *Analyst*, **149** (2024) 4464.

Separation of Lanthanides using a Mixed Ion Exchange Column with α -HIBA as Eluent

M. K. Das, V. G. Mishra[§]

Radioanalytical Chemistry Division, Bhabha Atomic Research Centre, Mumbai, India

[§]Email: vgmishra@barc.gov.in

Dynamically modified reversed phase chromatography efficiently separate lanthanides using α -hydroxyisobutyric acid (α -HIBA) as a complexing agent [1]. Lanthanide ions form complexes with α -HIBA, enabling separation based on stability of complexes and ionic interactions with a dynamically modified column. In this study, a mixed ion exchange column, IonPac CS5A (Dionex), incorporating both cationic and anionic exchange groups, was employed for the separation of lanthanides using α -HIBA in the eluent. Arsenazo(III) was used as a post-column reagent (PCR) for the detection of the lanthanide ions eluted from the column. The column's ability to retain both cationic and anionic complexes makes it an interesting choice for studying the elution behavior of lanthanides with α -HIBA. As per literature, lanthanide separation on the CS5A column using α -HIBA alone as the eluent, is not reported. A systematic study was carried out, which demonstrated that the heavier lanthanides (Lu to Tb) were eluted at a relatively lower concentration of the eluent, while the lighter lanthanides (La to Gd) exhibited stronger retention and hence required higher concentrations of the eluent. Several gradient profiles were examined for the elution indicating that the use of significantly high concentrations of α -HIBA facilitated the complete elution of all lanthanides with excellent separation. Fig. 1 represents the chromatogram obtained with the optimized elution conditions.

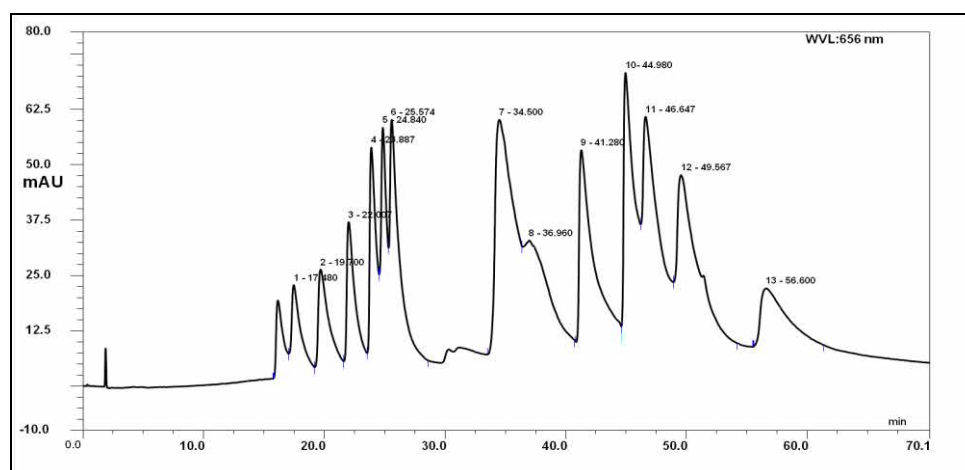


Fig. 1: A typical chromatogram obtained using the optimized elution profile. *Column:* Ion Pac CS5A, *Eluent:* α -HIBA with concentration ranging from 25-400 mM from 0 min to 60 min. *Detection:* UV-Vis, using Arsinazo(III) as PCR. *Sample:* standard mixture of 5 ppm each of lanthanides. *Peaks:* 1-Lu, 2-Yb, 3-Tm, 4-Er, 5-Ho, 6-Dy, 7-Tb, 8-Gd, 9-Sm, 10-Nd, 11-Pr, 12-Ce, 13-La.

Reference:

[1] V. G. Mishra, et. al., *Separation Science and Technology* **58** (2023) 2704.

Study of Effect of Linker Behavior on the Iodine Adsorption Capacity of Thorium Based UiO-66/67 MOFs

Abhishek Sharma^{1,3}, Bal Govind Vats^{2,3, §}, S. C. Parida^{1,3}

¹Product Development Division, BARC, Mumbai, India

²Fuel Chemistry Division, BARC, Mumbai, India

³Homi Bhabha National Institution, Anushakti Nagar, Mumbai, India

§Email: bgvats@barc.gov.in

Radioactive iodine is a fission product generated during the operation of a nuclear reactor. A typical 700 MWe nuclear power plant generate around 100-150 g of iodine depending on the fuel burnup [1]. Because of high volatility, it possesses severe environmental and health risks as iodine tends to preferentially bind with thyroid gland. At present, iodine separation from spent nuclear fuel (SNF) is carried out by liquid scrubbing with alkali hydroxide that may possess operating issues due to harsh conditions caused by alkali and low decontamination factor. In this regard, sorption of iodine on porous materials has emerged a viable technique. Metal-organic frameworks have emerged as the potential candidate for gas adsorption due to their high surface area, scope of tuning the topology, structure, functionality, pore design etc.

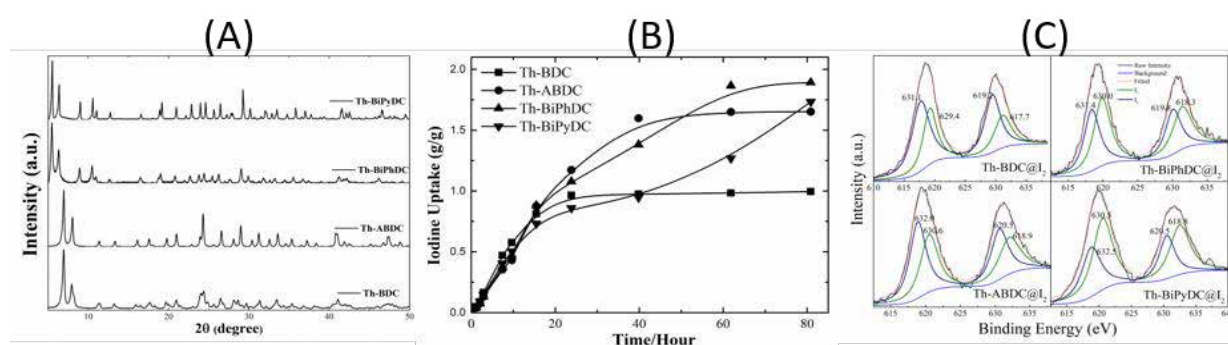


Fig.1: (A) XRD patterns of synthesized MOFs, (B) Iodine adsorption curves of the investigated MOFs, (C) XPS fitted curves of I 3d_{3/2} and I 3d_{5/2} peaks in I₂@MOFs

In the present study, we have synthesized four Th-based UiO-66/67 MOFs which comprises of Th₆(μ₃-O)₄(μ₃-OH)₄ cluster (Th) and organic linkers, namely 1,4-benzenedicarboxylic acid (BDC), 2-Amino-1,4-benzenedicarboxylic acid (ABDC), 1, 1'-Biphenyl-4, 4'-dicarboxylic acid (BiPhDC) and 2, 2'-Bipyridyl-5, 5'-dicarboxylic acid (BiPyDC). These synthesized MOFs were characterized by powder XRD (Fig. 1A) and IR spectroscopy. The iodine adsorption capacity of ThBDC, ThABDC, ThBiPhDC and ThBiPyDC (Fig. 1B) are 0.97, 1.65, 1.89 and 1.73 g/g, respectively. Further, it was observed that ThBiPhDC and ThBiPyDC frameworks partially collapse during solvent removal and hence are mechanically less stable. However, functionalizing BDC with an amino group, enhances the absorption capacity of the MOF without compromising its stability. The XPS studies (Fig. 1C) shows the absorbed iodine in the framework coexist as I₂ and I₃⁻ anion [2].

This study provides the strategy to increase MOF capacity for I₂ adsorption by introducing electron donating groups on the ring.

References:

1. Pepper, et. al., *Progress in Nuclear Energy*, **169** (2024) 105062.
2. Li, et.al., *Journal of the American Chemical Society*, **146**,20 (2024) 14048.

Fe(II)-Induced Immobilization of Selenium (VI) Oxyanion in Presence of Uranyl ions

Snigdha Srabane, ^{1,2} Sumit Kumar^{1,2,§}

¹Radioanalytical Chemistry Division, Bhabha Atomic Research Centre, Mumbai, India

²Homi Bhabha National Institute, Anushaktinagar, Mumbai, India

§Email: sumitk@barc.gov.in

Iron based materials have shown promise in reducing highly soluble selenium oxyanion, selenate, into a less soluble reduced form [1]. Owing to their surface mediated redox reaction, ferrous salts have been used in wastewater treatment leading to immobilization of the mobile oxyanions. The presence of redox-reactive elements, such as selenite, chromate, Mn, etc. can compete and impede this redox-induced immobilization procedure. It is therefore important to evaluate the role of such co-contaminants. Selenate enrichment in seleniferous soil and groundwater has been observed in Punjab region of India, which exhibit enhanced uranyl content [2]. In the present study, Fe(II)-induced immobilization of selenate oxyanion has been investigated in the presence of uranyl ion at near neutral pH to investigate the role of redox sensitive uranyl ion in the immobilization process.

The experimental procedure involves the aging of Fe(II) - selenate solution in the presence of Uranyl ions after mixing the individual solutions at pH ~3 and bringing the pH to 10 by adding 1 M NaOH solution in the anoxic condition. Molar ratio of U/Se was varied over 1.5 and 3 while the Fe(II) content was kept fixed at 10 mM. Part of the suspension was centrifuged after 6 hours, and assayed for dissolved Fe (UV Spectrophotometry using 1, 10-phenanthroline), U (U-233 LSC method) and Se concentration (Se-75 radiotracer method). Solid phases arising from the experimental solutions were analyzed by XRD for the mineral phase. The U(VI) containing solutions immediately become brown-blackish (unlike green-blackish in absence) on attaining near neutral pH indicating the oxidation of Fe(II) to Fe(III) and simultaneous hydrolysis to form (oxy)hydroxide of Fe(III). Solid phase appearing from the Fe-selenate-uranyl reaction mixture was found to exhibit complex XRD pattern with magnetite ($\text{Fe}^{\text{II}}\text{Fe}^{\text{III}}_2\text{O}_4$) as the dominant phase. Fig. 1 presents the kinetic profile of selenate removal from the aqueous phase with different concentration of uranyl ions. Interestingly uranyl presence accelerates the removal of selenate in 24 hours with increasing concentration (3mM) following pseudo first-order kinetics. Data in the study thus indicates uranyl-ions-prompted reducing action for selenate ion immobilization. For mechanism, uranyl ions sorption on hydrolyzed products of Fe(II) leads to formation of Fe(II)-Fe(III)-oxide surface which is actually responsible for selenate reduction. In presence of uranyl ions, the transformation of Fe(II) hydrolyzed product is actually gets catalyzed.

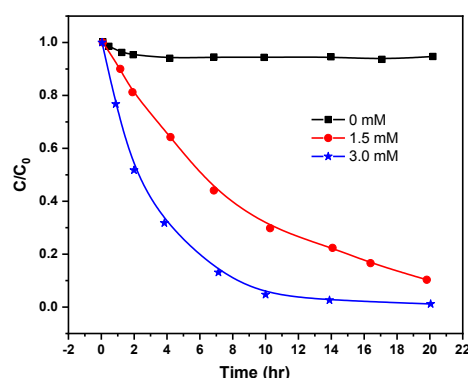


Fig. 1: Effect of Uranyl concentration on the removal of Se(VI) [1 mM]

Acknowledgements: Authors acknowledge the support and encouragement of Head, RACD.

References:

- [1] K. Zoroufchi Benis et al. *J. Hazard. Mat.*, **424** (2022) 127603.
- [2] M. G. Skalnaya et al., *Biol. Trace Elem. Res.*, **191** (2019) 10.

Neodymium Complexation by Tridentate Chelators: Speciation Studies by Absorbance and Calorimetry

Rama Mohana Rao Dumpala^{1, §}, Diksha P Dalvi², Shiny S Kumar¹, S. Jeyakumar¹

¹Radiochemistry Division, Bhabha Atomic Research Centre, Mumbai, India

²Department of Chemistry, K. J. Somaiya College of Science and Commerce, Vidyavihar, Mumbai University, Mumbai, India

§Email: rammohan@barc.gov.in

Neodymium (Nd), a technologically important metal ion, has emerged as a major contaminant in aquatic system in recent years owing to its surge in electrical and electronic applications as permanent magnets. The chelating molecules present in hydro and biospheres could substantially enhance its absorption and lead to transportation and migration of Nd from source [1]. The mechanistic understanding of Nd interaction with naturally relevant bio moieties present in flora and fauna are of primitive importance to estimate the toxicological effects of the metal ion. Nitrogen containing six membered aromatic pyridine and its derivatives abundantly exist in nature and play a vital role in the field of heterocyclic chemistry [2]. Pyridine derivatives are very important chemicals with wide biological applications. Hydroxy-pyridine dicarboxylic acid capable of forming tridentate chelate complexes with many metal ions, is one such naturally occurring pyridine skeleton moiety [3].

The $f \rightarrow f$ transitions in lanthanides are Laporte forbidden and majorly are insensitive to the coordination environment. Hypersensitive transitions show considerable changes in absorption or emission spectra to slight changes in coordination around them. For, Nd(III), transition ${}^4I_{9/2} \rightarrow {}^4G_{5/2}$ (centered at 576 nm) is hypersensitive transition. The present studies showed red shift and peak broadening of Nd(III) absorption spectra in 560-610 and 710-850 nm range (Fig. 1) on interaction with hydroxy-pyridine dicarboxylic acid (ligand). The absorption initially increased with increase in L/M ratio, after which it decreased with increase in L/M ratio. This intensity variation of hypersensitive transition band (560-610 nm), indicates an asymmetric complex formation at beginning to a symmetric complex formation at high L/M ratio. The speciation modelling also showed formation of three successive complexes ML, ML₂ and ML₃ by Nd³⁺ with the ligand. ML₃ being more symmetric than ML and ML₂, the intensities decreased with increasing L/M ratio. The log β values were found to be 9.18 ± 0.18 , 17.47 ± 0.29 and, 23.22 ± 0.56 respectively and matches with lanthanide tridentate chelate complexes. Calorimetric data showed completely endothermic enthalpies of complex formation as 17.97 ± 0.45 , 32.36 ± 0.54 and, 45.27 ± 0.74 kJ/mol respectively for all the three complexes, indicating the entropy driven complex formations.

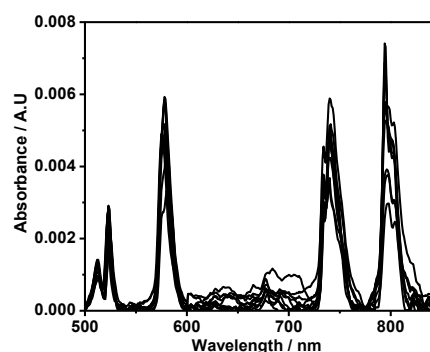


Fig. 1: Absorption spectra of Neodymium (Nd³⁺) on changing L/M ratio with addition of hydroxy-pyridine dicarboxylic acid to Nd³⁺ solution.

References:

- [1] K. Sultan, N. A. Shazili, *J. Rare Earths*, **27** (2009) 1072.
- [2] A. Ali et al., *J Drug Design Med Chem.*, **1** (2015) 1.
- [3] S. Abdolmaleki, M. Ghadermazi, A. Aliabadi, *Sci. Rep.*, **11** (2021) 15699.

Studies on Simultaneous Removal of Tc⁹⁹ & Ru¹⁰⁶ from Radioactive Low-Level Waste Using Mild Steel Wool in Acidic Conditions

Adwitiya Kar^{1,2}§, Anupkumar Bhaskarapillai^{2,3}, A.G. Shanmugamani¹,
S. Srinivasan¹, G. Srinivasa Rao¹, J. K. Gayen¹

¹ Integrated Nuclear Recycle Plant, Nuclear Recycle Board, BARC, Kalpakkam, India

² Homi Bhabha National Institute, Mumbai, India

³ Water and Steam Chemistry Division, BARC, Kalpakkam, India

§ Email: adwitiya@igcar.gov.in

Radioactive aqueous LLW is a highly voluminous alkaline effluent generated during the IX treatment of radioactive ILW. LLW is subjected to further treatment to ensure maximum removal of the radioactivity followed by its subsequent discharge to the Sea. Major radionuclides present in it are ⁹⁹Tc, ¹⁰⁶Ru & small quantities of ¹³⁷Cs, ⁹⁰Sr-⁹⁰Y. Typically, LLW is subjected to a two-step chemical treatment at pH 8.5 viz. (i) Co-decontamination of radionuclides (ii) Precipitation of the residual activity.

Literature suggests that Tc-mineralization can occur in iron oxy/hydroxide phases such as goethite/magnetite which are formed when mild steel corrodes in aqueous surroundings. MS wool has a very large surface area per unit mass compared to solid form. The corrosion process is facilitated inside aqueous LLW under acidic & O₂-rich conditions, generating iron oxy/hydroxide phases that can capture ⁹⁹Tc *in-situ* [1],[2]. Experiments were carried out under controlled parameters to exploit the ⁹⁹Tc-sequestration ability of MS wool as a pre-treatment step for the ⁹⁹Tc-rich LLW.

Combinations of Cu-turnings + MS wool were studied for feasibility of simultaneous remediation of ¹⁰⁶Ru by *in-situ* generated Cu₂O. Effects of turbulence, contact time, etc. were investigated.

Significant removal of ⁹⁹Tc (>90%) & ¹⁰⁶Ru (~50%) were observed at pH ~ 2.0. The final pH of the treated solution was ~5.0 – 6.0. About 10 % wool was consumed in 4 h. Removal efficiency reduced with increase in the solution pH. A single batch of MS wool was reused for multiple batches till complete degradation with minimal sludge was generated.

The preliminary studies have shown encouraging results as a pre-treatment step & further studies are ongoing.

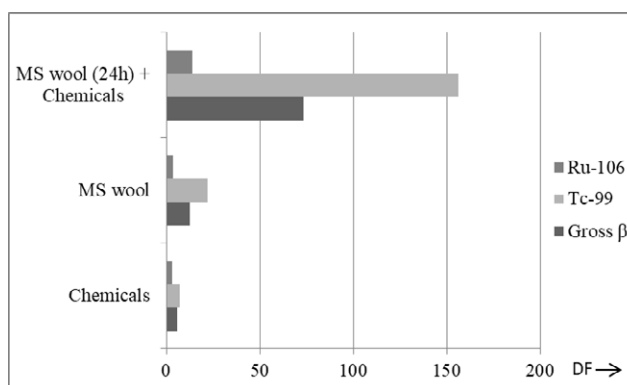


Fig. 1: Enhancement of decontamination factor (DF) in LLW w.r.t. gross β, ⁹⁹Tc & ¹⁰⁶Ru using *in-situ* corrosion of MS wool at an initial pH 2.0 as a pre-treatment step prior to chemical precipitation.

References:

- [1] J.G. Shah, et. al. U.S. patent -10,553,324 and EP3417461B1, 2020.
- [2] A. Ananthanarayanan, et al. *BARC Newsletter*, **361** (2018) 19.

Measurement of Nuclear Reaction Rates for Neutron Spectrum Characterization at the Maximum Flux Location in the Dry Tube of the KAMINI Reactor

Alakananda S.G^{1,2}, *Manish Chand*^{1,§}, *G.V.S. Ashok Kumar*¹, *K Sundararajan*^{1,2}

¹*Analytical Chemistry and Spectroscopy Division, IGCAR, Kalpakkam, India.*

²*Homi Bhabha National Institute, Mumbai, India.*

§ Email: mchand@igcar.gov.in

The KAMINI research reactor provides multiple irradiation facilities, including the PFTS, Thimble, Beam, and Dry tubes, each offering distinct neutron flux conditions ranging from 10^6 - 10^{11} n.cm⁻².s⁻¹. These facilities support diverse applications such as neutron activation analysis, isotope production, and material research. In this study, the neutron spectrum at the highest flux location inside the DT-1 was characterized using the foil activation method. Irradiations were performed at 10 kW reactor power for six hours using activation foils of Au, Fe, In, Ni, Co, Y, and Ti to investigate nuclear reactions such as (n, γ), (n, p), and (n, 2n), covering a range of threshold energies. The induced activity in the foils was measured using a 50% p-type coaxial high-purity germanium (HPGe) detector. Reaction rates were determined from the measured activities, providing insights into neutron interactions at this irradiation site as summarized in **Table 1**. Key activation products include ⁵⁹Fe, ⁵⁴Mn, ⁴⁸Sc, ^{115m}In, and ⁸⁸Y, among others. The gold equivalent neutron flux at DT-1 was also calculated and found to be 1×10^{10} cm⁻².s⁻¹. The reaction rates for higher threshold reactions, such as ⁴⁸Ti(n, p)⁴⁸Sc (E_{th} =3.2 MeV) and ⁸⁹Y(n, 2n)⁸⁸Y (E_{th} =9.4 MeV), were found to be 6–7 orders of magnitude lower than capture reactions. The neutron spectrum at DT-1 will be further analysed using the SAND-II code to unfold the complete energy distribution based on measured reaction rates with different threshold energy. The results will provide a detailed spectral characterization, identifying contributions from thermal, epithermal, and fast neutrons, thereby enhancing the characterization of neutron flux conditions in KAMINI for applications in radiochemical studies and reactor-based neutron metrology.

Table 1. The measured reaction rate for different nuclear reactions at DT-1.

Foil	Activation Product	Gamma Energy (keV)	Nuclear Reaction	Half-life (t _{1/2})	Measured Reaction Rate
Fe	⁵⁹ Fe	1099.2	⁵⁸ Fe(n, γ) ⁵⁹ Fe	45.1 (d)	7.75E-15
Co	⁶⁰ Co	1332.5	⁵⁹ Co (n, γ) ⁶⁰ Co	5.27 (y)	2.26E-13
Au	¹⁹⁸ Au	411.8	¹⁹⁷ Au(n, γ) ¹⁹⁸ Au	2.69 (d)	6.39E-13
In	^{115m} In	336.3	¹¹⁵ In(n,n') ^{115m} In	4.5 (h)	3.67E-17
Ti	⁴⁷ Sc	159.3	⁴⁷ Ti(n,p) ⁴⁷ Sc	3.341 (d)	3.64E-18
Ni	⁵⁸ Co	810.8	⁵⁸ Ni (n,p) ⁵⁸ Co	72 (d)	1.95E-17
Fe	⁵⁴ Mn	834.8	⁵⁴ Fe(n,p) ⁵⁴ Mn	310 (d)	2.77E-16
Ti	⁴⁶ Sc	1120.5	⁴⁶ Ti(n,p) ⁴⁶ Sc	83.83 (d)	2.13E-17
Ti	⁴⁸ Sc	1312.12	⁴⁸ Ti(n,p) ⁴⁸ Sc	1.821 (d)	6.83E-20
Y ₂ O ₃	⁸⁸ Y	1836.05	⁸⁹ Y(n,2n) ⁸⁸ Y	106 (d)	8.99E-19

References:

1. Manish Chand et. al., *J. Radioanal. Nucl. Chem.* **322** (2019) 147.
2. Manish Chand et. al., *J. Radioanal. Nucl. Chem.* **332** (2023) 4325.

Quantification of Minor and Trace Elements in Antidiabetic Herbal Formulations by Instrumental Neutron Activation Analysis Utilizing Self-Serve Facility of Dhruva Reactor

Arpita Datta^{1§}, Reetta Sara George¹, S. K. Samanta², R. Acharya^{3,4}

¹Amity Institute of Nuclear Science & Technology, Amity University Uttar Pradesh

²Radiochemistry Division, Bhabha Atomic Research Centre, Mumbai

³Isotope and Radiation Application Division, Bhabha Atomic Research Centre, Mumbai

⁴Homi Bhabha National Institute, Department of Atomic Energy, Mumbai

§Email: adatta@amity.edu

Diabetes mellitus has become a common health problem in recent years and may lead to multiple complications in human body. Herbal formulations are steadily gaining popularity as an alternative to synthetic medicines for controlling diabetics with lesser side effects due to the presence of bioactive phytochemicals along with essential elements like Cr, Zn, V etc [1-

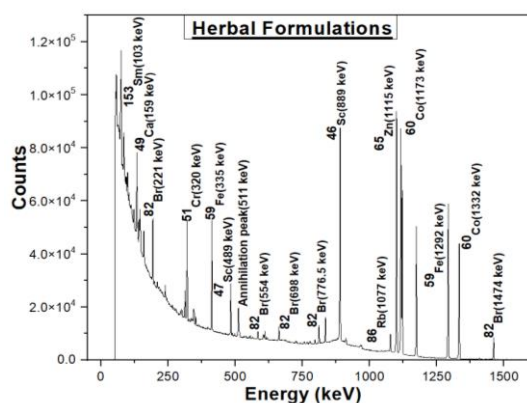


Fig 1. Typical gamma-ray spectrum of herbal formulation sample in NAA

2]. Present study is aimed to determine minor and trace elemental contents in fourteen antidiabetic herbal formulations using Instrumental Neutron Activation Analysis (INAA) by utilizing self-serve facility of Dhruva reactor (Fig.1). A total of twelve major, minor and trace elements such as Ba, Br, Ca, Co, Cr, Fe, K, Na, Rb, Sc, Sm, Zn, were determined in the herbal formulations. The quality of the results reported in the present study for the antidiabetic herbal formulation samples by INAA was validated by analysing biological certified reference material (CRM) mixed polish herbs (INCT-MPH-2). The analytical parameters assessed for each element in CRM with INAA in

the method validation are selectivity, limit of quantification, precision etc. Both Precision and selectivity for INAA method used in the present study were evaluated by performing the replicate (n=3) analysis and the RSD values are found to be within the range ($\leq 10\%$) for INAA. Limit of quantification was calculated from the spectrum sample i.e. background under the analyte peak. Results also indicated the presence of essential nutrients like Ca, K, Cr & Zn exhibiting the antidiabetic properties of herbal formulation as these nutrients act as a cofactor of various enzymes important for glucose metabolism, helpful to improve insulin sensitivity and manage blood sugar levels in human body. Estimated dietary intake (EDI) of the trace elements from the herbal formulation samples was determined and results were compared with the permissible limit as per Food Safety and Standards Authority of India (FSSAI) and the EDI of minor and trace elements in the samples obtained by INAA method are within the permissible limit as per FSSAI for most of the samples.

Authors from Amity University thank UGC-DAE-CSR (Mumbai Centre) for the Project (CRS-M-326) and financial grant to carry out R&D work at RCD, BARC, Mumbai.

References:

1. M. Kaur et al., *Eur. J. Med.*, **6** (2024) 226.
2. R. S. George et al., *J. Radioanal. Nucl. Chem.*, **332** (2023) 4301.

Influence of Organic and Inorganic Nutrients on Soil Physio-Chemical Parameters and Maize Yield Utilizing Instrumental Neutron Activation Analysis

Vaishali Dadwal^{1,2}, Deep Shikha^{1,§}, Sonika Gupta³,
Aditi Dalvi^{4,5}, Vimal Mehta¹, R. Acharya^{5,6}

¹Sri Guru Teg Bahadur Khalsa College, Punjab-140118, India

²Punjabi University Patiala, Punjab-147002, India

³Radiochemistry Division, Bhabha Atomic Research Centre, Mumbai - 400 08

⁴Analytical chemistry Division, Bhabha Atomic Research Centre, Mumbai - 400 085

⁵Homi Bhabha National Institute, Department of Atomic Energy, Mumbai – 400094

⁶Isotope and Radiation Application Division, BARC, Mumbai - 400085

§Email: deep_shikha79@yahoo.co.in

This study evaluated the effects of locally sourced organic inputs (Farm Yard Maure) and inorganic fertilizers (Muriate of Potash), on soil fertility and crop quality. A total of 12 samples from the Nawanshahr region of Punjab were subjected to elemental characterization, and various physicochemical parameters, including soil pH, electrical conductivity (EC), and organic carbon (OC), were also estimated. These included five soil samples, five maize crop samples, and two fertilizer samples. Instrumental Neutron Activation Analysis (INAA) was employed to determine elemental concentrations using reactor neutrons ($\sim 10^{13}$ n/cm²/s) at the Pneumatic Carrier Facility (PCF) of the Dhruva reactor, BARC. Geological Certified Reference Material (CRM), RGM-1 was used for quality control. Elements such as Na, Mn, Mg, Al, and Ca were identified, with results for RGM-1 showing good agreement with certified values, exhibiting Z-score within ± 1 . Elemental concentration ranges of these elements in crop samples, soil samples, and in fertilizers were measured. These findings underscore the importance of integrating nutrient management strategies to enhance soil fertility, increase crop quality. The relative method (equation 1) was used for elemental concentration calculation [1].

$$m_{x,\text{sample}} = m_{x,\text{std}} \cdot \frac{\text{CPS}_{x,\text{sample}} \cdot D_{x,\text{std}} \cdot C_{x,\text{std}}}{\text{CPS}_{x,\text{std}} \cdot D_{x,\text{sample}} \cdot C_{x,\text{sample}}} \quad (1)$$

Where $m_{x,\text{sample}}$ is the concentration of the analyte in the sample, $m_{x,\text{std}}$ concentration of the analyte in the std, CPS is the count rate of sample and std, D and C is the decay correction and counting correction factors respectively. Inorganic chemical fertilizers increased soil EC and calcium levels, while treatments with organic inputs improved pH, EC, and OC, enhancing soil quality. However, a weak correlation ($R^2 < 0.65$) was observed between elemental transfer from soil to crops.

The authors express gratitude to Dr. P.D. Babu, Centre Director, UGC-DAE CSR Mumbai Centre at BARC, for the UGC-DAE-CSR project and Dr R Acharya as Principal Collaborator (presently Head, IRAD, BARC)

Reference(s) :

[1] Sharma, N., et al., *Journal of Radioanalytical and Nuclear Chemistry*, **281** (2009):59

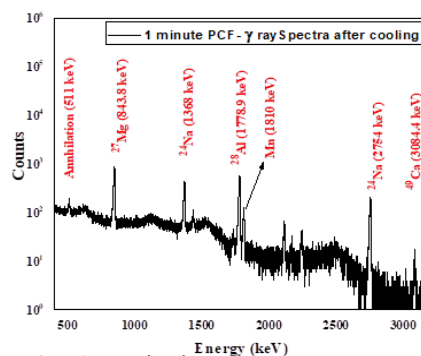


Fig. 1 Typical gamma-ray spectrum obtained by irradiation of in PCF at Dhruva for soil sample.

Neutron Attenuation Measurements in Borated Concrete and Comparison with Normal Concrete

D.V. Subramanian[§], Adish Haridas, D. Sunil Kumar,
J. Ashok Kumar, M. Elumalai, Himanshu Gupta, R. Preetha

Indira Gandhi Centre for Atomic Research, Kalpakkam, Tamilnadu 603102, India

[§]Email: dvs@igcar.gov.in

Different densities of concrete (2.4, 3.6, and 4.6 g/cc) are typically employed for neutron and gamma radiation shielding in various areas of nuclear reactors due to their cost effectiveness. Recently borated concretes, with 15%, 10% and 5% boron carbide (replacing fine aggregates) are designed with a density of 2.4 g/cc. Experiments are carried out to find their significance for neutron and gamma shielding and the attenuation results are compared with normal concrete. The experiment is done by stacking 5 numbers of borated concrete slabs of size $30 \times 20 \times 5$ cm at the south beam end of the KAMINI reactor and placing activation foils (such as Au, In, W, Cd and Zn) & thermo luminescent dosimeter (CaSO₄:Dy) (TLD) powder in between the slabs at different locations. The total thickness of the slabs is 29 cm. Activation foils are chosen to cover a broad spectrum of neutron energy, including thermal to fast neutron regions, and are exposed to 10kWt power for six hours. The neutron attenuation of the material is determined by utilizing the measured reaction rates of different locations after counting. Using the cumulative dose of different locations, the gamma attenuation pattern of borated concrete is obtained.

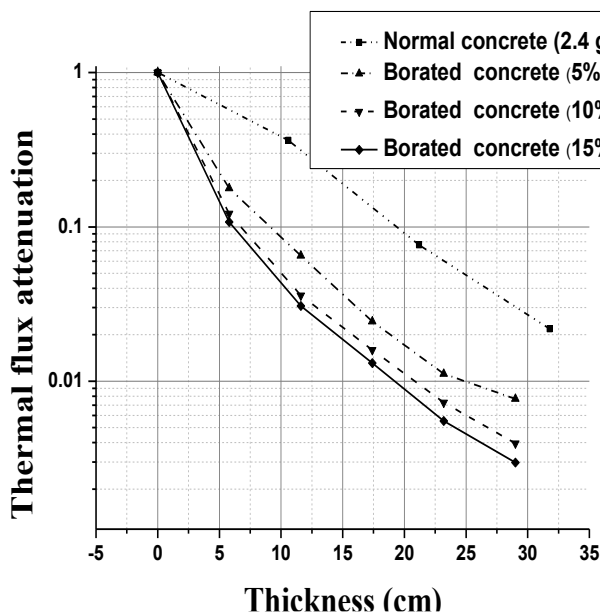


Fig. 1 : Thermal neutron flux attenuation

One of the thermal neutron flux attenuation of borated concretes is compared with normal concrete [1]. The comparative graph is given in Fig.1. With 19 cm thickness of 15% borated concrete, more than 100 times reduction is observed in thermal neutron flux. This is equivalent to 21 cm in 10% borated concrete, 24 cm in 5% borated concrete and > 35 cm in normal concrete. Hence it is clear that borated concrete (2.4g/cc) made with 15% B₄C is more effective for thermal flux attenuation. In case of fast neutron flux attenuation, the borated concretes with 15% & 10% B₄C are showing similar attenuation behaviour and are found to be more effective than normal concrete. Borated concretes show similar gamma dose rate attenuation as that of normal concrete.

The measured data will be used as a basic reference for further measurements and future validation studies.

References:

[1] D.V.Subramanian & Adish Haridas, "Neutron Attenuation measurements with normal concrete in the south beam end of KAMINI Reactor", PFBR/01115/DN/1208, (June-2020).

Semi-Quantitative Direct Non-Destructive Determination of Fe, Sn and Ni in Zirconium Alloy Samples using Wavelength Dispersive X-ray Fluorescence Spectrometer

M. Singh[§], L. Pradhan, A. D. Jadhav, A. Pandey, V. R. Sonar, A. Kelkar, D. B. Sathe, Aniruddha Kumar, R. B. Bhatt

Fuel Fabrication, INRP(O), NRB, Bhabha Atomic Research Center, Tarapur-401502 India

[§] Email: mamtasingh@barc.gov.in

Zirconium alloys, particularly Zircalloys, play a crucial role in nuclear reactor technology due to their excellent corrosion resistance and mechanical properties at elevated temperatures [1]. The typical composition of various Zr alloys used in nuclear industry is mentioned elsewhere and play very important role [2]. Ni was found to be responsible for enhanced H pickup fraction leading to hydrogen embrittlement. Sn improves strength and creep resistance. Fe and Ni led to the formation of brittle intermetallic compounds during cooling.

Wavelength Dispersive X-ray fluorescence (WDXRF) is a very useful non-destructive technique for the analysis of different types of samples with minimal sample preparation, rapid analysis, wide elemental range and versatility. A 200 W WDXRF with Pd target X-ray tube with LiF as a dispersion crystal, P10 gas (10% CH₄ and 90% Ar) at a flow rate of 7ml/min is used and measurement is done with Flow proportional counter detector. In this paper, an attempt has been made for direct non-destructive determination of Fe, Sn and Ni in Zr alloy samples using WDXRF spectrometer. The samples (dia. 30 mm) were cut from the actual clad tube of Zircaloy-2 and Zircaloy-4. During the analysis of the WDXRF spectra, the fundamental parameter (FP) method was employed. The FP approach is based on the theoretical relationship between the measured intensities of X-rays and elemental concentrations. To achieve a reliable quantification, the experimental set-up and instrumental parameters, such as incident/outgoing angles, sample matrix composition, as well as the X-ray detector characteristics were introduced within the ZSX software. The results thus obtained were compared with the literature reported values and were found in close agreement (Table 1).

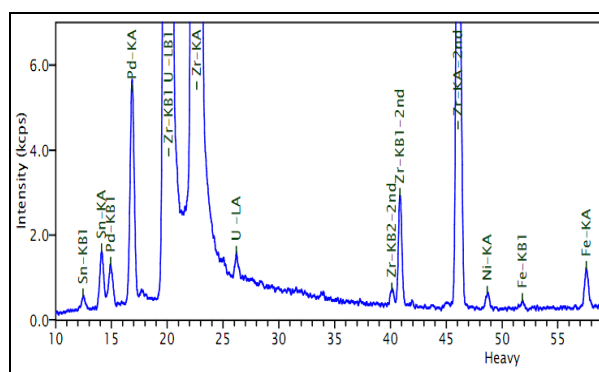


Fig. 1: WDXRF spectra of mirror finished Zircaloy-4 sample

S. No.	Standard Values (%)		WDXRF Values (%)
Zircaloy-2	Fe	0.07-0.20	0.29±0.15
	Sn	1.20-1.70	1.41±0.09
	Ni	0.05-0.15	0.07±0.14
Zircaloy-4	Fe	0.18-0.24	0.31±0.16
	Sn	1.20-1.70	1.44±0.10
	Ni	0.07-0.13	0.08±0.16

Table 1: Comparison of semi-quantitative values obtained for Fe, Sn and Ni using WDXRF with their reported standard values

Authors record their sincere thanks to colleagues of Lab, FF-INRP(O) during the course of this work.

References:

[1] Kaushik Sanyal et. al, *J. Synchrotron Rad.* **27** (2020), 1253–1261.

Assessment of Photo Peak Efficiency of BEGe Detector in Comparison with p-Type co-Axial HPGe Detector

S.J. Sartandel^{1,§}, V.A. Pulhani^{1,2}

¹Bhabha Atomic Research Centre, Environmental Monitoring and Assessment Division, India

²Homi Bhabha National Institute, India

§Email: sangjs@barc.gov.in

High-resolution gamma-ray spectrometry is one of the most widely used procedures to determine the concentrations of natural and artificial radionuclides in the environmental samples. Important step in the gamma spectrometric analysis is the full-energy peak efficiency (FEPE) calibration with respective energy for given measuring geometry. The detection system efficiency depends on parameters such as gamma ray energy, detector dimensions, its entrance window thickness, measurement sample geometry & matrix [1]. Thus selection of the appropriate detector is one of the crucial factors, as different detectors have varying capabilities and sensitivities.

For present study Canberra make p-type Broad Energy Germanium (BEGe) BE5030P and BSI make p-type coaxial extended range HPGe GCD-50 190X have been used. Both systems are 50% relative efficiency with thin entrance window of carbon fiber making it applicable for the extended range low energy. Photo peak efficiency evaluated using IAEA Reference PT-2024 quality control sample in 250ml geometry using Eq. (1).

$$\epsilon(E) = \frac{N}{A \gamma t} \quad \text{--- (1)} \quad \text{where } N\text{- net peak area, } A\text{- activity (Bq), } \gamma\text{- emission probability, } t\text{-time.}$$

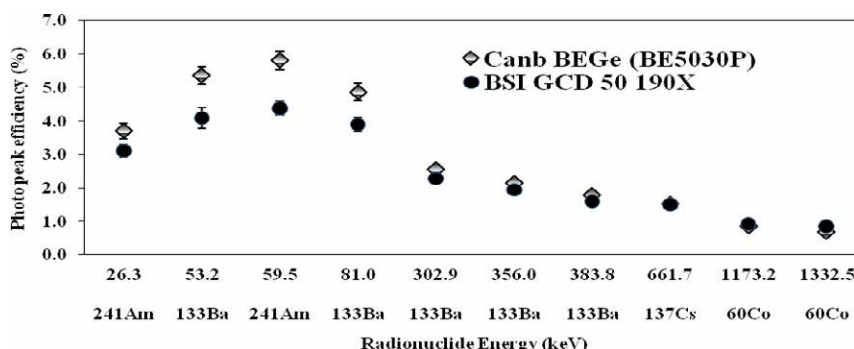


Fig. 1. Photo peak efficiency (IAEA PT2024) for BEGe and Coaxial P-Type HPGe Detector.

As observed from the fig 1, the BEGe detector showed relatively better efficiency at lower energy with 5.8% (²⁴¹Am) and 1.53% (¹³⁷Cs) compared to 4.4% (²⁴¹Am) and 1.5% ¹³⁷Cs by GCD-50 190X. Thus the evaluated % increase in the values was found to be 1.3% at 661.6 keV and 24% at 59.6 keV. For energies above 1MeV, coaxial GCD-50 showed relatively better efficiency of 0.93% and 0.85% compared to 0.85% and 0.68% at 1173.2 keV and 1332 keV respectively for ⁶⁰Co which amounts to 8.5% - 20% percentage increase in photo peak efficiency shown by GCD-50. BEGe detector has a short, fat shape which enhances the efficiency below 1 MeV for typical sample geometries and generally exhibits superior efficiency at low energies, due to its design that minimizes dead layer effects from the entrance window, while the coaxial HPGe detector excel at higher energies, but have lower efficiency at low energies. BEGe detector may make a better choice for assessment of radionuclides having low energy such as ²⁴¹Am and ²¹⁰Pb.

References:

[1] Özlem K, Sabiha V., *J Basic Clin Health Sci.*, **1** (2017) 18.

Investigating the Concentrations and Spatial Variability of Key Elements in Soil from Haryana India

R.C. Bhangare¹, M. Tiwari¹, P.Y. Ajmal¹, T.D. Rathod¹, S.K. Sahu^{§1,2}, V. Pulhani^{1,2}

¹Environmental Monitoring and Assessment Division, BARC, Mumbai, India

²Homi Bhabha National Institute, Mumbai, India

§ Email: sksahu@barc.gov.in

Soil is a vital resource for all life on earth. However, in current times it faces significant pollution challenges due to industrialization, agriculture, and urbanization, leading to resource degradation and ecosystem damage [1]. Toxic metals from sources like fertilizers, mining, and industrial activities degrade soil quality and threaten environmental safety, making monitoring and management very crucial [2]. This study is a part of nationwide monitoring of soil profile across India. In this study,

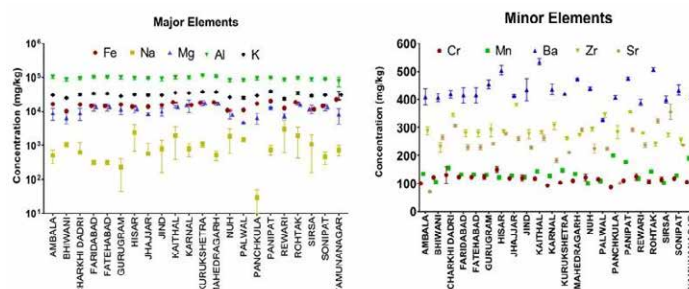


Fig 1: District wise concentration of Major and Minor elements

two soil samples collected from each taluk of all districts of Haryana, a state in India, were analysed using EDXRF technique. IAEA-433 was used as the SRM. The elemental concentrations in soil of Haryana are influenced by intensive agriculture, industrial emissions, and natural geochemical factors. Fig. 1 shows districtwise distribution of major, minor and Fig. 2 shows average concentration of trace elements in soils of Haryana. In major elements, highest soil concentration was found for Al with average value of 93567 ± 8211 mg/kg, while lowest was for Mg viz. 11215 ± 2836 mg/kg. In minor elements the maximum concentration was observed for Ba with average concentration of 433 ± 16 mg/kg while Cr was lowest with average concentration of 115 ± 8 mg/kg. In case of trace elements, maximum concentration was observed for Rb with a average value of 104 ± 15 mg/kg while lowest concentration was observed for Cs with value of 3 ± 2 mg/kg. Average U concentration in soil was 4 ± 1 mg/kg (DL=0.5 mg/kg). The levels of some heavy and toxic metals are observed to be elevated in this study which is in accordance with a previously reported study on Haryana [3]. Maximum total elemental concentration was observed in Kurukshetra soil as it had maximum concentrations of 3 major elements while minimum total soil elemental concentration was observed for Rewari district soil. Element wise amongst all districts, Panchkula and Panipat soils showed highest concentrations for a total of 5 elements each, while the soil from Bhivani showed lowest concentration for a total of 10 elements. This study offers a detailed distribution of elemental concentrations in soil in different districts. The findings are helpful in understanding regional soil composition, nutrient status, temporal changes from previous observations and its ecological implications.

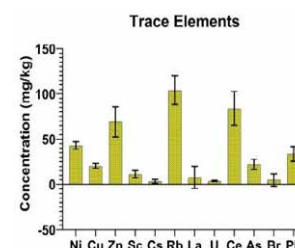


Fig 2: Average concentration of Trace elements

References:

- [1] Jin, Y., *Environ. Int.*, **124**, (2019) 320
- [2] Wu, Y., et al., *Conservation and Recycling* **181**, (2022) 106261
- [3] G Krishan et al., *Current World Environment* **13** (2018) 299

Evaluation of Experimental Detection Limit of B in Varying Matrices in External (in air) PIGE Using 3.5 MeV Proton Beam from FOTIA

Sonika Gupta^{1,§}, Priya Girikar¹, Suparna Sodaye¹, R. Acharya²

¹Radiochemistry Division, Bhabha Atomic Research Centre, Trombay, Mumbai-400085

²Isotope & Radiation Application Division, BARC, Trombay, Mumbai-400085

[§]Email: sonika_ta@barc.gov.in

Particle Induced Gamma-ray Emission (PIGE), an isotope specific ion beam analysis (IBA) technique, is performed using low energy (2-5 MeV) proton beam and it is capable of determining low Z elements mainly Li to S including B and its isotopic composition ($^{10}\text{B}/^{11}\text{B}$ atom ratio, IC) [1]. It involves measurement of prompt γ -rays of 429 and 718 keV from $^{10}\text{B}(p, \alpha\gamma)^7\text{Be}$, $^{10}\text{B}(p, p'\gamma)^{10}\text{B}$ and 2125 keV from $^{11}\text{B}(p, p'\gamma)^{11}\text{B}$ nuclear reactions. B based materials like B_4C find vast applications in nuclear technology as neutron absorbers due to high thermal absorption cross-section (3837 b) for $^{10}\text{B}(n, \alpha)^7\text{Li}$. External (in air) PIGE [2] is attractive for faster results with high sample throughput. Ext-PIGE facility at FOTIA with thin Ta-window (135/165 keV peak from ^{181}Ta serves for current normalization) is being utilized for R&D and commercial application for IC of B & B-10 isotope content certification. The objective of this work was to evaluate the detection limit (DL) of B in various matrices (from low Z (C) to high Z (Zr)) relevant to Indian power reactor program. Ceramic borides and B added structural materials with elements like Si, Ti, Fe & Zr are also proposed as future control and shielding materials. Various matrices namely graphite, cellulose, SiC, TiO_2 , Fe_2O_3 and ZrO_2 were mixed with natural B_4C (10 wt%) powder in 10:1 ratio with total mass of each sample 300 mg. Experiment was carried out at 3.5 MeV proton beam taking B_4C in graphite as standard and prompt γ -rays were measured online using a 40% HPGe detector system. A typical γ -ray spectrum of TiB_2 analysed by external PIGE is shown in the figure indicating peaks due to ^{181}Ta , ^{10}B & ^{11}B and ^{48}Ti . The most sensitive peak at 429 keV of ^{10}B was considered for concentration determination as well as DL evaluation taking natural IC corresponding 19.8 atom% of ^{10}B . The uncertainties in the measured B concentrations were found to be within $\sim 2\%$ with respect to added concentration in different matrices. The 3σ DLs (L_D) of B were calculated for different samples in a similar experimental condition, where σ refers to the square root of background under 429 keV peak. The L_D values in these matrices were found to be in the range of 50-123 ppm due to varying matrices from low to higher Z and L_D of B was found lower for graphite and higher for Fe & Zr matrices. In conclusion, though ext-PIGE is simple and gives faster results (5-10 min), the DLs for B were found to be poorer compared to vacuum chamber PIGE [1] due to slightly lower sensitivity and higher Compton background and L_D values are matrix dependent even at diluted sample with 10 wt% B concentration in graphite as major matrix.

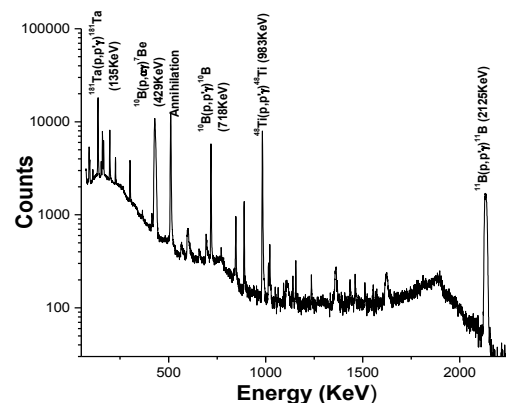


Fig. 1 γ -ray spectrum of TiB_2 in Ext-PIGE

Authors thank Director & Associate Director, RC&IG and Head, RCD for their support & encouragements. Authors thank Director, MRG, Head, IADD, Head, FOTIAS for their support and FOTIA Operation Crews for their help during the experiment.

Reference:

[1] Sumit Chhillar, et al, *Anal. Chem.*, **86** (2014) 11167.

[2] V Sharma, et al, *Journal of Analytical Atomic Spectrometry* **36**, 630-643.

EDXRF-Based Green Methodology for Direct Compositional Characterization of Actinides in UF₄-ThF₄-LiF

Kaushik Sanyal^{1,3}, Sangita Dhara^{1,3,§}, Pratik Das², R. V. Pai^{1,3}

¹Fuel Chemistry Division, Bhabha Atomic Research Centre, Mumbai, 400085, India

²Product Development Division, Bhabha Atomic Research Centre, Mumbai, 400085, India

³Homi Bhabha National Institute, Anushaktinagar, Mumbai, 400094, India

§ Email: sdhara@barc.gov.in

Molten Salt Reactors (MSRs) are promising advanced nuclear reactors with various benefits associated with them. They have higher efficiency, operate at low pressure therefore, less prone to accidents and have enhanced safety. Another advantage of MSRs is that it can adopt a variety of nuclear fuel cycles such as U-Pu, Th-U and Th-Pu cycles. This allows for extending the fuel resources as well. The Indian MSR proposed fuel was primarily based on the Th fuel cycle, leveraging the country's abundant thorium reserves [1]. The precise quantification of the fuel composition with respect to U and Th, is crucial for reactor performance, safety, as well as efficiency. Energy Dispersive X-ray Fluorescence (EDXRF) spectroscopy promises to offer a non-destructive, direct, rapid and reliable method for determining the elemental composition of MSR fuel with reasonable precision and accuracy [2]. Hence, an EDXRF based green methodology was developed for the direct compositional characterization of actinides in UF₄-ThF₄-LiF.

The working standards for calibration of the spectrometer were prepared by mixing weighed amounts of nuclear grade UF₄, ThF₄, and AR grade LiF in a pestle mortar. The three compounds were ground a multiple times 20-25 minutes by addition of acetone to obtain a reasonably good homogeneity and samples with lower particle size. Table 1 gives the composition of five working standards prepared as described above. Using these standards, the calibration plot was made for U and Th mol. percent Vs the intensity percent. The calibration plot for U determination is shown in Fig.1. A linear calibration plot was obtained with R² > 0.995 in case of both U and Th.

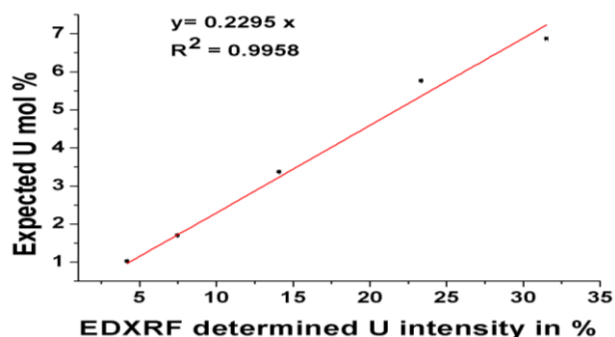


Fig 1. Calibration plot for uranium

S. No.	Li F	UF ₄	ThF ₄	U	Th
	(in g)			(in Mol. %)	
1.	0.112	0.018	0.385	1.02	22.39
2.	0.111	0.030	0.373	1.70	21.51
3.	0.113	0.060	0.341	3.37	19.64
4.	0.112	0.101	0.299	5.76	17.36
5.	0.113	0.122	0.279	6.87	16.04

Table 1. Composition of calibration standards

Samples of UF₄, ThF₄ and LiF mixtures as well as melts were analysed by EDXRF in order to validate the developed methodology. The U and Th mol. % in these samples were determined using the above calibration equation. The precision obtained was within 1% and the analytical results deviated from the expected values calculated on the basis of sample preparation, by 3% and 2% for U and Th, respectively.

References:

[1] P. K. Vijayan, et. al., *Pramana*, **85** (2015) 539.

[2] Sangita Dhara, S. Sanjay Kumar and N. L. Misra, *X-Ray Spectrometry*, **45** (2016), 268.

Assessment of Heavy Metals in Roadside Agricultural Field Soil Around Trombay

Rupali C. K. Kamat^{1§}, Sujata Gothankar¹, Sunita Singh¹, Vandana A. Pulhani^{1,2}

¹*Environmental Monitoring & Assessment Division, BARC, Mumbai, India*

²*Homi Bhabha National Institute, Mumbai, India*

§Email: chakor@barc.gov.in

Soil plays a crucial role in the biosphere and is vulnerable to a variety of pollutants, including heavy metals, which can enter through natural processes or human activities. Although the natural concentration of metals in soil is influenced by the underlying geogenic parent material, the excessive use of inorganic fertilizers and manure has been associated to higher levels of heavy metals in the soil [1]. Soil contamination by heavy metals poses a significant environmental risk, as these pollutants can enter the food chain, affecting both humans and animals, thus emphasizing the importance of thorough monitoring. This study aimed to evaluate the distribution of heavy metals in soils from roadside agricultural fields near Trombay, an area impacted by heavy traffic, waste dumping, and small-scale industries. Six sites were selected to collect composite soil samples from fields cultivating leafy vegetables along the roadside (5–15 m from the road). Approximately 1 kg of composite soil was collected by pooling five subsamples from various locations at each site. The samples were air-dried, sieved to remove debris, freeze-dried to remove moisture, and then ground into a fine powder. The powdered soil was mixed with cellulose powder and pressed into pellets for heavy metal analysis using EDXRF (Model EX 3600, Jordan Valley) with IAEA Soil-7 reference standard.

Table 1: Heavy Metal Concentration in Soil (mg kg⁻¹) from Roadside Agricultural Fields around Trombay

Location	Fe	Mn	Zn	Cu	Ni	Pb
AFS1	84713	1931.3	174.3	39	107.5	87.1
AFS2	93272	2175.3	129.1	37.6	98	94.7
AFS3	50028	1487	68	21.1	44	28.1
AFS4	81467	2424	125.7	33.5	49.8	16.4
AFS5	66464	991	130	24.6	37.4	60.5
AFS6	96530	1562.5	159.6	54.3	30.5	91.7
Average Present Study	78746	1761.9	131.1	35.1	61.2	63.1
Average Indian Roadside soil [2]	10995	325.7	88.9	42.3	77.3	54.7

Table 1 presents the heavy metal concentrations (mg kg⁻¹) in soil samples from roadside agricultural fields in the Trombay area. The average concentrations of metals were found to follow the order: Fe > Mn > Zn > Pb > Ni > Cu. Except for copper, the levels of all metals were significantly higher in Trombay compared to national average roadside soil levels. These elevated concentrations are likely due to excessive fertilizer use, untreated sewage, industrial wastewater irrigation, fungicide application, and the area's proximity to highways with heavy traffic.

References:

- [1] Yushu Shan et.al. *J. Soils Sediments*, **13** (2013) 720.
 [2] Vinod Kumar et.al. *Chemosphere*, **216** (2019) 449.

SRXRF Analysis of Serum Trace Elements in Breast Cancer Subtypes

B. Gowrinaidu^{1,§}, P. Sarita², G. J. Naga Raju³, S. Srikanth⁴, N. Srinivasa Rao², M. K. Tiwari⁵

¹Department of Physics, Government College (A), Rajamahendravaram, India.

²Department of Physics, GITAM School of Science, GITAM Deemed to be University, Visakhapatnam, India

³Department of Physics, JNTU-GVCEV, Vizianagaram, India

⁴Department of Engineering Physics, S.R.K.R. Engineering College (A), Bhimavaram, India

⁵Accelerator Physics & Synchrotrons Utilization Division, Raja Ramanna Centre for Advanced Technology, Indore, India

§Email: bgphy@gcrijy.ac.in

Analysis of serum trace elements in breast cancer patients (ductal carcinoma in situ and invasive ductal carcinoma) and healthy controls was performed using synchrotron radiation-based X-ray fluorescence (SRXRF) technique. The SRXRF experiments were conducted on the Microprobe Beamline-16 at the Indus-2 Synchrotron Radiation facility, located at the Raja Ramanna Centre for Advanced Technology (RRCAT), Indore, India [1]. The accuracy and reliability of the experimental method were confirmed using the International Atomic Energy (IAEA) reference material – animal blood (A-13). In the serum of two groups, sixteen trace elements were identified, and their concentrations were measured. The elements Cu, Zn, Mn, Fe and Se were significantly (<0.05) elevated in the breast cancer group with respect to healthy subjects. The observed serum trace elements were increased in invasive ductal carcinoma breast cancer patients when compared with ductal carcinoma in situ breast cancer patients. The figure shows the SRXRF typical spectrum of trace elements in the blood serum of breast cancer patients. The observed alterations in the specific trace elemental concentrations in the studied groups may have disrupted critical biological and biochemical pathways, thereby influencing pathological mechanisms that ultimately contributed to the initiation and progression of the carcinogenic process [2].

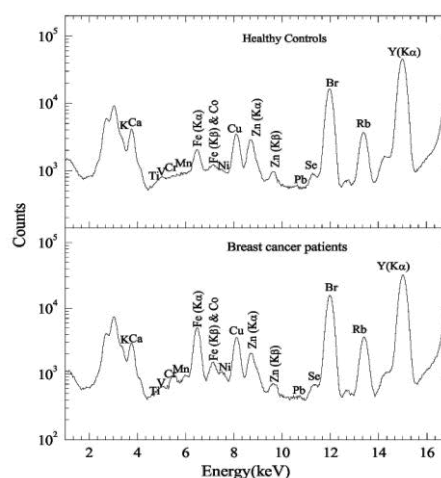


Fig. 1: Typical SRXRF spectra of serum trace elements in serum of in the groups.

The authors would like to thank the microprobe-XRF beamline (BL-16) team at Indus-2 Synchrotron Source, RRCAT, Indore, for beamtime allocation and technical support during experiments, and Mahatma Gandhi Cancer Hospital, Visakhapatnam, for permission to collect breast cancer patient serum samples.

References:

- [1] M.K. Tiwari et al., *Journal of Synchrotron Radiation* **20** (2013) 386.
- [2] Kristina Lossow et al., *Redox Biology* **42** (2021) 101900.

Estimation of KAMINI PFTS Neutron Flux Uncertainty by Foil Activation Method

G. Pandikumar[§], D.V. Subramanian, Adish Haridas

Indira Gandhi Centre for Atomic Research, Kalpakkam, India

[§]Email: pkg@igcar.gov.in

Gold sample is being used as a flux monitor in KAMINI reactor irradiation experiments. The flux obtained from the measured activity, with self-shielding correction, was showing considerable spread. In the present work, self-shielded neutron flux is obtained by gold activation. Using this, spread in the neutron flux for a specific reactor power is estimated.

Gold foils are irradiated at eight different reactor powers from 10W to 20kW. The activities from the gold samples are measured using 150% relative efficient HPGe detector. Due to strong resonance at 4.9eV in Au-197, the incident neutron flux gets perturbed. The incident neutron flux gets modified due to thermal flux depression factor, G_{th} and resonance self-shielding factor, G_{Res} . The resultant self-shielding factor, G , which indicates the ratio of perturbed neutron flux to actual incident neutron flux, is estimated using Hogdahl convention [1]. Figure 1 gives the variation of neutron flux with respect reactor power. Linear variation is observed from the analytical fit viz., $\phi = 6.678E+07 * P$ (flux (ϕ) and power (P)). The estimated neutron fluxes are normalised for 1W reactor power. These neutron fluxes found to have a spread from $6.2E+07$ to $7.1E+07$ n/cm²/s, which is about 14% with respect to mean value. Figure 2 gives the distribution of neutron fluxes corresponding to 1W reactor power. Statistical study shows that the estimated neutron flux best fits with normal distribution. Based on the fit, it is found that the mean is around $6.631E+07$ n/cm²/s. The standard deviation, 2σ , is found to be $0.56E+07$ n/cm²/s.

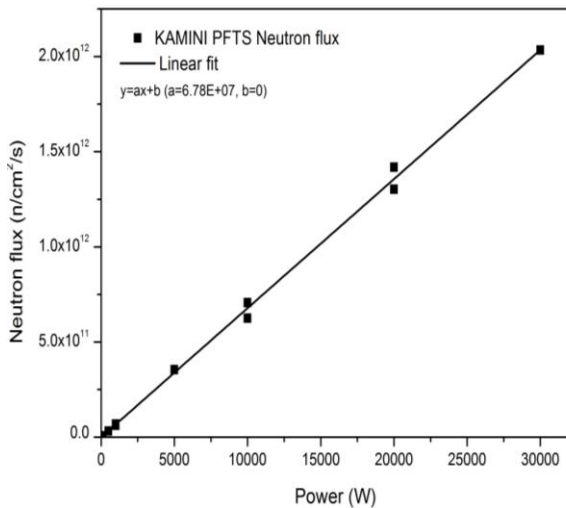


Fig. 1: Variation of neutron flux with reactor power

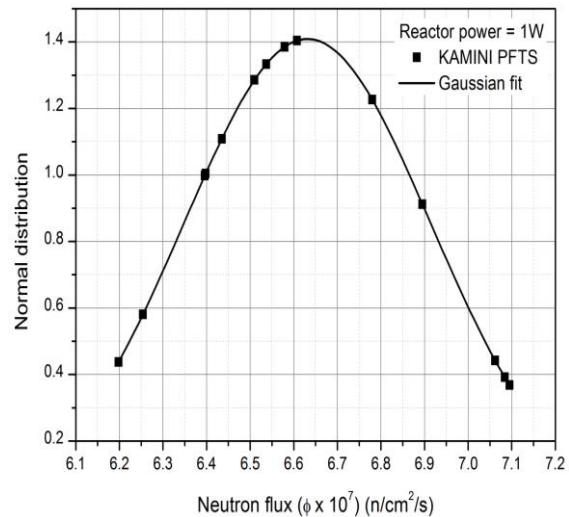


Fig. 2: Spread in neutron flux for 1W reactor power

Reference:

- [1] Stefaan Pomnie, et al., *Neutron activation analysis with K_o standardisation: General formalism and procedure*, **BLG-740**, Nuclear Spectrometry Radiation Protection Department, SCK-CEN, (September 1997).

Development of Direct X-Ray Fluorescence Based Methodology for the Determination of Fissile Atom Content in Fluoride Salt for Molten Salt Fuel Applications

K. Sanyal^{1,2,§}, B. Kanrar¹, R.V. Pai^{1,2}

¹Fuel Chemistry Division, Bhabha Atomic Research Centre, Mumbai-400094, India

²Homi Bhabha National Institute, Mumbai-400094, India

§ Email: ksanyal@barc.gov.in

The fuel used in Molten Salt Reactor (MSR) is continuously circulating fluoride molten salt which consists of fissile and fertile elements. The primary fuel salt consists of ²³³U (as UF₄) and Th (as ThF₄) along with other low Z fluorides like LiF, BeF₂ etc. For any types of fuel used in the reactor, one of the important quality control parameters is the determination of heavy metal contents (Th, U or Pu) present in the fuel. Recent work has proven the suitability of X-Ray Fluorescence (XRF) as an ideal technique for the compositional analysis of different types of fuels like oxide fuel, carbide fuel etc. [1]. The advantages of XRF method over several other methods are, it is simple, consumes lesser time for analysis and direct compositional analysis is possible without cumbersome dissolution of the sample. All these features made it an ideal technique for the compositional analysis of highly radioactive nuclear fuel salt mixture used in MSR. In this work, we have developed a direct XRF based method for the determination of uranium in (LiF, UF₄) fuel matrix. The working standard of the fluoride fuel sample was prepared by carefully mixing weighed amounts of UF₄ and LiF having different wt.% of U in the range of ~57 to 94 wt.%. The calibration standards of uranium were made in the form of pellets by mixing weighted amount of UF₄, Ga₂O₃ and boric acid. The U wt. % varied from 0.1 to 5. It was seen that while using Ga K_α line as an internal standard the matrix effect become severe even at 1wt% U concentration. However, while the Compton scattered peak of Rh K_α line was taken as an internal standard a linear calibration curve was obtained up to 5wt% uranium concentration. Fig. 1 shows the calibration curve for the determination of U wt% using XRF technique and Fig. 2 shows the EDXRF spectrum of one of pellets prepared using UF₄ and LiF salt mixture.

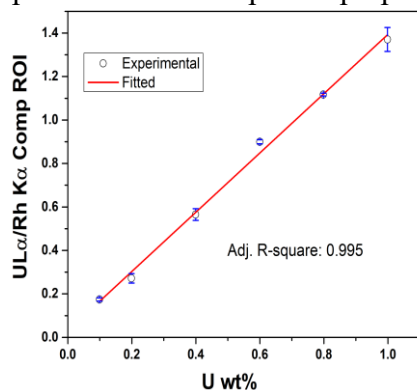


Fig. 1: Calibration curve for the determination of Uwt.% using XRF

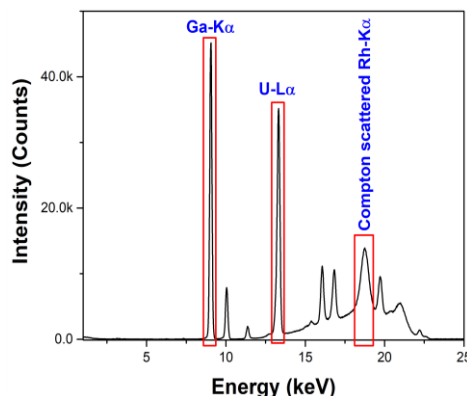


Fig.2: EDXRF spectrum of one of the pellets prepared using UF₄ and LiF salt mixture.

The U wt. % determined using the calibration curve obtained using Compton scattered peak was used to analyze some synthetic fluoride salt fuel mixture along with a real sample prepared by melting the molten salt fuel mixture. The results show that the developed method could determine U wt. % in these types of molten fuel salt mixture with an average accuracy within 5% and precision within 2%. A real molten salt (LiF and UF₄) ingot was prepared and analyzed with the developed method and the result was validated with ICP-OES technique.

References:

[1] K. Sanyal, et. al., *J. Analytical Atomic Spectrometry*, **37** (2022) 130.

Discoloration of Acidic Solution of Yellow 6 Lake Dye with 8 MeV ^1H Beam

A.A. Shanbhag^{1,§}, Sabyasachi Paul¹, S.C. Sharma², P. Srinivasan¹

¹Health Physics Division, BARC, Mumbai 400 085, India

²Nuclear Physics Division, BARC, Mumbai 400 085, India

§Email: shanbhag@tifr.res.in

In many cases the discoloration effect of dye solutions is found to be directly proportional to the radiation dose [1]. In this work, we have used a 8 MeV proton beam from the Pelletron accelerator at the BARC TIFR Pelletron Linac Facility (PLF) to study the discoloration effect on acidic solution of Yellow 6 Lake. Our aim is to do a preliminary investigation about the discoloration of dye solution by a proton beam to find potential applications in the development of a radiation dosimeter for low energy proton irradiation applications like seed mutation studies and radiation hardening studies of electronic components used in space applications. Yellow 6 Lake dye is an organic colouring pigment (Federal food, drug, and cosmetic complaint, CI No. 15985:1) that finds use in the manufacture of various cosmetic products. The preliminary results of these experiments are reported here. The Yellow 6 Lake dye solution was prepared by dissolving 0.2 g dye powder (dye content: 42% w/w) in a mixture of 90 ml of nano-pure water and 10 ml concentrated hydrochloric acid. During irradiation, each sample of 2.5 ml of this dye solution were irradiated in teflon holders in a specialised irradiation setup at the 6m facility of PLF. Multiple irradiations were performed between 3 to 21 minutes with a gap of 3 minutes and current was maintained at 22 nA resulting in absorbed doses of 12.67, 25.34, 38.02, 50.69, 63.36, 76.03 and 88.70 kGy dose respectively. After irradiation, the UV-Vis absorbance spectra of the un-irradiated & irradiated dye solutions were recorded using a spectrophotometer in the wavelength range between 200-800 nm. The wavelength of maximum absorbance (λ_{max}) (in terms of optical density) was found to be 477.5 nm. The degree of discoloration of the solutions was calculated by using the following formula:

$$\% \text{Discoloration} = \frac{[OD_{\text{unirradiated}} - OD_{\text{irradiated}}]}{OD_{\text{unirradiated}}} \times 100 \quad (1)$$

The acidic aqueous Yellow 6 Lake dye solution has shown significant discoloration after 8 MeV proton beam irradiation. The discoloration reaction followed first order kinetics. The results indicate that discoloration of dye solution by proton beam may find potential applications in the development of a radiation dosimeter in high dose ranges. Further experimental studies at proton energies up to 20 MeV and dose comparison with the well-established alanine-EPR dosimetry system are planned.

Authors acknowledge the authorities and staff of PLF for their support during the beam time experiment.

References:

[1] M. El-Banna et al., *Journal of Radioanalytical and Nuclear Chemistry*, **264** (2005) 657

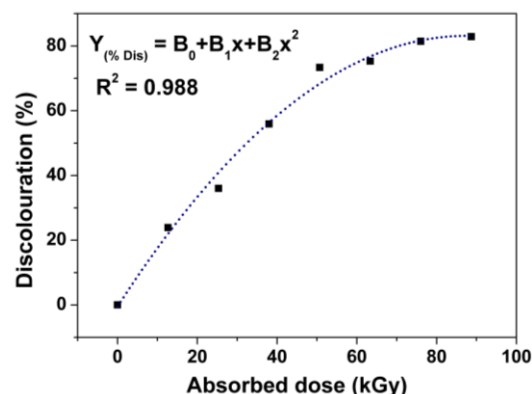


Fig. 1: Plot of Variation of %discoloration with radiation dose

Hydrogen Estimation for Post LOCA Tested Fuel Clads using Neutron Imaging

Shefali Shukla^{1,§}, T. Roy¹, Y.S.Kashyap¹, T.Sawarn³, M.Shukla^{1,2}, P.Singh^{1,2}

¹Technical Physics Division, BARC, India

²Homi Bhabha National Institute, India

³Post Irradiation Examination Division, BARC, India

§Email: shefali@barc.gov.in

Neutron imaging is an excellent nondestructive tool for hydrogen estimation in zirconium alloys. The neutron cross-section for zirconium and zirconium hydride differ by orders of magnitude allowing for measurement of very small (few ppm) amounts of hydrogen in zirconium matrix. Moreover, the technique is simple, requires no sample preparation and has been standardized for quantitative hydrogen estimation in zirconium alloys [1, 2]. LOCA is an accidental scenario resulting from a break in the coolant pressure boundary which results in cladding breakage eventually leading to high temperature oxidation of the cladding inner surface and absorption of huge amounts of hydrogen at certain locations around the burst. Identification of these sites and mapping of hydrogen profile along the clad length is important to understand the role of hydrogen in post LOCA mechanical failure. Neutron imaging being nondestructive can be used for this mapping before actual mechanical tests and the data correlated to understand the role of hydrogen in failure.

In this paper hydrogen profiling of fuel clads tested at oxidation temperatures ranging from 900°C to 1500°C using neutron imaging has been presented. The LOCA test included heating the test pin in flowing steam at near atmospheric pressure till the predetermined oxidation temperature, soaking at that temperature, cooling it down to 800°C and finally water quenching. This process resulted in ballooning deformation, rupture and hydrogen pick up by the clad. The hydrogen mapping in the fuel clad post-test was done using neutron imaging at the HS-3018 thermal neutron imaging beamline, Dhruva. The imaging facility was first calibrated for hydrogen estimation in the range of 10 to 7000 wppm using clad hydrogen standards. Neutron radiography studies were used for mapping the axial hydrogen profile while for circumferential and radial direction tomography was carried out.

Figure 1 shows the neutron radiograph as well as the axial hydrogen profile for the tested clad. The typical M shape around the burst centre for secondary hydriding is seen with maximum hydrogen pickup seen at 40mm around the burst. With neutron imaging hydrogen profile along the radial direction could also be mapped which is not possible using conventional techniques. This paper illustrates the importance of neutron imaging technique for nondestructive hydrogen estimation in fuel clads at a spatial resolution 100-150µm and the minimum distinguishable limit of 100wppm hydrogen.

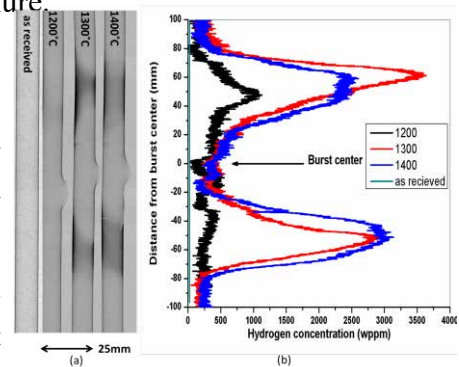


Figure 1: Neutron radiograph for samples tested at 1200°C, 1300°C and 1400°C along with as received sample. (a) Axial hydrogen profiles with burst centre at zero.

References:

- [1] Shefali Shukla et. al., *Journal of Nuclear Materials*, **580** (2023) 124414.
- [2] Shefali Shukla et. al., *Journal of Nuclear Materials*, **544** (2021) 152679.

Determination of Am-243 in the Fast Reactor Fuel Reprocessing Stream

T. Aneesh, Suraj Mondal, Sagunthala Devi, Bhavya S Nair
K Dhamodharan[§], K A Venkatesan, K Rajan

Reprocessing Group, IGCAR, Kalpakkam, Tamilnadu-603102

[§]Email: kdn@igcar.gov.in

The neutron captures by ^{242}Pu and its subsequent beta decay results in the formation of ^{243}Am in a nuclear reactor. The isotope ^{241}Am also converted to ^{243}Am by successive capture of neutrons. The alpha decay of ^{243}Am builds up neptunium (^{239}Np), subsequently it establishes secular equilibrium with ^{239}Np within two weeks due to shorter half-life of ^{239}Np (2.35 days). Therefore, ^{243}Am always associated with presence of ^{239}Np . In the present work, quantitative separation of ^{239}Np formed from ^{243}Am is carried out from a dissolver solution of the FBTR spent fuel and activity of the ^{239}Np was determined by recording the gamma spectrum [1]. The first step in the separation process involves dilution, acidity adjustment of the feed solution and converting oxidation state of all Np to Np (IV) using ascorbic acid and hydrazine mixture. In second step, extraction of Np (IV) into thenonyl trifluoro acetone dissolved in xylene (0.5M HTTA/xylene) was carried out. The quantitative recovery of Np into the organic phase (TTA/xylene) was obtained by providing multiple contacts with conditioned feed solution. The selective extraction of Np into organic phase eliminates the gamma interference from fission products and other minor actinides. And the concentration of ^{239}Np in the organic phase was analyzed by gamma spectrometry method using high purity germanium detector. The predominant photo peaks at 277.6 keV (14.4 % yield) and 228.2 keV (11.3 % yield) were used for the quantification of ^{239}Np activity. The activity of ^{243}Am in the dissolver solution was calculated by applying the first order decay kinetics from the time of separation of the equilibrium mixture and till the time of counting.

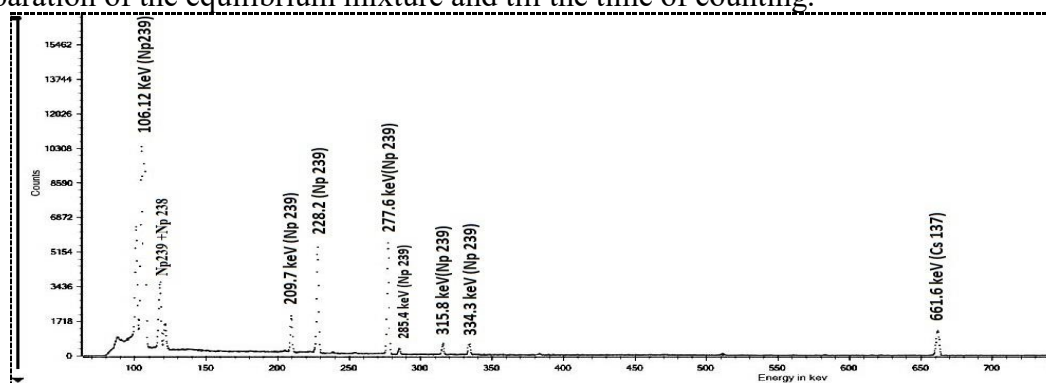


Fig. 1: γ spectrum (HPGe) of the TTA phase recorded after 2 hours of separation from ^{243}Am

The ^{243}Am activity in the dissolver solution was determined as 2.8 ± 0.3 mCi/L. The method described here is relatively easy and it does not require quantitative separation of Pu during ^{239}Np activity determination. The results from Fig 1 shows that gamma signature of $^{237}\text{Np}/^{233}\text{Pa}$ is insignificant. In order to have better peak area, it is preferred to have activity measurement of ^{239}Np within the first half life period of daughter of ^{243}Am .

References

[1] Jana Slimakova, et. al., *J. Radioanalytical and Nucl. Chemistry*, **298** (2013) 1179.

Determination of Neptunium-237 Concentration of by Extractive Alpha Spectrometry Method

T. Aneesh, S.Usha, Neeraja Chandran¹, K.Dhamodharan[§], K A Venkatesan, K. Rajan

Reprocessing Group, IGCAR, Kalpakkam, Tamilnadu-603102

[§] Email: kdn@igcar.gov.in

It is well known that, ^{237}Np is one of the minor actinides present in spent fuel discharged from a nuclear reactor. Its formation in the nuclear reactor is essentially attributed to following nuclear reaction; $^{238}\text{U} (n, 2n) \rightarrow ^{237}\text{U} \rightarrow ^{237}\text{Np} + \beta$; $^{235}\text{U} (n, \gamma) \rightarrow ^{236}\text{U} (n, \gamma) \rightarrow ^{237}\text{U} \rightarrow ^{237}\text{Np} + \beta$. Alpha decay of ^{241}Am can also result in the formation of ^{237}Np . The formation of ^{237}Np in fast reactor (FR) depends on cross section value of (n, 2n) reaction on ^{238}U & incident energy of neutron, and it is noted that the concentration of ^{237}Np present in FR is significantly more than the concentration present in the thermal reactor spent fuels. Therefore, attempts have been made to determine its concentration present in dissolver solution of spent fuel discharged from FBTR. Since, the concentration of plutonium (Pu) in FR spent fuel is 100-200 times higher than that of spent fuel from thermal reactors, very high separation factor is required from Pu for the analysis of Np in dissolver solution by radiometric technique.

Though, various methods were reported for the separation of Np from Pu, these methods did not ensure the quantitative separation of Np from Pu. In the present work, a known volume of aliquot of dissolver sample was diluted with 1M HNO_3 and the valence of Np was adjusted to Np (IV) using 0.1 M ascorbic acid (AA) & 0.1 M hydrazine nitrate (HN). The resultant aqueous solution was equilibrated

with a known volume of 0.5 M HTTA in xylene for 20 minutes. The D for Np(IV) for this condition was determined with the help of ^{239}Np tracer and found to be 9.4, hence two sequential contacts were given for quantitative recovery of Np. The equilibrated layers were collected and Np present in the loaded organic was stripped with 9 M HNO_3 by maintaining A/O ratio of 0.5. A known volume of aqueous phase consisting Np was delivered onto SS disc, dried, covered using mylar film and α spectrum was recorded. The aqueous strip product containing Np was evaporated near to dryness, conditioned with AA & HN, then subjected to second cycle extraction, stripping and finally analyzed for ^{237}Np by α spectrometry. Alpha spectrums are given in fig 1. The counts corresponding to peak area at 4.78 MeV was employed for quantification of ^{237}Np and its concentration in dissolver solution was determined to be $24.35 \pm 1.73 \mu\text{g/mL}$. Interferences from other actinide ions like U, Am were not observed as HTTA is selective extractant for tetravalent ions. The Th isotopes resulted from the alpha decay of ^{235}U & ^{238}U are beta emitters and did not interfere in the present method. A minimum of 2 cycles of purification [1] is mandatory for the quantitative separation of Np from Pu, and AA/HN was found to be promising reducing agent for rapid conversion of all Np to Np (IV).

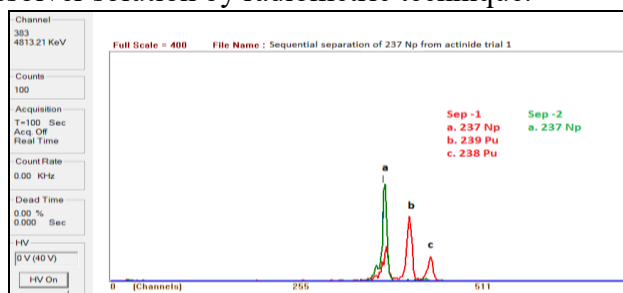


Fig. 1: Alpha spectrum of actinides recorded during the sequential separation of ^{237}Np from Pu.

References

- [1] B. Guillaume, J.P. Moulin, Ch. Maurice 'Chemical properties of neptunium applied to neptunium management in extraction cycles of PUREX process' Dounreay (UK), CEA-CONF- 7772

Introduction of Oxygen Non-Stoichiometry in Oxides and its Determination by Particle Induced Gamma-Ray Emission: a Feasibility Study

Y. Sunitha[§], D.V. Lakshmi pathy, A. A. Sukumar, Sk. Jayabun, G. L. N. Reddy

National Centre for Compositional Characterization of Materials,
BARC, ECIL Post, Hyderabad - 500062

[§]Email: sunitha@barc.gov.in

Oxygen non-stoichiometry makes oxides attractive materials for a wide range of applications beyond their traditional usage as dielectrics. The creation and control of oxygen vacancy-the entity attributable to non-stoichiometry- is crucial for harvesting and tailoring the functional properties of the oxides. The determination of oxygen is the most crucial aspect of such an exercise. The present study describes the measurement of oxygen non-stoichiometry in titanium dioxide ($\text{TiO}_{2-\delta}$) and manganese dioxide ($\text{MnO}_{2-\delta}$) powders post its introduction through vacuum heat treatment at ≤ 773 K. The non-stoichiometry is measured as metal to oxygen (M/O) ratio by particle induced γ -ray emission (PIGE), utilising the simultaneously occurring $^{48}\text{Ti}(p,\gamma)^{49}\text{V}$, $^{55}\text{Mn}(p,n\gamma)^{55}\text{Fe}$ and $^{18}\text{O}(p,p'\gamma)^{18}\text{O}$ nuclear reactions/inelastic scattering that emit 981, 931 and 1982 keV prompt γ -rays respectively [1]. This study represents the first instance of using PIGE, an ion beam based nuclear analytical technique, to determine the metal-to-oxygen ratio (M/O) in non-stoichiometric oxides. It holds particular significance in view of the inherent challenges in oxygen determination.

The powders were heat treated in a tubular furnace at $\sim 10^{-5}$ mbar for 2 h at each temperature. The PIGE experiments, on the other hand, were conducted with 4 MeV proton beams at the 3 MV Tandatron facility of the Centre and the prompt γ -ray spectra were recorded using a high purity germanium (HPGe) detector and MCA based data acquisition system.

The measured M/O ratios in titanium dioxide and manganese dioxide heat treated at different temperatures are shown in Fig.1. The precision of the measurements is better than 3%. Significant oxygen non-stoichiometry is observed in titanium dioxide and manganese dioxide at 673 K and 773 K respectively. Notably, the temperatures are considerably lower than those (e.g. 1000 K) employed elsewhere [2]. Results indicate a potential non-uniform distribution of oxygen vacancies in the powders. It can be probably alleviated by heat treatment for longer durations. The study shows that vacuum heat treatment can introduce oxygen vacancies in oxides while PIGE can be employed for the measurement of the ensuing oxygen non-stoichiometry.

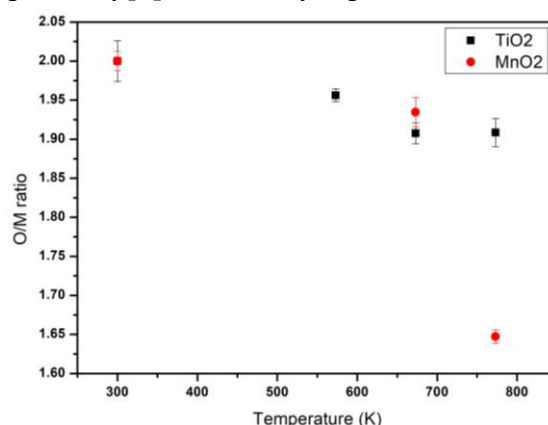


Fig. 1: O/M ratios of titanium dioxide and manganese dioxide heat treated at different temperatures.

References:

- [1] Y. Sunitha and Sanjiv Kumar, *J. Radioanal. Nucl. Chem.*, **314** (2017) 1803.
- [2] R.A. Bennett and N.D. McCavish, *Topics in Catalysis*, **36** (2005) 1–4.

Non-Destructive Evaluation of Accelerator Cathode Assembly

Anant Mitra^{1,§}, Dhruva Bhattacharjee^{2,3}, Lakshminarayana Y¹, Rajesh Acharya¹, S. Khader⁴,
Amitava Roy², Virendra Kumar^{3,4}, Umesh Kumar¹

¹Industrial Tomography & Instrumentation Section (ITIS), RC&IG, BARC, Mumbai, India

²Accelerator & Pulsed Power Division, BTDG, BARC, Mumbai, India

³Homi Bhabha National Institute (HBNI), Mumbai, India

⁴Radiation Technology Development Division (RTDD) BARC, Mumbai, India

§ Email: anantm@barc.gov.in

Electron beam accelerators (EBA) under the Department of Atomic Energy have diverse societal applications, including radiation sterilization of medical products, material modification for industry, and waste treatment. They also enhance food safety through irradiation, support healthcare in cancer treatment, and contribute to security via non-destructive testing and explosive detection. In EBA, accelerator cathode assembly is a critical component in high-energy particle accelerators, responsible for electron emission and beam generation. It typically consists of a lanthanum hexaboride (LaB₆) pellet, known for its high electron emissivity and thermal stability, housed within a vacuum-sealed structure. The assembly operates under extreme conditions, including high temperatures and strong electric fields, necessitating precise engineering to ensure reliability and performance.

This study presents a comprehensive non-destructive evaluation (NDE) of the accelerator cathode assembly using X-ray radiography and computed tomography (CT) scanning. These techniques enable the assessment of internal structural integrity, detection of potential defects such as cracks and voids, and precise dimensional analysis without causing any damage to the component. Although no physically defective sample was analyzed in this study, the applied NDE methodology has the capability to identify structural defects, contributing to quality assurance and reliability enhancement. However, functional defects, which require operational testing, remain beyond the scope of this evaluation. The findings are illustrated in the following figures: Figure 1 presents the cathode assembly, Figure 2 shows the X-ray radiograph highlighting internal features, and Figure 3 displays a CT slice offering cross-sectional details. This study highlights the effectiveness of non-destructive evaluation techniques in analyzing and replicating critical accelerator components.



Figure 1: Photograph of the cathode assembly.

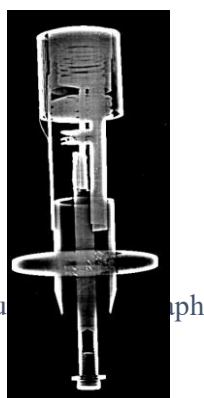


Figure 2: X-ray radiograph of the cathode assembly.

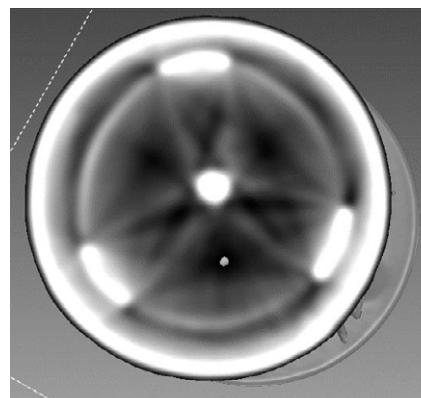


Figure 3: CT slice (Top view) of the cathode assembly.

References:

[1] Santanu Mondal et.al., *Open Ceramics*, **16** (2023), 100479.

Comparative Study of Air Borne Uranium Estimation using Radioanalytical and Chemical Methods

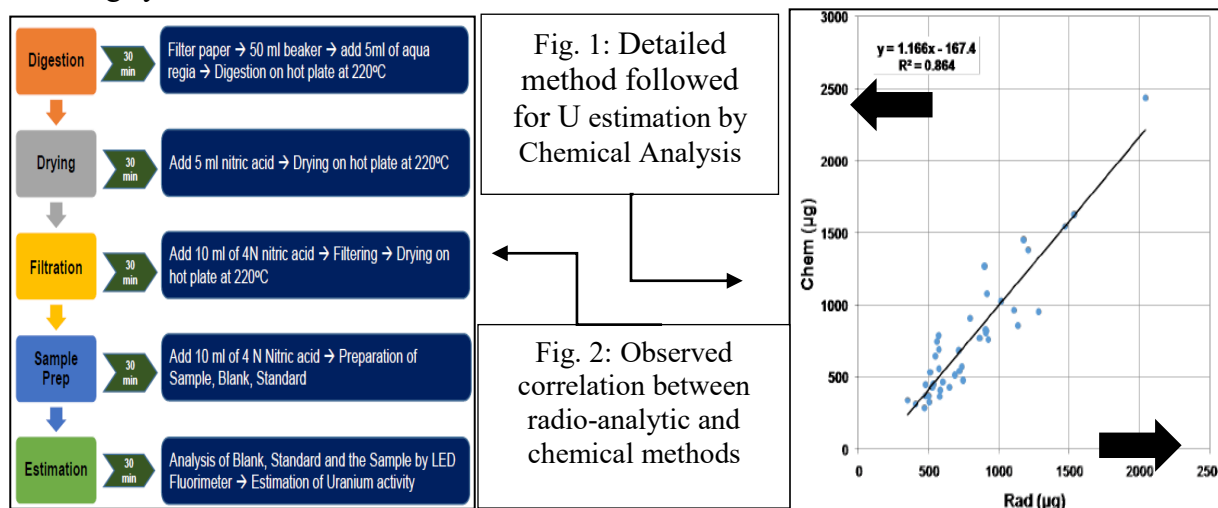
Nitin Kumari^{1,§}, Swaroopa Lakshmi², Amrit Pal Singh², K. Vishwa Prasad¹, Aditi C Patra¹, Probal Chaudhury¹, V.V.Mahesh Kumar², Komal Kapoor²

¹Bhabha Atomic Research Centre, Mumbai,

²Nuclear Fuel Complex, Hyderabad

§Email: nitkumari@barc.gov.in

Ambient air monitoring in all the powder handling areas of NFC is carried out by collecting the air samples on glass fibre filter papers and further counting the samples in ZnS(Ag) based Alpha counting system. The expected Air Activity can be calculated only 8 hours after sample collection. A new method based on filter paper digestion is used on experimental basis so that air activity can be estimated within 3 hours. Around 100 samples were collected from various areas of Oxide and Pelletizing plants by parallel sampling on 37 mm dia glass fibre filter for analysis by both radio analytical (existing) and chemical (developed) methods. In radioanalytical method, sample was counted after 4 hr, 8 hr and 5 day delay [1] for eliminating Radon and Thoron by using ZnS(Ag) based table top Alpha counting system.



For analysis by chemical method, samples were analysed using chemical method (Fig 1) and Uranium was estimated using LED Fluorometer. Sodium Pyro Phosphate solution was added to samples and pH was maintained at 7 for getting maximum fluorescence during estimation by LED Fluorometer. Resultant U content in the samples for both existing and developed methods were compared and 86% correlation has been found (Fig. 2). The 14 % non-correlation between both methods may be attributed to non-uniform deposition on filter paper, variation in operational parameters, residual Radon and Thoron progeny at the time of counting, inherent statistical spread, stray light interference etc. In conclusion, U analysis by chemical method is a quick and accurate technique requiring easy sample preparation, minimal effluent generation. Results indicate good correlation between existing and developed methods. Hence, this new method can be applied for any special/critical jobs in plants where in air borne U can be estimated quickly and plants can be informed for initiating timely corrective action thereby preventing exposure to operating personnel.

References:

[1] G. K. Srivastava, et al, *Radiation Protection Dosimetry*, **103** (2003) 371.

Simultaneous Determination of Uranium, Thorium and Plutonium in Nitric Acid Solution by K-edge Densitometry

M. Bootharajan¹, R. Gangadevi¹, B. Sreenivasulu^{1,2,§},
K. Sundararajan^{1,2}, C.V.S. Brahmananda Rao^{1,2}

¹Materials Chemistry and Metal Fuel Cycle Group, IGCAR, Kalpakkam-603102

²Homi Bhabha National Institute, IGCAR, Kalpakkam – 603102

§E-mail: bsrinu@igcar.gov.in

The Advanced Heavy Water Reactor (AHWR), which uses (Th, Pu)O₂ as fuel, is first of its kind to facilitate the early use of thorium for power generation[1]. Spent fuel from the AHWR is anticipated to contain approximately 2 to 4% fissile materials, including ²³³U and plutonium. The dissolver solution of AHWR will contain U, Pu and Th in nitric acid medium along with fission products (FPs). U and Pu can be estimated by potentiometry; whereas it cannot be employed for the estimation of Th due to its mono valency. K-edge densitometry (KED), non-consumptive technique was examined for the determination of high concentrations of uranium, thorium and plutonium in acidic solutions. In our laboratory, a hybrid KED system has been indigenously designed, developed, and installed within a glove box facility for the assay of uranium and plutonium [2]. The HKED method was calibrated and validated using a range of uranium (17–58 mg/mL) and plutonium (0.75–20 mg/mL) solutions, and results compared to the potentiometric method. In the current study, the HKED technique was applied to determine the concentrations of U, Pu and Th in simulated solutions.

In this context a stock solution containing Th, U and Pu about 73.8 ± 0.73 , 84.8 ± 0.42 and 22.4 ± 0.11 g/L, respectively were prepared in nitric acid medium. The concentration of Th, U and Pu in this stock solution was determined by HKED technique. Figure. 1 shows the typical KED spectrum of blank and Th, U and Pu in nitric acid solution. For each measurement by HKED, 5 mL of the stock solution containing Th, U and Pu in nitric acid was placed in a polypropylene vial. $\Delta\mu_k$ of U and Pu was determined for the existing geometry of the KED using standard Th, U and Pu solutions. Using these $\Delta\mu_k$ values, the concentrations of U and Pu in the MOX solutions were calculated,

and the results were compared with those obtained through potentiometric measurements for U and Pu and complexometry for Th. The concentration of Th, U and Pu determined by HKED was found to be about 73.03 ± 0.79 , 83.03 ± 0.94 and 22.90 ± 0.52 g/L, respectively with precision <1%. These results were found to be in good agreement with results obtained by potentiometry and complexometry values. This study indicates that HKED technique can be routinely employed for the simultaneous determination of actinides in HNO₃ solutions in presence of FPs without any radioactive waste generation.

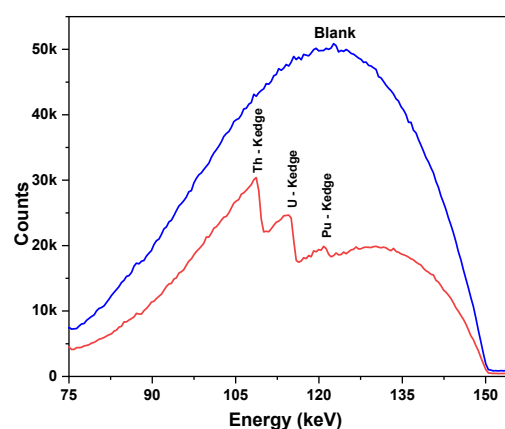


Fig. 1: Typical a) KED spectrum of Th, U and Pu in nitric acid solution b) blank

References:

- [1] P. S. Dhami et al., *Sep. Sci. Tech.* **45** (2010) 1147.
- [2] M. Bootharajan et al., *J. Radioanal. Nucl. Chem.* **324** (2020) 623.

Non-Destructive EDXRF Analysis of LaMnO₃-BaTiO₃ Multi-Functional Oxide Powders: Addressing the Spectral Overlaps

T.A. Chavan^{1,2}, P.S. Remya Devi^{1,2}, K.K. Swain^{1,2,§}

¹Analytical Chemistry Division, Bhabha Atomic Research Centre, Trombay, Mumbai, India

²Homi Bhabha National Institute, Anushakti nagar, Mumbai, India

§Email: kallola@barc.gov.in

LaMnO₃-BaTiO₃ composites are a class of multi-functional perovskites, which find immense applications as electrostatic energy storage materials, sensors, fuel cells and memory devices, owing to their high dielectric constants and saturation polarization [1]. To achieve these functionalities, fine-tuning the synthesis steps, along with compositional assessment at each stage, is inevitable [1]. Non-destructive, solid sample analysis is the need of the hour for such applications, where the samples are precious and / or refractory. In the present studies, LaMnO₃-BaTiO₃ composite powders were prepared via the well-established solid-state synthesis route, wherein all the four precursors: La₂O₃, MnCO₃, BaCO₃, TiO₂ were thoroughly mixed in various proportions and heated at 1200 °C - the optimized temperature, for 24 h. The composition of all the synthesized composites was determined using non-destructive energy dispersive X-ray fluorescence (EDXRF) spectrometry by Standard Less Fundamental Parameter (SLFP) mode. As is visible in the EDXRF spectrum (Fig. 1 and inset table), all 3 peaks: Ti-K_α, Ba-L_α and La-L_α are unresolvable. Even though La-L_β is well-separated, the Ti-K_β and Ba-L_β are overlapping. The energy resolution of silicon drift detector in EDXRF is 0.13 keV [2]. The direct spectral overlap was the major bottleneck, to obtain accurate analytical data. For addressing the severe overlap of La, Ba and Ti X-rays, various intensity corrections methods, namely: gross, net, digital filter and Gaussian fit, were adopted on synthetic standard composite, during the standard-less fundamental parameter approach of EDXRF [2, 3]. The % error in each method was assessed by comparing the measured and actual compositions. From % error values, it could be concluded that ‘digital filter’ is appropriate for quantification of MnO₂ in synthesized composite. Gaussian fit is appropriate for quantification of Ti, Ba and La oxides, where the spectral overlaps are significant. Table 1 shows the results of analysis on these composites. In the absence of reference materials, neutron activation analysis (NAA) was used as the reference technique for validation. Indistinguishability of NAA and EDXRF results for the composite was ascertained via t-test.

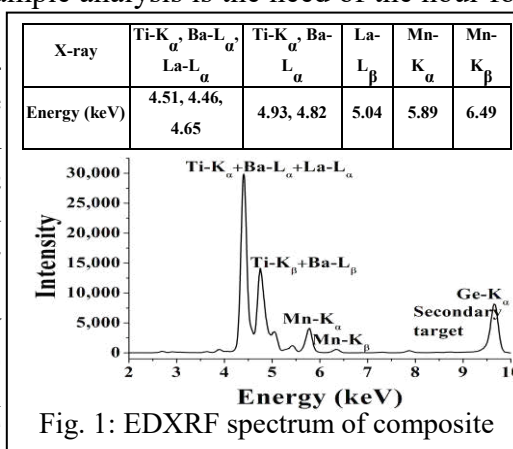


Fig. 1: EDXRF spectrum of composite

Table 1: Composition of the syn. LaMnO₃-BaTiO₃

ID	La ₂ O ₃ (%)	BaO (%)	MnO ₂ (%)	TiO ₂ (%)
1	3.04 ± 0.05	73.2 ± 1.6	1.22 ± 0.03	23.3 ± 0.1
2	13.3 ± 0.3	57.1 ± 1.1	6.12 ± 0.30	23.4 ± 0.9
3	35.5 ± 0.2	37.4 ± 0.2	17.6 ± 0.1	9.54 ± 0.11

Authors acknowledge the contributions of Dr. V.G. Gupta, Chemistry Division, BARC, and her doctoral student Ms. Jyoti Chahal, during the solid-state syntheses.

References

- [1] I.V. Lisnevskaya, et. al., *Int. J. Appl. Ceramic Technol.*, **13** (2016) 1125.
- [2] Operation manual, EX-3600/6600 spectrometers, Rev. **2.0**, Jordan Valley, Israel (2000).
- [3] P.S. Remya Devi, T.A. Chavan, K.K. Swain, *J. Anal. At. Spectrom.*, **37** (2022) 641.

Estimation of ^{227}Ac Activity in Lanthanum Samples using Gamma Spectrometry

Amar D. Pant^{1§}, Ritesh Ruhela², Anilkumar S. Pillai¹

¹Environmental Monitoring and Assessment Division, BARC, Mumbai, India

²Material Processing & Corrosion Engineering Division, BARC, Mumbai, India

§Email: amarp@barc.gov.in

Rare-earth elements (REE) form a range of alloys and compounds that have found broad and diverse applications in technology such as magnets, ceramics, electronics, chemical, optical, medical and nuclear. An issue frequently associated with REE production is presence of natural radioactivity associated with the rare earth minerals [1]. Trace level of actinium (^{227}Ac) impurity is found to be present in REE chloride samples, may be because of close similarity of physical and chemical properties of Ac and La, which pose a challenge in separation. ^{227}Ac is a beta emitter with a half-life of 21.8 years and due to its very low-intensity gamma lines it cannot be measured directly using gamma spectrometry. Therefore, the activity concentration of ^{227}Ac is estimated through its daughter product ^{227}Th using high resolution gamma ray spectrometry system [2]. The time required to attain the radioactive equilibrium between ^{227}Ac and ^{227}Th is three and a half months after the sample preparation. In the present work, the activity concentration of ^{227}Ac were analysed in LaCl_3 aqueous samples. Gamma spectrometry measurement was carried out using 60% HPGe detector coupled with 8K MCA system with an energy resolution of 1.9 at 1332 keV ^{60}Co . The efficiency calibration was carried out using standard ^{133}Ba and ^{152}Eu liquid sources in 20mL plastic vial geometry. The activity concentration of ^{227}Th was measured in different interval of time to ensure the radioactive equilibrium between ^{227}Ac and ^{227}Th is achieved. The activity build-up of ^{227}Th in sample is shown in figure 1. The gamma spectrum of lanthanum bearing sample is shown in figure 2. The gamma spectrum shows the presence of daughter products of ^{227}Ac i.e. ^{227}Th (235.96 keV), ^{223}Ra , ^{219}Rn , ^{211}Pb and ^{211}Bi radioisotopes and also the gamma lines of ^{138}La . The activity concentration of ^{227}Ac in the sample which is in radioactive equilibrium with ^{227}Th was found 0.9 ± 0.1 Bq/mL. The methodology and results presented here is useful for the measurement of low-level α active impurity of ^{227}Ac in the REE samples.

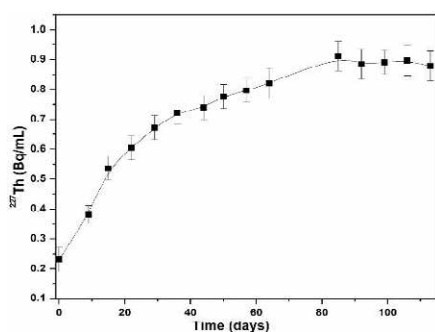


Fig. 1: Activity build-up of ^{227}Th with time.

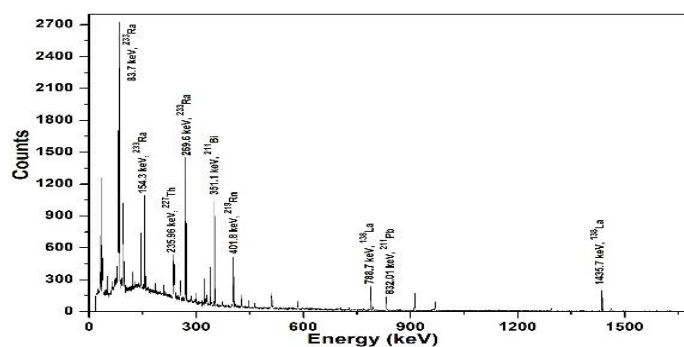


Fig. 2: Gamma spectrum of sample

References:

- [1] Pillai, P. M. B. et. al., *In National Symposium on Environment*, (2004), 178.
- [2] Marouli M. et. al., *Applied Radiation and Isotope*, **144** (2019) 34.

Occurrence of Trace Metals in Popularly Consuming Fruits and their Health Risk Assessment

Sugandhi Suresh^{1,§}, Harshali S Suryavanshi², Mahesh Tiwari^{1,3}, Vandana A Pulhani^{1,3}

¹Environmental Monitoring and Assessment Division, Bhabha Atomic Research Centre, India,

²The Institute of Science, Mumbai, India,

³Homi Bhabha National Institute, India- 400094

[§]Email: sugandhi@barc.gov.in

The major global public health concern in the present era is food security, as food may get contaminated via water, air, dust, microbial, chemical, pesticides, industrial effluents sources etc. A major quantity of essential nutrients and vitamins required for good human health are derived from fruits. Six numbers each of pome (apple, pear), berry (guava, orange) and stone (papaya, sapodilla) fruits were purchased from local fruit markets (Byculla and Dadar) at Mumbai. The edible (flesh), non-edible parts of the fruits were separated and the edible portion were taken up for analysis of trace elements (TEs). These flesh parts were oven dried at 60°C for 48 hours and ground to fine powder. The pellets were made by homogenization of the powder with cellulose and analysed for the concentration of TEs such as Mn, Fe, Cu, Ni, Zn, using Energy Dispersive X-ray Fluorescence. The Oriental Basma Tobacco leaves (certified reference material) was used for calibration and quality check. The health risk to humans was computed via indices like Estimated Daily Intake (EDI), Hazard Quotient (HQ) and Hazard Index (HI) using the following equations and the results are tabulated (Table 1).

$$\boxed{\text{EDI} = (C_m \times D_i \times C_f) / B_w} \quad \boxed{\text{HQ} = \text{EDI} / \text{RfD}} \quad \boxed{\text{HI} = \sum_{n=1}^i \text{HQ}_n; n = 1, 2, 3, \dots, n}$$

Where, C_m = Metal concentration (mg/kg); D_i = Daily intake (0.1kg/d) [1]; C_f = Fresh to dry weight conversion factor (0.085) for fruit; B_w = 70 kg [2]; RfD = Oral reference dose [3]

Table 1. Health risk estimate to humans from various types of fruits

Trace element	Pome			Berry			Stone		
	Conc. (mg/kg)	EDI (mg/kg/d)	HQ	Conc. (mg/kg)	EDI (mg/kg/d)	HQ	Conc. (mg/kg)	EDI (mg/kg/d)	HQ
Mn	22.8	0.003	0.02	21.1	0.003	0.02	73.0	0.01	0.06
Fe	168	0.02	0.02	360	0.05	0.05	536	0.07	0.09
Cu	11.1	0.001	0.03	10.9	0.001	0.03	12.8	0.002	0.04
Ni	11.1	0.001	0.07	10.7	0.001	0.06	11.4	0.001	0.07
Zn	13.0	0.002	0.01	11.9	0.001	0.01	20.0	0.002	0.01
HI			0.2			0.2			0.3

The Table 1 gives the concentration and the health risk indices with a standard deviation of 3-5%. It is observed that Fe concentration is higher than the other studied TEs in fruits. While, the concentration of other elements are of similar range except Mn in stone fruits, the EDIs in pome, berry and stone fruits are lower than the permissible limit of daily dietary intake (mg/d) for each metal (Mn: 4.1; Fe: 15; Cu: 2.5; Ni: 0.1; Zn: 15) [4]. The HQs in pome, berry and stone fruits are found to be less than unity, indicating no serious health risk to humans via ingestion pathway, which is further supported by the observed HI being < 1. Thus, the pome, berry and stone fruits are safe to consume with respect to TEs.

References

- [1] ICMR-NIN Expert Committee, Dietary Guidelines for Indians-2024.
- [2] US Environmental Protection Agency Exp Factors Handbook (2011) EPA/600/R-09/052F.
- [3] Regional Screening Level Summary Table (TR = 1E-06, HQ = 1), 2019; USEPA2019
- [4] A.M.Basha et al., Toxicology Reports (2014) 505-512.

Plutonium Estimation using Functionalized Nuclear Track Detector

Amol Mhatre[§], Chhavi Agarwal, R. Tripathi

Radiochemistry Division, Bhabha Atomic Research Centre, Trombay, Mumbai – 400 085

[§]E-mail: amolm@barc.gov.in

Solid state nuclear track detectors (SSNTDs) are one of the most sensitive detectors for detecting energetic heavy charged particles such as alpha and fission fragments. However, these detectors lack chemical selectivity, limiting their ability to distinguish between different radionuclides. Thus, to enhance their utility for selective detection in the presence of other radionuclides, it is necessary to impart chemical selectivity to SSNTDs [1, 2]. In this study, an attempt has been made to impart chemical selectivity to CR-39SSNTDs for the selective extraction of Pu(IV) ions. A thin polymer film of bis[2-(methacryloyloxy) ethyl]phosphate was anchored onto the surface of the CR-39 detector using UV-induced graft polymerization. The uptake of Pu at 2 mol.L⁻¹ HNO₃ by these modified CR-39 substrates was studied using PMT based scintillation counting with a polystyrene film. The Pu uptake in these substrates were observed to be 21%, which may be due to the hydrophobic nature of the CR-39 detector. An attempt to improve the hydrophilicity of the CR-39 sheet was made by exposing it to ozone for two time durations, 15 min and 1 hour. The Pu uptake was subsequently studied for these ozone-exposed samples along with the effect of varying monomer concentration. While there was no significant increase in Pu uptake on ozone exposure of 15 mins, however 1 hr exposure led to an increase in uptake to 52%. The Pu uptake was observed to significantly increase to ~ 85% on doubling the BMEP concentration. Alpha tracks were registered from the Pu-loaded poly(BMEP)-grafted sample at three different Pu activity levels (37, 88, and 161 Bq) in contact with the CR-39 detector. After exposure for a fixed time period, the exposed CR-39 detectors were chemically etched with 6 mol L⁻¹ NaOH at 70°C for 4 hours and examined under an optical microscope. Figure 1 shows the alpha track distribution of the CR-39 samples with different Pu activities. The observed alpha track density showed a linear correlation with Pu activity, confirming the effectiveness of the modified SSNTDs for selective Pu detection. These results demonstrate that the surface modification of CR-39 with suitable functional moieties can be a viable approach towards chemically selective SSNTDs.

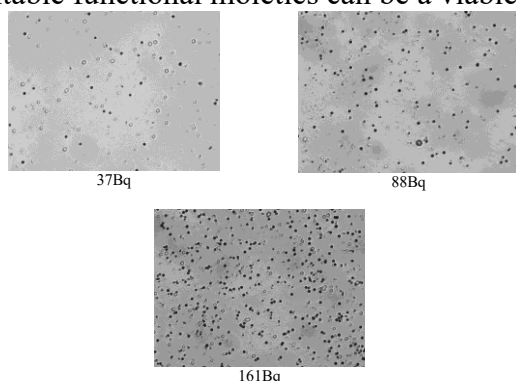


Fig. 1: Alpha tracks distribution at 40X magnifications using CR-39 detector exposed to Pu of different activities.

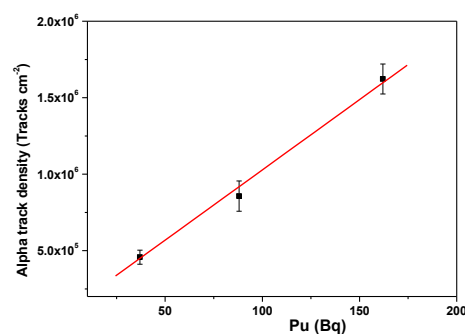


Fig. 2: Alpha track density (Tracks cm⁻²) as function of Pu activity (Bq) of the Pu loaded CR-39 Substrates.

References:

- [1] A.M.Mhatre, et al., *J Radioanal Nucl Chem*, **314** (2017)187.
- [2] A.M. Mhatre, et al, *J Anal At Spectrom*, **32** (2017) 1566.

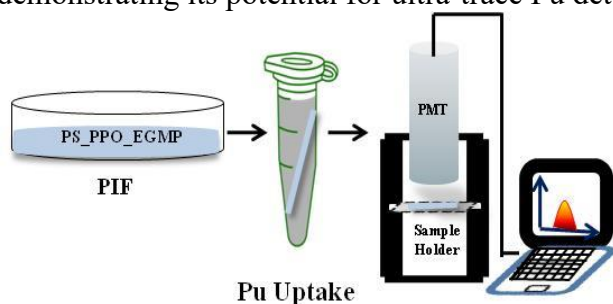
Development of Scintillating Phosphate Based Polystyrene Polymer Inclusion Films (PIFs) for Ultra-Trace Detection of Pu

Amol Mhatre[§], Chhavi Agarwal, R. Tripathi

Radiochemistry Division, Bhabha Atomic Research Centre, Mumbai – 400 085

[§]E-mail: amolm@barc.gov.in

Ultra-trace detection of plutonium (Pu) requires efficient pre-concentration methods, particularly for large-volume samples. In our earlier studies, Polystyrene (PS) based scintillation sensor was developed for the ultra-trace detection of Pu upto few mBq [1, 2]. However, the Pu adsorption capacity and the extraction efficiency in voluminous samples was found to be limited. This may be due to the availability of limited phosphate sites on the polymer substrate as the functional moieties were confined to the surface of the polymer. To address this limitation, an attempt was made to synthesize polystyrene based polymer inclusion film (PIF) with embedded fluor (PPO), phosphate moieties bis(2-(methacryloyloxy)ethyl) phosphate (BMEP). The prepared PIFs were also surface grafted with the same phosphate moieties (Scheme 1). The Pu uptake studies confirmed that both bulk and surface phosphate moieties were accessible for Pu in solution. However, the resulting PIF was found to be brittle and difficult to handle. This may be due to extensive crosslinking of the BMEP present in the bulk PIF matrix. In order to overcome this problem, the possibility to replace BMEP with another monomer having phosphate moieties i.e. ethyl glycol methacrylate phosphate (EGMP) was explored. The composition of EGMP-based PIFs was optimized for different monomer concentrations in both the bulk PS matrix and surface grafting. The newly developed PIFs were flexible and easy to handle. The Pu uptake studies were conducted using Pu activities of ~45 Bq and ~2500 Bq. For all EGMP compositions, Pu uptake at lower activity (45 Bq) was found to be remarkably high (~80%). A constant extraction efficiency at both activity levels could be achieved for the PIF with bulk EGMP amount as 0.08 g and 0.8 M EGMP as grafting monomer composition, which is crucial for accurate Pu quantification. Additionally, the effectiveness of the PIF for Pu pre-concentration from varying sample volumes (1–10 mL) was evaluated (Fig 1). The extraction efficiency remained stable across this volume range but significantly decreased at 20 mL. Furthermore, the substrate successfully extracted Pu at ultra-trace levels (4 mBq/mL) from a 5 mL solution, demonstrating its potential for ultra-trace Pu detection in large-volume environmental samples.



Scheme 1. Pu Uptake in polymer inclusion films (PIFs)

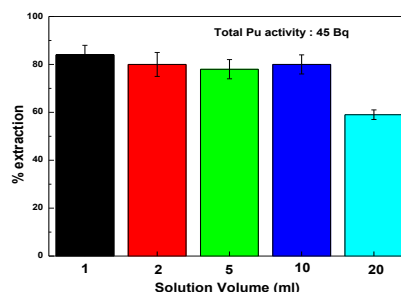


Fig. 1. Pu uptake in diff. sample volumes

References:

- [1] A. Mhatre, C. Agarwal, R. Tripathi, SESTEC-2024 Proceedings, 225.
- [2] A. Mhatre, C. Agarwal, R. Tripathi, ISMC-2024 Proceedings, MS-K-136.

Exploring Gamma Peak Identification for Sb, Eu, Co, and Zr in Cs Rich Condition: Challenges and Breakthroughs

Gopal Sharma¹, Chanchal Solanki ¹, Kankan Patra¹, V.K.Mittal¹,
Anoop Kelkar¹, D.B.Sathe¹, R.B.Bhatt¹

¹Nuclear Recycle Board, Bhabha Atomic Research Centre, Tarapur-401504, India

Email: kpatra@barc.gov.in

The nuclear industry is crucial for energy production, medical applications, and research, playing a key role in meeting global energy demands while reducing carbon emissions. However, managing radioactive waste, especially high-level liquid waste (HLW), remains a significant challenge. Gamma spectroscopy, using a Multi-Channel Analyzer (MCA), is essential for accurately identifying and quantifying radioactive isotopes in waste, enabling effective waste management. In MCA HPGe detector is used, the efficiency is 5.41×10^{-3} (peak efficiency) with respect to the 662 KeV. The resolution of the detector is ≤ 1.90 KeV FWHM at 1332 KeV, its diameter is 64.8 mm and length is 65.3mm. It is kept at a distance of 4.6 mm from the Al window (1.50 mm thick). This technology provides precise data that supports safe disposal, reduces environmental impact, and ensures compliance with safety standards. In this present study we have obtained ²⁴¹Am, ¹²⁵Sb, ¹⁵⁴Eu, ¹⁵⁵Eu ⁶⁰Co, ⁹⁵Zr peaks in presence of high concentration of Cs, which is real time critical challenges. Table 1 indicates the result before and after Ammonium molybdophosphate (AMP) resin pass solution of HLW. First the sample was passed through AMP resin to remove the Cs and then the spectrum for other radionuclides was studied. Identifying gamma peaks for these radionuclides using HPGe detector is critical for waste management. The primary challenge lies in the separation of ¹³⁷Cs. We have separated Cs using AMP resin, which often dominates and distorts smaller peaks from other radionuclides. Fig.1.a showed the only ¹³⁷Cs peaks which is before AMP pass, however after AMP pass, we have clearly obtained ²⁴¹Am, ¹²⁵Sb, ¹⁵⁴Eu, ¹⁵⁵Eu ⁶⁰Co, ⁹⁵Zr (Fig. 1(b)). By using this method, the primary challenges for identifying ²⁴¹Am, ¹²⁵Sb, ¹⁵⁴Eu, ¹⁵⁵Eu ⁶⁰Co, ⁹⁵Zr these isotopic peaks in HLW were overcome.

Table.1 Analysis result of HLW samples before and after AMP resin pass.

Sample	Gross α (Ci/L)	Gross β (Ci/L)	¹³⁷ Cs (Ci/L)	²⁴¹ Am (Ci/L)	¹²⁵ Sb (mCi/L)	¹⁵⁴ Eu (mCi/L)	¹⁵⁵ Eu (mCi/L)	⁶⁰ Co (mCi/L)	⁹⁵ Zr (mCi/L)
HLW Con before	2.72	169.82	50.80	2.01	--	--	--	--	--
HLW Con, after	--	--	365($\times 10^{-3}$)	2.69	59	765	289	3.42	94
Alpha spectrometer	--	--	--	2.09	--	--	--	--	--

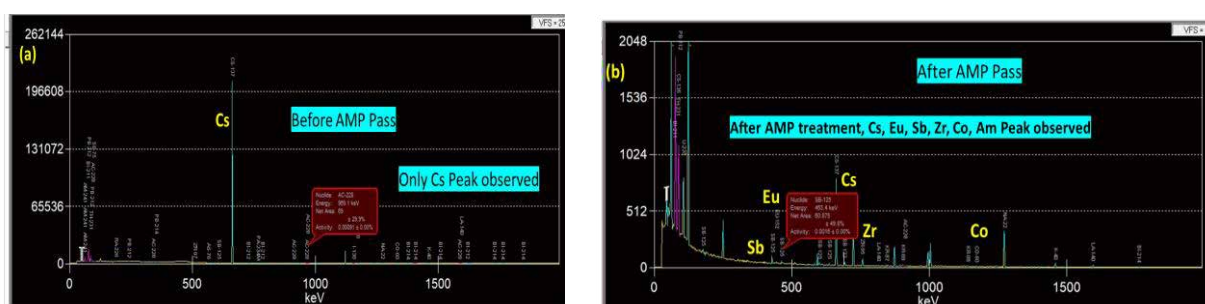


Fig. 1 (a) Gamma spectrometry before AMP pass, (b) after AMP resin pass
The authors acknowledge lab staff, FF, INRPO, BARC, Tarapur for their support.

References:

[1] D. F. Covell et.al., *Anal. Chem.* 131 (1959) 1785.

Determination of Boron Concentration and its Isotopic Composition (IC) in BORAL by PIGE

Purbali Das¹, Sudeep Kumar Samanta^{1,2}, Suparna Sodaye^{1,2,§}

¹Radiochemistry Division, Bhabha Atomic Research Centre, Mumbai – 400085

²Homi Bhabha National Institute, DAE, Anushaktinagar, Mumbai – 400094

§ Email: suparna@barc.gov.in,

Boron is used as neutron shielding due to its high thermal neutron absorption cross section, owing to $^{10}\text{B} (n, \alpha)^7\text{Li}$ (3837 barn). Boral is a promising neutron shielding material for nuclear reactors. Total B concentration and isotopic composition (IC) of ^{10}B are essential requirements for CQC (Chemical Quality Control) of finished product.

Boral has a complex matrix. Conventional wet-chemical analysis methods involve vigorous chemical treatment of dissolving the sample, which may lead to losses that needs to be accounted for. This may lead to added uncertainties in the measurements.

The developed external Particle Induced Gamma Ray Emission (PIGE) method for simultaneous IC and total concentration determination of B is advantageous as it is simple, rapid, non-destructive with minimal sample preparation and can be used for non-standard geometry samples.

At 6MV Folded Tandem Ion Accelerator (FOTIA), BARC using Prompt Gamma from nuclear reactions: $^{10}\text{B}(p,\alpha\gamma)^7\text{Be}$, $E_\gamma=429$ keV; $^{10}\text{B}(p,p'\gamma)^{10}\text{B}$, $E_\gamma=718$ keV; $^{11}\text{B}(p,p'\gamma)^{11}\text{B}$, $E_\gamma=2125$ keV were measured using ~40% relative efficiency HPGe placed at 45° to beam direction with fixed sample to detector geometry. 135 keV and 165 keV peaks of $^{181}\text{Ta}(p,p'\gamma)^{181}\text{Ta}$, from Ta window material were used as ex-situ beam current normalizer. To minimize matrix effects, synthetic standards were prepared by homogeneously mixing different concentrations of elemental boron powder with natural isotopic composition in pure aluminium powder. Direct “as received” sample chip of 1cm x 1cm were mounted in Mylar foil and irradiated for 15-30 min with $E_{\text{proton}}\sim 3.5$ MeV, $I\sim 12$ nA, $\phi\sim 3$ mm. Fig 1 is a typical PIGE spectrum of BORAL and table 1 gives the total concentration of B and its IC in BORAL as estimated.

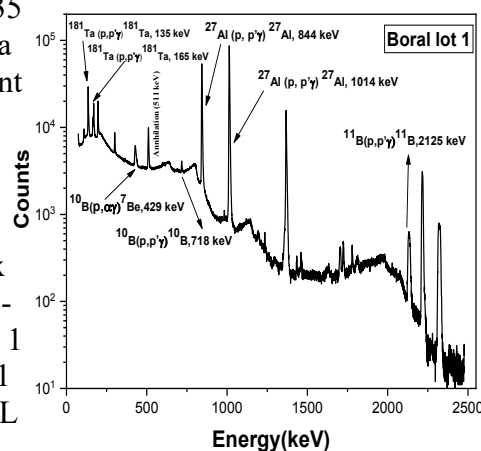


Fig. 1. PIGE spectrum of BORAL sample

Table 1. Determined values of B in BORAL

Sample	Standard	Determined Total B (wt.%) (using 429 keV)	Determined IC of B (^{10}B atom %) (using 429 keV)
Boral	Elemental B powder in Al powder	4.2 ± 0.5	20.2 ± 0.3

Authors thank Director, BARC Associate Director, RC&IG; Dr. S Jeyakumar, Head, RCD & Head, IADD for their encouragement, NPCIL for providing samples, members of FOTIA, members of electronics section for their assistance, Head, IRAD; Smt. Sonika Gupta, Smt. Priya V Mestry, Shri M G Desai & Shri R A Gaikwad for their support.

References

- [1] Sk Wasim Raja et al., *Analytica Chimica Acta*, 1202 (2022) 339686.
- [2] S K Samanta et al., *J. Radioanal. Nucl. Chem.*, 325 (2020) 923.

Polyoxometalate (POM) based Composite Material for the Determination of Americium in Synthetic Urine Samples

Suja A. Kumar^{1,3,§}, B. Mahanty^{2,3}, A. Bhattacharyya^{2,3}, P.D. Sawant¹

¹Radiation Safety Systems Division, BARC, Trombay

²Radio Chemistry Division, BARC, Trombay

³Homi Bhabha National Institute, Anushaktinagar, Mumbai-400 094, India

§Email: sujas@barc.gov.in

The detection and quantification of actinides in biological samples is crucial for assessing internal radiation exposure. However, the complex matrix of urine samples poses significant challenges for actinide analysis. This study reports the development of a Polyoxometalate (POM) based composite material for the determination of Am in synthetic urine samples. Diglycolamide, and multiple diglycolamide based ligands are generally used for the extraction of trivalent actinide and lanthanide ions [1]. The advantage of using POM is that they can be synthesized easily, with tuneable properties and showed high affinity for metal ion by lacunary POMs. Phosphotungstate based POM composite material exhibits high affinity towards Am, enabling efficient extraction and pre-concentration. A composite POM was developed and it was characterized using different techniques, like FTIR, NMR, SEM, photoluminescence. The K_d value for Am(III) at pH 6 was found to be very high ($\sim 4 \times 10^5$) in buffer medium [2]. At this pH, the used POM becomes a lacunary POM (PW₁₁) which has unsaturated oxo anions which can efficiently complex with Am(III). The loaded Am(III) was stripped using N-(2-Hydroxyethyl)ethylenediamine-N,N,N'-triacetic acid (HEDTA) (0.5 M) which indicated more than 95% stripping of Am(III) (Table 1). The reusability of the composite POM was tested by continuous uptake of Am(III) tracer which indicated the composite POM could uptake Am(III) quantitatively for seven repetitive experiments (Fig. 1). Finally, the composite POM was employed for Am(III) determination in synthetic urine sample [3]. The pH of the synthetic urine was adjusted to 6.0 (to simulate the condition of actual urine) by adding ammonia solution. A known amount of Am (~ 10000 cps/mL) was added into 2 mL of the synthetic urine sample in which 25 mg of the composite POM was also added. This was shaken for 2h in a thermo stated water bath. After 2 hrs, it was removed and centrifuged. The supernatant showed absence of Am which was quantitatively transferred to the composite POM. This innovative approach can offer a promising solution for the determination of Am in complex biological matrices, paving the way for improved radiation exposure assessment and nuclear safety monitoring.

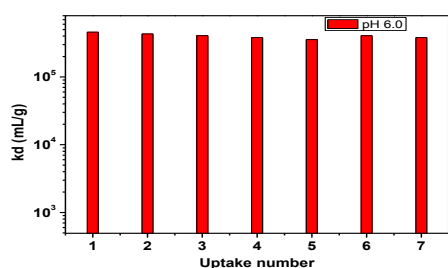


Fig. 1: Regular uptake of Am(III)

Stripping agent	% Stripping
1 M α -HIBA	0.01
0.01M EDTA	1
0.001M BTP	1
pH2	2
0.5 M Oxalic acid	40
0.5 M HEDTA	96

Table 1: Stripping of Am(III) from composite

References:

- [1] S. Ansari et al., *Chemical reviews*, **112**, 3, (2012)1751.
 [2] Suja A. Kumar et al., *SESTEC* 2024, 66.
 [3] ANSIN13.30: 2011, (R2017).

Determination of U²³⁵ Content in UO₂ Pellet by Gamma Ray Spectrometer with HPGe Detector using Enrichment Meter Principle

Vinod.K. Ray, U.B.Misra, Y. Balaji Rao[§]

Control Lab, Nuclear Fuel Complex, ECIL (PO), Hyderabad-500062

[§] E-mail: ybrclabnfc@gmail.com

Nuclear Fuel Complex (NFC) is responsible for manufacturing and supply of fuel sub-assemblies for all the operating nuclear power reactors in India. Heat Treated Uranium Peroxide (HTUP), Sodium Di-Uranate (SDU) and Uranium Ore Concentrate (UOC) are the raw materials used for producing UO₂ pellets as fuel by following well established chemical and mechanical processes. Measurement of U-235 content in UO₂ pellet is essential for qualifying them for intended applications.

Thermal ionization mass spectrometer (TIMS) [1] and alpha-spectrometry [2] are cited in the literature for this purpose. However, both the techniques are not preferred choices for an industrial lab with high analytical load as they involve elaborate sample preparation before measurements.

In view of the above, a simple and non-destructive gamma ray spectrometric (GRS) method has been developed for the measurement of ²³⁵U isotopic content using enrichment meter principle. The infinite thickness property of UO₂ pellet has been exploited in the present work. The developed method does not require any sample preparation and therefore makes the method non-destructive. A planar type high purity germanium (HPGe) detector has been used for spectra acquisition and 185.7 keV gamma ray emitted by ²³⁵U has been used for measurement of isotopic content in the present work.

Samples with ²³⁵U content from 0.7 to 2.6 % are taken for the measurements. The results obtained using GRS-HPGe are compared with TIMS and they are found to be in good agreement. The development of GRS-HPGe method has resulted in decrease of analysis time and analytical waste generation. The results of few typical samples are given below in Table 1.

Table 1: Analysis results of U-235 content using GRS-HPGe

S. NO	U-235 (wt %)	
	GRS-HPGe	TIMS
1	0.717 ± 0.005	0.714
3	2.094 ± 0.008	2.102
4	2.659 ± 0.010	2.662

References:

- [1] O. Pereira de Oliveira, W. De Bolle, S. Richter, A. Alonso, H. Kuhn, J.E.S. Sarkis, R. Wellum, *International Journal of Mass Spectrometry*, **246** (2005) 35.
- [2] A. Martin Sanchez, F. Vera Tome, J. Diaz Bejarano, M. Jurado Vargas, *Nuclear Instruments and Methods in Physics research*, **A313** (1992) 219.

N-13 Ammonia Production in Standard Niobium Target used for F-18 Production: Radiosynthesis and Quality Control

S.K. Nandy^{1,§}, A. Gopalkrishna², S. Chinnaessaki³, S.P. Kulkarni¹, N.S. Baghel¹

¹Radiation Medicine Centre (G), BARC, Mumbai

²Medical Cyclotron Facility, BRIT, Mumbai

³Low Level Counting Lab, BARC, HPD, BARC, Mumbai

[§]Email: saikatnandy1976@gmail.com

$^{13}\text{NH}_3$ is one of the oldest FDA approved PET radiopharmaceutical for evaluation of myocardial perfusion for clinical assessment of cardiac disorders [1]. In recent years, large scale on target production of $^{13}\text{NH}_3$ using ethanol containing water as target via $^{16}\text{O}(\text{p}, \alpha)^{13}\text{N}$ reaction and conversion of $^{13}\text{NO}_x$ to $^{13}\text{NH}_4^+$ through EtOH catalysis is reported in abroad as well as INDIA. We have explored the feasibility of $^{13}\text{NH}_3$ production in standard niobium target (Nb25) used for regular F-18 production. The brief procedure is as follows: STEP-I: Cyclotron irradiation (proton beam) of ethanol containing water to produce $^{13}\text{NH}_4^+$ STEP-II: Delivery of $^{13}\text{NH}_4^+$ along with target water to HOT CELL STEP-III: Trapping of $^{13}\text{NH}_4^+$ in pre conditioned CM cartridge. STEP-IV: Elution with physiological saline and collection in sterile, BET free vials through 0.22μ filters. The procedure is fully automated and total synthesis and QC time is 10 min. The whole procedure is carried out after obtaining regulatory permission. $^{13}\text{NH}_3$ is clear, colourless, free of any suspended particle, BET free and sterile. Radiochemical purity is $> 95\%$ (Fig.1). Half Life ($t_{1/2}$) is 10.39 ± 0.21 (n = 12) (Fig.2) confirming the formation of $^{13}\text{NH}_3$. HAVAR foil activated radio nuclidic impurities were determined by HPGe and Monte Carlo simulation and found to be in the range of few KBq - Bq. Following regulatory guidelines, we have maximum produced 106 mCi (~ 4 GBq) of $^{13}\text{NH}_3$ (without decay correction) using 10nM ethanol containing water as target for 30 min cyclotron irradiation with a beam current of $35\mu\text{A}$.

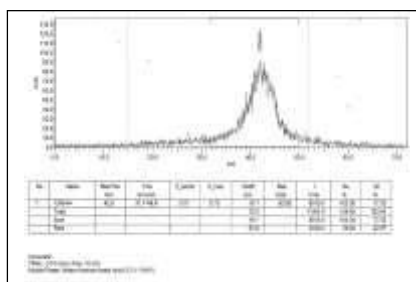


Fig. 1. Radio TLC of $^{13}\text{NH}_3$ in Water: Acetone: Acetic Acid 3:2:1 (V/V/V). R_f : 0.7

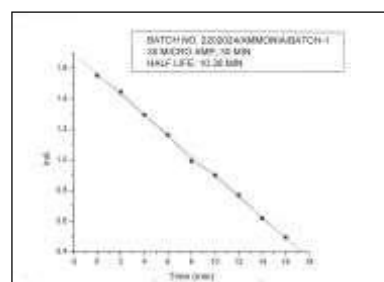


Fig.2: Half Life of $^{13}\text{NH}_3$: 10.38 min

Acknowledgements: The authors acknowledge the dedicated supports of all the staff members of RHCUC, RMC. Keen interest and support from retired Division Heads of RMC, Group Director (Medical Group) are also acknowledged.

References:

[1] A.K. Singh, et. al., *Indian Journal of Nuclear Medicine*, **37** (2022) 50.

Pre-clinical Studies for Clinical Translation of 16- α -¹⁸F –Fluoroestradiol

S.K. Nandy^{1,§}, Y. Shete², S. Rakshit¹, Y. Dhekale¹, S.P. Kulkarni¹, N.S. Baghel¹

¹Radiation Medicine Centre (G), BARC, Mumbai

²Radiation Medicine Centre (M), BARC, Mumbai

§Email: saikatnandy1976@gmail.com

Breast cancer is the world's most prevalent cancer including for India. Assessment of ER profile expression in biopsy tissue sample for assessment of ER positive breast cancer by immunohistochemical staining has several limitations [1]. ER positivity with immunohistochemistry indicates the presence, but not the functionality (activeness), which is most important for success in case of endocrine therapy using ER targeting drugs [2]. ¹⁸F-16 α -17 β -Fluoroestradiol (¹⁸F-FES) is an FDA approved (year 2020) PET radiopharmaceutical for the diagnosis of ER positive breast cancer as well as to determine the activeness (liveliness) including other advantages. A high yield, Sep-Pak® purification based fully automated radio synthesis procedure is developed for the production of ¹⁸F-FES [3]. The radiosynthesis procedure involves radiofluorination of the precursor MMSE and then acid hydrolysis with 2N HCl. Final elution with 10% ethanol containing water. The in vivo stability of the synthesized ¹⁸F-FES, ER expression as well functionality (activeness) and pharmacokinetics have been studied by PET/CT imaging of female rabbit and demonstrating accumulation of the tracer in ER expressing organ. Tumour uptake and retention [%ID/gm=5.98±0.82 (30min), 3.77 ± 0.17 (60min) & 4.48 ± 0.27 (120min) have been confirmed by bio-distribution study in tumour model (MCF-7, ER+). The tumour characteristics have been confirmed by histopathology and immunohistochemistry. The pre-clinical study confirms that the synthesized ¹⁸F-FES is suitable for clinical study.

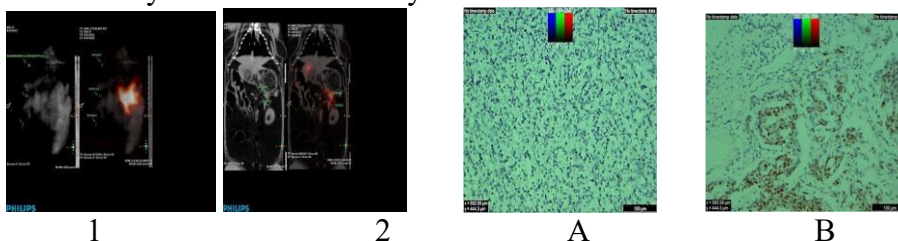


Fig. 1 & 2: ¹⁸F-FES uptake in NOD Breast nipple and Uterus (Normal ER Expressing organ)

Fig. 3 (A & B); A: IHC confirmation in SCID MCF-7 ER+ tumour model
B: Positive control, ER+ Human Breast Cancer Samples.

Acknowledgements: The authors acknowledge the keen interest and support from retired Division Heads of RMC, Group Director (Medical Group) as well as present Associate Director and Group Director.

References:

- [1] O'Brien, Sophia R. Edmonds, Christine E. Lanzo, Shannon M. Weeks et.al. *Radiographic* **43**, NO. 3: <https://doi.org/10.1148/rg.220143>. Feb 2023.
- [2] Salem K, Kumar Manoj, Powers Ginny L., Jeffery Justin J. et al. *Radiology*. 2018 Mar; **286** No.3: 856-864. doi: 10.1148/radiol.2017162956. Epub 2017 Sep 25.
- [3] Nandy Saikat, Banerjee Sharmila. *International Symposium on Trends in Radiopharmaceuticals (ISTR 2019)*, 28 October to 1 November 2019, Vienna, Austria. Abstract Book, PS1-50, Page-190

^{18}F -Sodium Tetra Fluoro Borate for Thyroid disorder and Thyroid Cancer: Radiosynthesis, Bio-evaluation & Histopathological Correlation

S.K. Nandy^{1,§}, Y. Shete², S. Rakshit¹, S.P. Kulkarni¹, N.S. Baghel¹

¹Radiation Medicine Centre (G), BARC, Mumbai

²Radiation Medicine Centre (M), BARC, Mumbai

[§]Email: saikatnandy1976@gmail.com

^{18}F -labelled Sodium Tetra Fluoro Borate (^{18}F]TFB), a substrate of human sodium/Iodide symporter (hNIS) is currently being evaluated worldwide as the first PET imaging agent of thyroid disorders and different types of thyroid cancer[1]. A high yield Sep-Pak purification based fully automated radiosynthesis procedure has been developed (unpublished). The synthesized ^{18}F -NaBF₄ was having RCP>95% in all batches. The pH (5~6) is suitable for IV injection. All the batches passed the BET and Sterility test. Biodistribution in male and female wistar rat, showed maximum uptake in thyroid but the uptake in other sodium iodide symporter expressing organs (like saliva, guts etc) were very low compared to thyroid. Female wistar rat thyroid had less uptake than male-similar to iodine uptake. The KClO₄ (specific inhibitor of sodium iodide symporter) blocked group, both male and female had very less thyroid uptake than the unblocked group. This other way proved that sodium tetra fluoro borate is also a specific inhibitor of thyroid. The H&E-stained slides showed the presence of active follicular cells required for sodium tetra fluoro borate uptake. Immunohistochemistry (IHC) with anti-sodium iodide symporter monoclonal antibody-based KIT (FP-5, specific for mouse, rat, and human) confirmed the presence of sodium iodide symporter in the thyroid tissue of male and female. Human thyroid tissue was kept as control during IHC (Fig.3 A&B). In-vitro cell binding assay using FRTL-5 cell line cannot be carried out due to import ban from Europe. PET/CT imaging study showed very distinct uptake in the thyroid of the rabbit (Fig. 1&2) and other mild sodium iodide symporter expressing organ.



Fig 1&2: ^{18}F -Sodium Tetra Fluoro Borate uptake in thyroid, salivary Gland, heart, gall bladder. Very Rapid blood clearance. No bone

Fig. 3 (A&B): A; IHC of human hNIS B: WISTAR RAT NaI Symporter IHC The arrow indicates the presence of sodium Iodide Symporter in thyroid which was Uptake removed during bio-distribution

Acknowledgements: The authors acknowledge the keen interest and support from retired Division Heads of RMC, Group Director (Medical Group) as well as present Associate Director and Group Director.

References:

- [1] M.J. Osoro, K. Sunasce et.al. *Eur J Nucl Mol Imaging* (2011) **37**, NO.2108-2116 <https://doi.org/10.1007/s.0259-010-1523-4>.

^{18}F -Labelled Phytochemicals for Breast Cancer Diagnosis

S.K. Nandy^{1,§}, S. Rakshit¹, Y. Shete², Y. S.P. Kulkarni¹, N.S. Baghel¹

¹Radiation Medicine Centre (G), BARC, Mumbai

²Radiation Medicine Centre (M), BARC, Mumbai

§Email: saikatnandy1976@gmail.com

Resveratrol, a naturally occurring stilbene, is known as a phytoestrogen due its ability to compete with natural estrogens for binding with estrogen receptor alpha (ER α) and estrogen receptor beta (ER β) with comparable affinity, and modulate the biological responses exerted by the receptors. The docking study revealed that Pterostilbene docked into ER- β (PDB Code:1X7R) active site with a very high affinity value (-42.723Kcal/mol) that is comparable to its ligand 17- β estradiol (-51.803Kcal/mol) [1]. While Resveratrol has three -OH groups attached to aromatic ring which exhibits enhanced resonance, it's analogue is only having one aromatic -OH group attached to benzene ring. Radiofluoroethylation is a very easy and well-established method for incorporation of radioactive fluorine in the molecule without much altering the geometry of the molecule and biological activity. Fully automated high yield radiosynthesis procedure with Sep-Pak[®] purification has been developed. Maximum radiofluorination was achieved by dissolving both Resveratrol and Pterostilbene in DMSO and adding catalytic amount of alkali for maximum deprotonation (Fig.1). The radiochemical purity is >95%. In order to check the potential of ^{18}F -Radiofluoroethylated derivative of Resveratrol (Trifluoro ethylated derivative) and of Pterostilbene, PET/CT imaging study was carried out in female rabbit to demonstrate the accumulation of the radiotracers in the normal ER expressing organs up to two hours post injections (Fig.2&3). Both the radiotracers showed good uptake in normal ER expressing organ of the female rabbit up to two-hour post injection and the uptake is comparable with 16- α -[^{18}F]-17 β -Fluoroestradiol. Further study in animal tumour model is required to prove its potential as ER+ breast cancer imaging agent.

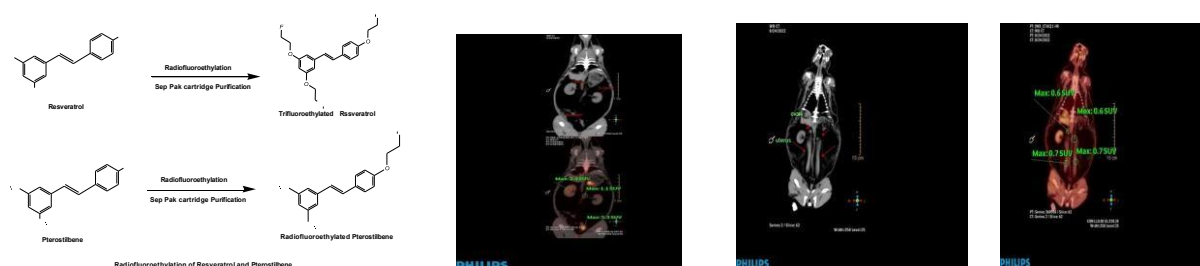


Fig.1 Radiofluoroethylation Fig.2. ^{18}F -trifluoroethylated Resveratrol. 2 hpi. Uterus, Kidney, Bladder accumulation

Fig. 3A & 3B ^{18}F -Fluoroethylated Pterostilbene Pterostilbene Uterus Uptake 1 hpi

Acknowledgements: The authors acknowledge the keen interest and support from retired Division Heads of RMC, Group Director (Medical Group) as well as present Associate Director and Group Director.

References:

[1] Tolba M.F., Abdel-Rahman. Z.S. *Scientific Reports*, 5:15239 (2015).

Development of Radiation Grafted Biodegradable Adsorbent for Ammonia Remediation in Water

N. Misra^{1,2,§}, M.G. Patil³, S. Rawat^{1,2}, S.A. Shelkar¹, V. Kumar^{1,2}

¹Radiation Technology Development Division, BARC, Mumbai, India

²Homi Bhabha National Institute, Mumbai, India

³Satish Pradhan Dnyansadhana College, Thane, India

§ Email: nilanjal@barc.gov.in

The presence of ammonia in water has been identified as a major threat to our aquatic eco systems and human health at large. With effective control and remediation measures being the need of the hour to counter this growing menace, this paper describes the development of a facile methodology for fabrication of efficient, low cost, biodegradable adsorbent for ammonia remediation. Radiation Induced Graft Polymerization (RIGP) technique was adopted to functionalize cotton cellulose fabric with styrene sulphonate groups (SS-g-cotton). Samples were characterized by TGA, FE-SEM and FTIR analytical techniques. Adsorption studies were carried out in batch process to optimize parameters such as pH, temperature, stirring rate and effect of competing ions. The SS-g-cotton adsorbent was observed to adsorb NH_4^+ at an optimum pH of ~ 7.0 with adsorption capacity of $\sim 15 \text{ mg.g}^{-1}$. Column adsorption experiments were also carried out on the SS-g-cotton samples using simulated ammonia containing wastewater. The RIGP mediated approach offers a facile technique to design cellulose based biodegradable adsorbents for potential large-scale ammonia remediation in the environment.

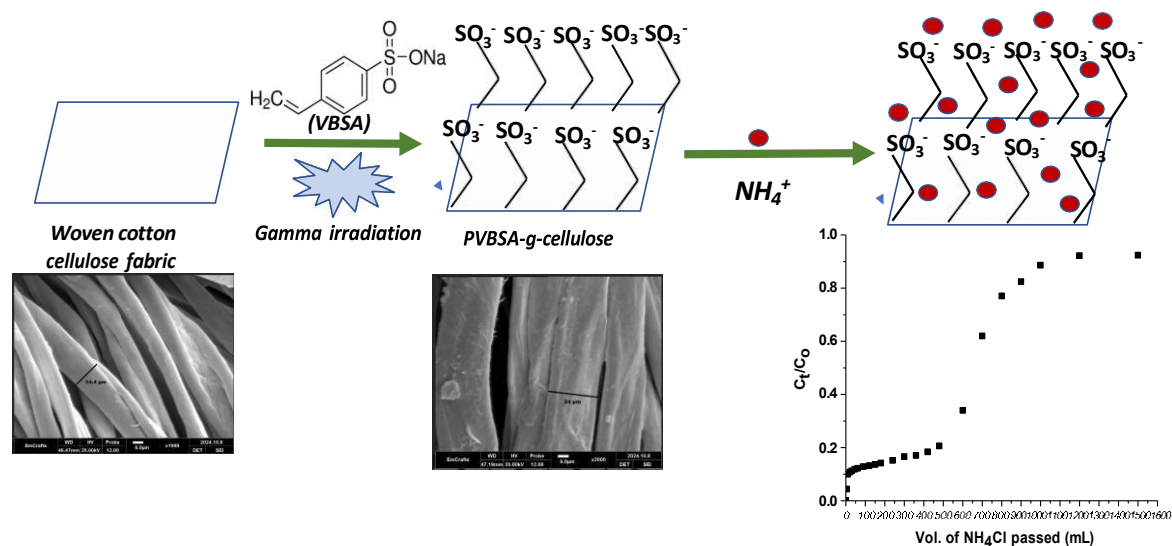


Fig. 1: Schematic of RIGP of SS onto cotton cellulose and NH_4^+ uptake by grafted adsorbent

Ensuring Consistency in Fluorine-18 Radiopharmaceuticals Production under GMP for Cancer Diagnosis: Lessons from Retrospective Analysis

R. Nanabala[§], A.K. Puthiyottumkara, T. George, A.K. Muhammed, D. Kottuparamban, J. Pokkat, S.K. Maniyoth, V. Pazhakkal, A.K. Joy, M.R.A. Pillai

Molecular Cyclotrons Pvt Ltd, Puthuvype, Ernakulam, 682508, Kerala.

[§]Email: ravi.teja131@gmail.com

DG is the gold-standard PET tracer for cancer diagnosis and treatment planning. However, its limited specificity for certain cancers and high brain uptake due to glucose metabolism can hinder the detection of certain diseases and cancers. Alternative radio-pharmaceuticals like [¹⁸F]FDOPA, [¹⁸F]FET, [¹⁸F]FCholine, [¹⁸F]FMISO and [¹⁸F]FPSMA-1007 are used for specific cancers and diseases. The production of these radiopharmaceuticals often face lower radiochemical yields as well as production inconsistencies in automated modules, affecting patient care [1]. With limited literature on troubleshooting and optimization, our study retrospectively analyses various ¹⁸F-

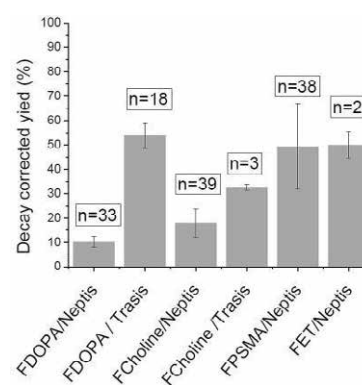


Fig 1: Radiochemical yields of ¹⁸F-radiopharmaceuticals

radiopharmaceuticals produced using two different automated modules in our facility to identify issues and implement troubleshooting strategies to improve radiochemical yields and production consistency. Fluorine-18 is produced using 11 MeV Siemens Eclipse HP cyclotron. [¹⁸F]FDOPA and [¹⁸F]FCholine cassettes were procured from ABX and Trasis, Belgium. [¹⁸F]FPSMA-1007 and [¹⁸F]FET cassettes and chemicals were sourced from ABX, Germany. The retrospective analysis focused on production parameters such as radiochemical yields, batch consistency, and failure rates. Troubleshooting included changes in software, module performance checks, and procedural optimizations. Fig.1 illustrates the radiochemical yields and number of batches for [¹⁸F]FDOPA, [¹⁸F]FCholine, [¹⁸F]FET, and [¹⁸F]FPSMA-1007. The Trasis module out-performed the Neptis module in terms of yields and consistency for [¹⁸F]FDOPA and [¹⁸F]FCholine production. Troubleshooting efforts for [¹⁸F]FCholine production using the Neptis module reduced the failure rate from 10% to 4%. For [¹⁸F]FDOPA, in the Trasis module, the failures were reduced from 50% to zero. No failures were observed for [¹⁸F]FPSMA-1007 and [¹⁸F]FET production using the Neptis module, with consistent production. All tracers achieved radiochemical purities > 96%. Retrospective analysis and targeted troubleshooting of ¹⁸F-radiopharmaceutical production significantly enhanced radiochemical yields improving the number of patients who will receive the radiopharmaceuticals.

References :

[1] R. Nanabala *et al.*, *Nuclear medicine and molecular imaging*, **56** (2022) 127.

Extended Surface Modification of Silicone-based Materials for Biomedical Application

R. Agarwal, S. Ray Chowdhury[§], Y. K. Bhardwaj

Radiation Technology Development Division, Bhabha Atomic Research Centre &
Homi Bhabha National Institute, Mumbai, India

[§]Email: rcsbhen@barc.gov.in, rohini@barc.gov.in

Silicone, also known as Polydimethylsiloxane (PDMS), is a versatile material with excellent properties. It is highly permeable to gases, optically transparent, and easy to manufacture. It has been widely used in various fields, from microfluidic fabrication processes to biomedical devices such as cochlear implants and urinary catheters [1]. This material is known for its excellent mechanical properties, including flexibility and is also cost-effective. However, silicone-based materials, including sheets and Foley catheters, are prone to biofouling. Chemically modifying PDMS is particularly challenging due to its relatively inert surface [2]. High-energy radiation is used to introduce chemical functionalities onto the surface, leading to enhancement of antifouling property [3]. In this study, the surfaces of silicone-based sheets and catheters are modified by grafting acrylic acid using Co-60 gamma radiation through a mutual irradiation technique. The maximum grafting yield of approximately 27% is achieved at the optimized grafting parameters, i.e., 8 kGy, 1.1 kGy/hr dose rate, 10% acrylic acid, and 50 mM Mohr's salt. Fourier Transform Infrared Spectroscopy (FTIR) analysis confirms the successful grafting of acrylic acid through the presence of a distinct carbonyl peak. The grafted materials are further modified by esterifying the grafted acrylic acid with α -terpineol, a natural antibacterial compound that disrupts bacterial cell walls and inhibits quorum sensing-mediated virulence and biofilm formation. This modification is done through a chemical synthetic route using N-ethyl, N'-dimethyl aminopropyl carbodiimide hydrochloride (EDC) and N-hydroxy succinimide (NHS) as coupling agents. A chemical yield of approximately 28% is obtained. The modified silicone materials are characterized using ATR-FTIR and thermogravimetric analysis, confirming the successful modification of the materials.

Table 1: % grafting yield obtained for (a) silicone sheet and (b) silicone-based foley's catheter at different radiation doses.

S. No.	Radiation dose/ kGy	% Grafting yield	
		Silicone sheet	Silicone-based foley's catheter
1	4	3	16
2	6	9	25
3	8	20	27
4	10	19	27

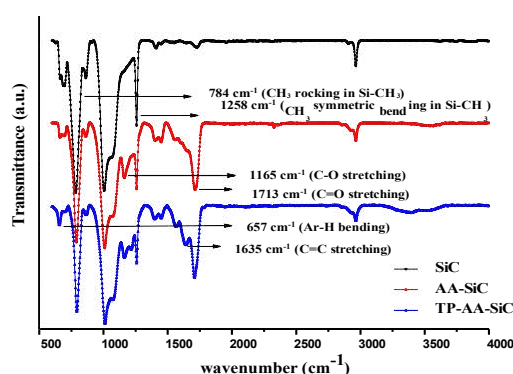


Figure 1: FTIR-spectrum of silicone, acrylic acid grafted silicone (AA-g-Si) and α -terpineol attached AA-g-Si

References:

- [1] Lam M. Migonney V. Falentin-Daudre C., *Acta Biomater.* **121** (2020) 68.
- [2] Magennis E. P. Hook A. L. Williams P. Alexander M. R., *ACS Appl. Mater. Interfaces.*, **8** (2016) 30780.
- [3] Agarwal R.; Kalambe S. C.; Chakraborty P.; Ray Chowdhury S; Pant H. J., *J. Appl. Polym. Sci.*, 0.1002/app.54871 (2023)

Intercomparison of Reference Standard Ionization Chamber of BARC for Dosimetry of Ir-192 Brachytherapy Source with IAEA

Greeshma K A[§], Sougata Rakshit, Sneha Chandrasekhar

Radiation Safety Systems Division, Bhabha Atomic Research Centre, Mumbai

[§]Email:greeshma@barc.gov.in

Brachytherapy is a type of radiation therapy in which radioactive sources are placed inside or close to tumor in the form of encapsulated seeds, wires or capsules. The High Dose Rate (HDR) Brachytherapy involves delivery of dose to tumors in the range of 15 to 20 Gray in multiple fractions for small interval of time. It is used to treat various cancers like breast cancer, head and neck cancer, lung cancer etc. Radiological Standards Group (RSG) of Radiation Standard Section (RSS) of Radiation Safety Systems Division (RSSD) calibrates approx.100 High Dose Rate (HDR) well type ionization chambers annually. Calibration involves finding the Reference Air Kerma Rate (K_R) of Ir-192 source by using primary standard graphite ionization chamber of 1002.4 cc volume and then deriving calibration coefficient (N_{RAKR}) of HDR well chamber of user in terms of Gy/h/A. $K_R = N_K \cdot (M_{u,c}/t) \cdot k_{sat} \cdot k_{air} \cdot k_{scatt} \cdot k_n (d/d_{ref})^2$ (corrected for saturation, air attenuation and scattering.) $N_{RAKR} = K_{R, corrected} / \mu \cdot K_{TP}$ (corrected for temperature and pressure to reference condition.) The key challenge for this calibration include determining source position of maximum current response inside the user well type chamber. In order to resolve this issue, the source was inserted into well chamber through standard guide tube and its movement was controlled by stepper motor system mounted in control unit. Also, the whole calibration was carried out by following Standard Operating Procedure which ensures consistency, accuracy and safety during the whole process. Another challenge during calibration is natural leakage current observed in the dosimeter due to presence of dirt/moisture in the RF connector of triaxial cable used between the well chamber and electrometer. This is resolved by removing moisture/dirt from connector ends by cleaning it using hot air blow. RSG, RSS recently participated in intercomparison of air kerma measurement standard conducted by IAEA/WHO secondary standards dosimetry laboratory using a reference standard well type ionization chamber. The calibration coefficient of the reference standard well type ionization chamber was evaluated both at BARC and IAEA. The result of intercomparison, R expressed in terms of the ratio of calibration coefficients estimated by RSG and IAEA was 0.987, with an uncertainty of 0.031. The result was within the acceptable range of $0.97 < R < 1.03$.

Table 1. Result of intercomparison

BARC				IAEA				Result R = (1) / (2)	Uc (k=2)
Air Kerma Rate	N_{RAKR} (1)	Uncert ainty	Trace ability	Air Kerma Rate	N_{RAKR} (2)	Uncert ainty	Trace ability		
8.6 mGy /hr	460.3 μGy/ hr/nA	1.6%	BARC	8.2 mGy /hr	466.1 μGy/ hr/nA	2.6%	PTB	0.987	3.1%

References:

- [1] International Atomic Energy Agency
- [2] Technical Reports Series No. 492, IAEA, Vienna (2023).

Preparation of Ethylene Vinyl Acetate/Jute Fabric Bio-composites with Improved Properties

A. Jha, S. A. Khader, S. Ray Chowdhury[§]

Radiation Technology Development Division, BARC, Mumbai-400085, India.

[§] Email: rcsbhen@barc.gov.in

Natural fibre-reinforced polymer composite is a great interest to researchers and industries. But the preparation of such composites with desired properties is challenging due to the difference in surface wettability (surface energy) of polymer and natural fibre [1]. Development of natural fibre-based polymer bio-composites with enhanced properties, and the reduction of loading of non-biodegradable polymer in the environment is the major objective of this study [2]. We selected ethylene vinyl acetate (EVA, VA content 28 wt%) as a polymer and jute as a natural fibre in a woven fabric (mat) form. Surface modification of jute fabric was done through gamma radiation assisted grafting of hydrophobic molecule dodecyl methacrylate (DMA). Attachment of DMA molecule on jute fabric turns the surface wettability of jute fabric closer to that of EVA. Then, EVA and jute fabric (JF) composites were prepared using pure jute fabric (PJF) and modified jute fabric (MJF) of different compositions. Increase of Young's modulus and yield strength for EVA/MJF composite were 1400% and 525% with respect to pure EVA as shown in Fig. 1 and Fig. 2. These enhancements were much higher compared to EVA/PJF composites (increase were 300% and 250% respectively w.r.t pure EVA) (Fig. 1 and 2). This occurred due to the improvement of interfacial strength of EVA/MJF composites. For the similar the reason, improvement of dynamic mechanical properties is also noticed.

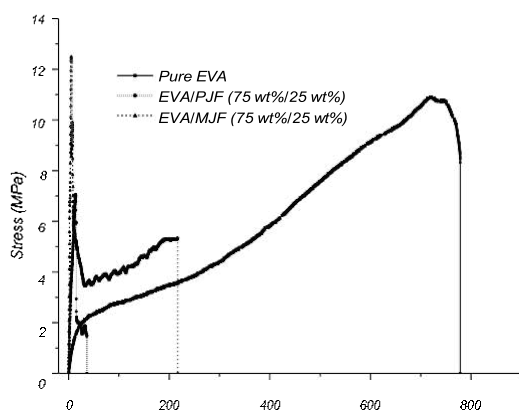


Fig. 1. Stress-strain plot of EVA and jute fabric composites

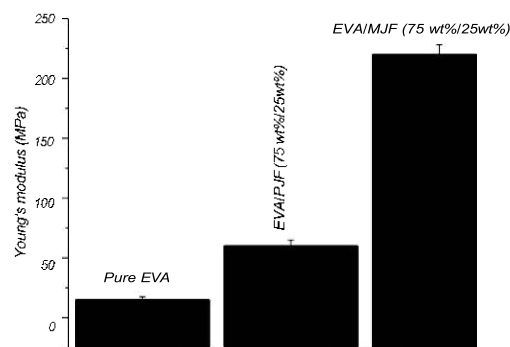


Fig. 2. Variation of Young's modulus of EVA and jute fabric composites

References:

- [1]. S.H. Patel and M.Xanthos, *Adv PolymTech* **20** (2001) 22.
- [2]. F. Sarker, P. Potluri, S.Afroj, V. Koncherry, K. S. Novoselov and N. Karim, *ACS Appl Mater Interfaces*, **11** (2019) 21166.

Formulation, Quality Control and Pre-Clinical Evaluation of [¹⁷⁷Lu] Lu- Labeled Glucuronic Acid Functionalized Hydroxyapatite Nanoparticles using Cold Kit for Potent Application of Nanoscale Brachytherapy

Sourav Patra^{1,2}, K. V. Vimalnath¹, Khajan Singh¹, Shishukant Suman^{1,2},
Rubel Chakravarty,^{1,2} Sudipta Chakraborty^{1,2,§}

¹Radiopharmaceuticals Division, BARC, Mumbai, India

²Homi Bhabha National Institute, Anushaktinagar, Mumbai, India.

§Email: sudipta@barc.gov.in

With recent advances in novel approaches to cancer therapy, application of nanoscale brachytherapy has emerged as a promising avenue since it involves direct delivery cytotoxic dose to the tumor uniformly with minimal uptake of non-target organ. In this regard surface functionalized inorganic nanoparticles provide attractive carrier platform for therapeutic radionuclides. In the present work, we have explored synthesis of glucuronic acid (GA) functionalized hydroxyapatite (HA) nanoparticles (GAHANp) and preparation of cold kits of GAHANp for radiolabeling with ¹⁷⁷Lu [$T_{1/2} = 6.65$ d, $E_{\beta}(\text{max}) = 497$ keV, $E_{\gamma} = 113$ (6.4%) and 208 keV (11.0%)]. For this, 5 mg of HA synthesized as reported earlier [1], was incubated with 50 mg of GA in aqueous medium at room temperature for 1 h under stirring condition at pH~6. The excess GA was removed using dialysis tube (MW cut-off 10 kDa). The reaction mixture was then lyophilized at -50°C and 1 mbar pressure to obtain five cold kits each containing 1 mg of HANp. The formation of surface functionalized HANp was ascertained from a randomly selected kit vial prepared using FTIR spectroscopy, where shifting of stretching vibration of -C=O group towards the lower frequency region indicates binding of Ca of HA with -C=O group of GA. The particle size distribution and zeta potential of the GAHANp in kit form were found to be 48 ± 3 nm and -32.6 ± 2.5 mV at pH ~6, respectively. For the radiolabeling with ¹⁷⁷Lu, content of one kit vial was dispersed in 1 mL de-ionized water and 50 μ L of [¹⁷⁷Lu]LuCl₃ (~ 25 mCi) was added at pH ~ 6 and incubated at room temperature for 1 hr. The radiolabeling yield was determined using radio-TLC and found to be >98%. The *in vitro* stability of [¹⁷⁷Lu]Lu-GAHANp formulation in physiological saline indicated that [¹⁷⁷Lu]Lu³⁺ ion did not leach out upto 2 weeks from the time of formulation. *Ex vivo* biodistribution study of the formulation was carried out in BALB/c mice bearing triple negative breast cancer (TNBC) after localized administration in the tumor. The percentage uptake of administered formulation at different time points post-injection is shown in Fig 1, which demonstrates significant retention of radiolabeled formulation in the tumor mass upto a period of 2 weeks of post-administration. These experimental observations indicated that [¹⁷⁷Lu]Lu-GAHANp formulation which was prepared using cold kit of GAHANp, could be envisaged as a promising agent for nanoscale brachytherapy.

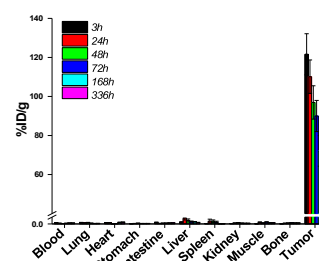


Fig.1: Ex vivo biodistribution in BALB/c mice bearing after intra-tumoral injection of [¹⁷⁷Lu]Lu-GAHANp

References:

[1] Patra S et al, *Ind. Eng. Chem. Res.* **62** (2023) 3194).

Studies on the Complexation Kinetics and Mechanism of Bone Uptake of ^{177}Lu -Complex of Bisphosphonate Amide of DOTA

Priyalata. S. S. Shetty^{1,2}, K. V. Vimalnath¹, Sharad P. Lohar¹, Sudipta Chakraborty^{1,2,§}

¹Radiopharmaceuticals Division, Bhabha Atomic Research Centre, Mumbai, India.

²Homi Bhabha National Institute, Mumbai, India

§Email: sudipta@barc.gov.in

One of the recent advancements in the palliative care of pain arising from metastatic bone lesions is the use of radiolabelled bisphosphonates. In this regard, ^{177}Lu -labelled bisphosphonate amide of DOTA (^{177}Lu]Lu-BPAMD) has shown excellent prospects. Toward this, an optimized protocol for the clinical dose formulation of ^{177}Lu]Lu-BPAMD using moderate specific activity carrier added (CA) ^{177}Lu was previously established [1]. The present article describes various intricate aspects of kinetics of complexation, kinetics and mechanism of uptake of ^{177}Lu]Lu-BPAMD on hydroxyapatite (HA) matrix which mimics the mineralized surface of bone. A comparative evaluation of these parameters is also reported for ^{177}Lu]Lu-BPAMD complex prepared using CA ^{177}Lu as well as no carrier added (NCA) ^{177}Lu .

In order to determine the complexation kinetics, varying amounts of BPAMD ligand was radiolabelled using CA as well NCA ^{177}Lu (~ 2.6 GBq activity in both the cases) at 100° C at different reaction times. The kinetics of uptake of BPAMD labelled with CA and NCA ^{177}Lu on HA particles were studied by varying the incubation period with a fixed amount of HA. An attempt was made to determine the mechanism of binding of Lu-BPAMD complex on HA using radiotracer technique by incubating the complex with ^{45}Ca -labelled HA particles and monitoring the release of ^{45}Ca radioactivity from HA matrix.

It has been observed that the kinetics of complex formation is significantly faster for ^{177}Lu]Lu-BPAMD prepared using NCA ^{177}Lu compared to CA ^{177}Lu , as shown in Table 1. Moreover, the complex could be prepared with significantly higher specific activity while using NCA ^{177}Lu . The uptake of NCA ^{177}Lu]Lu-BPAMD is also significantly faster on HA matrix as shown in Fig. 1. From the sorption studies of Lu-BPAMD on ^{45}Ca labelled HA, it was observed that once the bisphosphonate complex is adsorbed on the HA surface, the Lu^{3+} ion gradually replaces the Ca^{2+} from HA matrix as seen by the release of ^{45}Ca into the supernatant.

Table 1: Effect of variation of the amount of BPAMD and reaction time on the radiolabelling yield

BPAMD (μg)	% Radiolabelling Yield					
	15 min		30 min		60 min	
	c.a. ^{177}Lu	n. c.a. ^{177}Lu	c.a. ^{177}Lu	n. c.a. ^{177}Lu	c.a. ^{177}Lu	
10	11.5	19.5	14	22	15	
25	24	>99	45	>99	48	
50	57	>99	73	>99	79	>99
100	71	>99	98	>99	>99	

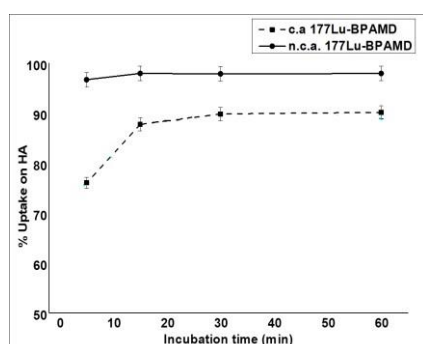


Fig. 1. Effect of incubation time on the % uptake on HA

References:

- [1] S. Chakraborty et.al, *Radiochimica Acta*, **108** (2020) 661.

Indigenous Synthesis of Fibroblast Activation Protein Targeted [$^{68}\text{Ga}/^{177}\text{Lu}$]-FAPI-2286 Peptide

Akanksha Jain, Manoj Kumar, Drishty Satpati[§]

Radiopharmaceuticals Division, BARC, Mumbai, India.

[§]Email: drishtys@barc.gov.in

Fibroblast activation protein (FAP) has elevated expression in cancer-associated fibroblasts (CAFs) that are actively involved in promoting tumor proliferation and metastasis. FAPI-2286 has been identified as selective FAP-targeted peptide and [$^{68}\text{Ga}/^{177}\text{Lu}$]-FAPI-2286 are in phase I clinical investigation. Hence with an aim of increasing cost-effective availability, effort was undertaken for indigenous synthesis of FAPI-2286 peptide for $^{68}\text{Ga}/^{177}\text{Lu}$ -labeling.

The linear peptide Hex-Cys-Pro-Pro-Thr-Gln-Phe-Cys-OH was synthesized manually using standard Fmoc protocol of solid phase peptide synthesis. The peptide was cleaved from the resin, purified and characterized by mass spectrometry. Subsequently, the linear peptide was cyclized using 1,3,5-tris(bromomethyl)benzene followed by conjugation with 2-aminoethanethiol. The cyclic peptide was further conjugated with 1,4,7,10-tetraazacyclodecan-1,4,7,10-tetraacetic acid-4-nitrophenylester (DOTA-PNP) using triethylamine as base. The final purified product, FAPI-2286 was characterized by ESI-MS. Expected mass ($\text{C}_{67}\text{H}_{99}\text{N}_{13}\text{O}_{18}\text{S}_3$): 1469.64; Mass obtained ($\text{M}+2\text{H}^+$): 735.83

Indigenously synthesized FAPI-2286 was radiolabeled with $^{68}\text{GaCl}_3$ and $^{177}\text{LuCl}_3$. ^{68}Ga -labeling was performed by addition of $^{68}\text{GaCl}_3$ (eluted from JSC, Russia generator using 0.1 N HCl) to the peptide (40 nmoles) dissolved in 1 M sodium acetate buffer (pH 4) and incubation at 90 °C for 10 min. The radiolabeling yield as determined by radio-HPLC (Fig.1) was found to be >95%. ^{177}Lu -labeling was carried out by addition of $^{177}\text{LuCl}_3$ (5 mCi) to the peptide (70 nmoles) dissolved in 1.5 M sodium acetate buffer (pH 5) followed by heating at 90 °C for 30 min. The radiolabeling yield (Fig.1) was found to be >90%.

Indigenously synthesized FAPI-2286 could be successfully characterized and radiolabeled with $^{68}\text{Ga}/^{177}\text{Lu}$.

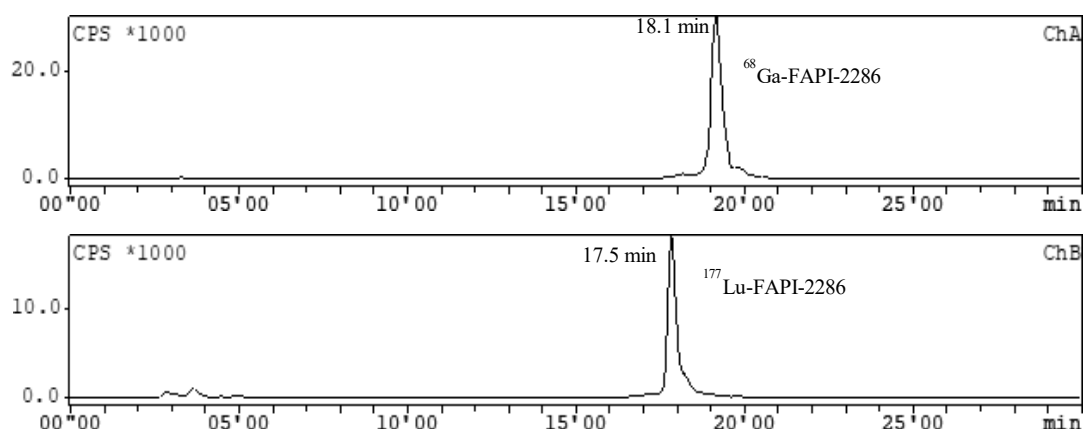


Fig.1: RP-HPLC chromatogram of ^{68}Ga -FAPI-2286 and ^{177}Lu -FAPI-2286

References:

[1] Zboralski D, et al. *Eur. J. Nuclear Medicine and Molecular Imaging*, **49** (2022) 3651.

Effect of Vegetation on Hydraulic Performance of a Horizontal Flow Constructed Wetland using Radiotracer

Sunil Goswami[§], J.S. Samantray, V. K. Sharma, R. Acharya

Isotope and Radiation Application Division, BARC, Mumbai-400085, India

[§]Email: gsunil@barc.gov.in

Constructed wetlands (CW) are human engineered systems that utilize natural process for treatment of wastewater. They have been highly applicable in developing countries, due to their characteristics like utilization of natural processes, simple construction, operation and maintenance, process stability and cost effectiveness. The design of constructed wetland requires multidisciplinary inputs involving biological and ecological sciences, aquatic chemistry, engineering hydrology and flow hydrodynamics [1]. The CW are heterogeneous in nature. Thus, they are prone to show deviation in the designed flow pattern and residence time for the treatment of wastewater. Thus, the aim of the present study is to measure mean residence time (MRT) and flow patterns of CWs using radiotracer technique. In this experiment, ~ 100 MBq of ^{99m}Tc ($t_{1/2}$: 6 h, E_{γ} : 140 keV) as sodium pertechnetate used in each run as radiotracer. The radiotracer concentration monitored at different planes across the width and outlet of CW using NaI(Tl) scintillation detectors connected to a computer controlled data acquisition system was set to record tracer concentration at an interval of once per minute as shown in Fig. 1.

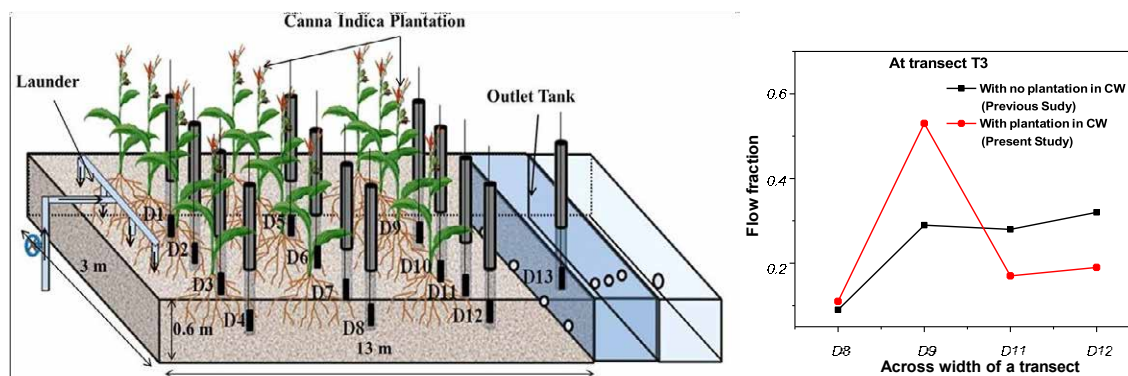


Fig. 1: Isometric view of horizontal constructed wetland for the radiotracer experiment

The radiotracer data obtained was treated and analyzed using a residence time distribution (RTD) analysis software. The data treatment steps includes background subtraction, tail correction, radioactive decay correction, zero shifting and normalization. The data was used to calculate MRT, dead volume and hydraulic efficiency of the CW. A four-parameter model i.e., tank in series exchanging with dead volume model prefixed with plug flow component was used to simulate the radiotracer data. From the measured experimental curves different parameters such as flow distribution, mean residence time, hydraulic efficiency index, effective volume fraction and short circuiting index of the wastewater in CW were estimated. Moreover, a flow model was developed to identify flow pattern and degree of mixing in the CWs. The model and hydrodynamic parameter were suggested, development of roots due to maturity of the plants, the overall flow behavior of wastewater inside the plant was approaching to the plug flow as desired and improve its hydraulic efficacy.

References:

[1] Persson, J., The use of design elements in wetlands. *Hydrology Research*, **36**, 2004, 113.

Post-Harvest Quality Assessment of Litchi Fruits (*Litchi Chinensis* Sonn.) through Edible Coatings and Gamma Irradiation

Mani Gopal¹, Singh Omveer¹, Rai Ratna¹, Lal Surendra¹, Joshi G. C.²

¹Department of Horticulture, ²Radiations and Isotopic Tracer Laboratory
G. B. Pant University of Agriculture and Technology, Pantnagar, Uttarakhand.

§Email: gaugm97@gmail.com

Litchi (*Litchi chinensis* Sonn.) also known as ‘Queen of fruits’ is an important subtropical fruit crop of the family Sapindaceae. It is beloved for its vibrant deep pink to red hue, delightful sweetness, and juicy aril. Its high perishability and susceptibility to pericarp browning are present challenges in transportation and marketing because litchi fruit has a very short life of 2-3 days at ambient temperature. Various methods have been adopted to mitigate post-harvest browning, including heat treatment, edible coating or waxing, vinyl resin plastic coating, ethylene bromide fumigation, gamma irradiation, etc. The present study aimed to enhance the shelf life and post-harvest quality of litchi fruit (cv. Rose Scented) through integrated treatments using *Aloe vera* and gamma irradiation. *Aloe vera*, a well-known medicinal plant, is widely recognized for its numerous medicinal and health benefits [1]. Irradiation has been extensively used in fruits and vegetables to prolong shelf life and maintain quality standards during storage. The joint expert committee of the FAO, IAEA, and WHO has approved a permissible irradiation dose of up to 10 kGy (100 kR) for food processing, as it does not pose any harmful effects on microorganisms or nutritional value [2]. The gamma irradiation processing was applied to samples weighing 2 kg for each treatment in the Radiations and Isotopic Tracer Laboratory (RITL, CBSH). Then, *Aloe vera* gel (10%, 20%, and 30%) combined with ascorbic acid (1%), hydrogen peroxide (1%) and Glycerol (1%) were applied as surface coating treatments. Treated samples along with untreated/control were stored at 5°C in 50µ LDPE bags. The fruits were subjected to periodical quantitative and qualitative analyses at every five-day intervals. The results found that 10 kR gamma irradiated litchi fruits when coated with 20% *Aloe vera* gel incorporated with 1% ascorbic acid as an antioxidant effectively decrease the physiological loss in weight (PLW) percentage [fig.1], preserved the post-harvest quality, extended the shelf life and reduced pericarp browning of litchi fruits for a longer storage period (up to 30-day) followed by fruits coated with gamma irradiation 10 kR + 10% and 30% *aloe vera* gel.

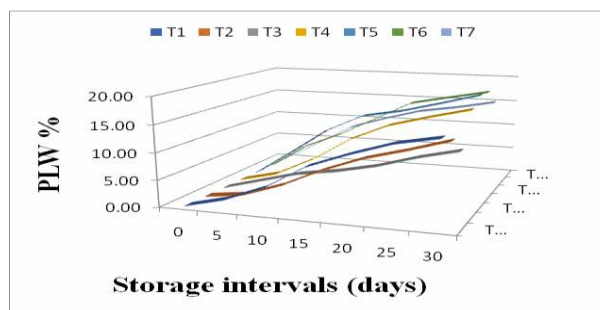


Fig. 1: Physiological Loss in Weight (%)

References:

- [1] Khalil *et al.*, *International journal of food science & technology*, **44**(2009): 927.
[2] Pandey *et al.*, *Radiation Physics and Chemistry*, **85**(2013):197.

Gamma Rays Induced Morphological and Biochemical Mutants in Bael (*Aegle marmelos*)

M. Rawat^{1,2§}, V. P. Singh³, S. Aswal⁴, G. C. Joshi⁵, J. Das⁶

^{1,§3,4} Department of Horticulture, ⁵Radiations and Isotopic Tracer Laboratory, G. B Pant University of Agriculture & Technology, Pantnagar, India. Uttarakhand, India, College of Agriculture Sciences, ^{2,6}Teerthanker Mahaveer University, Moradabad, U.P, India.

§ Email:- mandeeprawat107@gmail.com

Radiation technology plays a pivotal role in mutation breeding by enhancing genetic variability for crop improvement. Induced mutagenesis using gamma radiation is a highly effective approach due to its deep penetration and ability to generate novel genetic variations. Bael (*Aegle marmelos*), also known as the golden apple, is valued for its nutraceutical and pharmaceutical applications, with its leaves, fruits, roots, and bark exhibiting medicinal properties[1]. Moreover, its extensive reliance on open-pollination, complex cytogenetics, lack of standardized cultivars, and inconsistent fruit quality pose significant challenges. Additionally, bael has a prolonged juvenile phase, making conventional breeding approaches inefficient. To address these limitations, bael seeds were subjected to gamma irradiation at seven different doses (50 Gy, 100 Gy, 150 Gy, 200 Gy, 250 Gy, 300 Gy, and 350 Gy), along with an untreated control.

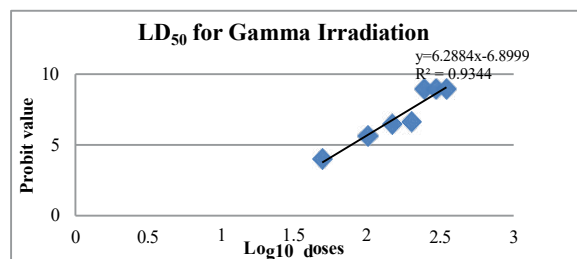


Fig1: Probit analysis based on corrected mortality rates of bael

The primary objective of this study was to induce genetic variability and identify promising mutants at the pre-bearing stage based on morphological and biochemical traits. The lethal dose (LD₅₀) was determined to be 77.68 Gy. Gamma-irradiated populations exhibited substantial morphological variations, particularly in plant height, leaf area, and internodal length. Notably, at 150 Gy, two distinct chlorophyll mutants—albino and viridis—were identified. Biochemical analyses revealed a dose-dependent increase in phenolic content, flavonoids, proline accumulation, catalase activity, antioxidant capacity, and total soluble protein, suggesting enhanced physiological responses to radiation-induced stress. These findings underscore the potential of gamma irradiation in generating beneficial genetic variability in bael for future breeding programs. The selected mutant lines are currently being evaluated for fruit and yield-related traits to identify elite genotypes with improved agronomic and commercial potential. This study lays the foundation for the development of high-yielding, early-maturing, and superior-quality bael cultivars, paving the way for genetic improvement and large-scale cultivation of this valuable crop.

References:

[1] V. P. Singh and Msira, K. K. *India Journal of Horticulture*, **67** (2010): 70- 47.

Corrosion Monitoring of Borosilicate Glass by Thin Layer Activation Method Utilizing Proton Beam from Pelletron

Jayashree Biswal^{1,2,§}, S. C. Sharma³, A. K. Gupta³, V. K. Sharma¹, R. Acharya¹

¹Isotope and Radiation Application Division, BARC, Mumbai 400085, India

²Homi Bhabha National Institute, Mumbai 400094, India

³Nuclear Physics Division, BARC, Mumbai 400085, India

§ Email: jbiswal@barc.gov.in

Borosilicate glasses are extensively utilized in various systems like rechargeable batteries, tissue engineering and for immobilization nuclear waste. Understanding the corrosion mechanism / leaching behaviour of these glasses in aqueous solutions is essential to reliably predict their long-term applications. Thin layer activation analysis (TLA) using a ion beam (proton, deuteron, ³He and ⁴He) is a nuclear method for measurement of surface loss of materials in the range of micrometers [1]. In the current work the leaching behaviour of titanium borosilicate glass has been studied using TLA method.

Borosilicate glass containing 10 wt% TiO₂ were prepared under programmed heating at 1200 °C temperature. The molten glass was first poured into a stainless steel cylindrical container and cooled to room temperature, followed by cutting of the glass to coupons of size 10 mm x 10 mm x 3 mm each. The glass coupons were irradiated with 12 MeV proton beam from BARC-TIFR Pelletron Accelerator, Mumbai. Vanadium-48 (half-life: 16 days, gamma energies: 983 and 1312 keV) radioisotope was produced on the surface of glass samples through nuclear reaction ⁴⁸Ti(p,n)⁴⁸V. The activity of each glass sample using HPGe detector system (Fig 1) was found to be ranging from 110-200 kBq. The gamma spectrum indicated, either there is absence of any other radionuclide impurity in the sample or their concentration is below the detection limit. The corrosion of these glass were studied in aqueous medium at 100 °C using ⁴⁸V as the radiotracer. The remnant activity on the glass sample with time of corrosion is shown in Fig 2. The change in the remnant activity with time will be utilized for estimation of the rate of corrosion in the experimental condition.

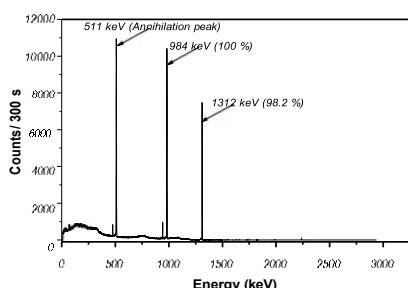


Fig. 1. Gamma spectrum of borosilicate glass containing ⁴⁸V

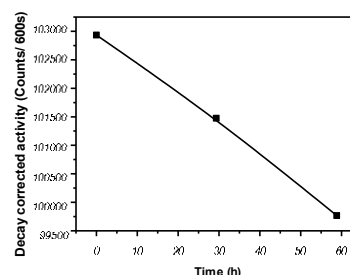


Fig. 2. Remnant activity versus time for glass corrosion in aqueous medium at 100 °C

References:

- [1] Stroosnijder, M.F. (1995). Thin Layer Activation in Materials Technology. In: Misaelides, P. (eds) Application of Particle and Laser Beams in Materials Technology. *NATO ASI Series*, **283**. Springer, Dordrecht.

In-Situ Monitoring of Natural Radioactivity Present in Sediments of Jampore Beach, Daman, India

Jayashree Biswal^{1,2,§}, Sunil Goswami¹, V. B. Yadav³, S. J. Sartandel³, J. S. Samantray¹,
V. Pulhani³, V. K. Sharma¹, R. Acharya¹

¹Isotope and Radiation Application Division, BARC, Mumbai 400085, India

²Homi Bhabha National Institute, Mumbai 400094, India

³Environmental Monitoring and Assessment Division, BARC, Mumbai 400085, India

§ Email: jbiswal@barc.gov.in

Natural radionuclides present in the sediments of coastal and river zones have received substantial attention in the past decades due to their diverse geochemical and physical properties. The information about the spatial and temporal distribution of these radionuclides are essential for the protection and management of the marine environment and for better understanding of oceanographic and sedimentological processes. The main source of natural radioactivity comes from three major radionuclides, such as, ²³⁸U, ²³²Th and ⁴⁰K; and their progenies. In the present paper, a study on in-situ measurement of natural radioactivity in Jampore beach, Daman, India has been reported. The in-situ monitoring of gross radioactivity or total gamma counting was carried out using a specially fabricated portable NaI(Tl) based gamma detector coupled with battery operated count rate meter (Fig. 1). The detector was placed in a PVC pipe, which was blinded at the bottom to prevent ingress of water to the detector system. The measurement was carried out in an area of 2 km x 600 m in the beach. For in-situ measurement, an imaginary grid was made with 200 m separation between adjacent measurement locations both in X & Y direction. The counts were measured at thirty locations. The latitude and longitude of each location was recorded using a hand-held GPS system. The total gamma count map of the beach is shown in Fig. 2. The total gamma counts in the sediment measured in-situ was found to be varying from 30 to 108 counts per second.



Fig. 1. NaI (Tl) detector connected to the count rate

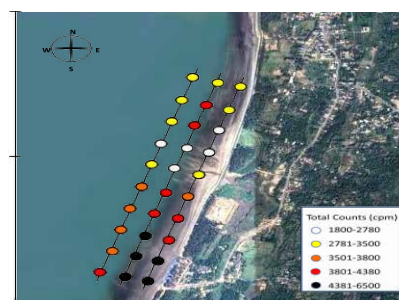


Fig. 2. Remnant activity versus time for glass corrosion in aqueous medium at 100 °C

References:

- [1] A. C. A. Velásquez, et al., (2022) *Beach sediment dynamics from natural radionuclides point of view*, In: *9th International Symposium "Monitoring of Mediterranean Coastal Areas: Problems and Measurement Techniques"*

Pr³⁺-Activated Phosphor for X-Ray Imaging

Annu Balhara^{1,2}, Priyansu Mishra,^{1,3} Mohit Tyagi^{2,4}, Santosh K. Gupta^{1,2,§}

¹Radiochemistry Division, BARC, Mumbai-400085, India

²Homi Bhabha National Institute, Mumbai-400094

³Mithibai College, Mumbai-400056, India

⁴Technical Physics Division, BARC, Mumbai-400085, India

§Email: santoshg@barc.gov.in

The combination of long persistent luminescence (PersL) and X-ray imaging capabilities in inorganic phosphors has garnered significant scientific interest, owing to their multifunctional applications ranging from radiation detection and imaging to anti-counterfeiting, optical storage, and medical diagnostics [1,2]. However, designing such materials with the appropriate defect structures and desired trap depths for ultralong PersL after UV and X-ray irradiation remains a significant challenge. Moreover, the ability to exploit multi-mode luminescence in a single material presents exciting possibilities for anti-counterfeiting applications.

In this regard, we have developed a bright orange-white emitting Ca₃Ga₂Ge₃O₁₂:Pr³⁺ phosphor (CGGO:Pr) with long-lasting PersL under both UV and X-ray irradiation (lasting > 60 minutes). Advanced synchrotron-based extended X-ray absorption fine structure (EXAFS) spectroscopy was employed to probe the local coordination environment of Pr³⁺ ions. The EXAFS analysis suggests that Pr³⁺ ions occupy both eight-coordinated Ca²⁺ sites and octahedral Ga³⁺ sites within the crystal structure. The CGGO:Pr phosphor, when embedded in a PMMA thin film, demonstrated persistent radioluminescence, and clear imaging of a screw on the CGGO:Pr-based PMMA film was achieved with high resolution (4 lp/mm), supporting its potential for X-ray detection and imaging applications (**Fig. 1**).

To further enhance the material's multifunctionality, we applied an aliovalent ion codoping strategy for trap engineering, which not only improved the PersL but also enabled multi-mode luminescence. The codoping of Er³⁺/Yb³⁺ ions allowed for selective tuning of the trap depths, with thermoluminescence measurements confirming the modulation of traps towards shallower depths. The resulting smart CGGO:Pr³⁺/Er³⁺/Yb³⁺ phosphor exhibited orange-white emission under 275 nm UV excitation, green emission under 380 nm UV excitation, and upconversion green emission under 980 nm near-infrared (NIR) irradiation.

The combination of triple-mode luminescence, long PersL, and X-ray imaging and detection properties in a single CGGO:Pr-based material underscores its potential for advanced

applications in anti-counterfeiting, security, radiation detection, and X-ray imaging. The insights gained from both experimental observations and theoretical calculations offer a deeper understanding of trap engineering and provide valuable guidance for designing next-generation PersL phosphors.

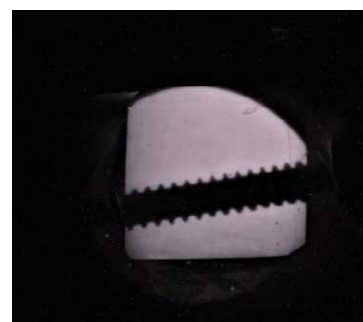


Fig. 1: X-ray imaging Pr³⁺ based phosphor film

References:

- [1] C. Richard and B. Viana, *Light: Science & Applications*, **11** (2022) 123.
- [2] Y. Wei and J. Wang, *ACS Applied Materials & Interfaces*, **16** (2024) 56519.

Radioluminescent and Persistent Phosphor for Potential X-ray Scintillator

Reshmi T. Parayil^{1,2}, Nitesh Kanojia^{1,3}, Mohit Tyagi^{2,4},
M. Mohapatra^{1,2}, Santosh K. Gupta^{1,2, §}

¹Radiochemistry Division, Bhabha Atomic Research Centre, Trombay, Mumbai-400085, India

²Homi Bhabha National Institute, Mumbai-400094

³Department of Physics, Institute of Chemical technology, Matunga, Mumbai-400019, India

⁴Technical Physics Division, Bhabha Atomic Research Centre, Mumbai – 400085

§ Email: santoshg@barc.gov.in

X-ray luminescence is an optical phenomenon where chemical compounds, known as scintillators, emit short-wavelength light when excited by X-ray photons [1, 2]. Due to X-rays' deep penetration ability and minimal autofluorescence background in biological samples, X-ray luminescence has gained significant attention as a promising optical tool for overcoming challenges in imaging, biosensing, and theragnostics. In recent years, the development of inorganic oxide-based scintillators has further broadened the applications of X-ray luminescence, including high-resolution X-ray imaging, autofluorescence-free biomarker detection, and non-invasive phototherapy for deep tissues. Additionally, X-ray luminescence shows great potential for overcoming the depth dependency of treatments for deep-seated lesions and for achieving synergistic effects in radiotherapy and phototherapy.

In this work, we employed a solvent-free solid-state reaction to synthesize Mn-doped spinel MgGa₂O₄ (MGO) in different annealing environments. We doped 2% Mn ions into MGO (MGO-Mn) and annealed the material in air, inert, and reducing atmospheres. The synthesized phosphor was characterized using X-ray diffraction (XRD), Fourier-transform infrared (FTIR) spectroscopy, energy dispersive X-ray spectroscopy (EDS), X-ray photoelectron spectroscopy (XPS), and Raman spectroscopy. The MGO-Mn annealed in a reducing atmosphere (MGO-Mn(R)) exhibited superior green emission with a photoluminescence quantum yield (PLQY) of approximately 64%. Moreover, the material demonstrated persistent emission for over 900 seconds, qualifying it as an afterglow phosphor.

In addition to afterglow, the material also exhibited X-ray excited luminescence, making it a multi-wavelength excitable material. The radioluminescence (RL) spectrum of MGO-Mn(R), shown in **Fig. 1**, displays spectral features similar to those observed under UV excitation, indicating that the emission originates from Mn²⁺ ions.

We also recorded the radioluminescence spectra as a function of X-ray voltage, ranging from 20 kV to 100 kV, with a constant current of 4 mA. Although the spectral features remained unchanged, the RL intensity increased monotonically with higher X-ray voltage. An important feature observed was the X-ray excited persistent luminescence of the material, which lasted for approximately 100 minutes.

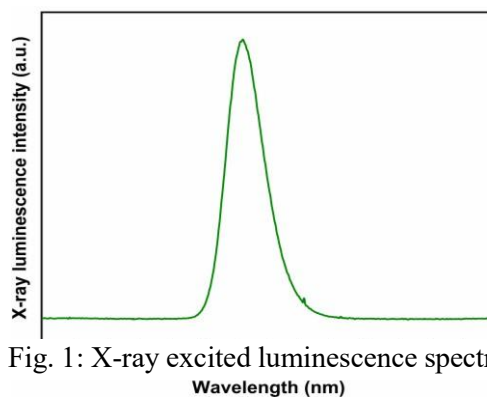


Fig. 1: X-ray excited luminescence spectra

References:

- [1] Y. Wei and J. Wang, *ACS Applied Materials & Interfaces*, **16** (2024) 56519.
- [2] C. Richard and B. Viana, *Light: Science & Applications*, **11** (2022) 123.

Optimization of Peptide-Based Chelators for ^{99m}Tc -Labeling

*Sonal Gupta^{*a,c}, Manoj Kumar^a, Ajit A. Kengar^c, Drishty Satpati^{a,b}*

^aRadiopharmaceuticals Division, Bhabha Atomic Research Centre, Mumbai, India;

^bHomi Bhabha National Institute, Mumbai, India;

^cKET's V. G. Vaze College, Mumbai University, India;

(*Email: sonalgupta.uk@gmail.com)

The well-established diagnostic radioisotope, technetium-99m is known to form stable complexes with N₃S chelator containing ligands. Incorporation of short peptide sequences bearing cysteine can constitute the N₃S chelator through amide nitrogens of amino acids and thiol group of cysteine. Biodistribution characteristics can be modulated by the use of different amino acids having different side chains and polarity.

Three different peptide sequences were incorporated into the A9 peptide targeting human epidermal growth factor receptor 2 (HER2) in breast cancers. N-terminus of A9 peptide was conjugated with three different group of amino acids: Gly-Gly-Gly-Cys (GGGC), Gly-Glu-Glu-Cys (GEEC) and Gly-Ser-Ser-Cys (GSSC). Different parameters (temp., buffer, ascorbic acid) were optimized for ^{99m}Tc labeling of the three peptide-chelator conjugates so as to obtain stable radiolabelled complex. ^{99m}Tc labeling (185 MBq) of peptide conjugates (300 μg) was performed in the presence of SnCl_2 (100 μg) as the reducing agent, sodium gluconate (5 mg) as the intermediate exchange ligand and sodium bicarbonate (10 mg) to maintain pH 7. Higher amounts of peptide were observed to be essential for stabilization of ^{99m}Tc -oxo core. Reaction components were incubated at 90°C for 30 min. and the radiolabeling efficiency of all the three complexes was determined by analytical RP- HPLC. Retention times of ^{99m}Tc -CGGG-rL-A9, ^{99m}Tc -CEEG-rL-A9 and ^{99m}Tc -CSSG-rL-A9 were 15.5 min, 15 min and 15.2 min respectively [Fig. 1]. The three complexes could be obtained in >95% radiolabelling yield but ^{99m}Tc -CEEG-rL-A9 and ^{99m}Tc -CSSG-rL-A9 were highly unstable, degrading to <5% within 1 h of preparation [Fig. 2]. However, ^{99m}Tc

CGGG-rL-A9 was observed to stable for 6 h after preparation. Hence the present study concludes that CGGG is the most suitable peptide-chelator system for ^{99m}Tc - labeling of peptides. Further investigation and evaluation studies shall be performed with ^{99m}Tc -CGGG-rL-A9

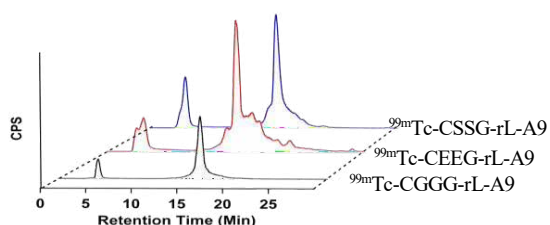


Fig. 1: Radio-HPLC of ^{99m}Tc -CGGG-rL-A9

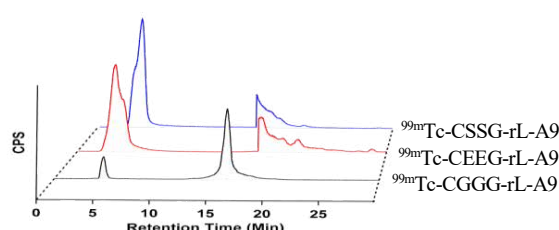


Fig. 2: Analysis of *in vitro* stability by RP-

Synthesis of [¹⁷⁷Lu]Lu-labeled-PCNA-Directed Dual Modal Conjugate for Treatment of Triple Negative Breast Cancer (TNBC)

Soumi Kolay¹ §, V Kusum Vats^{1,2}, Sandeep B. Shelar³, Mohini Guleria^{1,2}, Tapas Das^{1,2}

¹Radiopharmaceuticals Division, Bhabha Atomic Research Centre, Mumbai - 400085, India

²Homi Bhabha National Institute, Anushaktinagar, Mumbai - 400094, India

³Chemistry Division, Bhabha Atomic Research Centre, Mumbai - 400085, India

§Email: soumikolay@barc.gov.in

Proliferating Cell Nuclear Antigen (PCNA) plays a crucial role in DNA replication and repair. In rapidly proliferating cancer cells, PCNA is an attractive target for development of multi-modal agents for targeted cancer therapy [1]. Present study focuses on the development of a PCNA-targeting dual modal agent for selectively delivering therapeutic payloads to rapidly dividing cancer cells. A novel conjugate was synthesized by linking the PCNA-targeting peptide RWLVK to 5,10,15-tris(4-carboxymethoxyphenyl)-20-(4-carboxyphenyl) porphyrin via a Nuclear Localization Signal (NLS), another short peptide sequence (PKKKRKV). The porphyrin moiety in the conjugate enhances cellular uptake as well as enables the Photo Dynamic Therapy (PDT) upon light activation. To further enhance the therapeutic efficacy, the peptide sequence in the conjugate was modified with lysine-1,4,7,10-tetraazacyclododecane-1,4,7,10-tetraacetic acid (DOTA), allowing for radiolabeling with lutetium-177 (¹⁷⁷Lu), a beta-emitting radionuclide with proven therapeutic potential.

The conjugate was synthesized using solid-phase peptide synthesis method, followed by an appropriate protection-deprotection strategy to achieve site-specific conjugation. The conjugate was radiolabeled with ¹⁷⁷Lu with high radiochemical yield (>95%) under optimized conditions and the final radiolabeled product exhibited adequate stability in human serum. The conjugate's efficacy was assessed in various proliferating cancer cell lines, including TNBC derived MDA-MB-231 and fibrosarcoma-derived HT1080. The study reveals selective uptake and minimal dark toxicity of the radiolabelled agent but significant reduction in cell proliferation upon light exposure. Confocal microscopy confirmed intracellular localization without the need for additional fluorescent tagging due to the intrinsic fluorescence of porphyrin (Fig. 1). Cytotoxicity evaluation using the MTT assay demonstrated promising therapeutic potential, highlighting the effectiveness of PCNA-targeting strategies in specific breast cancer subtypes. This work presents an innovative approach for breast cancer treatment, integrating radiotoxicity and PDT for enhanced cancer cell selectivity and therapeutic outcomes.

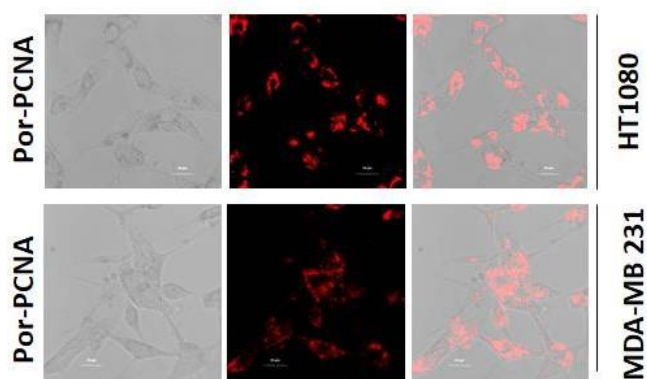


Fig. 1: Fluorescence cell images showcasing uptake of the porphyrin-PCNA conjugate in two different cancer cell lines

Reference:

[1] Wilson, K. A., et. al., *Chem. Biol. Drug Des.*, **91** (2018) 561.

Studying the Effect of Administration of Cold Antibody on Bio-Distribution of [¹⁷⁷Lu]Lu-Labeled-Antibody in Small Animal Model

Jeyachitra Amirdhanayagam¹, Soumi Kolay¹, Samrudhi Kar^{1,2},
Rohini P. E.³, Mohini Guleria^{1,2}, Tapas Das^{1,2§}

¹Radiopharmaceuticals Division, BARC, Mumbai- 400085, India

²Homi Bhabha National Institute, Anushaktinagar, Mumbai-400094, India

³SRM IST, Kattankulathur, Tamil Nadu-603203, India

§Email: tdas@barc.gov.in

Use of radiolabeled antibodies for targeting different types of cancers is currently in various stages of clinical trials worldwide. This type of treatment which involves the use of radiolabeled antibodies for cancer management is termed as radioimmunotherapy (RIT). Antibodies being proteins have high molecular weight (around 150 kDa) and exhibit slow pharmacokinetics and prolonged blood circulation thereby leading to high non-specific uptake in various organs [1]. To circumvent this, different administration regimens are being followed at Nuclear Medicine Centers during RIT. However, a systematic study outlining the optimized protocol for administration of cold/unlabeled antibody along with radiolabeled one has not yet been studied. In present work, a radiolabeled monoclonal antibody namely, [¹⁷⁷Lu]Lu-DOTA-Rituximab was prepared and animal studies were performed in healthy Balb/c mice model to evaluate the effect of administration of different amounts of cold antibody along with its radiolabeled counterpart. Bio-distribution studies with [¹⁷⁷Lu]Lu-DOTA-Rituximab, were conducted both with as well as without co-administration of 500 µg of the cold/unlabeled Rituximab. The results obtained revealed a reduction in the uptake of the radiolabeled antibody in organs such as liver and spleen upon co-injection with 500 µg of cold antibody. A separate experiment was also conducted wherein about 250 µg of cold Rituximab was injected about 1 h before the administration of the radiolabeled preparation. Another experiment by co-injecting the same amount of the cold antibody along with [¹⁷⁷Lu]Lu-DOTA-Rituximab, was also carried out. During pre-injection of cold Rituximab, an enhanced uptake of the radiolabeled antibody was observed in the majority of organs compared to when the same amount of cold was administered as co-injection in the animals (Fig. 1). The aforementioned observations clearly indicate the pronounced effect of administration regimen upon bio-distribution of radiolabeled antibodies.

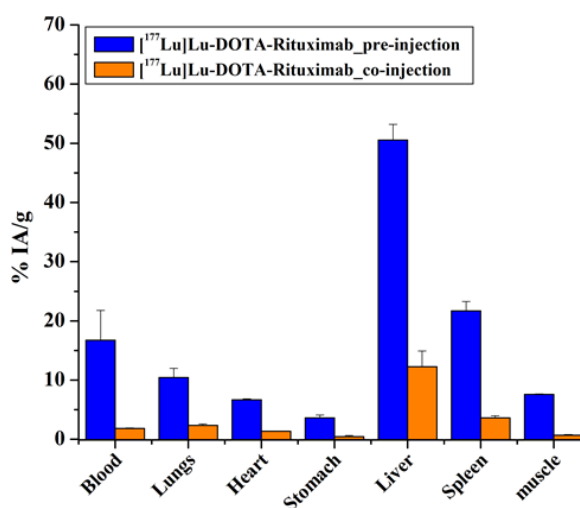


Fig. 1: Graphical depiction of uptake of radiolabeled Rituximab in major organs during pre-injection and co-injection of cold 250 µg Rituximab

References:

[1] H. Suzuki, K. Kannaka, T. Uehara, *Pharmaceuticals*, **17** (2024) 508.

Expression of Sodium-Iodide Symporter in Patients with Thyroglobulin Elevated and Negative ¹³¹Iodine Scan in Various Thyroid Cancer Types

Chandrakala Gholve^{1,§}, Vividh Raje², Yogita Shete¹, Swapnil Rane²,
Asawari Patil², Smita Gawandi¹, Roopal Agrawal¹, Sandip Basu¹, Nawab Singh Baghel¹

¹Radiation Medicine Centre, BARC, C/o TMH Annexe, Parel, Mumbai-400 012

²ACTREC, TMC, Navi Mumbai-410210

§Email: kalagholve@gmail.com

Sodium iodide symporter (NIS) is pivotal iodide transporter in thyroid tissue, essential for iodine metabolism and hormone synthesis. However, the molecular mechanisms leading to the impaired iodide uptake in thyroid tumors remain inadequately understood [1]. By elucidating the expression and localization of NIS, this study aims to shed light on the underlying alterations that contribute to iodine metabolism deficiencies, which will help in the management of radioactive iodine refractory (RAI-R) thyroid cancers. Our study aims to establish NIS expression and ¹³¹Iodine uptake in thyroglobulin elevated and negative ¹³¹I scan (TENIS) patients. This retrospective study employed immunohistochemistry to accurately localize NIS expression within human thyroid tissue samples obtained from patients diagnosed with thyroid carcinoma.

We included 38 TENIS patients, based on their radioactive iodine (RAI) uptake status in residual or metastatic lesions. All patients underwent total thyroidectomy followed by RAI therapy. Detailed clinical history data was collected. Histopathology & immunohistochemistry (IHC) staining was performed on 4-µm- thick formalin-fixed paraffin-embedded whole-tissue sections. The immunostaining pattern was graded as a percentage of positive tumor cells, and staining intensity (weak 1+, moderate 2+, or strong 3+) was noted along with the staining pattern (cytoplasmic or membranous).

As noted in the IHC analysis, 37 out of 38 patients with negative radioiodine scan showed dislocation of membranous expression of the NIS protein (Fig.1). These findings are in concordance with the available literature. Further research is required to understand the correlation between the translocation of membranous NIS and ¹³¹Iodine uptake in TENIS patients at the molecular level for better patient outcomes.

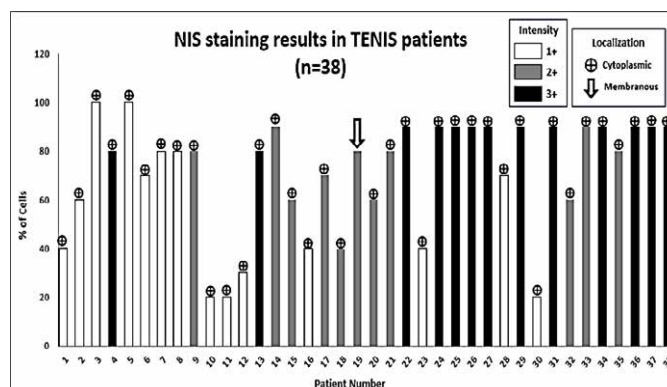


Fig.1: NIS staining results in TENIS patients

In conclusion, the insights gained from this research could pave the way for the development of innovative therapeutic strategies, including redifferentiation protocols or combination treatments that may restore iodine avidity in cancer cells. Ultimately, this study seeks to enhance the understanding of thyroid cancer biology, providing a foundation for improved patient management strategies in the face of iodine concentration challenges.

References:

[1] Y. Liu, et. al., *Drug Resistance Updates*. 68 (2023),100939.

Radiation and Plasma Fabricated Reusable Catalytic System for Catalytic Reduction of Cr(VI) to Cr(III)

S. Rawat^{1,2, §}, N. Misra^{1,2}, S.A. Shelkar¹, V. Kumar^{1,2}

¹Radiation Technology Development Division,

Bhabha Atomic Research Centre, Trombay, Mumbai, India

²Homi Bhabha National Institute, Anushaktinagar, Mumbai, India

§ Email: swarnima@barc.gov.in

Cr(VI) contamination in water bodies is a cause of severe concern, due to its widespread use in several industries and its numerous harmful health effects [1]. Cr(VI) compounds are known genotoxic carcinogen, therefore remediation of Cr(VI) is extremely important. One of the important remediation methods from Cr(VI) in water involves catalytic reduction of Cr(VI) to Cr(III), which is ~100 times less toxic due to its limited solubility and lower mobility [2, 3]. The present work reports green fabrication of a palladium nanoparticles (Pd NPs) based catalytic system using a combination of radiation and plasma processing for catalytic reduction of Cr(VI) in water. Radiation Induced Graft Polymerization (RIGP) was used to functionalize cellulose substrate with epoxy groups and subsequently, a plasma-based fabrication method was employed for synthesis and simultaneous immobilization of Pd NPs. The plasma-based approach that has been employed is environment friendly, as it is devoid of any organic solvents, chemical initiators, linkers, etc. and it also ensures minimal wastage of expensive metal precursor. Samples were characterized using FTIR, SEM, TGA, and XRF. The catalytic efficiency of the developed catalytic system towards Cr(VI) reduction, in the presence of formic acid as reducing agent was investigated, spectrophotometrically. Efficiency of >99.5 % towards Cr(VI) to Cr(III) could be achieved in batch mode, wherein 2 mM Cr(VI) could be reduced within 10 minutes. The catalytic system has exhibited storage stability of >3 months so far with ~90 % retention in activity.

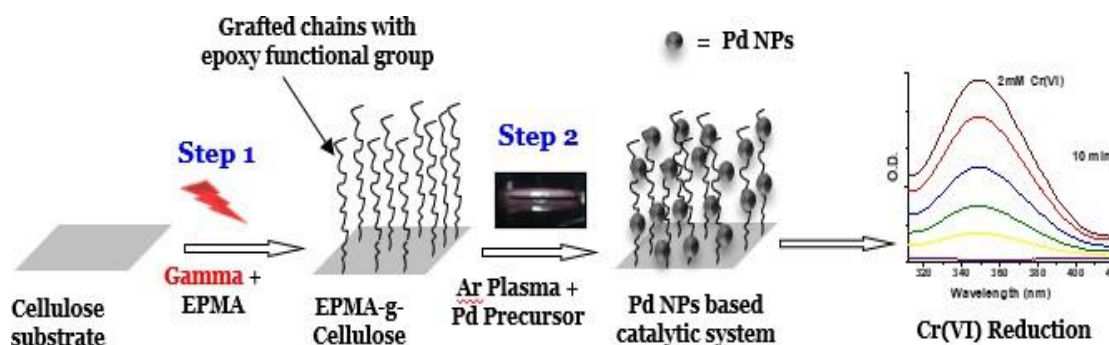


Fig. 1: Schematic of fabrication of Pd nanoparticles based catalytic system for Cr(VI) reduction

References:

- [1] C.C. Alvarez et al. *Trace Elem. Med. Biol.*, **65** (2021), 126729.
- [2] G. C. He et al. *Environ. Chem. Lett.*, **18** (2020), 561–576.
- [3] N. Misra et al. *Environ. Sci. Pollut. Res.*, 2018, **25** 16101-16110.

Sorption of Actinide by Phosphate Functionalized Teflon Scrap

R.B. Gujar^{1,§}, S.A. Ansari¹, A. Bhattacharyya¹
C.V. Chaudhari², K.A. Dubey², Y.K. Bhardwaj³

¹Radiochemistry Division, BARC, Mumbai – 400 85, India

²Radiation Technology Development Division, BARC, Mumbai – 400 085, India

³Radiochemistry and Isotope Group, BARC, Mumbai – 400 085, India

§Email: rgujar@barc.gov.in

Generally, the phosphate groups of ethylene glycol methacrylate phosphate (EGMP) show affinity for tetravalent and hexavalent actinides ions in a wide concentration range of nitric acid solution. However, they lack the selectivity towards Pu^{4+} ions over UO_2^{2+} ions. Studies have been shown that the selectivity of phosphate

groups for Pu^{4+} can be enhanced if the functional groups are in close proximity which helps in covalent binding with the metal ion [1]. At higher concentration of nitric acid (3-4 M HNO_3), one may not expect an ion-exchange mechanism for the sorption of Pu^{4+} and UO_2^{2+} ions by EGMP. Therefore, the sorption of these actinides must be taking place by their complexation with the phosphoryl ligating groups present in EGMP.

In this work, an attempt has been made to prepare glycidyl methacrylate grafted on PTFE scrap by gamma ray induced radiation grafting method (Fig 1). The epoxy group of poly-GMA (PGMA) grafted chains were allowed to react with *ortho*-phosphoric acid in THF by refluxing at 80°C [2]. Subsequently, the phosphate converted GMA-g-PTFE scrap material was studied for sorption of Pu^{4+} from nitric acid solution. As shown in Fig 2, the distribution coefficient (K_d) values for Pu^{4+} on the phosphate grafted Teflon was highest measured at 0.5 M HNO_3 , and remained constant up to 2 M HNO_3 .

Further increase in the feed acidity resulted in a sharp decrease in the K_d values. The uptake capacity of the material for Pu, measured at 0.5 M HNO_3 , was $5.0 \pm 0.1 \text{ mg/g}$. The sorption isotherm for Pu on the material followed monolayer chemisorption mechanism with maximum loading capacity of $5.6 \pm 0.1 \text{ mg/g}$, obtained from Langmuir isotherm model. The monolayer sorption energy, obtained from D-R isotherm model, was $15.1 \pm 0.5 \text{ kJ/mol}$. In order to check the feasibility of the material for the removal of Pu from a lean acidic waste, we prepared a column using 0.9 g of material in a 4 mm glass column (bed volume 1.63 cm^3). To this column, we passed 1000 mL of feed solution (3 M HNO_3) containing 170 μg of Pu. Our experimental observations indicated that the entire Pu was loaded on the column and clean solution free from Pu activity was coming out of the column. The results indicated a possible application of the present material for removal of Pu from an acidic feed.

References:

- [1] Sankararao Chappa, et. al., *J. Phys. Chem. B*, **120** (2016) 2942.
[2] S.T. Jadhav, et. al., *J. Radioanal. Nucl. Chem.*, **312** (2017) 413.

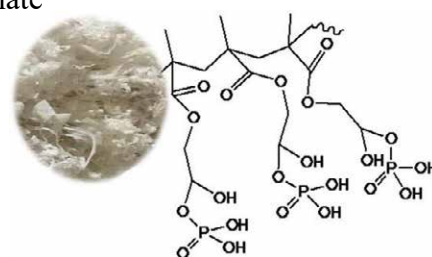


Fig. 1: Grafted phosphates on Teflon.

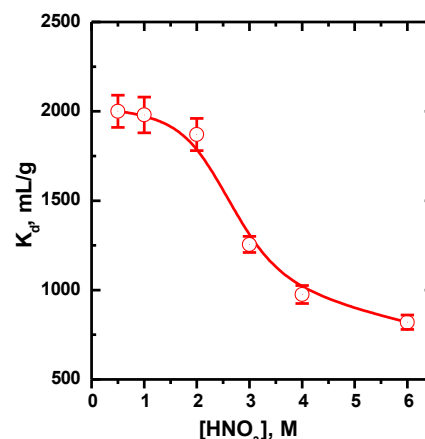


Fig. 2: Variation of K_d of Pu^{4+} with feed acidity.

Indigenous Development of ^{141}Ce -Point Source for Radiometry Assay of Nuclear Fuels

Manoj Kumar*, Drishty Satpati, Tapas Das

Radiopharmaceuticals Division, BARC, Mumbai-400 085, India

*Email: mkjangir@barc.gov.in

Radiometry is an important technique for assessment of nuclear fuel rods for detection and analysis of any packing flaws, failures or defects in the fuel assembly [1]. A radiation source, emitting gamma photons in the energy range of 100–150 keV is optimal for analysis of uranium and plutonium fuel pins due to energy of K-edges of uranium and plutonium being 115.6 keV and 121.8 keV, respectively. This is usually done using ^{57}Co as the point source ($E_\gamma=122$ keV). However, unavailability of ^{57}Co , an imported radioisotope prompted production of ^{141}Ce exhibiting nuclear characteristics [$t_{1/2}=32.5$ days, decay to ^{141}Pr (stable), $E_\gamma=145.4$ keV (48.5%)] [Fig.1] suitable for radiometry of nuclear fuels. ^{141}Ce can be produced by simple (n, γ) reaction employing natural Ce metal target. Though sensitivity of measurement may be slightly affected due to higher energy of ^{141}Ce but it serves as a cost-effective, import substitute of ^{57}Co for indigenous applications. Since the production of ^{141}Ce is need-based there are not many literature reports of its production. Working in this direction, we have attempted to develop ^{141}Ce point sources for radiometric applications. Parameters such as irradiation time, neutron flux and amount of target were optimized for the production of ^{141}Ce sources. Four batches of Cerium metal powder (25 mg, 50 mg, 70 mg & 100 mg) were loaded in small quartz tubes, sealed in aluminium cans and irradiated at a neutron flux of 0.26×10^{14} n.cm $^{-2}$.s $^{-1}$ for different time periods (30 - 45 days) in Dhruva reactor. Subsequently, the irradiated quartz tubes were recovered from aluminium cans and loaded into a custom-made aluminium holder [15 mm (H), 8 mm (ϕ), 1 mm (thick)]. [Fig.2]. Radioactivity of the point sources, thus obtained was in the range of 20-80 mCi as measured using pre-calibrated ionization chamber. Autoradiography experiments were carried out to confirm the uniformity of the point source. The uniform ^{141}Ce point source could be successfully fabricated indigenously and supplied to end users for performing radiometry assays.

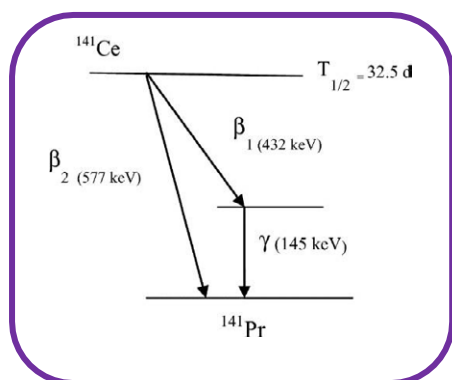


Fig. 1: Decay Scheme of ^{141}Ce

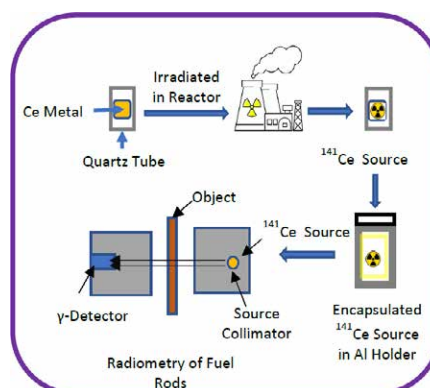


Fig.2: Flow Chart of ^{141}Ce process

References:

M.S. Rana, et. al., *Journal of Non-Destructive Testing & Evaluation*, Vol. 10/issue-1, 2011.

[¹⁷⁷Lu]Lu-Doxorubicin Loaded DHF-I crosslinked Radiopaque Microspheres towards Radio-Chemoembolization of Hepatocellular Carcinoma

Sayan Das^{1,2}, Mohini Guleria^{2,3}, Saikat Biswas¹, Santanu Dhara^{1§}, Tapas Das^{2,3§}

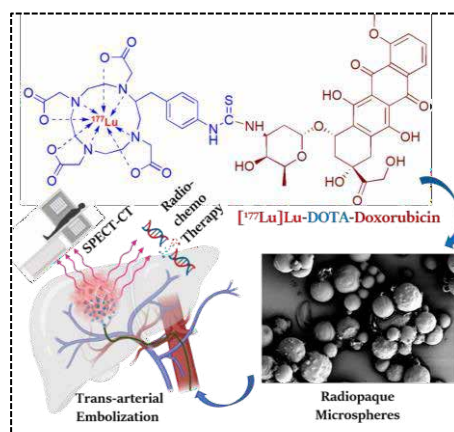
¹*Biomaterials and Tissue Engineering Group, School of Medical Science and Technology, IIT Kharagpur, Kharagpur-721302, India*

²*Radiopharmaceuticals Division, BARC, Mumbai-400085, India*

³*Homi Bhabha National Institute, Anushaktinagar, Mumbai-400094, India*

§Email: sdhara@smst.iitkgp.ac.in, tdas@barc.gov.in

Trans-arterial chemoembolization (TACE) is an effective palliative treatment for hepatocellular carcinoma, where micron sized (20-300 μm) drug eluting beads are administered in the tumor feeding hepatic artery. Major clinical problems associated with this therapy are - (a) in-vivo tracking of the microspheres post-administration, and (b) the side effects associated with high dose of chemotherapeutics [1]. To address this, we have developed an in-house build biocompatible radiopaque microsphere and loaded it with newly synthesized [¹⁷⁷Lu]Lu-DOTA-Doxorubicin, a potential radio-chemotherapeutic agent. Radiopaque chitosan microspheres have been prepared by emulsion crosslinking process using iodine bound 2,5-dimethoxy-2,5-dihydrofuran (DHF-I) as a biocompatible crosslinker. Scanning Electron Microscopy (SEM) shows the microspheres have the mean diameter of 25±7.6 μm, suitable for embolization application. FT-IR and XPS analyses as well as ninhydrin assay show the efficient crosslinking (>83±3.4 %) of the chitosan moiety by DHF-I. *In-vitro* degradation study of the developed microspheres shows <20 % degradation over the period of 21 days. Hemolysis assay and MTT assay with live-dead and Rhodamine-DAPI images on HepG2 and L929 cell line proves the hemocompatibility and biocompatibility of the radiopaque microspheres. For preparing radio-chemotherapeutic agent [¹⁷⁷Lu]Lu-DOTA-Dox, Doxorubicin (5.4 mg, 10 μM) was conjugated with *p*-NCS-benzyl-DOTA (8.2 mg, 15 μM) to prepare DOTA-Dox (37 °C, pH = 9.5, 24 h, purified by semi-preparative HPLC, characterized by FT-IR spectroscopy and LC-MS) and the conjugate (1.1 mg, 1 μM) was subsequently radiolabeled with [¹⁷⁷Lu]LuCl₃ (500 μCi, 18.5 MBq). Radiolabeling conditions (37 °C, pH= 5.6, 1 h) were optimized to obtain [¹⁷⁷Lu]Lu-DOTA-Dox with a radiochemical purity of >90% (confirmed by Radio-HPLC) and the preparation exhibited adequate radiochemical stability in PBS (pH = 7) and human blood serum (as confirmed by Radio-HPLC). *In-vitro* loading study of [¹⁷⁷Lu]Lu-DOTA-Dox (2.2 mg, 2 μM) in chitosan microspheres (5 mg) has shown 78±5 % loadability. *In-vitro* release study has been performed in PBS, which showed slow-release (>35%) pattern of [¹⁷⁷Lu]Lu-DOTA-Dox over 7 days (confirmed using Radio-PC). Albeit preliminary, our present study showed that in-house developed [¹⁷⁷Lu]Lu-DOTA-Dox loaded radiopaque microspheres have significant potential as a radio-chemoembolic agent.



References:

- [1] Clark TW. Complications of hepatic chemoembolization. *Semin Intervent Radiol.* 2006;**23**(2):119-125. doi:10.1055/s-2006-941442.

Comparative Analysis of Serum Thyroglobulin Quantification Using Indigenously Developed Immunoradiometric Assay Kit with Electrochemiluminescence Immunoassay in Thyroid Cancer Patients

C.S. Gholve^{1§}, S.N. Gawandi², S. Raut³ K. Ghosh⁴, N.S. Baghel⁵

^{1,2,5}Radiation Medicine Centre, BARC, C/o TMH Annexe, Parel, Mumbai-400 012

^{3,4}Biochemistry Department, TMH, Parel, Mumbai-400 012

§kalagholve@barc.gov.in

The major clinical application of measuring thyroglobulin (Tg) is monitoring the course of differentiated thyroid cancer (DTC) after total tumor resection. However, Tg autoantibodies (TgAb) in approximately 18% of thyroid cancer patients can interfere with various immunoassays, complicating accurate monitoring. Optimal performance goals are recommended for manufacturers, laboratories and physicians selecting a serum Tg method to use for serial long-term monitoring of thyroid cancer patients. Isotopic assays are considered gold standard methods, however, due to certain limitations non-isotopic assays are preferred. Interchangeability and standardization between Tg assays have not yet been achieved, even with the development of an international Tg standard CRM-457. In this study, Tg was measured by two different methods viz., an in-house immunoradiometric assay (IRMA) in our laboratory and an electrochemiluminescence immunoassay (ECLIA) using Roche Elecsys Tg II at Tata Memorial Hospital on aliquots of the same specimens stored at -20 °C. The study involved evaluating the performance of the two immunoassays as per the available infrastructure at the two centers. Procedures were as recommended by the respective manufacturers. Serum specimens from 37 thyroid cancer patients, aged 23-79 years with a male-to-female ratio of 1:2 were tested using both methods. Method comparisons were analyzed by linear regression method and correlation coefficient (r) was used to assess results between the two methods. The working ranges for Elecsys Tg II and in-house IRMA are 0.04-500 ng/ml and 0.1-300 ng/ml respectively. Reference range for Elecsys Tg II is 3.5-77 ng/ml whereas, for the IRMA method, we have 3 different ranges, a) Intact thyroid: undetectable (UD)-30 ng/ml b) Thyroidectomized (off T4): UD-14 ng/ml, c) Thyroidectomized (on T4): UD-3.5 ng/ml. The correlation coefficient obtained was 0.34 (p<0.05) and the linear regression equation observed was $y = 0.13x + 23.3$, showing a limited method comparability (see Fig.1). In conclusion, to accurately monitor serum Tg levels and detect recurrences of DTC, it is imperative to use the same assay method for all serial measurements as different assays are based on different principles giving limited comparability. At RMC, the IRMA kit has been used for more than 11 yrs and so far, has analyzed satisfactorily ~48, 000 samples. Preparing reagents in bulk for IRMA kit production reduces overall production costs, thus making it cost-effective and innovative.

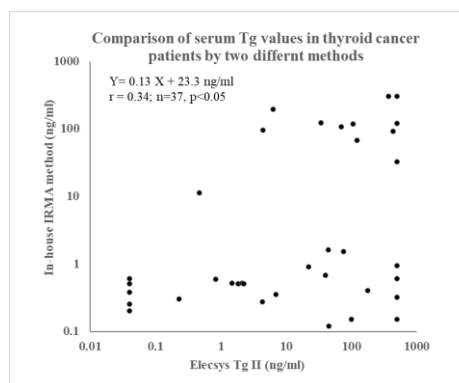


Fig. 1: Scatter plot of serum thyroglobulin levels obtained by in-house IRMA and Elecsys Tg II.

References:

- [1] C. Gholve et. al., *BARC Newsletter* (2022), Issue: **382**, 7-12.
- [2] C. Gholve and N.S. Baghel, *BARC Newsletter* (2024), Issue: **392**, 52-53.

Boron-Doped Bismuth Zinc Erbium Tellurite (TBBZE) Glass Matrix for Radiation Shielding Applications

Mo Anas Ahmad^{a§}, Virendra Singh^{a§}, Neeraj Singh^a, Neeraj Bisht^b, Yogendra Kumar Singh^c

^aDepartment of Physics, G. B. Pant University of Agriculture and Technology, Pantnagar, India

^bDepartment of Mechanical Engineering, G. B. Pant University of Agriculture and Technology, Pantnagar, India

^cDepartment of Industrial and Production Engineering, G. B. Pant University of Agriculture and Technology, Pantnagar, India

§Email: vs45us22@gmail.com, viren.pant@gmail.com

Exposure to ionizing radiation poses serious health risks, including DNA damage, cancer, and organ failure, emphasizing the need for effective shielding materials. Glass materials are excellent radiation shielding materials which offer benefits such as structural stability, optical transparency, and enhanced gamma-ray attenuation. This study investigates a novel tellurite-based glass system with the composition $(70-x)\text{TeO}_2-x\text{B}_2\text{O}_3-10\text{Bi}_2\text{O}_3-19\text{ZnO}-1\text{Er}_2\text{O}_3$, where x ranges from 0 to 30 mol%, synthesized via the conventional melt-quenching technique. The structural, optical, and radiation shielding properties of the glass samples were analyzed. X-ray diffraction (XRD) confirmed the amorphous nature, and UV-Vis spectroscopy showed an optical band gap values of ~ 3 eV, indicating that the addition of B_2O_3 content did not significantly affect the glass network structure. The density, measured by Archimedes' principle, was found in range of 6.027 g/cm³ to 5.400 g/cm³, and the oxygen packing density (OPD) varied from 65.155 g atom/L to 79.596 g atom/L, both correlating with increasing B_2O_3 content. The radiation shielding properties of the glass samples were calculated using XCOM software, with the results compared to those obtained from PhyXpsd simulations. The results obtained from both XCOM and PhyXpsd showed good agreement. Among all the prepared samples, TBBZE2 (7.5 mol% of B_2O_3 content), with a density of 6.133 g/cm³ and an OPD of 71.612 g atom/L, demonstrated superior radiation shielding performance. At 1.17 MeV, the mass attenuation coefficient (MAC) was 0.05483 cm²/g, and the half-value layer (HVL) was 2.06 cm, indicating strong gamma radiation attenuation capability of this glass. The mean free path (MFP) and effective atomic number (Z_{eff}) at 1.17 MeV were 2.973 cm and 24.61 , respectively, further confirming its shielding effectiveness. The glass transition temperatures and chemical bonding would be determined by DSC and FTIR methods, respectively; and the results are awaited. Based on the observations, it may be stated that TBBZE is a better high-energy radiation shielding glass matrix and the sample TBBZE2 [$62.5\text{TeO}_2-7.5\text{B}_2\text{O}_3-10\text{Bi}_2\text{O}_3-19\text{ZnO}-1\text{Er}_2\text{O}_3$] is a promising candidate for effective gamma radiation shielding.

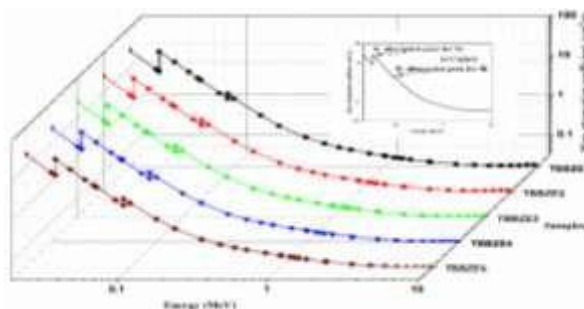


Figure 1 Mass attenuation coefficient of TBBZE glass samples

References :

[1]. Rautela, M. S., Singh, V., et. al., *Radiation Physics and Chemistry*, **224** (2024) 112071.

Studies on Gamma Radiation Stability of Curcumin

S. Show¹, S. Mitra^{2,3}, S. Lahiri^{1,4,§}, R. K. Nandi⁵, P. Banerjee¹

¹Department of Chemistry, Diamond Harbour Women's University, Sarisha, India

²Department of Environmental Science, University of Calcutta, Kolkata, India

³Present address: RIKEN Nishina Center for Accelerator Based Science, Wako, Japan

⁴Department of Physics, Sidho-Kanho-Birsa University, Purulia, India

⁵Department of Chemistry, Jadavpur University, Kolkata, India

§Email: susanta.lahiri.sinp@gmail.com

The present-day radioanalytical separation techniques explore the efficacy of nature resourced chemicals (NRC) as alternatives to synthetic chemicals. Earlier, we studied radiation stability of caffeine and catechin and used them in radiochemical separations [1]. The enol form of curcumin binds with various metal ions like Mn^{2+} , Fe^{3+} , Ni^{2+} , Cu^{2+} , etc. and make it potential radioisotope-metal chelator. The radiation stability of curcumin is an important parameter to decide its usage in radiochemical experiments. In this work, we have studied the stability of curcumin in γ -radiation environment in solid and aqueous form. Curcumin was extracted from turmeric powder following known methods [2]. 10 mg curcumin in solid form was exposed to ^{60}Co γ source where the dose was varied from 1 to 5 kGy. The irradiated curcumin was dissolved in de-ionized water and was characterized by UV-Vis, fluorescence and FTIR spectroscopy. To study the radiation stability in aqueous solution of curcumin, 0.0027 mM curcumin solution in de-ionized water was exposed to dose ranging from 0.1 kGy to 1.2 kGy. Solid curcumin was found to be structurally stable up to 5 kGy γ radiation (Fig. 1). However, in aqueous solution, the absorbance intensity of curcumin was found to decrease with increasing dose and absorbance maxima shifted to longer wavelength (Fig. 2). The fluorescence intensity was found to decrease with increasing dose suggesting degradation of curcumin moiety in aqueous form. Degradation efficiency reached up to 62% upon application of 1.2 kGy dose. Hydroxyl radicals produced by gamma radiolysis of H₂O can efficiently degrade any organic compound in aqueous phase. This degradation was found to be more pronounced in acidic medium compared to neutral or basic medium. The degradation can be controlled by addition of methanol.

Acknowledgements: Authors gratefully acknowledge Prof. Paramita Banerjee and Ms. Dipshikha Tamili of Dept of Food Technology and Biochemical Engineering, Jadavpur University for providing gamma irradiation facility. SS and SL acknowledge CSIR-ES project.

References:

- [1] S. Mitra et al., *Appl. Radiat. Isot.*, **183** (2022) 110148.
 [2] N. Nurjanah and E. Saepudina, *AIP Conf. Proc.*, **2168** (2019) 020065.

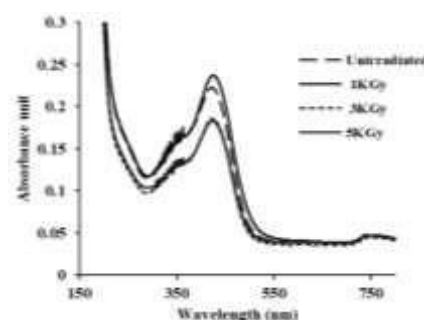


Fig. 1: UV-Vis Spectra of unirradiated and irradiated curcumin (solid)

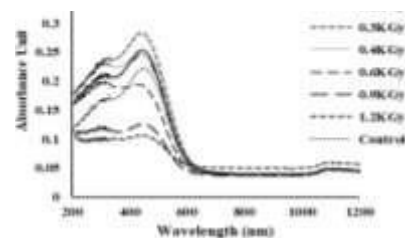


Fig. 2: UV-Vis Spectra of unirradiated and irradiated curcumin (aqueous)

A Large Scale Radiotracer Investigation in Heat Exchanger System of Refinery

Sunil Goswami[§], J. Biswal, J.S. Samantray, V. K. Sharma, R. Acharya

Isotope and Radiation Application Division, BARC, Mumbai-400085, India

[§]Email: gsunil@barc.gov.in

The hydrocracker unit (HCU) in a refinery was designed to process 300 metric tons per day (MT/day) of crude oil, converting it into various products such as liquid petroleum gas (LPG), naphtha, kerosene, and diesel. The unit comprises hydrocracking reactors loaded with catalysts and a series of heat exchangers. During the hydrocracking process, an exothermic reaction takes place, and the heated products are then passed through the heat exchanger system to preheat the incoming crude feed. Generally, if the sulfur content in the HCU's products exceeds the permissible limit, it is often due to a leakage of the crude feed stream into the reactor effluent stream. In one instance, after detecting such a leak in a refinery, repair work was conducted on the heat exchanger system. Following the repairs, a comprehensive radiotracer investigation was carried out to verify the effectiveness of the recent corrective measures aimed at addressing the sulfur leak in the refinery's heat exchanger system. The experimental setup for the radiotracer investigation to detect any potential leaks in the heat exchanger is illustrated in Fig. 1. In this study, the reactor-produced neutron activation product, Br-82, in the form of dibromobiphenyl, was utilized as the radiotracer [1]. For leak detection, approximately 30 mCi of Br-82 was injected as an impulse into the high-pressure crude oil feed line (marked in blue line, high pressure stream) of the system using a radiotracer injection system.

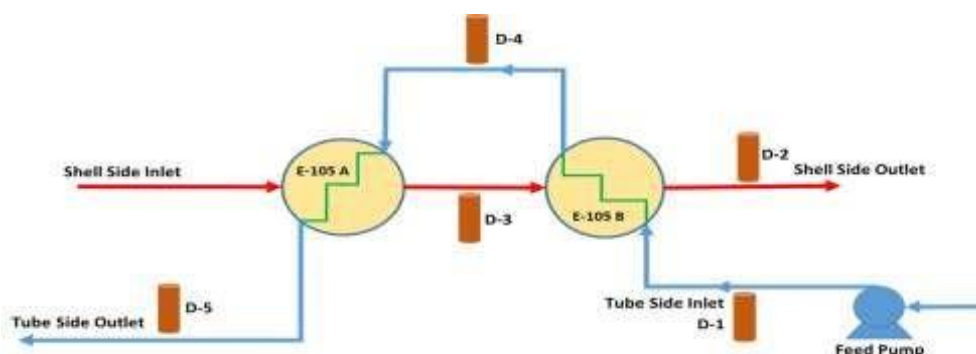


Fig. 1: Schematic diagram of exchangers and radiotracer setup

Subsequently, the movement of the radiotracer within the system was monitored at five strategically selected locations using NaI(Tl) detectors and data recorded at pre-set intervals of one second as Shown in Fig. 1. If a leak were present in the heat exchanger system, a radiotracer peak would be observed in detectors D2 and D3, which are located in the low-pressure stream (marked in red line). However, in this study, no radiotracer signal was detected in D2 and D3, confirming the absence of any leaks in the heat exchanger system. The reproducibility of the results was verified by conducting two repeated radiotracer measurements.

References :

- [1] Leak Detection in Heat Exchangers and Underground Pipelines Using Radiotracers, *IAEA Guide Book*, Training Course Series No. 38, IAEA, Vienna (2009).

Production of ^{89}Zr via Indigenously Developed Solid Target: Evaluation of Radiation Safety Parameters using the FLUKA Code

K. Kushwaha¹, B. Keshavkumar², N. S. Baghel¹, S. Banerjee^{3,4,§}

¹Radiation Medicine Centre, BARC, Mumbai 400012, India,

²Health Physics Division, BARC, Mumbai 400085, India

³Advanced Centre for Treatment, Research and Education in Cancer, TMC, Navi Mumbai 410210, India

⁴Homi Bhabha National Institute, DAE, Mumbai 400094, India

§Email: banerjeesharmila2207@gmail.com

An indigenous semi-automated solid target assembly has been developed at the Radiation Medicine Centre (RMC), for use in production of medically important radioisotopes, in the Medical Cyclotron Facility (MCF). It is necessary to ensure satisfactory radiation safety while using this target assembly for radioisotope production in the MCF. In view of this requirement, various radiation safety parameters have been evaluated theoretically, during ^{89}Zr production, using this solid target assembly.

A 150 μm thick yttrium target with irradiation condition of 25 μA proton current for 30 minutes was considered for the theoretical calculation. The radiation safety parameters such as neutron and photon yields, corresponding ambient dose-equivalent rates, production yield and photon ambient dose-equivalent decay rates with time, after end of bombardment (EOB), have been evaluated, during the production of ^{89}Zr via the $^{89}\text{Y}(p,n)^{89}\text{Zr}$ nuclear reaction route, using Fluka Monte Carlo code.

The neutron and photon yield and their corresponding ambient dose-equivalent rates are found to be $8.01\text{E}+04 \text{ cm}^{-2}\mu\text{A}^{-1}\text{s}^{-1}$, $3.33\text{E}+05 \text{ cm}^{-2}\mu\text{A}^{-1}\text{s}^{-1}$, $1.06\text{E}+02 \text{ mSvh}^{-1} \mu\text{A}^{-1}$ and $6.83 \text{ mSvh}^{-1} \mu\text{A}^{-1}$ respectively at 100 cm distance from the target assembly. With these illustrated dose rates, the calculated radiation field outside the 2 m thick concrete shielding is found to be well below the permissible limit ($< 1 \mu\text{Svh}^{-1}$). The theoretically estimated total activity of ^{89}Zr obtained is 5 mCi. Fig-1 illustrates that the photon dose-rate becomes reasonably low, $1.84\text{E}-02 \text{ mSvh}^{-1} \mu\text{A}^{-1}$ at 30 cm from the target assembly, after 6 h decay.

This study confirms that production of ^{89}Zr in sufficient quantity is feasible at RMC with adequate radiation safety. After irradiation the transfer of irradiated target disc to the chemical processing laboratory is semi-automated and personnel intervention is needed. Therefore, 6 h decay is essential to minimize the radiation exposure during this process.

References:

- [1] Battistoni G, Cerutti F, Fassò A, et al (2007) *The FLUKA code: Description and benchmarking*. In: *AIP Conference Proceedings*. AIP, pp 31–49.

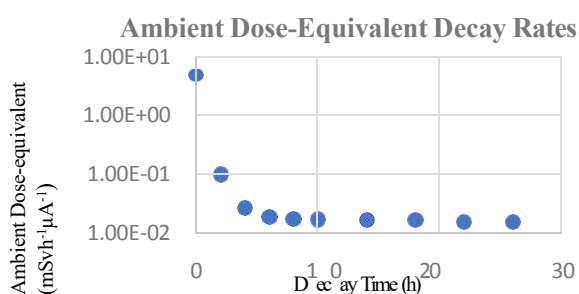


Fig-1 Ambient dose-equivalent

Effects of Gamma Radiation on Corrosion Behaviour and Hardness Properties of AA6061-T6

Deepa Singh^{1,2}, Neeraj Bisht^{1,2,§}, Virendra Singh^{3,4}, B.C. Chanyal^{3,4}

¹*Department of Mechanical Engineering, G .B. Pant University of Agriculture and Technology, Pantnagar (Uttarakhand), India*

²*College of Technology, Pantnagar (Uttarakhand), India*

³*Department of Physics, G .B. Pant University of Agriculture and Technology, Pantnagar (Uttarakhand), India*

⁴*College of Basic Science and Humanities, Pantnagar (Uttarakhand), India*

§Email: neerajbisht30@gmail.com

This study investigates the influence of varying doses of gamma (γ) radiation on the hardness and corrosion behaviour of an aluminium alloy (AA6061-T6) before and after exposure to simulated marine environments. The primary objective was to investigate the correlation between radiation exposure and hardness and corrosion resistance of the AA6061-T6 aluminium alloy. Multiple samples (20 mm \times 20 mm \times 3 mm) were exposed to varying doses ranging from 60 to 260 kGy and compared with an untreated control sample. The influence of γ -radiation was divided into two phases: In the first phase, the hardness of the untreated sample was 49.5 HRB while an increase in hardness to 55.5 HRB was observed for 60 kGy to 76.1 HRB for dosage of 180 kGy, however further increase of radiation dosage from 180 kGy to 260 kGy resulted in a drop in hardness to 60.1 HRB. In the second phase the effects of radiation on corrosion resistance and hardness due to simulated long-term marine exposure was studied. In the second phase, the various irradiated samples were immersed in distilled water with 3.5 % NaCl solution (seawater condition) for 12-days, followed by 7-day exposure to atmospheric conditions of February 2025 in Pantnagar. The results showed a negligible change of 0.03% in the untreated sample, whereas the samples exposed to high radiation doses of 260 kGy exhibited a maximum weight loss of 0.07%, demonstrating increased susceptibility to corrosion at higher radiation doses. At higher radiation dosage there was a higher susceptibility to corrosion. Upon simulated marine exposure, all the samples showed a significant reduction in hardness, the reduction pattern was however similar to what was observed before marine simulations. The hardness of the samples irradiated at 180 kGy showed maximum hardness. In conclusion, the hardness increased as the radiation dose increased upto 180 kGy (peak hardness), with a 53.8% increase from the initial hardness of 49.5 HRB to 76.1 HRB. However, a reduction in hardness was noted at high doses, with the 260 kGy sample recording a 21.2% loss at 60 HRB before exposure to seawater conditions. Corrosion negatively affected the hardness of AA6061-T6, as evidenced by a 27.7% loss in the hardness of the untreated sample and a 45.1% loss in the 260 kGy sample. The results reveal that hardness can be improved by gamma ray irradiation but the radiation dosage has to be optimized. The γ -ray treatment can be a viable method to improve mechanical properties of metals.

Increased Efficacy of ^{177}Lu -DOTA-BASS Antagonist Peptide Over ^{177}Lu -DOTA-TATE Agonist Peptide using ^{177}Lu of Low to Medium Specific Activity in AR42J Cells

Rani G. *, Shalaka Paradkar, Sheela M., Navin Sakhare, Laxman Ram, Sanjeev Kumar, Anupam Mathur, Vijay Kadwad, Usha Pandey

Radiopharmaceutical Laboratory, Board of Radiation and Isotope Technology,
Navi Mumbai, India.

*Email: rani@britatom.gov.in

^{177}Lu -DOTA-TATE (TATE= $\overline{\text{FCYWKTCCT}}$) is an established clinical agent used for treatment of sstr positive Neuroendocrine tumors (NET). TATE belongs to the family of agonist peptide that gets internalized into the cell post binding onto the sstr receptor. Since antagonists binds to more sites higher peptide amounts can be infused for patient treatment. Hence ^{177}Lu activity with medium to low specific activity (10-15 Ci/mg) on complexation with antagonist peptides can be therapeutically more effective than ^{177}Lu -DOTA-TATE for treatment of NET cancer types. In this view, *in vitro* cell uptake studies of ^{177}Lu -DOTA-BASS (antagonist peptide complex; BASS= $\overline{\text{FCYWKTCTCY}}$) in comparison to ^{177}Lu -DOTA-TATE were conducted at different specific activities to ascertain the aforementioned advantage. ^{177}Lu -DOTA-BASS and ^{177}Lu -DOTA-TATE complexes were prepared following identical protocols, except that complexes were prepared at different molar ratios (metal to peptide) of 1:5 in case DOTA-BASS and 1:2 for DOTA-TATE. The complexes were synthesized on reaction of $^{177}\text{LuCl}_3$ (100 mCi; 15 Ci/mg) with peptide in appropriate amount in acetate buffer (pH 5) at 90 °C for 45 min. The radiolabeling yields observed in each case as analyzed by HPLC [H_2O (0.1%TFA; A) + AcN (0.1%TFA; B) 0-4 min 95% A, 4-15 min 95%-5% A, 15-20 min 5% A, 20-25 min 5%-95% A and 25-30 min 95% A; Product: R_t ~16-17 min] and PC (AcN: H_2O / 1:1 v/v; Product: R_f 0.5-1.0) was more than 98%. A total of three formulations (0.65 mCi/nmol 0.3 mCi/nmol and 0.15 mCi/nmol) were prepared for carrying out the cell experiments. To ascertain the non-specific binding (NSB), triplicate wells were treated with excess cold peptide (DOTA-TATE or DOTA-BASS) 30 min prior to radiotracer addition. The specific uptake was calculated on subtraction of %NSB from total % uptake (Figure 1). ^{177}Lu -DOTA-BASS showed higher uptake than ^{177}Lu -DOTA-TATE at all the specific activities as known for the antagonist peptide. Also, the percentage decrease in the cell uptake results for antagonist peptide is far lower in comparison to agonist peptide. The latter point highlights the advantage of using radiolabeled antagonist over agonist peptide on using ^{177}Lu of low to medium specific activity for clinical utility.

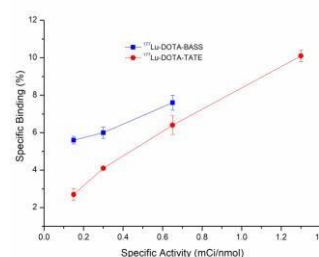


Figure 1: Cell binding results

Role of PET-CT Imaging in Neurobehavioral Studies Influenced by Pheromones in C57BL/6 Mice

Yogita Shete^{1,§}, Anushka Patil², Swati Baghul¹, Avik Chakraborty¹, Sandip Basu¹

¹ Radiation Medicine Centre, BARC, C/o TMH Annexe, Parel, Mumbai-400 012

² Department of Biotechnology, The Institute of science, Dr. Homi Bhabha State University

§Email: yogeshwarivet@gmail.com

Laboratory animals are utilized as an *in-vivo* test model for biomedical research and neurobehavioral studies to estimate the safety for clinical trials. The Pheromone essences affect the biochemical process and induces behavioural changes in the mice like anxiety, pain, stress and aggression. This altered behaviour has an additional impact on drug metabolism and organ pathology in experimental animals. Usually, physical examination of animals has the preferred method in neurobehavioral changes. However, it has limitations due to hiding behaviour shown in mice naturally. The real-time visualization method is required to understand the effect and mechanism with animal behaviour changes. This will help to compare the behavioural alteration and neuronal activity in the animals. The effect of volatile pheromones (*Eucalyptus oil*) evaluated by studying the behaviour panel test and its correlation with brain uptake using ¹⁸F-FDG radiopharmaceutical. Under this study, C57BL/6 mice (n=12) were divided as control and treated groups. *Eucalyptus oil* was used at different concentrations for a period of 5 weeks with a cotton ball. Clinical haematology and whole-body ¹⁸F-FDG PET-CT scan (dose 100µCi) done in both treatment and control mice. Animal behaviour studies showed no effect on nesting, grooming and locomotor activity in the treated but time taken for formation of nests was slightly more as compared to control animals. In elevated maze test exploration, no anxiety was seen in both the groups. In T- maze, no effect was seen on spatial learning and long-term spatial memory loss as compared to control. The observed and confirmed brain PET-CT scan in C57BL/6 mice showed significantly increased brain uptake in treated male and female animals (Max 6.8 and 5.1SUV) as compared to control group (Max 2.1 and 1.6 SUV) respectively. All of the animals that were treated saw an increase in olfactory uptake, which coincided with neurobehavioral nest formation during PET-CT uptake. Further no significant adverse haematological changes seen in both the groups. No adverse pathological changes seen in the brain post treatment, and it is comparable to control brain morphology (Fig.1). In conclusion, nuclear imaging techniques play a pivotal role in defining the metabolic activation of olfactory part in response to volatile stimulus but there is no alteration in the natural behaviour and adverse effect on the animals. Nuclear medicine technique is superior in understanding of neurobehavioral changes over the traditional animal behaviour method.

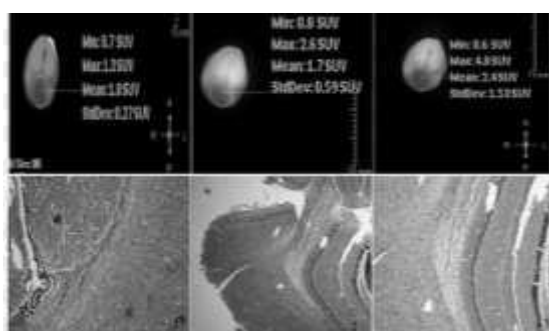


Fig.1: Brain PET-CT imaging and histology of C57BL/6 mice: Brain PET-CT showed increased uptake in treated animals as compared to control. Normal brain histopathology in both the group stained with H and E stain 100x

References:

[1] Uecker, A., et al. *Neurobiology of aging*, **21.5** (2000): 705

Radiation Grafting: An Innovative Strategy for Designing Tailored Surfaces

N. K. Goel^{1, §}, S.A. Shelkar¹, Sanju Francis, Virendra Kumar^{1,2}, Y.K. Bhardwaj^{1,2}

¹Radiation Technology Development Division,

Bhabha Atomic Research Centre, Trombay, Mumbai-400085, India

²Homi Bhabha National Institute, Anushaktinagar, Mumbai-400085, India

§Email: ngoel@barc.gov.in

Surfaces of synthetic polymers like PP, PE, PTFE or natural polymers cellulose etc. can easily be modified to design polymers with targeted functionality. Properties like hydrophilicity, ion exchangeability, pH sensitivity, thermo-sensitivity, antibacterial property etc., can easily be incorporated in to an existing polymer. The paper will provide an overview of grafting describing in detail the grafting process, grafting mechanism, grafting methods, and factors affect the grafting process.

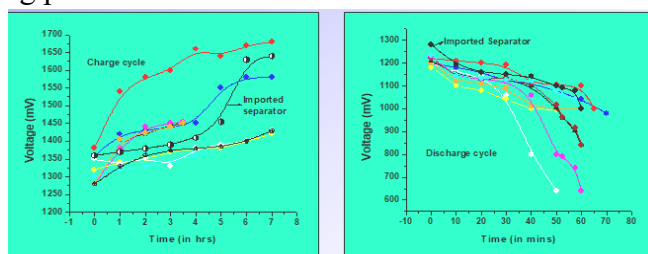


Fig.1. Charging-discharging of Ni/Cd batteries using grafted and imported battery separator

Two case studies will be presented where radiation grafting altered the surface to functionalise the base polymer PP and cotton to add ion exchangeability and antibacterial properties respectively. Radiation grafted PAA-g-PP was functionalised for adding carboxyl group for battery separator applications in Ni/Cd batteries [1]. The membranes grafted to an extent of ~20% were found to perform comparably with the presently being used by battery industry (Fig.1).

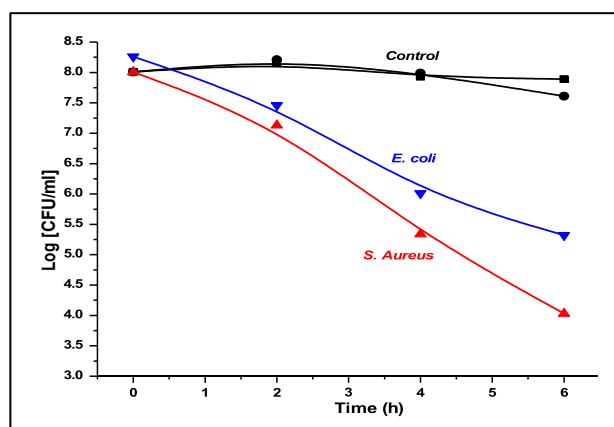


Fig.2. Antibacterial grafted cellulose

Antibacterial cotton refers to cotton fabric that has been treated or modified to have antibacterial properties, which help prevent the growth and spread of bacteria. In Fig. 2, quaternary ammonium-based monomer has been grafted to add antibacterial efficacy [2]. This modification can enhance the fabric's hygiene, reduce odour, and make it more suitable for applications where cleanliness is important, such as in medical textiles, sportswear, or everyday clothing.

References:

- [1] N.K. Goel, et. al., *Expr. Polym. Lett*, **3** (2009), 268
- [2] N.K. Goel, et. al, **80** (2011), 1233.

Performance Assessment of X-ray DRCT Image Display and Interpretation System for NDT Analysis of Concrete Specimens

Janaki S Nair², Lakshminarayana Y¹, Anant Mitra¹, Rajesh Acharya¹, Umesh Kumar¹

¹Industrial Tomography and Instrumentation Section, BARC, Mumbai, India

²Department of physics, Cochin University of Science and Technology, Kerala, India

§Email:laxmany@barc.gov.in

Non-destructive Testing (NDT) imaging is crucial for assessing the quality of ordinary concrete in structures like bridges and buildings, as well as Radiation Shielding Concrete (RSC) used in nuclear and medical facilities. X-ray Digital Radiography and Computed Tomography (DRCT) are key NDT tools for both concrete types. Before inspecting an object, evaluating the DRCT display system is essential for ensuring reliable inspections and high-quality radiographs. This paper presents the performance assessment of the DRCT display and interpretation system, along with the evaluation of ordinary and RSC for nuclear applications. Visual and quantitative assessments were done as per relevant international standard for the performance of the DRCT display system using the SMPTE RP 133 test pattern method. Key image quality parameters measured were contrast and brightness, uniformity, Modulation Transfer Function (MTF) at different spatial resolutions and temporal performance over three month period. Spatial resolution was characterized using the MTF as calculated below:

$$\text{MTF (\%)} = ((\text{GV}_{\max} - \text{GV}_{\min}) / (\text{GV}_{\max} + \text{GV}_{\min})) \times 100 \quad (1)$$

Where GV_{\max} and GV_{\min} represent maximum and minimum grey values, respectively.

Figure 1 shows line profiles of 100% contrast lines at center and in all four corners of the phantom which were used for MTF measurement. The data collected from temporal studies, including graphs for spatial resolution and uniformity, offers practical insights into system reliability. Uniformity study reveals grey squares at 50% picture level background were free from artifacts. Contrast and brightness testing shows 5% DDL patch in the 0% DDL patch and a 95% DDL patch in the 100% DDL patch were clearly perceptible. The experimental results show that the DRCT image display system meets the required performance standards, ensuring stable and accurate image rendering for industrial NDT applications. voids/air pockets have been detected in concrete specimen.

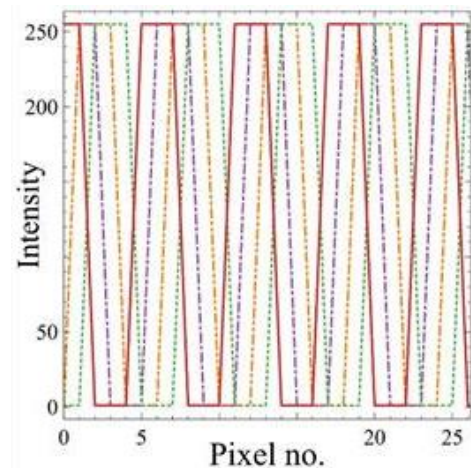


Fig.1:MTF measurement

Acknowledgement: The authors wish to express their sincere gratitude to the Associate Director of RC&IG at BARC, Mumbai, HBNI, and CUSAT for their continuous support and encouragement.

References:

- [1] ASTM E-2698, "Standard Practice for Radiological Examination Using Digital Detector Arrays", 2010.
- [2] J. E. Gray, "Use of SMPTE test pattern in picture archiving and communication systems", *J. Digit Imaging* 5, pp 54–58, 1992.

Influence of Gamma Irradiation on Physico-Chemical, Thermodynamic, Electro-Chemical, and Surface Properties of Superhydrophobic Coatings

Sonali B. Jadhavar¹, Prashant P. Chikode², Satish A. Mahadik³, Rajiv S. Vhatkar¹

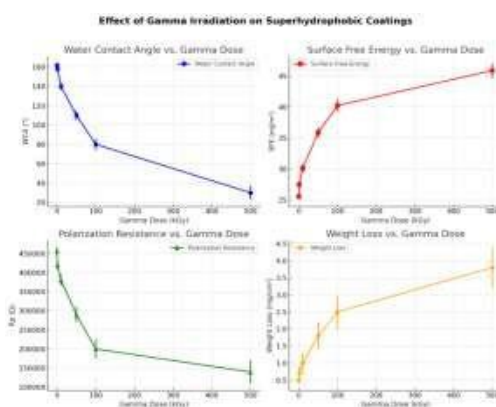
¹Department of Physics, Shivaji University, Kolhapur

²Department of Physics, Jaisingpur College, Jaisingpur

³Department of Physics, Sanjay Ghodawat University, Kolhapur

§Email: rsv_phy@unishivaji.ac.in

This study investigates the effects of gamma irradiation on ORMOSIL and polypropylene (PP) nanocomposite -based superhydrophobic coatings. ORMOSIL/PP nanocomposite coatings were synthesized via dip-coating and exposed to gamma irradiance doses ranging from 1 kGy to 500 kGy. The surface roughness decreased from 0.032 μm to 0.027 μm at 10 kGy, and the water contact angle (WCA) dropped from 162° to 30° at 500 kGy, indicating a transition from the Cassie-Baxter to the Wenzel state. Subsequently, surface free energy (SFE) increased from 25.58 mJ/m^2 to 45.89 mJ/m^2 , due to the formation of polar groups, which enhanced surface wettability. Gamma irradiation also led to a decline in corrosion resistance, with polarization resistance (R_p) decreasing from $4.569 \times 10^5 \Omega$ to $1.3945 \times 10^5 \Omega$ and inhibition efficiency dropping from 97.15% to 90.67%. Thermal analysis showed increased weight loss across various temperature ranges, highlighting accelerated degradation.



The activation energy (E_a) decreased from 24.79 J/mol at 0 kGy to 20.36 J/mol at 500 kGy, indicating weakened molecular bonds and faster phase transformations. Additionally, the band gap narrowed from 4.25 eV to 4.05 eV, improving optical absorption. These modifications suggest that gamma irradiation degrades superhydrophobic properties at high doses, altering their performance in ways that may limit their effectiveness in certain applications. Balancing irradiation benefits with surface stability will be key to advancing next-generation coatings for aerospace, nuclear, and medical applications.

References:

- [1] Y. Zhang, J. Zhang, Y. Liu, Superhydrophobic Surface with Gamma Irradiation Resistance and Self-Cleaning Effect in Air and Oil, *Coatings*. 10 (2020) 106.
- [2] A. Hooda, M.S. Goyat, J.K. Pandey, A. Kumar, R. Gupta, A review on fundamentals, constraints and fabrication techniques of superhydrophobic coatings, *Prog. Org. Coatings*. 142 (2020) 105557.

Investigating the Correlation Between Mechanical Properties and Water Absorption in Gamma-Irradiated Jute/SiC Composites for Enhanced Durability in Moisture-Sensitive Applications

Deepa Singh^{1,§}, Neeraj Bisht², Deepak Yadav², Sonika Chauhan²

¹Department of Mechanical Engineering, G .B. Pant University of Agriculture and Technology, Pantnagar (Uttarakhand), India

²College of Technology, Pantnagar (Uttarakhand), India

§Email: deepasingh092@gmail.com

This study investigated the effects of gamma radiation on the mechanical properties and water absorption of jute fiber-reinforced composites containing silicon carbide (SiC) filler. Natural fiber polymers, while versatile, are susceptible to water absorption, limiting their use in humid or outdoor conditions. Gamma irradiation aims to enhance durability by reducing moisture uptake. Composite samples were fabricated with varying fiber orientations (0°/90°, 30°/60°, 45°/45°) and SiC filler contents (2%, 5%, 8%). The composite with 2% SiC and 0°/90° fiber orientation exhibited the highest initial tensile strength. After achieving an optimal configuration, the resulting composites were exposed to gamma radiation doses (15–90 kGy). Tensile strength testing (UTM) revealed a slight increase up to 45 kGy. The highest tensile strength (64.8 MPa) was observed at 45 kGy, compared with the initial strength of 62 MPa of the control sample. However, further increases in radiation dose (75-90 kGy) led to a decrease in tensile strength, reaching 60.93 MPa at 90 kGy (Fig. 1) [1]. Gamma radiation has a limited positive effect on mechanical properties and can be detrimental at higher doses [2]. The impact of gamma radiation on water absorption, assessed by immersing the samples in distilled water for seven days, was more pronounced. Lower radiation doses (15-30 kGy) promoted crosslinking, reducing water absorption from 4.26% to 4.05%. At 45 kGy, water absorption reached a minimum of 3.89%, indicating optimal crosslinking. Higher doses (75-90 kGy) resulted in increased water absorption (up to 4.35%) due to degradation (Fig. 2) [2]. In conclusion, gamma irradiation effectively reduced water absorption, especially at 45 kGy. This makes these gamma treated composites suitable for applications like automotive interiors, outdoor construction, and agricultural equipment, which require moisture resistance. This study highlights the potential of gamma-treated natural fiber composites for enhanced durability in humid environments.

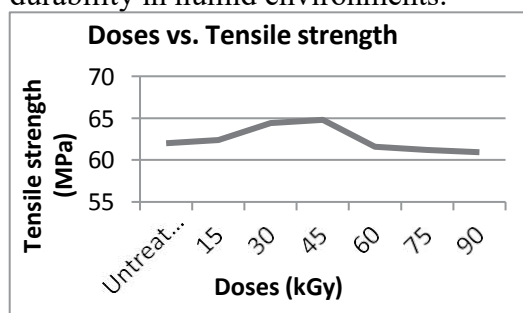


Fig. 1: Effect of gamma radiation on tensile strength

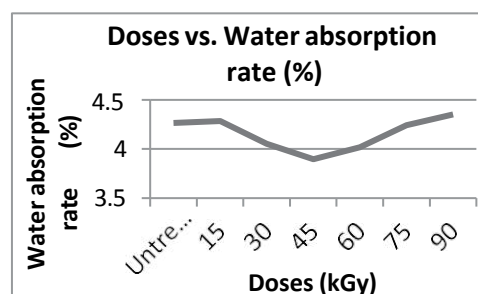


Fig. 2: Effect of gamma radiation on water absorption rate

References:

- [1] Motaleb, K. and Z. M., Islam or M. S. et.al., *Fibres & Textiles in Eastern Europe*, **27** (2019) 88.
- [2] Shifa, S. S. and Kanok, M. M. H. or Haque, M. S et.al., *Hybrid Advances*, **5** (2024), 100181.

Ultraviolet and Visible-Emitting Bi³⁺-activated phosphor with Efficient Radioluminescence under X-ray Excitation

Annu Balhara^{1,2}, Priyansu Mishra^{1,3}, Mohit Tyagi^{2,4},
Santosh K. Gupta^{1,2, §}, K. Sudarshan^{1,2}, S. Jeyakumar^{1,2}

¹Radiochemistry Division, Bhabha Atomic Research Centre, Mumbai-400085, India

²Homi Bhabha National Institute, Mumbai-400094, India

³Mithibai College, Mumbai-400056, India

⁴Technical Physics Division, Bhabha Atomic Research Centre, Mumbai-400085, India

§Email: santoshg@barc.gov.in

This study focuses on the luminescent properties of Ca₃Ga₂Ge₃O₁₂:Bi³⁺ (CGGO: Bi³⁺) phosphors for efficient radioluminescence and x-ray imaging. [1, 2] The Bi³⁺-doped phosphors exhibit strong emissions in the UV-A and blue regions under 275 nm UV and X-ray excitation (Fig.1a). Additionally, Bi²⁺ ions show near-infrared (NIR) emissions following X-ray excitation (Fig.1), highlighting the ability of these materials to emit across a broad spectrum from UV to NIR. This tunable luminescence makes the phosphors ideal candidates for anti-counterfeiting, optical storage, security, and biomedical imaging. Positron annihilation lifetime spectroscopy (PALS) studies (Fig.1b) were used to investigate the defect structures and the nature of the vacancies. With initial doping of Bi, the intensity of the second positron annihilation lifetime drastically increased along with decrease in the short lived positron lifetime and intensity showing huge trapping of positrons. However, trapping reduced at higher concentrations. Based on PALS data it can be concluded that initial doping resulted in cation vacancies due to aliovalent doping of Bi³⁺ at Ca²⁺ site while at higher doping concentration, antisite are being formed.

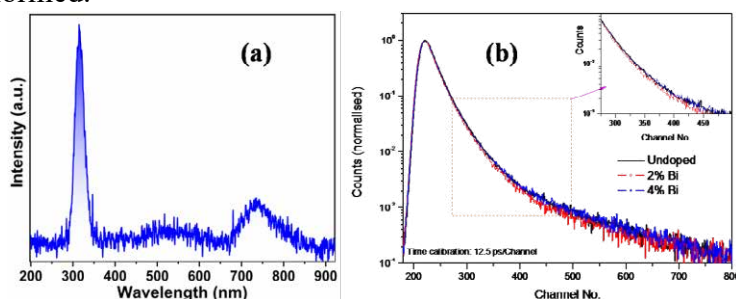


Fig.1: (a) X-ray excited emission and (b) Typical positron annihilation lifetime spectra of CGGO: Bi³⁺ phosphor

The phosphors also exhibited persistent luminescence and thermoluminescence properties, with studies revealing the trap levels and codoping effects of Bi³⁺ ions. These findings are essential for understanding the material's performance in applications that require long-lasting afterglow and stable emission under excitation. In conclusion, the Ca₃Ga₂Ge₃O₁₂:Bi³⁺ phosphors demonstrate strong radioluminescence across UV-A, blue, and NIR regions, making them promising candidates for X-ray imaging and health-related applications. The combination of broad emission spectra, robust performance under excitation and insights from DFT and PALS studies position these materials as valuable for advanced imaging technologies and biomedical diagnostics.

References:

- [1] Y. Wei and J. Wang, *ACS Applied Materials & Interfaces*, **16** (2024) 56519.
- [2] C. Richard and B. Viana, *Light: Science & Applications*, **11** (2022) 123.

Design and Fabrication of an Automated Module for Formulating Clinical Doses [^{177}Lu]Lu-DOTA-Trastuzumab Using Medium Specific Activity, Carrier Added [^{177}Lu]LuCl₃

Aaditya Shah^{1,*}, Arpit Mitra¹, Varun Nair¹, Mohini Guleria², Jeyachitra Amirdhanayagam², Anupam Mathur¹, Usha Pandey¹, Tapas Das²

¹Radiopharmaceutical Laboratory, BRIT, Navi Mumbai, India.

²Radiopharmaceuticals Division, Bhabha Atomic Research Centre, Mumbai, India.

*Email: aaditya.shah@britatom.gov.in

In recent years, radio-immunotherapy (RIT) using [^{177}Lu]Lu-DOTA-Trastuzumab has gained prominence in management of HER-2 overexpressed breast cancer patients. Here we have designed and fabricated an automated radiochemistry module for the formulation of patient doses of [^{177}Lu]Lu-DOTA-Trastuzumab using pre-synthesized freeze dried DOTA-Trastuzumab kit.

The indigenous automated module (Figure 1) developed comprised of (i) control unit and (ii) chemical processing unit. The control unit is Programmable Logic Controller (PLC) based where the flow of reagents is maintained using 3/2- or 2/2-way solenoid valves connected by 1/8" TEFZEL tubing and customized 1/4-28 flange-less ferrule type PEEK fittings. The chemical control unit is composed of (i) raw material vessel (ii) reaction vessel fitted with thermostat controlled dry heater (iii) two reservoirs and (iv) slot for holding purification column (PD-10).

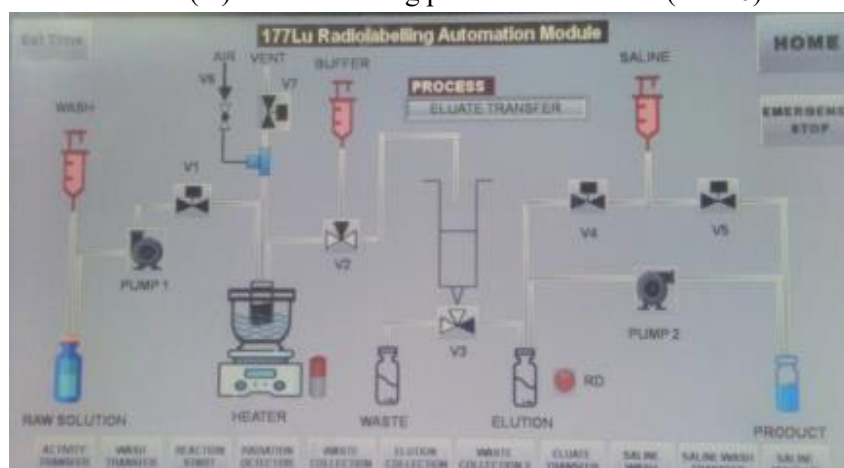


Fig. 1: Schematic of Automated Module

Briefly in a typical batch, [^{177}Lu]LuCl₃ (~ 50 mCi in 30 μL ; 22.41 mCi/ μg) was added to radiolabeled reaction mixture was transferred to preconditioned PD-10 column and [^{177}Lu]Lu-DOTA-Trastuzumab (24.8 mCi) was eluted using 0.2 M acetate buffer (pH 5.6) in collection vial. The purified [^{177}Lu]Lu-DOTA-Trastuzumab (24.8 mCi in 2.0 mL) was suitably diluted with saline so as to achieve final concentration ~ 8 - 10 mCi/mL. Finally, the [^{177}Lu]Lu-DOTA-Trastuzumab was passed through 0.22 μm PES membrane syringe filter to product collection vial. The radiochemical yield (RCY) of the formulation was 49.82 \pm 3.14% (n=3), while the radiochemical purity (RCP) of the formulation was 98.95 \pm 0.08% (n=3) as estimated by radio-TLC. To conclude, the present study merits the availability of cost-effective RIT for patients on a routine basis in hospital radiopharmacy settings using the developed automated radiochemistry module.

Single Optimized Protocol for Formulation of Multiple Patient Doses of Different [¹⁷⁷Lu]Lu- based Radiopharmaceuticals using Low Specific Activity, Carrier Added [¹⁷⁷Lu]LuCl₃

Sudeep Kumar Sahu^{1§}, Sangita Lad¹, Avik Chakraborty^{1,2}, Arpit Mitra³,
Megha Tawate^{1,2}, Mukti Kanta Ray¹, Sandip Basu^{1,2}

¹Radiation Medicine Centre, BARC, Mumbai, India.

²Homi Bhabha National Institute, Mumbai, India.

³Radiopharmaceutical Laboratory, BRIT, Navi Mumbai, India.

[§]Email: sudeep.sahu4@gmail.com

Peptide Receptor Radioligand Therapy (PRRT) using [¹⁷⁷Lu]Lu-labeled radiopharmaceuticals has gained prominence in therapeutic practices. The present work describes a single optimized protocol for radiochemical synthesis of multiple patient doses of [¹⁷⁷Lu]Lu-FAPI-46 and [¹⁷⁷Lu]Lu-PSMA-617 using carrier added (ca) [¹⁷⁷Lu]LuCl₃ with specific activity (SA) as low as 11–14 mCi/μg. Multiple patient doses of [¹⁷⁷Lu]Lu-FAPI-46 (~0.6 Ci equivalent to 3-4 patient doses, n=4) and [¹⁷⁷Lu]Lu-PSMA-617 (~1.2 Ci equivalent to 5-6 patient doses, n=5) were prepared using low specific activity [¹⁷⁷Lu]LuCl₃. Each of these [¹⁷⁷Lu]Lu-labeled formulations were carried out at metal:ligand molar ratios of 1:2.0 in 0.22M CH₃COONH₄ buffer containing gentisic acid (15 mg/mL). The radiolabeling reaction was carried out pH ~4.3 and incubated at 95°C for 60 minutes. The reaction mixture was further diluted with same buffer and final radioactive concentration for both the formulations were maintained at ~30 mCi/mL and further these formulations were filtered using 0.22 μm PES membrane syringe filter. The radiochemical purity (RCP) were estimated by radio-HPLC. The specific activity for each of these products was > 1.0 mCi/μg, while the peptide concentration per patient doses (200 mCi) was found to be < 190 μg compiling with EANM guidelines as describe in below Table. The consistent and reliable RCY and RCP of multiple [¹⁷⁷Lu]Lu-labelled tracers produced by single optimized radiochemistry protocol exhibits the versatility of the low specific activity, carrier added [¹⁷⁷Lu]LuCl₃ produced at medium flux research reactor by (n, γ) nuclear reaction. The formulated [¹⁷⁷Lu]Lu-PSMA-617 has shown desirable uptake in lesions of patients with prostate cancer.

Description	Specifications of [¹⁷⁷ Lu]Lu-PSMA-617 (Pluvicto™)	QC parameters of the produced [¹⁷⁷ Lu]Lu-FAPI-46	QC parameters of the produced [¹⁷⁷ Lu]Lu-PSMA-617
Characteristics of the Solution	Clear & Pale yellow color	Clear & Pale yellow color	Clear & Pale yellow color
pH	4.0 – 8.0	~ 5.0 – 6.0	~ 5.0 – 6.0
RAC	≥ 20 mCi/mL	~ 30 mCi/mL	~ 30 mCi/mL
SA of [¹⁷⁷ Lu]LuCl ₃	> 10 mCi/μg	12 – 14.76mCi/μg	11.25 – 14.76mCi/μg
RCY*	ND	(96.23±0.44)%	(96.4±0.44)%
RCP	> 98%	(99.31±0.47)%	(99.26±0.66)%
SA of Final Product	1-2 mCi of ¹⁷⁷ Lu/μg of Ligand	1.42±0.10 mCi/μg	1.13±0.13 mCi/μg

RAC: Radioactive Concentration, RCY*: Non-decay Corrected Radiochemical yield, ND: Not Defined, RCP: Radiochemical purity, #Single patient dose: 200 mCi, V: Total Volume of Injection

Energy-Dependent Attenuation Properties of Water-Soluble Inorganic Compounds in the 10 keV–1333 keV Gamma-Ray Regime: A Shielding- Oriented Study

Sneha Dinkar Sanap^{1,*}, S.R. Mitkari¹, Anil V. Raut², Pravina P. Pawar³

¹*Department of Physics, Shri. Siddheshwar Mahavidyalaya, Majalgaon, India*

²*Department of Physics, Vivekanand Arts, Sardar DalipSingh Commerce and Science College, Chhatrapati Sambhajanagar, India*

³*Department of Physics, Dr. Babasaheb Ambedkar Marathwada University, Chhatrapati Sambhajanagar, India*

**Email: snehasanap12@gmail.com*

This study investigates the gamma-ray shielding capabilities of zinc nitrate ($\text{Zn}(\text{NO}_3)_2$), a water-soluble inorganic compound, motivated by its unique combination of high effective atomic number (dominated by zinc, $Z = 30$), lightweight structure, and solubility properties advantageous for applications requiring flexible, portable, or eco-friendly shielding solutions, such as in medical imaging or temporary radiation containment. The mass attenuation coefficient (μ/ρ) was experimentally determined using narrow-beam geometry with a NaI(Tl) scintillation detector across photon energies (356-1333 keV), validated against Phy-X software. Experimental uncertainties, including statistical counting errors ($<2\%$) and thickness variations (± 0.01 cm), were systematically evaluated to ensure reproducibility. Results revealed that $\text{Zn}(\text{NO}_3)_2$ exhibits superior low-energy photon attenuation (μ/ρ peaks below 200 keV) compared to conventional materials like aluminum and polyethylene, while maintaining competitive performance with lead-oxide composites at higher energies (662 keV). Relaxation length (λ), half- and tenth-value layers (HVL, TVL), Z_{eff} , and N_{eff} demonstrates a pronounced thickness-dependent attenuation decline below 0.2 cm. $\text{Zn}(\text{NO}_3)_2$ offers an alternative to dense, toxic shields in scenarios prioritizing solubility, weight reduction, or environmental safety to address shielding challenges where traditional materials are impractical, balancing performance with functional adaptability [1-3].

Keywords: Phy-X; Mass Attenuation Coefficient; Gamma Ray; Shielding Materials;

Reference :

- [1] S.-C. Kim, Analysis of shielding performance of radiation-shielding materials according to particle size and clustering effects, *Applied Sciences*, **11** (2021) 4010.
- [2] N.J. AbuAlRoos, M.N. Azman, N.A.B. Amin, R. Zainon, Tungsten-based material as promising new lead-free gamma radiation shielding material in nuclear medicine, *Physica Medica*, **78** (2020) 48- 57.
- [3] M. Hasan, S. Sugiharto, S. Astutiningsih, Gamma radiation shielding properties of slag and fly ash- based geopolymers, *Atom Indonesia*, **47** (2021) 173-180.

Gamma Radiolytic Synthesis of Polybis[2-(methacryloyloxy)ethyl] Phosphate Stabilized Gold Nanoparticles: an Efficient Sensor for LSPR Shift Based Detection of U(VI)

S.A. Shelkar¹, N. Misra^{1,2,§}, S. Rawat^{1,2}, V. Kumar^{1,2}

¹Radiation Technology Development Division,

Bhabha Atomic Research Centre, Trombay, Mumbai-400085, India

²Homi Bhabha National Institute, Anushaktinagar, Mumbai-400085, India

§ Email: nilanjal@barc.gov.in

In this work, we report the facile synthesis of a polybis[2-(methacryloyloxy)ethyl] phosphate (PB2MP) stabilized gold nanoparticles system (PB2MP-Au NPs) using a chemical initiator free, toxic solvent free, room temperature based ⁶⁰Co-Gamma radiolytic synthesis approach. The method involves the simultaneous reduction of Au³⁺ precursor ions and their stabilization by the PB2MP polymer chains generated during the irradiation process. Parameters such as radiation dose, solvent polarity, monomer concentration and precursor concentration were optimized to arrive at uniformly dispersed, spherical nanoparticles, as determined by UV-visible spectrophotometry. TEM and Particle Size Analyzer data revealed the nanoparticle size to be in the region of 6-8 nm, with the hydrodynamic size being ~15 nm. Zeta potential measurements within the ±10 mV domain indicated the nanoparticles to be sterically stabilized. These nanoparticles were observed to undergo spectral shift in their LSPR band in the presence of trace amounts of U(VI) solution, with the decrease in OD being linearly proportional to the increase in U(VI) concentration in the range of 5-80 ppb, the limit of detection (LOD) being 0.2 ppb. The method was validated through quantification of U(VI) in water samples spiked with known U(VI) concentrations, the results being comparable to those reported using standard ICP-OES method.

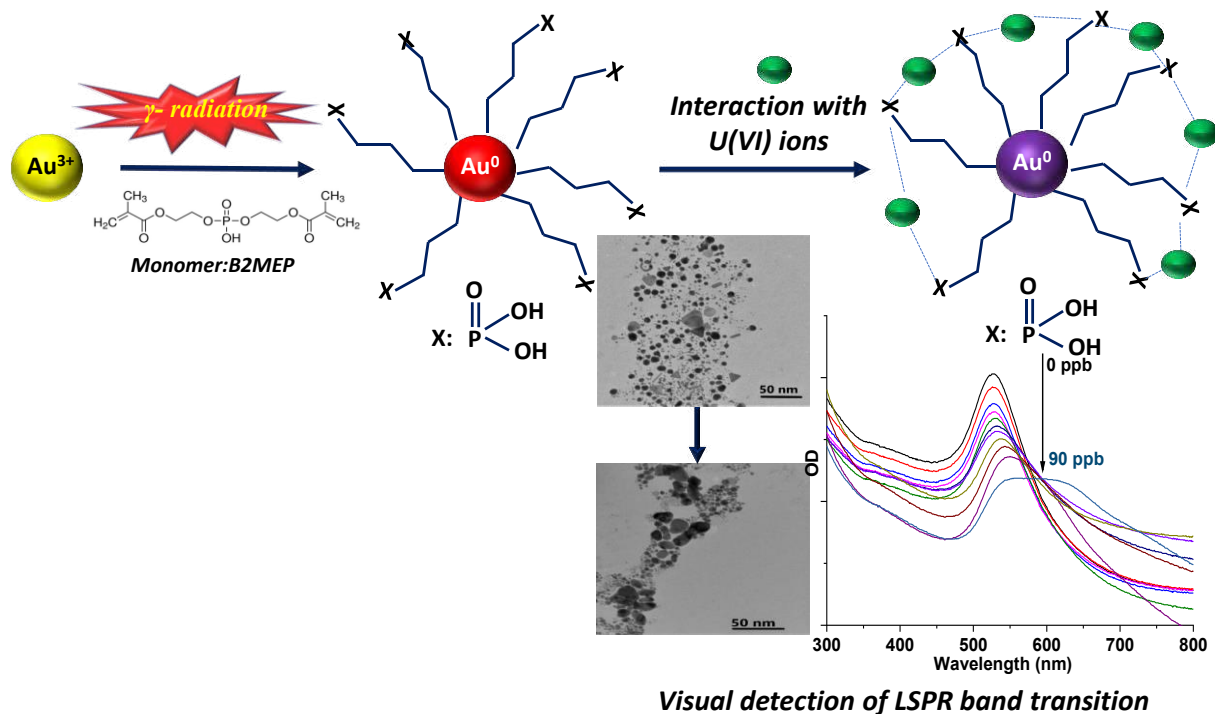


Fig. 1: Schematic of spectrophotometric detection of U(VI) using PB2MP-Au NPs

Analysis of Sedimentary Organic Carbon Sources in Mumbai Harbour Bay

V. B. Yadav^{1§}, Vandana A. Pulhani^{1,2}, A. Vinod Kumar^{1,2}

¹Environmental Monitoring and Assessment Division, BARC, Mumbai, India - 400 085

²Homi Bhabha National Institute, Anushaktinagar, Mumbai, India- 400 094

§Email: vbyadav@barc.gov.in

Coastal and estuarine environments play an important role in the global carbon and nitrogen cycles. The continental margin is essential for understanding biogeochemical processes at a global scale as these regions sequestered more than 90% of the carbon in marine system. Mumbai Harbour Bay (MHB), is heavily influenced by various anthropogenic activities, which significantly affect the composition and distribution of organic matter within sediments. In present study, stable isotope ratio of carbon and nitrogen ($\delta^{13}\text{C}$ and $\delta^{15}\text{N}$), and total organic carbon to total nitrogen ratio (TOC/TN) values in 4 core sediment samples (**Figure 1**), collected from MHB, were analysed using Isotope Ratio Mass Spectrometer (IRMS) system coupled with Elemental Analyser (EA) to understand the sources of sedimentary organic carbon. Stable isotopic ratios are expressed in delta (δ) notation and expressed relative to VPDB (Vienna Pee Dee Belemnite) scale and N_2 -air scale, respectively.

Table 1: Proportion of marine and terrestrial sources of organic matter in different cores

Core	Terrestrial Contribution (%)	Marine Contribution (%)
R1	46.60±11.24	53.40±11.24
R2	34.52±7.67	65.48±7.67
R3	28.71±5.35	71.29±5.35
R4	9.49±6.91	90.51±6.91



Fig. 1: Study Area

The average values for TOC (%), TN (%) and TOC/TN ratio at different sampling locations in the study area ranges from 1.86% to 2.29%, 0.16% to 0.22%, and 10.49 to 12.01, respectively. Similarly, the average values for $\delta^{13}\text{C}$ and $\delta^{15}\text{N}$ were found to vary from -23.53‰ to -21.12‰ and from 1.22‰ to 3.14‰, respectively. The organic carbon in the MHB is contributed by both the marine and terrestrial sources. A two end-member mixing model is used to estimate the fraction of the two organic carbon sources using $\delta^{13}\text{C}$ values measured in the individual cores using the method described by Krishna et al., (2018). The vertical profile of TOC and TN also suggest higher inputs of organic carbon towards the top layers of the sediment cores. While the northern region of the bay exhibits higher levels of organic matter, these sediments exhibit a greater influence from terrestrial sources compared to those from the southern part (**Table 1**). In the all the cores, strong to very strong positive correlation, between the TOC and TN indicates organic nitrogen constitutes the primary component of the TN. The relationship between $\delta^{13}\text{C}$ and TOC/TN are not statistically significant which indicates the selective degradation of sedimentary nitrogen during sediment diagenesis.

References:

[1] J. Krishna et al., *Journal of Geophysical Research: Biogeosciences*, **123** (2018) 463.

Trend Analysis of Gross Alpha and Gross Beta Activities in the Environment of Rawatbhata Rajasthan

S. N. Tiwari^{1,§}, A. K. Jain¹, M. Sisodia¹, Tejpal Menaria¹, M. C. Meena¹, I. V. Saradhi²

¹Environmental Survey laboratory, EMAD, BARC, Rawatbhata, 323307,

²Environmental Monitoring and Assessment Division, BARC, Mumbai-400085

§ Email: sntiwari@npcil.co.in

Continuous measurement of radioactivity in air borne particulate matter (PM) is important part of environmental monitoring programme at nuclear power plant site. Gross alpha and gross beta ($G\alpha$ & $G\beta$) activities in air is due to the naturally occurring radionuclides attached to aerosols, from potential releases from nuclear power plants and the long- term monitoring of $G\alpha$ & $G\beta$ provides information about trends and contribution from nuclear facilities, if any [1]. Weekly measured data of $G\alpha$ & $G\beta$ activities in airborne PM for the period 2001 to 2020 are used to study the distribution characteristics, temporal trend, and time series analysis at Rawatbhata Rajasthan site. Monitoring of $G\alpha$ & $G\beta$ is carried out by collecting PM on glass fibre filter paper of size 25cm x 20cm using Poltech make high volume air sampler with average flow rate of 1.1 m³/min. Weekly collected samples were counted for $G\alpha$ & $G\beta$ activities after delay of one week as per standard procedure [2]. During the study period, annual average concentration of $G\alpha$ & $G\beta$ activity in air PM varied from 0.03 to 0.1mBq/m³ and 0.6 to 1.4mBq/m³ respectively with measurement uncertainty of 2σ . Temporal variation of airborne annual geomean of $G\alpha$ & $G\beta$ activities during the period 2001-2020 is shown in Fig-1 and can be attributed to natural background fluctuations. Mann Kendall (MK) statistical test was used to detect any monotonic trend in measured data of $G\alpha$ & $G\beta$ activity during the study period. Statistical analysis of MK test reveals no significant trend of $G\alpha$ & $G\beta$ activities during the study period. MK test results along with statistical summary are presented in Table 1. The activity ratio of individual activity concentrations of $G\alpha$ & $G\beta$ are at the level of 0.1 that corresponds to normal ratio of ²¹⁰Po/²¹⁰Pb [3] and is comparable with most of studies conducted by Gam et.al, in Korea, Yang et.al, in Vietnam and Duenas et.al, in Spain. This finding also indicated that airborne $G\alpha$ & $G\beta$ activities in the environment are largely influenced by natural factors with negligible influence from nuclear facilities.

Table: 1 Statistical and Mann Kendall test result of $G\alpha$ & $G\beta$ activity

Parameter	Period	Range	GM	GSD	Median	Z value	P value	Trend
$G\alpha$	2001-2020	0.03-0.08	0.05	1.35	0.05	0.03	0.97	No trend
$G\beta$	2001-2020	0.61-1.39	1.09	1.26	1.13	0.32	0.74	No trend

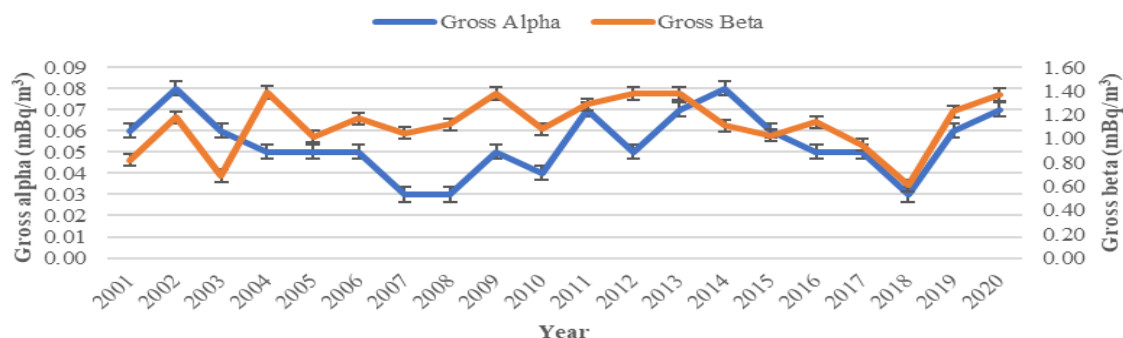


Fig. 1: Temporal variation of Geo Mean of $G\alpha$ & $G\beta$ activities (2001-2020)

References:

[1] Papastefanou, C., 2008, first ed. Radioactive aerosols, Vol 12, Elsevier Science

[2] Hegde et al, 1998, ERL Procedure Manual, BARC

[3] UNSCEAR, 2000, United Nations sales publication E.00.IX.3, United Nations, New York.

Assessment of Radiation Hazard Indices in Soil Samples and ^{222}Rn in Drinking Water of Southern Gulbarga District

S. Rajesh^{1, §}, R. Archanadevi², B. R. Kerur²

¹Department of Studies and Research in Physics, Smt V G Women's College Gulbarga, India

²Department of Physics Gulbarga University Gulbarga, India

§ Email: rajeshsiddanna@gmail.com

The human are exposed to radiation from a variety of sources including cosmic rays, natural radionuclides in water, air, soil and plants; and artificial radioactivity from fallout during nuclear testing and medical applications. This paper provides insights into the radioactivity levels in 30 samples from 3 sampling stations of the southern Gulbarga district. The environmental samples were measured for naturally occurring radionuclides (^{40}K , ^{238}U , and ^{232}Th). Southern Gulbarga district lies in the northern part of Karnataka, with a geographical area of 5000 sq. km. The northern part of the district represents a plateau, typical of Deccan Trap terrain, and is deeply indented with ravines. The study region represents undulating terrain with sparsely distributed knolls & tors.

A high-efficiency 4"X4" NaI scintillation detector-based gamma spectrometric system was adopted for the sample counting. The spectrum was analyzed by least squares spectrum analysis code is developed in FORTRAN with Visual Basic interface. The detector was surrounded by 3" thick lead shield on all sides to reduce the background radiations originating from the walls and cosmic rays. Efficiency calibration for the system was carried out using the IAEA standard (IAEA, RGU-1) uranium ore. The ^{222}Rn concentrations in drinking water collected from different places in the southern part of the Gulbarga district were determined by the Emanometry method. Drinking water samples were collected and analyzed from standard procedures used elsewhere (1). The radioactive elements present in soil and water will generate a significant component of the background radiation exposure of the population present in that area.

The activity of ^{40}K , ^{238}U and ^{232}Th were found to be in the range from 81 Bqkg⁻¹ to 362 Bqkg⁻¹, 12 Bqkg⁻¹ to 50.4 Bqkg⁻¹ and 10 Bqkg⁻¹ to 57.8 Bqkg⁻¹ respectively, Outdoor Annual Effective Dose rates from 0.023 to 0.081 mSvy⁻¹. By computing the various hazard indices, the detrimental gamma radiation effects brought on by the radionuclides found in these soil samples were evaluated. The external and internal hazard indices range from 0.110 - 0.392 mSvy⁻¹ and 0.158 - 0.421 mSvy⁻¹ respectively and found to be well within the limit of 1 mSvy⁻¹. The soil samples from the Southern Gulbarga district showed a mean absorbed dose range of 19 to 66 nGyh⁻¹ and. All the soil samples have shown the annual effective dose equivalents to be within the range as compared to the dose values available for other regions of the world. In situ measurements of effective dose at the sample location was performed using RadEye survey meter holding at 1m above the ground level. The absorbed dose values are compared with the RadEye Personal Radiation Dosimeter values. Radiological parameters were estimated for the natural radioactivity of all soil samples. Annual effective dose to the population also have been estimated using the conversion factor of 0.7 Sv/Gy as provided by UNSCEAR (2000) report.

Reference:

1. Archanadevi et al., *Radiation Protection Dosimetry*, **200** (2024) 1041.
2. UNSCEAR, Sources and Effects of Ionizing Radiation. United Nations Scientific Committee on the Effect of Atomic Radiation, United Nations, New York (2000).

Optimization of Parameters for the Determination of ^{226}Ra in Water via Cherenkov Radiation

Sudeshna Goswami^{1,§}, N. Chitra¹, Kothai Parthasarathy¹

¹Radiation Applications and Technology Division, Indira Gandhi Centre for Atomic Research, Kalpakkam, Tamilnadu, India, 603102

§ Email: sgoswami1997@igcar.gov.in

Accurate detection of ^{226}Ra in drinking, surface, and groundwater is essential for health-risk assessments and radiation dose calculations. This study focused on detecting the presence of ^{226}Ra in untreated water samples by exploring the Cherenkov radiation from ^{214}Bi and ^{214}Pb using the Hidex 300 SL liquid scintillation counter [1]. To ensure accurate Cherenkov measurements, experimental work must be precise, as Cherenkov counting efficiency is highly sensitive to colour presence. Even small traces of colour can reduce photon detection and lower counting efficiency. A colour quench correction curve was prepared using the yellow quenching agent $\text{K}_2\text{Cr}_2\text{O}_7$ by determining the efficiency of a set of 20 mL samples with varying quench levels, each containing the same activity of ^{226}Ra [see Fig. 1(a)]. An empirical formula was developed to relate Cherenkov counting efficiency to the net triple to double coincidence ratio (TDCR) value, yielding a counting efficiency of 55% with the net TDCR of 0.60 in low-quenched samples, with a minimum detectable activity (MDA) of ~ 1 Bq/L for 1000 min counting. The potential improvement of the method was explored by the addition of sodium salicylate (SS) as the wavelength shifter. Adding 10 mg g^{-1} of SS improved efficiency to $\sim 70\%$ without altering the background rate (0.132 s^{-1}), reducing MDA to 0.67 Bq/L. However, SS concentrations above 50 mg.g^{-1} resulted in excessively high efficiencies ($>100\%$) due to wavelength shifting and increased scintillation light production [2]. Spectra for double and triple counting modes, both with and without sodium salicylate, are presented [see Fig. 1(b)], illustrating the impact of sodium salicylate on Cherenkov counting efficiency and spectral characteristics. Sample volume variations (7–20 mL) showed no significant effect on efficiency [see Fig. 1(c)]. A comparison with conventional extractive liquid scintillation technique (LSC)-radon techniques showed Cherenkov counting as less efficient but advantageous due to its non-destructive, cocktail-free, and eco-friendly approach.

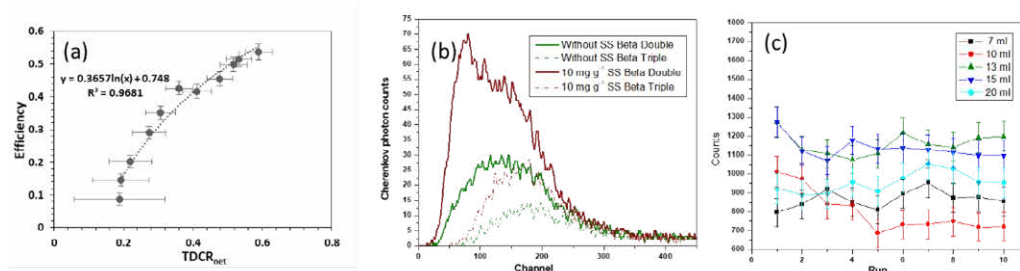


Fig 1. (a) Quench correction curve by TDCR approach (b) Cherenkov spectrum of ^{226}Ra and its daughters (with and without SS) (c) Effect of volume on Cherenkov photon counts

References:

- [1] I. Stojković et al., *Materials*, **14** (2021) 6719.
 [2] Y. Wang, *Appl. Radiat. Isot.*, **139** (2018) 175.

Radionuclide Transfer in Rice: Assessing Uptake in the Uranium-Mineralized Singhbhum Region, Jharkhand, India

Samim Molla^{1,2,§}, Ranjit Kumar¹, V. S. Srivastava¹, Aditi C. Patra^{1,2}, P. Chaudhury¹

¹Health Physics Division, Bhabha Atomic Research Centre, Mumbai-400085, India

²Homi Bhabha National Institute, Mumbai-400094, India

§ Email: samimm@barc.gov.in

Radionuclides present in the soil are transferred to the plants through uptake from the soil through roots and direct absorption through aerial parts of the plants. Food consumption is the primary cause of human exposure to radioactive elements that lead to ingestion doses [1]. India is the world's second-largest producer of rice (*Oryza sativa* L.), and it serves as a primary food for most of the population. However, comprehensive studies assessing radionuclide distribution and its transfer factors (TF) for rice cultivated in this region are scarce. This paper presents the activity of the radionuclide in the soil, rice, and soil-to-rice Tf for natural uranium series (²³⁸U, ²²⁶Ra and ²¹⁰Pb) radionuclides and ⁴⁰K for rice grown in natural field conditions around the Singhbhum region of Jharkhand. The areas are most commonly known for their near-surface and deep geological uranium mineralization and commercial uranium mining and milling.

The fully grown rice and corresponding soil samples were collected from 10 different locations in East Singhbhum and Seraikela Kharsawan districts of Jharkhand, India. Soil samples were collected from the rooting zones of paddy (up to 20 cm). The samples were processed as per IAEA-recommended procedures and radionuclides were analyzed using an HPGe gamma spectrometer (p-type, 50% relative efficiency). Certified reference materials such as RGU-1, RGTh-1, and RGK-1 were used for the efficiency calibration of the detector. ²³⁸U, ²²⁶Ra, ²¹⁰Pb, and ⁴⁰K activities in soil samples were varied from 27 ± 1 – 155 ± 2 , 28 ± 1 – 150 ± 3 , 52 ± 2 – 125 ± 2 , and 314 ± 5 – 647 ± 5 Bq.kg⁻¹, respectively. ²³⁸U, ²²⁶Ra, ²¹⁰Pb, and ⁴⁰K activities in the rice grains varied from ≤ 0.07 – 0.22 ± 0.07 , ≤ 0.09 – 0.46 ± 0.10 , ≤ 0.08 – 0.81 ± 0.14 , and 16 ± 0.4 – 46 ± 1 Bq.kg⁻¹, respectively with respective means of 0.13 ± 0.06 , 0.21 ± 0.15 , 0.35 ± 0.28 , and 26 ± 9 Bq.kg⁻¹. Using the results of the activity concentrations of radionuclides in the soil and in the rice samples, the soil-to-plant TF were estimated using Eq. (1).

$$TF = \frac{\text{Radionuclide activity in rice (Bq kg}^{-1} \text{ dry weight)}}{\text{Radionuclide activity in soil (Bq kg}^{-1} \text{ dry weight)}} \quad (1)$$

The soil to rice TF of ²³⁸U, ²²⁶Ra, ²¹⁰Pb, and ⁴⁰K from were varied from 1.2×10^{-3} – 5.6×10^{-3} , $< 7.0 \times 10^{-4}$ – 1.1×10^{-2} , $< 7.0 \times 10^{-3}$ – 1.3×10^{-2} , and 2.7×10^{-2} – 1.2×10^{-1} , respectively. The uptake of radionuclides from soil to rice grains did not exhibit a linear relationship, as it is influenced by multiple factors, including the physicochemical properties of the soil, the composition of irrigation water, and the chemical characteristics of the radionuclides. Therefore, the TF is a site-specific parameter, determined by a combination of factors rather than a single influence. The ingestion dose for the adult population from consuming rice (100 kg.y⁻¹ per person) was calculated as 0.01, 1.2, 5, and 16 μ Svy⁻¹ for ²³⁸U, ²²⁶Ra, ²¹⁰Pb and ⁴⁰K respectively [2]. This is significantly lower compared to the total ingestion dose of 290 μ Svy⁻¹ received from all sources. The findings provide valuable insights into the behaviour and transfer of radionuclides in environment, contributing to safe and sustainable operation of nuclear facilities in the Singhbhum region, Jharkhand.

References:

[1] Saeed et al., (2012). Rom J Phys, 57, 1417-1424.

[2] UNSCEAR (2000) Report to the General Assembly, Volume I, p. 140.

Short Term Prediction of Radon in a Dwelling Using an ARIMA Model

C. G. Sumesh^{1, §}, R. Shrivastava², P. Singhal^{1,3}, A. C. Patra^{1,3}, P. Chaudhury¹

¹Health Physics Division, ²Radiation Safety Systems Division, ³Homi Bhabha National Institute
Bhabha Atomic Research Centre, Trombay, Mumbai-400085, India

§Email: sumeshcg@barc.gov.in

Radon and its progeny are widespread in the environment, with concentrations that can vary significantly over time. Seasonal variations in radon levels are substantial, while diurnal variations typically vary by a factor of 2. Environmental factors such as relative humidity, temperature etc. influence radon concentrations. Studies indicate that radon levels increase with higher atmospheric relative humidity but decrease with rising temperatures. These variations are primarily attributed to diurnal changes in radon concentrations. Higher radon concentrations are generally observed in winter when dwellings are more tightly sealed with limiting air exchange.

Time series models based on Auto Regressive Integrated Moving Average (ARIMA) has been applied to predict radon concentrations [1-2]. In the present study, indoor radon concentration measurements during 18th December to 31st December 2024 at an interval of two hours were utilized to train the model. Here, temperature was used as an exogenous variable in the ARIMA model to refine the prediction of ARIMA model. Thereafter, prediction of indoor radon concentration and temperature were carried out for 01st January 2025. Even with only two weeks of measured data, model results (see Figures 1 (left) for temperature and (right) for radon concentration) were compared with observations and a good agreement was seen. This technique is useful for prediction of indoor radon concentration and may be further refined by introducing more parameters. Probable applications include prediction of radon concentration at underground mining sites.

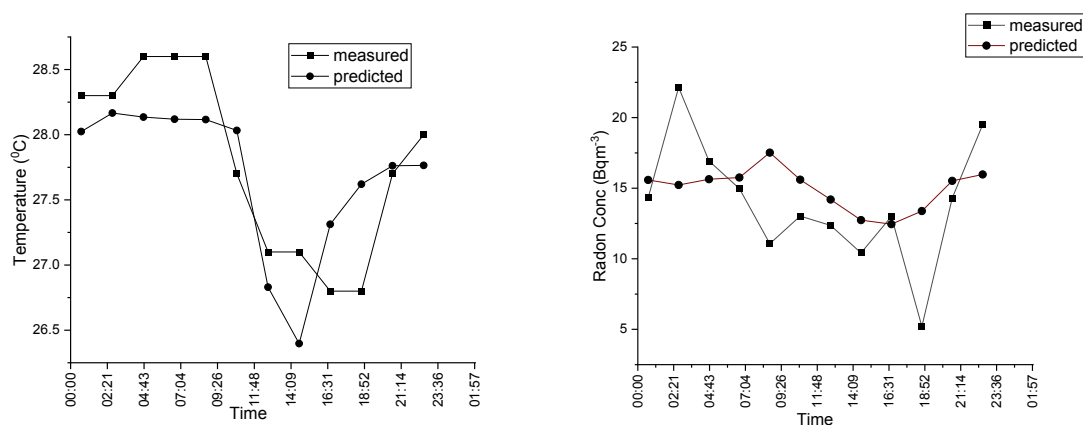


Fig-1: Predicted and observed time series of temperature (left) and Rn concentration (Bqm⁻³) (right)

References:

- [1] Marianna S et.al., *Frontiers in Earth Science*, **8** (2020), 575001.
- [2] Stránský V and Thnová L, *Radiation Protection Dosimetry*, **1** (2017) 177.

Radiological Assessment of Building Materials Around the Tummalapalle Uranium Mining Site

M. R. Dhumale^{1, §}, B. K. Rana², S. V. Bara¹, S. Chinnaesakki¹, A. C. Patra^{1, 3}, P. Chaudhury¹

¹Health Physics Division, BARC, Trombay, Mumbai

²Radiological Physics & Advisory Division, BARC, Trombay, Mumbai

³Homi Bhabha National Institute, BARC, Trombay, Mumbai.

§Email:mrarjun@barc.gov.in

Naturally occurring radionuclides (NORMs) such as ²³⁸U, ²²⁶Ra, ²³²Th, ⁴⁰K are present in Earth's crust and also in construction materials derived from natural materials. Some materials such as fly ash, phogypsum are found to have elevated levels of natural radioactivity. Soil and sand, essential components for manufacturing concrete, mortar, and bricks, are extensively used in the construction industry. Hence estimation of radioactivity content of such materials is crucial for evaluating potential radiation exposure to the occupants.

Twenty four number of samples including soil, sand, fly ash, natural gypsum, and mixed fly ash bricks (MFAB), were collected from the area around Tummalapalle site. Samples, dried at 110°C, were ground to fine powder, sieved (200 µm), and packed in sealed containers for one month to achieve secular equilibrium. Gamma spectrometry analysis was conducted using a p-type HPGe detector with 50% Relative Efficiency calibrated across 46–2614 keV energy. Parameters such as activity index, radium equivalent activity, absorbed dose rate, and external hazard index were calculated to assess health risks [1]. Mean NORM concentrations associated with building materials is presented in Table-1. Fig.1 and Fig.2 depicts the average Radium equivalent activity and Activity index associated with the materials respectively.

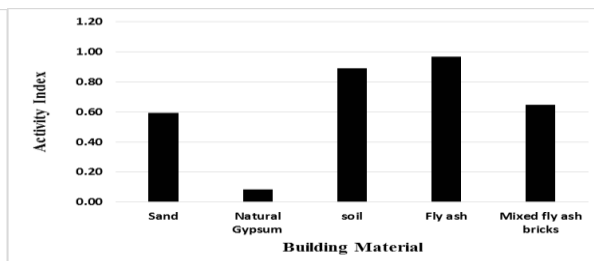
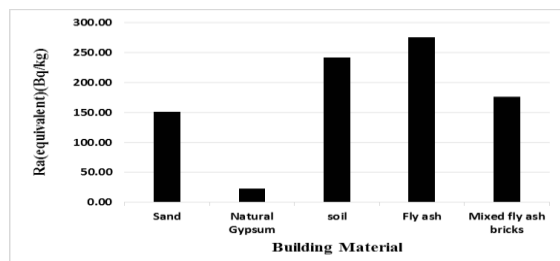


Fig. 1. Mean values of radium equivalent activity

Fig. 2. Activity Index of Building Material

Table1: Mean activity concentrations and Radiological parameters in building materials

Sample	Ra-226 (Bq/kg)	Th-232 (Bq/kg)	K-40 (Bq/kg)	Activity Index	H _{ex}	Ra _{eq} (Bq/kg)	Abs. Dose Rate (nGy/Hr)
Sand	18.3±1.0	35.7±1.0	1057.7±6.0	0.59	0.41	150.78	74.12
Nat. Gypsum	10.0±1.0	7.0±1.0	49.3±2.0	0.08	0.06	22.97	10.54
Soil	55.7±1.0	87.3±1.0	799.3±5.0	0.89	0.65	242.22	111.86
Fly Ash	93.0±2.0	112.6±2.0	285.6±4.0	0.97	0.75	276.00	122.89
MFAB	46.0±1.0	61.0±1.0	566.0±4.0	0.65	0.48	176.56	81.59

The evaluated activity index for the building materials ranges from 0.08 to 0.97 which is well below the limit to restrict dose at 1.0 mSv/y [2].

References:

[1] S.V. Bara et al., *J Radioanal Nucl. Chem.*, **291** (2012) 769.

[2] European Commission (2000), Radiation Protection No. 112.

Long-Term Monitoring of ^{226}Ra Activity in Groundwater Around the Uranium Mill Tailings Pond, Turamdih, Jharkhand

Ranjit Kumar^{1,§}, Samim Molla^{1,2}, V. S. Srivastava¹, A. C. Patra^{1,2}, P. Chaudhury¹

¹Bhabha Atomic Research Centre, Trombay, Mumbai 400 085, India

²Homi Bhabha National Institute, Mumbai 400 094, India

§ Email: ranjitks@barc.gov.in

To meet the growing demand for nuclear energy, uranium mining and processing have been increasing globally. In Turamdih, Jharkhand, the nation's second uranium milling facility was established in the year 2007 to process the ore produced by the Banduhurang open-pit mine and Turamdih and Mohuldih underground mines. Uranium milling produces almost all processed ore as waste called tailings, which contain a trace of unrecovered uranium and major radioactivity that was associated with the low-grade ore. Uranium and ^{226}Ra are naturally present in soil and rock in different quantities and are released into groundwater by natural weathering and anthropogenic activities. Among the daughter products of ^{238}U , the most important radionuclides is ^{226}Ra because of their radiological significance. ^{226}Ra is an alpha-emitting radionuclide with a 1622-year half-life, possesses only Ra(II) as its oxidation state in the environment, and has chemical characteristics similar to those of other alkaline earth metals. If radium is ingested, approximately 20% is absorbed and transported into the blood circulation, where it primarily builds up in the bones.

Estimation of radioactivity in groundwater around the tailings pond is important for proper environmental management. Groundwater samples from boreholes (15 nos.) around the tailings pond, Turamdih were collected monthly and analysed for radiochemical constituents. ^{226}Ra activity in water samples was estimated by the radon emanometry method [1].

The statistical analysis of the monitored data is shown in Table 1. The geometric mean (GM) of the ^{226}Ra activities during the last five years were varied from 13.1 to 18.1 mBqL^{-1} with respective geometric standard deviation (GSD) of 2.0 and 2.4. One-way analysis of variance (ANOVA) was carried out using statistical software (Origin Pro v. 2020) and the observed results showed that at the 95% confidence level, the population means of ^{226}Ra data over the years 2020 to 2024 are not significantly different.

The estimated ^{226}Ra activities are comparable to other reported data in literature such as 6.4–44.8 mBqL^{-1} in Mandya region, Karnataka, < 3.5–208 mBqL^{-1} in Jaduguda, Jharkhand, and 5.2–38.1 mBqL^{-1} in Narwapahar, Jharkhand. ^{226}Ra concentrations in monitoring wells are far less than the drinking reference level 1000 mBqL^{-1} [2].

Table 1: ^{226}Ra activity in Groundwater

Year	Nos. of data	^{226}Ra (mBqL^{-1})	
		Geo. Mean	GSD
2020	128	18.1	1.8
2021	173	13.1	2.0
2022	171	14.1	2.1
2023	168	15.2	2.1
2024	176	18.1	2.4

References:

[1] Bureau of Indian Standards (BIS) (2003), IS 14194-4.

[2] World Health Organization (WHO) (2011) Guidelines for Drinking-water Quality, 4th Ed 9: 211–216.

Bio Accumulation of ^{40}K in Seaweed Samples

B. S. Selvi^{1,§}, Thomas George¹, B. Vijayakumar¹, I. V. Saradhi²

¹Environmental Survey Laboratory, Kudankulam Nuclear Power project, Tamil Nadu 627120

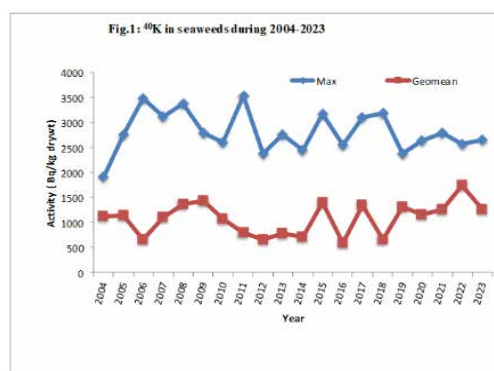
²Environmental monitoring and Assessment Division, BARC, Mumbai, India

[§]Email: bsselvi78@gmail.com

The marine organisms have the capacity of bio-accumulating radionuclides and toxic materials from water, making analyses of marine organisms an effective approach for evaluating the quality of the marine environment [1]. Among marine organism, seaweed is used as bio-indicator in monitoring radioactive contamination in the marine environment. The present work is aimed at determination of concentration of radioactive potassium (^{40}K) in seaweed samples collected around Kudankulam Nuclear Power Plant (KKNPP) during 2004-2023. The different types of seaweeds collected for this study are Sargassum (brown algae), Amphiroasp, Gracilaria, Laminaria, Sea grass, Spirunila and Ulva. About 1 kg of seaweeds was collected from the shorelines around Kudankulam on monthly basis from 2004 when the preoperational work of KKNPP commenced. The collected sea weeds were cleaned thoroughly with tap water to remove the adhering sand, dried in hot air oven at 110°C and ashed in a muffle furnace at 400°C . ^{40}K activity in the processed sample was determined using coaxial P type Hyper pure Germanium Detector with a well configuration having 110% relative efficiency and 2.0 keV resolution. Each sample was counted for 80000 seconds and achieved the MDA 5.0 Bq/kg dry wt.

Table 1: Species wise ^{40}K Conc in seaweed

Species	Nos	Range (Bq.kg ⁻¹ dry wt.)	GM	GSD
Amphiroa	11	102 – 431	156	2.49
Gracilaria	10	512– 3490	1997	1.88
Laminaria	5	277 – 3116	1325	2.36
Sargassum	153	42 – 3536	1603	2.13
Sea grass	15	110 – 2387	569	2.68
Spirulina	1	5550	-	-
Ulva	11	278 – 1958	665	1.78



Natural ^{40}K activities of different seaweed species are presented in Table 1. As shown in the table, there is a wide variation of ^{40}K activity among different sea weeds. This may be attributed to spatial and temporal differences and the age of sample collected. Additionally, in one sample of Spirunila, the activity of ^{40}K was 5550 Bq.kg⁻¹ dry wt. Spirunila is an edible blue-green seaweed that is packed with vitamins, minerals, antioxidants and protein and has a long history as a super food [2]. Figure 1 presents the maximum and the annual GM value of ^{40}K in seaweeds during 2004-23. ^{40}K activity levels ranging from 2200-3800 Bq.kg⁻¹ in edible seaweed samples collected in Malaysian sea [3]. Seaweeds are rich in ^{40}K because they absorb and accumulate minerals and trace elements from the ocean where potassium is abundant.

References:

- [1] M. F. Khan and S. G. Wesley, *Mar.Pollit.Bull.*, **62** (2011) 399.
- [2] Dr. Zilpah Sheik MD; <https://www.webmd.com/diet/spirulina-health-benefits>, 2024
- [3] M U Khandaker, *Elsevier, Algal Research* **38** (2019) 101386.

Assessment of Radiological Impact for Utilization of Uranium Mining Waste Rock in Paver Block Construction

Raghvendra Rathore, Pallavi Singhal[§], Aditi C. Patra, Pradeep Bhargava

Health Physics Division, Bhabha Atomic Research Centre, Mumbai, India

[§]Email: psinghal@barc.gov.in

The UCIL was established in 1967 with the goal of uranium mining in the country. As compared to other mines across the world, especially those in Canada and Australia, the percentage of uranium in Indian uranium ore is low and therefore mining activities generate a significant amount of unused residue, known as waste rock. Although some amount of this waste rock is used for mine backfilling; the remaining portion left in the waste yard utilizing a large amount of land and causing a socio-economic challenge. Presently UCIL has a huge amount of waste rock stored, requiring a substantial amount of space and careful handling. Furthermore, because of the rising demand for uranium and nuclear energy, this number is anticipated to rise significantly in the near future. These problems must be addressed immediately, and circular economy principle needs to be applied in uranium mining industry. In the past, it has been shown that many industrial wastes, such as fly ash from thermal power plants, steel slag, copper slag, phosphogypsum has been successfully utilized in construction industry. For this purpose, it is proposed to utilize these waste rocks in paver blocks construction. In 2023, the block paving market was estimated to be worth USD 5.231 billion. With a compound annual growth rate (CAGR) of 4.00% from 2024 to 2032, the block paving industry is expected to increase from USD 5.501 billion in 2024 to USD 7.551 billion by 2032[1]. For this, a typical Paver Block design in India is adopted [2] as shown in Figure 1 and dose rate were evaluated by QAD-CGGP code calculations for light Traffic area and commercial traffic area. The result shows that the external gamma radiation dose using this Paver Block will be 0.37 mSv^{-1} for light traffic areas and 0.51 mSv/year for heavy traffic areas (Commercial Traffic), which is far lower than the Atomic Energy Regulatory Board requirement for the unrestricted use of bulk materials in public domain [3]. Earlier we have assessed the radiological impact in using these waste rocks in road construction materials and observed that the external gamma dose rate will be $<1 \text{ mSv}^{-1}$ [4]. By preserving natural resources and encouraging a circular economy, this strategy not only tackles resource shortages but also advances environmental sustainability.

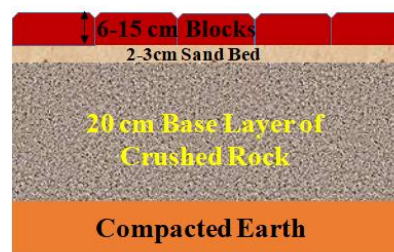


Fig. 1. Typical Paver Block design layout in India

Acknowledgements - The authors would like to acknowledge Sh. Probal Chaudhury, head HPD and Dr. D.K Aswal, Director HS&EG for their support.

References:

- [1] Block paving Market Research Report Source (MRFR/CO/1530-HCR)
- [2] Guidelines For The Use of Interlocking Concrete Block Pavement, The Indian Roads Congress (IRC:SP:63-2004).
- [3] AERB directive No. 01/2021, Radiation Substance or Material, AERB, Mumbai, 2021.
- [4] Singhal et. al. *Journal of Environmental Radioactivity* **282** (2025) 107613.

Cs Sorption Study on Different Organic Phases in Organic Rich Soil

Sukanta Maity[§], P. Sandeep, Suchismita Mishra, C. B. Dusane, Anilkumar S. Pillai

Environmental Monitoring and Assessment Division, Health Safety and Environment Group,
Bhabha Atomic Research Centre, Mumbai-400085, India

[§]Email: sukanta@barc.gov.in

Cesium (Cs) radioisotope (^{137}Cs) is significant fission product generated during nuclear fuel cycle, and have a probability of reaching the environment and human food [1]. Cs sorption studies in soils provide critical insights into its mobility and retention, particularly in environments with high organic matter content. Organic phases such as humic substances, fulvic acids, and decomposed plant residues play a significant role in the sorption process due to their high cation exchange capacities and surface functional groups. Understanding cesium's interaction with organic-rich soils is crucial for predicting its mobility, managing and mitigating risks associated with nuclear fallout or waste disposal.

A study was conducted to examine how changes in soil organic matter content and type affect the sorption behavior of Cs. Sorption experiments were performed on 10 soil samples collected from a deep forest area (forest area near south site of BARC, Trombay), divided into three sets: Set 1 (untreated soil containing both soluble and insoluble organic matter), Set 2 (soil with soluble organic matter removed), and Set 3 (soil with both soluble and insoluble organic matter removed). The experiments used distilled water spiked with a known Cs concentration ($13.33\ \mu\text{g/mL}$, totaling $400\ \mu\text{g}$). Cs analysis was performed using Atomic Absorption Spectrometry (AAS) (GBC, Avanta). As mobility of Cs can be expressed in terms of distribution coefficient (K_d), these were calculated and are represented in figure 1.

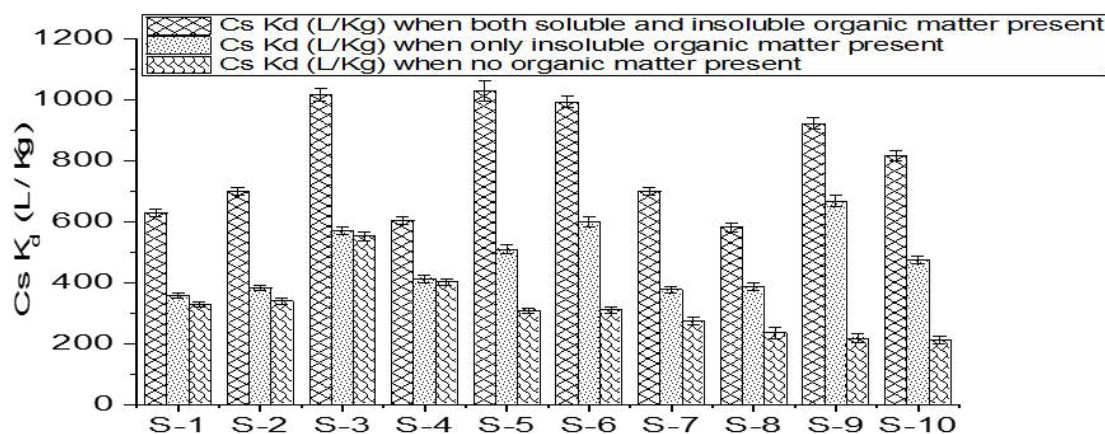


Fig. 1: Cs K_d variation w.r.t. organic matter of soil

The highest Cs K_d values were observed in samples containing both soluble and insoluble organic matter, while the lowest values were found in samples without any organic matter. Intermediate K_d values were recorded in samples where only insoluble organic matter was present. This study suggests that Cs sorption increases with higher organic matter content, regardless of whether it is soluble or insoluble. In soils with high organic matter, Cs mobility is likely to be lower. However, detailed experiments are needed for more precise conclusions.

References:

- [1] Parab, H. et al., *Progress in Nuclear Energy*, **127** (2020) 103419.

Long-Term Trends in Environmental Gamma Radiation Monitoring Using Thermoluminescent Dosimeters (TLDs) Around Variable Energy Cyclotron Centre, Kolkata

R. A. Takale[§], P. G. Shetty, M. Swarnakar, S. K. Sahu, V. Pulhani

*Environmental Monitoring and Assessment Division, Health Safety and Environment Group,
Bhabha Atomic Research Centre, Mumbai-400085, India*

[§]Email: takalera@barc.gov.in

Variable Energy Cyclotron Centre (VECC), Kolkata, is one of the premier nuclear science and accelerator technology centers of India. In addition to its own programmes of building the latest state of the art accelerators, the center provides R & D facilities to various branches of nuclear sciences. As a part of the assessment of the environmental impact of the Indian nuclear power programme, radiation surveys are being carried out on continuous basis in the environs of all the nuclear facilities using Thermoluminescent Dosimeters (TLD). This paper discusses the analysis of long-term environmental gamma radiation monitoring data generated around VECC using TLDs.

The environmental TL dosimeters used during the survey consist of indigenously developed CaSO₄:Dy based card TLDs. These TLDs have been thoroughly characterized based on ANSI 545 [1] criteria for the environmental radiation monitoring. These freshly prepared TL dosimeters were mailed to VECC on a quarterly basis. The exposed TLDs were retrieved back to BARC for the analysis. Annual values (mGy/a) for all the locations were evaluated based on the average quarterly values by normalizing to 365 days. Annual values for a particular year were evaluated only if, minimum of three quarterly values are available, to get representative exposure level at the location. Table 1 gives the annual average and standard deviation of locations around VECC premises for the year 2013-2023.

The average gamma radiation levels are seen in the range of 0.81 ± 0.05 mGy/a in VECC Garage to 1.29 ± 0.13 mGy/a in CED. Overall annual average of these locations for the period 2013-2023 was 1.05 ± 0.17 mGy/a. The annual average gamma levels are comparable with the values reported earlier 1.19 ± 0.25 mGy/a in 1984-1995 [2] and 1.09 ± 0.21 mGy/a in 1996-2012 [3]. This study illustrates how gamma radiation measurements using TLDs are a potentially valuable method for assessing radiological effects in VECC region.

References:

- [1] ANSI N-545 (1975).
- [2] Basu A. S.et.al., BARC/1997/E/007.
- [3] Takale R.A. et.al. (2014) IARPNC 2014.

Table. 1: Annual average dose rate in and around VECC premises.

Location Name	Ann avg mGy/a	Year
Medical Cyclotron	0.94 ± 0.22	2013-2023
VECC Housing	1.06 ± 0.10	2013-2023
D.G.Building	0.90 ± 0.12	2013-2023
Main Gate	0.91 ± 0.19	2013-2023
VECC Hostel	1.06 ± 0.10	2013-2023
Hudco	1.20 ± 0.10	2013-2023
Anjanghar	1.09 ± 0.09	2013-2023
Garage	0.81 ± 0.05	2021-2023
Kiosk (Security)	0.84 ± 0.03	2021-2023
S. J. Guest House	0.96 ± 0.04	2018-2023
Nagar Bazar	1.01 ± 0.08	2018-2023
Praffulla Kanan	1.27 ± 0.22	2013-2017
SINP	1.13 ± 0.16	2013-2020
CED	1.29 ± 0.13	2013-2020

Distribution of Primordial Radionuclides in Soil Samples from Haryana, India and their Radiological Significance

M Tiwari¹, S. K. Sahu^{1,2,§}, S. J. Sartandel¹, T. D. Rathod^{1,2}, M. Swarnkar¹,
R. C. Bhangare¹, P. Y. Ajmal¹, M. K. Mishra¹, V. Pulhani^{1,2}

¹Environmental Monitoring and Assessment Division, BARC, Mumbai – 400085, India

²Homi Bhabha National Institute, Anushakti Nagar, Mumbai – 400094, India

§Email: sksahu@barc.gov.in

Naturally occurring radionuclides (NORs), such as the uranium (^{238}U) series, the thorium (^{232}Th) series, and potassium (^{40}K), are ubiquitously distributed across the Earth's surface. Among these, NORs present in soil constitute the most significant source of radioactivity encountered by humans. Assessing the activity concentrations of these radionuclides in soil is crucial for evaluating the radiological characteristics [1]. In this study, surface soil samples were collected from 35 locations across the state of Haryana, India, and analyzed for their naturally occurring radionuclide content using gamma spectrometry. Gamma-ray spectrometry was performed with a 50% relative efficiency BSI make HPGe detector, coupled with an ITECH system and InterWinner-8 gamma spectroscopy analysis software. The photopeak detection efficiency for the specific sample geometry and gamma-ray energy of interest was evaluated using IAEA-certified reference materials (CRM) RGU and RGTh.

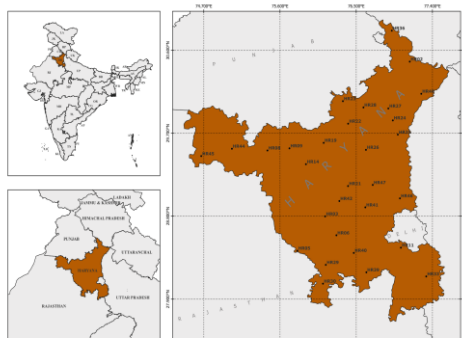


Fig. 1: Location of soil samples collected from Haryana.

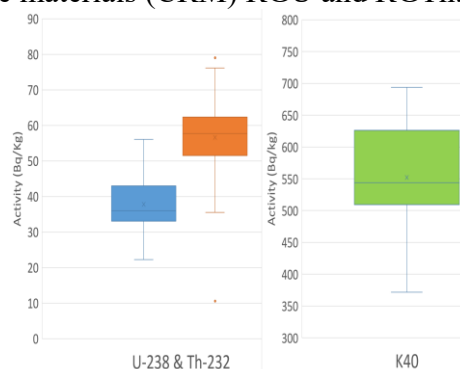


Fig. 2: Box and whisker plot of ^{238}U , ^{232}Th , and ^{40}K activity concentrations (Bq/kg).

The box-and-whisker plot of ^{238}U , ^{232}Th , and ^{40}K activity concentrations (Bq/kg) in soil from Haryana state is shown in Fig. 2. The data were used to calculate the radium equivalent activity (R_{eq}) in the soil, along with the absorbed dose (D) and the external (H_{ex}) and internal (H_{in}) hazard indices [1, 2]. The R_{eq} values ranged from 106.8 to 222.5 Bq/kg, with an average of 161.3 Bq/kg, the radium equivalent concentration much below the limit of 370 Bq/kg for safe material use, [1]. The H_{ex} values ranged from a minimum of 0.29 to a maximum of 0.60, with an average of 0.44. Similarly, H_{in} values ranged from 0.35 to 0.75, with an average of 0.55. The absorbed dose ranged from 50 to 102 nGy/h, with an average of 72 nGy/h. Overall, the measured concentrations of primordial radionuclides and the calculated radiological indices indicate that the soil from Haryana state does not exhibit any significant variations from the global average radionuclide concentration.

References:

- [1] S. Sakr et al., *Journal of Environmental Radioactivity*, **266** (2023) 107240.
- [2] K. M. Murthuza et al., *Materials Today: Proceedings*, **65** (2022) 2606.

Environmental Gamma Radiation Monitoring Around Upcoming NFC-Kota

P.G. Shetty, R.A. Takale, M. Swarnakar, S.K. Sahu[§], V. Pulhani

*Environmental Monitoring and Assessment Division, Health Safety and Environment Group,
Bhabha Atomic Research Centre, Mumbai-400085, India*

[§]Email: sksahu@barc.gov.in

NFC-Kota is a green field project being established adjacent to Heavy Water Plant, Rawatbhata (HWP-Kota), Rajasthan. This project is established as an extension to NFC-Hyderabad and is based on the technological procedures adopted at NFC-Hyderabad. NFC-Kota project envisaged to establish 37 element fuel bundle manufacturing facility to cater to fuel requirement of upcoming 4 x 700 MWe Pressurized Heavy Water Reactors (PHWRs). Preoperational gamma radiation monitoring forms a crucial activity in assessing the baseline radiological environment before commissioning any nuclear facilities. The monitoring of ambient air dose around the upcoming site was started from 2022 using CaSO₄: Dy based Thermoluminescent dosimeters (TLDs) on quarterly basis. These dosimeters were chosen for their precision, stability, and ability to measure low-dose radiation levels in environmental conditions. They were deployed at 25 locations, covering aerial distance of 30 Km from the upcoming site. This paper presents the three-year preoperational average annual ambient air dose values observed in the region during the period 2022-2024. Fig.1 shows three-year average annual air dose measurements at the 25 monitored areas using TLDs.

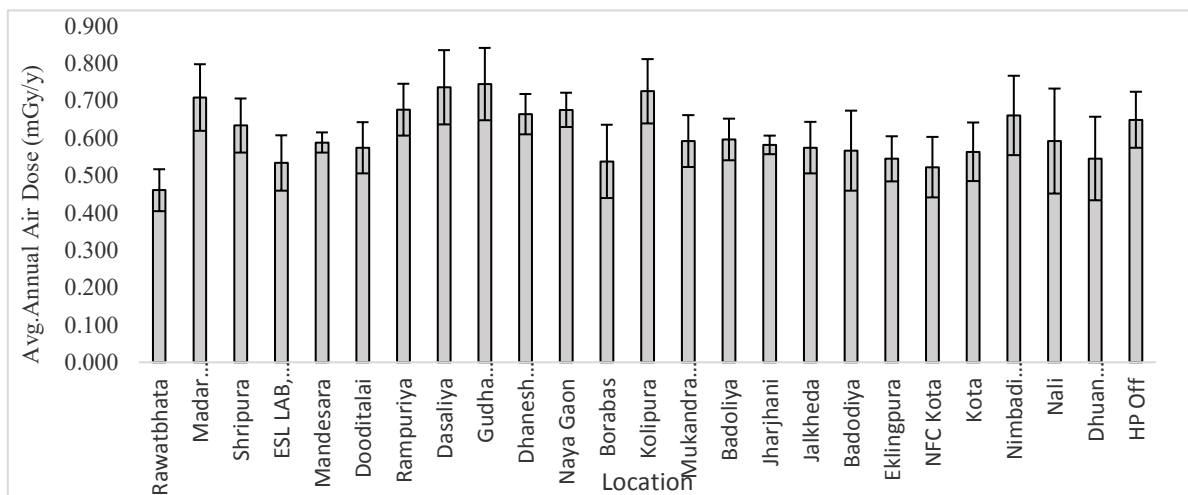


Fig. 1: Average Annual Air Dose (mGy/a) in the monitored areas

The average annual air dose levels across the monitored area exhibited spatial variability, ranging from 0.46 to 0.74 mGy/a with mean 0.61 ± 0.073 mGy/a. A comparison with average annual radiation level of 0.62 ± 0.09 mGy/a [1] at RAPS site in the same state indicates that the radiation levels in the monitored areas are comparable. This baseline data is crucial for assessing any potential impact of operational activities on ambient radiation levels and ensuring compliance with radiological safety standards.

References:

- [1] A. S. Basu et.al. BARC/1998/E/021 (1998)

Radiological Assessment of U-Mill Tailings and Mine Waste Rock-Based Construction Materials for Societal Applications

B. K. Rana^{1,*}, Samim Molla², B. K. Sahoo¹, Arshad Khan¹, B. K. Sapra¹

¹Radiological Physics & Advisory Division, BARC, Mumbai-400085, India

²Health Physics Division, Bhabha Atomic Research Centre, Mumbai-400085, India

*E-mail: barendragargi@gmail.com

India, the world's second-largest consumer of construction aggregates, requires about 5.5 billion tonnes annually. Uranium mining in Jharkhand and Andhra Pradesh generates substantial waste, about 60 million tonnes of waste rock at Banduhurang Mine and 50 million tonnes of silica-rich tailings in the Jharkhand region. When combined with sand and local materials, these can be used in construction. This study assessed the radioactivity of U-mill tailings and mine waste rock-based materials using an HPGe detector (50% RE). Energy and efficiency calibration were conducted across the 46.53–2614.53 keV range using IAEA-certified reference materials. The ²²²Rn exhalation rate from paver blocks (made with waste rock) and tailings brick walls was measured with an accumulation chamber and a portable radon monitor. Exhalation rates for Tailings Bricks-1, 2, and 3 (with 30%, 40%, and 50% tailings) were 0.0011, 0.0019, and 0.0026 Bqm⁻²s⁻¹, with error of 5-10%. After plastering, these dropped by 37%, 36%, and 19%. Paver blocks had a mean exhalation rate of 0.00273 ± 0.0005 Bqm⁻²s⁻¹, much lower than Jaduguda soil (0.08 ± 0.05 Bqm⁻²s⁻¹) [1]. Both tailings bricks and paver blocks met compressive strengths above Bureau of Indian Standards limits [2], posing insignificant radiological risks in outdoor. Blending with other materials reduced radioactivity to a safe level of 1 Bq/g as per AERB Directive No. 1/2010 is achieved in T1 category brick. Table 1 compares the radioactivity data for newly manufactured tailings bricks, paver blocks, and conventional materials. This study confirms that uranium tailings and waste rock can be safely and effectively used as construction materials for roads, bridges and non-residential building foundations.

Table 1: Radioactivity content in tailings bricks, paver block and conventional construction materials for comparison purpose.

Material (Nos.)	²²⁶ Ra (Bqkg ⁻¹)	²³² Th (Bqkg ⁻¹)	⁴⁰ K (Bqkg ⁻¹)	Ra _{eq} (Bqkg ⁻¹)
Bed Materials (5)	68.72 ± 4	65.24 ± 2	187.26 ± 9	176.4
Cement (4)	63.5 ± 3	51.1 ± 1	215.43 ± 7	153.2
Copper Tailings (5)	414.16 ± 6	18.58 ± 0.8	501.84 ± 8	479.4
Fly Ash (5)	82.6 ± 4	99.9 ± 2	206.8 ± 10	241.4
Gypsum (5)	567.86 ± 4	6.38 ± 0.5	10.7 ± 3	577.8
LD Slag (5)	6.58 ± 2	2.6 ± 0.6	<10.2	11.08
Lime (5)	13.82 ± 2	2.73 ± 0.6	16.5 ± 5	18.99
Sand (5)	15.74 ± 1	13.38 ± 0.5	565.26 ± 6	78.4
Tailings brick (T1, T2 &T3)	876.8±111	61.1±2.8	346.8±27.6	991±107
	1146.5±113.3	53.1±3.1	408.8±34	1254±140
	1431.5±166	69.1±3.7	503.7±42	1569±175
Paver blocks	1278±356.5	67.2±13	672.8±57	1426±379

Reference:

1. S. Jha et al., *J. Environ. Radioactivity*, **49**, (2000), 157.
2. Bureau of Indian Standards (BIS), 15658: Precast concrete blocks for paving – (CED 5: Flooring, Wall Finishing and Roofing), (2006).

Measurement of Radon Concentration in Air over the Eastern Coast of India: Implications of Heavy Mineral Deposits on Natural Background Radiation

Abinash Sahu^{1,§}, P. Prusty¹, A. Rout¹, P. Sahu², R.P. Patra¹, A.C. Patra^{1,3}, P. Choudhury¹

¹ Health Physics Division, BARC, Trombay, Mumbai – 400085, India

² ICAR-IIWM, Bhubaneswar, Odisha – 751023

³ Homi Bhabha National Institute, Anushaktinagar, Mumbai – 400094, India

§Email: abinash.sahu31@gmail.com

This study presents measurements of radon concentrations in the air over the eastern coast of India, an area characterized by heavy mineral deposits such as ilmenite, rutile, zircon, garnet, and monazite. These minerals, known for their natural radioactivity due to the presence of uranium and thorium in it, influence the radon emissions. Measurements were conducted using an ion chamber-based detector (AlphaGUARD) having 0.62 l pulsed ion chamber operating in both 3D spectroscopy and current mode, a widely recognized instrument for its accuracy and sensitivity. Key sites for radon measurement were selected based on proximity to mineral deposits, population density, and accessibility. By investigating spatial and temporal variations in radon levels, the study aims to assess the influence of heavy minerals on radon emissions and their potential implications for environmental radiation and public health. Spatial and temporal variations in radon concentrations were observed, with levels not exceeding internationally recommended safety limits of 200 Bqm⁻³ in any of the locations [1,2].

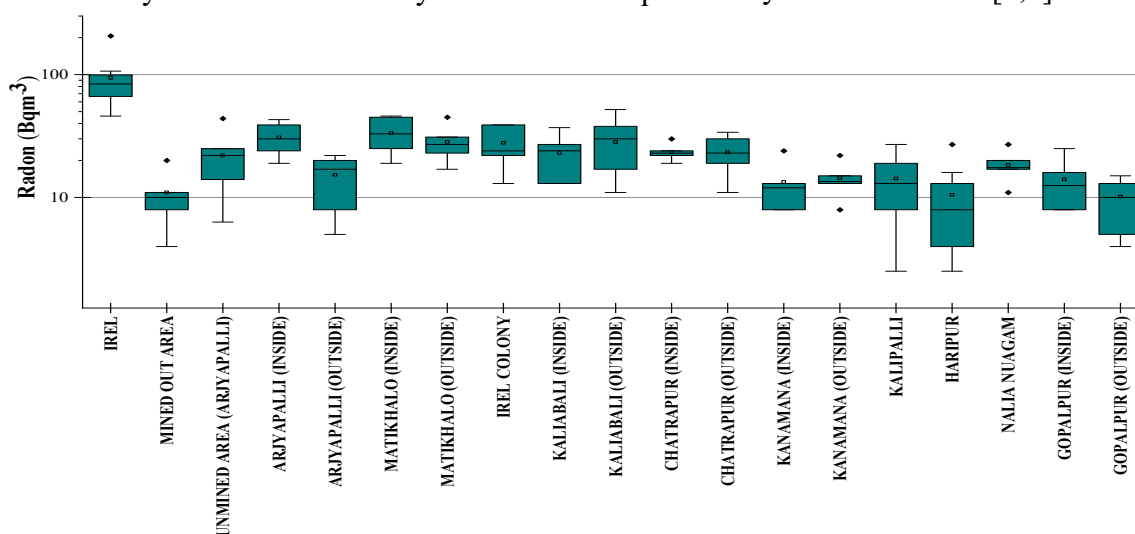


Fig.1: Radon activity in air of the eastern coast of India

The mean radon level in the area where the heavy mineral is mined out observed to be 11 ± 3.32 Bqm⁻³ and in the unmined area is 33 ± 4.80 Bqm⁻³. The instrument's performance was cross-checked using a standard reference source. The reduction in radon level from unmined area to mined out area is due to lesser presence of the source term monazite and zircon mineral in the beach sand. The average outdoor radon concentration in India is 10 Bqm⁻³.

References:

- [1] World Health Organization (2009): *WHO Handbook on Indoor Radon: A Public Health Perspective*.
- [2] A. Sahu et.al, *AOCR6*, February 07 – 11, 2023; S43.

Comparative Assessment of Uranium in Groundwater Around Operating Uranium Mining Facilities in Singhbhum Region, Jharkhand

S.K. Sahoo^{1,§}, V.N. Jha¹, Rajesh Kumar¹, A.M. Gupta¹, A.C. Patra^{1,2}, P. Chaudhury¹

¹Health Physics Division, Bhabha Atomic Research Centre, Trombay, Mumbai – 400 085

²Homi Bhabha National Institute, Trombay, Mumbai – 400 094

[§]Email: sksbarc@barc.gov.in

Seven uranium mines (Jaduguda, Bhatin, Narwapahar, Turamdih, Banduhurang, Mohuldih, and Bagjata) and two ore processing facilities (at Jaduguda and Turamdih) are operating in the Singhbhum region of Jharkhand since 1965. Radiation protection and environmental surveillance are integral part of the plant operation, since inception, to ensure the safety of occupational workers, members of the public and the surrounding environment. Monitoring of uranium in groundwater is one of the indicative parameters of any plausible impact on the surrounding groundwater. However, uranium is a naturally occurring low specific active radioactive element that occurs in groundwater with wide variation. In this study, the comparative assessment of uranium levels in groundwater around operating uranium mining sites in Singhbhum region has been carried out. Seven uranium mines are operating in Singhbhum thrust belt of Jharkhand are grouped into three zones considering the close proximity among the sites. Jaduguda zone comprises of Jaduguda, Bhatin and Narwapahar uranium mine and their surroundings, Turamdih zone comprises of Turamdih, Banduhurang and Mohuldih mines and their surroundings while Bagjata zone comprises the surrounding area around this mine.

Groundwater samples were collected around uranium mining facilities in pre-monsoon season (April – June, 2022) following the standard protocol and analysed for its uranium content using LED induced Fluorimeter by standard addition method. Water quality was also assessed for understanding correlation of parameters. Strict quality assurance and quality control measures were adopted to ensure the data quality [1].

Uranium content in groundwater around Jaduguda, Turamdih and Bagjata zones was found to vary in the range of <0.2 – 24.5 µg/L (n=51); <0.2 – 39.3 µg/L (n=20) and <0.2 – 46.3 µg/L (n=47), respectively and found to be well within the AERB stipulated drinking water limit of 60 µg/L. Spatial distribution of uranium in all the three zones is ascribed to heterogeneous surface mineralogy and underlying hydrogeological process across the region. Gibb's plot indicates host rock-groundwater interaction is the predominant geological process in the region. Findings reveal that the variation of uranium in this area is natural, which can be correlated to regional geology of Singhbhum Thrust Belt, hydrogeochemical parameters and environmental influences.

Reference:

[1] S.K. Sahoo et.al., *Current Science*, **120** (2021) 1482.

Natural Radio Nuclides in Fish Consumed at Visakhapatnam

P. Padma Savitri^{1,*}, B. Ramesh¹, J. Sudhakar¹, R. Balaram¹, Manoj Warriar², A.D.P. Rao³

¹Environmental Monitoring and Assessment Division, BARC, Visakhapatnam, India

²Computational Analysis Division, BARC, Visakhapatnam, India,

³Nuclear Physics Department, Andhra University, Visakhapatnam, India

*Email: ppsavitri@barc.gov.in

Activity concentration of natural radionuclides varies in fish at different places depending on differing background values. Visakhapatnam is a maritime district with a major fishing harbor. Varieties of fish under study were procured from markets. There are no radiological facilities operational during sampling period in the studied region. The objective is to establish site specific baseline database of natural radionuclides in fish. The edible parts were processed, stored in standard geometry box as per standard procedure [1]. Concentration of ²²⁶Ra, ²³²Th and ⁴⁰K were determined using 3"x3" NaI gamma-ray spectrometer. The samples were counted for 25000s using Genie-2000 Inspector basic spectroscopy software. Geometrical ash weight of the sample was around 150g. The density correction factors were applied to correct the difference in the densities of samples and standards. Efficiency calibration of the spectrometry system was carried using IAEA reference materials such as RGU-I, RGTh and RGK with self attenuation correction. The full width half maximum was 44 KeV with a resolution of 6.7% for ¹³⁷Cs (662 KeV) peak. Activities were determined by respective energies as given in [1]. The combined uncertainty has been estimated by considering the errors due to counting statistics, gamma emission probability and absolute efficiency. Self attenuation correction was carried by assuming that fish samples powder as cellulose matrix and RGu is in silica. Figure 1 presents activity concentration in 15 varieties of sea, fresh water fish which are analyzed for the first time in this region. Concentration of ⁴⁰K was in the range 21±9.6 to 176±6.4 Bq/kg of edible weight where as ²²⁶Ra, ²³²Th are insignificant. This is to be expected as potassium is widely distributed in marine environments and is involved in the metabolism of fish. Activities in fish varied by species as it depends on physiology of the fish. The concentrations were in the comparable range with reported values in studies done at Visakhapatnam, South India [1, 2]. Results indicate that natural radioactivity in consumable fish is not of concern and thus will help for public awareness.

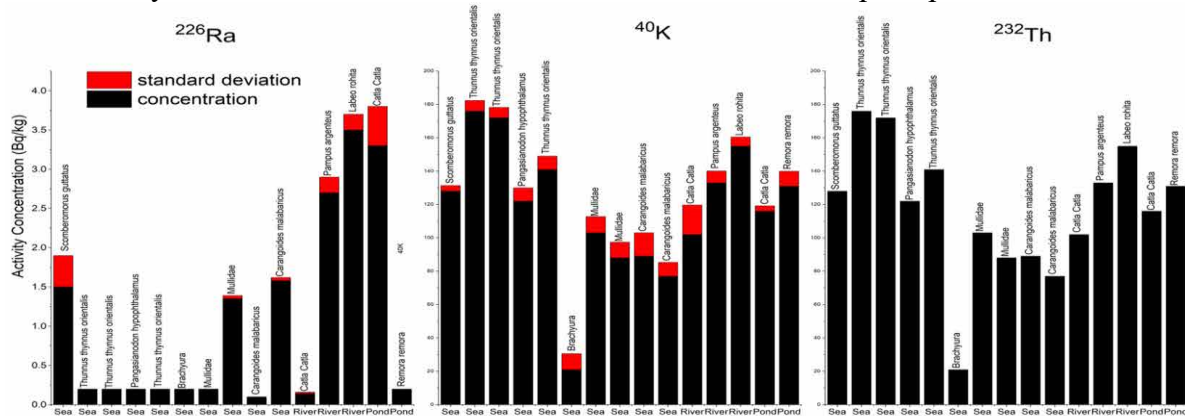


Fig. 1. Radioactivity concentration in different varieties of fish at Visakhapatnam

References:

- [1] Patra A.C et al, *J Radioanal Nucl Chem* 300 (2014) 903.
- [2] G. Shanti J. Thampi et.al., *Nucl. Instr. Methods in Physics Research A*, 619 (2010) 436.

Weathered Microplastics as Uranium Carriers: Sorption Behavior in Simulated Marine Conditions

Sonali Yadav^{1,2,§}, Sabyasachi Rout^{1,2}, Vandana Pulhani^{1,2}

¹Bhabha Atomic Research Centre, Trombay, India

²Homi Bhabha National Institute, Mumbai, India

§ Email: sonaliy@barc.gov.in

Microplastics (MPs), defined as plastic particles smaller than 5 mm, are emerging contaminants of high eco-toxicological concern due to their persistence, ubiquity, and ability to adsorb and release harmful substances [1]. These particles can act as vectors for heavy metals, including uranium (U), in aquatic environments. This study explores the changes in physicochemical properties of four commonly found microplastics: polypropylene (PP), polyethylene terephthalate (PET), high-density polyethylene (HDPE), and low-density polyethylene (LDPE) after exposure to simulated marine conditions and evaluates their U sorption behavior. To replicate environmental weathering, pristine MPs (approximately 4 g per type) were enclosed in nylon mesh bags (250 μm mesh size) and immersed in seawater-filled aquarium placed on a rooftop for four months. After retrieval, the samples were thoroughly cleaned with sterilized seawater and air-dried. Fourier transform infrared (FTIR) spectroscopy revealed significant oxidative degradation of the MPs. Notable changes included the formation of carbonyl groups in PP (1650 cm^{-1} peak), hydroxyl and carbonyl groups in HDPE and LDPE (3353 cm^{-1} and 1660 cm^{-1} peaks), and increased intensity of $-\text{C}-\text{O}-$ peaks in PET (1179 cm^{-1} and 1027 cm^{-1}). Crystal Violet staining revealed that biofilm biomass has increased on all the MPs. Subsequently, U sorption experiments were conducted by taking 200 mg of each weathered MP samples with 20 mL of 200 $\mu\text{g L}^{-1}$ U solution. Voltammetry analysis revealed that weathering-induced surface alterations enhanced U sorption capacity in all MP types, with the extent of sorption varying by polymer type as shown in Table 1. The results revealed the role of environmental weathering in transforming MPs into active carriers of U in marine environments, highlighting their potential impact on aquatic ecosystems.

Table 1: Apparent Distribution Coefficients (K_d) of U across various types of MPs.

Type of MPs	Range (L kg^{-1})
Polypropylene (PP)	93-103
Polystyrene (PS)	8-10
High Density Polyethylene (HDPE)	12-24
Low Density Polyethylene (LDPE)	141-200

Reference:

[1] S. Yadav, et.al, *Journal of Environmental Science and Health, Part A*, **57**(2022), 575.

Indigenously Developed Sampling System for Radiocarbon Species in Air

Sabyasachi Rout^{1,2,§}, Sonali Yadav^{1,2}, Vandana Pulhani^{1,2}

¹Bhabha Atomic Research Centre, Trombay, India

²Homi Bhabha National Institute, Mumbai, India

§ Email: srout@barc.gov.in

Carbon-14 (^{14}C) is a beta-emitting radionuclide with a half-life of 5730 yr. It has both cosmogenic and anthropogenic origins, with the latter as a byproduct or specialized product in nuclear reactors, reprocessing facilities, and research initiatives[1]. Nuclear facilities represent the major source of ^{14}C release into the atmosphere. Monitoring atmospheric ^{14}C near such facilities is essential to ensure regulatory compliance and environmental radioactivity assessment. Nuclear reactors, such as Boiling Water Reactors (BWRs), Pressurized Water Reactors (PWRs), and Pressurized Heavy Water Reactors (PHWRs), released ^{14}C primarily in oxidized and reduced form. The speciation of these releases varies by reactor type. PWRs predominately release ^{14}C in hydrocarbon form (primarily as CH_4), BWRs emit 5-20% hydrocarbons along with oxidized forms such as CO_2 , and PHWRs primarily release oxidized form (approximately 80 % as CO_2) and about 20 % as hydrocarbons. Although hydrocarbons and reduced forms are released initially, they eventually oxidize in the atmosphere to form stable oxidized species. This necessitates efficient sampling and speciation techniques for monitoring atmospheric ^{14}C near nuclear facilities. We designed and developed an automated system for the simultaneous sampling and speciation of atmospheric ^{14}C . The system integrates multiple stages for capturing the inorganic and organic species of ^{14}C . Key features include an initial sampling stage where air is drawn through the system using an air pump, followed by removal of moisture using silica gel as desiccant. The moisture free air is then passed through set of 3 bubblers in series containing 2 M NaOH (ultrapure) solution for trapping ^{14}C as CO_2 . The CO_2 free air is then directed through a furnace containing a 0.5 % Pt- Al_2O_3 catalyst at 550 °C, converting all the hydrocarbons and CO to CO_2 . All the trapping units are maintained at a controlled temperature of 20°C to prevent evaporative loss. Finally, the oxidized form is trapped in second set of bubblers containing 2 M NaOH solution. The system is equipped with CO_2 , temperature and humidity sensors placed after each sampling stage to monitor operational efficiency. For field-testing, sampling was carried out in the Mumbai coastal area (see in Fig. 1) and it was found that atmospheric ^{14}C as CO_2 varies between 220–230 Bq/kg C, compared to the background value of 228 Bq/kg C. In CH_4 form, it ranges from 190–200 Bq/kg C. The developed system demonstrated high efficiency in the simultaneous sampling of atmospheric ^{14}C species. This innovation enables accurate speciation and monitoring of these radionuclides in ambient environments, contributing to improved regulatory compliance and environmental safety near nuclear facilities.

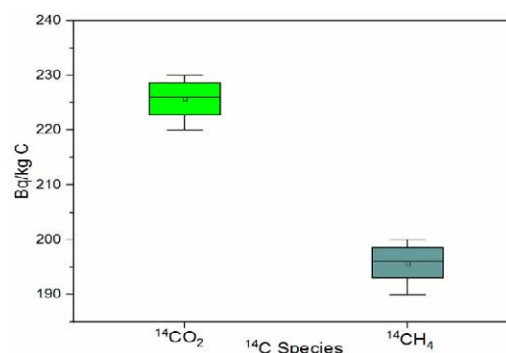


Fig.1: Activity of the ^{14}C species in air

References:

- [1]. IAEA, Management of Waste Containing Tritium and Carbon-14, Technical Reports Series No. 421, IAEA, Vienna (2004)

Modifying the UiO-66 (Ce) Functionality to Boost Uranium Sorption from Real Water Samples

Jay Singh Dubey¹, Adish Tyagi², Pallavi Singhal^{1,§}, Gourab Karmakar^{2,§}, Aditi C. Patra¹

¹Health Physics Division, Bhabha Atomic Research Centre, Mumbai, India

²Chemistry Division, Bhabha Atomic Research Centre, Mumbai 400085.

[§]Email: psinghal@barc.gov.in, gourabk@barc.gov.in

Nuclear power is increasingly viewed as a solution to the growing global energy demand and the challenges posed by climate change [1]. Large-scale extraction of uranium from seawater is seen as crucial for sustainable nuclear power generation [2]. Herein, UiO-66-NH₂ (Ce) was synthesized and subsequently modified to phosphoryl amide-functionalized UiO-66-NHPOPh₂ (Ce) for their application in uranium extraction. The samples were characterized by FT-IR spectroscopy, PXRD, TGA, SEM-EDX and BET surface area analysis. Uranium sorption studies were carried out to check the feasibility of these sorbents. The influence of pH and contact time on uranium uptake was systematically investigated. pH-dependent adsorption studies revealed over 95% and 99% sorption for UiO-66-NH₂ (Ce) and UiO-66-NHPOPh₂ (Ce) respectively in the pH range of 3-9, with maximum adsorption observed at pH 5, mirroring the pH range of most naturally occurring water bodies. Time dependent sorption measurements suggest that the sorption is very fast for UiO-66-NH₂ (Ce)MOF and >95% sorption has been achieved after 1 min of interaction and ~98% after 60 min. Similar experiment with UiO-66-NHPOPh₂ (Ce)MOF suggest >99.5% sorption within 1 min of interaction. It was observed that the sorption follows chemisorptions process. Interestingly, phosphoryl amide functionalized MOF exhibited a higher uranium sorption capacity across a wide pH range compared to amine functionalized MOF. Moreover, the sorption capacity of UiO-66-NHPOPh₂ (Ce) MOF, estimated at 95 mg of U/g of sorbent using the Langmuir isotherm model, surpassed that of many other reported sorbents (see Figure 1). Adsorption studies conducted with tap water, drinking water and seawater demonstrated uranium sorption from real samples.

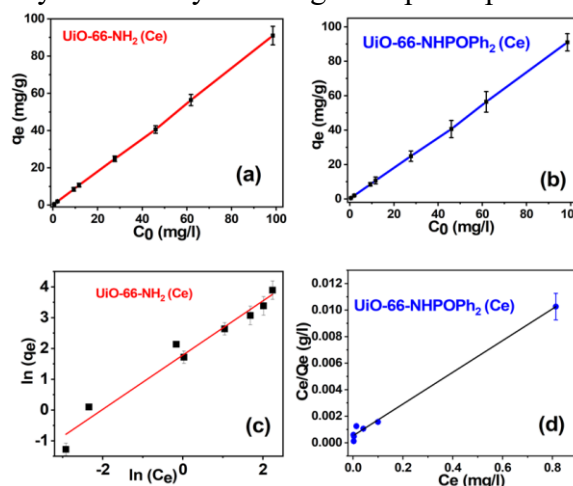


Fig. 1. (a and b) Plot of mass of uranium sorbed with initial uranium concentration. $V/m = 1$ mL/mg and sonication time was 60 min for UiO-66-NH₂ (Ce)MOF and $V/m = 2$ mL/mg and sonication time was 1 min for UiO-66-NHPOPh₂ (Ce)MOF. Experiments were carried out at pH 5. (c and d) Fitting of sorption isotherm experiment results into different models for UiO-66-NH₂ (Ce) and UiO-66-NHPOPh₂ (Ce)MOF.

Acknowledgements - The authors would like to acknowledge Sh. Probal Chaudhury, Head HPD and Dr. D. Aswal, Director HS&EG for their support.

References:

[1] Singhal et. al., *Curr. Nat. Sci. Eng.* **1** (2024) 12.

[2] Singhal et. al., *Journal of Industrial and Engineering Chemistry* **90** (2020) 17.

Modifying the ZIF-8 Functionality to Boost Uranium Sorption from Real Water Samples

Pallavi Singhal^{1, §}, Jay Singh Dubey¹, Adish Tyagi², Gourab Karmakar², Aditi C. Patra¹

¹Health Physics Division, Bhabha Atomic Research Centre, Mumbai, India

²Chemistry Division, Bhabha Atomic Research Centre, Mumbai 400085.

§Email: psinghal@barc.gov.in

The use of nuclear power is a key solution to meet the rising energy demand [1]. The large-scale extraction of uranium is considered essential for ensuring the long-term sustainability of nuclear energy [2]. Zeolitic imidazolate frameworks, ZIF-8 were synthesized for extraction of U. The synthesized products were characterized by FT-IR spectroscopy, PXRD, TGA, SEM-EDX and BET surface area analyser.

Uranium sorption studies were carried out to check the feasibility of these sorbents in extracting uranium. First, the pH dependent sorption studies were carried out to determine the working pH range of the synthesized sorbent. Initially the experiments were performed with 1 ppm uranium with $V/m = 1\text{ mL/mg}$, but U could not be detected in laser fluorimetry. Detection was feasible when the studies were performed with 10 ppm uranium concentration and $V/m = 1\text{ mL/mg}$. The results are shown in Fig. 1A. It is clearly observed from Fig. 1A that MOF adsorb >99% uranium in pH range of 2-9 suggesting the suitability of this MOF in different applications. Time dependent sorption experiment suggest that the sorption is very fast and >99% sorption was achieved after 1 min of interaction as shown in Fig. 1B. The experimental results were fitted into different models and the results indicated that the sorption process followed pseudo-second order kinetics thereby suggesting chemisorption process. Sorption capacity was determined by adding different concentration of uranium (1-60 ppm) to the MOF. The results are best fitted into Langmuir isotherm (Fig. 1C). The maximum sorption capacity using Langmuir isotherm model was found to be 250 mg of U/g of sorbent which is much higher as compared to many other sorbents. Recyclability of the material is tested by carrying out the experiment at different cycles without uranium desorption to make it simpler and more economical as shown in Fig. 1D. The experiments were performed with 10 ppm uranium keeping $V/m = 5\text{ mL/mg}$. It can be seen that the MOF can sorb almost 50% uranium till 5 cycles without any desorption.

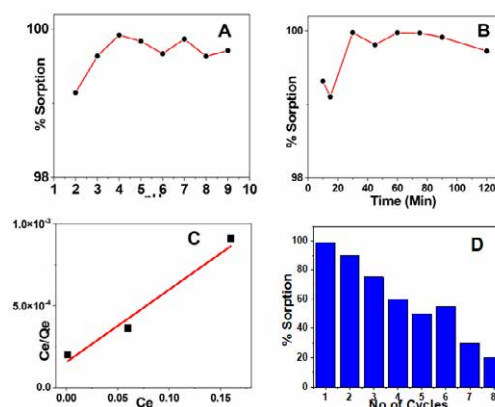


Fig. 1: Plot of % uranium sorption with (A) pH and (B) Time. Initial uranium concentration = 10 ppm and $V/m = 5\text{ mL/mg}$. (C) Fitting of sorption isotherm experiment results into Langmuir models. (D) Recyclability experiment with different no of cycles.

Acknowledgements: The authors would like to acknowledge Sh. Probal Chaudhury, Head HPD, Dr. Niharendu Choudhury, Head, ChD for their support.

References:

[1] Singhal et. al. *Curr. Nat. Sci. Eng.* **1** (2024) 12.

[2] Singhal et. al. *Journal of Industrial and Engineering Chemistry* **90** (2020) 17.

Measurement of Naturally Occurring Radioactive Materials (NORM) in Kutni Village near South Purulia Shear Zone

Sayantana Mitra¹, Sumana Mukherjee¹, Anil Sharma², Soumalya Kundu², Aditi Das², Pankaj K. Giri², Rajarshi Raut², Sandeep S. Ghugre², Chiranjib Barman^{1,§}

¹Department of Physics, Sidho-Kanho-Birsha University, Purulia, India

²UGC-DAE CSR, Kolkata Centre, LB 8 Sector III, Bidhannagar, Kolkata, India

§ Email: chiranjib-barman@skbu.ac.in

Kutni village in the Purulia district of West Bengal is located in close to the South Purulia Shear Zone (SPSZ) and holds significant geological importance due to the presence of uranium-thorium-bearing lithologies [1, 2]. This study aims to assess the distribution of naturally occurring radioactive materials (NORMs), such as ^{238}U , ^{232}Th , ^{40}K in soil and rock samples collected from this area. Qualitative estimation of these radionuclides was performed using a NaI(Tl) detector at Sidho-Kanho-Birsha University, Purulia followed by quantitative analysis using a 30% High Purity Germanium (HPGe) detector at the UGC-DAE CSR, Kolkata Centre. Calibration has been done with ^{226}Ra standard (IAEA448; 50g kept in Petri dish in secular equilibrium; similar geometry of the samples). Absolute efficiency is 0.45% and 0.26% with FWHM of 2.59 keV (resolution: 0.74%) and 1.64 keV (resolution: 0.27%) at 351.93 keV and 609.31 keV gamma line of ^{238}U (or ^{226}Ra) respectively. The same source of ^{226}Ra is also used for the energy and efficiency calibration of the NaI(Tl) setup. Results from the NaI(Tl) detector exhibit maximum activity of ^{238}U of 1263.54 ± 24.53 Bq/kg, while for ^{232}Th and ^{40}K , the highest activities are 105.95 ± 3.71 Bq/kg and 1550.31 ± 18.41 Bq/kg, respectively. The activities obtained in this study are higher than the global averages of these radionuclides (^{238}U : 35 Bq/kg, ^{232}Th : 45 Bq/kg; ^{40}K : 420 Bq/kg) [1]. The results obtained from the NaI(Tl) detector are in reasonable agreement with those from the measurements using the HPGe detector with superior energy resolution and reliable quantification, and are marginally (~7%) greater than the aforementioned maximum activities (see Fig. 1). Radiological hazard indices including the absorbed dose rate and annual effective dose due to the exposure of the radionuclides are also estimated in this study. Elevated levels of these radionuclides may be attributed as a consequence of uranium mineralisation in this region as reported in previous studies [2]. It may be noted that the use of fertilizers in agricultural fields near the sampling locations contributes significantly to ^{40}K activity levels. This study highlights the significance of comprehensive radioactivity assessment in this region for ascertaining its impact on environment and public health. Such endeavours are expected to provide the necessary premise to correlate these findings with geological and anthropogenic factors for a deeper understanding of NORM distribution and its implications.

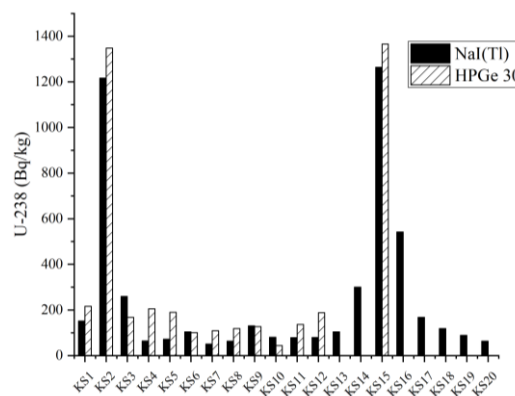


Fig. 1: Comparison between NaI(Tl) and HPGe Data

References:

- [1] Mitra, S., et al., *Environ. Geochem. Health.*, **46-2** (2024) 66.
- [2] Mandal, A., et al. *GSTF Journal of Geological Sciences*, **1(1)** (2014) 83.

Evaluation of Step-Wise Decontamination of Actinide Spiked Soil Sample

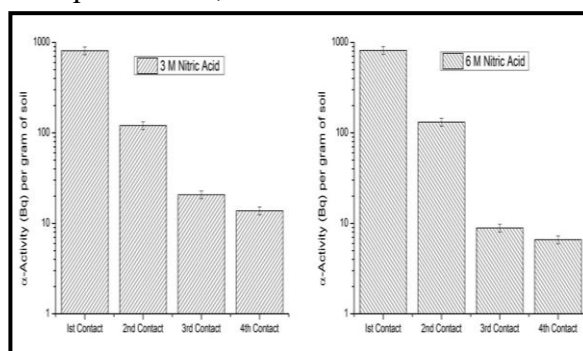
Saparya Chattaraj[§], Hemachandar V, Dinesh K. Patre, D. P. Rath, Ashokkumar P

Health Physics Division, Bhabha Atomic Research Centre, Mumbai, 400085, India

[§]Email: saparya@barc.gov.in

Radioactivity content assessment in the soil samples encountered in the facility is an integral part of the environmental monitoring. The radionuclides in the soil are expected to be embedded deep into the matrix, hence accounting for the total activity will require its leaching out into a water soluble matrix. Mechanistically, nitric acid is known to form soluble nitrates with actinides [1]. In a recent study, maximum extraction of actinides from soil sample was observed to level off at 3M-6M of HNO₃, while varying the nitric acid concentration from 0.1M to 6M, in a single contact [2]. The remaining radioactivity in the soil after the first round of contact was important to analyse. Furthermore, the number of steps of HNO₃ contact necessary for removal of majority of the radioactivity from the soil sample was necessary for a comprehensive understanding.

Nearly 1g of each dried and homogenised soil sample acquired from the facility surroundings were spiked with a maximum of 1 kBq of Nat. U, dried and crushed into fine powder. The samples were taken in centrifuge tubes and treated with 5 ml of 3M and 6M nitric acid in separate sets at ambient conditions. The samples were subjected to ultrasonic agitation for one hour, followed by centrifugation at 10,000 rpm for 15 minutes. The visibly clear supernatants were separated, and 1 mL aliquots were successfully plancheted without any residue. The planchets were subjected to gross alpha counting using calibrated ZnS(Ag) counter.



spiked soil sample

The average efficiency of the counter being 25%. The remaining soil samples in the centrifuge tubes were further treated with 5 mL of the same acid. The above mentioned process was repeated for several rounds until the remaining alpha activity is reduced significantly. Fig 1. shows similar trend of stepwise extraction was observed for both 3M and 6M nitric acid solutions. 85% alpha activity was extracted in the first step itself, followed by 10% activity in the second round. In the subsequent two rounds decontamination of the remaining 2% of the activity in the soil sample was achieved.

It may be concluded that alpha activity estimation in soil sample with 3M-6M nitric acid solutions will require atleast two rounds of contact for leaching out of ~95% of the activity into the aqueous medium.

Acknowledgements: The authors are grateful to Sh. Probal Choudhury, Head HPD, BARC for his encouragement and support. Thanks are due to staff members of RC&IG for providing the required technical help.

References:

- [1] A.D. Prakash et al., *Ann. Nucl. Energy*, **194** (2023) 110102
- [2] D.K. Patre et al., *Proceedings in 35th IARP National Conference*, 2025

Radiological Mapping of Environment Around the Upcoming Fuel Fabrication Facility at Kota

Anil Goyal¹, Daksha^{1§}, Anshi¹, Richa Sharma¹, S. K. Srivastava¹,
C G Sumesh², Aditi C Patra^{2,3}, Probal Chaudhury²

¹Health Physics Unit, Health Physics Division, BARC, NFC-Kota, Rawatbhata-323303

²Health Physics Division, Bhabha atomic Research Centre, Mumbai-400085

³Homi Bhabha National Institute, BARC, Trombay, Mumbai

§Email: daksha@nfc.gov.in

Nuclear fuel complex-Kota, a green field project at Rawatbhata site Rajasthan is an upcoming fuel fabrication facility at advanced stage for producing of 500MT per annum natural uranium fuel bundles to PHWRs. Generation of baseline data for uranium in environmental matrices is a prerequisite to assess the impact due to plant operation. Groundwater and soil were collected from 25 locations for uranium estimation and environmental TLD were deployed for background gamma radiation.

Uranium concentration in groundwater were directly analyzed using LED fluorimeter while uranium in soil samples were estimated through acid digestion followed by solvent extraction using ethyl acetate as solvent and fluorescence measurement. The exposure assessment using environmental TLD was carried out following standard procedures. Uranium concentration in groundwater were observed to range from 0.3 to 7.1 ppb with average of 1.5 ppb. Uranium in soil samples were observed to be in the range of 0.3 to 2.0 ppm with an average of 1.1 ppm. The quarterly background radiation exposure through environmental TLD was observed to be in the range of 133 to 221 μ Gy with mean of 174 μ Gy. The radiological mapping for uranium in groundwater and soil was carried out through kriging interpolation method and presented in Fig.1 (a) and Fig.1 (b). The contour map of quarterly background radiation exposure is presented in Fig.1 (c).

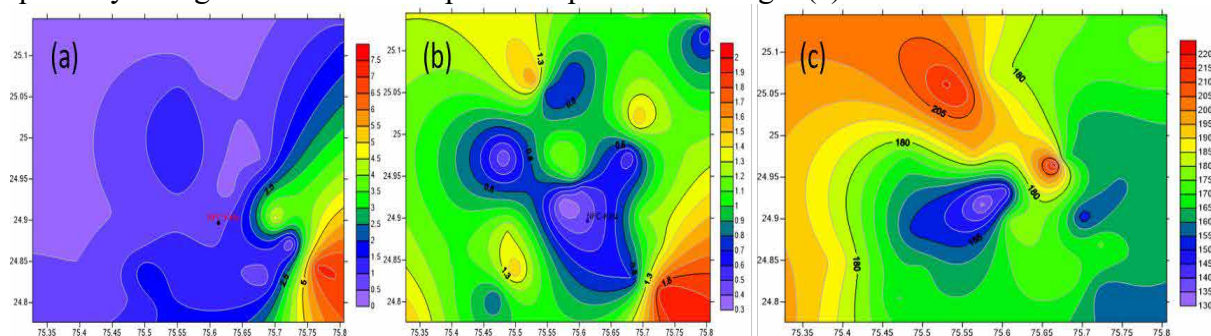


Fig 1: (a) Contour plot of uranium in groundwater, (b) Contour plot of uranium in soil, and (c) Gamma radiation exposure (μ Gy/quarter)

Uranium level in groundwater were found to be below the guideline value of 60ppb and 30 ppb prescribed by AERB and WHO, respectively. The radiological mapping of environment around the facility serves as baseline to assess the long-term impact to the environment due to fuel fabrication operations at NFC-Kota.

Reference:

[1] Operation Manual for LED Fluorimeter, LF-2, Quantalase Enterprises Pvt Ltd.

Assessment of Radon, Thoron Concentration and Inhalation Dose in Rural and Urban Dwellings of Aligarh District

R. L. Sharma^{1§}, A. K. Mahur², S. Sharma¹, S. A. Ali³

¹Institute of Technology and Management, Aligarh, India-202140

²Vivekananda College of Technology and Management, Aligarh, India- 202001

³Department of applied Physics, Aligarh Muslim University, Aligarh, India--202001

§ Email: roshanamu007@gmail.com

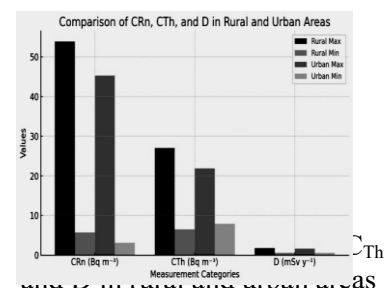
The study evaluates radon (C_{Rn}), thoron (C_{Th}), and inhalation dose (D) in rural and urban dwellings using a twin-cup dosimeter along with LR-115 type-II non-pelliculable Solid State Nuclear Track Detectors (SSNTDs). The study employed SSNTDs for passive monitoring of radon and thoron levels. The detectors were deployed in selected rural and urban homes and later chemically etched using a 2.5N NaOH solution at 60°C for 90 minutes. Track densities were then counted using an optical microscope, and concentrations were derived using the following equations:

$$C_R \left(\frac{Bq}{m^3} \right) = \frac{T_m}{dS_m} \quad (1) \quad C_T \left(\frac{Bq}{m^3} \right) = \frac{(T_f - dC_R S_{rf})}{dS_{rf}} \quad (2)$$

Where, CR = radon concentration, CT = thoron concentration, Tm = track density in the membrane compartment, Tf = track density in the filter compartment, d = Exposure time Sensitivity factor for membrane compartment ($S_m = 0.019 \pm 0.003 \text{ Tr/cm}^2/\text{d/Bq/m}^3$) Sensitivity factor for radon in filter compartments ($S_{rf} = 0.020 \pm 0.004 \text{ Tr/cm}^2/\text{d/Bq/m}^3$) Sensitivity factor for thoron in filter compartment ($S_{rf} = 0.016 \pm 0.005 \text{ Tr/cm}^2/\text{d/Bq/m}^3$). The inhalation dose (D) in mSv y⁻¹ was estimated using the relation:

$$D = \{(0.17 + 9F_R)C_R + (0.11 + 32F_T)C_T\} \times 7000 \times 10^{-3} \quad (3)$$

Where 0.4 and 0.1 are the equilibrium factors for radon and thoron respectively Field measurements in rural dwellings show C_R and C_T concentrations ranging from $5.7 \pm 0.7 \text{ Bq m}^{-3}$ to $53.9 \pm 5.3 \text{ Bq m}^{-3}$ and $6.51 \pm 0.8 \text{ Bq m}^{-3}$ to $27.0 \pm 3.0 \text{ Bq m}^{-3}$, respectively, with a maximum inhalation dose of 1.8 mSv y^{-1} . Urban homes exhibit slightly lower C_R and C_T values, ranging between $3.1 \pm 0.4 \text{ Bq m}^{-3}$ and $45.3 \pm 4.9 \text{ Bq m}^{-3}$, and $7.9 \pm 2.1 \text{ Bq m}^{-3}$ to $21.9 \pm 2.2 \text{ Bq m}^{-3}$, respectively, with a maximum inhalation dose of 1.6 mSv y^{-1} . Variations in radon and thoron levels are linked to construction materials and ventilation, with higher C_R values in dwellings using granite flooring. A comparative bar chart highlighting higher radon levels in rural areas, possibly due to differences in building structures and soil compositions. The findings suggest all measured values remain below the WHO action threshold of 100 Bq m^{-3} ensuring minimal health risks. Findings from this study emphasize the necessity of proper ventilation and material selection in housing to mitigate radiation exposure risks. Further research is recommended to develop guidelines for safer rural housing practices.



Reference:

[1] Sharma R L. et al. *J Radioanal Nucl Chem.* <https://doi.org/10.1007/s10967-024-09503-9>

Influence of Soil Organic Matter on the Distribution of Radionuclides in Soil Systems around Kaiga: A Correlation Study

Sanyam Jain^{1,2,§}, S. Rout^{2,3}, V. Pulhani^{2,3}, M. S. Vishnu¹, I. V. Saradhi³

¹Environmental Survey Laboratory, EMAD, BARC, Kaiga, India

²Homi Bhabha National Institute, Anushaktinagar, Mumbai, India

³Environmental Monitoring and Assessment Division, BARC, Mumbai, India

§Email: sanyam@barc.gov.in

Soil organic matter (SOM) plays a crucial role in the retention and mobility of radionuclides in the environment [1]. Understanding these interactions is essential for environmental monitoring, soil contamination assessments, and remediation planning. Earlier studies reported the SOM and radioactivity in the soil around Kaiga, but their correlation was underexplored [2]. Given the organic-rich nature of Kaiga's soil, investigating its interaction with radionuclides is essential. This study investigates the relationship between SOM and activity of ²²⁶Ra, ²³²Th, ⁴⁰K, and ¹³⁷Cs in soil systems around Kaiga, Karnataka, through a statistical correlation analysis. For this study, 60 soil samples were collected from 5 different locations in the Kaiga region and analyzed for radionuclide activity using a High-Purity Germanium (HPGe) detector-based gamma spectrometry system. SOM content was determined using the Loss on Ignition (LOI) method, which provides an estimation of organic matter by measuring weight loss after combustion at high temperatures.

The Pearson correlation coefficients revealed a strong positive correlation between SOM and ¹³⁷Cs (0.80***) as well as SOM and ²²⁶Ra (0.65***), indicating that higher organic matter content enhances the retention of these radionuclides. Additionally, a very strong correlation (0.92***) was observed between ²²⁶Ra and ²³²Th, which may be attributable to their shared geological origin. A moderate positive correlation was also observed between SOM and ²³²Th (0.53***), which suggests that organic matter also influences ²³²Th retention, albeit to a lesser extent. In contrast, ⁴⁰K exhibited an insignificant correlation with SOM (-0.14), and showed a weak negative correlation with ¹³⁷Cs (-0.28*), though both the elements are monovalent and belong to the same group suggesting differing environmental behaviour. These findings highlight the importance of SOM in controlling the fate of both natural and anthropogenic radionuclides. The strong association of ²²⁶Ra, ²³²Th, and ¹³⁷Cs with SOM suggests that organic matter-rich soils may act as reservoirs for these radionuclides,

potentially influencing their bioavailability and migration in ecosystems around Kaiga. However, more soil parameters are required to be analyzed and correlated to gain a comprehensive understanding of radionuclide behaviour in different soil conditions.

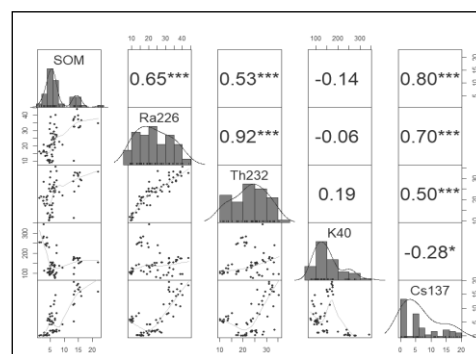


Fig. 1: Correlation plot of SOM vs. activity concentration (***) and * indicate significance level, $p < 0.001$ and $p < 0.05$ resp.)

References:

- [1] C. Xu et.al., *J. Environ. Radioact.*, **153** (2016) 156.
 [2] J. P. James et.al., *J. Environ. Radioact.*, **102** (2011) 1070.

Assessment of Groundwater Recharge Through Defunct Dug Wells Using Environmental Stable and Radioisotopes

Anushree Ghosh¹, Tirumalesh Keesari^{1, 2§}, A. Jaryal¹, A. Roy¹,
D. Pant¹, H.V. Mohokar¹, S.N. Kamble¹, R Acharya^{1,2}

¹Isotope and Radiation Application Division, BARC, Mumbai, India

²Homi Bhabha National Institute, BARC, Mumbai, India

§ Email: tirumal@barc.gov.in

An isotope hydrological study was carried out in the Nuapada district of western Orissa to evaluate the impact of defunct dug wells on groundwater recharge through isotope techniques. Due to irregular rainfall and frequent droughts, groundwater resources have been indiscriminately exploited in this region leading to water quantity and quality issues [1]. Among the methods proposed to boost groundwater quality and quantity, one is the use of abandoned/defunct dug wells to improve rainwater recharge to groundwater. It is therefore important to evaluate the efficacy of these dug wells to achieve sustainable development of groundwater systems in this region.

The main objective of this study is to estimate the contribution of dug well recharge to groundwater and to assess the groundwater dynamics using isotopic tools. The major water bearing formations are Granite and Granite Gneiss and two types of aquifer systems are found here, viz., i) unconfined aquifer extended up to a depth of 30 m and ii) confined aquifer with maximum thickness of 200 m. The water samples were collected from three test sites where rainwater, collected on the roof top, was filtered using custom-built units and the filtered water was allowed to infiltrate to groundwater through dug wells (Fig. 1a). Environmental isotopes (²H, ¹⁸O, ³H) were measured in water samples collected from handpumps, dug wells, tube wells and surface water bodies. The stable isotope measurements were performed using isotope ratio mass spectrometer and environmental tritium was measured using liquid scintillation counter.

Stable isotope data suggests three types of groundwaters, viz., i) rainwater recharged, ii) mixture of rainwater and regional groundwater and iii) contributed from evaporated surface water sources (Fig 1b). Based on the tritium content it can be inferred that groundwater has modern recharge. It is also observed that wells near the defunct dug wells showed higher tritium and the values were close to that of local rain water (Fig. 1c). End member mixing analysis was performed to quantify the recharge contribution through dug wells, which was found to range from 5% to 42% in pre-monsoon and 82% in post-monsoon season.

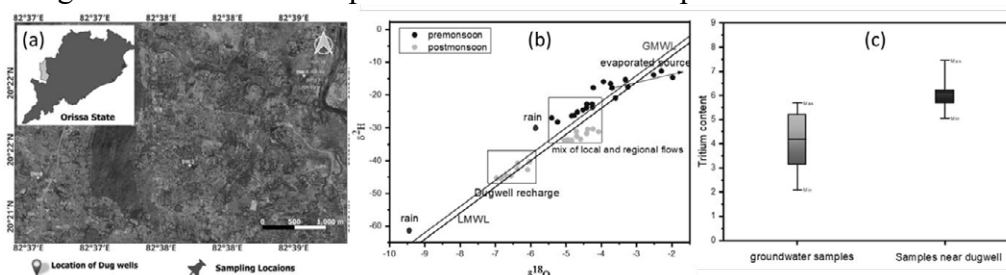


Fig. 1 a) Location map of study area, b) $\delta^2\text{H}$ vs $\delta^{18}\text{O}$ plot of water samples, c) Box-whisker plot of tritium content (in TU) of water samples

References:

- [1] Groundwater information booklet, Nuapada district, Orissa, Central Ground Water Board, May 2012

A Study on the Groundwater Dynamics in Coastal Aquifers of Eastern India Using Environmental Tritium and Radiocarbon Dating Techniques

Annadasankar Roy^{1,2}, Diksha Pant^{1,2}, H. V. Mohokar¹, Ajay Jaryal¹, Sanjit Kumar Sahu³, Anushree Ghosh¹, Prakash Chandra Mishra³, Raghunath Acharya¹, Tirumalesh Keesari^{1,2,§}

¹Isotope and Radiation Application Division, BARC, Mumbai, India

²Homi Bhabha National Institute, Anushaktinagar, Mumbai, India

³Department of Environmental Science, Fakir Mohan University, Balasore, India

§ Email: tirumal@barc.gov.in

Groundwater sustainability is a major concern for water resource management authorities and it is more complex and challenging in the case of coastal aquifers. India has a long coastal line of approximately 7500 km [1] in length and groundwater salinization is one of the major issues in coastal regions. Studies on the issue of groundwater sustainability of these large aquifer systems are limited. Balasore district of Odisha falls in the eastern part of India and the groundwater availability is constrained by complex contamination processes from F⁻ leaching to salinization to groundwater depletion. Natural environmental radioisotopes (³H and ¹⁴C) were used in this study to evaluate groundwater dynamics and sustainability, which are essential parameters for groundwater management and policy implementation. The ³H and ¹⁴C sampling in groundwater from selected monitoring wells was carried out during pre and post monsoon seasons of year 2022 (Fig. 1a). A total of 26 and 22 groundwater samples for environmental tritium were collected during pre and post monsoon seasons, respectively, while 15 locations with negligible ³H content were selected for groundwater ¹⁴C dating.

A comparative analysis of ³H variations during pre and post monsoon season is provided in Fig. 1b. The values indicate that groundwater dynamics increased considerably in the region after monsoon season, suggesting significant recharge from rainwater. The spatial distribution of ³H data during post monsoon season suggests that groundwater is more dynamic in the hard rock parts of the coastal aquifer system (Fig. 1a). This observation agrees with the geological framework of the area. The ¹⁴C results in groundwater suggest residence time values varying from 16 ka to 27 ka (uncorrected). These paleowater pockets were found to be situated towards coastal boundary of Balasore and these were mostly associated with highly saline groundwater samples. Based on this study, it can be concluded that certain parts of the Balasore coastal region contain highly saline paleowater pockets and further groundwater development may risk the availability of freshwater resources.

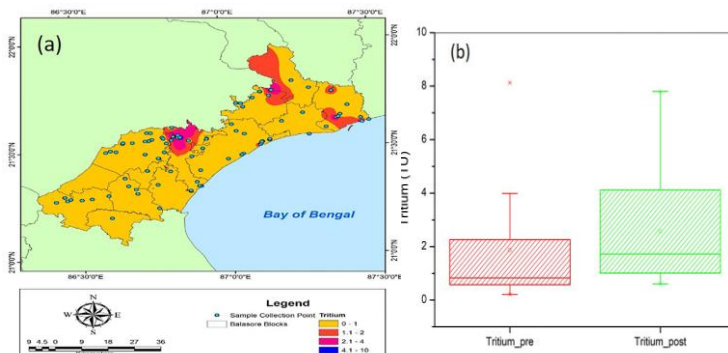


Fig. 1: (a) Sampling locations and spatial distribution of groundwater tritium content during 2022; (b) tritium content during pre and post monsoon season.

References:

[1] P. Prusty and S. Farooq, *HydroResearch*, **3** (2020) 61.

Measurement of Activity Size Distribution of Radon Progeny using SSNTD-Based Cascade Impactor

R.P. Rout[§], R.Mishra, R. Prajith, S. Jalaluddin, Arshad Khan, B. K. Sapra

Radiological Physics and Advisory Division, BARC, Mumbai, India

[§]Email: rprout@barc.gov.in

As the deposition of radon and thoron progeny in various regions of respiratory tract is mainly governed by their size, it is important to measure their Activity Median Diameter (AMD) in order to know which region is likely to get more dose [1]. In the present study, we have developed a LR-115 SSNTD based simple technique, namely D-LPI (DRPS/DTPS loaded Low Pressure Impactor) to measure the AMD of radon and thoron progeny and validated its results with the commercially available Scanning Mobility Particle Sizer (SMPS) from GRIMM, Germany.

D-LPI consists of an 11 stage Low pressure cascade impactor with varying cut-off size from less than 0.1 μm to more than 21.3 μm . The Filter Papers (FPs) kept on impaction plate in each stage of the conventional LPI were replaced with LR-115 SSNTD based Direct Radon Progeny Sensor (DRPS) and Direct Thoron Progeny Sensor (DTPS) to collect the progenies at a calibrated flow rate of 10 Lpm as shown in Fig 1. The alpha's emitted by these deposited progenies will register tracks in the LR-115 films which can be analyzed to get the AMD.

Experimental measurement of AMD of radon and thoron progeny was carried out in an 8 m³ calibration chamber using both D-LPI and SMPS. After sampling of progenies, the track densities in the DRPS and DTPS were determined by standardized chemical etching, followed by track counting. From the log-probability plot of cumulative track density versus cut-off size (d) as shown in Fig. 2, AMD and GSD (Geometric Standard Deviation) were determined as follows:

$$AMD = d(50\%) \text{ \& \ } GSD = d(84\%) / d(50\%) \quad (1)$$

AMD of radon and thoron progeny using D-LPI were found to be 0.20 μm (GSD 2.88) and 0.17 μm (GSD 2.65), respectively, which are in close agreement with the values of 0.21 μm (GSD 2.71) and 0.16 μm (GSD 2.63), measured by SMPS.

The developed system will be more convenient to measure the AMD of radon and thoron progeny as the tracks registered in the SSNTD film are permanent.

References:

[1] ICRP 137 (2017), Occupational Intakes of Radionuclides: Part 3. Ann. ICRP 46(3/4).

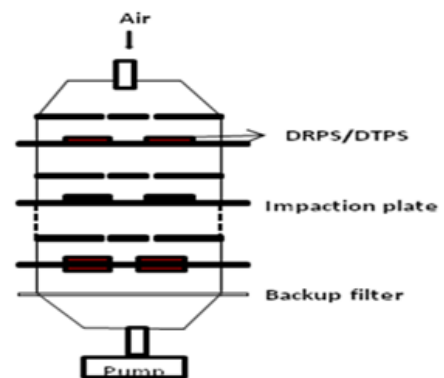


Fig. 1: Schematic diagram of D-LPI

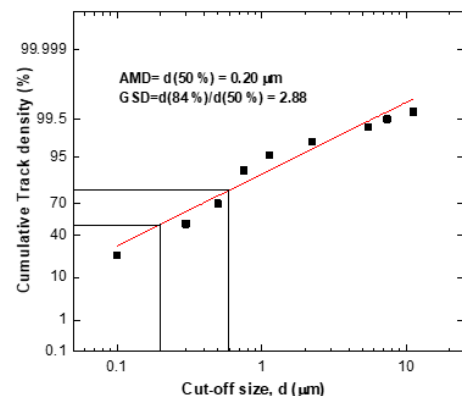


Fig. 2: Log-probability plot of cumulative track density versus cut-off size for radon progeny

Measurement of Radon Mitigation Factor of Synthetic and Natural Fibers

R. Prajith[§], R.P. Rout, R.Mishra, Arshad Khan, B. K. Sapra

¹Radiological Physics & Advisory Division, BARC, Mumbai, India

[§]Email: rama@barc.gov.in

Radon mitigation is essential in high radon background areas to decrease the inhalation dose as well as in underground laboratories where radon can be a background for high energy physics experiments. In the present work, the Radon Mitigation Factor (RMF) for various radon barrier materials has been tested using an indigenously developed diffusion sampler based on ISO/TS 11665-13:2017 [1].

The diffusion sampler consists of two SS chambers; Source chamber (SC) and Receiver chamber (RC) with a volume of 800 cm³ each. Barrier material (area 78.5 cm²) to be tested is placed between these 2 chambers (Fig 1a). 90 nCi Radium powder source is kept in SC, such that radon gas diffuses through the barrier material to reach the RC. Both the chambers are connected to two separate continuous Radon monitors (RnDuO) to simultaneously measure radon in both the chambers.

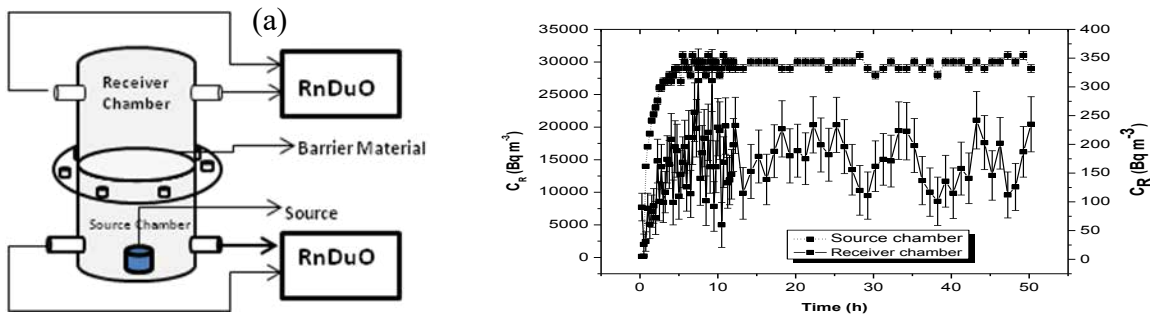


Fig 1(a) Experimental set up and (b) Radon concentration for Aluminised PET in two chambers

Various synthetic polymers like Aluminised PET, polyester, PVC and natural fibers, namely bamboo towel and banana fiber paper have been studied and the RMF is calculated as,

$$RMF (\%) = (C_{SC} - C_{RC}) / C_{SC} \times 100 \quad (1)$$

where, C_{SC} and C_{RC} are radon concentration in SC and RC respectively. Fig 1b shows the Radon concentration verses time in SC and RC with Aluminised PET (150 μm) as barrier material. RMF values of different barrier materials measured in the present study are shown in Table 1. It was observed that RMF of synthetic fibres is more than that of the natural fibres.

Table 1: Radon mitigation factor of some synthetic and natural fibers

Type of material	Polymer	Thickness	RMF (%)
Synthetic polymer	Aluminised PET	150±2 μm	99.2±3.5
	polyester	150±2 μm	98.7±2.1
	PVC	150±2 μm	99.9±3.2
Natural fiber	bamboo towel	150±5 μm	89.8±1.9
	Banana fiber	150±8 μm	91.0±1.5

References:

- [1] ISO/TS11665-13:2017-Measurement of Radioactivity in the Environment-Air: Radon 222.

Distribution of ^{210}Po and ^{210}Pb Activity in Soil of Chittorgarh, Rajasthan

Tejpal Menaria^{1§}, D.S. Rathore², S.N. Tiwari¹, I.V. Saradhi¹

¹Environment Monitoring and Assessment Division, BARC, Mumbai, India

²Mohan Lal Sukhadiya University Udaipur, India

§ Email: tejmenaria76@gmail.com

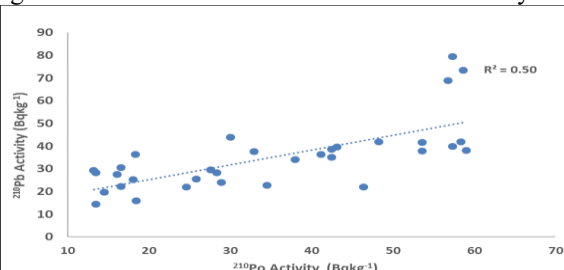
Radionuclides ^{210}Po ($T_{1/2}$ 138 days) and ^{210}Pb ($T_{1/2}$ 22.3 years) are daughter products of the uranium series. ^{210}Pb undergoes beta decay to form ^{210}Bi , which further decays to ^{210}Po by beta particle emission. ^{210}Po undergoes α decay to form ^{206}Pb . The rapid decay of ^{222}Rn in the atmosphere generates ^{210}Po and ^{210}Pb , which adsorb onto aerosols and return to earth's surface and their activity depends on the geological formation and atmospheric aerosol particles. The mean atmospheric residence time of ^{210}Po varies between 15 to 75 days, with a mean of 26 ± 3 days, while ^{210}Pb is continuously deposited from the atmosphere in association with aerosols at a rate of about $55 \text{ Bq}(\text{m}^2\text{y})^{-1}$ [1]. Though studied in various media (soil, water, air, sediment, biota, and food), data on ^{210}Po and ^{210}Pb in soil is limited. This study aims to generate baseline soil data in Chittorgarh.

About 10 g of soil samples from clean top layer soil up to 5 cm depth, was processed by using standard IAEA wet acid digestion procedure [2]. This sample was digested under an IR lamp for 8 h, and then treated with a mixture (20 mL) of HNO_3 and HCl (1:3) at 85°C on a hot plate for 3 h. It was then refluxed with the same acid mixture (30 mL) for 4 hours, filtered, and extracted with 0.5 M HCl . ^{210}Po was collected by auto deposition on a silver disc in an ascorbic acid medium at 90°C for 4 h. The silver disc was rinsed with deionized water and ethanol, and then counted on both sides using the $\text{ZnS}(\text{Ag})$ detector. This aliquot was stored for a year to allow ^{210}Po build up from its parent (^{210}Pb). Auto deposition of ^{210}Po on silver disc was repeated to estimate ^{210}Po from ^{210}Pb using build up correction for the growth period [3]. Quality and recovery (87.6%) of this method were validated by analyzing ^{208}Po source (IAEA sample) with alpha spectrometry.

The salient features of radioactivity of ^{210}Po and ^{210}Pb in the soil samples are tabulated in Table-1. In the study area, the activity of ^{210}Po and ^{210}Pb were found to be similar to the reported in literature [4]. As shown in Fig-1, moderate correlation ($R^2 \leq 0.5$) exists between the activity of ^{210}Pb and ^{210}Po in the soil, suggesting that ^{210}Pb and ^{210}Po are from similar geological and lithological formation of surface soil of this region.

Parameters (N=31)	Activity (Bqkg^{-1})		Ratio ($^{210}\text{Po}/^{210}\text{Pb}$)
	^{210}Po	^{210}Pb	
Range	13.1-59.2	14.4-79.6	0.5-2.1
Mean \pm SD	34.6 ± 14.3	34.9 ± 10.4	0.9 ± 0.3
Skewness	0.2	1.6	0.7
Kurtosis	-1.4	2.8	1.0
25 th Percentile	18.4	25.1	0.7
75 th Percentile	48.3	39.6	1.2

Fig-1: Correlation between ^{210}Po and ^{210}Pb activity



References:

- [1] F. El-Daoushy and G. Garcia-Tenorio, G., *Sci. Total Environ.*, **69**(1988) 19.
- [2] IAEA, *Int. J. Radiat. Biol.*, **IAEA/AQ/12**(2009).
- [3] H. Xiaolin, et al, *J. Radioanal. Nucl. Chem.*, **249**(3) (2001), 587.
- [4] N. Venunathan, and Y. Narayana, Y., *J. Radiat. Res. Appl. Sci.*, **9**(4) (2016) 392.

Radiocarbon Dating of Tree Rings Using Accelerator Mass Spectrometry

Anushree Ghosh¹, Tirumalesh Keesari^{1,2§}, Pankaj Kumar³, Leema Saikia³,
Shreyas Managave⁴, Chandra Kant Salunke⁵, Himanshu Mishra⁵

¹Isotope and Radiation Application Division, BARC, Mumbai, India

²Homi Bhabha National Institute, BARC, Mumbai, India

³National Geochronology Facility, Inter University Accelerator Centre, New Delhi, India

⁴Indian Institute of Science Education and Research, Pune, Maharashtra, India

⁵Architectural and Structural Engineering Division, BARC, Mumbai, India

§Email: tirumal@barc.gov.in

Tree ring dating supports historical reconstruction, geochronology, archaeology, and palaeoscience. Classical analysis of ring width, density, and stable isotopes of C, O, and H offers reliable climate-sensitive proxies [1]. While dendrochronology is commonly used, it is limited in trees lacking clear annual or seasonal rings. In such cases, radiocarbon dating provides accurate age estimation. This study aimed to determine the age of trees using radiocarbon dating and correlate it with historical plantation records. Wood samples were collected from the stumps of fallen raintrees (*Albizia saman*) inside the BARC premises. The tree sections along with sampled tree rings for radiocarbon dating are presented in Fig. 1a and 1b. Tree rings were sampled using a custom drilling tool, and alpha cellulose was extracted using standard base-acid-base-acid-bicarbonate (BABAB) treatment. Samples were then combusted and graphitized using Automated Graphitized Equipment (AGE), converting CO₂ to graphite under hydrogen atmosphere in presence of an iron catalyst. The graphite samples were then radiocarbon dated with the AMS system at National Geochronology facility, IUAC [2]. The blank corrected ¹³C/¹²C and ¹⁴C/¹²C ratios were normalized with a known standard material (NISTSRM-4990: OXII), corrected for δ¹³C values and converted to fraction modern value and then to a calendar dates using bomb pulse calibration curve for northern hemisphere (Fig. 1c & 1d). The radiocarbon data indicate that trees Log-2 and Log-3 date back to 1962–1963 and 1963–1964, confirming their status as some of the earliest transplanted trees in BARC.

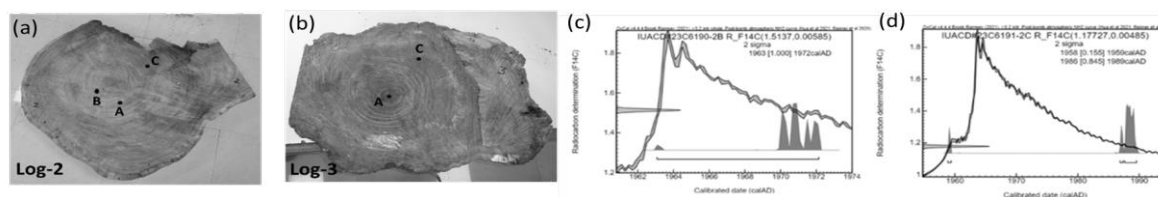


Fig. 1 (a) & (b): photographs of raintree stumps, (c) & (d): radiocarbon values of the wood samples superimposed on the bomb pulse calibration curve for north hemisphere (Bomb 21 NH2)

Acknowledgement: Authors would like to thank Chairman, AEC and Director, BARC for their keen interest in this study and AD, RC&IG and Head, IRAD for their constant support.

References:

- [1] R. T. W. Siegwolf, J. R. Brooks, J. Roden, M. Saurer, Stable isotopes in tree rings, 2022, Springer publishers
- [2] P. Kumar et al., *Nucl. Instrum. Methods Phys. Res. B.*, **361** (2015) 115.

Measurement of $^{232+228}\text{Th}$ in Fine and Coarse Fractions of Airborne Aerosols in Monazite Mining and Processing Facilities

P. Prusty[§], A. Sahu, A. Chakrabarty, A. Rout, R. P. Patra, P. Chaudhury

Health Physics Division, Bhabha Atomic Research Centre, Mumbai, India

[§]Email: parthap@barc.gov.in

Monazite mining is pivotal for the third stage of India's nuclear power program because it is the foremost source of thorium and the key fuel element for this stage, allowing India to bring into play its abundant thorium reserves for generating nuclear energy. The mining and processing of monazite generates airborne particulates, which contain alpha-emitting thorium isotopes. Measurements were carried out in monazite mining areas and monazite processing facility to estimate the activity concentration of $^{232+228}\text{Th}$ in PM_{10} and $\text{PM}_{2.5}$.

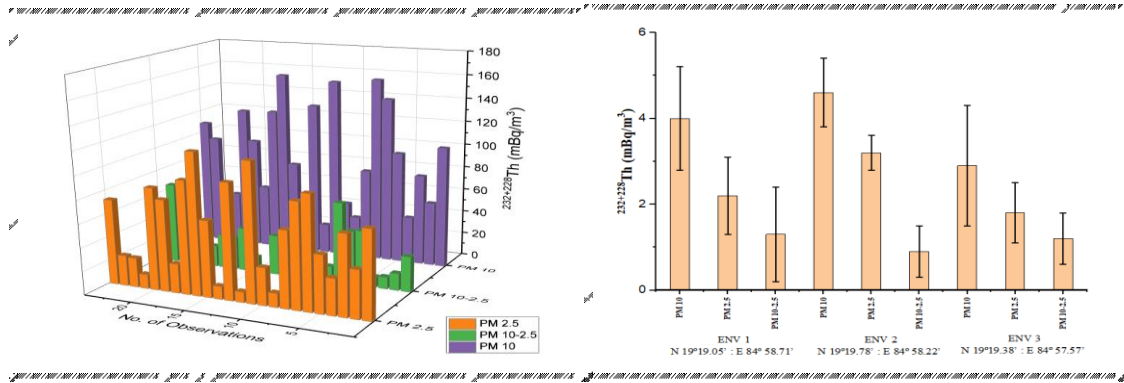


Fig 1: $^{232+228}\text{Th}$ activity in airborne particulates of monazite processing facility

Fig 2: $^{232+228}\text{Th}$ activity in airborne particulates of monazite mining facility

The mean long-lived alpha ($^{232+228}\text{Th}$) activity in PM_{10} , fine particulate ($\text{PM}_{2.5}$) and coarse fraction ($\text{PM}_{10-2.5}$) in the mining area was 3.8 ± 2 , 2.4 ± 1.2 & 1.1 ± 1.3 mBq.m^{-3} , respectively (Fig 2). Similarly, 24 occupational areas were monitored and $^{232+228}\text{Th}$ activity in PM_{10} , $\text{PM}_{2.5}$ and coarse fraction ($\text{PM}_{10-2.5}$) are shown in Fig. 1, with average values of 78.3 ± 25.2 , 47.9 ± 28.3 and 21.5 ± 9.0 , respectively. The thorium activity levels in the sampling locations is well below the DAC value i.e. 160 mBq.m^{-3} as recommended by AERB. The contribution of ^{230}Th is not taken into account during the measurement as it is the daughter product of ^{238}U and the abundance of thorium is approximately thirty times higher than uranium in monazite mineral. The aerosol sampling was done by ECOTECH AAS 127 MFC sampler and the alpha counting was carried out using a well-calibrated ZnS (Ag) scintillation detector. The long-lived alpha activity is more in PM_{10} fraction because it has larger aerosol concentration, which provides larger surface area to adsorb the radionuclides. The outcomes of the study will help to assess the radiation dose received by occupational workers due to the inhalation of thorium-bearing aerosol using the dose coefficient assigned by the regulatory agencies and to enhance the radiation protection policies in beach sand mining industries.

References:

[1] Assessment of ^{232}Th particulates released from the processing of monazite; P Prusty, A Sahu, et. al, AOCRP6, 07-11 Feb 2023.

Assessment of ^{210}Po Activity in Stream Sediments Around a U Ore Processing Facility, India

Sarjan Singh^{1,§}, N. K. Sethy¹, N. M. Soren², A. C. Patra¹, P. Chaudhury¹

¹Health Physics Division, Bhabha Atomic Research Centre, Mumbai, India

²HP Unit, Uranium Corporation of India Limited, Jaduguda, India

[§]Email: sarjans@barc.gov.in

The U industry generates tailings and effluents containing radionuclides and heavy metals, which can disperse into water bodies and sediments if not managed properly. Sediments act as both a source and a sink for radionuclides, influencing their transport and bioavailability, potentially leading to human exposure. ^{210}Po a U-series radionuclide, is significant due to its high specific activity, α emission energy (5.4075 MeV) and toxicity. It bioaccumulates in organisms with a $t^{1/2}$ of 138 days. Monitoring ^{210}Po in sediments near uranium facilities like UCIL Jaduguda is crucial for assessing its environmental migration and the effectiveness of effluent management strategies. The study was conducted near the UCIL Jaduguda uranium processing facility, where treated effluents are discharged into local water bodies. Sludge samples from the primary reservoir of UCIL's Effluent Treatment Plant, are collected as the source term. Deposited by effluent from the tailings pond (TP), the sludge is returned to TP once the reservoir reaches its capacity. Sediment samples were collected from six sites: upstream (Rohinbera (S1), Dungridih (S2)), and downstream (Gandhi Market (S3), Shiv Mandir (S4), RCP Bridge (S5), Moubhandar Bridge (S6), Subernarekha river). Samples were air-dried, sieved, and homogenized. 5 g of each sample was acid-digested at 120–140 °C. ^{210}Po was measured using the spontaneous deposition method, where the digested sample was treated with 0.5 N HCl and stirred at 90 °C for 6 h on a silver disc for deposition, followed by α counting [1]. Method validation using ^{209}Po (SRM 4326a, NIST) showed 98% recovery at 95% CI, ensuring accuracy.

The naturally occurring ^{210}Po in sediments ranges from 30 to 200 Bq.kg⁻¹, indicating background levels. A 4220 Bq.kg⁻¹ in the sludge sample, serving as the source term. Post-treatment, effluent enters the Juria Nala, where S3 (within plant premises) shows localized accumulation. This is primarily due to the occasional overflow of effluent exceeding the ETP capacity (200 m³.h⁻¹) in rainy season, leading to fine tailings settling in low-flow zones, such as Juria Nala D/S sediments.

However, levels decrease at Shiv Mandir (S4) and further dilute at RCP Bridge (S5), nearing background levels. At Moubhandar Bridge (S6), ^{210}Po returns to natural levels, confirming complete dilution. A slight increase in Juria D/S remains localized, indicating effective dilution along the discharge path, minimizing environmental ^{210}Po migration.

Table 1. ^{210}Po activity across various locations

Location	^{210}Po (Bq Kg ⁻¹)
Rohinbera, Juria U/S	44 ± 10
Dungridih, Juria U/S	54 ± 08
Gandhi Market, Juria D/S	1025 ± 116
Shiv Mandir, Gara D/S	163 ± 24
RCP Bridge, Gara D/S	67 ± 17
Moubhandar Bridge, S/Rekha D/S	30 ± 07

References:

- [1] D. B. Sharma et al., *J. Radioanal. Nucl. Chem.*, **331** (2022) 1323.

Radiological Parameters of Environmental Water Samples: Radiological Safety at OSCOM, Chhatarpur, Odisha

Annapurna Rout[§], A. Sahu, P. Prusty, R. Patra, Aditi C. Patra, P. Chaudhury

Health Physics Division, Bhabha Atomic Research Centre, Mumbai, India

[§]Email: annapurnar@barc.gov.in

The Orissa Sand Complex (OSCOM), Chhatarpur, Odisha is the largest division of IREL for producing monazite, a commercially suitable rare earth mineral that also contains radioactive uranium and thorium. As a result, radiation safety is essential during the mining and extraction of rare earths. According to WHO (2011), access to safe drinking water is a basic human right and critical for health protection, making quality control vital. Drinking water may contain radioactivity that could present a risk to human health. The radioactivity in groundwater comes mainly from radionuclides of the natural decay chains ^{238}U and ^{232}Th , and ^{40}K in soil and bedrock [1]. To address this, Health Physics Unit (HPU) of Radiation Protection Section (Nuclear Fuels), HPD, BARC located at OSCOM IREL (India) Ltd., is being assigned to monitor the radiological safety of plant and surrounding environment [2].

Sites within a 10 km radius of the plant fall under this surveillance. These areas show naturally high radiation background. Borehole water samples from these locations are collected quarterly and analyzed for physicochemical and radiological parameters. Gross α/β measurement is one of the simplest radioanalytical procedures applied widely as a screening technique in the field of radioecology, environmental monitoring and industrial applications as well. Dual counter i.e., a plastic scintillation counter (composite detector with a combination of plastic and ZnS (Ag) scintillators) is used for α and β measurements.

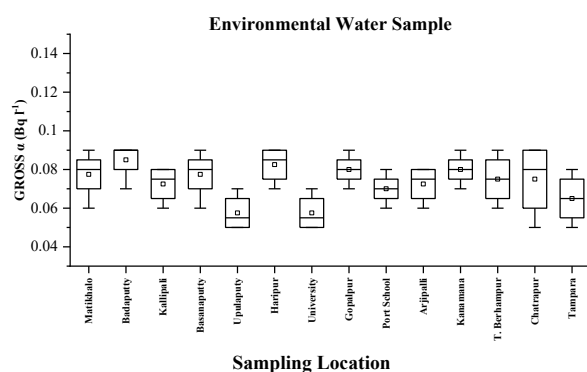


Fig. 1: Gross alpha activity of water samples.

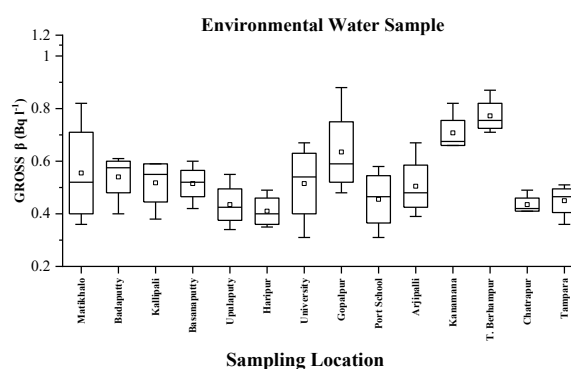


Fig. 2: Gross beta activity of water samples.

In 2023, environmental water samples showed gross α activity ranging from 0.07 ± 0.017 to 0.09 ± 0.038 Bq.l⁻¹, and β activity from 0.41 ± 0.005 to 0.77 ± 0.01 Bq.l⁻¹. These are average quarterly values and remain below the IS 10500 limits i.e. 0.1 Bq.l⁻¹ and 1.0 Bq.l⁻¹ for α and β emitters, respectively. These values depend on the radionuclide content of water, which is indirectly related to monazite abundance of the soil. The radiological analysis of water samples is monitored regularly to ensure radiological safety of drinking water in and around OSCOM.

References:

- [1] A. Malanca et.al., *Appl Radiat Isot*, **49** (7) (1998) 893.
- [2] A. Sahu et.al., Radiation protection and environmental surveillance in and around OSCOM, IREL Ltd. At Chatrapur, Odisha, Annual Report, 2021.

Study of Elemental Profile of Soil and Plant Samples Using EDXRF Technique Near National Highway Pantnagar, Uttarakhand

Smriti Kandpal¹, G. C. Joshi^{1,2*}, Mahesh Tiwari³, R. S. Srivastava¹, Anil Kumar⁴

¹ Department of Physics, ² Radiations & Isotopic Tracers Laboratory,
G B Pant University of Ag. & Tech., Pantnagar, Uttarakhand

³ Environmental Monitoring and Assessment Division, BARC, India

⁴ Department of LPM, G B Pant University of Ag. & Tech., Pantnagar, India

§ Email: girishjoshi.bpp@gbpuat.ac.in

Soil and plants are essential components of ecosystems, serving a vital role in supporting life on Earth, whereas soil is believed to have a capacity for receiving and decomposing pollutants [1]. Elemental analysis of soil and plants is essential for assessing soil health, such as plant growth and development, and improving productivity [2]. The present study was an attempt to determine the elemental profile of plants and soil collected from the National Highway running through Pantnagar and from Model Floriculture Centre to detect environmental pollution and identify the plant to absorb the heavy metals. An EDXRF analysis was conducted on 18 samples collected and a total of 27 elements Sc, Ti, V, Cr, Mn, Fe, Co, Ni, Cu, Zn, Na, Mg, Al, Si, K, Ca, Ba, Pb, La, Ce, U, Th, Rb, As, Zr, Sr, and Cd were identified in soil samples and same elements were detected in plant leaf samples except Pb. The NIST 2709a and INCT-OBTL5 standards were used in analysis of soil and plant samples respectively. The results are presented in Fig. 1 and Fig. 2.

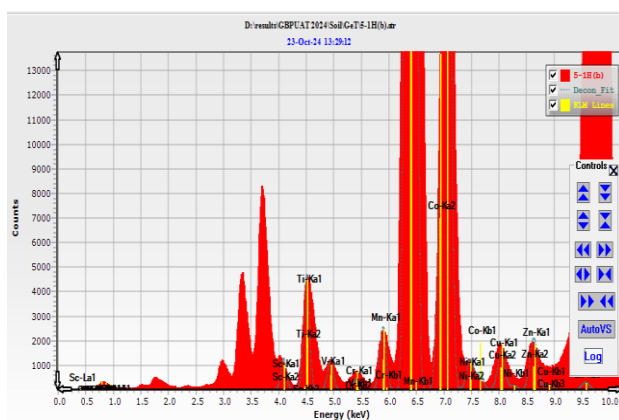


Fig.1.EDXRF spectra of soil sample S1Hb

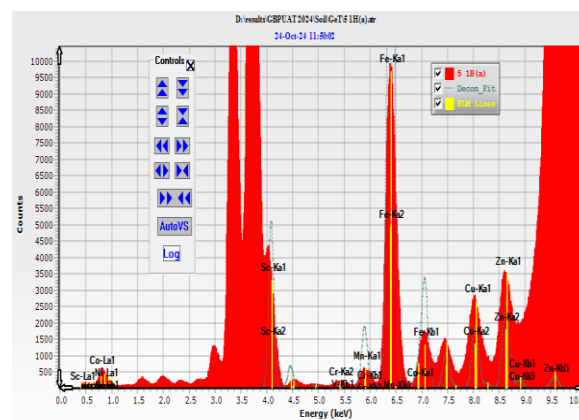


Fig.2. 3EDXRF spectra of Plant sample S1Ha

The interpretation of data was done on the basis of Principal Component analysis (PCA) and pollution indices were used to determine contamination in soil and plants sample.

Thus, the present study affirms that a moderate contamination was observed in the soil by cadmium and plants *Dalbergia sissoo* (Sheesham) has the capacity to absorb heavy metals. Therefore, *Dalbergia sissoo* (Sheesham) should be strategically planted to minimize heavy metal pollution and minimize the contamination levels. Moreover, to understand the impact due to anthropogenic activity should be identified, surveyed and analysed to maintain soil and plant health and to promote the environmental sustainability.

References:

- [1] J. C. Young et.al., *J. water Pollut. Contr. Fed.*, **53** (1981) 1253.
- [2] G. C. Joshi and H.M., Agrawal, *J. Radioanal. Nucl. Chem.*, **198(2)** (1995) 475.

Baseline Radiological Assessment in Soil Samples from Uranium Mining Site at Rohil

S. V. Bara^{1§}, M. R. Dhumale¹, S. Chinnaesakki¹,
P. Lenka¹, A. C. Patra^{1,2}, Probal chaudhury^{1,2}

¹Health Physics Division, BARC, Mumbai, India

²Homi Bhabha National Institute, Mumbai, India

§Email: sheetalk@barc.gov.in

Sustainable development requires balancing environmental health with the efficient use of natural resources. A pre-operational database is essential to protect human health and the environment from pollutants resulting from industrial and technological activities. This study assesses natural and anthropogenic radioactivity in soil samples from the Rohil region to establish a baseline for environmental monitoring and radiological safety. As a primary medium for radionuclide accumulation, soil serves as a vital indicator of both natural and anthropogenic radiation sources. Rohil, located in the Sikar district of Rajasthan, has been identified as a new uranium (U) mining site, with a medium-tonnage deposit (~8,000 tonnes) of polymetallic, metasomatitic uranium ore grading 0.06% [1].

26 soil samples were collected around U mining site at Rohil. Samples were dried, sieved (70 mesh), and sealed in 250 cc containers to allow radioactive equilibrium between radium and its progeny. Samples were analyzed using a high-resolution gamma-ray spectrometry system with a 50% relative efficiency p-type HPGe detector coupled with 64 k DSP MCA module. The detector is shielded using graded shielding of 100 mm lead, 9 mm copper with nickel electroplating. Calibration used standard reference materials (RGU and RGTh) covering the energy range from 46 keV to 2614 keV. Natural radioactivity due to the presence of ²³⁸U, ²³²Th, and their daughter products, ⁴⁰K, and ¹³⁷Cs were estimated, with activity concentration calculated using standard formula [2]. Table 1 presents the activity levels of these radionuclides, while Table 2 shows the calculated radiological parameters. As soil is often used in construction, the activity index was also evaluated. Activity levels in soil and the evaluated radiological parameters are in line with national average [3].

Table1. Concentration of radionuclides in soil.

	Activity (Bq/Kg)				
	²³⁸ U	²²⁶ Ra	²³² Th	⁴⁰ K	¹³⁷ Cs
Min	14.0	19.0	33.0	493.0	≤ 0.2
s.d.	0.6	0.7	0.6	8.3	
Max	45.0	43.0	73.0	620.0	2.4
s.d.	1.1	1.1	0.9	5.0	0.08
Avg	27.0	30.0	52.0	543.0	1.4
s.d.	0.6	0.2	0.4	3.0	0.04

Table.2 Evaluated radiological parameter in soil

Radium Equivalent Activity (Bq/Kg)	Absorb dose rate (nGy/hr)	Effective dose rate (mSv/yr)	Activity Index
104.6	47.5	0.3	0.4
190.2	89.0	0.5	0.7
145.1	66.5	0.4	0.5

References:

[1] D. Kumar et.al., MPDI, **151** (2022) 1

[2] S. Chinnaesakki et al, *J. Radioanal. Nucl. Chem.*, **294** (2012) 143.

Particle Size Distribution and Dose Estimation in Uranium and Rare Earth Chloride Processing Plants

Ajesh Kumar[§], S. M. Harikumar, Aditi C. Patra, Probal Chaudhury

Health Physics Division, Bhabha Atomic Research Centre, Trombay, Mumbai, India

[§]Email: ajeshks@barc.gov.in

Occupational radiation workers in uranium and rare earth chloride processing plants are exposed to radioactive aerosols through inhalation. The size of these particles affects the internal radiation dose they receive. This study analyzed airborne dust in these facilities to determine the Mass Median Aerodynamic Diameter (MMAD) and Activity Median Aerodynamic Diameter (AMAD). MMAD represents the median particle size by mass, which is crucial for understanding particle transport and deposition behaviour in lungs. Meanwhile, AMAD accounts for activity-weighted distribution, directly impacting inhalation dose assessments. Air samples were collected using an Andersen Cascade Impactor with seven stages, operating at 45 LPM for 5000 seconds at each location. The collected samples were analyzed for mass concentration and radioactivity (Gross alpha counting). The results showed that particle size distribution depends on process conditions, aerosol formation, and material properties. MMAD ranged between 3.8 – 4.0 μm, while AMAD ranged between 4.4 – 4.68 μm. Table 1 presents data from the Uranium Recovery Plant, Rare Earth Extraction Plant, and Solvent Extraction Plant. Fig. 1 and 2 represents the plots for MMAD and AMAD in Uranium Recovery Plant (URP)

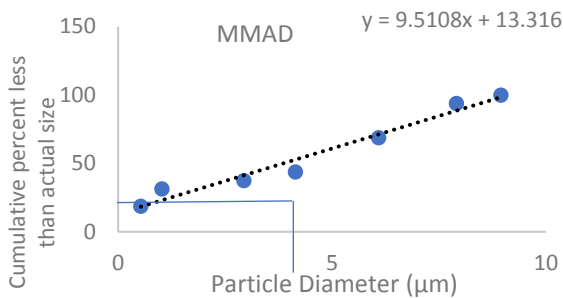


Fig. 2: MMAD, URP

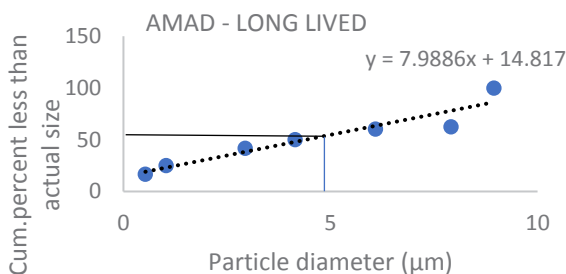


Fig. 1: AMAD, URP

Table 1: MMAD and AMAD in various plants

S No	Plant	MMAD	AMAD
1	URP	3.85	4.4
2	REP	3.92	4.56
3	SEP	3.98	4.68

The observed AMAD value (4.5 μm) falls between the ICRP dose coefficients for 3 μm and 5 μm AMADs. Considering the uncertainties in air activity measurements and the conservative approach of ambient air dosimetry, the 5 μm AMAD dose coefficient recommended by ICRP Publication 119 remains appropriate. This supports the continued use of current dose assessment methods for radiological protection in uranium and rare earth chloride processing plants.

References:

[1] G. Johnston et.al, *Health physics*, 60 (1991) 781.

Fly Ash to Pollucite: A Long-Term Storage Option for Cesium of Low-Level Radioactive Waste

Y. Raghavendra^{1,2,§}, Jayaprakasam Selvakumar^{2,4}, Anupkumar Bhaskarapillai^{1,2},
A.L.Rufus^{1,2}, T. V. Krishna Mohan^{1,2}, S.N. Achary^{2,3§}

¹Water and Steam Chemistry Division, BARCF, Kalpakkam, India

²Homi Bhabha National Institute, Anushaktinagar, Mumbai, India

³Chemistry Division, BARC, Mumbai, India

⁴Nuclear Recycle Board, Bhabha Atomic Research Centre, Mumbai, India

§ Email: sachary@barc.gov.in

The management of Cs in low level waste, particularly the Cs contaminated soil has drawn attention after the Fukushima nuclear reactor accident. For Cs management, fixing it in a pollucite matrix is considered a practical approach due to its thermal and geochemical stability. Investigations to isolate/trap Cs from the contaminated soil by zeolites/K-chabazite, has opened up exploratory research on synthetic and natural zeolites. Recently, K-chabazite, synthesized from fly-ash through alkali fusion followed by hydrothermal technique, has showed Cs exchange capacity of 2.25 mmol.g⁻¹ [1,2]. To convert Cs-exchanged chabazite into a pollucite lattice, hydrothermal reactions were conducted on K-chabazite in the presence of Cs ions. The transformation to Cs-pollucite was achieved in 20 hours at 248 °C. Similar results were obtained using Cs-exchanged K-chabazite beads with 25% bentonite as a binder. Highly crystalline Cs-pollucite formed when excess Cs was present, while lower Cs concentrations led to a mix of K-chabazite and pollucite phases. With the 50% Cs exchanged samples, both chabazite and pollucite phases were observed. This suggests that all the Cs of the Cs exchanged K-chabazite can be fixed as pollucite by a post hydrothermal reaction. The synthesised pollucite from the K-chabazite showed high thermal stability and only a small weight loss (~2%), while heating to 1100°C in thermogravimetric studies. This can be due to a possible decomposition of adsorbed materials on the pollucite, which were not noticed in XRD. This report in conjunction with earlier studies presents a mode to transform fly-ash, a waste material from coal fired power plants to usable ion exchange material and then to a stable waste immobilization matrix for Cs. This study also presents a viable process for managing Cs-exchanged zeolites by converting them into pollucite, which otherwise forms at temperature above 1000°C.

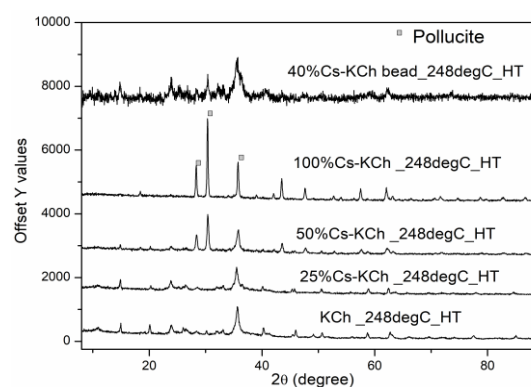


Figure-1. XRD pattern of the products of different hydrothermal reactions.

References:

1. Y. Raghavendra et al., *JOM*, **73** (7) (2021) 2111.
2. P. A. Nishad et al., *Chem. Eng. J.*, **499** (2024) 156354.

Estimation of Effective Radiation Dose Due to ^{222}Rn in Groundwater of Gogi Region, Yadgir District

R. Archanadevi, B. R. Kerur[§]

Department of Physics Gulbarga University Kalaburagi, Karnataka, India

[§]Email: kerurbrk@gmail.com

Radon (Rn) is the most important radioactive element among the radionuclides from a radiation protection point of view. Since Rn continuously escapes from water to the atmosphere and indoor air by household activities of water, Rn in water may be considered as an important secondary source for indoor Rn exposure. This paper presents radioactivity data from 10 samples collected across three zones (0–10 km, 10–20 km, and 20–30 km) covering approximately 900 sq. km in the Gogi region. The study area is a plateau typical of Deccan Trap terrain, marked by deep ravines and undulating southern parts with scattered knolls and tors.

The concentration of ^{222}Rn in drinking water collected from different locations in Gogi was measured using the Emanometry method, following standard procedures [1]. At each location, a 1-litre water sample was collected. Physicochemical parameters, such as pH, conductivity, and TDS were also measured to assess their influence on Rn levels and associated health risks. A weak correlation was observed between Rn and these parameters. Annual effective doses from Rn, via inhalation and ingestion, were calculated using parameters given by [2].

Table 1: Range of Radon Activity and radiological parameter from study region

S.N.	Sampling Area	Range	^{222}Rn Activity Bq.L ⁻¹	Inhalation $\mu\text{Sv.y}^{-1}$	Ingestion $\mu\text{Sv.y}^{-1}$	Total dose $\mu\text{Sv.y}^{-1}$	Lung $\mu\text{Sv.y}^{-1}$	Stomach $\mu\text{Sv.y}^{-1}$
1	Gogi	Min	1.55±0.1	3.89	0.324	4.21	0.468	0.03
		Max	44.97±1.3	113.3	9.443	122.7	13.6	1.33
		Mean	20.57±0.7	51.83	4.319	56.144	6.22	0.52

The ^{222}Rn concentrations, inhalation dose, ingestion dose, and equivalent effective dose due to ^{222}Rn in drinking water to the public of the study area are summarized in Table 1. The ^{222}Rn concentration in the drinking water sample is found to vary from 1.55 to 44.97 Bq.L⁻¹. The highest ^{222}Rn activity concentration in the water sample is found to be 44.97 in Gogi K village and the lowest ^{222}Rn activity concentration in Karakalli village, which is found to be 1.55 Bq.L⁻¹. The results obtained from this study reveal that higher Rn concentration was observed in some groundwater where the geology is characterized by granite as the most extensive unit. Regions with high concentrations of radium- and uranium-bearing granitic rocks are expected to exhibit elevated levels of Rn in groundwater. The dose contribution from this source to the lungs and stomach is calculated by multiplying the inhalation and ingestion dose with the tissue weighting factor for the lungs and stomach, respectively. Therefore, a plan for a health risk assessment study should be taken up.

References:

- [1] D. R. Rangaswamy et al., *J. Radioanal. Nucl. Chem.*, **307** (2016) 907.
- [2] UNSCEAR, Sources and Effects of Ionizing Radiation. United Nations Scientific Committee on the Effect of Atomic Radiation, United Nations, New York (2000).

Environmental Aspects of Release of Iodine-129, Performance of Mitigation Processes and Management of Secondary Waste

Umadevi K.^{1,2}§, Prasad Dabhade², Pradeep Kumar Sharma¹, Santhosh Kumar Satpati³

¹Nuclear recycle Board, Bhabha atomic Research Centre, Mumbai, India

²Chemical Engineering group, Bhabha atomic Research Centre, Mumbai, India

³Nuclear Fuels Group, Bhabha atomic Research Centre, Mumbai, India

§Email: umadevi@barc.gov.in

From the perspective of radiation dose to public, I^{129} is one of the most harmful radionuclides present in the gaseous waste stream released during the normal operation of radiochemical facilities at the back end of nuclear fuel cycle. Caustic scrubbing and fixed bed adsorption using suitable adsorbents are two well-known methods that can quantitatively remove iodine from the gaseous waste stream before it is discharged to atmosphere. This paper incorporates the scientific outcome of the experimental studies conducted in a laboratory scale fixed bed adsorber for removal of iodine from simulated gaseous waste stream. Two types of silver attached porous adsorbents, viz, silver exchanged zeolite (Ag^0X) and silver attached silica gel (AgS) are synthesized in the laboratory for the adsorption experiments.

From experiments, the mass transfer co-efficient for the caustic scrubber packed column was established, which was found to be largely affected by the gas flow rate (Fig.1). Incorporating all the affecting parameters, a correlation for overall mass transfer co-efficient was developed. Similarly, for the silver based adsorbent synthesized, the breakthrough curves were established through fixed bed experiments. The dynamic adsorption capacity (mg/g of adsorbent) was found to be affected by the percentage of silver present in the adsorbent and temperature of the adsorbent bed (Fig.2).

Even though isolation of I^{129} from the biosphere cannot be guaranteed for the timescale of its radioactive decay, its dispersion into environment can be controlled by proper management of the secondary waste to convert iodine into a stable waste form suitable for long term storage. Proposed techniques for the secondary waste treatment are also incorporated.

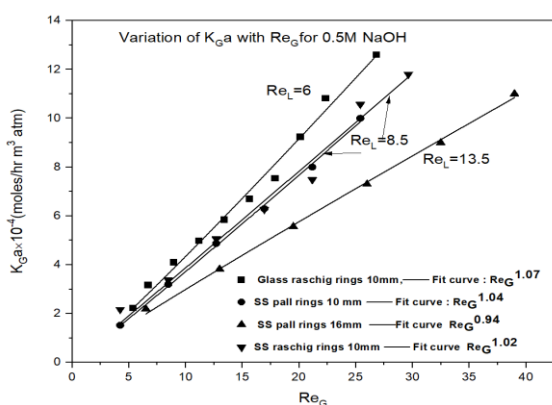


Fig. 1: Variation of overall mass transfer co-efficient with gas flow rate in caustic scrubber

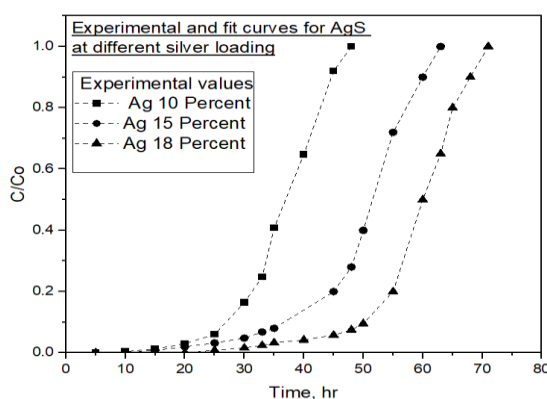


Fig. 2: Breakthrough curves for AgS for different silver loadings

Acknowledgements: Dr. P.A. Hassan, Dr. Jeyakumar, Dr. V. Sudarsan and Chemistry Division, BARC for their support in synthesizing the adsorbents, analysis, and characterization studies respectively.

Assessment of the Activity Concentrations of ^{238}U , ^{232}Th , and ^{40}K in Stone Samples from the Koppal Districts of Karnataka, India

Nagraj Channappa, Jayashri B Mutugar, Basavaraj Rachappa Kerur[§]

Department of Physics, Gulbarga University, Kalaburagi, India.

[§]Email: kerurbrk@gmail.com

Gamma's background in the environment comes from natural and manmade sources, including cosmic, terrestrial, and surrounding building materials. The samples were collected from the Koppal district, brought to the laboratory for crushing and sieving with a 0.355 mm sieve and stored in a sealed plastic container for four weeks to achieve radioactive equilibrium. The collected stones belong to the Deccan trap terrain. The 4" x 4" NaI(Tl) Scintillation detector gamma spectrometer is used to estimate the activity concentration of radionuclides. For the selected radionuclides of ^{238}U , ^{232}Th , and ^{40}K , activity concentrations were calculated using the energies of 1764, 2614, and 1460 keV, respectively. The Minimum Detectable Activity (MDA) values were found to be, 1.2 for ^{238}U , 1.8 for ^{232}Th , and 20.2 for ^{40}K in the present geometry. The activity concentration values are shown in the below table. In the Karatagi and Yalburga area, which is part of the granitic zone, the concentration of uranium was found to be higher than that of thorium. The obtained values are less than the national and world average values reported in the United Nations Scientific Committee on the Effects of Atomic Radiation (UNSCEAR 2000) report.

Table: Activity Concentration of ^{238}U , ^{232}Th , and ^{40}K in Koppal District stone samples

Sl. No	Location	No. of Samples in each Taluka	Range	Activity Concentration (Bq/Kg)		
				^{238}U	^{232}Th	^{40}K
01	Koppal	10	Minimum	12.4±0.3	56.4±0.2	664.4±3.2
			Maximum	46.6±0.4	102.2±0.3	1015.7±4.4
			Average	19.5±0.7	81.7±0.3	802.1±4.9
02	Karatagi	10	Minimum	135.7±0.3	75.7±0.4	613.6±3.6
			Maximum	299.4±0.9	152.1±0.5	1242.6±6.1
			Average	208.9±0.9	119.9±0.9	956.8±6.2
03	Gangavathi	10	Minimum	80.5±0.6	96.9±0.3	628.0±6.6
			Maximum	158.5±0.8	286.5±0.5	1188.3±7.5
			Average	121.1±0.7	190.2±0.4	855.4±7.6
04	Kushtagi	10	Minimum	53.7±0.5	60.6±0.3	608.9±3.9
			Maximum	86.8±0.7	86.5±0.3	1143.5±5.9
			Average	61.2±0.8	70.7±0.5	866.6±6.2
05	Kanakagiri	10	Minimum	21.7±0.5	93.5±0.2	494.2±4.4
			Maximum	82.8±0.5	156±0.3	1028.4±5.2
			Average	44.0±0.6	102.3±0.3	810.4±5.3
06	Kuknoor	10	Minimum	13.6±0.1	49.9±0.2	727.1±3.8
			Maximum	56.3±0.5	138±0.3	1139.7±5.0
			Average	25.2±0.7	101.8±0.5	975.3±5.4
07	Yelburga	10	Minimum	54.7±0.4	64.9±0.2	354.8±5.4
			Maximum	189.6±0.6	146.1±0.4	1008.4±6.3
			Average	132.4±0.6	101.3±0.5	513.8±6.7

References:

[1] Kerur et al., *Acta Geophysica*. **61** (4), (2013) 1046.

Assessment of Radioactivity in Solid Waste Generated Due to Operation of Rare Earth Extraction Plant in Odisha

Rajendra P. Patra^{2,§}, A. Sahu², A. Rout², P. Prusty², A. C. Patra¹, P. Choudhury¹

¹Health Physics Division, Bhabha Atomic Research Centre, Trombay, Mumbai, India

²H P Unit, IREL OSCOM, Chhatrapur, India

§Email: patrabarc@gmail.com

In Rare Earth Extraction plant (REEP) Monazite is processed to produce mixed Rare Earth chloride (MRCL), Rare earth flake, Tri-sodium phosphate, Thorium nitrate and Nuclear grade ammonium di uranate (NGADU) at IREL(I) Ltd, OSCOM, Odisha. The main radioactive wastes generated due to processing of monazite are: Thorium and Uranium residues, leftover radioactive materials after the extraction of REEs. The aim of the study was to quantify the radioactivity generated due to processing of monazite.

Four types of solid waste generated due to the operation of Rare Earth Extraction Plant (REEP), OSCOM were insoluble muck, ETP cake, Lead Barium slurry and Iron Carbonate cake. Annually 5000t to 6000t capacity monazite is processed in REEP, OSCOM. The gross alpha, gross beta activities and concentration of ²²⁸Ra are shown in Fig.1.

The gross alpha radioactivity is 1007.5 Bq.g⁻¹ in insoluble muck is, 965.5 Bq.g⁻¹ in iron carbonate cake, 2511 Bq.g⁻¹ in Lead barium slurry and 1187.16 Bq.g⁻¹ in ETP solid waste. The gross beta radioactivity 866.16 Bq.g⁻¹ in insoluble muck, 1071.6 Bq.g⁻¹ in iron carbonate cake, 5676.8 Bq.g⁻¹ in lead barium slurry and 1000.6 Bq.g⁻¹ in ETP solid waste. The concentration of ²²⁸Ra in different types of Solid waste generated during the operation of rare earth extraction plant are 309.16 Bq.g⁻¹ in insoluble muck, 141.5 Bq.g⁻¹ in iron carbonate cake, 4715.6 Bq.g⁻¹ in Lead barium slurry and 261.0 Bq.g⁻¹ in ETP solid waste.

The external gamma exposure rates measured in these four solid radioactive waste generated during the operation of rare earth extraction plant varies from 7.6 $\mu\text{Gy.h}^{-1}$ - 10.0 $\mu\text{Gy.h}^{-1}$ in insoluble muck, 4.2 $\mu\text{Gy.h}^{-1}$ - 6.4 0 $\mu\text{Gy.h}^{-1}$ in Iron carbonate cake, 20.0 $\mu\text{Gy.h}^{-1}$ - 40.0 $\mu\text{Gy.h}^{-1}$ in Lead barium slurry and 5.3 $\mu\text{Gy.h}^{-1}$ -8.2 Gy.h⁻¹ in ETP solid waste. The solid waste generated due to processing of monazite is transported safely under supervision of radiological safety officer with proper RSWP and PPEs and disposed in specially designed trenches as per waste disposal guidelines.

References:

- [1] P.M.B. Pillai, Proc. of Internat. Symp. On Norm, Sevilla, Spain, March 19-22, (2007). IAEATECDOC.

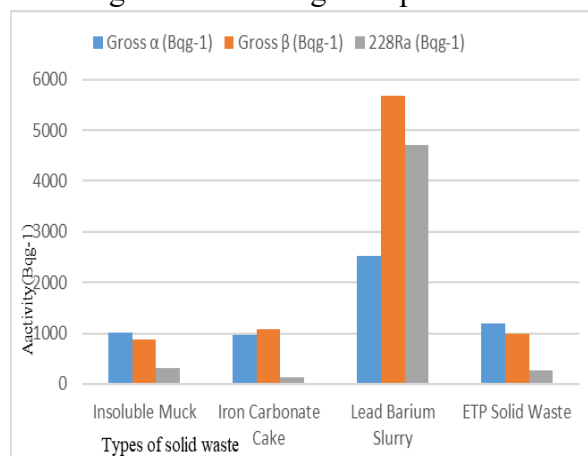


Fig. 1: Radioactivity in solid waste

Variation of Outdoor Natural Gamma Absorbed Dose Rate in Air Across the Indian Himalayan Region

Hasem Ali[§], Pratip Mitra, Saurabh Srivastava, G. Priyanka Reddy, Saurabh Garg

Environmental Monitoring and Assessment Division, BARC, Mumbai, India

[§]Email: hasem@barc.gov.in

As part of the Indian Environmental Radiation Monitoring Network (IERMON) initiative, a long-term study was conducted to monitor natural (cosmic and terrestrial) gamma absorbed dose rate in outdoor air, using permanently installed Geiger–Mueller (G-M) detector-based environmental radiation monitors (ERMs), at 19 monitoring locations across varying altitudes (Fig.1) in the Indian Himalayan Region (IHR). This study provides an unprecedented, comprehensive analysis of gamma dose rate distribution in high-altitude mountainous terrains.

The measured mean dose rates (D) ranged from 77 ± 3 nGy h⁻¹ (altitude 22 m) to 235 ± 4 nGy h⁻¹ (altitude 4270 m), with corresponding annual effective doses (AED) varying from 0.10 ± 0.01 mSv y⁻¹ to 0.29 ± 0.01 mSv y⁻¹. The shortest period of measurement for any ERM was more than one year. Control chart of the hourly dose rate values measured by one of the representative ERM reveal that only 2.58% data points exceeded the control limits of $\pm 3\sigma$ around the mean. The findings reveal that the natural gamma absorbed dose rate in air in the IHR generally exceed both the Indian and global averages [1]. A strong positive correlation (Pearson's $r = 0.903$) was observed between D and altitude. The cosmic dose rate (D_{cosmic}) was calculated for each location using the EXPACS model [2] and subtracted from D to determine the terrestrial dose rate ($D_{terrestrial}$). D_{cosmic} becomes the dominant contributor above 3000 m. $D_{terrestrial}$ varied significantly, likely due to varying concentrations of ²³⁸U, ²³²Th, and ⁴⁰K in different geological formations. Seasonal variations revealed lower D values during the monsoon, likely due to reduced radon emanation, while D values were found to be also low during winter snowfall.

These findings establish a baseline dataset for public radiation exposure assessment in the IHR and provide a critical reference for detecting any future radiological anomalies.

We extend our heartfelt gratitude to all the members of IERMON Group of EMAD, BARC and to all the agencies and institutions that facilitated the installation of ERMs.

References:

- [1] UNSCEAR *Report to the General Assembly with scientific annexes* (2000), United Nations, New York.
 [2] T. Sato, *PLOS ONE*, **10(12)** (2015): e0144679.

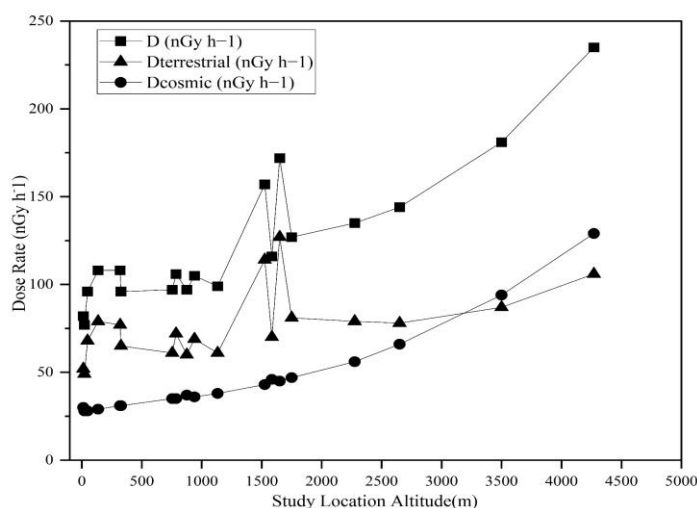


Fig. 1: Variation of dose rate (D) in air (total, cosmic and terrestrial) with altitude across the 19 monitoring locations.

Understanding the Groundwater-Surface Water Interactions in Yamuna Plains of Noida Region using Environmental Tritium

Diksha Pant^{1,2,§}, H. V. Mohokar¹, A. Roy^{1,2}, Tirumalesh Keesari^{1,2}, Dipankar Saha³

¹ Isotope and Radiation Application Division, BARC, Mumbai, India

² Homi Bhabha National Institute, BARC, Mumbai, India

³ Central Ground Water Board, Western Region Faridabad, India

§ Email: diksha@barc.gov.in

Tritium is produced in stratosphere by cosmic ray interaction with nitrogen, it is oxidized and enters troposphere through leaks and becomes part of water cycle. Tritium decays by beta emission (18.6 KeV) and has a half-life of 4500 days. Tritium being integral part of water acts as a very useful tracer for estimating residence time of water. However, since the concentration of natural tritium is very low, it is preconcentrated in natural water samples by electrolytical enrichment method and counted for beta activity using liquid scintillation counter [1]. The minimum detection limit of the liquid scintillation counter is 0.7 TU (1σ) for counting time of 500 min. with a counting efficiency of 25%.

The dynamics of groundwater and its interaction with surface water source (River Yamuna) in Noida region was evaluated using environmental tritium data. For this purpose, fifty-six water samples were collected for rain (4 nos.), river water (2 nos.) and groundwater (24 nos.) with a depth range of 12-122 meters below ground level (m bgl) distributed across the geographical area of 1442 km² during both pre and post monsoon seasons.

Vertical distribution of tritium data (Fig. 1) indicates three different clusters of water. Tritium content of rainwater and river water (cluster i, 9.5 to 10.5 TU) is similar with slight increase in river water tritium during post monsoon that can be attributed to increased stream flow and addition of water from parent source from higher altitude. The Ranney wells (Cluster ii, 5 to 8.5 TU) having tritium concentrations higher than the deep groundwater samples indicating active recharge. During the post-monsoon season a slight increase in tritium content is observed in the Ranney wells indicating recharge contribution during the post monsoon season. The groundwater samples with depths 40 to 120 m bgl show low tritium (cluster iii, 1.5 to 2.7 TU) suggesting slow recharge through regional flows. The environmental isotopes and tritium data suggest active interconnection between the well present in the flood plain region compared to the well far away from the river.

Acknowledgements: The authors acknowledge Dr. Y.K. Bhardwaj, AD, RC&IG and Dr. R. Acharya for their constant support and encouragement. Shri Sagnik Das, Hydrogeologist, WAPCOS is sincerely acknowledged for his cooperation during the field sampling.

References:

- [1] U. Morgenstern and C. B. Taylor CB (2009) *Isotopes Environ Health Stud.*, 45(2) (2009) 96-117.

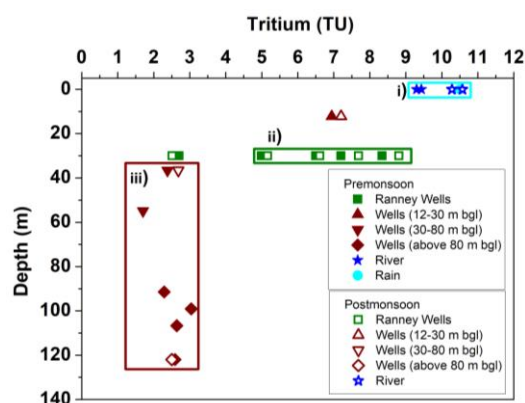


Fig. 1: Depth profile of tritium concentration.

Natural Radioactivity Levels in Some Environmental Soil Samples of the Belagavi Region, North West Karnataka, India

Jayashri B Mutugar, Nagraj Channappa, Basavaraj Rachappa Kerur[§]

Department of Physics, Gulbarga University, Kalaburagi, India.

[§]Email: kerurbrk@gmail.com

The natural radioactivity concentrations of ^{238}U , ^{232}Th , and ^{40}K in soil samples from Belagavi District in Karnataka, India, were measured to assess the radiological impact on the environment and public health. Soil samples were collected from three different locations within the district; The ASTM procedure was followed for the sample collection and preparation for gamma energies. A high-resolution figure illustrating the gamma spectrometric setup and measurement procedure is provided (Fig. 1). The 4" x 4" NaI (TI) Scintillation detector gamma spectrometer is used to estimate the activity concentration of radionuclides. The average activity concentrations of ^{238}U , ^{232}Th , and ^{40}K were found to be 26.8 ± 0.2 Bq/kg, 48.3 ± 0.3 Bq/kg, and 150.7 ± 1.6 Bq/kg, respectively, in Savadatti soil samples; 28.5 ± 0.2 Bq/kg, 34.3 ± 0.4 Bq/kg, and 135.7 ± 1.3 Bq/kg, respectively, in Ugargol; and 22.8 ± 0.2 Bq/kg, 54.4 ± 0.4 Bq/kg, and 219.9 ± 1.7 Bq/kg, respectively, in Belavadi soil samples. The activity concentrations are shown in Table 1. Belavadi in Bailhongal Taluka is characterized by rocky terrain and sedimentary formations, with limestone and granite-rich soil that can impact natural radioactivity distribution. Ugargola, in Athani Taluk, is primarily an agricultural and rural settlement, featuring red loamy soil with high mineral content, which influences the accumulation of radionuclides. The study assessed soil radioactivity levels using the Radium Equivalent Activity (Ra eq) and External Hazard Index (H ex), finding safe limits. It emphasizes continuous monitoring of environmental and public health, comparing findings with global safety limits set by UNSCEAR.

Table 1: Activity Concentration of Belagavi Districts Samples

Sl. No.	Location	Range	Activity Concentration (Bq/kg)		
			^{238}U	^{232}Th	^{40}K
1	Savadatti	Minimum	19.9 ± 0.1	39.2 ± 0.1	138.1 ± 1.5
		Maximum	43.9 ± 0.1	60.7 ± 0.2	258.0 ± 1.2
		Average	26.8 ± 0.2	48.3 ± 0.3	150.7 ± 1.6
2	Ugargol	Minimum	21.1 ± 0.1	26.2 ± 0.2	115.9 ± 1.2
		Maximum	33.0 ± 0.2	46.4 ± 0.1	149.2 ± 1.3
		Average	28.5 ± 0.2	34.3 ± 0.4	135.7 ± 1.3
3	Belavadi	Minimum	18.1 ± 0.1	50.0 ± 0.1	180.0 ± 1.6
		Maximum	26.6 ± 0.1	62.8 ± 0.2	252.4 ± 1.7
		Average	22.8 ± 0.2	54.4 ± 0.4	219.9 ± 1.7



Fig.1. 4"X4" NaI(Tl) scintillation detector based gamma ray spectrometer

Acknowledgements: The authors sincerely express their gratitude to the Department of Physics, Gulbarga University, Kalaburagi, for providing the necessary facilities.

References:

- [1] S. Rajesh et al., Assessment of Natural Radioactivity Levels in Soil Samples of Bidar District by Gamma Spectrometry, (2015).

Studying Back Diffusion in Accumulators for Radon Flux Measurements Using OpenFOAM

D. Rana^{1,2,§}, N.K. Sethy^{1,2}, R. L. Patnaik^{1,2}, M. K. Singh^{1,2}, A. C. Patra², P. Choudhuri²

¹HP Unit, Jaduguda, India

²Bhabha Atomic Research Centre, Mumbai, India

§ Email: ranadibs@barc.gov.in

Radon exhalation is a key factor in radon studies, especially in uranium mineralized areas, where accurate radon flux measurement is essential for assessing potential health risks, such as lung cancer, and ensuring environmental safety by providing reliable data for risk assessment and mitigation strategies. Back diffusion refers to the process where accumulated radon gas inside an accumulator chamber reduces the concentration gradient between the soil and the chamber, thereby slowing the radon flux over time. As a result, the flux measured with the accumulator in place (bound flux) is lower than the flux measured without the accumulator (free flux). Since back diffusion always occurs when an accumulator is in place, only bound flux can be directly measured. The bound-to-free flux ratio is crucial for accurately predicting radon flux in such systems. The aim of this study is to quantify the bound flux and the bound-to-free flux ratio using OpenFOAM simulations. This modeling approach allows for more accurate flux predictions by evaluating how accumulator design influences radon flux measurements.

In this study, the soil system is characterized by a radon diffusion length of approximately 59 cm. Two accumulator designs are analyzed: one with a circular face and the other with a square face. The radius of the cylindrical accumulator is set equal to the radon diffusion length, a novel approach compared to previous studies where the accumulator diameter was either much smaller or larger than the diffusion length [1]. The square accumulator's side length is calculated to have the same cross-sectional area as the cylindrical one. The cylindrical accumulator has a diameter and height of 60 cm, while the square accumulator has a side length of 53.17 cm. Flux variations for both designs are shown in Fig 1, with free-to-bound flux ratios of 0.58 for the cylindrical accumulator and 0.42 for the square accumulator. The flux pattern indicates that radon migrates in opposite directions at the boundary of the accumulator before eventually escaping into the atmosphere, demonstrating the phenomenon of back diffusion.

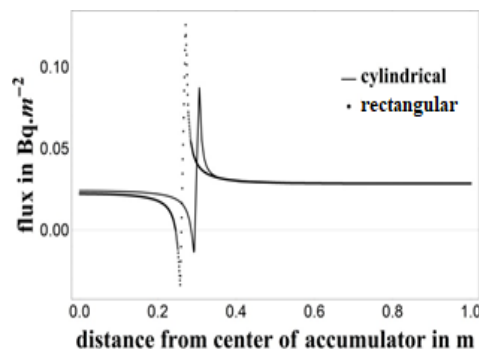


Fig 1. Flux Variation

References:

[1] Y. S. Mayya, *Radiation Protection Dosimetry*, **111** (2004) 305.

Study of Seasonal Variation of Outdoor ^{222}Rn Concentration at a Location Nearby Uranium Mining and Milling Facility

R.L. Patnaik^{1,2,§}, M. K. Singh^{1,2}, Dibyendu Rana^{1,2}, N. K. Sethy^{1,2},
V. N. Jha², A. C. Patra²

¹Health Physics Unit, Jaduguda, Jharkhand, India

²Bhabha atomic Research Centre, Anushaktinagar, Mumbai, India

§ Email: rpatnaik@barc.gov.in

Inhalation of Radon (^{222}Rn) and its daughter products contributes a major fraction (52%) of total dose to human beings from all possible source of natural radioactivity [1]. Radon released from the different surrounding matrix is dispersed into the environment thus becoming a potential source of internal exposure. Radon is ubiquitous, seasonal and diurnal variations in the radon level are reported by many researchers. Releases from minerals industries containing uranium series radionuclides may lead to increase in the existing radon level in the environment and can modify the radiological environment surrounding the mining facilities. A study was carried out to record the variations in the outdoor ^{222}Rn concentration in the HPU campus, which is at a distance of ~500 m away from the Uranium mining and milling facility at Jaduguda during prominent summer, rainy and winter seasons. The yearly temperature level in this region varies from as low as 6 to 7 °C in winter to as high as 45 to 46 °C in summer.

Continuous ^{222}Rn Concentrations were measured outdoor using digital Radon Detector, a compact device (AirThings Corentium) based on the alpha spectrometry (silicon photodiode). The system was mounted at a place 1m above ground in outdoor air. In view of the compact design the technical specifications and user manual were adopted for deciding the operational conditions for the measurements. Radon concentration in natural ambient condition was recorded for Average values of ^{222}Rn concentrations for one day, seven-day and long-term has been recorded throughout Summer, Rainy and winter season. The measured radon levels were comparable with the reference AlphaGUARD professional radon monitor.

The results obtained showed that of one day average value of outdoor ^{222}Rn concentration varied from 10 to 87, 10 to 65 and 31 to 167 Bq.m⁻³ in summer, rainy and winter seasons respectively. Corresponding average values worked out were 29±16, 24±11 and 92±39Bq.m⁻³ respectively. The long term (>7 days) average value of outdoor ^{222}Rn concentration observed in that particular location ranged from 38 to 59, 17 to 28 and 31 to 49 Bq.m⁻³ in summer, rainy and winter seasons, respectively. Corresponding average values worked out for long term measurements were 44±5, 23±2 and 40±6 Bq m⁻³, respectively. The one-day maximum activity concentration of radon was recorded during the winter. This might be due to the weather condition on that particular day. Radon is ubiquitous, seasonal and diurnal variations in the atmospheric radon level are anticipated. The results of the present study are attributed to local geological and weather condition. Continuous measurements of ^{222}Rn concentration in outdoor environment confirmed to the wide variability of observed values as per the seasonal variation and weather conditions at a place. The long-term average value of radon concentration was observed as anticipated for a uranium mineralogy area in Singhbhum Thrust belt.

References:

- [1] UNSCEAR (2008), Sources, Effects and Risks of Ionizing Radiation. Report to the General Assembly, with annexes, United Nations, New York.

^7Be in Fresh Water Sediment in Kadra Reservoir at Kaiga Region

R M Joshi^{1,§}, M S Vishnu, I. V. Saradhi²

¹Environmental Survey Laboratory, EMAD, Kaiga, India

²ESS, EMAD, BARC, Mumbai, India

§ Email: rmjoshi@barc.gov.in

^7Be a cosmogenic radionuclide ($t_{1/2} = 53.3$ days), formed in upper atmosphere and deposited to aquatic and terrestrial through wet and dry deposition. Having partition coefficient (k_d) $\sim 10^5$, ^7Be is often used as a tracer in studies on atmospheric deposition and sediment transport [1]. In this paper, ^7Be concentration in fresh water sediment samples and its relationship with rainfall at Kaiga region is presented. Sediment samples around depth of 2 cm were collected from Kadra reservoir in Hartuga village, where four Pressurized Heavy Water Reactors are under operation. The collected samples are processed and analyzed as per standard procedure [2]. Samples are counted in p-type coaxial High purity Germanium detector with 50% relative efficiency. 477.6 keV γ energy is used for estimating ^7Be concentration. Annual mean value ^7Be concentration in sediment during 2007-2024 ranges from 5.6 to 40.2 Bq.kg⁻¹ (GM = 17.1 Bq.kg⁻¹ GSD=1.6). A clear monthly variation of ^7Be is observed as shown in Fig. 1. Also, there exists a sharp increase during month of August and September. This increase can be attributed to high rainfall and fresh inputs of ^7Be through run-off from soil erosion in catchment areas. To further understand variation in ^7Be , concentration in sediment are correlated with rainfall as annual average rainfall at Kaiga is about 3500 mm. Monthly percentage rainfall contributions of each month during monsoon season (June - September) were estimated, whereas Jan to May and Oct- Dec months are considered as others than monsoon season. During monsoon season, percentage contribution of rainfall for July month is 34.7% followed by June (25.0%), August (23.3%) and September (9.4 %). The percentage contribution of other than monsoon season period is 7.6 %. It was observed that during months of June and July, rainfall percentage is high but ^7Be in sediment is less. This may be due to shorter time for settling, dynamic movements of water and sediment and continuous release of water from Kadra dam during June and July month. Higher concentration of ^7Be during August and September is due to fresh inputs through runoff and complete sedimentation. Lower ^7Be in sediment may be due to low deposition flux (dry deposition), radioactive decay.

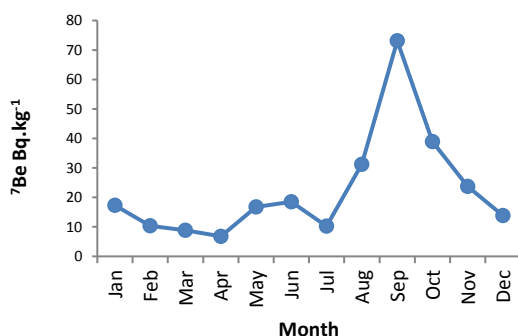


Fig. 1. Monthly Mean ^7Be in sediment

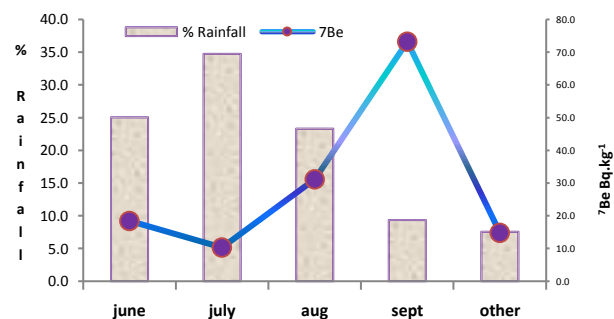


Fig. 2. ^7Be variation with Percentage Rainfall

References:

- [1] Taylor et al., Assessing recent soil erosion rates through use of ^7Be , IAEA, Springer, 2019.
- [2] BARC, ERL Procedure Manual, Health Physics Division, (Mumbai, BARC), (1998).

Assessment of Radon Levels and Their Correlation with Physicochemical Parameters in Water Sources of Dakshina Kannada District

Neha S¹, Latha T¹, Rishika¹, Greeshma K V¹, Rita Crasta^{1§}, Suresh S²

Department of post graduate studies and research in Physics, St Aloysius, Mangalore, India

Department of Physics, M.P.E Society's S.D.M Degree College, Honnavar, India

[§]E-mail: rita.crasta@gmail.com

Determining radon concentration in groundwater is crucial for assessing health hazards and developing effective mitigation strategies. Various geological factors influence radon concentration in groundwater. In this study, groundwater samples were analyzed using the Emanometry technique, employing a radon bubbler and a Lucas scintillation cell. A total of 80 groundwater samples were collected from four locations: Mulky, Moodabidre, Panambur, and Konaje. Additionally, physicochemical parameters, including pH, Electrical Conductivity (EC), Total Dissolved Solids (TDS), and the concentrations of sodium and potassium, were measured to examine their correlation with radon levels.

The radon activity in groundwater samples ranged from 1.40 Bq.L⁻¹ to 12.44 Bq.L⁻¹, with an average concentration of 3.93 Bq.L⁻¹. The variation in ²²²Rn concentration was found to be influenced by the geological characteristics of the study area. Higher radon concentrations were observed in lateritic regions, whereas lower levels were recorded in alluvial soil areas, with the least concentration detected in sandy soil near coastal regions. The estimated annual effective dose due to radon activity in groundwater varied from 3.83 μ Sv.y⁻¹ to 29.67 μ Sv.y⁻¹, with an average of 10.38 μ Sv.y⁻¹. The estimated annual effective dose due to radon inhalation and ingestion was compared with international safety standards, including WHO guidelines, which recommend a maximum contaminant level of 100 Bq.L⁻¹.

The physicochemical parameters measured in the groundwater samples are as follows: Electrical Conductivity (EC): ranged from 0.03 to 1.74 μ S.cm⁻¹, with an average of 0.23 μ S.cm⁻¹. pH varied between 5.62 and 7.59, with an average value of 6.58. TDS ranged from 5 to 243 mg.L⁻¹, with an average of 34.65 mg.L⁻¹. Sodium concentration: Spanned from 0.8 to 73.2 ppm, averaging 8.1 ppm. Potassium concentration: ranged from 0.5 to 15.5 ppm, with an average of 3.8 ppm. All measured parameters were within the maximum permissible limits for drinking water. A weak positive correlation was observed between ²²²Rn concentration and the physicochemical parameters (Fig. 1), indicating that while these factors may influence radon levels to some extent, other geological and environmental conditions play a more significant role. This study emphasizes the need for regular ground water monitoring and public awareness to mitigate radiological and environmental hazards.

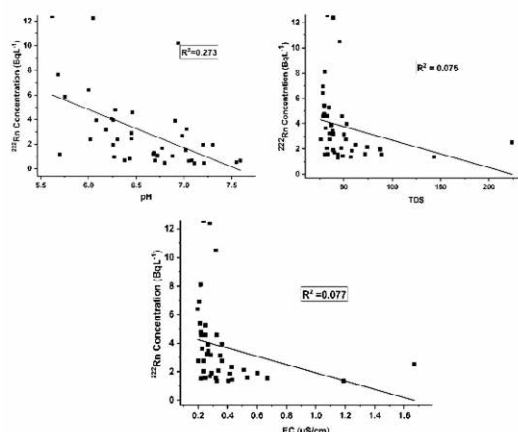


Fig. 1: Correlation of ²²²Rn concentration with pH, TDS and EC

References:

- [1] A. M. Bagher et al., *Int. J. Renew. Sustain. Energy*, **3(3)** (2014) 59.
- [2] S. Suresh, et al., *J. Radiat. Res. Appl. Sci.*, **13(1)** (2020) 12.

Pre-operational Environmental Radiation Mapping Around Gorakhpur Haryana Anu Vidyut Pariyojana (GHAVP)

Vaibhav Bhujbal^{1, §}, MVR Narsaiah¹, Jaivendra Kumar²,
Anil Kumar², Deepak Kumar², Shashank S. Saindane¹

¹RSSD, Bhabha Atomic Research Centre, Mumbai – 85

²EM&AD, Bhabha Atomic Research Centre, Mumbai – 85

§Email: vaibhavb@barc.gov.in

The objective of radiation monitoring is to establish baseline radiation dose rate data in the Emergency Planning Zone (EPZ) area around the proposed construction site of the new nuclear power plant at Gorakhpur Haryana Anu Vidyut Pariyojana (GHAVP), Haryana. The data will be used as reference pre-operational data EPZ. The radiation monitoring covers the EPZ and an area extending up to 30 km, encompassing 215 villages and 25 specific locations within the nuclear power plant site. Radiation dose rates were measured, and soil samples were collected at multiple locations within EPZ and an area extending up to 30 km to obtain a representative range of environmental radiation level.

Background radiation level monitoring was carried out with instruments calibrated in a standard laboratory. These included Geiger-Müller tube-based survey meter and an online monitoring system equipped with a GPS-enabled NaI(Tl) detector for continuous dose rate logging and spectrum analysis. A calibrated portable plastic scintillator-based detector was also used for radiation monitoring and to compare readings with those of other calibrated instruments. These radiation monitoring instruments were kept at appropriate location and at suitable height in the vehicle, thereby ensuring minimum shielding by the vehicle body [1]. Radiation levels of the raw materials used for road and house construction including heaps of aggregates, sand, and other construction elements in the EPZ area were also measured.

The measured background radiation levels, ranging from 60 to 200 nGy.h⁻¹, confirms to be within the range specified in literature [2]. The gamma-ray spectrometric analysis of soil samples and raw materials, conducted using a P-type HPGe system with 50% relative efficiency, revealed the presence of ²³⁸U, ²³²Th and ⁴⁰K with concentrations as given in Table 1.

Table 1	Activity Range (Bq. kg ⁻¹ dry wt.)		
	²³⁸ U (Location)	²³² Th(Location)	⁴⁰ K(Location)
Min	20.74 ± 1.61(Kajal Hedi)	33.84 ± 1.85 (Shekupur)	395.69 ± 8.19 (Khajuri Jati)
Max	39.11 ± 1.23 (Chankothi)	65.4 ± 2.05 (Kuleri)	707.03 ± 7.94 (Kuleri)
Average	31.42 ± 1.72	51.58 ± 1.96	444.86 ± 8.35

The environmental radiation level monitoring provides valuable pre-operational radiation data for the proposed nuclear power plant construction site and its Emergency Planning Zone (EPZ). The results of radiation monitoring around GHAVP site confirms that the background radiation levels up to 30 km radial distance from proposed NPP are inline as specified in the literature [2, 3].

References:

- [1] S. S. Saindane et. al, National Symposium on Environment (NSE-18), Anantapur, March 11-13, 2013.
- [2] M. K. Mishra et. al., *J. Environ. Radioact.*, **262** (2023) 107146.
- [3] The UNSCEAR 2000 Report: Sources and Effects of Ionizing Radiation

Uranium Partitioning in Soils from NFC Kota campus

V. K. Thakur¹, P. Lenka¹, Gopal P. Verma^{1,2}, S. K. Srivastava¹, A. C. Patra^{1,2§}, P. Chaudhury¹

¹Health Physics Division, Bhabha Atomic Research Centre, Trombay, Mumbai – 400 085

²Homi Bhabha National Institute, Trombay, Mumbai – 400 094

§Email: aditic@barc.gov.in

In order to assess scenarios involving radionuclide release, disposal or remediation, it is essential to have idea of the solid-liquid distribution coefficient (K_d). K_d of soil is an important parameter used to predict radionuclide-soil interaction and subsequent transport [1]. In this study, K_d was determined for garden soils in NFC Kota campus, which are expected to receive treated water with uranium concentration exceeding 60 ppb.

Soil samples were collected in duplicate, using standard procedures. They were dried in hot air oven at 105°C, passed through 2 mm mesh sieve, homogenized, subject to physico-chemical characterization and estimation of K_d for uranium. The pH, electrical conductivity, particle size distribution and organic matter content were estimated using standard procedures [2]. The estimation of K_d for uranium was carried out using laboratory batch method [3]. The sorption kinetics of uranium was estimated using a contact time of around 90 hours at a solid: liquid ratio of 1:30. The U-spiked demineralized water samples were kept in contact with soil on a rotary shaker. Uranium analysis was carried out using LED Fluorimetry [2].

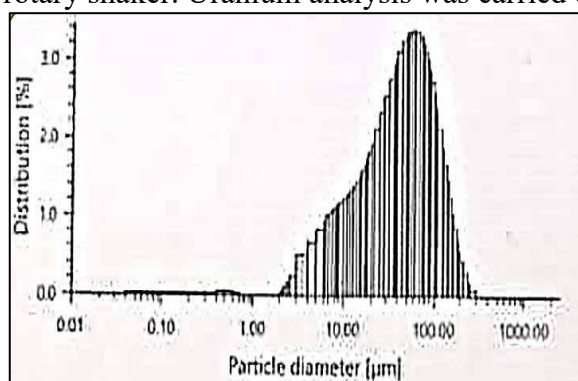


Fig 1. Particle size of soil

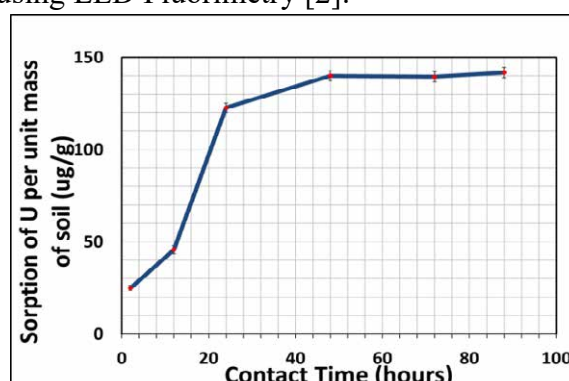


Fig 2. Sorption of U on soil

The average pH, electrical conductivity and organic matter content of the silty-clay-loam soils were 6.4, 847 $\mu\text{S}\cdot\text{cm}^{-1}$ and 0.2%, respectively. The average K_d value for the soils was observed to be 547 $\text{L}\cdot\text{kg}^{-1}$. Recommended $K_d(\text{U})$ values of 40, 200, 200 and 2,000 $\text{L}\cdot\text{kg}^{-1}$ have been mentioned for sand, loam, clay, and organic soils, respectively [4]. Hence it can be concluded that $K_d(\text{U})$ for these soils are similar to silt-clay-loam type soils and within globally reported values.

References:

- [1] Vandenhove et al., *Environ. Pollut.*, **145** (2007) 587.
- [2] Patra A.C. et al., *J. Environ. Management* 92 (2011) 919.
- [3] EPA, Understanding Variation in Partitioning Coefficients, K_d , Values: Volume II: Review of Geochemistry and Available K_d Values for Cadmium, Caesium, Chromium, Lead, Plutonium, Radon, Strontium, Thorium, Tritium and Uranium. EPA 402-R-99-004B, 1999.
- [4] Sheppard et al., *J. Environ. Radioactiv.* **89** (2006) 115.

Phosphonate Modified MOF-808 (Ce) for the Remediation of Uranium from Aqueous Solution

Nitin Gumber^{1,2}, Rajesh V. Pai^{1,2}§

¹Fuel Chemistry Division, Bhabha Atomic Research Centre, Mumbai – 400085

²Homi Bhabha National Institute, Anushakti Nagar, Mumbai – 400094.

§Email: rajeshvp@barc.gov.in

Metal Organic Frameworks as the name suggest comprises of an inorganic metal/ cluster and an organic linker to give rise to a 3D framework possessing excellent properties like high surface area and pore volume [1]. The fascinating field of MOFs has emerged exponentially over the last few years with diverse applications in fields ranging from catalysis, drug delivery, gas separation, adsorption etc. To sustain nuclear power production, a reliable and long term source of uranium is required. The presence of uranium in aqueous solutions specifically sea water is a major source which constitutes ~ 450 million tons all around the world. Thus, the state of the art materials like MOFs can be utilized efficiently to recover U from different aqueous waste streams.

In present work, Ce based MOF-808 was synthesized using $(\text{NH}_4)_2\text{Ce}(\text{NO}_3)_6$ as the metal source and trimesic acid as linker. It was further post modified using methyl phosphonic acid to yield phosphonate grafted MOF-808 (Ce) termed as PG-MOF-808 (Ce). Both the MOFs were characterized using XRD, FT-IR and TGA. The successful synthesis was confirmed through the presence of characteristics MOF-808 peaks as shown in XRD in Fig.1.

The uranium adsorption studies were carried out under different conditions like pH variation, adsorption kinetics, adsorption isotherm, cyclic reusability etc. The maximum adsorption for MOF-808 was observed at pH 8 while the phosphonate based MOF exhibited highest adsorption at pH 5 as shown in Fig. 2. The adsorption kinetics revealed higher rate of adsorption for bare MOF (~ 90 minutes) in comparison to PG-MOF-808 (Ce) which attained saturation after 270 minutes. This might be due to the requirement for U to diffuse inside the pores where P=O/P-OH group are situated in case of PG-MOF-808 (Ce). Adsorption isotherms revealed maximum experimental adsorption capacity for PG-MOF-808 (Ce) and was higher (~ 240 mg/g) compared to bare MOF with capacity of ~ 157 mg/g.

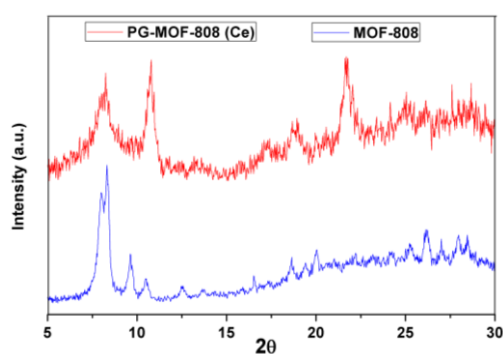


Fig. 1. XRD Patterns of MOF-808 (Ce) and PG-MOF-808 (Ce).

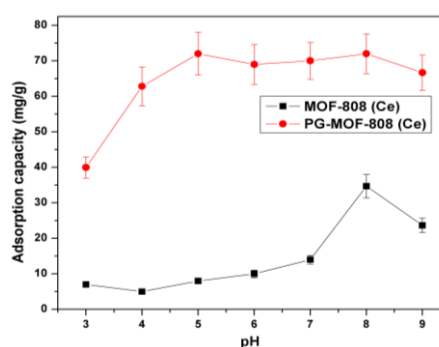


Fig. 2. Variation of adsorption capacity with change in pH for both MOFs.

References:

- [1]. G M. Lammert, C. Glibmann, H. Reinsch, N. Stock, *Crystal Growth & Design*, **17** (2016) 1125.

Characterization of Contaminated Water Using Stable and Radioisotope Signatures

Bhumika Kumari^{1,2}, Hemant Mohokar¹, Diksha Pant¹, Tirumalesh Keesari^{1,2,§}

¹ Isotope and Radiation Application Division, BARC, Mumbai

² Homi Bhabha National Institute, Anushaktinagar, Mumbai

§ Email: tirumal@barc.gov.in

Several anthropic derived organic contaminants are deteriorating the quality of water and impacting the aquatic habitat adversely. In this study, contaminated groundwater samples were examined to determine the dyes contributing to Dissolved Organic Matter (DOM). Water samples were also measured for environmental tritium to understand if the contamination is a recent phenomenon. Approximately one liter of water sample was collected from tube wells in the Padra region of Gujarat where groundwater contamination was reported. The water samples were filtered and filled in pre-washed high-density polyethylene containers. The recharging nature of the groundwater was evaluated using environmental tritium (³H). The tritium content of the water samples was measured using a Quantulus 1220 Liquid Scintillation Counter (LSC) after electrolytic enrichment [1]. The precision of tritium measurement was 0.5 TU (3σ criterion), where 1 TU is one atom of tritium in 10¹⁸ atoms of hydrogen, which is equivalent to 3.2 pCi/L of water. For DOM studies, the samples were acidified to pH 2-3 using high-pure concentrated HNO₃ and passed through the Solid Phase Extraction (SPE) cartridge (Inertsep HLB-FF, GL Science) for DOM extraction. The extracted DOMs as well as some commonly used industrial dyes were measured for the stable isotopes (δ¹³C, δ¹⁵N, and δ³⁴S) using Elemental Analyzer – Isotope Ratio Mass Spectrometry (EA-IRMS). The concentration of the DOM found to vary from 0.1 to 50 mg/L and the Platinum – Cobalt color scale showed an intensity ranging from 40 to 1200. The extraction efficiency of the cartridge was estimated using Fulvic Acid (FA) and

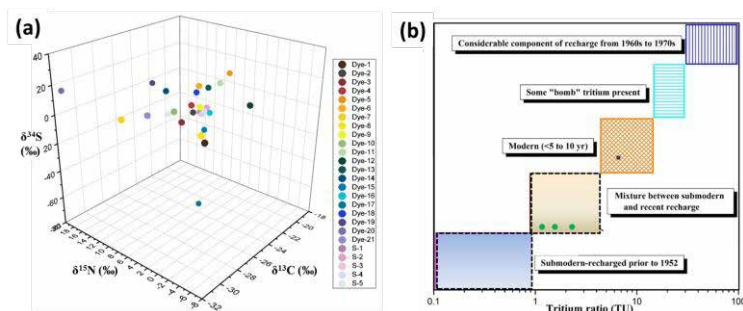


Fig. 1 a) δ¹³C, δ¹⁵N, and δ³⁴S values of dyes and contaminated samples and b) Tritium content of water samples and qualitative ages.

found to be 89%. The contaminated water samples showed δ¹³C, δ¹⁵N, and δ³⁴S values in the range of -26.53 to -23.47‰, 4.78 to 7.64‰ and -3.61 to 0.31‰ respectively. A comparison of the isotope values of contaminated samples with commercial dyes suggested that among 21 tested dyes, 6 dyes viz., Disperse Blue 14 (Dye-2), Acid Orange 8 (Dye-3), Acid Blue 25 (Dye-9), Eriochrome Black - T (Dye-12), Acid Black 194 (Dye-14) and Reactive Yellow 145 (Dye-15) contribute DOM to contaminated waters (Fig. 1a). Tritium content of the contaminated waters was found to range from 1.3 to 5.8 TU, suggesting that the contamination is a recent phenomenon and mixing with old groundwater is prominent (Fig. 1b). This study emphasizes the effectiveness of stable and radioisotopes in providing a deeper understanding of the source of contamination and its dynamics.

Reference(s):

[1] U. Morgenstern, CB Taylor, *Isotopes Environ Health Stud.*, **45**(2) (2009) 96.

Estimation of ^{40}K in the Human Body Using Shadow Shield Whole Body Counter

Jayan M P[§], Krishnakumar P, Amit Bhatnagar, Sureshkumar M K

Health Physics Division, Bhabha Atomic Research Centre, Mumbai, India

[§]Email: jayan@barc.gov.in

Whole-body counting (WBC) system is used to quantify the radionuclide incorporated into body. Natural potassium is a mixture of three isotopes: ^{39}K , ^{40}K and ^{41}K with mass percentages of 93.08%, 0.0118% and 6.91% respectively, in which ^{40}K is a radionuclide emitting γ -ray of 1.46 MeV [1]. Hence, human body is always subjected to irradiation from ^{40}K . With appropriate shielding for the WBC, it is possible to measure the ^{40}K content in human body [2].

The WBC system consists of a 5"x3" NaI(Tl) detector, arranged inside a shadow shield with a scanning bed. The calibration of the system was carried out with a BOMAB phantom, using KCl solution. ^{40}K body burden were measured for 40 male and 10 female workers.

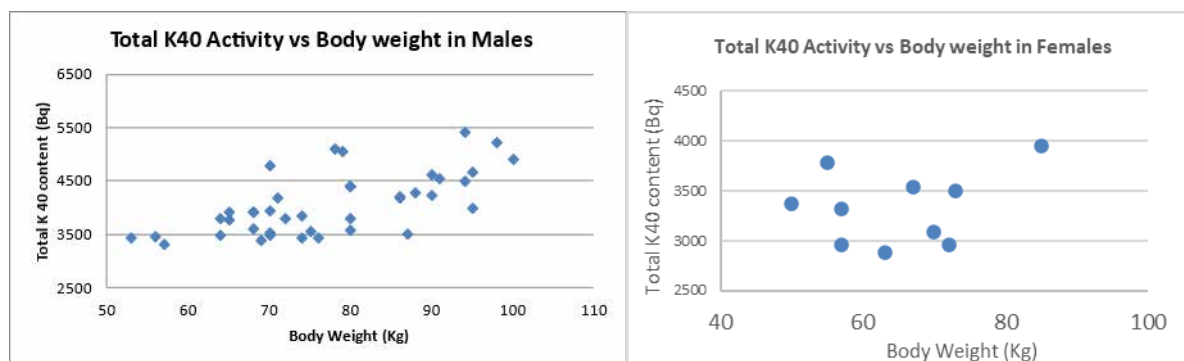


Fig.1: Plot of Total ^{40}K activity vs Body weight for Male and Female Radiation workers.

The counting efficiency of the WBC system was 6.39×10^{-5} cps/Bq for ^{40}K . The minimum detectable activity (MDA) for ^{40}K was estimated as 2462 Bq. The ^{40}K content in males and females are given in Fig.1. ^{40}K body content ranged from 3313 ± 172 to 5409 ± 220 Bq (mean 4064 Bq) for males and 2887 ± 161 to 3949 ± 188 Bq (mean 3337 Bq) for females respectively. From the results it is observed that the ^{40}K body content is higher in males than the females. In the present study the average height and weight of females (159.5 cm and 64.9 kg) was lower than that of males (169.9 cm and 77 kg). Thus the lower in ^{40}K body content in females may be ascribed to their possible lower lean body mass [2]. The annual internal effective dose from ^{40}K for males ranges from 112 to 190 $\mu\text{Sv/y}$ with an average dose of 148 $\mu\text{Sv/y}$ and for females ranges 114 to 188 $\mu\text{Sv/y}$ with an average dose of 146 $\mu\text{Sv/y}$. The concentration of ^{40}K observed here is in the same range as in other studies and the annual dose rate received in the measured workers is also within the bracket as reported in UNSCEAR [3].

References:

- [1] CY Lan, PS Weng., *Health physics*. **57** (1989) 743.
- [2] M.T Taha et.al, *Journal of Radiation Research and Applied Sciences*, **15** (2022) 353.
- [3] Sources and Effects of ionising radiation, UNSCEAR 2000.

Electrochemical Decontamination of Radioactive Metallic Surfaces with Fixed Contamination

Arkaprava Layek, Ruma Gupta[§]

Fuel Chemistry Division, Bhabha Atomic Research Centre
Mumbai, India 400085

[§] Email: rumac@barc.gov.in

The effective decontamination of radioactive metallic surfaces with fixed contamination is a critical challenge in nuclear facility maintenance and decommissioning. We have already established an in-house strippable gel based decontamination method for loose contamination. This study further extends to a systematic electrochemical approach for the removal of fixed alpha contamination from metallic surfaces using an optimized electrolytic process. Radioactive contamination on metallic surfaces poses significant risks in nuclear decommissioning. According to literature studies, over 98% of radionuclides are found within the first 10 μm of the metal surface, with decreasing contamination levels at greater depths. Effective decontamination requires removal beyond 10 μm to reach clearance levels.

A controlled contamination assessment was conducted on an alpha-active planchet with an initial radioactive contamination level of 5401.62 cpm. Electrochemical decontamination was performed using a DC power supply, where the anode was connected to the contaminated metal surface and the cathode consisted of a graphite rod with an HDPE cloth-based decontamination head saturated with 4M nitric acid. This setup enabled electron transfer from the anode to the cathode, initiating oxidation-reduction reactions to dissolve and remove radioactive contaminants into the electrolyte solution. The electrochemical treatment significantly reduced radioactivity levels to 1.5 cpm, achieving a decontamination factor (DF) of approximately 3600 in just 5 minutes, corresponding to a decontamination efficiency of 99.96%. The findings validate electrochemical decontamination as a highly effective and rapid method for removing fixed alpha contamination while preserving the integrity of the underlying metal surface. Electrochemical decontamination offers a non-destructive, efficient alternative to conventional decontamination techniques. This approach holds great potential for nuclear decommissioning and radioactive waste management, enhancing radiation safety protocols and reducing long-term environmental risks.

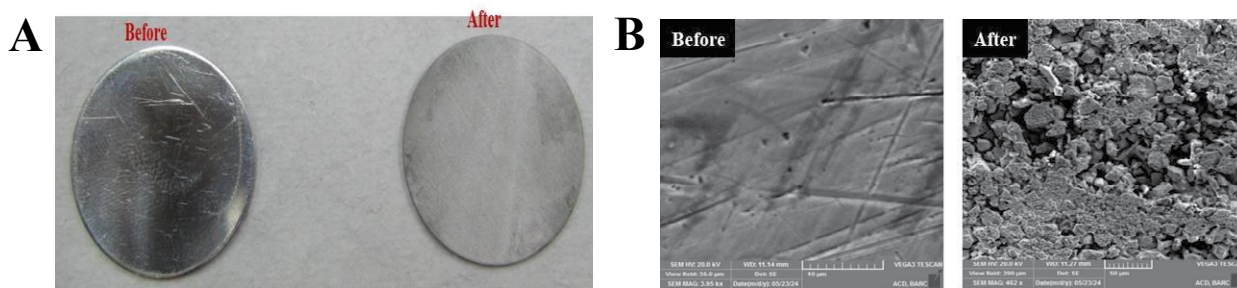


Fig 1: A) steel planchet before and after electrochemical decontamination B) SEM image of steel planchet before and after electrochemical decontamination.

References:

[1] Sushil M. Patil et al, *Journal of Applied Polymer*, **141** (2024) e55904.

Advanced Statistical Approach for Tracing Uranium Yellow Cake Origins via Coupled LIBS-Chemometrics Analysis

Anannya Banerjee¹, Subhankar Manna², Anandhu Mohan³, Santosh K. Satpati²,
Rajesh V. Pai^{1,3}, Arnab Sarkar^{1,3,§}

¹ Fuel Chemistry Division, BARC, Mumbai 400 085, India

² Uranium Extraction Division, BARC, Mumbai 400 085, India

³ Homi Bhabha National Institute, Anushaktinagar, Mumbai 400 094, India

§ Email: arnab@barc.gov.in

This work highlights the application of statistical approach in the Indian context for the geographical origin identification of uranium yellow cakes coupled with Laser Induced Breakdown Spectroscopy (LIBS)-chemometrics. Globally, the importance of nuclear forensics towards strengthening the security against the unauthorized uses of important materials has been demonstrated by the methodology used in LIBS [1] proving that it's a viable technique. Due to its robustness, easy sample preparation and micro-destructivity, LIBS is a value addition in the field of nuclear forensics compared to other lengthy techniques like TIMS. The parameters distinguishing the sample from one another is the difference in the spectral signature pattern depending upon the region of collection/processing. For this study, eight samples from four different origins of India was collected and the samples were pelletized using high pressure. LIBS spectra was recorded after optimizing experimental parameters like Q switch delay and gain using a Nd:YAG laser(532 nm) forming a plasma. After finding the optimum region of analysis in the LIBS spectra and properly clustering the samples on application of Principle Component Analysis (PCA), the viability of the coupled model was tested statistically. For this purpose, statistical parameters like Youngden's index (J) was used (Fig. 1).

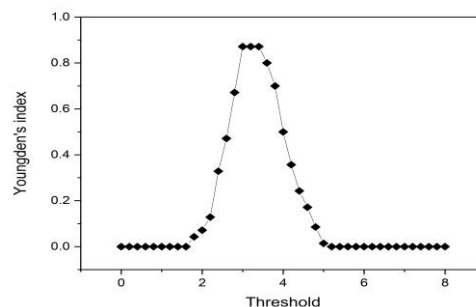


Fig. 1: A representative J curve

For understanding the performance of the model, further a machine learning model-based approach called confusion matrix was created. Apart from one sample, in each case, the accuracy of the prediction of the model was >90%. Further to understand the strength of the machine learning based model, different statistical curves like Receiver Operating Characteristics (ROC) curve was constructed. The ROC curve gives the idea of the model performance by changing the thresholds [2]. In most of the cases ROC curve has given peak diagnostic performance at 1, which indicates the superiority classification capability of the model. The model was further analyzed by calculating statistically important parameters such as specificity and sensitivity which brought about exemplary result in most of the cases. In summary, it can be concluded that this statistical based approach towards proving the effectiveness of the coupled chemometrics-LIBS is a value added addition in the field of Nuclear Forensics from an Indian approach.

References:

- [1] Sirven et al., *J. Anal. At. Spectrom.*, **24** (2009) 451.
- [2] Unnikrishnan et al., *RSC Advances*, **3** (2013) 25872.

Development of a Supervised Machine Learning Algorithm for Non-Destructive Burn-up Verification of Simulated PHWR Spent Fuel Pin

Sabyasachi Patra^{1,3,§}, Satyam Kumar¹, Y.S. Rana², Rahul Tripathi^{1,3}

¹ Radiochemistry Division, BARC, Mumbai-400085

² Research Reactor Services Division, BARC, Mumbai-400085

³ Chemical Sciences Discipline, Homi Bhabha National Institute, Mumbai-400094

§ Email: spatra@barc.gov.in

One of the important minor actinides present in the spent fuel (uranium based) from a nuclear reactor is plutonium. This underscores the need for stringent control and safeguards to monitor and secure spent nuclear fuel during its long-term storage in facilities [1]. Gamma-ray spectrometry (GRS) plays an important role in nuclear security, though it cannot directly quantify Pu present in spent fuel because of the high radioactivity of fission products (FPs) present in the sample. GRS is conventionally used to verify spent fuel inventories by correlating the measured relative FP activities with operator-declared burn-up. In a previous study, we demonstrated that absolute quantification of multiple FPs in a typical PHWR spent fuel pin is possible by high-resolution gamma-ray spectrometry [1]. Taking advantage of the absolute assay of FPs, a data mining algorithm has been developed in the present work for prediction of burn-up of a PHWR spent fuel pin using supervised machine learning (ML) principle, inspired by the k-nearest neighbour (KNN) model. We developed a Python-based ML code, SPINFOR, trained on expected γ -ray activities of seven FPs (half-lives: 30 years to 250 days) at various burn-ups and cooling times. FPs covering wide range of the half-lives make the code sensitive to cooling time variation over a several years. The FP inventories at different burn-ups ranging between 1000 to 7000 MWD/Te and at different cooling times were obtained using standard depletion code, and were used for training the code SPINFOR. The burn-up and the cooling time indices for a set of measured FP activities were thus predicted based on finding the best collective matching of the measured activities with the trained activity matrices. SPINFOR has been validated using a simulated γ -ray spectrum of a PHWR spent fuel pin (burn-up: 5000 MWD/Te, cooling time: 5 years), demonstrating its ability in estimating fuel burn-up and cooling time (Fig. 1). The recently developed GNDA methodology [2] has been suitably adapted for the assay of FPs in the simulated spent fuel pin prior to the ML analysis.

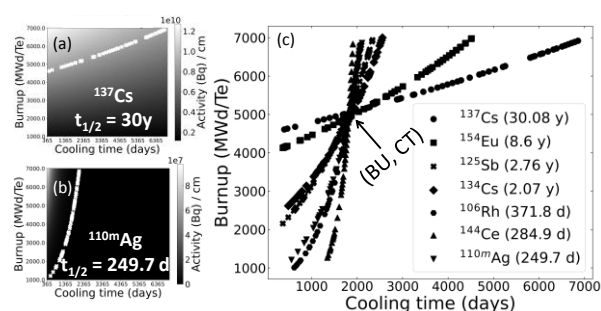


Fig. 1: Representative burn-up (BU) vs. cooling time (CT) training matrices showing ¹³⁷Cs and ^{110m}Ag activities (colourmap) with mining of respective test FP activities shown as blue markers (a,b) and predictive solution of burn-up and cooling time based on finding the best collective matching of the mined coordinates (c).

References:

- [1] S. Patra et al, Proceedings of the fifteenth biennial DAE-BRNS symposium on Nuclear and Radiochemistry, 2021, INIS Reference number: 53116468.
- [2] S. Patra, A.M. Mani, S. Kumar, R. Tripathi, *Anal. Chem.*, **96** (2024) 2857.

Development of a Monte Carlo Methodology for Response Function Analysis of Plutonium Alpha Spectra

Sabyasachi Patra^{1,3,§}, R. Suvethaa^{2,#}, Satyam Kumar¹, Rahul Tripathi^{1,3}

¹ Radiochemistry Division, Bhabha Atomic Research Centre, Mumbai-400085

² Department of Chemistry, Lady Doak College, Madurai-625002

³ Chemical Sciences Discipline, Homi Bhabha National Institute, Mumbai-400094

§Email: spatra@barc.gov.in

Alpha spectrometry is a highly effective radiometric tool for the low-level assay of fissile materials such as plutonium in environmental and nuclear forensic samples. However, given the proximity of the alpha particle energies, the spectral overlap between different isotopes is substantial in plutonium alpha spectrometry, making the straight forward isotopic assay difficult. The present study attempts to simulate the surface barrier alpha detector response for different isotopes of plutonium and ²⁴¹Am by Monte Carlo method [1]. The detector parameters such as the detector deadlayer and the detector resolution have been iteratively optimized using an in-house Monte Carlo code (developed in python-3.8) by matching the simulated detector response of ²³⁸Pu with experimental spectrum (Fig. 1). The code takes a

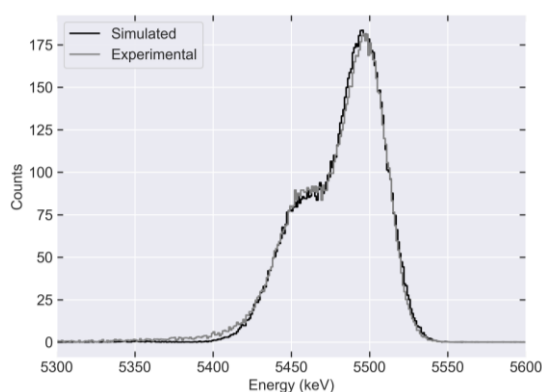


Fig. 1: Co-plot showing the experimentally measured and Monte Carlo simulated alpha particle spectra of ²³⁸Pu with the optimized detector parameters. [Black: simulated; Grey: experimental]

maximum of 5 minutes to run on a desktop PC with an i5 processor and Windows OS. Detector response functions of all the alpha emitting isotopes of Pu and ²⁴¹Am have thus been generated using the same code at the optimized detector parameters. Test alpha spectra of typical power reactor grade plutonium sample (about 70 wt% ²³⁹Pu) at a given burn-up and different ages (between 5 to 100 years of cooling) have been obtained by mathematical mixing of the detector efficiency normalized detector responses for various isotopes at a given isotopic composition. In all the cases, the experimentally obtained response of ²³⁸Pu has been mixed with Monte Carlo simulated detector responses for other isotopes to generate the test spectra. Finally, another code has been written in python-3.8 to analyse the test spectra by response function fit to obtain the absolute isotopic inventory of different Pu and ²⁴¹Am isotopes. Considering the alpha peak at ~5.5 MeV in the test spectra to be a representative of a “proof of concept” experiment (as this peak contains experimental input for ²³⁸Pu), the absolute activity (and mass) of ²³⁸Pu and ²⁴¹Am could be obtained from the analysis within 10% of the expected masses in spite of the significant spectral overlap. The comparison with experimental data of ²³⁸Pu provides an initial validation/benchmarking of the code. We plan to carry out comprehensive benchmarking with comparisons against more complex experimental spectra.

#Formerly, Masters project student at Radiochemistry Division, BARC.

References:

Radiochemical Separation of Protactinium Using Anion Exchange Method in Uranium Rich Matrices for Application in Chronometry

Prabhath Ravi K[§], Suchismita Mishra, Sathyapriya R Sreejith

Environmental Monitoring and Assessment Division, BARC, India

[§]Email: ravip@barc.gov.in / prabhathravi@gmail.com

Development of simple methodologies for separation of radionuclides for age determination of nuclear materials is challenging. Typical recovery of $94.1 \pm 2.5\%$ was reported for Pa from bioassay samples spiked with ^{231}Pa [1]. Same methodology was adopted for Pa separation from U-ore samples. Separation of Pa from uranium rich materials like U-ore was carried out using Dowex 1x8 anion exchange resin (exchange capacity of $\sim 1.2 \text{ meq.ml}^{-1}$) for studying the ^{235}U - ^{231}Pa radiochronometer. 1 g of U-ore sample sourced from UCIL, Jaduguda was digested in a microwave digester using HNO_3 , HF and HClO_4 reagents. ^{233}Pa prepared by neutron activation of ^{232}Th in PCF facility of Dhruva at a neutron flux of $\sim 10^{13} \text{ n.cm}^{-2}.\text{s}^{-1}$ was used as tracer. Digested sample in 8N HNO_3 was loaded onto anion exchange column, followed with 8N HNO_3 and 8N HCl washing in succession before eluting with freshly prepared 0.1M HF in 1M HCl . 312 keV gamma line of ^{233}Pa was used for quantification of Pa radiochemical recovery. Oxidation of Pa to Pa(V) by adding a pinch of NaNO_2 in the loading solution is a crucial step in the separation of Pa and should be done before loading to the column for effective Pa separation. Flow rate of reagents and eluent

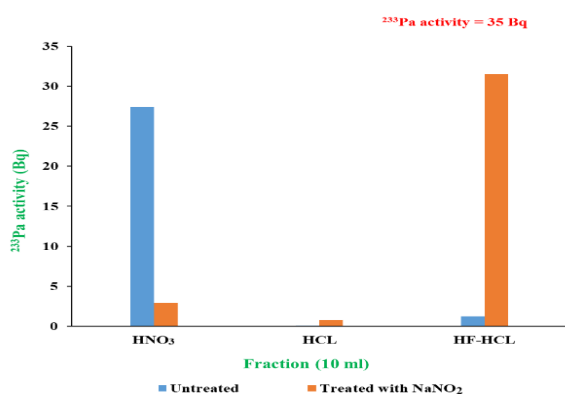


Fig. 1: Elution profile of ^{233}Pa in pure tracer solution

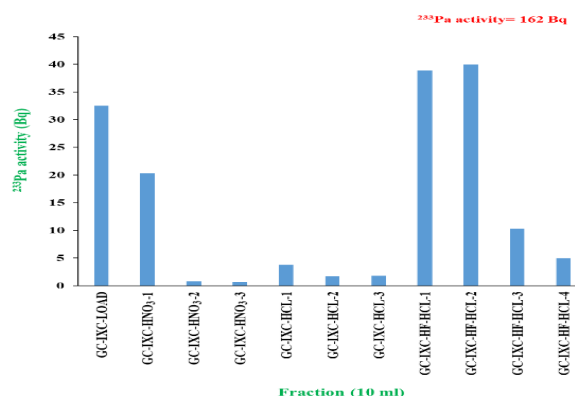


Fig. 2: Elution profile of ^{233}Pa with fine flowrate adjustment in U-ore sample

should be finely controlled for better Pa separation (0.2 ml.min^{-1}). Chemical recovery of $90 \pm 3\%$ was observed for Pa in a pure tracer solution. In case a real digested ore sample, the recovery was found to be $63 \pm 2\%$ under the same elution conditions. Further studies are planned for improving the Pa chemical recovery.

Acknowledgements: PRK would like to thank Sh. B Vijayakumar, OIC, ESL, KKNPP, Sh. R K B Yadav, Head, EPRS and Probal Chaudhury, Head, HPD for their support and encouragements. Authors would like to thank Sh. I V Saradhi, Head, ESS, Dr. Anilkumar S Pillai, Head, NFS and Dr. A Vinodkumar, Head, EMAD for their suggestions and support.

References:

[1] S. P. Prabhu et al., *Radiation Protection and Environment*, **33(3)** (2010) 137.

Implementing Artificial Neural Network Base Modelling for Estimating Elemental Concentration from Overlapping Line of Rb/U

B. Kanrar^{1,§}, K. Sanyal^{1,2}, R.V. Pai^{1,2}

¹Fuel Chemistry Division, Bhabha Atomic Research Centre, Mumbai-400094, India

²Homi Bhabha National Institute, Mumbai-400094, India

§Email: buddha@barc.gov.in

Uranium and its compounds are technologically important materials having a variety of applications in the form of catalysts, magnetic, materials, electrodes and most important nuclear fuel [1]. Rubidium is an important fission product formed during fuel irradiation and therefore many rubidium uranates are reported in the literature [1]. Systematic studies to assess the analytical parameters obtained in the total reflection X-ray fluorescence (TXRF) determinations of interfering elements Rb and U using artificial neural network base modelling reported in the present manuscript.

We have utilized an artificial neural network (ANN) based algorithm which is a variant of multivariate chemometric method for modelling the overlapping line of Rb/U for estimating elemental concentration of the same. Total 26 sets of samples were prepared, each containing mixture of Rb and U having different concentrations ratios ranging from 86 to 0.2 (Rb/U concentration ratio). Known concentration of Sr was added as internal standard. About 20 μ L of each sample was deposited on quartz sample supports and TXRF spectra were recorded for each sample 4 times. In the presently developed methodology, ANN model is trained, validated and tested with a calibration dataset that consists of 104 TXRF spectra from 26 sets of samples mentioned above. The predictability of the trained model was assessed by Standard Error of Prediction (SEP) parameter and defined as:

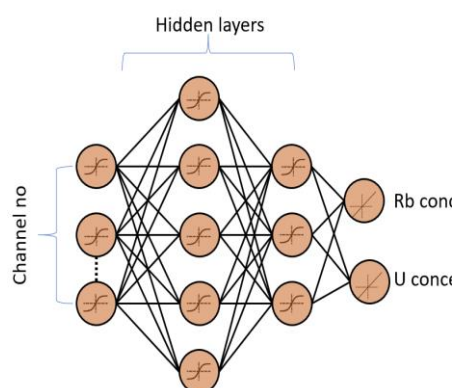


Fig 1: Basic ANN architecture

$$SEP(\%) = \sqrt{\frac{1}{N} \sum_{i=1}^N (C_s - C_p)^2} \quad (1)$$

Known concentration of Sr was added as internal standard. About 20 μ L of each sample was deposited on quartz sample supports and TXRF spectra were recorded for each sample 10 times. The Python 3.9.7 version was utilized to implement the ANN model. For handling data, an easy-to-use data structure and data analysis tool called Pandas was used. After optimizing all the parameters (i.e., ANN architecture, activation function and epochs no)[2], the relative error and precision for the U/Rb quantifications in test dataset were evaluated using the optimized ANN model. A relative error of 8.76% and 1.81% were obtained for U and Rb concentration determination. A precision of 5.47% and 7.60% were obtained by the regression on the test dataset.

References:

- [1] S. Dhara, A.Khooha, A.K. Singh, M.K. Tiwari, N.L. Misra; *Spectrochimica Acta Part B*, **144**(2018), 87–91
- [2] B. Kanrar, K. Sanyal, A. Sarkar and R. V. Pai, *Journal of Analytical Atomic Spectrometry*, **38**(2023), 1841–1850

Development of Instrumentation for on-line Measurement of DC Current Using Non Contact Method for the Electrolytic Conversion of Metal Oxide into Metal

Ajay Kumar Keshari^{1,§}, J. Prabhakar Rao¹, N. Sanil¹, V. Arunkumar¹, L. Shakila¹,
R. Kumaresan^{1,2}

¹Homi Bhabha National Institute (HBNI)

²Materials Chemistry & Metal Fuel Cycle Group

Indira Gandhi Centre for Atomic Research, Kalpakkam - 603102, Tamil Nadu, India

§ Email: ajayanau@igcar.gov.in

An instrumentation setup was designed and developed for the non contact measurement of DC current (0-200 A) in an electrochemical cell for the conversion of metal oxide to metal using direct-oxide electrochemical reduction (DOER) method. The setup consists of an electrochemical cell, sensor, hardware, and software. During electrolysis, continuous measurement and logging of current through individual electrodes (anode and cathode) is required to monitor and control the process accurately to convert the metal oxide to metal. The block diagram of the instrumentation setup is shown in Fig. 1.

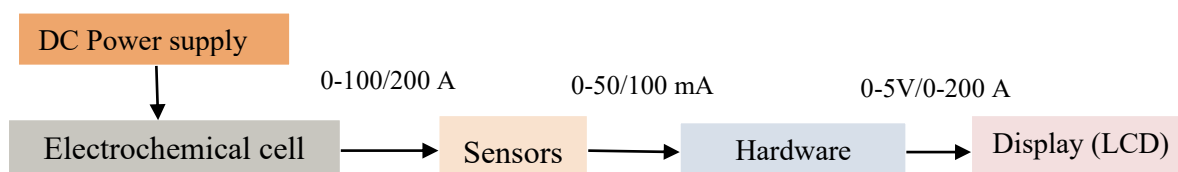


Fig. 1 The block diagram of instrument of an electrochemical cell for the measurement of current

The sensor measures the dynamic currents of the electrode and provides a 50 mA output for a 100 A sensor and gives a 100 mA output for a 200 A sensor with an accuracy of $\pm 0.5\%$. The multichannel hardware was developed to measure the high DC currents of 100 and 200 A of the anode and cathode of the electrochemical cell using signal conditioning and data processing based on the 8051 microcontroller. The signal conditioning unit converts sensor current into voltage using a high impedance operational amplifier. The data processing unit processes the amplified data and sends it to the LCD for the display of high DC current. The hardware also provides the analog output from 0-5 V to integrate with other modules and for further processing. This multichannel instrumentation setup was tested and validated with the standard inputs, and the corresponding results are presented in Fig. 2 (a) & (b). The accuracy and sensitivity of the developed instrument were evaluated as $\pm 0.5\%$ and 0.5 mA/A and are portable, compact, and remote data collection into the control room compared to commercial instruments. The instrumentation setup was installed into the glove box and tested in a 2 kg DOER facility for converting uranium oxide into uranium metal.

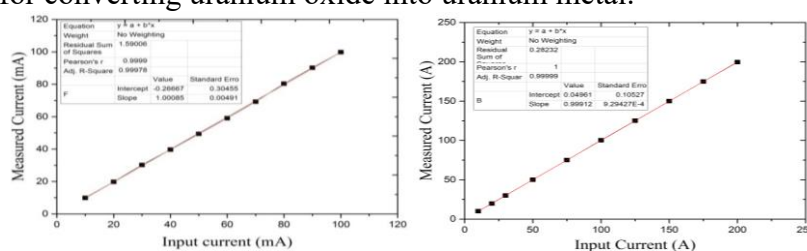


Fig. 2 (a) and (b) Calibration and validation of multichannel hardware with the standard currents

Reference(s):

[1] E. Y. Choi and J. Lee, *Journal of Nuclear Materials*, **494** (2017) 439-447.

Coincidence Ion Beam Analysis (CIBA) facility

A. A Sukumar, D. V. Lakshmipathy, Y. Sunitha, Sk. Jayabun, G. L. N. Reddy[§]

National Centre for Compositional Characterisation of Materials (NCCCM), BARC,
Hyderabad, India, 500062

[§]Email: glreddy@barc.gov.in

Coincidence and anti-coincidence measurement techniques are being used in nuclear physics, radioactivity metrology, and in the nuclear analytical measurements to enhance the precision and reliability of particle detection. By employing coincidence techniques, it is possible to achieve greater sensitivity, precision, and interference-free determination of elemental composition in nuclear analytical experiments.

At NCCCM-BARC, Hyderabad, we have established a Coincidence Ion Beam Analysis facility. For this, we have employed a high-speed, four-channel digitizer, which eliminates the need for traditional spectroscopy amplifiers, constant fraction timing discriminators, universal coincidence modules, counters, etc. This compact desktop system integrates four independent 16k-channel digital MCAs for nuclear spectroscopy. Key features of the system include four detector inputs with simultaneous data acquisition, 14-bit flash ADCs with a sampling rate of 100 MS/s per channel, and a time resolution of up to 10 ns. The digitizer is equipped with a DPP-PHA Firmware, that is a Digital Pulse Processing-Pulse Height Analysis algorithm making it a spectroscopy acquisition system providing energy (i.e. pulse height) and timing information. Additionally, the system captures portions of the waveform for debugging, monitoring, and pulse shape analysis.

The digitizer is controlled via the multiparametric DAQ in physics applications. It enables coincidences and anti-coincidences both within and across boards. The system features list mode operation, storing pulse height and time-stamp data for each event across all channels. This allows for offline coincidence spectroscopy analysis using the time-stamped events.

Using CIBA facility the Elastic Recoil Coincidence Spectroscopy (ERCS) as well as coincidence Nuclear Resonance Reaction Analysis measurements were carried out. ERCS is used for sensitive determination and depth profiling of light elements [1]. Figure 1 shows ERDA spectra from two different detectors as well as coincidence recoil spectra of thin mylar foils carried out in transmission mode. Well isolated background free signal of hydrogen can be seen in the coincidence spectra. CIBA can be applied to Ion Beam Induced Prompt nuclear reactions, such as $^{19}\text{F}(p, \alpha\gamma)^{16}\text{O}$, $^{31}\text{P}(\alpha, p\gamma)^{34}\text{S}$, $^{10}\text{B}(p, \alpha\gamma)^7\text{Be}$ etc., to achieve better sensitivity.

The various experimental geometries and nuclear reactions for carrying out CIBA will be discussed.

References:

[1] B. L. Cohen, C. L. Fink and J. H. Degnan, *Journal of Applied Physics* **43** (1972) 19.

dedicated CAEN CoPASS software for

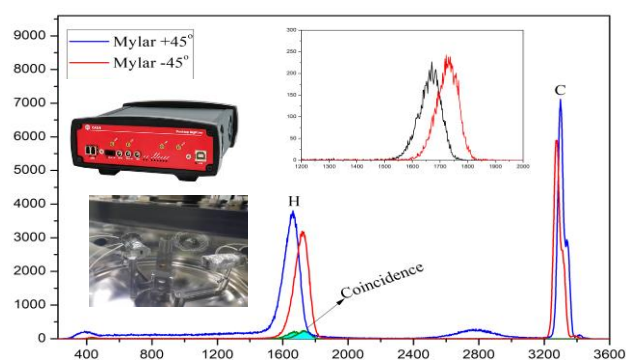


Figure 1. ERDA spectra from two detectors positioned at 90° w.r.t each other. Inset shows the coincidence recoil spectra of hydrogen

Characterization of ASIC Based Indigenous Neutron Area Flux Monitor with BARC-make BF₃ filled neutron detector

P. Bahre¹, M. K. Jha¹, T. Bhattacharjee^{1,§}, P. Maity¹, S. Ghosh¹,
A. Banerjee^{1,3}, S. Mazumder¹, T. Samanta^{1,3}, S. S. Desai²

¹ Computer and Informatics Group, Variable Energy Cyclotron Center, Kolkata, India

² Solid State Physics Division, Bhabha Atomic Research Center, Mumbai, India

³ Homi Bhabha National Institute, Mumbai, India,

§Email: btanu@vecc.gov.in

Neutron Flux Monitors (NFM) play an important role in radiological safety at nuclear facilities. An effort towards indigenous development for medical accelerator as per IAEA guidelines is presented [1]. NFM incorporates Application-Specific Integrated Circuit (ASIC) developed by VECC and BF₃ filled neutron detectors, developed by SSPD, BARC. The key feature of this system is its ability to discriminate gamma and background noise from thermal neutron better than the available one in the market. The NFM consists of a Charge Sensitive Pulse Converter (CSPC) module, a Digital Controller Module (DCM) and a neutron detector. VECC003 (Fig. 1) is a low noise charge-sensitive preamplifier and shaper chip, designed and fabricated with 180 nm CMOS technology at SCL Chandigarh [2]. The ASIC offers a dynamic range of 500 fC and a sensitivity of 2 V/pC, producing a shaped output with a 1 μs peaking time of a neutron pulse. The sensitivity of the BARC-make BF₃ filled neutron detector is 0.3 cps/nv and another with 4 cps/nv [3] is being tested. The NFM offers better efficiency as compared to commercial [4] as the application is for public, patients and radiation workers at medical accelerator [1].



Fig. 1: An ASIC 28 Pin DIP VECC003

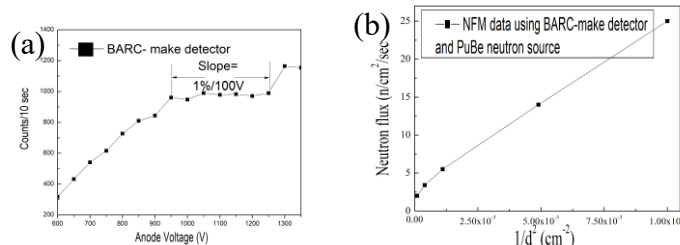


Fig. 2: a) Anode bias Curve and b) Detector response with variable source-detector distance with a 50 mCi neutron source

The electronics of the NFM was tested successfully in the laboratory with count rates of up to 100 kHz. The NFM module was characterized using Pu-Be source using a commercial as well as the BARC-make detector. Fig. 2a shows the counting plateau obtained for the BARC-make detector mounted in this module. Fig 2b shows the linear variation of this detector's response with source distance following inverse square law. Validation of the NFM module was conducted at the Multipurpose Test Facility, Dhruva reactor, where neutron flux of about 40,000 nv was successfully measured. The NFM proves its effectiveness for neutron detection in the gamma background of ~1 R/hr with neutron count-rate ~ 10⁴ per sec. The performance of NFM highlights its potential for deployment in neutron environments with better sensitivity than commercial one [4]. Details of these developments and characterization will be presented.

References:

- [1] Neutron monitoring, IAEA safety reports series 2023, ISSN 1020–6450; no. 115, p169.
- [2] P. Bahre et.al, *DAE-BRNS Symposium on Nuclear Physics*, 65 (2021) 776.
- [3] S. S. Desai, *J. Phys: Conf. Ser.*, 528(2014) 012037 and *Rad. Meas*, 144 (2021) 106593.
- [4] <https://www.ecil.co.in/RIDFinalCatalog.html#NFM>

Automation of Indegenous Integrated Segmented & Tomography Gamma Ray Scanning System

Rajesh T. Jadhav[§], Chhavi Agarwal, Rahul Tripathi, Suparna Sodaye

Radiochemistry Division, BARC, Trombay, Mumbai - 400 085, India

[§] Email: rtjadhav@barc.gov.in

The assay of low-density 200 L waste drums containing low to intermediate levels of radioactivity, required for inventory and safeguard purpose, is a critical application of gamma-based non-destructive assay (NDA) techniques. It presents significant challenges due to the complex and varied waste composition [1]. Single tomographic assay requires large number of measurements (3060 measurements each for emission and transmission mode). Therefore, it is practically impossible to carry out the measurements manually. To address these challenges, the Integrated Segmented and Tomographic Gamma-ray Scanning System (ISTGSS) has been developed and routinely deployed by RC&IG for analyzing such heterogeneous samples [2]. This work details the automation of indigenous ISTGSS for performing segmented, radial, tomographic, and helical transmission and emission scanning with integrated data storage and analysis. The system can be used for complete tomographic information or segment wise assay of heterogeneous sample depending on the available time and assay requirements. All the parameter settings for the ISTGSS, including data acquisition and analysis, have been integrated under computer control through serial communication protocols such as USB and RS232. The automation system comprises of hardware and software components. The hardware component includes an Arduino Mega 2560 Microcontroller board as the master controller for controlling the motion of the waste drum (translational, rotational and vertical), along with the shutter and collimator positioning. The software aspect involves Visuino software for microcontroller programming. This software provides a graphical integrated environment which helps user program microcontrollers and microprocessors with the help of easy to use visual interface. Along with this, LabVIEW (Laboratory Virtual Instruments Engineering Workbench) version 2016, a Windows-based graphical programming language, has been used for user-friendly interface development, real-time data acquisition, and analysis. Figure 1 shows the front panel of the automation software for tomographic transmission mode. The accuracy of the automated system was validated by calibrating the number of pulses given to the servo motor driver with its physical measurement.

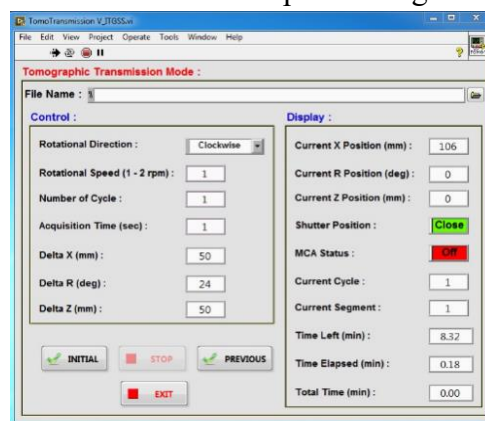


Fig 1. Front Panel of the LABVIEW based automation software for tomographic transmission mode.

The integration of automated control and data acquisition into ISTGSS enhances operational efficiency and reliability, ensuring precise and accurate assay of nuclear waste drums.

Authors thank Head, RCD for his support and encouragement.

References:

- [1] E.R.Martin et al., *Los Alamos National Laboratory report*, LA-7059 (1977).
- [2] R.J. Estep et al., *Los Alamos National Laboratory report*, LA-UR-93-1637 (1993).

Measurement of Radiation and Transmutation in H₂O&D₂O Electrolysis

Ankit Kumar^{1§}, K. P. Rajeev¹, Pankaj Jain², R. G. S. Pala³

¹ Department of Physics, IIT Kanpur, Kanpur, India

²Space, Planetary & Astronomical Sciences & Engineering, IIT Kanpur, Kanpur, India

³ Chemical Engineering, IIT Kanpur, Kanpur, India

§ Email: ankitkumar5111994@gmail.com, ankt@iitk.ac.in

The Department of Physics at Indian Institute of Technology Kanpur (IITK) has initiated a critical analysis of Low Energy Nuclear Reactions (LENR), based on the original Fleischmann-Pons electrolysis experiments, which reported neutrons, tritium, and gamma emissions obtained with an energy input < 5 eV [1]. These findings were considered sceptical as such possibilities were at odds with the established nuclear theory. Despite initial doubts [2], LENR has opened new possibilities for understanding how condensed matter could influence nuclear reaction rates [3], and fostered advancement in theory and applications of metal-hydrogen storage [4].

To verify such chemically induced nuclear reactions, we studied light water electrolysis where pure metals and their alloys underwent nuclear transmutations. While we could not find correlated gamma emissions using sodium-iodide detectors, these experiments were pivotal in shaping our subsequent research. The details of transmutation correlation with photons will be presented at the conference. Our latest work utilizes a Solid-state nuclear track detector, Columbia Resin-39 (CR-39), to detect potential particle emissions in D₂O electrolysis. The detectors are placed in contact with the cathode to register the particle tracks emissions. The main challenge of this work was characterizing the nature of the emitted particles. To address this, we used radiators and performed control experiments, which confirmed that both charged particles and neutrons were emitted during electrolysis experiments. Additionally, we also emphasize the role played by magnetic fields in enhancing emission rates by up to four times in our experiments. While changing the cathode material in such experiments, we found that the particle track density on CR-39 followed the order: Pt > Pd > Ni. Our experiments confirm nuclear activity in low-voltage electrolysis and introduce reproducible techniques to observe these effects. The details of observation and interpretations will be discussed at the conference.

A recent analysis by our theory team, published in Physical Review C, emphasizes the role of resonance states in achieving observable nuclear reaction rates ($\sim 10^{-20}$ reactions/second) using second-order perturbation theory within the current theoretical framework [5].

References:

- [1] M. Fleischmann and S. Pons, *Journal of Electroanalytical Chemistry and Interfacial Electrochemistry*. **261(2)**, (1989) 301.
- [2] A. J. Leggett and G. Baym, *Nature*. **340**, (1989) 45.
- [3] V. A. Chechin, V. A. Tsarev, M. Rabinowitz, and Y. E. Kim., *International Journal Theoretical Physics*. **33**, (1994) 617.
- [4] Z. W. Seh, et al., *Science* **355**, (2017) eaad4998.
- [5] K. Ramkumar, H. Kumar, P. Jain., *Physical Review C*, **110**, (2024) 044605.

Glove Box Adaptation, Performance Evaluation of O-N, O-H Twin Determinator System and Related Studies at FRFCF

S. Sasma^{1,§}, B. Sivakumar¹, P. Kumarsekaran¹, P. K. Singh¹, G. Sivasankaran¹, R. B. Bhatt^{1,2}

¹FRFCF, Nuclear Recycle Board, Bhabha Atomic Research Centre, Kalpakkam- 603102

²Fuel Fabrication, INRP (O), Tarapur, India

§ Email: ssom@igcar.gov.in

Fuel Fabrication Plant of Fast Reactor Fuel Cycle Facility (FRFCF) at Kalpakkam is mandated for the fabrication and supply of Uranium & Plutonium based fuel for Fast Breeder Reactor. Ensuring high-quality fuel pins is essential for the reactor's safe and efficient operation. The fabrication process includes rigorous quality control steps starting from raw materials e.g. pin hard ware, feed U/Pu oxide powder, to interim products like fuel pellets and finally the fuel pins. One crucial parameter is determining non-metallic impurities such as nitrogen and hydrogen. Recently, FRFCF acquired an Oxygen-Hydrogen (O-H) and Oxygen-Nitrogen (O-N) twin determinator, modified for use with a glove box (GB). The furnace was placed inside the GB, while detectors and controllers remained outside, ensuring proper alignment [1]. A special leak tight Teflon gland with copper bar was designed for furnace power supply which made the operation and maintenance of the equipment safe inside GB.

This study outlines the adaptation and performance evaluation of the equipment using various standard samples and stainless steel (SS) samples. The ELTRA ONH 2000 employs inert gas fusion with an impulse furnace that heats the sample to approximately 2300°C to remove oxygen, nitrogen, and hydrogen. High-purity N₂ and He are used as carrier gases for the OH and ON modes, respectively. Detection methods include a Thermal Conductivity Detector for nitrogen and hydrogen and an Infrared (IR) cell for oxygen detection as CO₂. After the system's adaptation, it was tested and verified to be operational. With a minimum analysis time of about 4-5 minutes and the solid-phase determination method, this approach was found to be more suitable for radio analytical applications than the wet chemical Kjeldahl method for nitrogen analysis. Calibration was conducted using standard steel pins to measure oxygen, nitrogen, and hydrogen levels in stainless steel samples. Multi-point linear calibration curves were obtained, showing a correlation coefficient greater than 0.998 for O, N, and H (See Figure 1), which enhances the confidence in unknown sample analysis over a wide range compared to commonly used single-point calibration methods. For repeatability testing, ~ 0.4 g SS samples were cut from a bulk SS sample and analyzed for O, N, and H content. The results, presented in Table 1, demonstrate good accuracy and precision better than 10%.

Table 1. Results for O & N content in Standard and samples.

	O (ppm)	N (ppm)	H (ppm)
Std(cert)	31±2	202±3	4.5±0.4
Std(obs)	29±2	204±6	4.6±0.4
Sample1	55±4 (n=7)	770±27 (n=7)	>calib. range
Sample2	82±8 (n=7)	762±58 (n=7)	>calib. range

Std(cert)&Std(obs) are Certified and observed values of standard respectively.

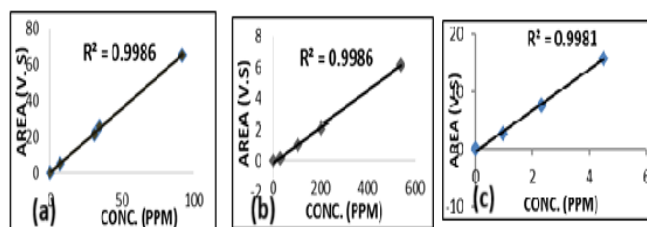


Fig.1: Calibration plot for (a) O & (b) N (c) H

References:

[1] D.R. Raut et al, *In the Proceedings of NUFUC-2022* (2022) 113.

Integrator Circuit to Measure Giga-ohm Resistor of Charge Sensitive Loop of HPGe Detector

N.Tawade^{1,§}, S.Vishwasrao², C. Datrik², S. Sodaye¹

¹ Radiochemistry Division, BARC, Mumbai, India

² Product Development Division, BARC, Mumbai, India

§ Email: nstawade@barc.gov.in

The High Purity Germanium (HPGe) Detector is an advanced, high-resolution gamma-ray detection system extensively used to probe complex multiple gamma-ray emitting isotopes with precision [1]. The superior energy resolution and energy rate limit of the HPGe detector are primarily governed by the feedback capacitor (C_f) and resistor (R_f) embedded in the charge integrator circuit of its preamplifier. The resistor value in this circuit is very high, typically ranging from 1 to 5 Giga-ohms, depending on the required resolution and energy rate limit of the detector [2]. However, accurately measuring such a high resistance value presents significant challenges. Conventional electronic measuring instruments, such as digital multi-meters, have a measurement limitation of up to only 200 Mega-ohms. Consequently, direct measurement of these high resistance values using standard equipment is not feasible. Additionally, when multiple resistors are combined to achieve the required high resistance, the presence of such large resistance values may introduce a significant loading effect, potentially affecting the measurement. To address these challenges, a dedicated integrator circuit was designed to facilitate the testing and measurement of such high-value resistors, as illustrated in Figure 1. The circuit operates by generating a ramp signal, whose slope is determined by the characteristics of the resistor under test.

$$\frac{dV_o}{dt} = \frac{V_i}{R_i C_f} \quad (1)$$

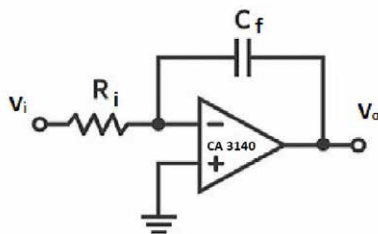


Fig. 1: Circuit diagram of Integrator



Fig.2: Output of integrator

The high value resistor was removed from the HPGe charge sensitive loop and measured using the circuit shown in Figure 1. A capacitance of $C_f = 1\text{nF}$ was used in the measurement. A constant input voltage, $V_i = 1\text{V}$, was applied to the circuit. The resulting output voltage (V_o) followed a ramp function as shown in Figure 2. The ramp signal was observed on oscilloscope and the slope of the ramp was measured to be 1V/sec . Then using equation (1), the value of resistance (R_i) was determined as $1\text{G}\Omega$. Hence, it is concluded that Giga ohms resistance can be determined using above method.

Authors thank Head, RCD for his keen interest and constant encouragement.

References:

[1] Glenn F. Knoll, 3rd edition (1999).

[2] Germanium Detectors user's manual, Canberra Industries, Inc., Meriden, U.S.A., 2002.

Performance Study of Indigenous Readout Electronics for HPGe Detectors in Low Level Gamma Spectroscopy and Counting Applications

Tushar A. Kesarkar^{1, §}, Saikat Das¹, Sudheer K.M.¹, Sourav Mukhopadhyay¹, V.B. Chandratre^{1#}, R.S. Shastrakar^{1#}, Vaishali Shedam¹, Sandeep Kumar¹, K. Hari Prasad¹, Menka Sukhwani¹, P.V. Bhatnagar¹, S Chinnaesakki²

¹ Electronics Division, Bhabha Atomic Research Centre, Mumbai
² Health Physics Division, Bhabha Atomic Research Centre, Mumbai
 § Email: tushark@barc.gov.in

The readout electronics for high resolution HPGe detector is required to exhibit ultra-low noise performance with high linearity over wide dynamic range. A standalone bench-top 16k channel Integrated Multi-channel Analyzer (IMCA) module is developed indigenously for HPGe detector-based gamma spectroscopy applications. This paper presents the performance study results of IMCA with commercial 30% efficiency p-type HPGe detector for low level gamma spectroscopy and counting application.

The IMCA comprises a high voltage (HV) module, a low voltage (LV) supply module, a spectroscopy amplifier and a multichannel analyzer. It is interfaced to the in-house developed ANUSPECT gamma spectrum analysis (GSA) software for online & offline analysis.

In the present test setup (see Fig.1), the IMCA provides ~ 3.3 kV HV bias to the detector and ±12 V LV supply to its preamplifier. The preamplifier output is amplified in the IMCA with a gain of ~ 15 V/V and shaped to a unipolar semi-gaussian pulse with a shaping time constant (τ) of ~ 6 μ s. The pulse height (energy) spectrum built in 16k channels of the IMCA is analyzed using ANUSPECT.

The long-term spectrum for Co-57 and Co-60 lab sources, accumulated for a live time of ~ 80 hours (see Fig.2), exhibited negligible drift in the peak centroid for 122 keV and 1332.5 keV peaks, respectively, as shown in Table-1.

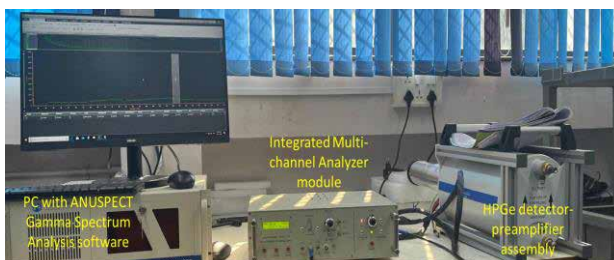


Fig.1: Setup for IMCA performance testing



Fig.2: Long-term spectrum of Co-57 and Co-60 (shown in ROI-1) sources with IMCA setup

Table1: IMCA long term test results

Live Time (sec)	Peak Energy (keV)	Peak Ch No	FWHM (keV)	Peak Energy (keV)	Peak Ch No	FWHM (keV)
13,000	122.09	598.70	0.95	1332.64	7242.45	1.81
1,80,000	122.09	598.65	0.97	1332.61	7242.35	1.81
3,00,000	122.08	598.61	0.96	1332.63	7242.39	1.81

The performance stability of the IMCA is in-line with the commercial HPGe detector systems used in low-level gamma spectroscopy and counting applications. Further, IMCA can also support higher count rate applications by selecting a lower shaping time constant.

Authors are thankful to NISS, ED, BARC for providing ANUSPECT software.

Neutron Measurement in 10 MeV Electron Accelerator Environment Using CR-39 Track Detector

G.S. Sahoo^{1, §}, Sabyasachi Paul^{1,2}, S.P. Tripathy^{1,2}, N. Chaudhary^{2,3} and P. Srinivasan¹

¹ Health Physics Division, Bhabha Atomic Research Centre, Mumbai, India

² Homi Bhabha National Institute, Anushaktinagar, Mumbai, India

³ Accelerator & Pulse Power Division, Bhabha Atomic Research Centre, Mumbai, India

§Email: gssahoo@barc.gov.in

In electron accelerator, the neutron production follows two way process, i.e., the high energy electrons produce the bremsstrahlung photons which then produce neutrons via photonuclear reaction. Neutron production in 10 MeV electron accelerator environments near the threshold energy for different targets has already been studied by Sahoo *et al.* [1]. The experimental validation of the simulation results is the main objective of the present study where neutrons were measured using CR-39 at a very close proximity of the target. The accessibility of other types of active neutron detectors near the target is a challenge due to larger dimensions. The intense gamma field and RF interference also affect the active detectors. CR-39 being insensitive to gamma radiation in terms of track formation is a useful detector for neutron detection in mixed radiation field.

In this work, the irradiation was carried out at Electron Beam Centre. 10 MeV electrons were allowed to incident on 1.8 mm thick Ta target which was supported by 8 mm thick Al. CR-39 detectors were attached to the Al support and the detectors were irradiated for 30 minutes. The electron fluence rate on the Ta target was calculated to be 1.655×10^{16} electrons cm^{-2} per hour. After irradiation, the detectors were subjected to chemical etching and tracks were analysed through optical microscope and image analysis software. From the track density, the neutron fluence was obtained by using the calibration factor determined through Am-Be neutron source. The neutrons fluence for the same experimental set up was also estimated by FLUKA Monte Carlo simulation. The neutrons spectrum (in Fig. 1) from FLUKA simulation is peaked at ~ 0.2 MeV and extends up to 1.9 MeV. The neutron production threshold for Ta is 8.1 MeV [2] which leads to the maximum neutron energy of 1.9 MeV. The neutron yield per primary electron from the FLUKA was found to be 1.593×10^{-7} ($\pm 1.1\%$). From Fig.1, it can be observed that, the spectrum is dominated by fast neutrons, hence could be detected by CR-39 detector. Fig.2 shows the images of developed tracks in CR-39 from which the neutron fluence was measured to be 2.55×10^8 n/cm². Normalising with respect to incident electron fluence, the neutron yield per primary electron was found to be 3.083×10^{-8} ($\pm 13.5\%$).

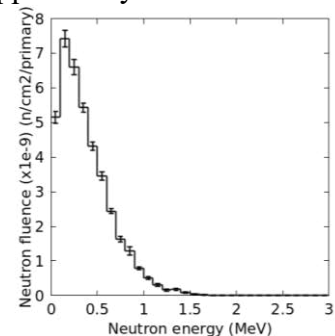


Fig. 1: Neutron spectrum in CR-39 from FLUKA simulation.

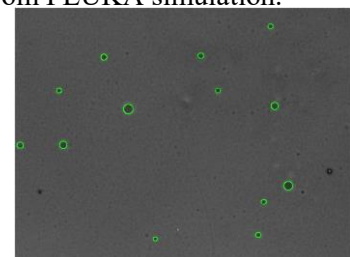


Fig. 2: Track images

The authors express their sincere thanks to L. Mishra, S. S. Gaikwad, P. Patade, R.B. Chavan, Mukesh Kumar and Meghnath Sen for their help during irradiation.

References:

- [1] G.S. Sahoo, S.P. Tripathy and M.S. Kulkarni, *Appl. Radiat. Isot.* 181 (2022)110080.
 [2] S.S. Dietrich and B.L. Berman, *Atomic Data Nucl. Data Tables* 38 (1988) 199.

Development of Instrumentation for the Fabrication of Fuel Microspheres Using the Sol-Gel Method

Ajay Kumar Keshari^{1,§}, S. Balakrishnan¹, J. Prabhakar Rao¹, Dasarath Maji¹,
Abhiram Senapati¹, V. Suresh Kumar¹, T. V. Prabhu¹ and V. Jayaraman^{1,2}

¹Materials Chemistry & Metal Fuel Cycle Group, IGCAR, Kalpakkam, India

²Homi Bhabha National Institute, IGCAR, Kalpakkam, India

§ Email: ajayanu@igcar.gov.in

An instrumentation setup was designed and developed for the sol-gel process to automate the dispensing of broth solution to prepare uniformly sized microspheres of uranium oxide fuel. Due to the handling of radioactive material and its associated complex fuel fabrication by sol-gel, the development of an automation setup was investigated for the fabrication with minimal human intervention and for remote operation. The instrumentation setup consists of a feed tank, sensors, hardware, and software. A broth solution containing uranium nitrate and complexing agents such as hexamethylenetetramine and urea was prepared by the standard route. This broth solution is maintained at less than 5°C to avoid the formation of gel prior to the fabrication process. The droplet dispensing setup was able to deliver the fuel solution at a constant flow (20 ml min⁻¹) from the feed tank to a nozzle. A vibrator attached to the nozzle dispenses the broth solution as droplets into silicone oil at 90°C. As the level of fuel solution decreases in the feed tank, the argon gas pressure above it also decreases. This change in level and pressure is provided as feedback to the pressure regulator, which increases the pressure in the feed tank. Such a feedback mechanism maintains a constant flow of broth solution through a mass flow controller. The hardware and software were designed and developed with a PID controller to control the process & various parameters, display & save the various parameters in a file for the study of process parameters towards fabrication with respect to flow, time, pressure, etc., and validation and qualification of the microspheres fuel. The instrument has various unique features, viz., setting flow rate, chamber pressure, percentage opening of valves, etc. The photograph of the droplet dispensing system is shown in Fig. 1.



Fig. 1 The photograph of the droplet dispensing system

The system consists of two modes- automatic and manual, for the dispensing of broth solution. The electronic control unit was connected to a PC through LAN for collecting data into the PC for automatic operation to minimize the radiation to operating personnel. The hardware is based on the 8051 microcontroller. The signal conditioning unit measures and processes all inputs using the data processing unit and sends data to the PC through LAN for study of microsphere characteristics. The system can be operated as a standalone system (HMI) or through a PC. All the parameters of the system are displayed in a standalone display unit. The system was tested and validated with water, silicone oil, and nitrate solution. The instrumentation has been deployed on the site for the fabrication of fuel of uranium oxide.

Reference(s):

[1] M. Brykala, et al, Archives of Metallurgy and Materials, **65** (2020) 1397-1404.

Validation of An Automated FBTR End Plug Metrology System

Rajashree Dixit[§], Gagan Deep Kaur and Amrit Prakash

Radiometallurgy Division, Bhabha Atomic Research Centre, Mumbai.

[§] Email: Rajashree@barc.gov.in

Fast Breeder Test Reactor (FBTR) is an integral part of the second stage of the Indian three stage nuclear program [1, 2]. The FBTR fuel is made up of Mixed carbide (U, Pu) C to oblige to the reactor prerequisite. The fuel is mixed and milled to pelletization and then positioned in a stainless steel clad which is further hermetically sealed with end plugs to form a fuel element. These fuel elements play a vital role in containing the radiation and its integrity is of utmost importance for optimum functioning of the reactor. To ascertain the equitable in-reactor life of the fuel element it is imperative to ensure the quality of the fuel element and its components. This is made certain by following intrinsic quality control steps in FBTR fuel fabrication process. One such step is metrology. In this paper our interest lies with the metrology of end plugs of fuel element. The FBTR fuel elements have 2 end plugs viz. top end plug and bottom end plug (Fig 1). These components are 100% inspected for 14-17 dimensions on either plug respectively including length, breath, angles, radius, etc measurement for each carving. The inspection process was done manually and prone to human error owing to the tedious process and high throughput. Thus an automated system was fabricated for the FBTR end plug metrology system. The system was based on shadowgraphy using telecentric LED illuminator, imaging sensor (CCD or CMOS camera) along with bi-telecentric lens and GUI-based measurement software. Validation of the system was taken up to ensure the acceptance of the designed system in production. The validation of parameters like accuracy and precision of the system were carried by using 25 standard samples of top plug and bottom plug. Multiple dimensions were first measured by 3 skilled and qualified personnel's using profile projector, micrometers, etc to record average values followed by measurement in the system. Fig 2 shows readings of the total length measurement on the bottom plug. It was observed that all the measurements lies within the 3σ variation of the mean value of each reading. The confidence and reliability test was also done using standards considering binomial distribution based on accept/reject criterion. The sample size for reliability was as per the sampling plan MIL-STD-105E. The repeatability of better than $2\mu\text{m}$ and measurement accuracy of better than $5\mu\text{m}$ was obtained. Thus the system thus designed was validated for operator independent accurate and repeatable data for end plug metrology.

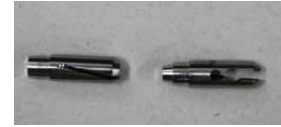


Fig. 1: FBTR top plug (left) and FBTR top plug (right).

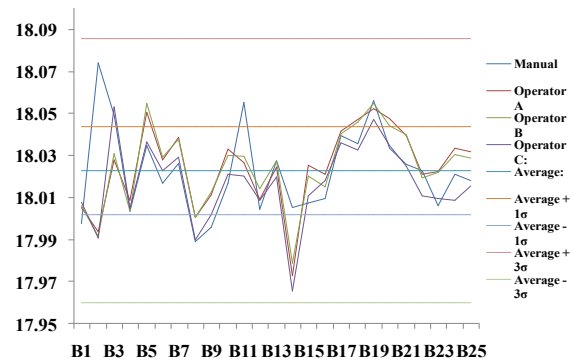


Fig. 2: FBTR bottom plug length readings.

The authors appreciate the help and support extended by our colleagues.

References:

- [1] G Srinivasan et al, *Nuclear Engineering and Design*, **236** (2006) 796-811.
- [2] Journey of FBTR - Reaching further heights - 50 years journey of FBTR, Indira Gandhi Centre for Atomic Research, Kalpakkam, India, April 30, 2022.

Removal and Scraping of Two Nos. of 110 KW Furnace No 1 & 2, at ADU Facility by Using ALARA Principle

Akhilesh Panigrahi[§], Kumar Awinash, Rajkumar, Rohit Ameta, K.S. Vasudevan

Reprocessing & Waste Management, Nuclear Recycle Board, BARC, Tarapur

[§]Email: akhileshp@barc.gov.in

Ammonium-Di-Uranate (ADU) facility is used for converting Uranyl Nitrate solution received from U purification cycle of reprocessing plant to U₃O₈. Process of conversion involves the calcination of intermediate product using resistance furnaces. The old 110kW bogie hearth furnace (resistive heating) has experienced operational challenges due to magnetostriction-induced vibration in the conductive heating elements and aging effect for continuous operation of >15 years. These two old 110kW ADU furnaces were degraded and needed to replace with new furnace of same capacity. The replacement includes radiation survey, decontamination, cutting, dismantling, material handling, waste disposal, industrial safety and isolation activity using ALARA (As-Low-As-Reasonable-Achievable) principle.

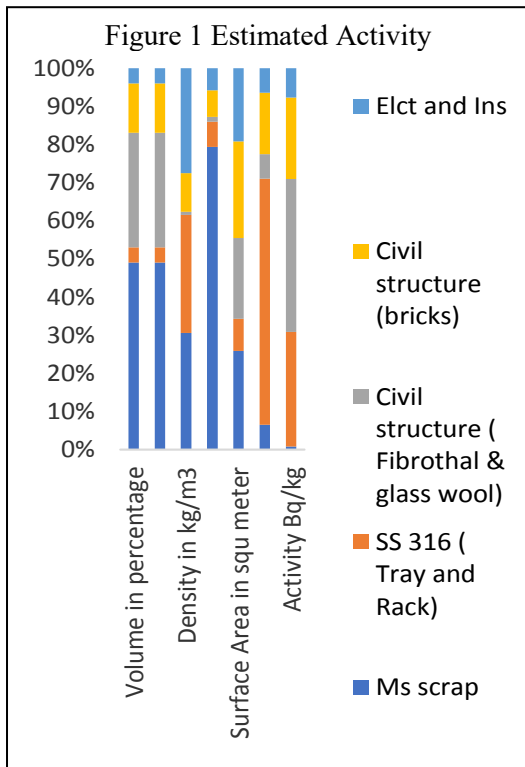


Table 1 Estimated Collective Exposure

S N	Work	Pers ons	Duratio n (Min)	Radiati on mR/Hr	ent ries	Dos e
1	Decontamination	5	180	1	3	7
2	Removal of Uranium dust.	2	180	1	2	12
3	Shifting of trays	2	30	1	1	1
4	wet mopping of bogie	4	60	0.5	1	2
5	Health Physics survey	4	20	0.5	1	0.7
6	Retrieval of tray stack	3	120	1	2	12
7	Installation of Scaffoldings	3	120	0.5	2	6
8	Door/Counterweight Removal	3	120	0.5	3	9
9	Removal of Doors and Counter Weights to ADU Floor	4	120	0.5	3	12
10	Removal of Electrical	4	120	0.5	3	12
11	Furnace Insulation Removal	5	120	0.5	3	15
12	Removal of Scrap Material	15	120	0.5	3	45
13	Gas Cutting of Door Structure	4	120	0.5	4	16
14	Off Gas System Line Removal	4	120	0.5	2	8
15	Gear Box Assembly Removal of Doors and Trolley	4	120	0.5	3	12
16	Removal of Motor of Gear Box Assembly	4	120	0.5	3	12
17	Furnace Tray Structure (SS316) Removal and Cutting by Cutting Wheel	3	120	0.5	5	15
18	Removal of Furnace Bricks and Foundation	4	120	0.5	3	12
19	Furnace Metal Wall Structure	4	120	0.5	8	32
Estimated Collective Exposure in Man Ram						234
In P-mSv						2.3

The replacement of two nos of 110kW furnace with one 220kW furnace involved radiation and industrial hazard. Total waste was estimated based on weight, volume, and density. Radiation surveys were done and collective exposure and alpha activity were estimated. The complete work has been carried out in supervision of industrial and health physicist with in allowable radiation safety limits. Solid (3.264 m³ / 9838.34 kg):- MS door, high temperature bricks, SS316 tray rack, Fibrothal and glass wool etc. will be disposed in yellow cat-1 disposal waste drum. Total Estimated Collective Exposure was 2.34 p-mSv and Estimated Alpha Activity was 0.605Bq/g which was very less than 4000Bq/g. The collective dose was estimated by multiplying no of person and duration they spend in field and amount of radiation at the working place. Also, the complete work was done below these estimated data.

Comprehensive Quality Assurance Tests for Large Area Dual Phosphor Contamination Monitors as Per Standards

I Vijayalakshmi[§], A. Dhanasekaran, Kothai Parthasarathy

Indira Gandhi Centre for Atomic Research, Kalpakkam, India

[§] Email: vijisan@igcar.gov.in

ANSI 42.17A provides comprehensive guidelines for the performance specification of portable Instruments used by Health Physicist [1]. The specifications provided can be classified as relevant to the instrumentation and maintenance section and the health physics as an equipment user. ANSI N42.17, Section 7 elaborates on the accuracy, probe surface sensitivity, photon energy dependence, beta energy dependence, neutron energy dependence, photon radiation overload and Angular dependence as specifications for the radiation response. The performance of three large-area dual phosphor contamination monitors (DPCM) capable of measuring alpha and beta, gamma radiation simultaneously are studied and reported in this paper. The DPCM consists of a 17x10 dual phosphor detector (3 mg/cm²ZnS(Ag) coated over a 0.25 mm thick EJ200 equivalent plastic scintillator) integrally coupled to a photomultiplier tube. The readings are displayed in user-selected units cps, cpm, Bq, dpm, Bq/cm² or dpm/cm² with the help of associated electronics. The accuracy, probe surface sensitivity and energy dependence are measured using 10 x 10 cm² sources ²⁴¹Am, ³⁶Cl and ⁹⁰Sr-⁹⁰Y. The detector is a flat panel type and measures the surface contamination. Hence, uniformity in response throughout the surface is studied instead of angular dependence. The detector surface is divided in to 15 grids of area~11.5 cm² and the response is studied for sources ²⁴¹Am and ⁹⁰Sr-⁹⁰Y (area ~3.5 cm²). Further, the standard demands that the beta energy dependence be studied for at least three sources covering energies <0.4 Me, 0.4 to 1.0 MeV and > 1.0 MeV. Thus, ⁹⁹Tc, ³⁶Cl and ⁹⁰Sr-⁹⁰Y disc sources are used to study the detector response and the ¹⁴C response is studied to check the performance for <0.2 MeV. Three monitors are subjected to the tests to examine the instrument-to-instrument variation.

Table 1. Criteria for Acceptance as per standards

Property	Criteria	
Accuracy	$0.9 \leq R \leq 1.10$	* Interpreted from the environmental condition requirement.
Beta energy dependence 0.2 to 3.5 MeV	$0.5 \leq R \leq 1.5$	
*Uniformity in Response	$\pm 15\%$	# Required criteria for simultaneous alpha, and beta gamma measuring instruments not covered in ANSI but stipulated in Ref. 2
#Alpha source response in the beta channel	< 10%	
#Beta source response in the alpha channel	< 1%	

The three monitor's reading accuracy for the 100 cm² source ²⁴¹Am varied between 0.97 to 1.03, ³⁶Cl varied between 0.96 to 1.04 and for ⁹⁰Sr-⁹⁰Y varied between 0.98 to 1.02. The ³⁶Cl beta source response is kept as the reference because the most commonly encountered fission product beta energies lie in that range. The beta energy dependence lay between 0.7 – 1.3 for source ⁹⁹Tc and ⁹⁰Sr-⁹⁰Y. The response of the ¹⁴C source is < 0.3 and acceptable as the endpoint energy of ¹⁴C falls below the standard's energy range of 0.2 – 3.5 MeV. The spatial responses in all the grids are observed to be within $\pm 15\%$ for alpha and beta sources. No alpha source response is observed in the beta channel and vice-versa. Based on the experimental observations, It is concluded that all three monitors have been tested as per standard and found to be functioning satisfactorily. These quality assurance tests not only boost the confidence of the health physicist but also help to provide more accurate results.

References:

- [1] ANSI (2003), ANSI-N42.17A
 [2] IS (2006), IS-11866

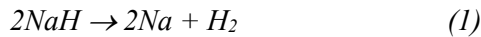
Control Instrumentation for Fuel Cell Based Hydrogen Mitigation System for Secondary Cold Trap Regeneration

R. Karunakaran[§], M. Lavanya V.A Faizal, N. Murugesan, P. Manikandan, Hrudananda Jena, Rajesh Ganesan, V. Jayaraman

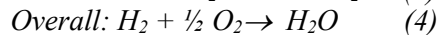
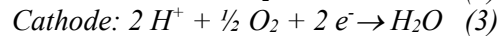
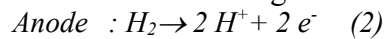
¹Materials Chemistry & Metal Fuel Cycle Group, IGCAR, Kalpakkam – 603 102, INDIA.

[§] Email: karunar@igcar.gov.in

In sodium-cooled fast reactors (SFR), cold traps (CT) are used to control the H₂ and O₂ impurities in liquid Na by trapping them as NaH and Na₂O. However, on its continuous usage, CTs are saturated with these impurities and need regeneration. The secondary cold trap (SCT) of the prototype fast breeder reactor (PFBR) is mainly loaded with NaH impurity and needs regeneration every 5 years. During the regeneration of SCT, a large quantity of H₂ is produced (Eq 1) and its mitigation is an important step towards reactor safety [1].



For safe H₂ mitigation, an automated polymer electrolyte membrane fuel cell-based H₂ mitigation system (FC-HMS) was developed. The electrochemical reactions are given in the equations (2-4).



In order to use fuel cell in automated mode in the plants for longer operation hours, a dedicated control instrument (CI) (Fig. 2) was designed and developed for the first time. CI uses H₂ mass flow controller (MFC) output as feedback to draw a suitable current from the fuel cell. In the H₂ removal studies set-up, CI was integrated with MFCs for H₂ and N₂, a 3 kW fuel cell stack (72Nos of fuel cells), ELB and hydrogen sensor (Fig.1). The H₂ removal experiment using CI in automated mode was carried out by passing H₂ with various flow rates up to 5.0 standard litres per minute (SLPM). CI controlled the fuel cell current according to the H₂ flow rate automatically and H₂ concentration also was measured. All the data (Fig 3) were measured online remotely and were recorded by the CI software. The quantity of H₂ removed by the fuel cell was calculated from the measured cell current (*i*) using the equation 5.

$$H_2 \text{ removed at STP(SCCM)} = i \times Z \times n = i \times \frac{6.96 \text{ sccm}}{i} \times 72 \quad (5)$$

where, *n* = No of cells FC, *Z*= 6.96 SCCM/A (standard cubic centimetre/Ampere)

The H₂ removal efficiency was calculated using the inlet and outlet (i.e., unburnt) H₂ flow rates. Using CI, automated H₂ removal experiment on laboratory scale was demonstrated with efficiency of ~ 95% while maintaining outlet H₂ concentration less than 4% upon diluting with N₂. The automated FC-HMS (capacity 5000 SCCM level) was demonstrated successfully.

References:

1. C. C. McPheters, S. B. Skladzien, D. J. Raue, ANL-79-100 (1980) 1-14.

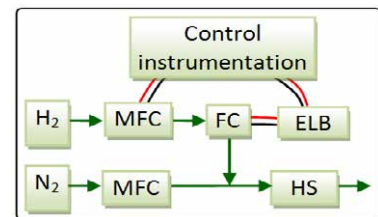


Fig.1: Schematic of CI for fuel cell based H mitigation system

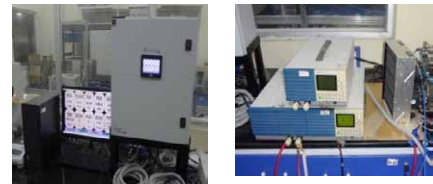


Fig.2: Fuel cell CI with remote data acquisition system

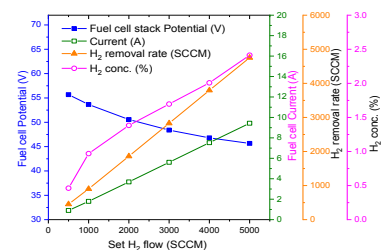


Fig.3 Online measurement of experimental parameters using CI

Design and Fabrication of Segmented Temperature Controller with a Furnace to Study Positron Annihilation Lifetime Spectroscopy at High Temperatures

Ghanshyam Meena^{1§}, Sandeep Vishwasrao², Chhaya P. Koli¹, Sibhu Soren¹,
Vishal Chougule¹, Suparna Sodaye¹

¹Radiochemistry Division, RC & IG, BARC, Mumbai, India

² Product Development Division, RC&IG, BARC, Mumbai, India

§ Email: gmeena@barc.gov.in

To carry out positron annihilation studies at high temperatures, a microcontroller controlled small muffle furnace is required which is having two windows to detect gamma pulses at 180°. Such systems are not readily available in market and requires customised designing and fabrication. A microcontroller based segmented temperature controller with a small copper furnace was designed and fabricated. The furnace is 25 x 20 mm in size, which was sealed in aluminum box of size 10x10 x 8 cm. A 15V/2A power supply was designed and fabricated for the heater. A K type thermocouple was fixed at the bottom of the furnace, which is having contact with the sample boat, to minimize the temperature reading error. The thermocouple senses temperature and amplify using AD595 [1] and sends amplify signal to C8051f120 [2] microcontroller. The microcontroller processes the data and gives the control output signal to the power control circuit, which controls the power of the heater as per set point value. Once the desired temperature is achieved, it triggers the data acquisition using Multi Channel Analyzer (MCA) [3]. The set point is defined by the user in the PC using an interfacing software, which was developed in visual Basic 6.0. The communication between the PC and microcontroller is made through RS232 communication. The system was tested for temperatures up to 200° C and found working satisfactorily within $\pm 1^\circ\text{C}$. Measurements have been taken at different temperature values between 0 to 200°C and run over a period of 4 -7 hrs at a given temperature. This unit has facilitated the automated data acquisition for positron annihilation lifetime spectroscopy at higher temperatures.

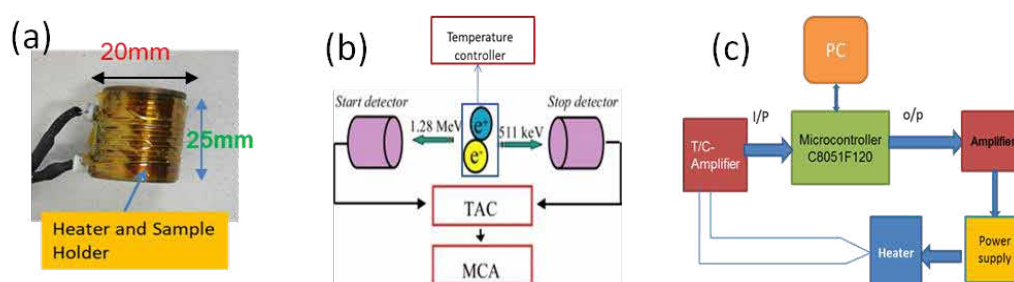


Fig1: (a) Photograph of furnace, (b) Schematic of detector setup and (c) Block diagram of temp. Controller

The authors thank Head, RCD for his constant support and encouragement. Thanks are due to Dr. D. Dutta and Dr. S Mukherjee for their support.

References:

[1] <https://www.analog.com/en/products/ad595.html>

[2] <https://www.silabs.com/mcu/8-bit-microcontrollers/c8051f12x-f13x>

[3] "MCA-3 Series / P7882, multichannel analyzer / dual input multiscaler user manual", Oberhaching, Germany: FAST ComTec Communication Technology GmbH, 2016.

Comparative Analysis on Efficiency Variation for Alpha Spectrometry System

Riya Gupta,[§] Anish A. Ansari, D. K. S Pandey, U.V. Deokar, J.P.N. Pandey

Health Physics Division, Bhabha Atomic Research Centre, Mumbai, India

[§] Email: riyag@barc.gov.in

The ORTEC BSU-020-450-AS Dual Alpha Spectrometer is an instrument used for the estimation of alpha activity in environmental samples, featuring dual channels that allows simultaneous measurements of two samples. The spectrometer employs passivated ion-implanted silicon detector (PIPS) with an active area of 450 mm². A mixed standard source containing Pu-239, Am-241, and Cm-244, of activities of 258 Bq, 257 Bq, and 161 Bq, respectively having uncertainty of ± 3 %, used to measure the efficiency. In this study, the variation in detector efficiency with source distance has been analysed. The best-fit method applied for curve fitting, and the fitting parameters calculated for various sources [1]. The experimental setup has the detector operated at 50 V within the 3–9 MeV range. Measurements utilized SS- planchated 15 mm diameter mixed alpha sources (Pu-239, Am-241, and Cm-244) placed at distances ranging from 4 to 40 mm in 4 mm increments. A minimum vacuum of 100 mTorr is maintained throughout all measurements. To account for peak tailing effects, the Region of Interest (ROI) for each measurement underwent careful optimization which extended the ROI to include 30 channels to the right of the peak and 100 channels to the left of each peak, ensuring an accurate representation of the alpha peaks.

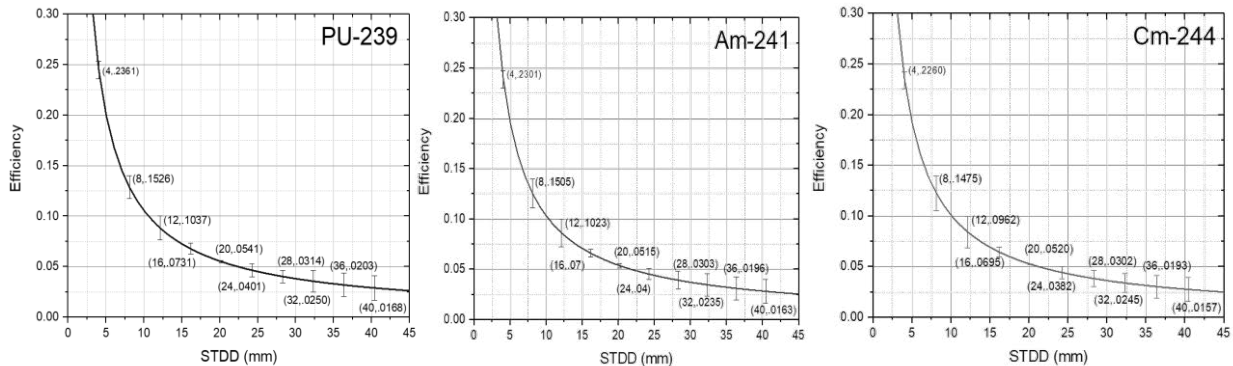


Fig 1: Eff vs STD for Pu-239 Fig 3: Eff vs STDD for Am-241 Fig 2: Eff vs STDD for Cm-244
 Results obtained from the detector efficiency with source distance experiment shown in Figure 1-3. The plot has efficiency in y-axis and source distance (mm) in X-axis. Maximum efficiency at 4mm was ≈23% for all three sources. Their best fit was obtained considering power law functions of the form $y = a \cdot x^{-b}$ and corresponding $R^2 \geq 0.96$. The parameters of the fitting curves, “a” and “b” are 0.8925 and 0.927 for Pu, 0.8732 and 0.9282 for Am, and 0.8583 and 0.9301 for Cm as shown in fig.1. It can be concluded that the efficiency of the alpha spectrometer decreases with source distance, following the equation y (efficiency) = $a \cdot x^{-b}$. The values of a and b are nearly the same for all three sources, but ‘a’ shows a slight decreasing, while ‘b’ has increasing trend. This suggests that efficiency reduces as the energy of the isotopes increases. Future studies with broader alpha energy ranges, could further explore energy-dependent efficiency variations.

References:

[1]V. S. P. S. D.D. Rao, *Applied Radiation and Isotopes*, **70** (2012) 1519-1525

Low Resolution Gamma Spectroscopy (LRGS) for Waste Drum Assay

J. A. Mason^{1,§}, S. Ramesh², A.C.N. Towner¹, N A Troughton¹, H.R. Turner¹

¹ A.N. Technology, Wallingford, UK

² ANTECH, Chennai, India

§Email: Mason.John@antech-inc.com

Nuclear waste from nuclear power plants and research institutes is commonly placed into 200 L drums before storage or disposal. The disposal of the waste drum requires a record of radiological characterization of its contents & dose rate, and evaluation for no external contamination. High resolution gamma spectroscopy (HRGS) is used for the characterization of waste in drums, owing to its high resolution (2 keV at 1332 keV (^{60}Co)), which allows accurate identification of γ -emitting isotopes. However, this approach cannot be used for non γ emitting radioisotopes, such as ^{90}Sr and its daughter ^{90}Y (β emitters), ^{55}Fe (e^- capture). Commonly a fingerprint or nuclide vector is used to infer the activity of the unmeasurable isotopes. Additionally, HPGe detectors require liquid nitrogen to obtain spectroscopically acceptable data. An alternative approach is to use low-resolution gamma spectroscopy (LRGS) which uses low resolution detectors such as sodium iodide (NaI) can operate at room temperature and whilst the resolution at 1332 keV is in the range of 65 to 70 keV, which is sufficient to quantify isotopes having good fingerprint. The LRGS approach has been widely used for the measurement of power station wastes [1], uranium processing wastes [2] and is a recognized alternative to HRGS measurements [3]. Typical fingerprints for fission products are dominated by ^{137}Cs , activation products by ^{60}Co and transuranics by ^{241}Am , and so focusing on these three isotopes covers the majority of radioactive wastes. The LRGS is sufficiently sensitive that it can sense all kinds of radioactive wastes. This paper describes the development and testing of a LRGS system for the measurement of waste drums. The system has been designed for safe and practical operation in a nuclear environment with the detectors, electrical and electronic components in an IP54 rated enclosure. The robust turntable has an integrated weigh-scale and engraved rings to ensure that the drum is centred. With three shielded and temperature-stabilized NaI detectors, the system has a high efficiency. A correction factor for the overlap of the field of view of the detectors is applied to the measurements. The system software is designed for easy operation and provides secure storage and access to the measurement results. In addition, it has tools to support the management of background and standardization measurements, calibration, measurement control data, fingerprints.



Fig. 1: The LRGS Drum monitor

References:

- [1] J Dean, *Applied Radiation and Isotopes*, 67(5), (2009), p. 678.
- [2] P.A. Clark *et al.* *Proceedings of the 9th International Conference on Radioactive Waste Management and Environmental Remediation* (2003), p. 859
- [3] Ed. L. Keightley, *NPL Good Practice Guide 34, Radiometric Non-Destructive Assay* (2012), p.28

In-House Design and Development of a Bi-Amperometer to Analyse Uranium and Plutonium Using Redox Titrimetric Method

Ghanshyam Meena^{1,§}, Sandeep Vishwasrao², Chhaya P. Koli¹, Sibhu Soren¹, Vishal Chougule¹,
Suparna Sodaye¹, Jayashree S Gamare³, Kavita Jayachandran³

¹Radiochemistry Division, Bhabha Atomic research Centre, Mumbai, Maharashtra, India

² Product Development Division, Bhabha Atomic research Centre, Mumbai, India

³ Fuel Chemistry Division, Bhabha Atomic research Centre, Mumbai, Maharashtra, India

§Email : gmeena@barc.gov.in

An analog Bi-amperometer was designed and developed for Redox titrimetric methods for analysis of Uranium and Plutonium. The current instrument being used for endpoint detection in these methods are analog type and the components are obsolete which makes their upkeep difficult. Hence, an in-house instrument was designed and developed using latest components and the values are displayed in digital format.

A small potential of 100-200mV applied to a pair of identical platinum electrodes dipped in a solution containing a reversible system and this will cause the flow of current as the reaction progresses. Oxidation occurs at the anode while reduction occurs at cathode. If concentration over potential is not involved, flow of current will increase linearly with the applied potential. At the end point, current becomes equal to the background current, which is in nano-ampere range.



The performance of the instrument has been tested with actual experimental solutions in lab and the results were in good agreement with existing analogue instrument. In the analogue instrument, the end point was seen in μA current range, but with the digital instrument, the end point is seen up to nA current range. Detail studies and further improvisation are in progress.

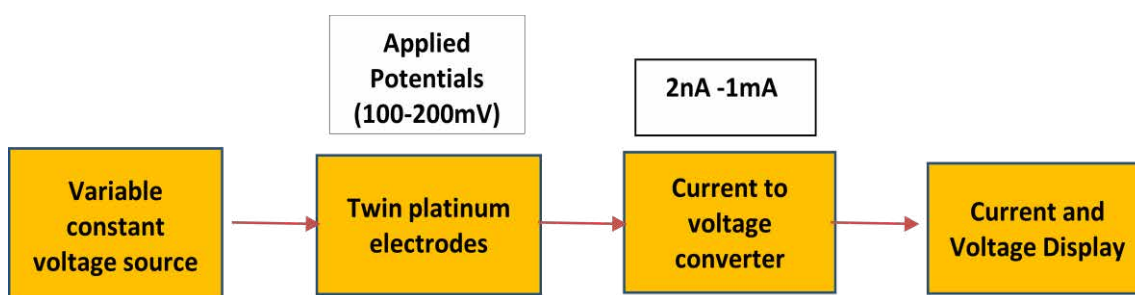


Fig1: Block diagram of the instrument

The authors thank Head, RCD for his kind support and encouragement. Also, acknowledge the kind support of Dr. Arnab Sarkar, FCD.

Refurbishment of Preamplifier in HPGe Detectors

C. Datrik^{1,§}, S.Vishwasrao¹, N. Tawade², Suparna Sodaye²

¹ Product Development Division, BARC, Mumbai, India

² Radiochemistry Division, BARC, Mumbai, India

§ Email: datrikes@barc.gov.in

High Purity Germanium (HPGe) Detectors are sensitive to ionizing radiation such as X-rays or Gamma rays [1]. The charge generated in the detector is proportional to energy of radiation falling on it and it is converted into a voltage pulse by charge sensitive preamplifier [2]. The preamplifier has one differentiator & one integrator circuit with pole-zero cancellation as shown in figures 1a and 1b. The charge sensitive preamplifier components are prone to failure in surge current. The tantalum capacitors are used in the preamplifier circuits. The tantalum capacitor consists of tantalum powder as anode, a Ta₂O₅ oxide layer as dielectric, and a cathode that can be MnO₂. Transient voltage or a current spike applied to tantalum electrolytic capacitors with solid manganese dioxide can short some of the tantalum capacitors. So, excessive current drawn through the filter circuit may lead to failure of inductors. The maximum DC surge current, which the tantalum capacitors can safely withstand during operation, is dependent on UR/ESR, where UR and ESR are rated voltage and own equivalent series resistance of the product.

As case study, it was observed in the some of the HPGe detector preamplifiers there was no signal output and DC shift was observed. When tracing the signal output at each stage of the preamplifier it was found that the tantalum capacitor was getting short in most cases after replacement and there was no improvement in the output signal. After retracing, it was observed that the components along the series of tantalum capacitor such as inductor, transistor had also gone bad due to excessive current flows through the short capacitor. The procurement of similar preamplifier board is costly as well as time consuming as they have to be imported. Finally, replacing all these components brought the HPGe to working condition and revenue has been saved.

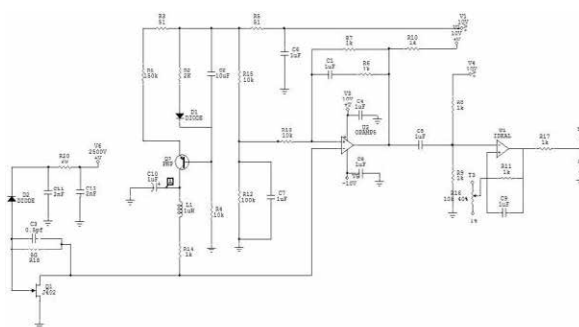


Fig.1a : Preamplifier board Fig. 1b : Preamplifier circuit

Acknowledgements: Authors thank Head, PDD and Head, RCD for their keen interest and constant encouragement.

References:

[1] "Radiation Detection and Measurement", Glenn F. Knoll, 3rd edition (1999).

[2] "Germanium Detectors user's manual", Canberra Industries, Inc., Meriden, U.S.A. (2002).

Authors Name	Page No.
A	
Achary S.N.	266
Acharya R.	152, 153, 158, 194, 198, 199, 213, 254, 255
Acharya Rajesh	169, 219
Adnan Akber	17
Agarkar P.	86, 93, 113
Agarwal Chhavi	131, 144, 175, 176, 292
Agarwal R.	53, 188
Agarwal Raghav	43
Agrawal Roopal	205
Ahmad Mo. Anas	211
Ajmal P.Y.	157, 239
Alakananda S.G	151
Alexander Rajath	57
Ali Hasem	271
Ali Manjoor	112
Ali S.A.	252
Amarendiran P.	89
Ambade Rajwardhan N.	195
Ameta Rohit	300
Amirdhanayagam Jeyachitra	204, 223
Anandhanarayanan V.	142
Aneesh T.	107, 166, 167
Ansari Anish A.	304
Ansari S.A.	118, 207
Anshi	251
Anshul Kumari	133
Aono Tatsuo	8
Archanadevi R.	229, 267
Arunkumar V.	61, 65, 289
Ashok Kumar G.V.S.	142, 151
Ashok Kumar J.	154
Ashokkumar P	92, 250
Aswal S.	197
Awinash Kumar	300
B	
B.K. Sreedhar	64
Baghel N.S.	181, 182, 183, 184, 185, 205, 210, 214
Baghul Swati	217
Bahre P.	291
Balaji V.	132
Balakrishnan S.	103, 298

Authors Name	Page No.
Balamurugan M.	141
Balaram R.	244
Balasubramonian S.	94
Balasurendran J.	88
Balhara Annu	47, 87, 145, 200, 222
Bamal Sumit	49
Banerjee A.	291
Banerjee Anannya	32, 68, 70, 284
Banerjee D.	22, 127
Banerjee P.	110, 212
Banerjee Rumu H.	57
Banerjee S.	214
Bano Shehanaz	29, 124
Bara S.V.	233, 264
Barman C.	56
Barman Chiranjib	249
Basu Sandip	205, 217, 224
Bera S.	60, 90
Bhandari Shapath	44
Bhangare R.C.	157, 239
Bhanja Kalyan	74
Bhardwaj Y. K.	188, 207, 217
Bhargava Pradeep	236
Bharti Bhavana	47
Bhaskarapillai Anupkumar	150, 266
Bhatnagar Amit	282
Bhatnagar P.V.	296
Bhatt R. B.	100, 108, 110, 139, 155, 177, 294
Bhattacharja Rudrashis	97
Bhattacharjee Dhruva	169
Bhattacharjee T.	291
Bhattacharyya A.	118, 129, 179, 207
Bhattacharyya S.	56
Bhojane S.M.	79
Bhujbal Vaibhav	278
Biju K.	59
Bikash K.N.	82, 102
Bisht Neeraj	55, 211, 215, 221
Biswal Jayashree	39, 198, 199, 213
Biswas S.	95
Biswas Saikat	209
Bootharajan M.	90, 171
Bouniol Pascal	19

Author Index

Authors Name	Page No.
Brahmananda Rao C.V.S.	5, 82, 89, 90, 91, 101, 102, 125, 126, 137, 138, 143, 171
Burger Arnold	31
C	
Caër Sophie Le	19
Chakrabarty A.	260
Chakraborty Avik	217, 224
Chakraborty P.	98, 99
Chakraborty Sudipta	191, 192, 195
Chakravarty Rubel	191, 195
Chand Manish	151
Chandanshive V.	79
Chandramohan P.	132
Chandran Neeraja	167
Chandrasekhar Sneha	189
Chandratre V.B.	296
Channappa Nagraj	269, 273
Chanyal B.C.	55, 215
Chattaraj Saparya	92, 250
Chatterjee S.	56
Chaudhari C.V.	207
Chaudhary N.	57, 297
Chaudhury P.	170, 231, 232, 233, 234, 242, 243, 251, 260, 261, 264, 265, 270, 274, 279
Chauhan Sonika	221
Chavan T.A.	172
Cheeta Pawan Kumar	133
Chikode Prashant P.	220
Chinnaesakki S.	181, 233, 264, 296
Chitra N.	230
Chopra Manish	134
Choudhary Mahesh	42, 57
Choudhury Niharendu	134
Chougule Vishal	303, 306
Chourasia Aditi	144
Chowdhury S. Ray	53, 188, 190
Chowta S.D.	95
Crasta Rita	277
D	
Dabhade Prasad	268
Dadwal Vaishali	153
Dagre V.S.	59
Daksha	251

Authors Name	Page No.
Dalvi Aditi	153
Dalvi Diksha P.	122, 149
Danu L. S.	49, 58
Das Aditi	249
Das Arindam	98, 99
Das Atanu	116, 117
Das D.	51
Das J.	197
Das M.K.	146
Das Pratik	159
Das Purbali	178
Das Saikat	296
Das Sanjay Kumar	64
Das Sayan	209
Das Tapas	195, 203, 204, 208, 209, 223
Dasgupta S.	56
Dash Bibek	136
Datrik C.	295, 307
Datta Arpita	152
Datta J.	56
De Sukanya	58
Deb S.B.	27, 67, 69, 109
Deep Shikha	153
Deokar U.V.	304
Desai S.S.	291
Desigan N.	94, 96, 97, 141, 142
Devi P.S. Remya	172
Devi Sagunthala	166
Dhamodharan K.	104, 107, 166, 167
Dhanasekaran A.	301
Dhankar K.	52
Dhanuradha S.V.V.	17
Dhara S.	85, 159
Dhara Sandip Kumar	84
Dhara Santanu	209
Dhekale Y.	182
Dhumale M.R.	233, 264
Dixit Rajashree	299
Dubey Jay Singh	247, 248
Dubey K.A.	207
Dubey Punit	43, 58
Dumpala Rama Mohan Rao	83, 112, 122, 149
Dusane Ajit R.	10

Authors Name	Page No.
Dusane C.B.	237
Dutta D.	44, 53
E	
Elumalai M.	154
F	
Faizal V.A	302
Femina F.N	125
Francis Sanju	218
G	
G Rani	216
Gaidhani S.R.	10
Gamare Jayashree S.	306
Gandhi A.	49
Ganesan Rajesh	103, 302
Ganesh Vemuri Lakshmi	101, 125, 126, 143
Gangadevi R.	171
Ganjave Bharat R.	195
Garg Saurabh	271
Gawandi S.N.	210
Gawandi Smita	205
Gayen J.K.	133, 150
George Reetta Sara	152
George T.	187
George Thomas	235
Gholve C.S.	210
Gholve Chandrakala	205
Ghosh Anushree	254, 255, 259
Ghosh Chanchal	84
Ghosh K.	210
Ghosh Pabitra	104
Ghosh S.	291
Ghugre Sandeep S.	249
Ginish Kumar P.	79
Giri Pankaj K.	249
Girikar Priya	158
Goel N.K.	218
Goel Shelly	134
Gogoi D.	98
Golda K. S.	43
Gopakumar	101, 125, 126, 143
Gopinadhanpillai	
Gopalkrishna A.	181
Goswami Preeti	71, 72
Goswami Sudeshna	230

Authors Name	Page No.
Goswami Sunil	194, 199, 213
Gothankar Sujata	160
Gowrinaidu B.	161
Goyal Anil	251
Goyal Priya	87, 135
Guchhait S.R.	108
Gujar R.B.	106, 207
Guleria Mohini	203, 204, 209, 223
Gumber Nitin	111, 280
Gupta A.K.	198
Gupta A.M.	243
Gupta Himanshu	154
Gupta K.K.	95
Gupta Riya	304
Gupta Ruma	145, 283
Gupta S.N.V.M.S.	81
Gupta Santosh K.	47, 51, 88, 100, 200, 201, 222
Gupta Sonal	202
Gupta Sonika	153, 158
Gupta Y. K.	34
H	
Haba H.	13
Hadi Khaled	17
Hanuman V.V.	75
Hari Prasad K.	296
Haridas Adish	154, 162
Harikumar S.M.	265
Hemalatha V.	80
Herin Thibaut	19
J	
Jadhav A. D.	155
Jadhav Rajesh T.	292
Jadhav Sachin B.	195
Jadhavar Sonali B.	220
Jain A.K.	228
Jain Akanksha	193
Jain Pankaj	293
Jain Sanyam	253
Jaison P.G.	71, 72, 115
Jalaluddin S.	256
Jaryal A.	254, 255
Jayabun Sk.	168, 290
Jayachandran Kavita	145, 306

Author Index

Authors Name	Page No.
Jayaraman V.	142, 298, 302
Jena Hrudananda	302
Jeyakumar S.	63, 78, 93, 113, 122, 149, 222
Jha A.	190
Jha M.K.	291
Jha V.N.	243, 275
Jhingan Akhil	43
Joshi G.C.	196, 197, 263
Joshi R.M.	276
Joy A.K.	187
K	
K Biju	50
K V. Greeshma	277
K. Sundararajan	37, 80, 90, 142, 151, 171
K.A. Greeshma	189
K.C. Sandeep	74
K.M. Sudheer	296
Kadam Apeksha	111
Kamaraju I.V.N.S.	60
Kamat Rupali C. K.	160
Kamble S.N.	254
Kandpal Smriti	263
Kanekar A.S.	85, 93
Kanojia Nitesh	201
Kanrar B.	163, 288
Kapoor Komal	170
Kar Adwitiya	150
Kar Aishwarya S.	116, 117
Kar Samrudhi	204
Karmakar D.	83
Karmakar Dipita	135
Karmakar Gourab	247, 248
Karthick R.	104
Karunakaran R.	302
Kashyap Y.S.	165
Kaur Gagan Deep	299
Kavasi Norbert	8
Keesari Tirumalesh	254, 255, 256, 272, 281
Kelkar A.	99, 107, 109, 138 154, 177
Kengar Ajit A.	202
Kerur B.R.	229, 267
Kerur Basavaraj Rachappa	269, 273
Kesarkar Tushar A.	296

Authors Name	Page No.
Keshari Ajay Kumar	289, 298
Keshavkumar B.	214
Keskar Meera	121
Khader S. A.	169, 190
Khadilkar H.V.	79
Khan Arshad	241, 256, 257
Khan Sahiralam	195
Kiran	43
Kodandaramanand J.	97
Kolay Soumi	203, 204
Koli Chhaya P.	303, 306
Kottuparamban D.	187
Krishna Mohan T.V.	60, 132, 266
Krishnakumar P.	282
Kulkarni S.	52, 73, 76
Kulkarni S.P.	181, 182, 183, 184, 185
Kumar Ajay	43, 48, 49, 58
Kumar Ajesh	265
Kumar Amit	112
Kumar Anil	263, 278
Kumar Aniruddha	155
Kumar Ankit	293
Kumar C. Krishna	99
Kumar Deepak	278
Kumar Jaivendra	278
Kumar Mahesh V.V.	170
Kumar Manoj	193, 202, 208
Kumar Mohit	43
Kumar P.V. Nagendra	81, 124
Kumar Pankaj	259
Kumar Phanindra M.	73, 76
Kumar Pranaw	112, 115
Kumar Rajeev	49
Kumar Rajesh	243
Kumar Ranjit	231, 234
Kumar Sandeep	296
Kumar Sanjeev	216
Kumar Satyam	48, 285, 286
Kumar Shiny S	85, 86, 93, 113, 122, 149
Kumar Suja A.	179
Kumar Sumit	121, 148
Kumar Sunil	73, 76, 154
Kumar Suresh V.	298
Kumar Umesh	169, 219

Authors Name	Page No.
Kumar V.	186, 206, 226
Kumar Virendra	169, 218
Kumaresan R.	36, 61, 62, 65, 289
Kumari Bhumika	281
Kumari Khushboo	67, 69, 109
Kumari Nitin	170
Kumari Vinita	114
Kumarsekaran P.	294
Kundu Soumalya	249
Kushwaha K.	214
Kutty V.K.M.	98, 99
L	
Lad Sangita	224
Lahiri S.	56, 212
Lakshmi Swaroopa	170
Lakshminarayana Y.	169, 219
Lakshmipathy D.V.	168, 290
Lal Surendra	196
Lalnuntluangi Rebecca	49
Lalremruata B.	49
Latha T.	277
Lavanya M.	302
Lawitlang S.	49
Layek Arkaprava	145, 283
Lenka P.	264, 279
Lohar Sharad P.	192
M	
M Sheela	216
M.P. Jayan	282
Mahadik Satish A.	220
Mahanty B.	38, 106, 129, 179
Mahur A.K.	252
Maity P.	291
Maity Sukanta	237
Maji Dasarath	298
Maji S	80
Malarvizhi B.	64
Managave Shreyas	259
Mani Gopal	196
Manikandan P.	302
Maniyoth S.K.	187
Manna Subhankar	284
Mason J. A.	305
Matei Liviu	31

Authors Name	Page No.
Mathur Anupam	223
Mazumder S.	291
Meena Ghanshyam	303, 306
Meena M.C.	228
Mehta Vimal	153
Menaria Tejpal	228, 258
Mhatre Amol	48, 131, 144, 175, 176
Mishra G.	58
Mishra Himanshu	259
Mishra M.K.	239
Mishra Prakash Chandra	255
Mishra Priyansu	200, 222
Mishra R.	256, 257
Mishra Satyabrata	96, 97, 104
Mishra Suchismita	237, 287
Mishra Sujata	136
Mishra Utkarsha	43
Mishra V.G.	146
Misra N.	186, 206, 226
Misra U.B.	180
Mitkari S.R.	225
Mitra Anant	169, 219
Mitra Arpit	223, 224
Mitra Pratip	271
Mitra S.	212
Mitra Sayantan	249
Mittal V.K.	139, 177
Modak B.	88
Mohan Anandhu	32, 68, 70, 284
Mohandas J.	98
Mohandas Jaya	99
Mohapatra M.	92, 105, 127, 201
Mohapatra P.K.	87, 95, 106, 130, 135
Mohokar H.V.	254, 255, 272, 281
Molla Samim	231, 234, 241
Mondal Jayanta	66
Mondal Suraj	166
Monika	49
Mor J.	45, 46
Muhammed A.K.	187
Mukherjee Anwasha	62
Mukherjee G.	56
Mukherjee S.	52, 56, 110
Mukherjee Sumana	249

Author Index

Authors Name	Page No.
Mukhopadhyay Chandan	104
Mukhopadhyay Sourav	296
Muniasamy L.	60
Murugesan N.	302
Mutugar Jayashri B.	268, 272
N	
Naga Raju G.J.	161
Nagar Adityamani	83, 130, 135
Nagar B.K.	72, 75
Nair Bhavya S.	166
Nair Janaki S.	219
Nair Varun	223
Nanabala R.	187
Nandi R.K.	212
Nandy S.K.	181, 182, 183, 184, 185
Narsaiah M.V.R.	278
Navamani N.	91
Nayak A.K.	29
Nayak B.K.	49
Nayak N.	93
Nedumaran S.	62
Nelliyil R. B.	45, 46
O	
Omveer Singh	196
P	
P Pravina	225
Padma Shruti B.	132
Pai R.V.	3, 111, 159, 163, 280, 284, 288
Pakhui Gurudas	62
Pal Kuntal Kumar	84
Pala R.G.S.	293
Palai Manisankar	80
Panda Pratyasha	136
Panda Soumitra	129
Pandey A.	155
Pandey D. K.	304
Pandey J.P.N.	304
Pandey Usha	223
Pandikumar G.	162
Panigrahi Akhilesh	300
Panja Suman	100
Pant Amar D.	173, 254
Pant Diksha	255, 272, 281

Authors Name	Page No.
Paradkar Shalaka	216
Parayil Reshmi T.	201
Parida Pratyusha	136
Parida S.C.	25, 79, 147
Parthasarathy Kothai	230, 301
Pasupuleti Kalpana	66
Pathak Nimai	127
Pathak Sachin	119, 120
Patil A.N.	66
Patil Anushka	217
Patil Asawari	205
Patil M.G.	186
Patil Prashant	119, 120
Patkare Geeta R.	128
Patnaik R.L.	274, 275
Patoju Sai Dilip	62
Patra A.C.	170, 231, 232, 233, 234, 236, 242, 243, 247, 248, 251, 261, 262, 264, 265, 270, 274, 275, 279
Patra Kankan	139, 177
Patra R.P.	242, 260, 262, 270
Patra Sabyasachi	48, 285, 286
Patra Sourav	191
Patre D.K.	92, 250
Paul Sabyasachi	164, 297
Paul Sriya	43, 58
Pazhakkal V.	187
Petrov V.G.	12
Pillai Anilkumar S.	173, 237
Pillai M.R.A.	41, 187
Pokkat J.	187
Poyet Stéphane	19
Prabhakar Rao J.	289, 298
Prabhath Ravi K	287
Prabhu T.V.	298
Pradeep Arjun	64
Pradhan L.	155
Prajapati Rishabh	43
Prajith R.	256, 257
Prakash Amrit	1, 299
Prasad Arvind	96
Prasad V.V.S.A.	10
Preetha R.	154
Prusty P.	242, 260, 262, 270

Authors Name	Page No.
Pulhani V.	156, 157, 160, 174, 199, 227, 238, 239, 240, 245, 246, 253
Puspalata R.	132
Puthiyottumkara A.K.	187
R	
Raghavendra Y.	266
Rai Abhishek Kumar	77
Raja Sk Wasim	54
Rajan K.	26, 107, 142, 166, 167
Raje Vividh	205
Rajeev K.P.	293
Rajeev R.	141
Rajesh Pushpalata	60, 104
Rajesh S.	229
Rajeswari S.	82
Rajkumar	300
Rakshit S.	182, 183, 184, 185
Rakshit S.K.	77, 79, 119, 120
Rakshit Sougata	189
Ram Laxman	216
Ram Ramu	195
Ramachandran K.	48
Ramakrishnan R.	60
Ramanathan N.	140
Ramanjaneyulu P.S.	73, 76
Ramesh B.	244
Ramesh S.	305
Rana B.K.	233, 241
Rana D.	274, 275
Rana Y.S.	285
Rane Swapnil	205
Rao A.	85, 86, 93
Rao A.D.P.	244
Rao Balaji Y.	29, 81, 124, 180
Rao Brahmaji J.S.	142
Rao G. Jogeswara	103
Rao G. Srinivasa	98, 99, 133, 150
Rao N. Srinivasa	161
Rashidi Amjad Al	17
Rath D.P.	92, 250
Rathod T.D.	157, 239
Rathore D.S.	258
Rathore N.S.	100
Rathore Raghvendra	236

Authors Name	Page No.
Ratna Rai	196
Raut Anil V.	225
Raut Rajarshi	249
Raut S.	210
Raut Vaibhavi V.	78
Ravi Jammu	141
Rawat M.	197
Rawat S.	186, 206, 226
Ray Mukti Kanta	224
Ray Vinod. K.	180
Reddy C. Santosh	75
Reddy G. Priyanka	271
Reddy G.L.N.	168, 290
Reddy Venkat G	64
Reshmi T.P.	105
Revathy T.	101, 126, 138
Rishika	277
Robert Selvan B.	140
Rohini P. E.	204
Rout A.	242, 260, 262, 270
Rout R.P.	256, 257
Rout Sabyasachi	245, 246, 253
Roy A.	254, 255, 272
Roy Amitava	169
Roy T.	165
Rufus A.L.	266
Ruhela Ritesh	114, 123, 173
S	
S Neha	277
S. Suresh	277
Sabarathinam Chidambaram	17
Sadhukhan Jhilam	43
Saha Abhijit	27, 67, 69, 79, 109
Saha Debasish	104, 142
Saha Dipankar	272
Sahoo B.K.	241
Sahoo G.S.	297
Sahoo S.K.	243
Sahu A.	260, 262, 270
Sahu A.K.	139
Sahu Abinash	242
Sahu P.	242
Sahu S.K.	114, 157, 238, 239, 240
Sahu Sanjit Kumar	255

Author Index

Authors Name	Page No.	Authors Name	Page No.
Sahu Sudeep Kumar	224	Shafeeq Muhammed	128
Saikia Leema	259	Shah Aaditya	223
Saindane Shashank S.	278	Shah Raju V.	115
Saket Ranjeet	116	Shakila L.	61
Sakhare Navin	216	Shakilaand L.	289
Salunke Chandra Kant	259	Shanbhag A.A.	164
Sam E.D. Shiny	79	Shanmugamani A.G.	150
Samanta S.K.	152	Sharathbabu M.	119, 120
Samanta Sudeep Kumar	178	Sharma Abhishek	147
Samanta T.	291	Sharma Anil	249
Samantray J.S.	194, 199, 213	Sharma D.B.	118
Samui P.	79	Sharma Gopal	177
Sanap Sneha Dinkar	225	Sharma M.K.	77
Sandeep P.	237	Sharma Pradeep Kumar	268
Saneesh N.	43	Sharma R.L.	252
Sanil N.	61, 65, 289	Sharma Richa	251
Santra S.	49	Sharma S.	252
Sanyal K.	163, 288	Sharma S. K.	46, 47
Sanyal Kaushik	159	Sharma S.C.	164, 198
Sapra B.K.	241, 256, 257	Sharma Shikha	112
Saradhi I.V.	228, 235, 253, 258, 276	Sharma V.K.	55, 194, 198, 199, 213
Sarathi Partha	108	Shastrakar R.S.	296
Sarita P.	161	Shastry K.	52
Sarkar Arnab	32, 68, 70, 284	Shedam Vaishali	296
Sarma Debajit	23	Shelar Sandeep B.	203
Sartandel S.J.	156, 199, 239	Shelkar S.A.	186, 206, 218, 226
Sasi Bhushan K.	70, 71	Shete P.P.	35
Sasmal S.	294	Shete Y.	182, 183, 184, 185, 205, 217
Sathe D.B.	100, 108, 110, 139, 155, 177	Shetty Madhuri	21
Satpati Drishty	193, 202, 208	Shetty P.G.	238, 240
Satpati S.K.	66, 284	Shetty Priyalata S.S.	192
Satpati Santhosh Kumar	268	Show S.	212
Satyakumar S.	10	Shrivastava R.	232
Savitri P. Padma	244	Shukla M.	165
Sawant P.D.	129, 179	Shukla Shefali	165
Sawarn T.	165	Sil Suvra	62
Saxena M.K.	73, 76, 78, 117	Singh Amrit Pal	170
Selvakumar J.	133, 266	Singh D.K.	108
Selvi B. S.	235	Singh Deepa	215, 221
Senapati Abhiram	298	Singh Jitendra	74
Sengupta A.	83, 87, 95, 130, 135, 139	Singh Khajan	191
Sengupta Pranesh	57	Singh Kulwant	57
Sengupta Somnath	137	Singh M.	53, 155
Sethy N.K.	261, 274, 275	Singh M.K.	274, 275

Authors Name	Page No.
Singh Namrata	43, 58
Singh Neeraj	211
Singh P.	165, 197
Singh P.K.	294
Singh Ritu	105
Singh Sarjan	261
Singh Shweta	43, 58
Singh Sunita	160
Singh Tej	15
Singh Virendra	211, 215
Singh Yogendra Kumar	211
Singhal Pallavi	232, 236, 247, 248
Sinharoy Prithwish	127
Sisodia M.	228
Sivakumar B.	294
Sivakumar P.	96, 142
Sivasankaran G.	294
Sodaye Suparna	158, 178, 292, 295, 303, 306, 307
Solanki Chanchal	177
Sonar V.R.	155
Soren Sibub	303, 306
Srabanee Snigdha	148
Sreejith Sathyapriya R	287
Sreenivasulu B.	82, 89, 90, 91, 101, 102, 125, 137, 138, 171
Srikanth S.	161
Srinivasan P.	59, 164, 297
Srinivasan S.	133, 150
Sriram S.	80
Srivastava A.	83, 86, 111, 112, 113, 119, 120
Srivastava Dinesh	81, 124
Srivastava R.S.	263
Srivastava S.K.	251, 279
Srivastava Saurabh	271
Srivastava V.S.	231, 234
Suba M. Amutha	140
Subramanian D.V.	154, 162
Sudarshan K.	47, 51, 222
Sudhagar S.	142
Sudhakar J.	244
Sugathan P.	43
Sugilal G.	95
Sukhwani Menka	296

Authors Name	Page No.
Sukumar A. A.	168, 290
Suman Shishu kant	191
Suman Vitisha	50
Sumesh C.G.	232, 251
Suneesh A.S.	103, 140
Sunitha Y.	168, 290
Suresh A.	89, 91
Suresh Sugandhi	174
Sureshkumar M.K.	282
Suryavanshi Harshali S.	174
Suvethaa R.	286
Swain K.K.	172
Swarnakar M.	238, 240
T	
Takale R.A.	238, 240
Tale K.V.	10
Tawade N.	295, 307
Tawate Megha	224
Telmore Vijay M.	115
Thakur B.D.	79
Thakur Smita	129
Thakur U.K.	63
Thakur V.K.	279
Thomas R. G.	58
Tiwari Mahesh	113, 156, 160, 173, 238, 262
Tiwari S.N.	228, 258
Towner A.C.N.	305
Tripathi R.	6, 48, 144, 175, 176, 285, 286, 292
Tripathy S.P.	297
Troughton N.A.	305
Turner H.R.	305
Tyagi Adish	247, 248
Tyagi Mohit	200, 201, 222
U	
Umadevi K.	268
Umasankari K.	49
Upadhyay Mahima	43, 58
Usha S.	167

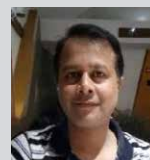
Author Index

Authors Name	Page No.
V	
V Hemachandar	92, 250
Vasudevan K.S.	300
Vats Bal Govind	128, 147
Vats V. Kusum	42, 203
Venkatesan K.A.	94, 96, 97, 104, 107, 166, 167
Verboom W.	106
Verma Gopal P.	279
Verma Poonam	63
Verma Rishi	66
Vhatkar Rajiv S.	220
Vigyan Nikhilesh Nav	123
Vijayakumar B.	235
Vijayalakshmi I.	301
Vimalnath K.V.	191, 192
Vinod Kumar A.	227
Vishnu M.S.	253, 276
Vishwa Prasad K.	170
Vishwasrao S.	295, 303, 306, 307
W	
Wadawale A.P.	118
Wagh P.J.	108
Warrier Manoj	244
Y	
Yadav A.K.	88
Yadav Deepak	221
Yadav Kartikey K.	108
Yadav Sonali	245, 246
Yadav V.B.	199, 227



Dr. Aishwarya Soumitra Kar is currently serving as a Scientific Officer 'G' in Radioanalytical Chemistry Division, BARC. She earned her M.Sc. in Chemistry from the Indian Institute of Technology, Roorkee in 2004, and her Ph.D. in Chemistry from the HBNI, Mumbai in 2014. During her academic tenure, she was awarded a Gold Medal for achieving the highest C.G.P.A. in both Chemistry and the overall Sciences category at IIT, Roorkee. Dr. Kar belongs to the 48th batch of the BARC Training School, and her primary research interests lie in the speciation of radionuclides. She is the recipient of DAE Group Achievement Award in 2014. She has authored about 50 research papers in peer-reviewed journals.

Dr. Sadhan Deb has over 25 years of experience in the field of analytical chemistry, with a particular focus on the development and optimization of techniques for the characterization of nuclear materials. Throughout his career, he has contributed significantly to the advancement of robust analytical methodologies, several of which are now routinely employed in chemical quality assurance of nuclear components. His primary area of specialization lies in the quantification of trace metallic elements using spectrometric techniques, including ICP-MS and ICP-OES. Currently, he is engaged in the development and application of direct solid sampling methods using ETV-ICP-OES. He has more than 30 publications in peer reviewed international journals.



Dr. Seraj Ansari graduated in Chemistry from The University of Mumbai in 2000 and received Doctoral Degree from the same University in 2008. He did Postdoctoral Research at Lawrence Berkeley National Laboratory, USA. He joined Radiochemistry Division of BARC in 2009. His research interest includes the complexation thermodynamics and separation of actinides with state of art designed organic ligands. He is a member of National Academy of Sciences India (NASI). He is the author of about than 160 research papers in the leading International Journals with citation index more than 5600, *h*-index of 38 and *i*-10 index of 113 (Google Scholar).

Dr. S.K. Rakshit joined BARC, Mumbai in the year 2000, and since then, he is working in the field of high temperature thermodynamics of materials relevant to material science and nuclear technology. He received Ph.D. (Chemistry) from the University of Mumbai in the year 2010. He has contributed significantly to develop a high-volume assay calorimeter for the department, and his work in BARC has led to 5 DAE awards and more than 25 research papers in peer-reviewed journals. He is the recipient of TA Instruments – ITAS Young Scientist Award - 2010. His current area of research interest is thermodynamic studies on materials relevant to nuclear technologies and molten salt system and calorimetric assay of nuclear materials.



Dr. Subbiah Jeyakumar obtained his M.Sc. in Chemistry from Madurai Kamaraj University, Madurai. Later, he obtained PhD in analytical chemistry from the University of Mumbai. He joined the Fuel Chemistry Division of BARC, Mumbai in 1988. He is an expert in the field of chemical quality control of nuclear fuels and chemical characterisation of reactor materials. His field of research interests are CQC of nuclear fuels and reactor materials, HPLC, ion chromatography, pyrohydrolytic separations and capillary electrophoresis. Currently, he is the Head, Radiochemistry Division, BARC.

Shri M.K. Saxena, former Head, Radioanalytical Chemistry Division, RC&I Group, joined BARC in 1988. His research interests include trace element quantification using mass spectrometry, total gas analysis, O, N, H & C determinators. He has developed methodologies for determining the isotopic composition of actinides using TIMS and gamma spectrometry. Additionally, he has a keen interest in thermal analysis through DSC. In 2018, he served as Course Director for the IAEA International workshop on state system of accounting, organized by the Global Centre for Nuclear Energy Partnership (GCNEP). Shri Saxena has received several DAE Group Achievement Awards and has authored over 50 publications in peer-reviewed international journals.



Dr. Y. K. Bhardwaj joined BARC in the year 1989. He has been working in the field of high energy radiation processing of materials for environmental, agricultural and industrial applications. This includes radiation crosslinking of polymers, their blends & composites for sensing applications, shape memory polymers, high-performance coatings, water soluble polymers for healthcare stimuli responsive hydrogels and designing grafted matrices for environmental pollution mitigation. For his contribution to the field of radiation processing of materials he was bestowed upon DAE Science and Technical Excellence Award in year 2010. He has more than 130 papers in peer reviewed journals, has co-authored fourteen book chapters and has a patent to his credit. Currently he is Outstanding Scientist and Associate Director, RC&I Group of BARC, Mumbai.